

Trends in Radiopharmaceuticals (ISTR-2005)

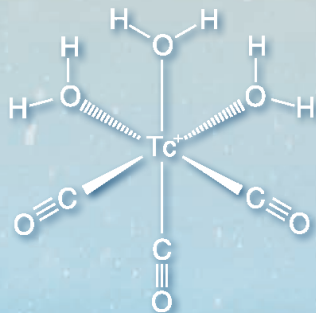
Proceedings of an International Symposium
Vienna, 14–18 November 2005

Vol. 1



IAEA

International Atomic Energy Agency



TRENDS IN
RADIOPHARMACEUTICALS
(ISTR-2005)

VOLUME 1

The following States are Members of the International Atomic Energy Agency:

AFGHANISTAN	GREECE	NORWAY
ALBANIA	GUATEMALA	PAKISTAN
ALGERIA	HAITI	PALAU
ANGOLA	HOLY SEE	PANAMA
ARGENTINA	HONDURAS	PARAGUAY
ARMENIA	HUNGARY	PERU
AUSTRALIA	ICELAND	PHILIPPINES
AUSTRIA	INDIA	POLAND
AZERBAIJAN	INDONESIA	PORTUGAL
BANGLADESH	IRAN, ISLAMIC REPUBLIC OF	QATAR
BELARUS	IRAQ	REPUBLIC OF MOLDOVA
BELGIUM	IRELAND	ROMANIA
BELIZE	ISRAEL	RUSSIAN FEDERATION
BENIN	ITALY	SAUDI ARABIA
BOLIVIA	JAMAICA	SENEGAL
BOSNIA AND HERZEGOVINA	JAPAN	SERBIA
BOTSWANA	JORDAN	SEYCHELLES
BRAZIL	KAZAKHSTAN	SIERRA LEONE
BULGARIA	KENYA	SINGAPORE
BURKINA FASO	KOREA, REPUBLIC OF	SLOVAKIA
CAMEROON	KUWAIT	SLOVENIA
CANADA	KYRGYZSTAN	SOUTH AFRICA
CENTRAL AFRICAN REPUBLIC	LATVIA	SPAIN
CHAD	LEBANON	SRI LANKA
CHILE	LIBERIA	SUDAN
CHINA	LIBYAN ARAB JAMAHIRIYA	SWEDEN
COLOMBIA	LIECHTENSTEIN	SWITZERLAND
COSTA RICA	LITHUANIA	SYRIAN ARAB REPUBLIC
CÔTE D'IVOIRE	LUXEMBOURG	TAJIKISTAN
CROATIA	MADAGASCAR	THAILAND
CUBA	MALAWI	THE FORMER YUGOSLAV REPUBLIC OF MACEDONIA
CYPRUS	MALAYSIA	TUNISIA
CZECH REPUBLIC	MALI	TURKEY
DEMOCRATIC REPUBLIC OF THE CONGO	MALTA	UGANDA
DENMARK	MARSHALL ISLANDS	UKRAINE
DOMINICAN REPUBLIC	MAURITANIA	UNITED ARAB EMIRATES
ECUADOR	MAURITIUS	UNITED KINGDOM OF GREAT BRITAIN AND NORTHERN IRELAND
EGYPT	MEXICO	UNITED REPUBLIC OF TANZANIA
EL SALVADOR	MONACO	UNITED STATES OF AMERICA
ERITREA	MONGOLIA	URUGUAY
ESTONIA	MONTENEGRO	UZBEKISTAN
ETHIOPIA	MOROCCO	VENEZUELA
FINLAND	MOZAMBIQUE	VIETNAM
FRANCE	MYANMAR	YEMEN
GABON	NAMIBIA	ZAMBIA
GEORGIA	NETHERLANDS	ZIMBABWE
GERMANY	NEW ZEALAND	
GHANA	NICARAGUA	
	NIGER	
	NIGERIA	

The Agency's Statute was approved on 23 October 1956 by the Conference on the Statute of the IAEA held at United Nations Headquarters, New York; it entered into force on 29 July 1957. The Headquarters of the Agency are situated in Vienna. Its principal objective is "to accelerate and enlarge the contribution of atomic energy to peace, health and prosperity throughout the world".

PROCEEDINGS SERIES

TRENDS IN
RADIOPHARMACEUTICALS
(ISTR-2005)

PROCEEDINGS OF AN INTERNATIONAL SYMPOSIUM
ORGANIZED BY THE INTERNATIONAL ATOMIC ENERGY AGENCY
AND HELD IN VIENNA, 14-18 NOVEMBER 2005

In two volumes

VOLUME 1

INTERNATIONAL ATOMIC ENERGY AGENCY
VIENNA, 2007

COPYRIGHT NOTICE

All IAEA scientific and technical publications are protected by the terms of the Universal Copyright Convention as adopted in 1952 (Berne) and as revised in 1972 (Paris). The copyright has since been extended by the World Intellectual Property Organization (Geneva) to include electronic and virtual intellectual property. Permission to use whole or parts of texts contained in IAEA publications in printed or electronic form must be obtained and is usually subject to royalty agreements. Proposals for non-commercial reproductions and translations are welcomed and considered on a case-by-case basis. Enquiries should be addressed to the IAEA Publishing Section at:

Sales and Promotion, Publishing Section
International Atomic Energy Agency
Wagramer Strasse 5
P.O. Box 100
1400 Vienna, Austria
fax: +43 1 2600 29302
tel.: +43 1 2600 22417
email: sales.publications@iaea.org
<http://www.iaea.org/books>

© IAEA, 2007

Printed by the IAEA in Austria
November 2007
STI/PUB/1294

IAEA Library Cataloguing in Publication Data

International Symposium on Trends in Radiopharmaceuticals (2005 : Vienna, Austria)

Trends in radiopharmaceuticals : ISTR-2005 : proceedings of an international symposium / organized by the International Atomic Energy Agency and held in Vienna, 14–18 November, 2005. — Vienna : IAEA, 2007.

p. ; 24 cm. (Proceedings series, ISSN 0074–1884)

STI/PUB/1294

ISBN 92–0–101707–3

Includes bibliographical references.

1. Radiopharmaceuticals — Congresses. 2. Nuclear medicine — Congresses. I. International Atomic Energy Agency. II. Series: Proceedings series (International Atomic Energy Agency).

IAEAL

07–00497

FOREWORD

The growth of nuclear medicine depends on advances in radiopharmaceutical development and discovery, as well as improvements in instrumentation. The field of radiopharmaceuticals has witnessed continuous evolution thanks to the contributions of scientists from diverse disciplines such as chemistry, physiology and pharmacology. The IAEA has been supporting activities in the field of radiopharmaceuticals, which has resulted in significant capacity building in the above fields in Member States. Many Member States have developed manufacturing facilities through technical cooperation projects for the large scale production of radiopharmaceuticals which helped the growth of nuclear medicine in those countries. IAEA efforts through coordinated research projects have also helped in advancing research activities in the development and utilization of new products in many Member States.

The International Symposium on Trends in Radiopharmaceuticals (ISTR-2005) was organized in order to provide scientists and professionals from 70 countries working in the field of radiopharmaceuticals and related sciences with the opportunity to present their research to an international audience. Sessions covered the most relevant topics of radiopharmaceuticals chemistry, including radionuclide production, radiochemical processing, manufacturing and quality control, quality assurance, latest advances in radiopharmaceuticals research, good manufacturing practices and regulatory aspects. On the basis of the invited presentations, papers and panel discussions during ISTR-2005, several areas of possible future international cooperation were identified.

This publication comprises two volumes and constitutes a record of the symposium and includes a summary as well as invited papers presented. A CD-ROM containing the unedited contributed papers which were presented in the two poster sessions of the symposium is included in volume 2.

The IAEA gratefully acknowledges the contribution made by the various participants to the success of this symposium, in particular to M.M. Vora for his technical editing of the papers.

EDITORIAL NOTE

The Proceedings have been edited by the editorial staff of the IAEA to the extent considered necessary for the reader's assistance. The views expressed remain, however, the responsibility of the named authors or participants. In addition, the views are not necessarily those of the governments of the nominating Member States or of the nominating organizations.

Although great care has been taken to maintain the accuracy of information contained in this publication, neither the IAEA nor its Member States assume any responsibility for consequences which may arise from its use.

The use of particular designations of countries or territories does not imply any judgement by the publisher, the IAEA, as to the legal status of such countries or territories, of their authorities and institutions or of the delimitation of their boundaries.

The mention of names of specific companies or products (whether or not indicated as registered) does not imply any intention to infringe proprietary rights, nor should it be construed as an endorsement or recommendation on the part of the IAEA.

The authors are responsible for having obtained the necessary permission for the IAEA to reproduce, translate or use material from sources already protected by copyrights.

CONTENTS OF VOLUME 1

SUMMARY	i
---------------	---

TECHNETIUM CHEMISTRY AND RADIOPHARMACEUTICALS: I (Session 1)

Technetium-99m radiopharmaceuticals: Current situation and perspectives	3
<i>A.M. Verbruggen</i>	
^{99m} Tc labelled minigastrin for tumour targeting: Optimization of labelling and peptide sequence.	21
<i>E. von Guggenberg, M.P. Béhé, C. Decristoforo</i>	
Design and synthesis of isoniazide mimetic conjugated with DTPA, potential ligand of novel radiopharmaceutical and contrast agent for medical imaging, bis (amide) of diethylenetriaminepentaacetic acid: DTPA-Bis(INH)	31
<i>A.K. Mishra, P. Panwar, K. Chuttani, N. Kumar, P. Mishra, R.K. Sharma, R. Sharma</i>	
Antimicrobial peptide ^{99m} Tc-UBI 29-41 for infection diagnosis: Kit formulation and a preliminary clinical study	43
<i>G. Rodríguez, P. Oliver, J. Vilar, V. Trindade, A. Robles, A. López, G. Lago, H. Balter, M.M. Welling, E.K.J. Pauwels</i>	

TECHNETIUM CHEMISTRY AND RADIOPHARMACEUTICALS: II (Session 2)

Preparation and evaluation of third generation technetium-99m radiopharmaceuticals.	55
<i>G. Ferro-Flores, C. Arteaga de Murphy, F. de M. Ramirez, M. Pedraza-López, J. Rodríguez-Cortés, L. Meléndez-Alafort</i>	
Detection of deep venous thrombosis in an experimental animal model using radioactive labelled tirofiban GPIIb/IIIa inhibitor	65
<i>E. Janevik-Ivanovska, I. Djorgoski, A. Andonovski, V. Milenkov, S. Miceva-Ristevska, G. Janoki</i>	

Preparation of in-house Dextran and its clinical applications in sentinel node studies, Siriraj Hospital	83
<i>N. Tojinda, S. Chiewvit, B. Khiewvan, S. Dumrongpisutikul, A. Ratanawichitrasin, S. Taweepraditpol</i>	

Comparative study of ^{99m}Tc -EMB and native EMB and the role of ^{99m}Tc -EMB in resistant mycobacterial imaging	95
<i>N. Singh, A.K. Singh, A. Bhatnagar, G. Mittal, T. Ravindranath</i>	

TECHNETIUM CHEMISTRY AND RADIOPHARMACEUTICALS: III (Session 3)

Technetium radiopharmaceuticals: Applications in nuclear cardiology . . .	103
<i>R.M.T. Giubbini</i>	

Imaging oncogene mRNA for early diagnosis of cancer	113
<i>N. Shanthly, M.R. Aruva, K. Zhang, C.A. Cardi, T. Xiobing, E. Wickstrom, M.L. Thakur</i>	

Synthesis and evaluation of ^{99m}Tc -Kanamycin and ^{99m}Tc -Isoniazid for infection imaging	149
<i>M. Jehangir, A. Mushtaq, S.A. Malik, S. Roohi</i>	

Preparation of ^{99m}Tc -pentavalent DMSA and its uptake by benign bone diseases	167
<i>N. Boucekkine, S.A. Zemoul, F. Mouas, R. Benlabгаа, S. Hanzal, A. Khelifa, F. Mechken, M. Habeche, K. Bellazoug, B. Benchelaghem, S.E. Bouyoucef</i>	

NOVEL TECHNETIUM CHEMISTRY AND RADIOPHARMACEUTICALS: I (Session 4)

What role for ^{99m}Tc radiopharmaceuticals in the age of molecular imaging?	171
<i>A. Duatti</i>	

^{99m}Tc EDDA/HYNIC-TOC: A suitable radiopharmaceutical for radioguided surgery of neuroendocrine tumours	183
<i>J. Fettich, S. Repse, M. Snoj, M. Zitko-Krhin, S. Markovic</i>	

Comparative in vitro and in vivo evaluation of a series of novel bombesin-like peptides	185
<i>E. Gourni, P. Bouziotis, M. Paravatou, S. Xanthopoulos, S.C. Archimandritis, A.D. Varvarigou, M. Fani, G. Loudos</i>	
[^{99m} TcN]-N-benzyl piperidine dithiocarbonate: A potential sigma receptor imaging agent	197
<i>D. Satpati, K. Bapat, S. Banerjee, K. Kothari, H.D. Sarma, M. Venkatesh</i>	
^{99m} Tc labelled peptide F11: A new potential $\alpha_v\beta_3$ integrin antagonist for scintigraphic detection of tumours	205
<i>A. Perera, A. Prats, A. Hernández, O. Reyes, M. Bequet, N. Santiago, R. Leyva, E. Fernandez, G. Pimentel</i>	
HYNIC-TOC labelled with ^{99m} Tc via an instant kit formulation: Preclinical results	217
<i>M. Ciavaro, E. Obenaus, G. Fiszman, S.G. de Castiglia</i>	

**INDIGENOUS CAPACITY BUILDING
IN RADIOPHARMACEUTICALS (Session 5)**

Indigenous capacity building in radiopharmaceuticals: Saudi Arabian experience	227
<i>M.M. Vora</i>	
Trends in indigenous radioisotope and radiopharmaceutical production in Bangladesh	241
<i>M.Z. Abedin, M.A. Haque</i>	
Experience in the production of Pakgen ⁹⁹ Mo– ^{99m} Tc generators	249
<i>M.M. Ishfaq, H. Nizakat, K.M. Bashir, M. Jehangir</i>	
BIONT — A new centre for PET radiopharmaceuticals production in central Europe	265
<i>P. Rajec, F. Macásek, P. Kováč</i>	
Capacities and current activities of the Cyclotron and Nuclear Medicine Department at NRCAM	271
<i>K.K. Moghaddam</i>	

REACTOR BASED RADIONUCLIDES AND GENERATORS

(Session 6)

Production of therapeutic radionuclides in medium flux research reactors	285
<i>M. Venkatesh, S. Chakraborty</i>	
The continuing important role of high flux research reactors for production of therapeutic radioisotopes	301
<i>F.F. Knapp, Jr., S. Mirzadeh, M.A. Garland</i>	
Technological line for the production of carrier free ^{188}Re in the form of sterile isotonic solution of sodium perrhenate(VII)	323
<i>E. Iller, Z. Zelek, M. Konior, K. Sawlewicz, J. Staniszevska, R. Mikolajczak, U. Karczmarczyk</i>	
Hydroxyapatite based ^{99}Mo – $^{99\text{m}}\text{Tc}$ and ^{188}W – ^{188}Re generator systems.	333
<i>F. Monroy-Guzmán, V.E. Badillo-Almaraz, J.A. Flores de la Torre, J. Cosgrove, F.F. Knapp, Jr.</i>	
Fostering development efforts towards (a) small scale local production of ^{99}Mo from LEU targets and (b) gel generator for $^{99\text{m}}\text{Tc}$ using (n, γ) ^{99}Mo : The IAEA role.	349
<i>N. Ramamoorthy, I. Goldman, P. Adelfang</i>	

NOVEL TECHNETIUM CHEMISTRY

AND RADIOPHARMACEUTICALS: II (Session 7)

Novel technetium chemistry and radiopharmaceuticals: Tc(V), Tc(III) or Tc(I) – which way to go for keeping Tc radiopharmaceuticals alive?	355
<i>R. Alberto, S. Kunze, S. Mundwiler, B. Spingler</i>	
New $^{99\text{m}}\text{Tc}$ -cysteine piperidine compound as a specific brain imaging agent	365
<i>M. Saidi, M. Trabelsi, A. Mekni</i>	

Tricarbonyltechnetium(I) complexes with neutral bidentate ligands — N-methyl-2-pyridinecarboamide and N-methyl-2-pyridinecarbothioamide: Experimental and theoretical studies	367
<i>J. Narbutt, M. Zasepa-Lyczko, M. Czerwinski, R. Schibli</i>	
Modified bombesin analogue with technetium tricarbonyl precursor as prostatic radiodiagnostic agent	375
<i>B.L. Faintuch, E. Muramoto, L. Morganti, R.M. Chura-Chambi, N. Nascimento, E.G. Garayoa, P. Blauenstein, P.A. Schubiger</i>	
Synthesis and characterization of ^{99m} Tc-metomidate as the ^{99m} Tc(I)-tricarbonyl-(R)-bipyridinyl-MTO-conjugate	383
<i>R. Schibli, M. Stichelberger, F. Hammerschmidt, M.L. Berger, I. Zolle</i>	
Direct labelling of Lipiodol with [¹⁸⁸ Re(CO) ₃]-chelates	395
<i>M.M. Saw, F.X. Sundram, T.S. Andy Hor, Y.Y. Kai, R. Alberto</i>	

SUMMARY

The International Symposium on Trends in Radiopharmaceuticals (ISTR-2005) was held on 14–18 November 2005 in Vienna. Two hundred and twenty participants attended the symposium, of which 142 were from developing Member States. Seventy Member States participated in the symposium, of which 52 were developing Member States. Eighty-three of the 220 participants were female scientists, mostly from developing Member States.

The symposium was opened by W. Burkart, Deputy Director General, Department of Nuclear Sciences and Applications, followed by A.M. Cetto, Deputy Director General, Department of Technical Cooperation, who spoke on the role of technical cooperation in promoting radiopharmaceuticals and nuclear medicine in Member States. Additional remarks were made by I. Carrio, President, European Association of Nuclear Medicine; M.L. Thakur immediate past President, Society of Nuclear Medicine; and M.C. Lee, President, World Federation of Nuclear Medicine and Biology.

A total of 156 papers were presented at the symposium, of which 66 were oral presentations, including 21 invited talks in the 16 scientific sessions; the remaining 90 papers were presented in two poster sessions. In addition there were two round table discussion on “Cyclotron PET Facilities” and “GMP and Regulatory Aspects” and the closing session which summed up the important contributions and achievements of the symposium.

The chemistry of technetium, radiopharmaceuticals research, development of new formulations and some of the relevant applications were covered in the four sessions devoted to these topics. There has been slow progress in the introduction of new technetium radiopharmaceuticals to the market in recent years, despite the good developmental efforts and the fact that technetium based radiopharmaceuticals are economic and universally available. The high cost of toxicity studies and clinical trials, together with competition from PET and other imaging modalities such as MRI and spiral CT come in the way of converting good research outputs into products. Industry driven and funded research initiatives for an assigned clinical target where there is an established lack of agents seems to be one way to solve the above scenario. Promoting a more efficient clinical use of new ^{99m}Tc radiopharmaceuticals by approaching the relevant authorities to encourage a less strict and less complex procedure for approval of new radiopharmaceuticals and making the products available to a broad selection of radiopharmacy and nuclear medicine practitioners were some of the suggestions.

SUMMARY

PET using ^{18}F FDG has shown the highest growth rate in recent times. However, despite the several positive developments, none of the ^{18}F radiopharmaceuticals except ^{18}F FDG has come to the large clinical arena and greater efforts are needed to develop them as useful clinical products. The various options for automation of the synthesis of new PET radiopharmaceuticals were also presented.

Application of therapeutic radiopharmaceuticals is one of the fastest growing areas of nuclear medicine and this was amply reflected by the number of presentations in the therapeutic radiopharmaceutical sessions, both oral and poster. Lutetium-177 has caught the attention of several scientists and interesting studies on the development of therapeutic radiopharmaceuticals with this isotope were reported. Radiosynoviorthesis using radiolabelled particulates is a complementary therapy for arthritis. Details of the production and large animal clinical studies were presented. The merits of using alpha particle carrying radiopharmaceuticals for targeted therapy were discussed; the disadvantage being the non-availability of the isotopes in large quantities worldwide for which there is no immediate solution.

Radionuclide production is an important area for the development and routine use of radiopharmaceuticals and several Member States operate nuclear reactors and cyclotrons for production of medically important isotopes. Various options available with the medium flux and high flux research reactors for the production of medically useful isotopes were discussed. The capability of a high flux research reactor to produce near theoretical specific activity was demonstrated in the case of ^{177}Lu . The IAEA's efforts towards promoting the use of LEU for production of ^{99}Mo in consonance with the RERTR programme were highlighted in an IAEA sponsored paper.

The use of cyclotrons for the production of radioisotopes for nuclear medicine applications has been increasing very rapidly. A large number of new establishments have been set up in the last few years which have medium energy cyclotrons (11–18 MeV), radiochemistry and PET–CT machines. The use of high energy (>40 MeV) machines has not increased significantly. Major research activities are directed towards improving the production yield of radionuclides by using better targetry and more efficient radiochemical processing methods.

Success stories on radiopharmaceutical capacity building achieved through IAEA technical cooperation programmes were presented by several Member States. Details of regular production of $^{99\text{m}}\text{Tc}$ generators, kits, ^{131}I products and operation of cyclotrons for SPECT and PET radiopharmaceuticals production undertaken in several Member States through such technical cooperation programmes were presented.

SUMMARY

Major issues on how to support the growth of PET in Member States was the theme of a panel discussion on cyclotron–PET facilities. The different types of cyclotron facility and the essential needs of these different categories of installations were discussed. FDG–PET is a cost effective modality which is more accurate than a CT–MRI scan for most disorders, as metabolic activity precedes changes in anatomy. The clinical utility of PET is 90% in oncology and 5% each in neurosciences and cardiology. The major utility of PET in oncology is in the detection of unknown primary, staging and restaging, follow-up, recurrence of radiation necrosis, efficacy evaluation of expensive chemotherapy, etc. However, PET is not a replacement for conventional nuclear medicine using ^{99m}Tc and use of the latter technique will continue to grow.

A panel discussion on current good management practice (GMP) in radiopharmaceuticals production was held during the meeting. The quality standards such as ISO and GMP and the need to have GMP for radiopharmaceuticals production were discussed. The type of clean room facilities, hot cells and production boxes needed for such facilities as well as the need to harmonize the conflicting considerations on radiation safety and microbiological safety were deliberated.

Fifteen commercial exhibitors participated in the symposium. The exhibitors included hot cell manufacturers, synthesis module suppliers and radiopharmaceutical companies other than general laboratory suppliers. The exhibition provided an opportunity for the participants to interact with the suppliers and get to know the new developments and products in the radiopharmaceutical field.

The various conclusions and recommendations arising out of the symposium are given below:

- The focus of the symposium was on the vital aspects of high practical value, e.g. production and quality control of products for widespread distribution and utilization; emerging importance of PET tracers; radio-nuclide therapy, especially the role of ^{177}Lu ; setting up of a cyclotron–PET facility; and issues in GMP of radiopharmaceuticals.
- The symposium reflected the considerable impact on capacity building made by Member States to undertake developmental tasks in various areas of radiopharmaceuticals. The IAEA's support through its technical cooperation projects for establishing facilities for the local production and utilization of radiopharmaceuticals has been employed to good effect by several Member States.
- The role of the IAEA's coordinated research project mechanism was 'visible' through several contributed papers from various Member States.

SUMMARY

- Major professional bodies in the field, namely the European Association of Nuclear Medicine, the Society of Nuclear Medicine, the Society for Radiopharmaceutical Sciences and the World Federation of Nuclear Medicine and Biology participated in the symposium. Such partnerships and involvement will help to achieve synergy and greater impact.
- Programmes and appropriate interactive mechanisms have been established to facilitate the use of new radiopharmaceutical developments in the clinical arena.
- Cyclotron–PET facilities in Member States need to be encouraged. Programmes on generator based PET radionuclides that will expand the scope of PET to more centres, in addition to improving the utility of existing PET facilities, are to be taken up.
- The use of therapeutic radiopharmaceuticals is increasing and appropriate programmes should be established to increase their availability in Member States.
- The participants emphasized the need for holding periodic conferences in the radiopharmaceutical sciences as this is one of the most highly visible and useful means of discussing the applications of radioisotopes.

TECHNETIUM CHEMISTRY AND
RADIOPHARMACEUTICALS: 1

(Session 1)

Chairpersons

S. GOMEZ DE CASTIGLIA
Argentina

F.F. KNAPP, Jr.
United States of America

TECHNETIUM-99m RADIOPHARMACEUTICALS

Current situation and perspectives

A.M. VERBRUGGEN

Laboratory of Radiopharmacy,

Katholieke Universiteit Leuven,

B-3000 Leuven, Belgium

Email: alfons.verbruggen@far.kuleuven.ac.be

Abstract

The ^{99m}Tc radiopharmaceuticals currently in clinical use in nuclear medicine have been developed from the mid-1960s up until the early 1990s by a combination of coincidence, trial and error and rational design. Further development of Tc chemistry (tricarboxyls, Hynic, conjugates, etc) created new opportunities and resulted in promising new ^{99m}Tc labelled tracer agents but no new 'Tc essential' radiopharmaceuticals have been approved within the last 15 years. Both scientific and economic reasons are the cause of this stagnation, such as the difficulty of preserving biological activity upon derivatization of a biologically active compound with a ^{99m}Tc complex, the high cost of development and limited return on investment of diagnostic drugs, and the increasing performance and competition of other imaging modalities. Ongoing developments in detector characteristics and SPECT camera design may be expected to result in continued investment and interest in ^{99m}Tc compounds and other SPECT tracer agents.

1. INTRODUCTION

Thanks to the favourable physical and imaging characteristics of ^{99m}Tc and the convenient availability of a broad series of ^{99m}Tc radiopharmaceuticals for diagnosis of a variety of diseases, ^{99m}Tc radiopharmaceuticals have been a cornerstone of nuclear medicine over the last 35 years of the 20th century. Attractive properties of this radionuclide include:

- (a) Its continuous availability at low cost from safe and well performing commercial ^{99m}Tc generators.
- (b) Its low radiation dose to patients and manipulators resulting from its short physical half-life (6.02 h) and the absence of particular radiation, except for a negligible percentage of beta-minus decay (<0.001%).

VERBRUGGEN

- (c) The ease of shielding the 140 keV gamma rays (an attenuation factor of about 10 for 1 mm of lead).
- (d) The energy of the gamma rays is ideal for efficient detection by Anger cameras and limited absorption in tissues. As a result, excellent images can be generated after a safe injection of up to 1100 MBq of a ^{99m}Tc radiopharmaceutical.

As a result of these nearly optimal characteristics of ^{99m}Tc , a large number of researchers from industry and academia has since the mid-1960s put a lot of effort into the development of new and specific ^{99m}Tc radiopharmaceuticals. This has resulted, especially in the late 1970s and 1980s, in a large number of useful novel ^{99m}Tc labelled tracer agents, of which several but not all have been introduced into clinical use. The intensity and success of the research in this field can be illustrated by the fact that a search in PubMed (www.ncbi.nih.gov/entrez) yields almost 40 000 scientific papers dealing with ^{99m}Tc over the period from 1963 to November 2005 (see Table 1). PubMed Central is the National Institutes of Health (NIH) free digital archive of biomedical and life sciences journal literature.

TABLE 1. NUMBER OF SCIENTIFIC PAPERS IN PUBMED (UP TO NOVEMBER 2005) ON ^{99m}Tc LABELLED RADIOPHARMACEUTICAL AND SOME RELATED TRACERS

Search term	Hits
Technetium	38 186
Mertiatide	607
Sestamibi	4012
Tetrofosmin	849
Exametazime	2547
Bicisate	411
TRODAT-1	80
DatSCAN	90
Hynic	125
FDG	8300

SESSION 1

2. SUCCESSFUL DEVELOPMENT OF ^{99m}Tc RADIOPHARMACEUTICALS

For most ^{99m}Tc radiopharmaceuticals developed up to the mid-1970s — ‘the old generation’ — and also for a number of recently introduced ^{99m}Tc labelled proteins or antibodies, the exact structure of the Tc compound is not known and the way of binding Tc has been characterized poorly or even not at all. Radiopharmaceuticals belonging to this class are:

- (a) ^{99m}Tc labelled colloids based on colloidal sulphur, antimony sulphide, rhenium sulphide, stannous sulphide, SnO_2 , denatured albumin particles (<7 μm diameter);
- (b) ^{99m}Tc labelled larger (10–100 μm) and smaller (nanometre size) particles — albumin aggregates and microspheres, Technegas;
- (c) $^{99m}\text{Tc(III)}$ -succimer (DMSA);
- (d) ^{99m}Tc -pentetate (DTPA);
- (e) ^{99m}Tc -diphosphonates (MDP, HDP, DPD);
- (f) ^{99m}Tc labelled albumin;
- (g) ^{99m}Tc labelled antibodies (or fragments) — arcitumomab (CEA-Scan), fanolesumab (Neutrospec, no longer in use because of serious side effects), anti-granulocyte Ab (Leukoscan, BW 250/283).

For some of these tracer agents, the preparation contains multiple components of unknown structure (e.g. ^{99m}Tc -diphosphonates) or the Tc binding compound contains several binding sites for the metal (e.g. proteins). Although it would be difficult to obtain approval for such preparations at this moment, they continue to be used in nuclear medicine on the basis of their well-established clinical value.

From the mid-1970s on, researchers in radiopharmaceutical companies and research institutes have been successful in developing especially designed and well-characterized ^{99m}Tc complexes (or in some cases discovered their useful properties by coincidence) and a number of these tracer agents have become radiopharmaceuticals that are still in use (Fig. 1). It concerns:

- (a) ^{99m}Tc complexes with derivatives of phenylcarbamoylmethylimino-diacetic acid, substituted on the phenyl ring with methyl (Hida, ^{99m}Tc -lidofenin, 1976), ethyl (Ehida, ^{99m}Tc -etifenin, 1978), isopropyl (Disida, ^{99m}Tc -disofenin, 1980) or methyl and bromine (Brida, ^{99m}Tc -mebrofenin, 1982, currently the agent of choice) substituents. They form a dimeric anionic complex with Tc(III) that allows functional hepatobiliary imaging and can be used as a replacement for radioiodinated rose bengal. The first

VERBRUGGEN

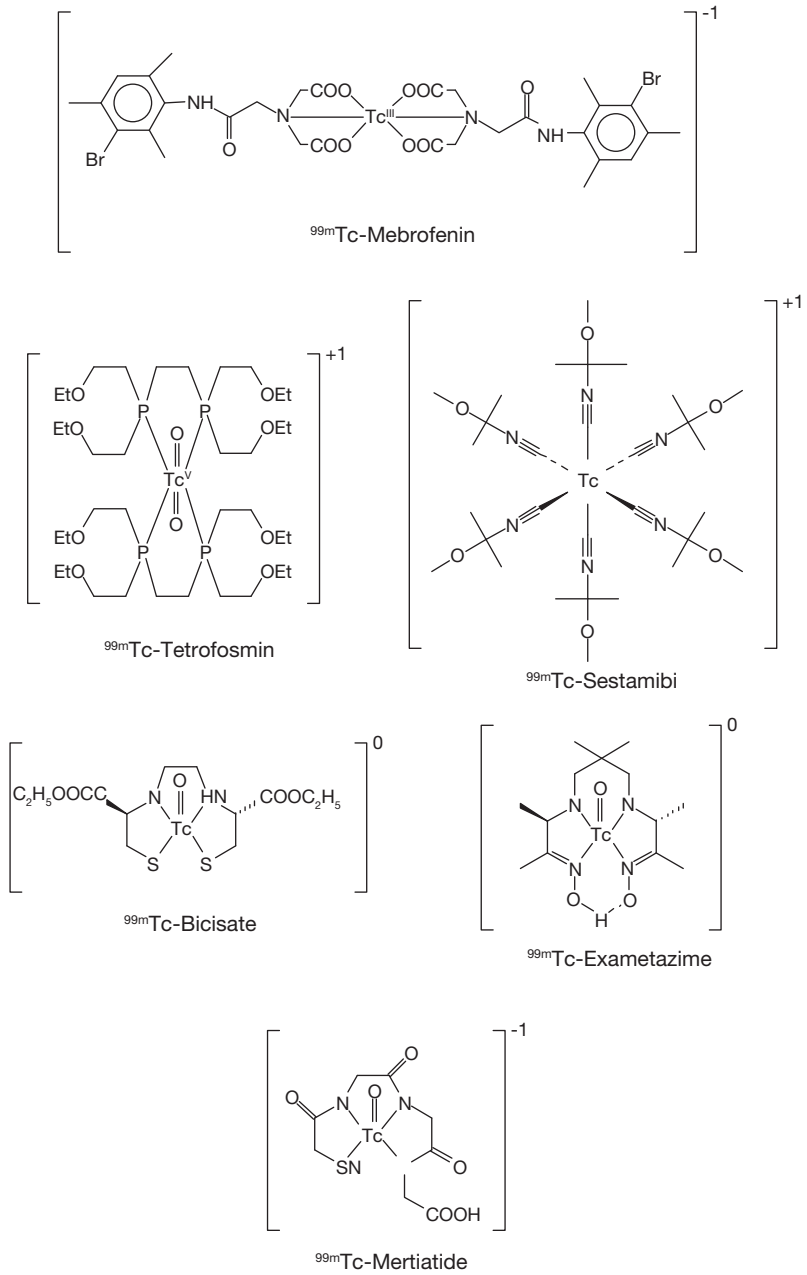


FIG. 1. Structure of the most successful ^{99m}Tc radiopharmaceuticals.

SESSION 1

representative of this series, ^{99m}Tc -lidofenin, was designed by Loberg et al. [1] in an attempt to develop a Tc derivative of lidocaine as a myocardial perfusion agent, but it turned out not to be taken up in the myocardium but excreted rapidly via the liver and gall bladder into the intestines.

- (b) ^{99m}Tc -mertiatide (^{99m}Tc -MAG3) was developed by Fritzberg and co-workers in 1985 [2] as a ^{99m}Tc labelled replacement for radioiodinated 2-iodohippuric acid (Hippuran) for renal function studies. It was the first of a series of Tc(V)O-tetradentate ligand complexes to have received approval as a radiopharmaceutical. It is assumed that its TcO-N-CH₂-COOH sequence mimics the carbonylglycine (CO-NH-CH₂-COOH) side chain of hippuric acid, which is believed to be important for recognition of the tracer agent by tubular transport proteins and in this way for a rapid plasma clearance and excretion into the urine via active tubular transport.
- (c) ^{99m}Tc -sestamibi is a monocationic complex of Tc(I) with six isonitrile ligand molecules. It was reported in 1988 [3] and can be prepared using the commercial labelling kit Cardiolite. It was the first successful ^{99m}Tc labelled substitute for ^{201}Tl -thallous chloride for myocardial perfusion imaging and diagnosis of myocardial infarction. Although it shares with Tl⁺ the positive charge, supposed to be a prerequisite for transport by Na⁺/K⁺-ATPase (also known as the Na⁺/K⁺ pump) and therefore a starting point during the rational development, its mechanism of uptake in myocytes has been shown to be largely different from that of Tl⁺, so the successful design was rather accidental. On the basis of the number of scientific papers (4012 hits in PubMed for sestamibi (Table 1), probably to be combined with many of the 1700 hits for mibi; more hits than for pertechnetate) this is up to now the most successful and most intensively used ^{99m}Tc radiopharmaceutical.
- (d) Among many other newly developed ^{99m}Tc agents with useful properties for myocardial imaging (namely ^{99m}Tc complexes with teboroxime, furifosmin, N-NOET, etc.), only ^{99m}Tc -tetrofosmin became also a generally accepted radiopharmaceutical for cardiac imaging. It is easy to prepare at room temperature using commercially available Myoview labelling kits. Compared with ^{99m}Tc -sestamibi, it can be considered as a 'me too' radiopharmaceutical with identical indications. Its later introduction into clinical practice might explain its lower popularity. Indeed, the number of hits in PubMed for 'tetrofosmin' is, surprisingly, almost a factor of five less than for sestamibi. Nevertheless ^{99m}Tc -tetrofosmin was developed only three years later [4] and has some more favourable characteristics: a higher myocardial uptake and higher heart to liver

activity ratio in clinical studies at rest and, in addition, it can be prepared at room temperature compared with a required boiling step for ^{99m}Tc -sestamibi. Apparently, nuclear medicine physicians adhere to a radiopharmaceutical that provides them with clinically useful images and information. Technetium-99m-tetrofosmin, which was already developed 15 years ago, is the latest new ‘Tc essential’ radiopharmaceutical to have gained approval for medical use.

- (e) ^{99m}Tc -exametazime (^{99m}Tc -d,l-HM-PAO, prepared using Ceretec labelling kit) was developed in 1985 as the first ^{99m}Tc tracer to replace N-isopropyl-p-[^{123}I]iodoamphetamine for cerebral perfusion imaging [5]. Its retention in the brain is due to conversion to a more polar metabolite, possibly as a result of an interaction with glutathione. The same conversion is also taking place in other organs and cells and this property is being used to label blood cells with ^{99m}Tc by incubation with ^{99m}Tc -exametazime. As a matter of fact, nowadays, ^{99m}Tc -exametazime is used mainly for the labelling of white blood cells for infection imaging and only to a limited degree for brain scanning. A search via PubMed on ‘exametazime’ yields clearly fewer hits than for sestamibi that was developed three years later.
- (f) ^{99m}Tc -bicisate (^{99m}Tc -L,L-ECD, prepared using a Neurolite labelling kit) is a second approved radiopharmaceutical for measuring regional cerebral perfusion. It was developed in 1988 [6] and is more stable than ^{99m}Tc -exametazime, has a more favourable dosimetry and yields brain images with a better contrast. As a result it is now the preferred brain scanning agent but is not useful for cell labelling. Its retention in brain cells is due to a rapid hydrolysis of one of the ester functions to an acid that is ionized at physiological pH, a phenomenon that is happening mainly in primates and to a much lesser extent in other animals. The ionized and thus more polar metabolite cannot easily pass the blood–brain barrier out of the brain. As a ‘me too’ tracer agent for localization of stroke in patients in whom stroke has already been diagnosed and for the evaluation and localization of altered regional cerebral perfusion associated with functional impairment in patients with other neurological disorders such as dementia, head trauma and epilepsy, it scores significantly lower than the first developed but now less frequently used ^{99m}Tc brain tracer ^{99m}Tc -exametazime in a PubMed search (411 hits).

SESSION 1

3. PROGRESS IN TECHNETIUM CHEMISTRY AND NEW COMPOUNDS

No new ^{99m}Tc essential radiopharmaceuticals have received approval for general medical use since 1992. However, there have been during this period a number of interesting new developments in the Tc field, of which the most prominent are:

- (a) ^{99m}Tc -Trodar-1 is a conjugate of a derivative of cocaine with a $^{99m}\text{Tc(V)}$ oxo-diaminodithiol complex (Fig. 2) developed by Kung and co-workers [7] in 1995. Clinical studies have established its usefulness for diagnosis of Parkinson's disease thanks to its affinity for the dopamine transporter, although this is lower than that of the approved radioiodinated analogue, ioflupane (DatSCANTM). The in vitro binding to the dopamine transporter was assessed using the surrogate Re complex, Re-Trodar-1, and a K_i value of 14 nM was found. The ratio of specific to non-specific binding of ^{99m}Tc -Trodar-1 appears to be lower than that of ^{123}I - β -CIT (1.66 as opposed to 7). It is the first and until now only ^{99m}Tc compound for receptor studies in the brain. It is not yet commercially available in the form of a labelling kit, but remains in the clinical trial phase. This explains the relatively low number of PubMed hits (82), but also on ioflupane the number of scientific papers is still limited (92 PubMed hits).

The use of hydrazinonicotinamide (Hynic) as a bifunctional chelating agent has proven successful for ^{99m}Tc labelling of mainly peptides and proteins, such as thrombus binding peptides, chemotactic peptides, octreotide

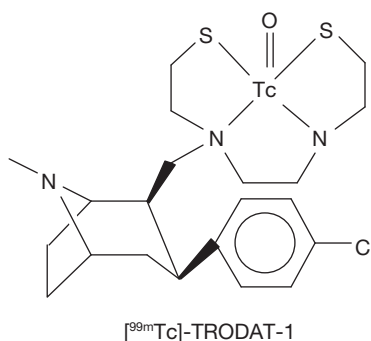


FIG. 2. Structure of ^{99m}Tc -TRODAT-1.

derivatives and annexin, at very low concentrations. Binding of Tc proceeds via the hydrazino group which acts as a monodentate ligand and requires the use of a coligand such as tricine or ethylenediamine diacetic acid (EDDA) (Fig. 3), but the exact nature of the formed complexes is not yet fully elucidated, also because of the presence of isomers. Promising results have been obtained with ^{99m}Tc -Hynic annexin V [8] (but clinical trials have been stopped and the compound is not commercially available) and ^{99m}Tc -Hynic labelled somatostatin analogues [9]. The latter yield higher quality images than ^{111}In labelled octreotide and have proven their clinical usefulness [10]. However, up to now there has been approval for clinical use only on a local basis and, for a number of reasons, development into a generally available radiopharmaceutical does not seem to be likely in the near future.

The most exciting development in the field of ^{99m}Tc chemistry during the last 15 years is without doubt the development by Alberto and co-workers [11] of a convenient method of labelling biomolecules with a Tc-tricarbonyl core. A $\text{Tc}(\text{CO})_3(\text{H}_2\text{O})_3$ precursor can be prepared easily using CO gas and sodium borohydride as reducing agent or, more reproducibly, easily and safely, using the commercially available IsolinkTM labelling kit that contains potassium

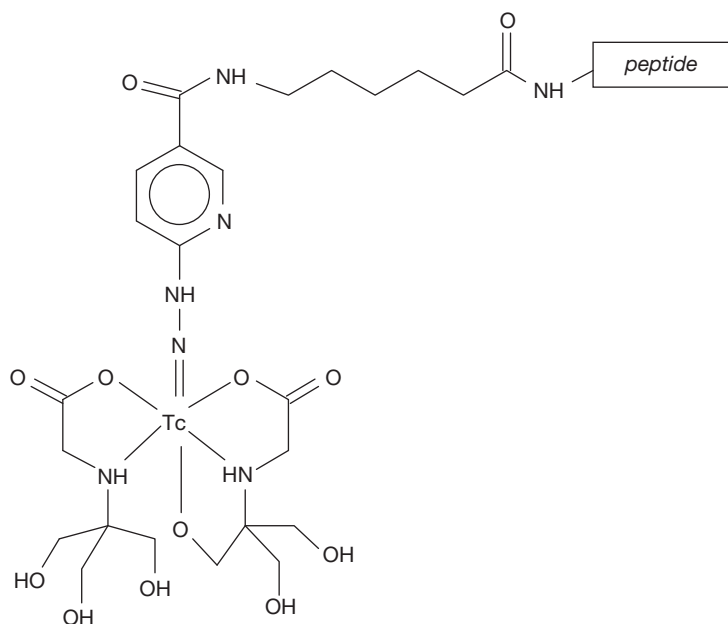


FIG. 3. Labelling of a peptide with ^{99m}Tc after conjugation with 6-aminohexanoic acid (spacer) coupled to Hynic. In the example shown, tricine is used as coligand.

SESSION 1

boranocarbonate [$\text{Na}_2(\text{H}_3\text{BCO}_2)$] as both reducing agent and source of CO. The water molecules of this precursor undergo efficient ligand exchange with a wide variety of donor ligands (Fig. 4), preferentially tridentate, to form compact Tc(I) complexes with diverging properties with respect to charge, size and lipophilicity and thus also to biological properties. By the proper choice of tridentate ligand, the final $^{99\text{m}}\text{Tc}$ -tricarbonyl labelled biomolecule conjugate can be neutral, anionic or cationic. Despite an intensive search by several groups for new $^{99\text{m}}\text{Tc}$ labelled radiopharmaceuticals on the basis of this chemistry, no Tc-tricarbonyl labelled tracer agent has been approved yet for clinical use nor is one awaiting introduction.

4. CHALLENGES FOR NEW $^{99\text{m}}\text{Tc}$ RADIOPHARMACEUTICALS

The success of the currently used $^{99\text{m}}\text{Tc}$ radiopharmaceuticals and the promising new developments may not mask the fact that there are also reasons for concern about the future of this class of tracer agent. As already mentioned, very few new $^{99\text{m}}\text{Tc}$ labelled tracer agents still reach the stage of clinical studies or approval. Several examples exist of newly developed $^{99\text{m}}\text{Tc}$ labelled tracer agents with useful or even excellent properties for clinical application that have not become or are no longer an approved radiopharmaceutical: $^{99\text{m}}\text{Tc}$ -BATO's (heart (Teboroxime) and brain perfusion imaging), $^{99\text{m}}\text{Tc}$ -MRP20 (brain perfusion imaging), $^{99\text{m}}\text{Tc}$ -N-NOET (myocardial perfusion) and its ester analogue (brain perfusion), $^{99\text{m}}\text{Tc}$ -furifosmin (myocardial perfusion), $^{99\text{m}}\text{Tc}$ -ethylene dicysteine ($^{99\text{m}}\text{Tc}$ -EC, renal function), $^{99\text{m}}\text{Tc}$ -hydroxyacetyltriglycine ($^{99\text{m}}\text{Tc}$ -HAG3) and $^{99\text{m}}\text{Tc}$ -tetrapeptides (renal function), $^{99\text{m}}\text{Tc}$ -dimercaptopyrionyl-HSA (ventriculography, gastrointestinal bleeding), $^{99\text{m}}\text{Tc}$ labelled octreotide derivatives (Hynic or tetraamine derivatized, detection of tumours), $^{99\text{m}}\text{Tc}$ -Hynic-annexin V (imaging of apoptosis) and $^{99\text{m}}\text{Tc}$ -HL91 (hypoxia imaging).

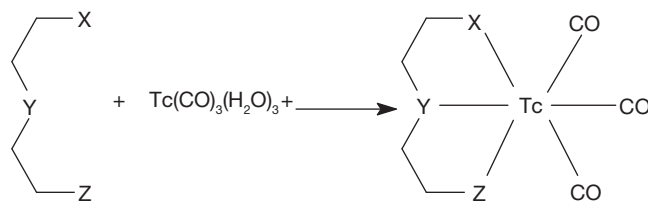


FIG. 4. Reaction of a tridentate ligand (X, Y, Z = N, O, S or P) with $\text{Tc}(\text{CO})_3(\text{H}_2\text{O})_3$.

VERBRUGGEN

The reason for this evolution and the stagnancy in approval of new ^{99m}Tc radiopharmaceuticals is due to different, mainly economic, factors. Most of these factors apply to both PET and SPECT radiopharmaceuticals, but some are specific for ^{99m}Tc labelled agents:

- (a) Authorities require adherence to stricter regulatory rules and diagnostic drugs must fulfil almost all requirements imposed for therapeutic drugs. As a result, the cost for development of a radiopharmaceutical has become increasingly high, mainly because of the required toxicological and clinical studies. The cost of developing a drug for diagnostic imaging to commercialization is in the US \$100–200 million range, whereas a blockbuster imaging drug has current sales of only \$200–400 million [12], making it hardly attractive for a company.
- (b) Starting materials for labelling kits for ^{99m}Tc radiopharmaceuticals must now also be prepared under GMP conditions, but chemicals of this high a quality are not readily available for all kits. Owing to the high costs associated with GMP production of starting compounds, some radiopharmaceutical companies have already abandoned the production of some labelling kits (e.g. DMSA, DTPA, HSA).
- (c) Owing to the high cost of developing a radiopharmaceutical, the price per dose of new tracers must be high and this in turn limits the use and thus the revenues, creating in this way a negative spiral. This situation holds true both for SPECT and PET tracers.
- (d) Companies will have a limited return on investment if the number of patients that will benefit from a new drug is not sufficiently (very) high.
- (e) There is almost no interest anymore from companies in developing a ‘me too’ radiopharmaceutical as it is more difficult to obtain approval for such agents (the applicant has to prove advantages and improvements). Moreover, experience (e.g. with ^{99m}Tc -tetrafosmin and ^{99m}Tc -bicisate) has shown that for a ‘me too’ compound, it is difficult to bridge the (sales) gap with the first agent of its class, once this has gained acceptance in the medical community.
- (f) The structural characterization of some new tracer agents (Hynic compounds, radiolabelled proteins) may be difficult, which will hamper and slow down approval.
- (g) Derivatization of a biologically active or interesting compound (BAC) with a ^{99m}Tc complex usually significantly alters the biological properties, except in the case of large molecules such as proteins, antibodies and some peptides. Coupling of a BAC with a Tc complex not only increases the molecular mass with at least about 300 dalton (Fig. 5), which constitutes a challenge for diffusion of the resulting tracer agent over the

SESSION 1

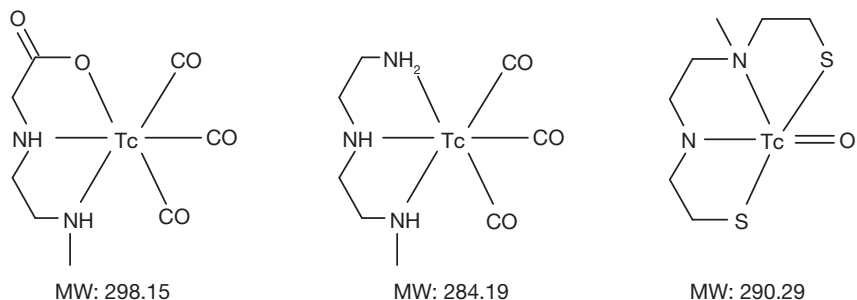


FIG. 5. The molecular mass of the smallest Tc complexes is about 300 (here two Tc-tricarbonyl complexes and a Tc(V)O-N₂S₂ complex are shown). Derivatization of a biomolecule with a Tc complex, mostly via a linker, thus increases the molecular mass by at least 300.

blood–brain barrier, but may also modify the polarity and charge with respect to the original BAC. As a result, the challenge of designing a ^{99m}Tc labelled agent for receptor imaging is enormous, especially with respect to ligands for brain studies.

- (h) Nuclear medicine procedures experience an increasing competition from in vitro assays (e.g. for thyroid studies) and other imaging modalities that are no longer limited to morphological images but which may also provide functional information (spiral CT for lung studies, fMRI for brain studies, echocardiography, etc.). Owing to the unique characteristics of PET cameras, studies using ^{99m}Tc radiopharmaceuticals (or other SPECT tracers) are hampered by an inferior sensitivity, a lower spatial and temporal resolution and inaccurate quantification compared with PET tracers. Especially because of this last reason but also as a result of some of the other mentioned factors, there has been in the University Hospital of Leuven during the last few years a clear trend of a gradually and continuously decreasing number of examinations using a ^{99m}Tc radiopharmaceutical (Fig. 6) compared with PET tracers (Fig. 7). In particular, PET studies using ¹⁸F-fludeoxyglucose (¹⁸F-FDG) for oncological studies have increased exponentially. In this respect, it is striking that ¹⁸F-FDG, which has only been used intensively for oncological diagnosis since 1995 has more than twice the number of hits in PubMed (about 8500) compared with the most successful ^{99m}Tc agent, i.e. ^{99m}Tc-sestamibi. Only kidney studies using ^{99m}Tc-meritide or ^{99m}Tc-succimer maintain their relative position and the use of colloidal ^{99m}Tc for sentinel node scintigraphy is sharply increasing, but the number of these examinations is small compared with, for example, bone and heart studies.

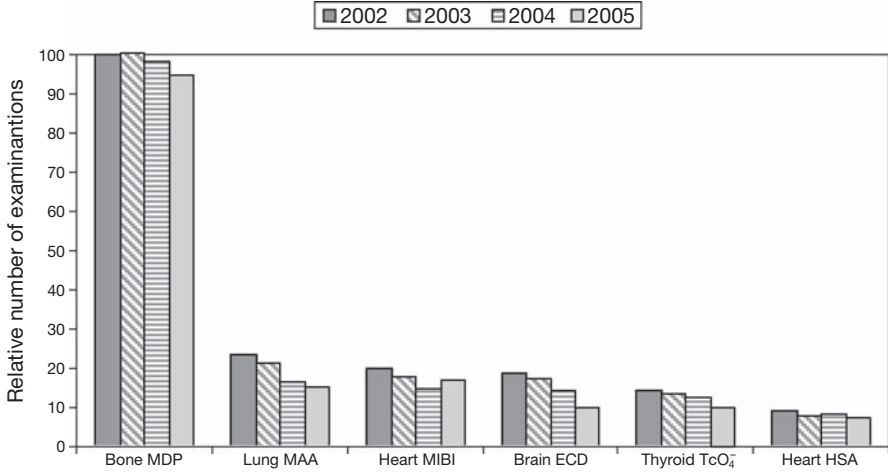


FIG. 6. Evolution of the relative number of some radioisotopic examinations using a ^{99m}Tc radiopharmaceutical at the University Hospital of Leuven over the last four years. The number of bone scans in 2002 has arbitrarily been set at 100 and the other figures are the relative number of bone scans expressed as a percentage.

The impact of PET tracers on the development and the use of ^{99m}Tc radiopharmaceuticals can be illustrated by additional examples:

- (a) ^{99m}Tc-depreotide (NeoTect™) has been developed by researchers at Diatide by rational and ingenious design of a peptide that contains both a

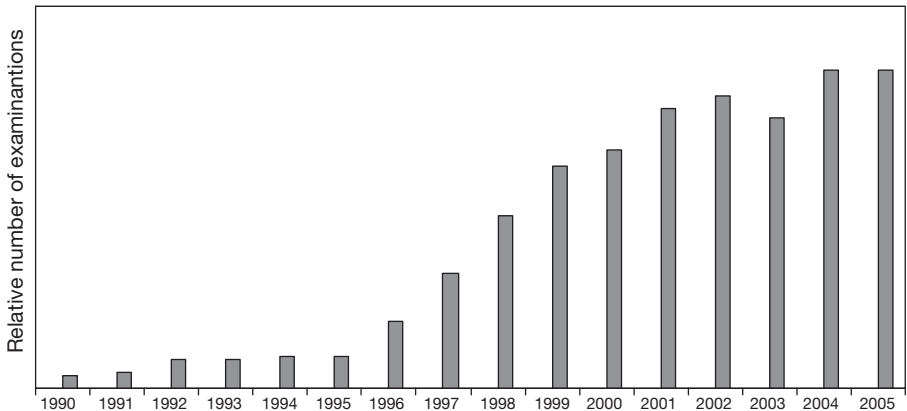


FIG. 7. Evolution of the relative number of PET scans at the University Hospital of Leuven since 1990. The number of PET scans in 2004 has arbitrarily been set at 100.

SESSION 1

domain binding with high affinity to somatostatin receptors, which are predominantly subtypes 2, 3 and 5, and a second structural moiety able to bind Tc (Fig. 8). It has a high sensitivity and specificity for lung cancer lesion detection and has received FDA approval for this indication. However, PET with ^{18}F -FDG has a similar sensitivity and specificity for lesion identification in this disease, yields images with superior resolution and is currently far more widely used [13]. It is doubtful whether $^{99\text{m}}\text{Tc}$ -depreotide will continue to be commercially available.

- (b) Gallium-68 is a positron emitting radionuclide that can be routinely obtained from a commercially available $^{68}\text{Ge}/^{68}\text{Ga}$ generator. Several clinical studies using ^{68}Ga labelled Dotatoc (Fig. 9), a conjugate of the macrocyclic complexing agent DOTA with an octreotide derivative with high affinity for somatostatin receptors, have shown the superiority of this PET tracer agent in terms of quality of images and sensitivity for tumour imaging compared with ^{111}In -octreotide. Using ^{68}Ga -Dotatoc, >30% additional lesions were detected. PET using ^{68}Ga -DOTATOC results in high tumour to non-tumour contrast and low kidney accumulation and

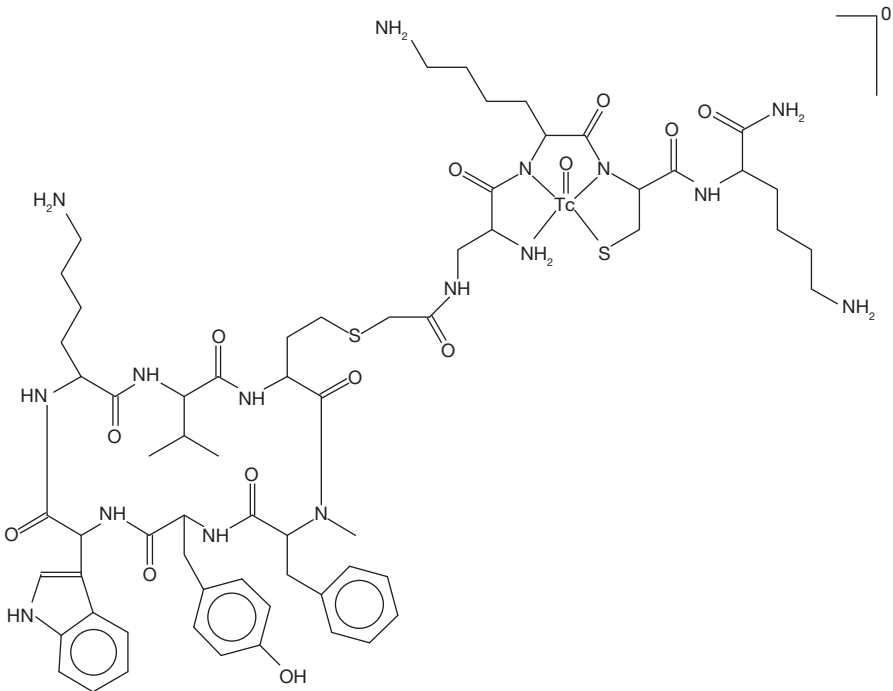


FIG. 8. Structure of Tc-depreotide.

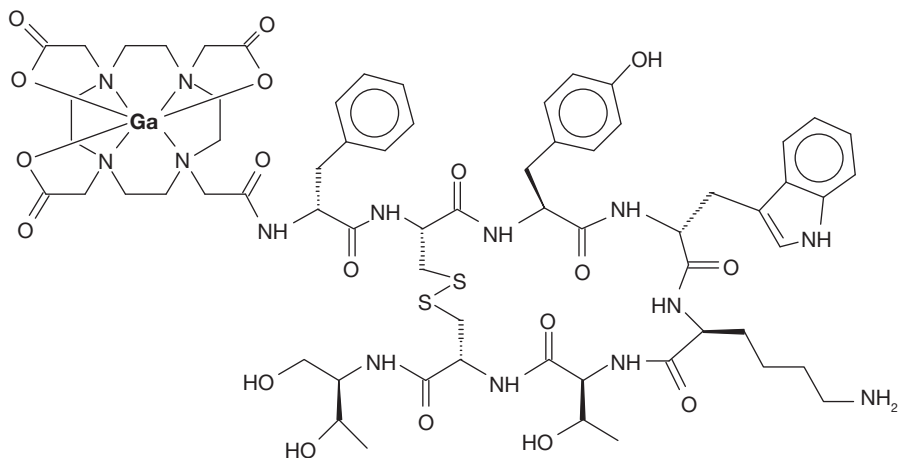


FIG. 9. Structure of Ga-DOTATOC.

yields higher detection rates compared with ^{111}In -octreotide scintigraphy [14]. It thus may be expected that the octreotide derivatives labelled with $^{99\text{m}}\text{Tc}$ via Hynic conjugation [9] or tetraamine conjugation [15] will not be developed further into approved radiopharmaceuticals in view of the superiority of the ^{68}Ga labelled peptide.

Also in the field of research on new tracer agents, it is clear that the relative contribution from studies on $^{99\text{m}}\text{Tc}$ compounds has been decreasing for many years while development of PET tracers is expanding continuously. This can be concluded from the relative numbers of abstracts in these respective fields at the consecutive symposiums on radiopharmaceutical chemistry (shown for two years in Fig. 10).

5. PERSPECTIVES FOR THE FUTURE

The balance between, on the one hand, factors favourable for new $^{99\text{m}}\text{Tc}$ radiopharmaceuticals and a continuing predominant role for such compounds in nuclear medicine and on the other hand the challenges experienced nowadays does not suggest a bright future for the $^{99\text{m}}\text{Tc}$ tracer agents; on the contrary. However, the ongoing research for new $^{99\text{m}}\text{Tc}$ complexes with specific applications, to a large extent in the field of Tc-tricarbonyl compounds and designed for molecular imaging purposes, and recent developments with

SESSION 1

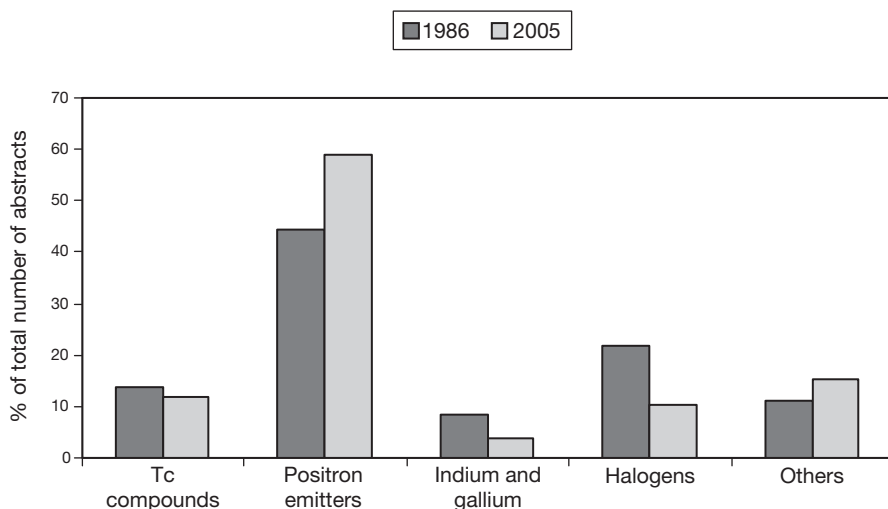


FIG. 10. Percentages of abstracts in the respective field given at symposiums of radiopharmaceutical chemistry in 1986 and 2005.

respect to SPECT instrumentation are valuable elements that may offer promising future opportunities for SPECT radiopharmaceuticals in general and ^{99m}Tc compounds in particular.

To remain competitive in diagnostic medicine, SPECT urgently needs gamma cameras with higher spatial resolution. There are perspectives that such improvement may be expected in the not too distant future thanks to crystal and collimator developments. New types of detector, such as Cd(Zn)Te strip crystals in combination with appropriate collimators, can offer a higher resolution (<1 mm) than PET cameras, which are limited in this respect by the range of the positrons. This material also has a somewhat greater intrinsic efficiency than the NaI(Tl) detectors [16], possibly resulting in a higher sensitivity than with the current SPECT cameras. These developments are still at the stage of SPECT cameras for small animal imaging, but translation towards cameras for clinical use is a logical progression, although the cost might be relatively high. Appropriate software development should also result in quantification of SPECT images with an accuracy similar to that now achievable for PET studies. Finally, the availability and increasing use of SPECT-CT cameras constitute favourable conditions for a continuing interest in existing and new ^{99m}Tc labelled SPECT tracers.

6. CONCLUSION

The favourable properties of ^{99m}Tc and the availability of high performance and valuable ^{99m}Tc radiopharmaceuticals formed the basis of a privileged position for ^{99m}Tc compounds up to ten years ago. Since then, the growing competition from PET compounds and from other imaging modalities has resulted in a declining use of ^{99m}Tc radiopharmaceuticals and lower investments in new agents labelled with ^{99m}Tc . With the successful further development of newer types of SPECT cameras with higher resolution and sensitivity and the possibility of accurate quantification, the use of ^{99m}Tc radiopharmaceuticals will gain renewed interest and they will continue to be a cornerstone of nuclear medicine, complementary but not superior to PET compounds.

ACKNOWLEDGEMENT

I wish to thank J. Cleynhens for his valuable help in preparing the manuscript.

REFERENCES

- [1] LOBERG, M.D., et al., Development of new radiopharmaceuticals based on N-substitution of iminodiacetic acid, *J. Nucl. Med.* **17** 7 (1976) 633–638.
- [2] FRITZBERG, A.R., et al., Synthesis and biological evaluation of technetium-99m MAG3 as a hippuran replacement, *J. Nucl. Med.* **27** 1 (1986) 111–116.
- [3] TAILLEFER, L., et al., Myocardial perfusion imaging with ^{99m}Tc -methoxyisobutyl-isonitrile (MIBI): Comparison of short and long time intervals between rest and stress injections: Preliminary results, *Eur. J. Nucl. Med.* **13** 10 (1988) 515–522.
- [4] HIGLEY, B., et al., Technetium-99m-1,2-bis[bis(2-ethoxyethyl)phosphino]ethane: Human biodistribution, dosimetry and safety of a new myocardial perfusion imaging agent, *J. Nucl. Med.* **34** 1 (1993) 30–38.
- [5] ELL, P.J., et al., Regular cerebral blood flow mapping with ^{99m}Tc -labelled compound, *Lancet* **2** 8445 (1985) 50–51.
- [6] VALLABHAJOSULA, S., et al., Technetium-99m ECD: A new brain imaging agent : in vivo kinetics and biodistribution studies in normal human subjects, *J. Nucl. Med.* **30** 5 (1989) 599–604.
- [7] KUNG, H.F., et al., Imaging of dopamine transporters in humans with technetium-99m TRODAT-1, *Eur. J. Nucl. Med.* **23** 11 (1997) 1527–1530.

SESSION 1

- [8] OHTSUKI, K., et al., Technetium-99m HYNIC-annexin V: A potential radiopharmaceutical for the in-vivo detection of apoptosis, *Eur. J. Nucl. Med.* **26** 10 (1999) 1251–1258.
- [9] DECRISTOFORO, C., MATHER, S.J., Preparation, ^{99m}Tc -labeling, and in vitro characterization of Hynic and N3S modified RC-160 and [TYR3]octreotide, *Bioconjug. Chem.* **10** 3 (1999) 431–438.
- [10] GABRIEL, M., et al., ^{99m}Tc -EDDA/HYNIC-Tyr(3)-octreotide for staging and follow-up of patients with neuroendocrine gastro-entero-pancreatic tumors, *Q. J. Nucl. Med. Mol. Imaging* **49** 3 (2005) 237–244.
- [11] ALBERTO, R., et al., A novel organometallic complex of technetium for the labeling of biomolecules: Synthesis of $[\text{}^{99m}\text{Tc}(\text{OH}_2)_3(\text{CO})_3]^+$ from $[\text{}^{99m}\text{TcO}_4]^-$ in aqueous solution and its reaction with a bifunctional ligand, *J. Am. Chem. Soc.* **120** (1990) 7987–7988.
- [12] NUNN, A.D., The cost of developing imaging agents for routine clinical use, *Invest. Radiol.* **41** 3 (2006) 206–212.
- [13] WEINER, R.E., THAKUR, M.L., Radiolabeled peptides in oncology: Role in diagnosis and treatment, *BioDrugs* **19** 3 (2005) 145–163.
- [14] HOFMANN, M., et al., Biokinetics and imaging with the somatostatin receptor PET radioligand ^{68}Ga -DOTATOC: Preliminary data, *Eur. J. Nucl. Med.* **28** 12 (2001) 1751–1757.
- [15] NIKOLOPOULOU, A., et al., Tetraamine-modified octreotide and octreotate: Labeling with ^{99m}Tc and preclinical comparison in AR4-2J cells and AR4-2J tumor-bearing mice, *J. Pept. Sci.* **12** 2 (2006) 124–131.
- [16] ZENG, G., GAGNON, D., CdZnTe strip detector SPECT imaging with a slit collimator, *Phys. Med. Biol.* **49** 11 (2004) 2257–2271.

^{99m}Tc LABELLED MINIGASTRIN FOR TUMOUR TARGETING OPTIMIZATION OF LABELLING AND PEPTIDE SEQUENCE

E. VON GUGGENBERG*, M.P. BÉHÉ**, C. DECRISTOFORO*

*Clinical Department of Nuclear Medicine,
Medical University Innsbruck,
Innsbruck, Austria
Email: clemens.decristoforo@uibk.ac.at

**Department of Nuclear Medicine,
Philipps-University of Marburg,
Marburg, Germany

Abstract

Gastrin/CCK receptors are overexpressed in a number of tumours such as medullary thyroid carcinoma, small cell lung cancer and gastrointestinal neuroendocrine tumours. Imaging of gastrointestinal neuroendocrine tumours with radiolabelled Gastrin analogues is of clinical importance, especially if Somatostatin receptor scintigraphy is negative. Therefore Gastrin analogues binding to the CCK-2 receptor are promising candidates for nuclear medicine imaging. Recently, a Minigastrin derivative (eEEEEAYGWMDf) was labelled with ¹³¹I, ¹¹¹In and ⁹⁰Y and evaluated in patients. However, ^{99m}Tc still would be the label of choice for routine applications owing to its availability, low cost, low radiation dose for the patient and optimal gamma energy profile. Today, a number of radiolabelling approaches are available, especially based on new Tc cores allowing radiolabelling of peptides at high specific activities, even if data on the comparison of these approaches are rare. The authors were especially interested in the comparison of 2-Hydrazino-nicotinic-acid (HYNIC) derivatized peptides compared with approaches using ternary ligand systems for labelling with the [Tc(CO)₃(H₂O)₃]⁺ core concerning in vitro and in vivo imaging properties. The paper describes the development of ^{99m}Tc analogue and the optimization of radiolabelling approaches and peptide sequence for targeting Gastrin/CCK receptor positive cells in vivo. Data are also presented on the comparison of radiolabelling approaches for peptides with ^{99m}Tc.

1. MATERIALS AND METHODS

1.1. Materials

All reagents were purchased from Aldrich-Sigma Chemical Co., except where otherwise stated, and used as received.

Two Minigastrin sequences, eEEEEAYGWMDf (MG0) and eAYGWMDf (MG11) were derivatized both with HYNIC at the aminoterminal, as well as MG0 with a HIS derivative (N_α-His)Ac for Tc-carbonyl labelling. Peptides were synthesized by piChem (Graz, Austria) with a purity of >95% as analysed by RP-HPLC and MS. ¹²⁵I-Tyr¹²-Gastrin I was purchased from Perkin Elmer Life Science (Boston, United States of America). Na ^{99m}TcO₄⁻ was obtained from a commercial ⁹⁹Mo/^{99m}Tc generator (Ultratechnekow, Mallinckrodt, Netherlands).

1.2. HPLC

A Macherey & Nagl Nucleosil 120-5 C18 250 × 4.6 mm column, flow rates of 1 mL/min, and UV detection at 220 nm was used with the following gradient: acetonitrile (ACN)/0.1% TFA/H₂O:t: 0–3 min 0% ACN, 3–5 min 0–25% ACN, 5–20 min 25–40% ACN, 20–25 min 40–60% ACN, 25–28 min 60–0% ACN, 28–33 min 0%.

1.3. Purification by solid phase extraction

For purification of the radiolabelled peptide for stability studies, a solid phase extraction method was used. The radiolabelling mixture was passed through a C18-SEPPAK-Mini cartridge (Water, Milford, MA, USA). The cartridge was washed with 5 mL physiological solution and the radiolabelled peptide eluted with 50% ethanol. This method efficiently removed all hydrophilic, non-peptide bound impurities (mainly ^{99m}TcO₄⁻, ^{99m}Tc coligands).

1.4. ^{99m}Tc labelling

1.4.1. HYNIC-MG-derivatives

Tricine as coligand: In a rubber sealed vial, 3 µg of HYNIC-MG was incubated with 0.5 mL of Tricine solution (70 mg/mL in water), 0.5 mL of ^{99m}TcO₄⁻ solution (>200 MBq) and 20 µL of tin-(II)-solution (10 mg of SnCl₂·2H₂O in 10 mL of nitrogen purged 0.1N HCl) for 20 min at room temperature or 75°C.

SESSION 1

Ethylenediaminediacetic acid (EDDA) as coligand: In a rubber sealed vial, 10 µg of HYNIC-MG was incubated with 0.5 mL of EDDA solution (20 mg/mL in pH6–7), 0.5 mL of $^{99m}\text{TcO}_4^-$ solution (400 MBq) and 20 µL of tin(II)-solution (10 mg of $\text{SnCl}_2 \cdot 2\text{H}_2\text{O}$ in 10 mL of nitrogen purged 0.1N HCl) for 30 min at room temperature and for 15 min at 100°C.

1.4.2. $[\text{}^{99m}\text{Tc}(\text{OH})_3(\text{CO})_3]^+$ -MG derivatives

(N_α -His)Ac-MG11: Carbonyl aquaion $[\text{}^{99m}\text{Tc}(\text{OH})_3(\text{CO})_3]^+$ was prepared using the IsoLINK kit (Mallinckrodt Medical, Netherlands). To the kit 1 mL of $^{99m}\text{TcO}_4^-$ solution (3–4 GBq) was added and incubated for 10 min at 100°C followed by 1.0 mL NaH_2PO_4 1M for neutralization. Peptide labelling: in a rubber sealed vial 20 µg of (N_α -His)Ac-MG were incubated with 0.5 mL of carbonyl precursor (800 MBq) for 30 min at 75°C.

1.5. Stability

The stability of the radiolabelled peptides in aqueous solution was tested by incubation of the reaction mixture purified by solid phase extraction at a concentration of ~500pM peptide/mL in phosphate buffer as well as in a solution containing 10 000-fold molar excess of cysteine or histidine over the peptide at pH7.4 at 37°C up to 24 h. Stability in fresh human plasma was measured in parallel. After incubation, plasma samples were precipitated with ACN and centrifuged (1750g, 5 min). Degradation of the ^{99m}Tc complexes were assessed by HPLC.

For protein binding assessment, the solid phase extraction purified complexes were incubated at a concentration of ~50pM peptide/mL in fresh human plasma at 37°C and analysed up to 4 h by size exclusion chromatography (MicroSpinTM G-50 Columns; Sephadex G-50). Protein binding of the ^{99m}Tc complex was determined by measuring column and eluate in a gamma counter.

For incubation in kidney and liver homogenates, kidneys or liver freshly excised from rat were rapidly rinsed and homogenized in 20mM HEPES buffer pH7.3 with an Ultra-Turrax T25 homogenator for 1 min at RT. The radiopeptides were incubated with fresh 30% homogenates at a concentration of ~500pM peptide/mL at 37°C up to 2 h. Samples were precipitated with acetonitrile, centrifuged (1750g, 5 min) and analysed by HPLC method 1.

1.6. Receptor binding studies

The binding affinity of the cold peptide conjugates was tested in a competition assay against ^{125}I -Tyr¹²-Gastrin. Rat pancreatic tumour (AR42J) cell membranes were used as the source for gastrin receptors. For membrane preparation, cells were homogenized three times for 10 s at 4°C with an Ultra-Turrax T25 homogenator in 20mM HEPES buffer pH7.3/10mM MgCl₂/10μM Bacitracin and protein concentration was assessed to 50 μg/100 μL (Bredford assay). In a Multiscreen well plate (glass fibre filters; Whatman GF/C) 50 μL competitor solution of increasing concentrations (0.001–1000nM in 1% BSA/10mM MgCl₂/10μM Bacitracin), 50 μL of radioligand solution (50 000 counts/min in 1% BSA/10mM MgCl₂/10μM Bacitracin) and 100 μL of membrane solution (50 μg protein/tube) were incubated in triplicates for 2 h at RT. Incubation was interrupted by filtration of the medium and rapid rinsing with ice-cold washing buffer (200 μL, followed by 50 μL 15mM TRIS/139mM saline pH7.4) and filters were counted in a gamma counter. The IC₅₀ values were calculated following non-linear regression with Origin software (Microcal Origin 5.0, Northampton, MA, USA).

1.7. Internalization studies

For internalization experiments AR42J cells were seeded at a density of 1×10^6 cells per well in 6 well plates (Greiner Labortechnik, Germany) and grown to confluency for 48 h. On the day of the experiment, cells were washed twice with ice-cold internalization medium prepared by RPMI1640 supplemented by 1% (v/v) fetal bovine serum. The cells were supplied with fresh medium (1.2 mL) and incubated with 300 000 counts/min of the radiolabelled peptide (150 μL in PBS/0.5% BSA buffer, corresponding roughly to 200fM total peptide) and either PBS/0.5% BSA buffer alone (150 μL, total series) or with 10μM human Minigastrin in PBS/0.5% BSA buffer (150 μL, non-specific series). The cells were incubated at 37°C in triplicates for each time point of 30 min, 1 h and 2 h incubation. Incubation was interrupted twice by removal of the medium and rapid rinsing with ice-cold internalization medium. Thereafter, the cells were incubated twice at ambient temperature in acid wash buffer (50mM glycine buffer pH2.8, 0.1M NaCl) for 5 min, a period sufficient to remove over 90% of membrane bound radioligand. The supernatant was collected (membrane bound radioligand fraction) and the cells were rinsed with PBS/0.5% BSA. Cells were lysed by treatment in 1N NaOH and cell radioactivity collected (internalized radioligand fraction). The internalized and non-internalized fractions were determined by measuring radioactivity on a gamma counter and the internalized fraction versus the selected 5, 15, 30, 60 and 120

min time intervals was expressed as a percentage of total activity and a percentage of bound activity.

1.8. Biodistribution

Normal biodistribution studies were performed in Balb/c mice (Charles River, Germany). On the day of the experiment three mice received the radioactive conjugate (1 MBq/mouse, corresponding to 0.15–0.2 µg peptide) intravenously injected into the tail vein. They were sacrificed by cervical dislocation 4 h post-injection. Different organs and tissues (blood, lung, heart, stomach, spleen, liver, pancreas, kidney, muscle, intestine) were removed. The amount of radioactivity was determined with a gamma counter. Results were expressed as a percentage of the injected dose per gram of tissue (%ID/g).

1.9. Tumour uptake studies in nu/nu mice (Charles River, Germany)

For the induction of tumour xenografts, AR42J cells were subcutaneously injected at a concentration of 10×10^6 cells/mouse and allowed to grow for 14 d. On the day of the experiment three mice were injected with ^{99m}Tc labelled peptide (1 MBq/mouse, corresponding to 0.15–0.2 µg peptide) with and without addition of 50 µg Minigastrin and treated as described above. Tumours and other tissues (blood, lung, heart, stomach, spleen, liver, pancreas, kidney, muscle, intestine) were removed. The amount of radioactivity was determined with a gamma counter. Results were expressed as a percentage of the injected dose per gram of tissue (%ID/g) and the tumour to organ ratios were calculated.

1.10. Metabolic stability

To evaluate the in vivo degradation of the conjugate urinary excretion products were characterized by RP-HPLC.

2. RESULTS

At specific activities $>1\text{Ci}/\mu\text{mol}$ both MG0 and MG11 could be labelled with yields $>90\%$ independently of the labelling approach and peptide sequence. Lipophilicity as determined by HPLC was in the order $^{99m}\text{Tc}(\text{CO})_3\text{-(N}_\alpha\text{-His)Ac-MG0} > ^{99m}\text{Tc-HYNIC-MG11} > ^{99m}\text{Tc-HYNIC-MG0}$. Typical HPLC profiles of labelling solutions are shown in Fig. 1.

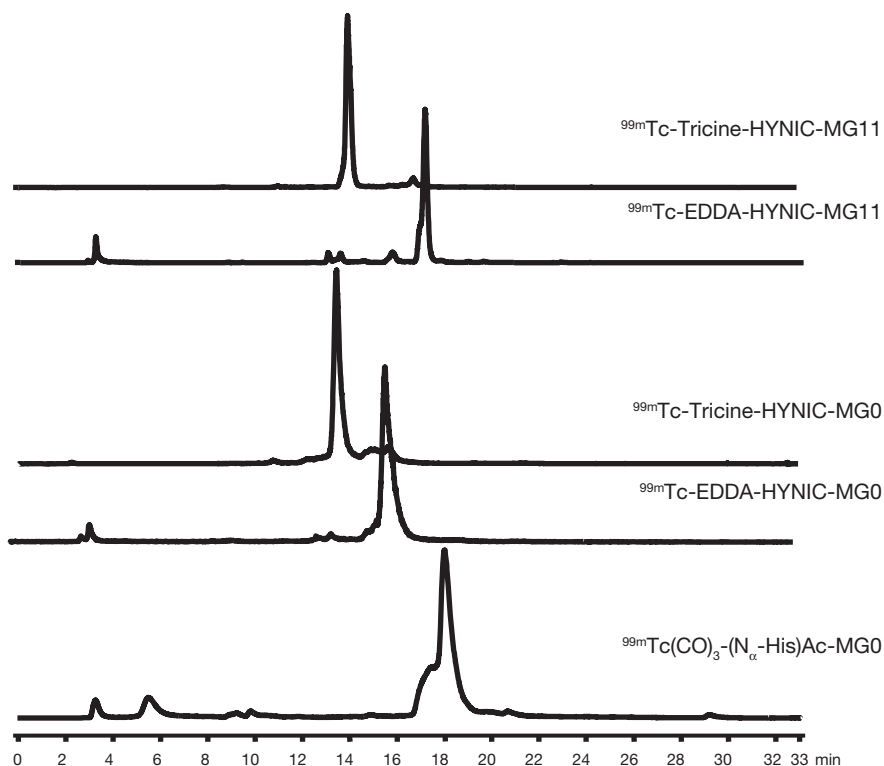


FIG. 1. Radio-HPLC of different labelling mixtures including retention times of the main ^{99m}Tc labelled Minigastrin peak; HPLC: C-18 Nucleosil 120-5 M&N column, $\text{H}_2\text{O}/\text{ACN}/0.1\%$ TFA gradient.

Stability experiments of all ^{99m}Tc -labelled conjugates revealed a high stability of the label in PBS and serum as well as towards challenge with histidine and cysteine. The ^{99m}Tc -Tricine-HYNIC-derivatives showed a slight decrease in in vitro stability and were therefore not further investigated in vivo. Incubation in kidney and liver homogenates resulted in rapid degradation of all conjugates, with somewhat lower degradation rates in liver. ^{99m}Tc -HYNIC-MG11 showed lower stability in comparison with both MG0-derivatives. Plasma protein binding was lower for HYNIC derivatized peptides, with lowest levels for ^{99m}Tc -MG11.

All peptides revealed high affinity for the Minigastrin receptor in the nanomolar range. Internalization behaviour was very rapid for all labelled conjugates in the order $^{99m}\text{Tc}-(\text{N}_\alpha\text{-His})\text{Ac-MG0} > ^{99m}\text{Tc-EDDA/HYNIC-}$

SESSION 1

MG11 > ^{99m}Tc -EDDA/HYNIC-MG0, with maximum values >10%. Comparative uptake values at different time points are shown in Fig. 2.

Overall biodistribution was comparable with rapid renal excretion and very low unspecific retention in most organs, revealing very promising distribution and excretion patterns with low blood and liver levels and low intestinal excretion. With ^{99m}Tc -EDDA-HYNIC-MG0, a very high kidney uptake and retention was observed in contrast to ^{99m}Tc -(N_α -His)Ac-MG0. Figure 3 shows typical behaviour of these derivatives in normal mice and rats. Maximum tumour uptake was found 4 h post-innoculation with highest tumour uptake levels of 8.1% ID/g for ^{99m}Tc -EDDA-HYNIC-MG0 and 7.1% ID/g for ^{99m}Tc -EDDA-HYNIC-MG11. These values were reduced by >60% by co-injection of cold Minigastrin. Technetium-99m-(N_α -His)-Ac-MG0 showed much lower levels of specific tumour accumulation (1.2% ID/g). Kidney uptake and retention was dependent on both the peptide sequence and the labelling approach, with very high levels for ^{99m}Tc -EDDA-HYNIC-MG0 (>100% ID/g),

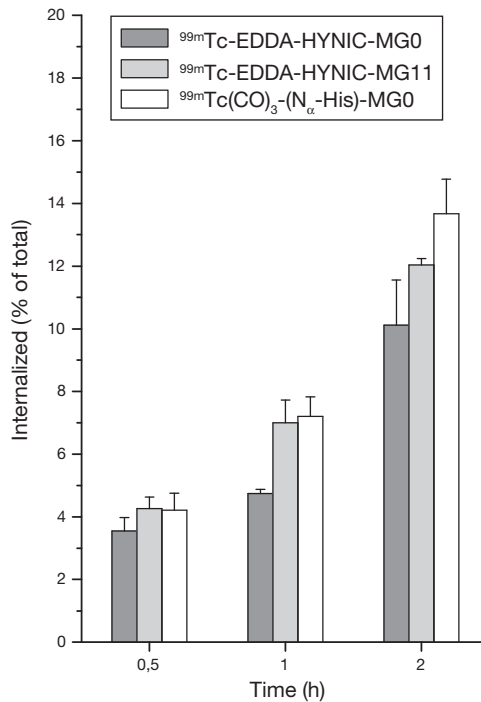


FIG. 2. Internalization in Minigastrin receptor positive cells of ^{99m}Tc labelled Minigastrin derivatives.

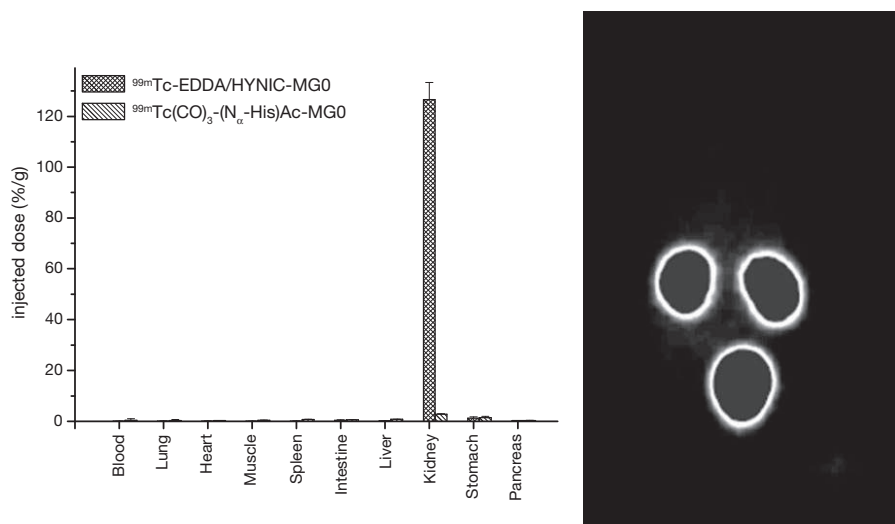


FIG. 3. Biodistribution of ^{99m}Tc-HYNIC labelled compared with ^{99m}Tc-(CO)₃ labelled MG0 showing very high accumulation in kidneys for the HYNIC derivative in balb/c mice (left) and in rats with additional high accumulation in the bladder (gamma camera image (right)).

but much lower levels for ^{99m}Tc-EDDA-HYNIC-MG11 (2.0% ID/g) and ^{99m}Tc-(N_α-His)-Ac-MG0 (1.8% ID/g). Figure 4 summarizes uptake in kidney, stomach (receptor expressing organ) and tumour of all three derivatives under study in the mouse tumour model.

3. CONCLUSION

For radiolabelling of peptides targeting specific receptors, both the peptide sequence and the labelling approach have to be optimized in the development of a suitable radiopharmaceutical. The results in ^{99m}Tc labelling of Minigastrin derivatives show that high stability and hydrophilicity are necessary for suitable pharmacokinetics, but labelling strategy also considerably influences both tumour uptake and kidney retention. Technetium-99m-EDDA-HYNIC-MG11 showed advantages over ^{99m}Tc-MG0 analogues, with much lower kidney retention without impairing uptake in tumour. Technetium-99m-EDDA-HYNIC-MG11 seems to be a promising candidate for imaging CCK-2 receptor positive tumours.

SESSION 1

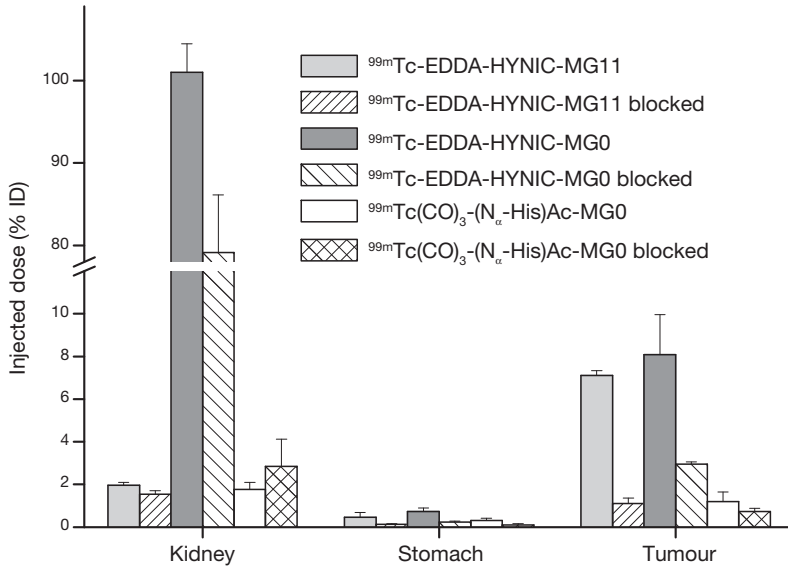


FIG. 4. Uptake of ^{99m}Tc labelled Minigastrin derivatives in major tissues in a AR42J-nude mouse tumour model. Specific uptake is seen in tumour and stomach with comparable uptake values for ^{99m}Tc -HYNIC derivatives, HYNIC-MG0 with high kidney uptake compared with HYNIC-MG11.

ACKNOWLEDGEMENT

Cost B12 Programme of the EC.

REFERENCES

- [1] GOTTHART, M., et al., Scintigraphy with In-111-DTPA-D-Glu1-Minigastrin and In-111-DTPA-D-Phe1-Octreotide in patients with gastrointestinal neuroendocrine tumors: Results of the first 60 patients, *Eur. J. Nucl. Med. Mol. Imaging* **30** (2003) S181.
- [2] BEHR, T.M., et al., Targeting of cholecystokinin-B/gastrin receptors in vivo: Preclinical and initial clinical evaluation of the diagnostic and therapeutic potential of radiolabelled gastrin, *Eur. J. Nucl. Med.* **25** (1998) 424-430.

- [3] BÉHÉ, M.P., BECKER, W., GOTTHARDT, M., ANGERSTEIN, C., BEHR, T.M., Improved kinetic stability of DTPA-DGlu as compared with conventional monofunctional DTPA in chelating indium and yttrium: Preclinical and initial clinical evaluation of radiometal labelled minigastrin derivatives, *Eur. J. Nucl. Med. Mol. Imaging* **30** (2003) 1140–1146.
- [4] BEHR, T.M., BÉHÉ, M.P., Cholecystokinin-B/Gastrin receptor-targeting peptides for staging and therapy of medullary thyroid cancer and other cholecystokinin-B receptor-expressing malignancies, *Semin. Nucl. Med.* **32** (2002) 97–109.
- [5] LIU, S., EDWARDS, D.S., ^{99m}Tc-labeled small peptides as diagnostic radiopharmaceuticals, *Chem. Rev.* **99** (1999) 2235–2268.
- [6] VON GUGGENBERG, E., et al., ^{99m}Tc-Labeling, in vitro and in vivo evaluation of HYNIC and (N_α-His)-acetic acid modified [D-Glu¹]-Minigastrin, *Bioconjug. Chem.* **15** (2004) 864–871.

DESIGN AND SYNTHESIS OF ISONIAZIDE MIMETIC CONJUGATED WITH DTPA, POTENTIAL LIGAND OF NOVEL RADIOPHARMACEUTICAL AND CONTRAST AGENT FOR MEDICAL IMAGING BIS (AMIDE) OF DIETHYLENETRIAMINEPENTAACETIC ACID: DTPA-BIS(INH)

A.K. MISHRA, P. PANWAR, K. CHUTTANI, N. KUMAR,
P. MISHRA, R.K. SHARMA, R. SHARMA
Division of Cyclotron and Radiopharmaceutical Sciences,
Institute of Nuclear Medicine and Allied Sciences,
Delhi, India
Email: akmishra@inmas.org

Abstract

The structure of isonicotinic acid hydrazide (INH) was coupled to diethylenetriaminepentaacetic acid (DTPA) via amide linkage. The overall yield of three steps synthesis starting from DTPA is above 80%. In particular, complexation of DTPA moiety with ^{99m}Tc showed excellent results as the metallopharmaceutical for medical imaging. The main objective of the present research was to develop a novel INH derivative based on DTPA, which forms stable complexes with most of the lanthanides and transition metals in the periodic table. A second objective was to introduce a chelating group without compromising the biological activity of the anti-infective drug for the diagnosis of infection using nuclear medicine. The DTPA-Bis(INH) was synthesized in high yield using a simple synthetic procedure and was characterized using mass spectroscopy in ESI positive mode ($[\text{M}+\text{H}^+]$ was found to be 632.2). Moreover, the complex with the DTPA-Bis(INH) is reflected in increased kinetic ability of the stabilized ^{99m}Tc complex compared with the unmodified INH. The complex was successfully labelled with the ^{99m}Tc radionuclide with more than 95% labelling efficiency. Radiochemical purity was ascertained chromatographically (ITLC and C18 RP chromatography) using different solvent systems. Blood kinetics in rabbits and biodistribution in mice was studied. Blood kinetics showed rapid first pass clearance with a biological half-life, $t_{1/2}$ (F), of 11 min. The ability of DTPA-Bis(INH) to target the infection site in vivo was assessed in gamma scintigraphic studies of normal rabbit and a rabbit with induced infections. From the present work it can be concluded that the radiolabelled DTPA-Bis(INH) accumulates at the site of infection.

1. INTRODUCTION

Tuberculosis and malaria together result in an estimated 5 million deaths annually worldwide. The spread of multidrug resistance in the most pathogenic causative agents, *Mycobacterium tuberculosis* and *Plasmodium falciparum*, underscores the need to identify active compounds with early diagnostic properties. Despite the worldwide ravages of tuberculosis and malaria, chemotherapeutic regimens against these two diseases have remained largely unchanged. Isoniazide (isonicotinic acid hydrazide (INH) [1–3] has been utilized as a front line agent in drug mixtures to treat *M. tuberculosis*. INH is highly effective for the treatment of experimentally induced tuberculosis in animals and is notably superior to streptomycin.

Unlike streptomycin, INH penetrates cells with ease and is just as effective against bacilli growing within cells as it is against those growing in culture media. It is generally recognized that INH is a ‘prodrug’ which is activated through an oxidation reaction catalysed by an endogenous enzyme. This enzyme, katG, which exhibits catalase-peroxidase activity converts INH to a reactive species capable of acetylation of an enzyme system found exclusively in *M. tuberculosis*. Evidence in support of the activation of INH reveals that INH resistant isolates have decreased catalytic activity associated with the deletion of the catalase gene, katG [4]. Furthermore, reintroduction of the gene into resistance organisms results in restored sensitivity of the organism to the drug. Reaction of INH with catalase-peroxidase results in the formation of isonicotinaldehyde, isonicotinic acid and isonicotinamide which can be accounted for through the reactive intermediate isonicotinoyl radical (I) or perisonicotinic acid (II).

Evidence has been offered both for and against the reaction catalysed by catalase-peroxidase activated by INH with a portion of the enzyme inhA, an enzyme involved in the biosynthesis of mycolic acids. The mycolic acids are important constituents of the mycobacterial cell wall in that they provide a permeability barrier to hydrophilic solutes. The enzyme inhA produced under the control of the gene inhA, is a NADH dependent enoyl reductase protein, which is thought to be involved in double bond reduction during fatty acid elongation. INH specifically inhibits long chain fatty acid synthesis [5, 6].

INH is readily absorbed following oral administration and is well tolerated in most patients. Peripheral neuritis and a variety of neurological manifestations are the most important dose dependent effects. These are due to interference with utilization of pyridoxine and its increased excretion in the urine. Pyridoxine is given prophylactically to prevent neurotoxicity even at higher doses.

SESSION 1

For a successful use of the isotope in antibiotic labelling, it has to be conjugated with an anti-infective drug by using the chelate approach. Thus, the prerequisites of fast complex formation and good radiochemical yield have to be fulfilled to avoid non-specific binding, to avoid label transfer in vivo to the competing serum protein, and to preserve the affinity of the INH complex conjugate.

Polyaminopolycarboxylic acid based chelating agents have given successful performances in labelling antibodies with some metallic radio-nuclides, especially ^{111}In , and various other lanthanides. The anhydride derivatives of diethylenetriaminepentaacetic acid (DTPA) are generally easier to synthesize because of the commercial availability of DTPA and are more cost effective, which prompted the design of an infection imaging agent based on DTPA conjugated to anti-infective drugs.

This paper reports on the achievement of the first aspects with a new DTPA conjugated INH. The works reported in the literature have shown that the DTPA conjugated [DTPA-B-(SLeX)A] form stable complexes with lanthanides and transition metals [7]. Moreover, the complex with the INH-DTPA is reflected in increased kinetic capability of the stabilized $^{99\text{m}}\text{Tc}$ complex compared with the unmodified INH. These studies have been continued to cover the conjugation of chelating moieties to label anti-infective drugs, which are an additional benefit in avoiding non-specific binding of $^{99\text{m}}\text{Tc}$ for use as infection imaging agents.

2. MATERIALS AND METHODS

2.1. Materials

2.1.1. Chemicals

Isoniazid (INH), DTPA bis anhydride, dimethylformamide (DMF) anhydride and triethylamine were purchased from Aldrich (Sigma Co.). Technetium was procured from the Regional Center for Radiopharmaceuticals (Northern region), Board of Radiation and Isotope Technology (BRIT), Department of Atomic Energy (India).

2.1.2. Instrumentation

HPLC analysis was performed employing a Beckman C-18 reversed phase column (250 mm × 4.6 mm). A mobile phase 0.05% TFA/methanol (7:1; v/v) and a flow rate of 0.5 mL/min were used. Mass spectroscopic analysis was

obtained using Agilent 1100 coupled with LC operation in ESI positive mode. A type GRS23C gamma ray spectrometer (serial no. 458-425 of Electronics Corporation of India Ltd) was used for determining the amount of activity (γ emitter) in the samples. A Siemens model DIACAM scintillation camera (planar) with pinhole collimator was used for the imaging of animals.

2.1.3. Animals

Female mice of Balb/c strain, weighing 40–50 g, were used for biodistribution studies. Rabbits of New Zealand strain weighing 3–3.5 kg were used for blood kinetics, serum protein binding study and imaging. The animals were selected at random from the stock colony maintained in the animal in-house facility. The animals were reared on laboratory 'chow' pellets, fed ad libitum and had free access to food and water at all time. The room was maintained at $25^{\circ}\text{C} \pm 2^{\circ}\text{C}$.

2.2. Synthesis of DTPA-Bis(INH) conjugate

DTPA (0.1 g; 0.28 mmol) was dissolved in 2 mL of DMF (anhyd.). INH (0.0844 g; 0.62 mmol) was then added. 2.2 molar equivalent of triethylamine (257.6 μL) was added. The reaction was allowed to proceed for 24 h. Completion of the reaction was checked by running TLC plates in 0.05% TFA/methanol (3:2; v/v) (R_f for INH: 0.89; R_f for DTPA-Bis(INH): 0.75). Triethylamine and DMF were evaporated under reduced pressure at 50°C using a rota-evaporator. The product was lyophilized and stored at -20°C until required. The chemical purity of the DTPA-Bis(INH) conjugate was examined by analytical HPLC on a Beckman C-18 reverse phase column (250 mm \times 4.6 mm). (INH, $t_R = 5.767$ min, DTPA-Bis(INH) $t_R = 6.1333$ min). The solvent system used 0.05% TFA/methanol (7:3 v/v) with a flow rate of 0.5 mL/min over 20 min. Using the same column, DTPA-Bis(INH) ($t_R = 6.1333$ min) was separated from INH ($t_R = 5.767$ min) and mass spectroscopic analysis was undertaken. A mass spectrum was obtained using Agilent 1100 coupled with LC in ESI positive mode. Elemental analysis of $\text{C}_{26}\text{H}_{33}\text{N}_9\text{O}_{10}$: C (49.44%); H (5.27%); N (19.96%); O (25.33%). Formula weight of DTPA-Bis(INH): 631.24. ESI positive mode $[\text{M}+\text{H}^+]$ at 632.3 [m/e]: 631.24.

2.3. Radiochemical synthesis of $^{99\text{m}}\text{Tc}$ -DTPA-Bis(INH)

Covalent attachment of a strong chelating agent MDL to INH provides binding sites to which reduced $^{99\text{m}}\text{Tc}$ may be strongly bound. Technetium-99m

SESSION 1

labelled DTPA-Bis(INH) conjugate was prepared by a simple reduction method using $\text{SnCl}_2 \cdot 2\text{H}_2\text{O}$ as the reducing agent.

Radiolabelled DTPA-Bis(INH) conjugate was prepared by dissolving 2.0 mg of the reaction product in 1 mL of distilled water. To this solution 150 μg of stannous chloride (1 mg/mL solution made in 1N HCL) was added. The pH of the solution was finally adjusted to 7.5 using 0.5M NaHCO_3 . The solution was then passed through a 0.22 μm Millipore filter. Finally, 2 mCi of activity was added drop wise and the mixture was incubated at room temperature for 15 min.

2.3.1. *Quality control of $^{99\text{m}}\text{Tc}$ -DTPA-Bis(INH) conjugate*

The radiochemical purity and labelling efficiency of the product was ascertained by ascending instant thin layer chromatography (ITLC). The ITLC strips were utilized as the stationary phase and acetone as the mobile phase. The procedure involved spotting 2 μL samples of DTPA-Bis(INH) radiopharmaceutical onto chromatography strip 10 cm in length. After developing in the solvent, the strips were cut into two portions (top:bottom: 1:3) and activity in each portion was measured in the form of counts using a gamma scintillation counter. Percentage activity at the origin and the solvent front was determined. The $^{99\text{m}}\text{Tc}$ -DTPA-Bis(INH) conjugate remained at the origin and free technetium travelled with the solvent front ($R_f = 0.9-1.0$). The percentage of colloid was determined using pyridine:acetic acid:water (3:2.5:1) as the mobile phase. The radiochemical purity was found to be greater than 95%.

2.3.2. *In vitro stability study*

In vitro stability studies were carried out by incubating the reaction mixture over various time intervals. Percentage radiolabelling was calculated for 0, 1, 2, 3, 4 and 24 h.

2.3.3. *In vivo stability study*

This study was done to evaluate the stability of $^{99\text{m}}\text{Tc}$ labelled DTPA-Bis(INH), after administering the radiopharmaceutical into the blood stream of the test organism. The in vivo stability study was carried out by injecting 18.5 MBq of radiolabelled compound through the dorsal ear vein. Blood was withdrawn from the other ear vein at different time intervals from 5 min to 24 h. Every time the blood was withdrawn, the ITLC was run in acetone and the percentage radiolabelling and free $^{99\text{m}}\text{Tc}$ were determined. Blood kinetics studies were done on normal rabbits whereby 18.5 MBq of radiolabelled

compound was injected intravenously through the dorsal ear vein. Blood was withdrawn from the other ear vein at different time intervals from 5 to 24 h. Persistence of activity in the circulation was calculated assuming total blood volume as 7% of the body weight.

2.4. Biological evaluation

2.4.1. Scintigraphy in rabbits

For this, 18.5 MBq of a radiolabelled compound was injected intravenously through the dorsal ear vein of the rabbit. Images were taken using a planar gamma camera equipped with a pinhole collimator. Images were obtained at 1 h post-injection and 24 h post-injection.

2.4.2. Biodistribution study

Normal mice were used for the biodistribution study and 1.48 MBq of radiolabelled compound was injected in the tail vein of each mouse. Mice were dissected at 1 h, 2 h, 4 h and 24 h. Different organs were taken out, weighed and counted in a gamma counter. Uptake of radiopharmaceutical in each sample was calculated and expressed as percentage injected dose per organ.

3. RESULTS AND DISCUSSION

3.1. Synthesis

The synthesis of DTPA-Bis(INH) is shown in Fig. 1. Synthesis of conjugated INH was performed as reported in the literature [7]. The reaction was monitored on HPLC and showed a peak only at 6.13 min, which was confirmed by mass spectra ESI positive mode (Fig. 2).

The DTPA-Bis(INH) complex was successfully labelled with ^{99m}Tc with more than 95% labelling efficiency. It was sufficiently stable up to 24 h. Such a high labelling yield and high stability are the prerequisite conditions for a good radiopharmaceutical. Such a high labelling efficiency and stability are attributed to the presence of defined multidentate chelating system. Variation in the amount of $\text{SnCl}_2 \cdot 2\text{H}_2\text{O}$ and pH had a significant influence on the labelling yield. When the concentration of $\text{SnCl}_2 \cdot 2\text{H}_2\text{O}$ was varied between 50–300 μg , keeping other factors constant, the optimal yield was obtained with 150 μg of stannous chloride. The percentage of colloid formed was 2.88%,

SESSION 1

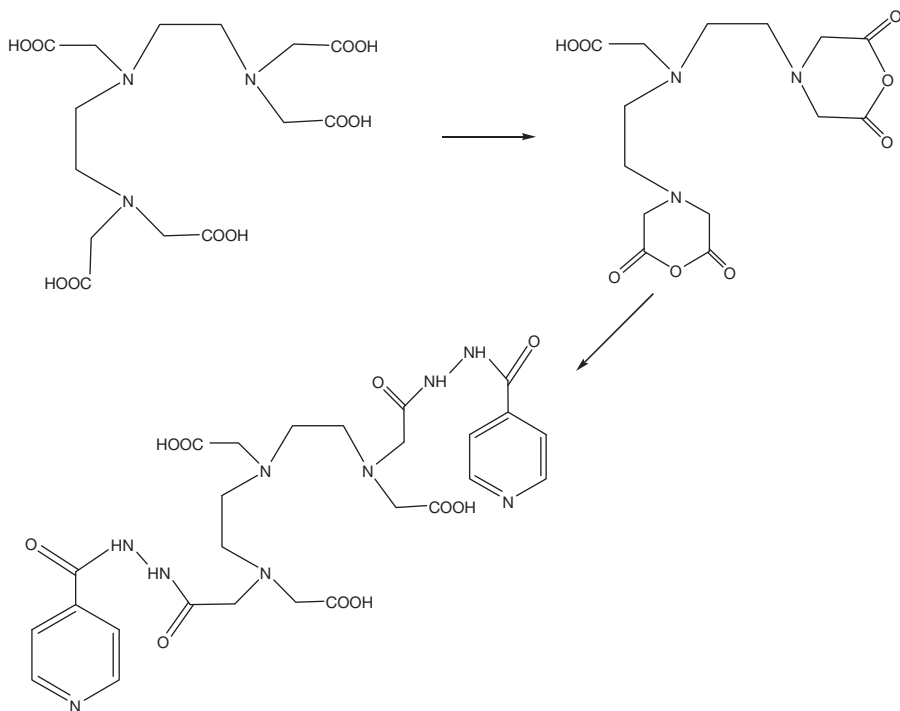


FIG. 1. Synthesis of Bis(amide) of diethylenetriaminepentaacetic acid: DTPA-Bis(INH).

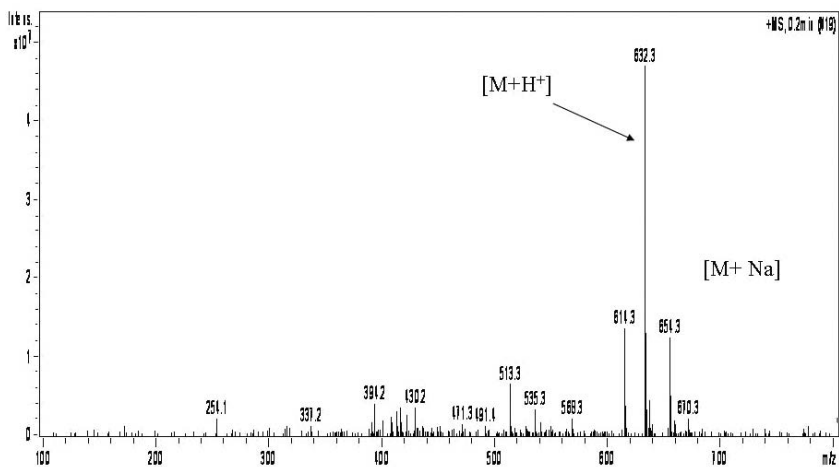


FIG. 2. Mass spectrum of DTPA-Bis(INH) in ESI (positive mode).

which increased with increasing concentration of stannous chloride. Variation in pH also affected the labelling efficiency. The optimum pH was found to be 7.5. At pH7.5, all the carboxyl groups of DTPA deprotonated as good binders for ^{99m}Tc . Thus, the complex between DTPA-Bis(INH) and ^{99m}Tc at pH7.5 is more stable than at an acidic pH. Figure 3 shows results of the in vitro studies on the DTPA-Bis(INH) complex in physiological conditions over a period of 24 h.

The conjugated INH was labelled with a specific activity of 20–30 mCi/mg of antibiotic. Labelling efficiencies were measured by ascending paper chromatography on ITLC-SG strips. The results of radiolabelling of the conjugate were found to be $98.5 \pm 0.30\%$. The ITLC-SG results in acetone showed that 1.5–2% or less free pertechnetate ran with the solvent front ($R_f = 0.7-1.0$). This indicated that pertechnetate was reduced almost entirely. Use of 10% NH_4OAc and methanol 1:1 as a solvent for migration showed all the activity occurred on the base of the ITLC-SG strips, indicating the radiolabelled conjugate, not the other species.

Radiolabelled conjugates were challenged with (25–100mM) of cysteine to test the stability of the radiolabelled DTPA-INH. Major transcomplexation of ^{99m}Tc to 25mM cysteine was observed for unmodified INH that was found to be 45%. DTPA-INH showed 5.9% transcomplexation of ^{99m}Tc to 25mM cysteine. More than 97% of the radioactivity remains associated with the conjugate after a 2 h challenge at 37°C with cysteine.

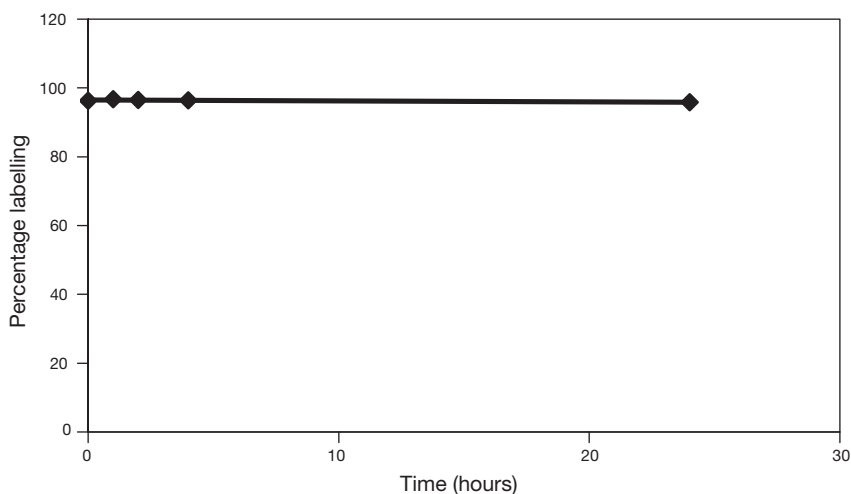


FIG. 3. In vitro stability studies of DTPA-Bis(INH) under physiological conditions.

3.2. Blood kinetics

Blood kinetics data of radiolabelled drug were obtained at various time intervals. The blood kinetics study showed very rapid first pass blood clearance with approximately 60% clearance by 5 min and >85% clearance by 1 h. Blood clearance $T_{1/2}$ equalled 11 min and shows very fast first order kinetics (Fig. 4). Such fast kinetics are due mainly to the highly hydrophilic nature of the drug.

3.3. Scintigraphy

Imaging of a normal rabbit and a rabbit with induced tuberculosis was carried out using a gamma camera. The images obtained for a normal rabbit 1 h and 24 h post-injection correlate fairly well with the blood kinetics and biodistribution studies. An appreciable activity can be noticed only in liver, kidney and urinary bladder. In experimental rabbits, a similar pattern was obtained 1 h post-injection but images taken at 24 h post-injection clearly show accumulation of radiopharmaceutical at the tubercular site (Fig. 5).

3.4. Biodistribution

Biodistribution data of radiolabelled drug were obtained at various time points; the results are shown in Table 1. Results clearly indicate that the major route of excretion of radiopharmaceutical is renal, since very high activity occurs in the kidney. However, the activity 1 h post-injection is much higher in the kidney than in the intestine. Most of the clearance of the drug, almost 80%,

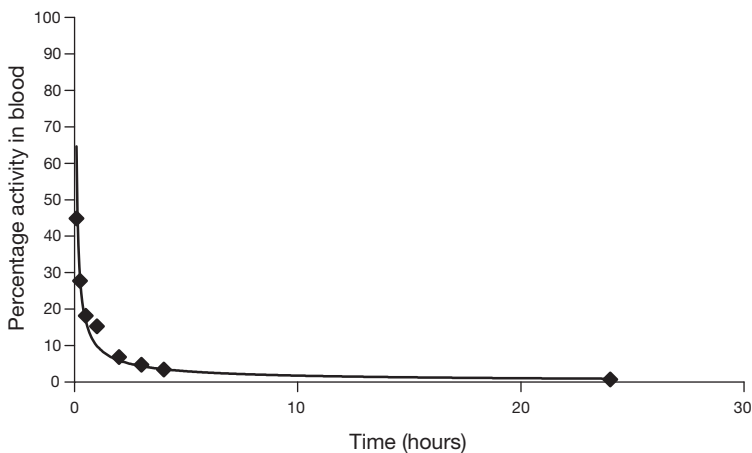


FIG. 4. Blood kinetics of DTPA-Bis(INH) in rabbit.

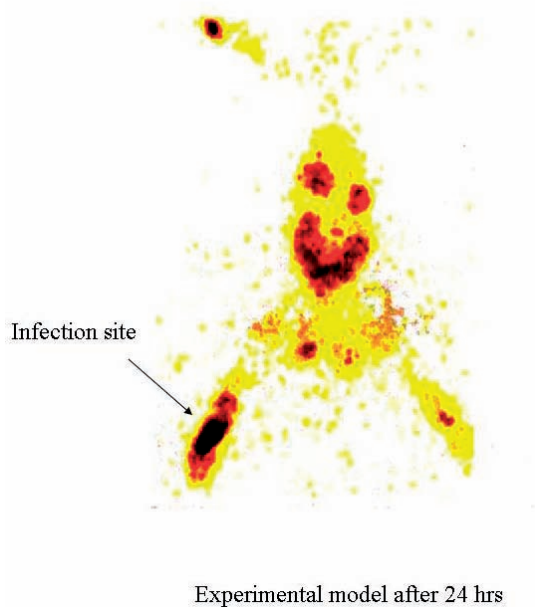


FIG. 5. Whole body gamma scintigraphy of $^{99m}\text{Tc-DTPA-Bis-INH}$ in rabbit bearing tubercular (*M. tuberculosis*) infective lesion in left leg at 24 h.

TABLE 1. BIODISTRIBUTION OF $^{99m}\text{Tc-DTPA-BIS(INH)}$ IN MICE

Organ/tissue	1 h	2 h	4 h	24 h
Blood	8.00 ± 0.070	6.09 ± 0.710	3.20 ± 0.170	0.700 ± 0.110
Heart	0.24 ± 0.014	0.17 ± 0.020	0.14 ± 0.010	0.007 ± 0.001
Lung	0.91 ± 0.060	0.66 ± 0.080	0.63 ± 0.110	0.040 ± 0.010
Liver	6.30 ± 0.580	6.25 ± 0.110	5.20 ± 0.330	0.500 ± 0.040
Spleen	0.34 ± 0.100	0.20 ± 0.005	0.17 ± 0.020	0.035 ± 0.010
Kidney	7.65 ± 0.520	6.70 ± 0.280	5.96 ± 0.700	0.350 ± 0.050
Stomach	0.88 ± 0.060	0.76 ± 0.050	0.78 ± 0.070	0.180 ± 0.030
Intestine	4.63 ± 0.620	8.56 ± 0.760	12.82 ± 1.23	1.340 ± 0.160
Muscle	0.38 ± 0.030	0.41 ± 0.040	0.52 ± 0.030	0.260 ± 0.050
Bone	1.32 ± 0.180	1.52 ± 0.210	1.25 ± 0.420	0.220 ± 0.030
Brain	0.31 ± 0.030	0.28 ± 0.060	0.36 ± 0.050	0.120 ± 0.002

SESSION 1

took place in the first hour post-injection, as determined from the blood kinetics study. Correlating both these observations, it can be concluded that most of the radiopharmaceutical (about 80%) is excreted mainly through the renal route. However, activity 4 h post-injection is concentrated more in the intestine than in the urine. A biodistribution study again showed a very fast clearance of the radiopharmaceutical from the blood. As far as accumulation of radiopharmaceutical in the RES is concerned, it showed accumulation mainly in the liver, very little accumulation in the lungs and almost negligible concentration in the spleen. Negligible accumulation occurred in the heart and brain. However appreciable accumulation is seen in bone, thus, this radiopharmaceutical can also be used effectively in diagnosing tuberculosis associated with bones.

This investigation focused on the possibilities and limitations of a ^{99m}Tc labelled INH. However, ^{99m}Tc labelled antimicrobial compounds, such as ciprofloxacin [8] and antimicrobial peptides [9, 10], may be the more promising radiopharmaceuticals that distinguish between bacterial infections and sterile inflammatory processes in humans [11]. The antibiotic ciprofloxacin and the human neutrophil peptides have been introduced in nuclear medicine as tracers that preferentially detect bacterial infections. A major drawback with these imaging agents is labelling directly with undefined radiochemistry. To overcome this disadvantage of known procedure for direct labelling, the antibiotic used employs a chelate technology to modify the antibiotics to label with radionuclide.

Antibiotic such as INH have been utilized as front line agents in drug mixtures to treat *M. tuberculosis*. In the present study, conjugates of the INH have been generated using DTPA anhydride as a chelating agent. This chelate has anhydride as the reactive group which allows INH conjugation and carboxylic and amide groups for radiolabelling with ^{99m}Tc . The two molecules of INH also enhance the hydrogen bonding with INH receptors and do not alter its binding with NADH. The use of this chelating agent to prepare radioconjugates makes rapid clearance from blood circulation and normal organs possible compared with directly radiolabelled antibiotics as previously described [12].

4. CONCLUSION

The DTPA-Bis(INH) shows substantial promise for diagnosis of tubercular sites, especially in patients with extrapulmonary tuberculosis. From the present work it can be concluded that radiolabelled DTPA-Bis(INH) accumulates at the site of infection. It is important to note that the complex is

highly hydrophilic in nature and is retained at the site of infection even after 24 h and not simply washed away. This indicates that some specific mechanism must be involved in the accumulation of radiopharmaceutical at the site of infection, other than the enhanced permeability and retention effect.

ACKNOWLEDGEMENTS

The authors would like to express their gratitude to Dr. R.P. Tripathi, Director INMAS, for providing the necessary facilities. The work was supported by the Defence Research and Development Organization, Ministry of Defence, under R&D project INM-302.

REFERENCES

- [1] BANERJEE, A., et al., inhA: Gene encoding a target for Isoniazide and Ethiomamide in *Mycobacterium tuberculosis*, Science **263** (1994) 227.
- [2] FLOYD, K., et al., Resources required for Global Tuberculosis Control, Science **295** (2002) 2040.
- [3] GARBE, T.R., et al., Isoniazide induces expression of the antigen 85 complex in *Mycobacterium tuberculosis*, Antimicrob. Agents Chemother. **40** 7(1996) 1754.
- [4] GUPTA, R., et al., Responding to market failures in tuberculosis control, Science **293** (2001) 1049.
- [5] KUO, M.R., Targeting tuberculosis and malarial through Inhibition of Enoyl Reductase, J. Biol. Chem. **278** 23 (2003) 20859.
- [6] LEI, B., et al., Action mechanism of antitubercular isoniazide: Activation by *Mycobacterium tuberculosis* KatG, isolation and characterization of inhA inhibitor, J. Biol. Chem. **275** 4 (2000) 2520.
- [7] FU, Y., et al., Synthesis of a Silyl Lewis mimetic conjugated with DTPA, potential ligand of new contrast agents for medical imaging, Eur. J. Org. Chem. (2002) 3966.
- [8] VINJAMURI, S., et al., Comparison of ^{99m}Tc infecton imaging with radio-labelled white cells imaging in the evaluation of bacterial infection, Lancet **347** (1996) 233.
- [9] WELLING, M.M., et al., Imaging of bacterial infections with ^{99m}Tc-labeled human neutrophil peptide, J. Nucl. Med. **40** (1999) 2073.
- [10] WELLING, M.M., et al., Technetium-99m labelled antimicrobial peptides discriminate between bacterial infections and sterile inflammations, Eur. J. Nucl. Med. **27** (2000) 292.
- [11] NIBBERING, P.H., et al., Radiolabelled antimicrobial peptides for imaging of infections, Nucl. Med. Commun. **19** (1998) 1117.
- [12] BRYANT, R.E., et al., Effect of abscess environment of the antimicrobial activity of ciprofloxacin, Am. J. Med. **87** (1989) 23.

ANTIMICROBIAL PEPTIDE ^{99m}Tc -UBI 29-41 FOR INFECTION DIAGNOSIS

Kit formulation and a preliminary clinical study

G. RODRÍGUEZ*, P. OLIVER*, J. VILAR**, V. TRINDADE*,
A. ROBLES*, A. LÓPEZ*, G. LAGO**, H. BALTER*,
M.M. WELLING***, E.K.J. PAUWELS***

*Department of Radiopharmacy,
Nuclear Research Center, Faculty of Sciences,
University of the Republic,
Email: grodri@cin.edu.uy

**Nuclear Medicine Center,
Clinical Hospital, Faculty of Medicine,
University of the Republic,

Montevideo, Uruguay

***Leiden University Medical Center,
Leiden, Netherlands

Abstract

Antimicrobial peptides that show specific binding to pathogens are potential precursors for the differential diagnosis of infections. The ubiquicidin derived peptide UBI 29-41 labelled with ^{99m}Tc was previously studied as part of the design of a radio-pharmaceutical showing good physicochemical and biological properties. In searching for the clinical application of this labelled peptide, the research focused on the optimization of a lyophilized kit composition, labelling parameters such as time and temperature of incubation, as well as on storage conditions. The best labelling results were obtained for a kit containing 50.0 μg of UBI 29-41, 4.4 μg of SnF_2 , 13.6 μg of $\text{Na}_2\text{P}_2\text{O}_7$ and 70.0 μg of KBH_4 , incubated with the pertechnetate in a boiling bath for 5 min. Radiochemical purity was higher than 95%. It showed a good stability at room temperature over 24 h. Studies of stability in human serum and cysteine challenge tests were performed, rendering good results. The kit was stable for more than five months at 4°C. Biological evaluation on mice with *S. aureus* induced infection indicated a differential uptake between normal and infected tissue. On the basis of promising preclinical results of ^{99m}Tc -UBI 29-41, a patient with a hip prosthesis was studied. The results obtained encourage more work on its possible future routine use in nuclear medicine.

1. INTRODUCTION

Differentiation of infections from sterile inflammatory lesions is an important goal in the development of radiopharmaceuticals for nuclear medicine.

Technetium-99m labelled cationic antimicrobial peptides derived from ubiquicidin (UBI) have high potential for use in this application [1].

On the basis of the authors previous research work [2], this investigation focused on UBI 29-41, containing the residues 29-41 of a cationic α -helical domain of human UBI, bearing the following sequence: Thr-Gly-Arg-Ala-Lys-Arg-Arg-Met-Gln-Tyr-Asn-Arg-Arg, 1693 Da [3]. A kit formulation was designed to obtain a labelled peptide with adequate properties for clinical trials and easy to apply on a routine basis [4]. Several formulations based on the use of tin fluoride and potassium borohydride as reducing agents and sodium pyrophosphate as an intermediate ligand were investigated. The radiochemical characteristics as well as the stability of the labelled molecules were determined. Biological performance was ascertained by biodistribution in a pathological animal model for bacterial infection.

As a result of the promising results obtained, a lyophilized kit formulation was selected and the first patient was studied.

2. MATERIALS AND METHODS

The UBI 29-41 peptide was synthesized at the Leiden University Medical Center as described before [1]. Chemical products were analytical grade and available from Sigma-Aldrich.

Lyophilized kits contained from 2.2 to 13.2 μg of SnF_2 , 6.8–40.0 μg of $\text{Na}_2\text{P}_2\text{O}_7 \cdot 10\text{H}_2\text{O}$, 70–100 μg of KBH_4 and 50 μg of UBI 29-41, and were prepared using as a reference the results obtained with a liquid formulation. The kit was directly labelled adding 1 mL of $^{99\text{m}}\text{Tc}$ -sodium pertechnetate (up to 1850 MBq) from a generator (CIS, France or Tecnonuclear, Argentina) and incubating at room temperature and at 100°C for different periods of time.

Radiochemical purity controls as well as the stability of the labelled peptide were evaluated by the following methods:

- (a) Instant thin layer chromatography (ITLC-SG) using saline solution (NaCl 0.9%), methylethylketone, or 0.1% trifluoroacetic acid in water ($\text{H}_2\text{O}/\text{TFA}$ 0.1%) as solvents.
- (b) Reverse phase high performance chromatography (RP-HPLC) on a C18 column (MCH-5, n-capp, Varian, Ireland or Deltapak, Waters, United

SESSION 1

States of America) with 0.1% (w/w) trifluoroacetic acid in water (eluent A) and 0.1% (w/w) trifluoroacetic acid in acetonitrile (eluent B), flow 1 mL/min, gradient programmed as follows: 0–3 min 100% A, 3–13 min from 100% A to 100% B, 13–18 min 100% B, 18–23 min from 100% B to 100% A.

- (c) Sep-pak: extraction on a C18 cartridge (Waters) previously activated with 5 mL methanol, 5 mL water and 5 mL 0.1% acetic acid and air dried. The sample (20–100 μ L) was applied on the cartridge and was rinsed with 5 mL of 0.1% acetic acid; trapped peptide was eluted with 5 mL of methanol in 1 mL fractions.
- (d) Stability of the labelled peptide was evaluated in diluted human serum (20%) at 37°C at various time intervals (5, 30, 60, 120 min and 24 h). Thirty milligrams (in 200 μ L) of the radiolabelled peptide was added to 200 μ L of diluted serum.

For the cysteine challenge, a solution of 10 mg/mL cysteine was diluted in phosphate buffer saline 0.2M, pH7.0 to 1, 0.1, 0.01 and 0.001 mg/mL. Mixtures of 10 μ L of each solution and 90 μ L of radiolabelled peptide solution were incubated for 1 h at 37°C and were compared with a blank sample. Each mixture was controlled by ITLC-SG.

Biodistribution studies were undertaken in an animal model consisting of mice having a bacterial infection induced by an intramuscular injection (24 h before the study) of 0.1 mL bacterial culture (10^8 cfu/mL) of *S. aureus* ATCC 25923 (American type cell culture catalogue number 25923) in the right hind limb. The animal model as well as all vivo biological procedures were done under the recommendations of the National Committee of Animal Experimentation. The labelled peptide (0.1 mL) was injected intravenously and the activity uptake in the different organs/tissues was determined after cervical dislocation at 1 h post-injection. Data were expressed as a percentage of the injected dose per gram (%ID/g). Target (infected/inflamed thigh muscle) to non-target (contralateral thigh muscle) (T/NT) ratios were calculated. The presence or absence of viable bacteria in muscle was evaluated microbiologically by in vitro assay.

From the promising results obtained, a patient with a suspected infected prosthesis was studied. The previous clinical data were great pain and high local temperature with elevated C reactive protein and erythrocyte sedimentation rate. In addition, the patient had had, within the previous five years, three reinterventions of the right hip owing to repeated infected prosthesis. This study was done with National Ethical Committee authorization and the prior informed consent of the patient.

After injection of 333 MBq of the labelled peptide, a dynamic study using a Elscint SP-4 gamma camera with a high resolution collimator was performed. The predetermined areas of interest, near both hips, were selected to quantify accumulation of the tracer. Static images were performed at 15 and 30 min and at 1, 2, 3, 4 and 24 h. The ratio of right hip prosthesis versus contralateral normal area, T/NT, was calculated at various intervals in order to determine the ideal acquisition time. Whole body anterior and posterior images were also acquired at 3 h.

3. RESULTS

The different physicochemical controls used were all successful for radiochemical purity determination of the labelled peptide, but in the case of Sepapak purification, high non-specific adsorption was observed.

Lyophilized formulation II rendered a radiochemical purity higher than 90% when the incubation time was up to 2 h at room temperature or 5 min at 100°C. These results reveal that there exists a difference between the kinetics of formation of the ^{99m}Tc -UBI 29-41 obtained by the liquid formulation (previous works) and the lyophilized forms. The best results were obtained for a kit containing 50.0 μg UBI 29-41, 4.4 μg SnF_2 , 13.6 μg $\text{Na}_2\text{P}_2\text{O}_7 \cdot 10\text{H}_2\text{O}$, 70 μg KBH_4 (formula II). Labelling with up to 1850 MBq of ^{99m}Tc -pertechnetate at an incubation temperature of 100°C for 5 min rendered a labelled molecule with a radiochemical purity higher than 95% (Fig 1).

The in vitro stability (at room temperature) of the kit (formula II) was confirmed for more than 24 h (Fig. 2).

The stability of ^{99m}Tc -UBI 29-41 in human diluted serum showed practically no release of radioactivity during the first hour of incubation (Fig. 3).

The cysteine challenge test indicated that more than 10% of the labelled peptide was transchelated for cysteine concentrations higher than 0.01 mg/mL (82.5 μM) as shown in Fig. 4.

Biological distribution in the animal model is shown in Fig. 5. The renal clearance was >60% ID within 1 h of administration. The T/NT ratio was 3.2. These results are similar to liquid preparation developed previously [2].

Scintigraphic images of the patient are presented in Fig. 6. It was observed that very early dynamic images showed equal perfusion in both hips (at 30 and 60 min). Accumulation of the radiotracer was significant in the probable infected hip compared with the normal one. The focus of accumulation was determined at the femoral proximal bone sector near the prosthesis. This result is evidence that uptake is selective and allows a differentiation of the process during the first hour of the study. The kinetics of elimination from

SESSION 1

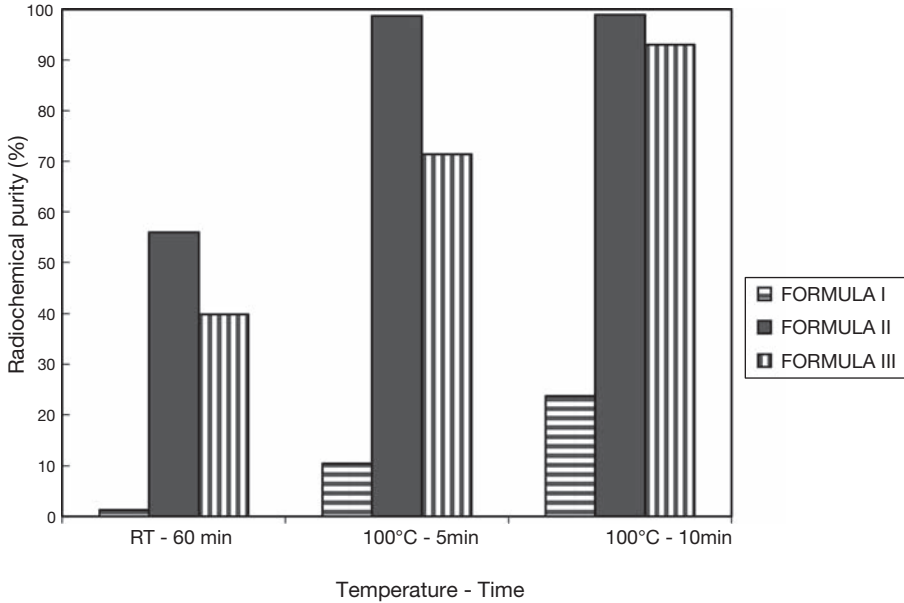


FIG. 1. Radiochemical purity (%) at different conditions of incubation for several formulations: formula I: 50.0 μg UBI 29-41, 2.2 μg SnF_2 , 6.8 μg $\text{Na}_2\text{P}_2\text{O}_7 \cdot 10\text{H}_2\text{O}$, 70 μg KBH_4 , formula II: 50.0 μg UBI 29-41, 4.4 μg SnF_2 , 13.6 μg $\text{Na}_2\text{P}_2\text{O}_7 \cdot 10\text{H}_2\text{O}$, 70 μg KBH_4 , formula III: 50.0 μg UBI 29-41, 13.2 μg SnF_2 , 40.0 μg $\text{Na}_2\text{P}_2\text{O}_7 \cdot 10\text{H}_2\text{O}$, 100 μg KBH_4 .

the site seem to be fast as the images, at longer durations, reveal a less significant T/NT ratio. Nevertheless, more clinical research is needed to confirm these preliminary results.

4. CONCLUSIONS

From the results obtained, it may be concluded that the kit formulation II was optimal, reaching more than five months stability. The UBI derived peptide UBI 29-41 directly labelled with $^{99\text{m}}\text{Tc}$ is easily produced with high radiochemical purity and is stable for more than 24 h. Stability in the presence of cysteine was compatible with levels of the analyte in normal individuals (7.9 μM). Technetium-99m-UBI 29-41 shows specific uptake in infected tissues, thus being a promising tracer for bacterial infection specific imaging. The kit formulation allows for its safe handling, compatible with its use in nuclear medicine centres.

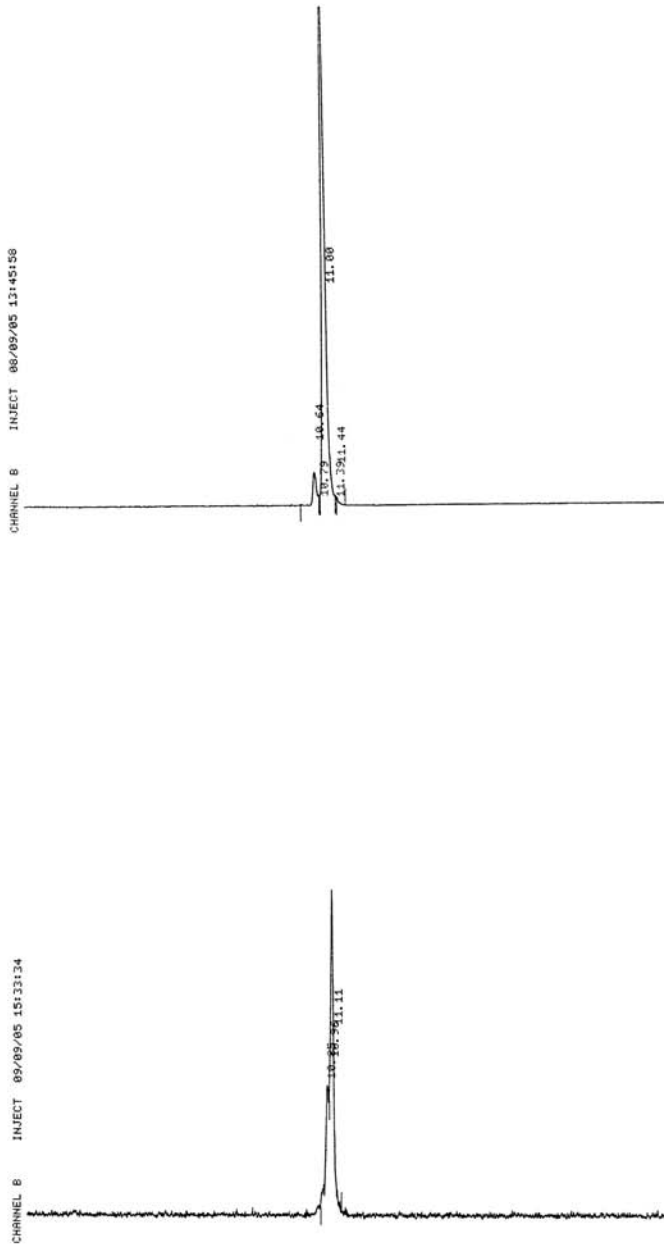


FIG. 2. HPLC of the ^{99m}Tc -UBI 29-41 at 0 h and 27 h post-labelling.

SESSION 1

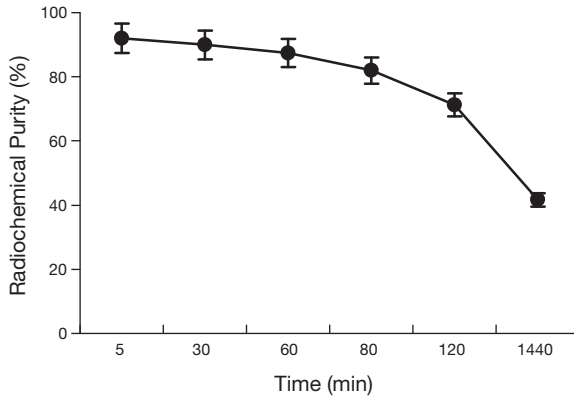


FIG. 3. Stability of ^{99m}Tc -UBI 29-41 in human diluted serum expressed as radiochemical purity in ITLC-SG-NaCl 0.9%.

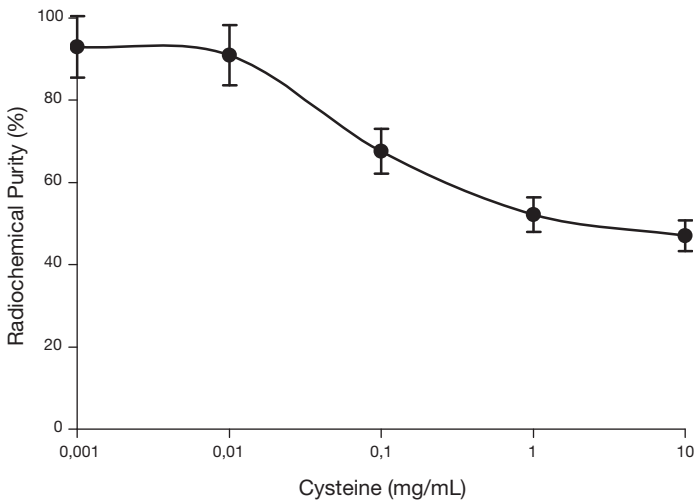


FIG. 4. RCP (%) of ^{99m}Tc -UBI 29-41 after cysteine challenge.

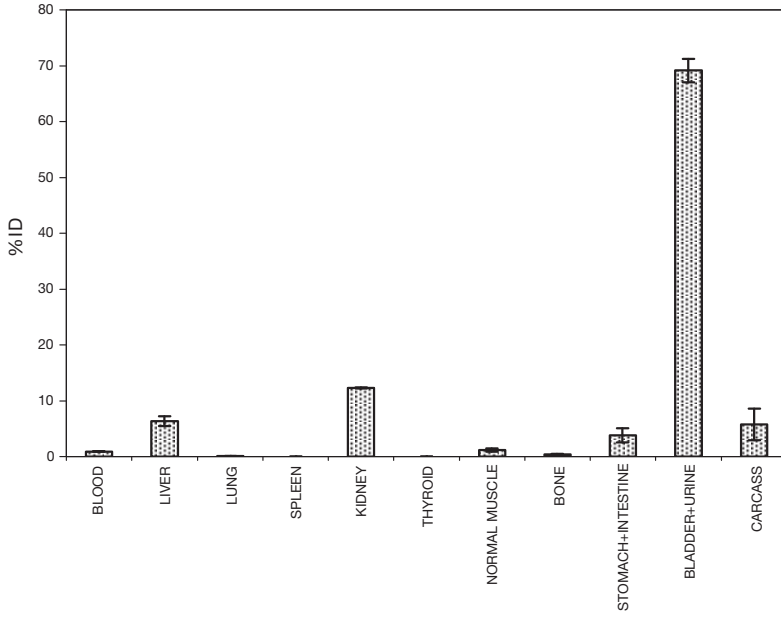


FIG. 5. Biodistribution in mice.

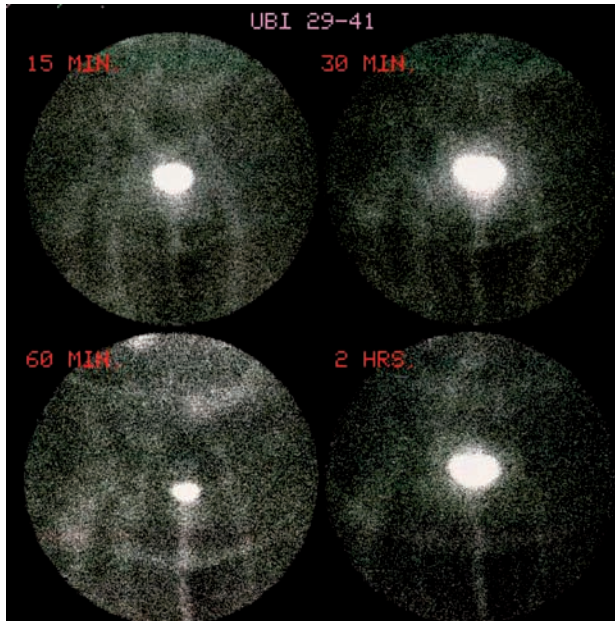


FIG. 6. Scintigraphic images of the patient at 15 and 30 min , and 1 and 2 h.

SESSION 1

More research work is in progress in order to establish the shelf life of the lyophilized kit as well as to confirm the promising results obtained in the first clinical study.

REFERENCES

- [1] WELLING, M.M., et al., Radiochemical and biological characteristics of ^{99m}Tc -UBI-29-41 for imaging of bacterial infections, *Nucl. Med. Biol.* **29** (2002) 413–422.
- [2] SOUTO, B., et al., “ ^{99m}Tc radiopharmaceuticals for infection imaging: Kits development and validation”, Development of Kits for ^{99m}Tc Radiopharmaceuticals for Infection Imaging, IAEA TECDOC-1414, IAEA, Vienna (2004).
- [3] LUPETTI, A; WELLING, M.M; PAUWELS, E.K.J, NIBBERING, P.H., Radiolabelled antimicrobial peptides for infection detection, **3** (2003) 223–229.
- [4] MUHAMMAD SAEED AKHTAR, et al., Antimicrobial peptide ^{99m}Tc -Ubiquitin 29–41 as human infection-imaging agent: Clinical trial, *J. Nucl. Med.* **46** 4 (2005) 567–573.

BIBLIOGRAPHY

BECKER, W., The contribution of nuclear medicine to patient with infection, *Eur. J. Nucl. Med.* **22** (1995) 1195–1211.

DE KOSTER, H.S., et al., The use of dedicated peptide libraries permits the discovery of high affinity binding peptides, *J. Immunol. Methods* **187** (1995) 179–188.

HNATOWICH, D.J., et al., Labeling peptides with Technetium-99m using a bifunctional chelator of a N-hydroxysuccinimide ester of mercaptoacetyltryglycine, *J. Nucl. Med.* **39** (1998) 56–64.

SIGNORE, A., et al., Peptide radiopharmaceuticals for diagnosis and therapy, *Eur. J. Nucl. Med.* **28** (2001) 1555–1565.

VALLABHAJOSULA, S., Technetium 99m labelled chemotactic peptides: Specific for imaging infection?, *J. Nucl. Med.* **38** (1997) 1322–1326.

WELLING, M.M., PAULUSMA-ANNEMA, A., BALTER, H.S., PAUWELS, E.K.J., NIBBERING, P.H., Technetium labelled antimicrobial peptides discriminate between bacterial infections and sterile inflammations, *Eur. J. Nucl. Med.* **27** (2000) 292–301.

TECHNETIUM CHEMISTRY AND
RADIOPHARMACEUTICALS: II

(Session 2)

Chairpersons

A. DUATTI
Italy

J. KÖRNYEI
Hungary

PREPARATION AND EVALUATION OF THIRD GENERATION TECHNETIUM-99m RADIOPHARMACEUTICALS

G. FERRO-FLORES*, C. ARTEAGA DE MURPHY**,
F. DE M. RAMIREZ*, M. PEDRAZA-LÓPEZ**,
J. RODRÍGUEZ-CORTÉS**, L. MELÉNDEZ-ALAFORT*

*Instituto Nacional de Investigaciones Nucleares,
Estado de México
Email: gff@nuclear.inin.mx

**Instituto Nacional de Ciencias Médicas y Nutrición Salvador Zubirán

Mexico City, Mexico

Abstract

The preparation and evaluation of three different ^{99m}Tc labelled peptides as third generation radiopharmaceuticals is presented. Lys³-Bombesin ([Lys³]BN), ubiquickidin 29-41 (UBI 29-41) and Tyr³-octreotide (TOC) were prepared as instant kit formulations to be labelled by direct or indirect methods with ^{99m}Tc in order to evaluate in vivo prostate malignancies, infection processes and lung cancer respectively. Radiochemical purity of >93% was obtained. Also, high in vitro and in vivo stabilities and preservation of the molecular recognition were observed. It is demonstrated that ^{99m}Tc -EDDA/HYNIC-[Lys³]BN detects GRP receptor positive tumours in mice, ^{99m}Tc -UBI 29-41 detects infection foci in humans and ^{99m}Tc -EDDA/HYNIC-TOC is useful in patients with lung cancer.

1. INTRODUCTION

Bombesin (BN) is a peptide that was initially isolated from frog skin and belongs to a large group of neuropeptides with many biological functions. The human equivalent is the gastrin releasing peptide (GRP) and its receptors (GRP-r) are over expressed in a variety of malignant tumours. The strong specific BN-GRP-r binding is the basis for labelling BN with radionuclides [1–5]. Technetium-99m-DADT-[Lys³]BN, [DTPA¹,Lys³(^{99m}Tc -Pm-ADT),Tyr⁴]BN,

$^{99m}\text{Tc}(\text{I})\text{-PADA-AVA-BN}$, $^{99m}\text{Tc}\text{-Cys-6-amino-n-hexanoic acid-BN}$ and $^{64}\text{Cu}\text{-DOTA-[Lys}^3\text{]BN}$ have been prepared to be used in nuclear medicine for malignant tumour detection and for staging of breast and prostate cancers and their lymph nodes [1–8].

Scintigraphy with radiolabelled peptides, such as the somatostatin (SST) analogues, has been used to demonstrate the presence in vivo of SST receptors in neuroendocrine tumours. Technetium-99m-EDDA/HYNIC-Tyr³-octreotide ($^{99m}\text{Tc}\text{-HYNIC-TOC}$) has shown high in vitro and in vivo stabilities, rapid background clearance, relatively low accumulation in non-target tissues and rapid detection of SST receptor positive tumours [9–13].

The availability of simple, efficient and reproducible radiolabelling procedures is essential to develop radiopharmaceuticals for routine clinical use. Although the technology of $^{99m}\text{Tc}\text{-HYNIC}$ involves an indirect labelling procedure where the hydrazinonicotinamide (HYNIC) bifunctional chelator is conjugated to the peptide and the ethylenediamine-N,N'-diacetic acid (EDDA) used as coligand to complete the technetium coordination sphere, it can be obtained easily from instant freeze dried kit formulations [14, 15].

Technetium-99m labelled ubiquicidin peptide 29-41 fragment ($^{99m}\text{Tc}\text{-UBI}$) has been proposed as a new radiopharmaceutical for infection imaging [16, 17]. UBI is a cationic human antimicrobial peptide fragment (MW 1.69 kDa) with the amino acid sequence Thr-Gly-Arg-Ala-Lys-Arg-Arg-Met-Gln-Tyr-Asn-Arg-Arg, therefore with six positively charged residues. Studies of its biodistribution in mice have shown a fast renal clearance with minimal hepatobiliary excretion. Technetium-99m-UBI is bound to bacteria in vitro and is accumulated at sites of infection in experimental animals [16, 17].

In this work, the preparation of [Lys³]BN, UBI 29-41 and Tyr³-octreotide (TOC) as instant kit formulations to be labelled by direct or indirect methods with ^{99m}Tc in order to evaluate in vivo prostate malignancies, infection processes and lung cancer respectively, is presented.

2. GENERAL METHODOLOGY

[Lys³]BBN and TOC were conjugated to HYNIC [15, 18] and UBI 29-41 used as a free ligand [19–21]. Structures of the corresponding peptides were built and the optimized structures, in the best stable configurations, were calculated by molecular mechanics and quantum mechanical calculations. The technetium cation was added and the potential energy of the final structure evaluated. In order to correlate the calculated and experimental results, in vitro stability tests with cysteine challenge, human serum, dilution in saline solution and binding assays to bacteria or receptor specific cells were performed for

SESSION 2

each labelled peptide. The components of the lyophilized kits were selected to produce a direct ^{99m}Tc labelling for UBI 29-41 and ^{99m}Tc -EDDA/HYNIC-peptide for $[\text{Lys}^3]\text{BBN}$ and TOC [2, 3]. In vivo studies involved infected mice or implanted tumour cells in athymic mice. Whole body images from patients with suspected infection or lung cancer were acquired.

3. RESULTS AND DISCUSSION

Molecular mechanics and quantum mechanical calculations were essential tools in explaining experimental results associated with molecular recognition and stability. For $[\text{Lys}^3]\text{BN}$, it was possible to demonstrate that the only site available to introduce HYNIC as technetium chelator was Lys^3 , even if reaction conditions are carried out at pH7, obtaining a very high thermodynamic stability without interference in the stereospecificity of the C-terminal eight residues which are believed to contain the domain responsible for receptor recognition (Fig. 1). In the case of UBI 29-41, a peptide without cysteine residues, Lys and Arg^7 could be the specific site to coordinate ^{99m}Tc in the UBI structure, in which the Arg^7 amino group has a structural arrangement

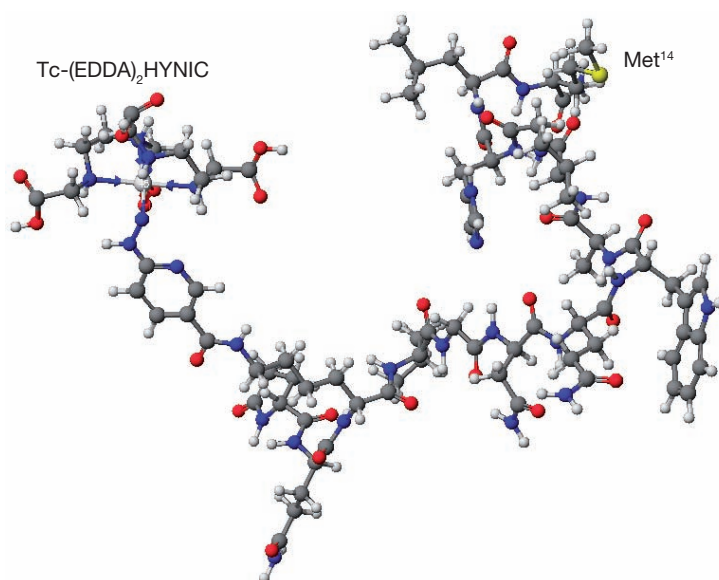


FIG. 1. Calculated structure of $\text{Tc}-(\text{EDDA})_2\text{HYNIC-BN}$ ($E = 105 \text{ kcal/mol}$).

facing the Lys amino group and forming a good chelating cage for the technetium cation [19].

Technetium-99m-EDDA/HYNIC-[Lys³]BN, ^{99m}Tc-UBI 29-41 and ^{99m}Tc-EDDA/HYNIC-TOC obtained from lyophilized kits showed radiochemical purities over 93%, high in vitro and in vivo stabilities, and preservation of the molecular recognition after a simple kit reconstitution without further purification. Lyophilized formulations showed high stability during the storage at 4°C for 3–6 months.

The ^{99m}Tc-EDDA/HYNIC-[Lys³]BN in vitro study results showed a high stability in serum and cysteine solutions, specific receptor binding and rapid internalization. Biodistribution in PC3 tumour bearing nude mice revealed a rapid blood clearance and specific binding towards GRP receptor positive tissues such as pancreas and PC3 tumours (Fig. 2). Conjugation of HYNIC to BN for the preparation of ^{99m}Tc-EDDA/HYNIC-[Lys³]BN modifies the lipophilic and pharmacokinetic properties of BN, producing a radiopharmaceutical with low hepatobiliary clearance and predominantly renal excretion. This is an important result because most of the ^{99m}Tc labelled BN analogues have a tendency to accumulate in the liver and intestine as a result of their high lipophilicity and hepatobiliary clearance [1–5]. The high radioactivity accumulation might interfere during the detection of BN/GRP receptor positive cancers and their metastases in the abdominal areas.

Biokinetic data of ^{99m}Tc-EDDA/HYNIC-TOC in humans obtained from lyophilized formulations showed a fast blood clearance with a mean residence time of 0.3 h. Images showed an average tumour/blood (heart) ratio of 4.3 ± 0.7

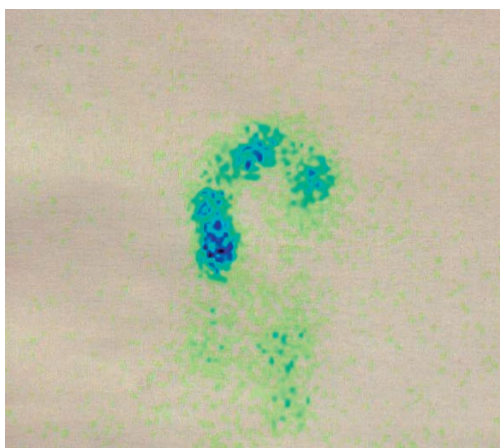


FIG. 2. Tumour, pancreas and kidney uptake of ^{99m}Tc-EDDA/HYNIC-[Lys³]BN in PC3 tumour bearing nude mice.

SESSION 2

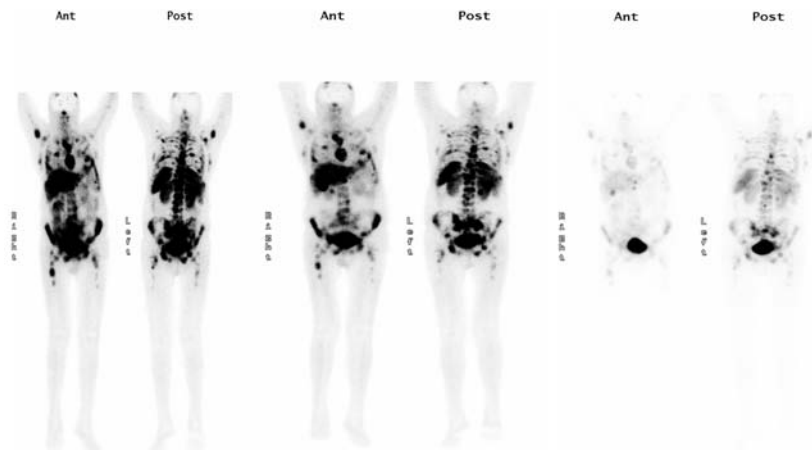


FIG. 3. Patient with metastatic neuroendocrine tumour. Anterior and posterior views at 1, 2 and 24 h after ^{99m}Tc -EDDA/HYNIC-TOC administration.

in receptor positive tumours at 1 h (Fig. 3). The mean radiation absorbed dose calculated for a study using 740 MBq was 24, 21.5, 5.5 and 1.0 mSv for spleen, kidney, liver and bone marrow respectively and the effective dose equivalent was 4.4 mSv [15].

Sugars such as glucose, mannitol and trehalose have been traditionally used as lyoprotectants because they can reduce the degradation of dried proteins. The peptide alone does not give sufficient solid residue (cake) after drying, therefore substances such as diluents should be added to provide a cake with uniform colour, texture and sufficient strength to prevent crumbling during storage. For $[\text{Lys}^3]\text{BN}$ and TOC, the final kit lyophilized formulation containing 20 μg of HYNIC-peptide, 20 μg of stannous chloride, 10 mg of EDDA, 20 mg of tricine and 50 mg of mannitol produced good cake appearance and stability. This was not the case for UBI, since all the sugars tested affect significantly the peptide reactivity towards the ^{99m}Tc metal. As previously proposed, Lys and Arg⁷ could be the specific site to coordinate ^{99m}Tc in the UBI structure, as glucose, mannitol and trehalose exhibit a reducing character, the presence of a sugar in the medium could modify slightly the stereochemical-structural arrangement of the amino acids with the consequent change in the final configuration and conformation of the structure. Despite the absence of diluents in the formulation, the cake does not appear crusty or crumbly because the mass is very small, providing a formulation with rapid reconstitution and high radiolabelling yields. The final kit was then made up of two vials, one lyophilized containing 25 μg of UBI 29-41 peptide and 10 μg of

stannous chloride as a reducing agent, and another containing 30 μ l of 0.1M sodium hydroxide to carry out the labelling reaction at pH9.0 [21].

In vitro testing demonstrated that ^{99m}Tc -UBI was specifically bound to the bacteria when it was compared with two different ^{99m}Tc labelled cationic peptides, ^{99m}Tc -Tat-1-Scr and ^{99m}Tc -Tat-2-Scr, used as control [22]. Biokinetic studies of ^{99m}Tc -UBI demonstrated a fast renal clearance with minimal hepatobiliary excretion and capability to detect infection foci in humans [23]. Adverse reactions were not observed in patients who tolerated the studies well and the sites of infection were successfully detected (Figs 4 and 5). Technetium-99m-UBI 29-41, easily prepared by a direct method from a kit formulation, has adequate biokinetic properties and can be used to detect infection foci in patients with fever of unknown origin or who are undergoing antibiotic treatment.

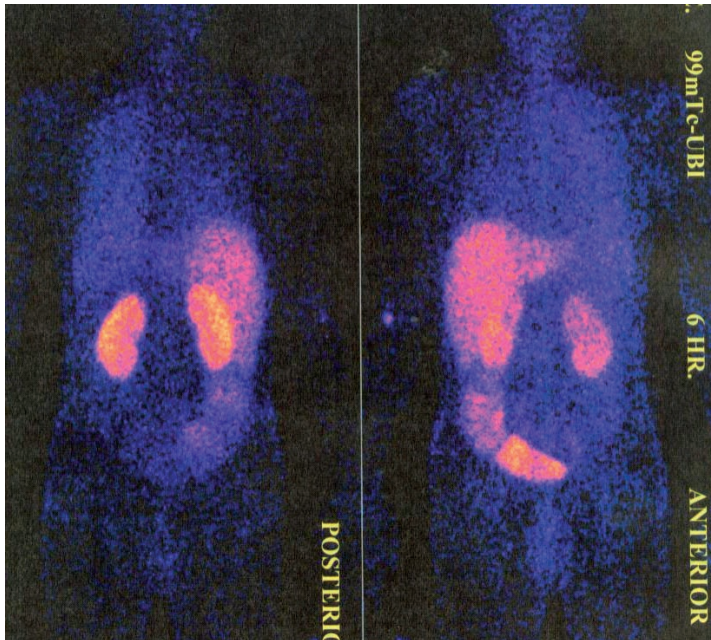


FIG. 4. Patient with colon infection process. Anterior and posterior views at 6 h after ^{99m}Tc -UBI 29-41 administration.

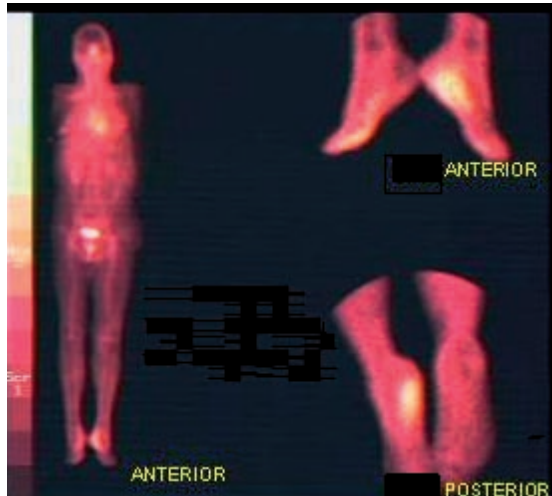


FIG. 5. Patient with osteomyelitis on left foot. Anterior and posterior views at 15 min after ^{99m}Tc -UBI 29-41 administration.

4. CONCLUSIONS

Technetium-99m-EDDA/HYNIC-[Lys³]BBN, ^{99m}Tc -UBI 29-41 and ^{99m}Tc -EDDA/HYNIC-TOC obtained from lyophilized kits, showed radiochemical purities of over 93%, high in vitro and in vivo stabilities and preservation of the molecular recognition after a simple kit reconstitution without further purification. Technetium-99m-EDDA/HYNIC-[Lys³]BN has a demonstrated capability to detect GRP receptor positive tumours in mice. Technetium-99m-UBI 29-41 prepared by a direct method has adequate biokinetic properties and the capability to detect infection foci in humans. Technetium-99m-EDDA/HYNIC-TOC has been useful in patients with lung cancer.

ACKNOWLEDGEMENTS

This work was supported by the CONACyT-Mexico and the IAEA.

REFERENCES

- [1] BAIDOO, K.E., et al., Design, synthesis, and initial evaluation of high-affinity technetium bombesin analogues, *Bioconjug. Chem.* **9** (1998) 218–225.
- [2] LA BELLA, R., et al., In vitro and in vivo evaluation of a ^{99m}Tc (I)-labeled bombesin analogue for imaging of gastrin releasing peptide receptor-positive tumors, *Nucl. Med. Biol.* **29** (2002) 553–560.
- [3] VARVARIGOU, A.D., et al., Synthesis, chemical, radiochemical and radiobiological evaluation of a new ^{99m}Tc -labelled bombesin-like peptide, *Cancer Biother. Radiopharm.* **17** (2002) 317–326.
- [4] SMITH, J.C., et al., Radiochemical investigations of ^{177}Lu -DOTA-8-Aoc-BBN[7-14] NH_2 : an in vitro/in vivo assessment of the targeting ability of this new radiopharmaceutical for PC-3 human prostate cancer cells, *Nucl. Med. Biol.* **29** (2003) 101–109.
- [5] CHEN, X., et al., microPET and autoradiographic imaging of GRP receptor expression with ^{64}Cu -DOTA-[Lys³]Bombesin in human prostate adenocarcinoma xenografts, *J. Nucl. Med.* **45** (2004) 1390–1397.
- [6] SCOPINARO, F., et al., Technetium labelled bombesin-like peptide: preliminary report on breast cancer uptake in patients, *Cancer Biother. Radiopharm.* **17** (2002) 327–335.
- [7] SCOPINARO, F., ^{99m}Tc -bombesin detects prostate cancer and invasion of pelvic lymph nodes, *Eur. J. Nucl. Med. Mol. Imaging* **30** (2003) 1378–1382.
- [8] LIN, K.S., et al., A new high affinity technetium-99m-bombesin analogue with low abdominal accumulation, *Bioconjug. Chem.* **16** (2005) 43–50.
- [9] DECRISTOFORO, C., et al., ^{99m}Tc -HYNIC-[Tyr³]-octreotide for imaging somatostatin-receptor-positive tumors: preclinical evaluation and comparison with ^{111}In -octreotide, *J. Nucl. Med.* **41** (2000) 1114–1119.
- [10] DECRISTOFORO, C., et al., ^{99m}Tc -EDDA/HYNIC-TOC: A new ^{99m}Tc -labelled radiopharmaceutical for imaging somatostatin receptor-positive tumours: first clinical results and intra-patient comparison with ^{111}In -labelled octreotide derivatives, *Eur. J. Nucl. Med.* **27** (2000) 1318–1325.
- [11] GABRIEL, M., et al., An intrapatient comparison of ^{99m}Tc -EDDA/HYNIC-TOC with ^{111}In -DTPA-octreotide for diagnosis of somatostatin receptor-expressing tumors, *J. Nucl. Med.* **44** (2003) 708–716.
- [12] PLACHCINSKA, A., et al., Clinical usefulness of ^{99m}Tc -EDDA/HYNIC-TOC scintigraphy in oncological diagnostics: a preliminary communication, *Eur. J. Nucl. Med. Mol. Imaging* **30** (2003) 1402–1406.
- [13] PLACHCINSKA, A., et al., ^{99m}Tc -EDDA/HYNIC-TOC scintigraphy in the differential diagnosis of solitary pulmonary nodules, *Eur. J. Nucl. Med. Mol. Imaging* **31** (2004) 1005–1010.
- [14] VON GUGGENBERG, E., et al., Radiopharmaceutical development of a freeze-dried kit formulation for the preparation of [^{99m}Tc -EDDA-HYNIC-D-Phe¹, Tyr³]-octreotide, a somatostatin analog for tumor diagnosis, *J. Pharm. Sci.* **93** (2004) 2497–2506.

SESSION 2

- [15] GONZÁLEZ-VÁZQUEZ, A., et al., Biokinetics and dosimetry in patients of ^{99m}Tc -EDDA/HYNIC-Tyr³-Octreotide obtained from lyophilized formulations, *Appl. Rad. Isot.* (2005) (in press).
- [16] WELLING, M., et al., Technetium-99m labeled antimicrobial peptides discriminate between bacterial infections and sterile inflammations, *Eur. J. Nucl. Med.* **27** (2000) 291–301.
- [17] WELLING, M., et al., Radiochemical and biological characteristics of ^{99m}Tc -UBI 29-41 for imaging of bacterial infections, *Nucl. Med. Biol.* **29** (2002) 413–422.
- [18] FERRO-FLORES, G., et al., Preparation and evaluation of ^{99m}Tc -EDDA/HYNIC-[Lys³]Bombesin for imaging of GRP receptor-positive tumours, *Nucl. Med. Commun.* (2005) (in press).
- [19] MELÉNDEZ-ALAFORT, L., et al., Lys and Arg in UBI: A specific site for a stable ^{99m}Tc complex?, *Nucl. Med. Biol.* **30** (2003) 605–615.
- [20] FERRO-FLORES, G., et al., Molecular recognition and stability of ^{99m}Tc -UBI 29-41 based on experimental and semiempirical results, *Appl. Rad. Isot.* **61** (2004) 1261–1268.
- [21] FERRO-FLORES, G., et al., Kit for Instant Tc-99m Labeling of the Antimicrobial Peptide Ubiquicidin 29-41, *J. Radioanal. Nucl. Chem.* **266** (2005) 307–311.
- [22] FERRO-FLORES, G., et al., In vitro and in vivo assessment of ^{99m}Tc -UBI specificity for bacteria, *Nucl. Med. Biol.* **30** (2003) 597–603.
- [23] MELÉNDEZ-ALAFORT, L., et al., Biokinetics of ^{99m}Tc -UBI 29-41 in humans, *Nucl. Med. Biol.* **31** (2004) 373–379.

DETECTION OF DEEP VENOUS THROMBOSIS IN AN EXPERIMENTAL ANIMAL MODEL USING RADIOACTIVE LABELLED TIROFIBAN-GPIIb/IIIa INHIBITOR

E. JANEVIK-IVANOVSKA*, I. DJORGOSKI**, A. ANDONOVSKI*,
V. MILENKOV***, S. MICEVA-RISTEVSKA*, G. JANOKI[†]

*Institute of Pathophysiology and Nuclear Medicine, Faculty of Medicine
Email: janevik@yahoo.com

**Institute of Biology, Faculty of Natural and Mathematics Science

***Institute of Blood Transfusion

Skopje, The Former Yugoslav Republic of Macedonia

[†]NFJC Research Institute of Radiobiology and Radiohygiene,
Budapest, Hungary

Abstract

Detection of acute deep venous thrombosis (DVT), including biochemical information on thrombus formation, is one of the most important issues in clinical nuclear medicine. Thus, development of radiolabelled small peptide or peptidomimetic ligands that can bind platelets and their specific expressed receptor have been suggested as a new approach to detect clot location and, more essentially, determine the age and morphology of the evolving thrombus. This new approach has focused on the use of a series of radiolabelled platelet GPIIb/IIIa receptor antagonists. Tirofiban N-(butylsulfonyl)-4-O-(4-(4-piperidyl)-L-tyrosine is a non-peptide tyrosine derivate. The aim of the study was to introduce radioactive labelled tirofiban as a specific imaging agent for acute DVT. Iodine-125-tirofiban labelling was performed using the Iodo-gen method with a >95% yield. Technetium-99-tirofiban labelling in the presence of a stannous reducing agent was obtained with a >95% yield. Both labelled preparations have a fast blood clearance in the normal rat model (without induced thrombosis). More than 80% of the injected dose was eliminated from the circulation in the first hour after injection. Biodistribution and visualization of the labelled molecule was carried out using an experimental model of thrombosis in the male Wistar rat. Planar images were obtained 30 min and 60 min after application of $2-6 \times 10^6$ counts/min ^{99m}Tc-tirofiban, as well as 2 h and 24 h after application of $1.6-2.1 \times 10^6$ counts/min in the rat's tail vein. Sensitivity

and specificity were determined using the ratio 'left leg positive for DVT' and 'right leg negative for DVT'. The obtained ratio was 1.76 after 1 h, 1.99 after 3 h and 2.06 after 24 h in the case of iodine labelled tirofiban, and 1.54 after 30 min and 5.04 after 60 min with ^{99m}Tc -tirofiban. These values were considered as positive in the detection of acute DVT. The results from experimental studies show that radiolabelled tirofiban could be helpful in the further clinical investigation of patients with acute DVT.

1. INTRODUCTION

Venous thromboembolism is a complex vascular disease with a multifactorial pathogenesis that results in significant morbidity and mortality. The first and more common manifestation is deep venous thrombosis (DVT), which usually arises in the deep veins of the calf and spreads upwards. Pulmonary embolism, the second and more serious manifestation, occurs as a complication of DVT proximal to the deep calf veins [1]. DVT is the product of a hypercoagulable state, coupled with a period of stasis, occurring in a low shear environment, resulting in the formation of a fibrin rich thrombus that also contains some platelets and erythrocytes. All available imaging procedures (duplex ultrasound, magnetic resonance and contrast venography as a standard test for validating new diagnostic procedures) do not reflect the metabolic activity of the clot and therefore they may overestimate the presence of active clots [2]. Only nuclear medical examinations can provide an image that includes information on thrombus formation. Numerous tracers have been reported as being useful for detecting DVT [3]. These studies targeted several components of the thrombus, i.e. fibrinogen, white blood cells and platelets. However, direct labelling of these components was not satisfactory for the imaging of acute DVT because the critical need was to detect a molecular marker of acute state that is not present in old, organized thrombus. Recent advances in biotechnology permit the use of highly specific synthetic peptide or small non-peptide molecules, which are involved in the acute stages of DVT formation and can be labelled efficiently with radioisotopes (^{125}I , ^{99m}Tc).

This new approach has focused on the use of a series of radiolabelled platelet GPIIb/IIIa receptor antagonists [4, 5]. The GPIIb/IIIa receptors are expressed on the membrane surface of activated platelets and play an integral role in platelet aggregation and thrombus formation [6]. Initial actions in thrombus formation frequently involve the activation of platelets by thrombogenic conditions and their subsequent aggregation. Platelet aggregation is mediated by fibrinogen, which binds via the Arg-Gly-Asp (RGD) sequence to the GPIIb/IIIa receptor expressed on activated platelets. Since the GPIIb/IIIa receptors are expressed only on the membrane surface of activated platelets,

SESSION 2

with 50 000–90 000 GPIIb/IIIa binding sites per platelet [7], the GPIIb/IIIa receptor makes an excellent target for the development of an imaging agent than bound with high specificity to activated rather than to unactivated platelets. They would be differentially incorporated in the thrombus (activated platelets) and the circulating platelets (resting or relatively less activated) [8, 9].

These molecules represent glycoprotein (GPIIb/IIIa) receptor antagonists and they act as true biochemical markers of active thrombosis [10, 11].

Commercially available ^{99m}Tc -apcitide (AcuTect), previously known as ^{99m}Tc -P280, is a small synthetic peptide containing RGD sequence, which binds to the GPIIb/IIIa receptor. Regarding published data, ^{99m}Tc -apcitide is the first imaging agent used in clinical studies and is highly accurate in the non-invasive detection of acute DVT, especially thrombosis involving the deep veins of the calf [12, 13].

The authors' idea to use the small non-peptide derivate or peptidomimetic ligands with high specificity for the GPIIb/IIIa receptor and incorporate a convenient radionuclide for imaging purposes was initiated from the already existing data presented using labelled peptides and GPIIb/IIIa receptor antagonists in the diagnosis of acute DVT. One promising GPIIb/IIIa receptor antagonist is tirofiban (AggrastatTM, Merck, Inc.), a novel non-peptide tyrosine derivate that inhibits fibrinogen binding [14] (Fig. 1).

Tirofiban is a small molecule, also known as L-700,462 and MK-0383, which inhibits platelet aggregation and subsequent thrombus formation. This GPIIb/IIIa receptor blocker is primarily used in the prevention of the progression of unstable angina to myocardial infarction [15–17].

Gamma emitters such as ^{99m}Tc and ^{125}I are the radionuclides that can be used for visualization during in vivo imaging with a gamma camera and quantified by direct counting of tissue samples in a well-type gamma counter.

During this process, experimental animal models of DVT are established and modified afterwards, according to the needs of a particular line of research [18, 19].

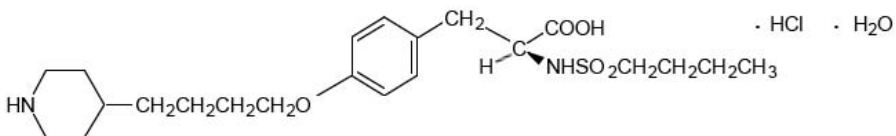


FIG. 1. Tirofiban (tirofiban hydrochloride monohydrate) *N*-(butylsulfonyl)-*O*-[4-(4-piperidinyl)butyl]-*L*-tyrosine monohydrochloride monohydrate.

1.1. Objectives

The aim of the study was to evaluate tirofiban as a specific imaging agent to the GPIIb/IIIa receptor in the experimental animal model with activated platelets during the process of the platelet aggregation and thrombus formation, and to evaluate its radiochemical and biological behaviour. The animal model based on thrombosis induced mechanisms has been designed to study this potential imaging agent [19].

2. MATERIALS AND METHODS

2.1. Materials

2.1.1. Tirofiban

The structure of tirofiban (tirofiban hydrochloride monohydrate) N-(butylsulfonyl)-O-[4-(4-piperidinyl)butyl]-L-tyrosine monohydrochloride monohydrate is shown in Fig. 1. Tirofiban hydrochloride monohydrate is a white to off-white, non-hygroscopic, free flowing powder, with a molecular weight of 495.08. It is very slightly soluble in water.

2.1.2. Isotopes

2.1.2.1. Iodine-125

Iodine-125 in the form of NaI, specific activity >600 GBq/mg and radioactive concentration 3700 MBq/cm³, was obtained from IZOTOP-Institute of Isotopes Co. Ltd.

2.1.2.2. Technetium-99m

Technetium-99m-pertechnetate was obtained from a commercial ⁹⁹Mo/^{99m}Tc generator (10 GBq) (Schering /CIS-biointernational).

2.2. Radiolabelling

2.2.1. Iodination of tirofiban with ¹²⁵I

Iodine-125-tirofiban labelling was performed using an Iodo-gen [20] coated tube containing 10 µg of Iodo-gen, tirofiban (0.2mmol) dissolved in

SESSION 2

buffer (ethanol 96%/PBS 0.01M, pH7.3, 1:3 vol./vol.) and 37 MBq ^{125}I (specific activity 28 000 MBq/cm³). The reaction mixture was mixed and incubated at room temperature for 10 min.

Radiochemical purity was analysed by TLC strip in 1N HCl. The percentage labelled yield was recorded by gamma scanner (Veenstra Instrumenten B.V. VCS-103 V1.06).

2.2.2. Labelling of tirofiban with $^{99\text{m}}\text{Tc}$

Tirofiban was labelled using the method of direct labelling under nitrogen. The kit freeze dried formulation contains a mixture of tirofiban (20nmol) dissolved in buffer (ethanol 96%/PBS 0.01M, pH7.3, 1:3 vol./vol.) and stannous chloride (10nmol) as a reducing agent. Sodium ($^{99\text{m}}\text{Tc}$) pertechnetate (specific activity 740–4500 MBq/mL) containing 100 MBq/mL was added and the reaction mixture incubated for 15 min at room temperature.

The quality control was done by paper chromatography and instant thin layer chromatography (ITLC) using two solvents – 95% acetone and saline. The percentage labelled yield was recorded by gamma scanner (Veenstra Instrumenten B.V. VCS-103 V1.06).

2.3. Blood clearance

Iodine-125-tirofiban and $^{99\text{m}}\text{Tc}$ -tirofiban were both injected intravenously into rats. Blood samples were drawn from the previously prepared carotid vein using a sterile syringe at 5, 15, 30, 45 min and 1, 2, 4, 6 and 24 h after injection. All samples were of the same volume and their radioactivity measured in a gamma counter and compared with a standard.

2.4. In vitro platelet binding

The binding study was performed with rat and human platelets isolated and treated according protocol for platelet labelling (TROMBO-SCINT). Platelets were incubated for 30 min with tirofiban radiolabelled with $^{99\text{m}}\text{Tc}$ and ^{125}I . The percentage of binding was measured after one and two washing steps.

2.5. Animal studies

Male Wistar rats weighing 220–250 g were used throughout the study, anaesthetized by intraperitoneal injection of water solution of Nesdonal (concentration 20 mg/kg body weight).

2.5.1. Experimental animal model [12, 21]

Venous thrombosis was induced by ligation of the femoral vein in rats whose blood was made hypercoagulable by intravenous administration of tissue thrombin [19, 22]. For the thrombosis model, the body temperature of the rats was maintained at 37°C. In brief, a short incision was made in the skin and subcutaneous tissue in the left groin region and the femoral neurovascular sheath was gently exposed [23]. An approximately 10 mm long portion of the left femoral vein, distal to the inguinal ligament was isolated by rubbing it against the blade of a pair of forceps and this segment was collapsed. The collapsed segment of femoral vein between the clamps was traumatized by striking and the twenty units of thrombin (in 0.2 mL saline) were injected into the segment with a needle. A semiconstricting ligature was placed downstream to prevent the clot from slipping away.

2.6. Imaging

The thrombi developed in the rats were visualized using tirofiban radiolabelled with ^{99m}Tc and ^{125}I . Planar images were obtained 30 min and 60 min after application of $2\text{--}6 \times 10^6$ counts/min in 50–100 μL ^{99m}Tc -tirofiban or 1 h and 24 h after application of $1.6\text{--}2.1 \times 10^6$ counts/min in 50 μL of ^{125}I -tirofiban in the rat's tail vein. Syringes should be measured before and after injection in order to determine accurately the radioactivity of material injected. The sensitivity and specificity of the radiopharmaceuticals were determined using the ratio 'left leg positive for DVT' and 'right leg negative for DVT' using the ROI technique.

2.7. Biodistribution

The biodistribution studies were carried out using the same experimental model of thrombosis in male Wistar rat and by injection of the radiolabelled products. After the desired time period had elapsed, the animals were sacrificed and the samples of organ of interest (heart, lung, liver, spleen, kidney, thrombotic and normal tissue) were collected and placed in pre-weighed counting tubes. These were then counted in a gamma counter together with a standard prepared from a known dilution of the injected material (preferably prepared at the time of injection). The total activity injected into each rat was determined and the activity remaining in the tail subtracted. The uptake of the labelled products in each tissue was calculated and the specific uptake of the products quantified using ratio 'left leg positive for DVT' and 'right leg negative for DVT'.

3. RESULTS

This study used a rat model of DVT to evaluate radiolabelled tirofiban, platelets GPIIb/IIIa antagonist for its potential use in the detection of rapidly growing venous thrombi. Two different methods of labelling were selected using ^{125}I and $^{99\text{m}}\text{Tc}$ as radioisotopes.

3.1. Labelling of tirofiban with ^{125}I

The specific activity of the radiolabelled product was $1.8\text{--}2.1 \times 10^{14}$ Bq/mol. The percentage of the obtained complex after labelling was more than 90% per mol/L HCl, and the free iodine (^{125}I) less than 5% (Fig. 2). The labelled product was stable without changing the percentage of labelling over one week at room temperature (Fig. 3).

3.2. Labelling of tirofiban with $^{99\text{m}}\text{Tc}$

The specific activity of the radiolabelled product was 9.2×10^{18} to 1.0×10^{19} counts/min/mol.

The percentage of obtained complex after labelling was more than 95% (in acetone), more than 85% (in saline), with the free pertechnetate ($^{99\text{m}}\text{TcO}_4^-$) less than 5% (Fig. 4).

The labelled product was stable without changing the percentage of labelling after 2 h at room temperature.

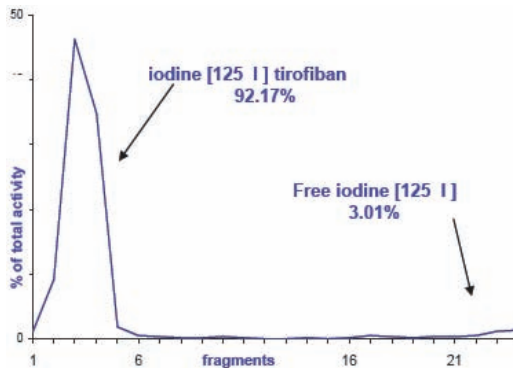


FIG. 2. TLC radiochromatograms of ^{125}I -tirofiban in 1M HCl.

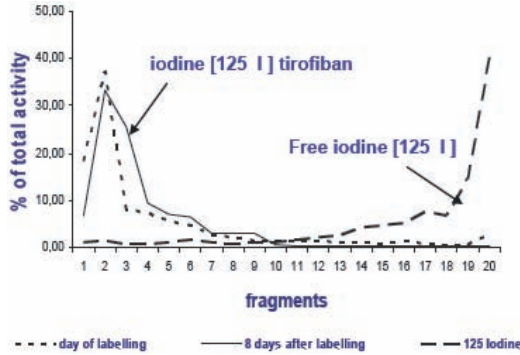


FIG. 3. Stability of radiochemical purity of ¹²⁵I-tirofiban.

After determination of radiochemical purity, it was concluded that both products could be tested for in vitro binding using normal platelets from humans and rats.

3.3. In vitro platelet binding

The binding study made for in vitro stability of platelets showed that ^{99m}Tc labelled tirofiban has a higher percentage of binding compared with ¹²⁵I-tirofiban (Fig. 5). The stability of binding did not change after two washing steps.

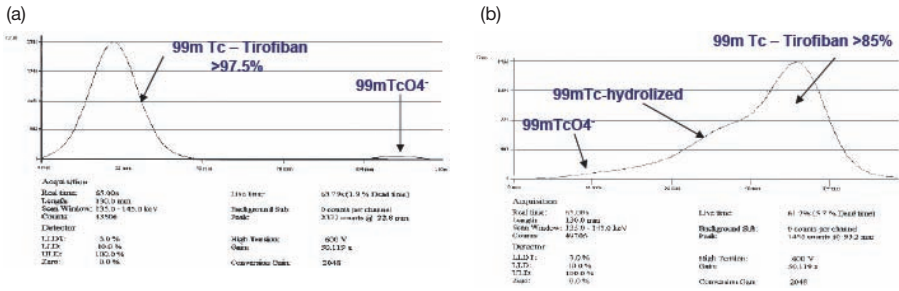


FIG. 4. ITLC radiochromatograms of ^{99m}Tc-tirofiban in (a) 95% acetone (b) saline.

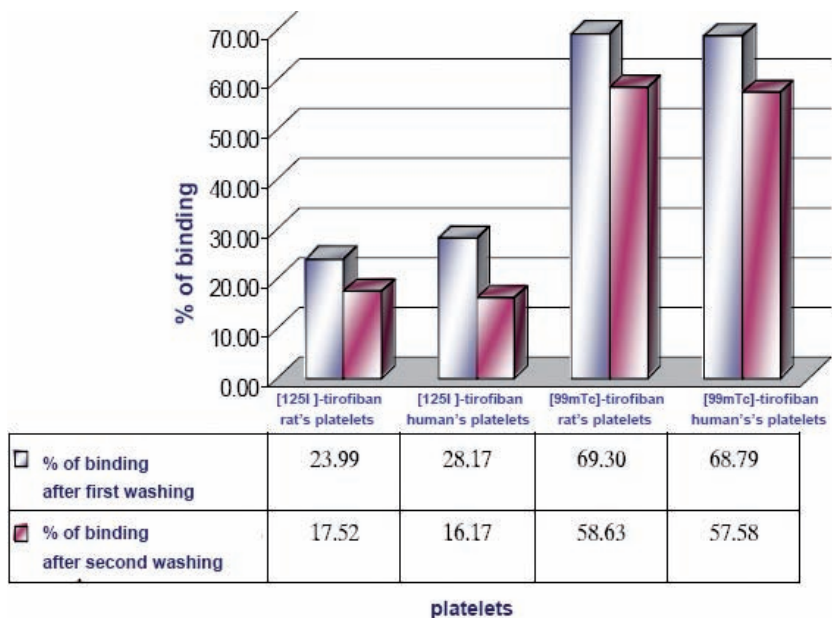


FIG. 5. In vitro binding of rat and human platelets isolated and treated with radiolabelled tirofiban.

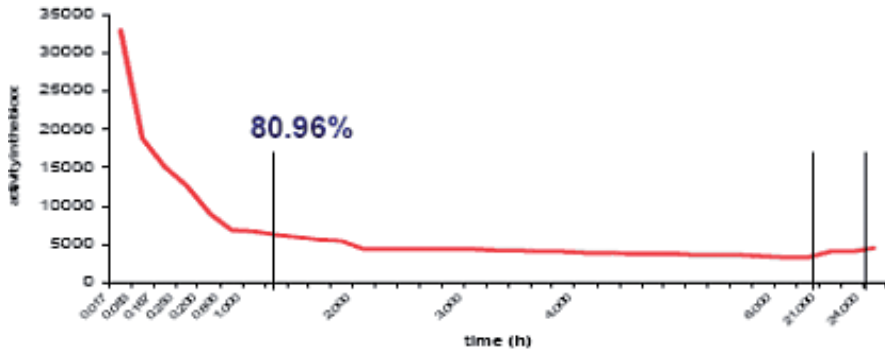
3.4. Blood clearance

The results showed that more than 80% of injected dose using two labelled preparations of tirofiban were eliminated from the circulation in the first hour after injection (Fig. 6).

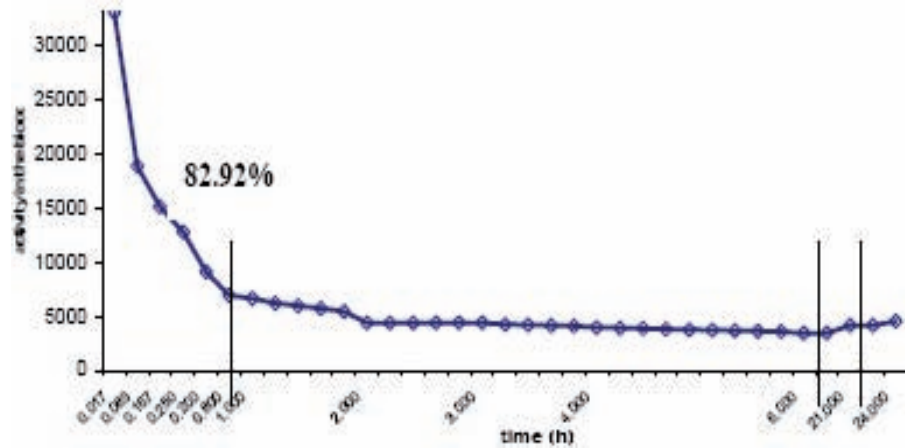
The two labelled products were compared with each other in the animal imaging and biodistribution experiments.

3.5. Imaging studies

Whole body images of distribution of ^{125}I -tirofiban in normal and experimentally induced thrombosis in rats 1 h and 24 h after administration are presented in Fig. 7. At 1 h and 24 h post-injection, experimentally induced thromboses are visualized compared with the normal rat distribution of the tracer. Biological data demonstrated that ^{125}I -tirofiban accumulated in the thyroid and the liver. This accumulation could be related to free iodine for thyroid and normal distribution of circulated platelets in the liver and the spleen.



(a)



(b)

FIG. 6. Blood clearance of radiolabelled tirofiban in normal rat (a) ^{125}I -tirofiban (b) $^{99\text{m}}\text{Tc}$ -tirofiban.

Whole body images of distribution of $^{99\text{m}}\text{Tc}$ -tirofiban in normal and experimental induced thrombosis in rats 30 and 60 min after administration are presented in Fig. 8.

At 30 min and 60 min, experimental induced thromboses are visualized compared with the normal rat distribution of the tracer. As previously shown, $^{99\text{m}}\text{Tc}$ -tirofiban was also accumulated in the liver. This accumulation could be related to the normal distribution of circulated platelets in the liver and the spleen.

3.6. Biodistribution studies

Biological distribution data for the two labelled products at different times after IV administration are presented in Fig. 9, for ^{125}I -tirofiban, and Fig. 10 for $^{99\text{m}}\text{Tc}$ -tirofiban. These biodistribution studies demonstrated some different behaviour. Results obtained from the radioactivity distribution of ^{125}I -tirofiban at 1 h and 24 h after IV administration clearly present a significantly higher liver and spleen uptake when compared with the $^{99\text{m}}\text{Tc}$ -tirofiban. This is in accordance with the presence of destroyed platelets carrying radioactive tirofiban. However, the radiolabelled products were rapidly cleared from the circulation as represented by a low percentage of radioactivity in the heart and lung.

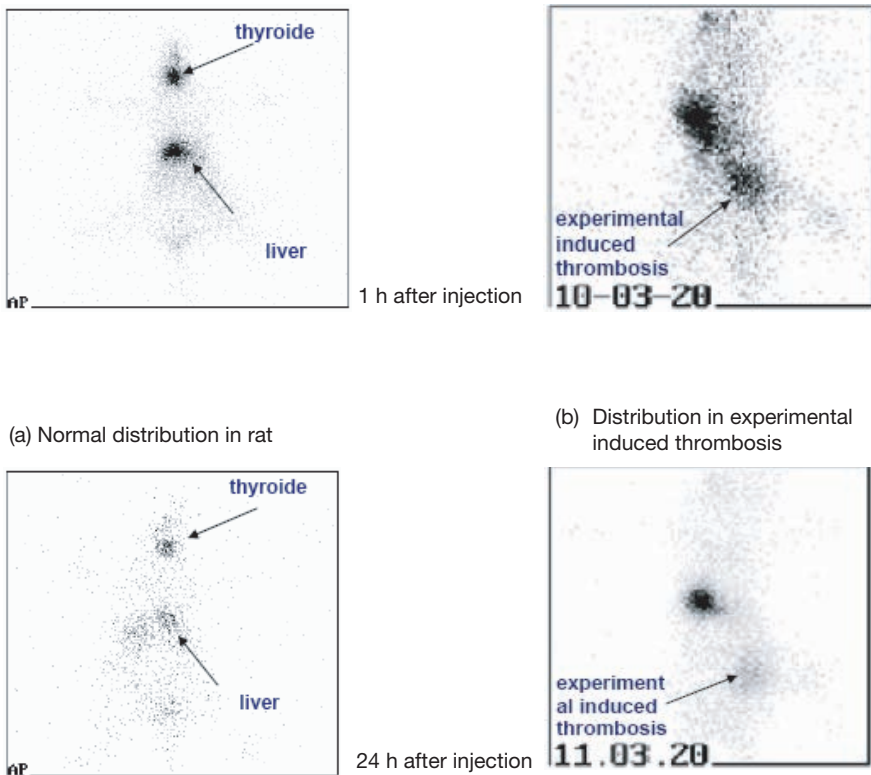


FIG. 7. Gamma camera images after IV injection of ^{125}I -tirofiban in rats.

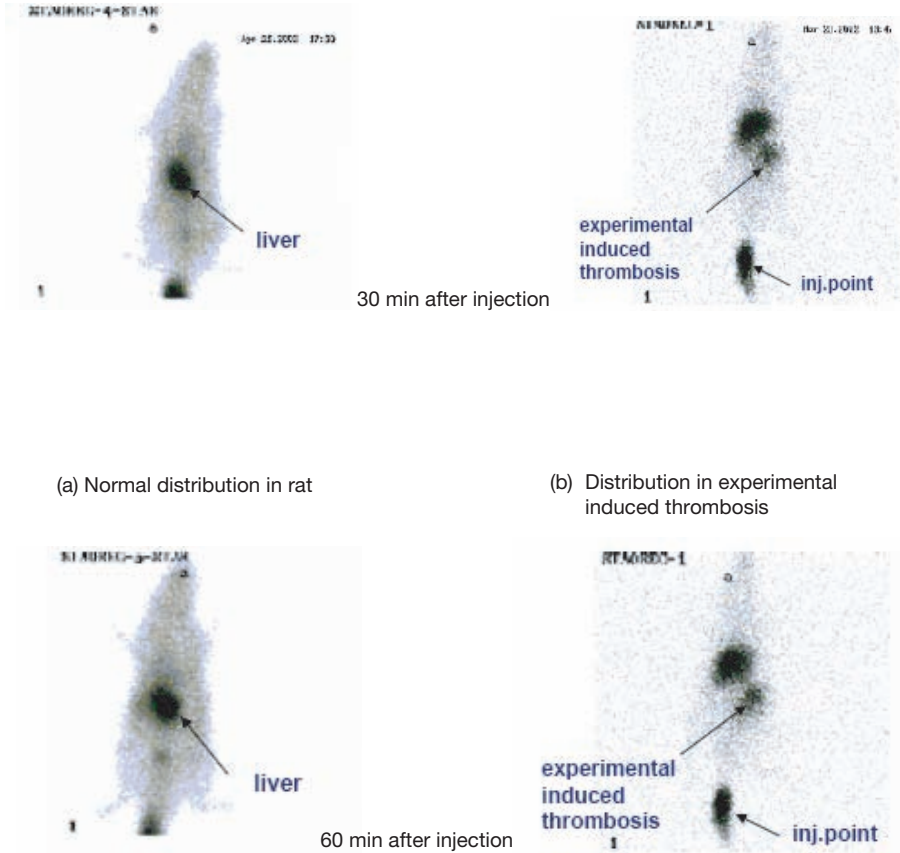


FIG. 8. Gamma camera images after IV injection of ^{99m}Tc -tirofiban in rats.

The obtained ratio 'left leg positive for DVT' and 'right leg negative for DVT' was 1.76 after 1 h, 1.99 after 3 h and 2.06 after 24 h in the case of iodine labelled tirofiban (Fig. 22) and 1.54 after 30 min and 5.04 after 60 min when the tirofiban was labelled with technetium (Fig. 12). These values were considered as positive in the detection of acute DVT.

4. DISCUSSION

Blood coagulation has long been considered an important factor in the pathogenesis of venous thrombosis. The relative contribution of stasis, altered

SESSION 2

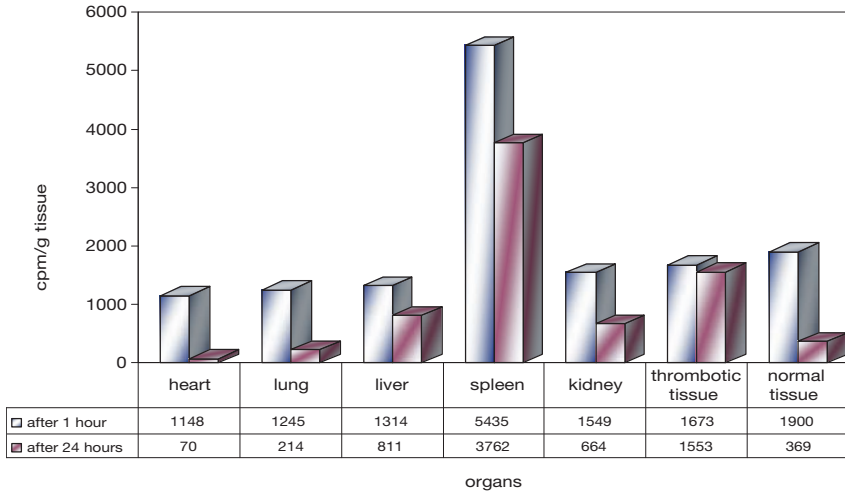


FIG. 9. Biodistribution studies in experimentally induced thrombosis in rats after injection of ¹²⁵I-tirofiban. Biodistribution profiles after rat sacrifice.

coagulability of the blood, vessel wall damage and circulation of leucocytes or platelets to the pathogenesis of venous thrombosis remains in dispute. On the other hand, it is known that a hypercoagulable state contributes significantly to the thrombotic process. Animal models based on these activation mechanisms

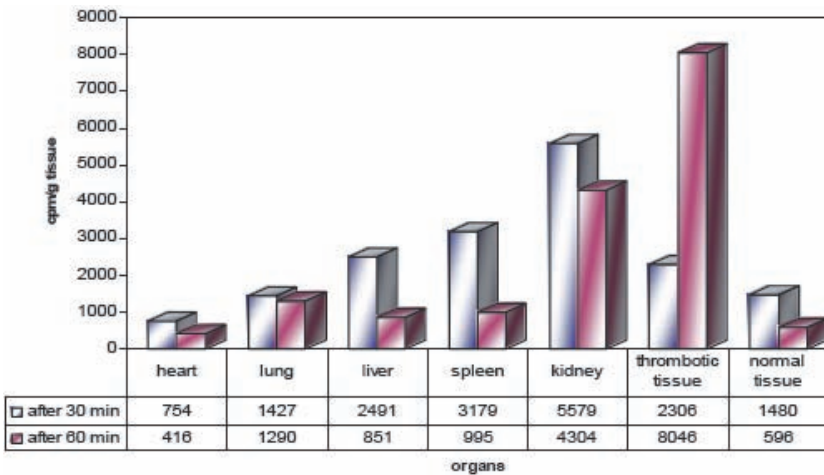


FIG. 10. Biodistribution studies in experimentally induced thrombosis in rats after injection of ^{99m}Tc-tirofiban. Biodistribution profiles after rat sacrifice.

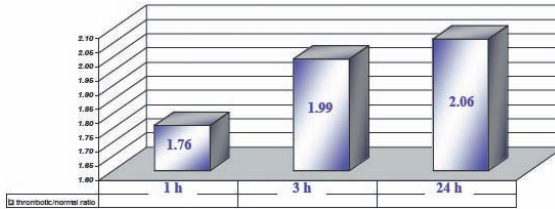


FIG. 11. Left thrombotic/right normal leg ratio using ROI technique from gamma camera images after injection of ^{125}I -tirofiban.

have been designed as a means of studying potential imaging agents for diagnosis of acute DVT. The venous stasis thrombosis model consists of inducing blood stasis in the femoral vein of rats after prior injection of a procoagulant.

A radionuclide imaging agent that binds to platelets being incorporated into an active thrombus but one which, if not bound, clears rapidly from the blood would have great potential for acute DVT detection.

Platelets expressed from the cell surface of GPIIb/IIIa receptors undergo the conformational change that makes them available for binding fibrinogen. Cross-linkage of activated platelets by the bivalent fibrinogen molecule to form a hemostatic plug is the primary episode of thrombosis. An imaging agent, ideally labelled with $^{99\text{m}}\text{Tc}$ and capable of binding actively and specifically to the GPIIb/IIIa receptor on activated platelets, would give images of active or acute venous thrombosis.

The aim of the study was to evaluate tirofiban as a specific imaging agent to GPIIb/IIIa receptors in the case of experimentally induced acute DVT in the rat experimental model. Radionuclide imaging offers considerable potential as a successful diagnostic agent which would address a few important criteria, i.e. rapid, non-invasive, cost effective and accurate.

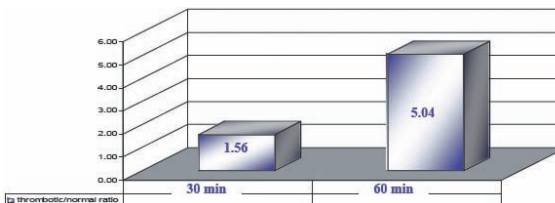


FIG. 12. Left thrombotic/right normal leg ratio using ROI technique from gamma camera images after injection of $^{99\text{m}}\text{Tc}$ -tirofiban.

SESSION 2

The published data [7, 13, 19] indicate that radiolabelled tirofiban binds preferentially to GPIIb/IIIa receptors on activated platelets and can differentiate acute DVT from chronic venous thrombosis. Radiolabelled tirofiban is a functional rather than anatomical imaging modality.

The use of radiotracers allows an understanding of the bioavailability process, biodistribution and kinetics of any molecule labelled with an isotope, a procedure which does not alter the molecule's biological properties. In the current work, technetium (to evaluate tirofiban as a specific imaging agent to GPIIb/IIIa receptor in the case of experimental induced acute DVT in the rat experimental model) and iodine (^{125}I) labelled tirofiban were chosen as radiotracers for biodistribution and imaging studies in the experimental thrombosis induced in rats. Technetium labelling was chosen for its favourable radiation and physical characteristics, ready availability, possibility of labelling and low cost.

Iodine (^{125}I) has been indicated for innumerable applications owing to its easy, simple and safe radioiodination system, labelled product stability and ease of detection.

Commercially available technetium–apcicide (AcuTect), previously known as $^{99\text{m}}\text{Tc}$ -P280, which binds to the GPIIb/IIIa receptor, is the first imaging agent used in the clinical studies to detect acute DVT [24, 25]. In this study, although the $^{99\text{m}}\text{Tc}$ –apcicide images obtained at 2 h after tracer injection show the greatest overall accuracy in comparison with earlier images, combined analysis of image sets from at least two time points (30 min and 60 min) provides greater accuracy in the detection of acute DVT in the patients. These results correlate with data obtained from the animal model. Technetium-99m-tirofiban is accurate in the detection of acute DVT, especially 60 min after application. The results obtained from the animal design experimental studies showed that the ratios 'left leg positive for DVT' and 'right leg negative for DVT' for the radiolabelled preparation of tirofiban are well within the range of that expected for a successful imaging agent.

5. CONCLUSION

Animal models provide convenient screening tools for radiolabelled products before a new radiopharmaceutical is further developed in clinical trials.

The tirofiban labelled with two different isotopes (^{125}I and $^{99\text{m}}\text{Tc}$) was found to have good thrombus uptake in in vivo experiments.

Obtained data indicate that radiolabelled tirofiban binds preferentially to GPIIb/IIIa receptors on activated platelets and can differentiate acute DVT from chronic venous thrombosis.

These results can be helpful in the further clinical investigation of patients with acute DVT.

REFERENCES

- [1] HYERS, T.M., Venous thromboembolism, *Am. J. Respir. Crit. Care Med.* **159** (1999) 1–14.
- [2] BLUM, J.E., HANDMAKER, H., Role of small-peptide radiopharmaceuticals in the evaluation of deep venous thrombosis, *RadioGraphics* **20** (2000) 2287–2293.
- [3] HIRSH, J., LEE, A.Y.Y., How we diagnose and treat deep vein thrombosis, *Blood* **99** (2002) 3102–3110.
- [4] KLEIMAN, N.S., Pharmacokinetics and pharmacodynamics of glycoprotein IIb-IIIa inhibitors, *Am. Heart J.* **138** (1999) S263–S275.
- [5] PEARSON, D.A., et al., Thrombus imaging using technetium-99m-labeled high-potency GPIIb/IIIa receptor antagonists: Chemistry and initial biological studies, *J. Med. Chem.* **39** (1996) 1372–1382.
- [6] COLLER, B.S., Cell adhesion in vascular biology: Platelet GPIIb/IIIa antagonists: The first anti-integrin receptor therapeutics, *J. Clin. Invest.* **99** (1997) 1467–1471.
- [7] THAKUR, M.L., et al., Imaging vascular thrombosis with 99mTc-labeled fibrin alpha-chain peptide, *J. Nucl. Med.* **41** (2000) 161–168.
- [8] VERSTRAETE, M., Synthetic inhibitors of platelet glycoprotein IIb/IIIa in clinical development, *Circulation* **102** (2000) e76–e80.
- [9] WEISS, D.J., et al., Platelet kinetics in dogs treated with a glycoprotein IIb/IIIa peptide antagonist, *Toxicol. Pathol.* **28** (2000) 310–316.
- [10] EDWARDS, D.S., et al., New and versatile ternary ligand system for technetium radiopharmaceuticals: Water soluble phosphines and tricine as coligands in labeling a hydrasinicotinamide-modified cyclic glycoprotein IIb/IIIa receptor antagonist with 99mTc, *Bioconjug. Chem.* **8** (1997) 146–154.
- [11] BARRETT, J.A., et al., Biological evaluation of 99mTc-labeled cyclic glycoprotein IIb/IIIa receptor antagonists in the canine arteriovenous shunt and deep vein thrombosis model: Effects of chelators on biological properties of [99mTc] chelator-peptide conjugates, *Bioconjug. Chem.* **7** (1996) 203–208.
- [12] LISTER-JAMES, J., MAUER, A., Thrombus imaging with a technetium 99m labeled, activated platelet receptor binding peptide, *J. Nucl. Med.* **213** (1996) 207.
- [13] LIU, S., et al., Labeling cyclic glycoprotein IIb/IIIa receptor antagonists with 99mTc by the performed chelate approach: Effects of chelators on properties of [99mTc] chelator-peptide conjugates, *Bioconjug. Chem.* **7** (1996) 196–202.

SESSION 2

- [14] AGGRASTAT: (Tirofiban). Approved: 06/04/01 EMMCO West, Inc. Board of Directors Approval 22/08/01 DOH Approval.
- [15] MERCK & CO. INC., AGGRASTAT® (TIROFIBAN HYDROCHLORIDE INJECTION PREMIXED), COPYRIGHT © MERCK&CO., Inc., 1998.
- [16] SMITHERMAN, T., Tirofiban Monograph, UPMC Pharmacy and Therapeutics Committee Formulary Review (1998).
- [17] TIROFIBAN HYDROCHLORIDE, INJECTION, AGGRASTAT®: SUMMARY BASIS OF APPROVAL EQUIVALENT. Document received from FDA with redactions. Applicant: Merck & Co., INC. Food and Drug Administration NDA Number: 20-912. Department of Health & Human Services 20-913 (Premixed) Public Health Service NDA - U.S.A. Approval Date: 5/14/98.
- [18] JESKE, W., CALLAS, D.D., FAREED, J., "A survey of animal models to develop new and novel antithrombotic agents", *New Therapeutic Agents in Thrombosis and Thrombolysis* (SASAHARA, A.A., LOSCALZO, J.L., Eds) (1997) 9–28.
- [19] HERBERT, J.M., BERNAT, A., MAFFRAND, J.P., Importance of platelets in experimental venous thrombosis in the rat, *Blood* **80** 9 (1992) 2281–2286.
- [20] PIERCE CHEMICAL COMPANY, Instructions: 28600X. IODO-GEN® Iodination reagent, (1993).
- [21] OLFERT, E.D., CROSS, B.M., McWILLIAM, A.A. (Eds), *Guide to the care and use of experimental animals*, Canadian Council on Animal Care Vol. 1, 2nd edn (1993).
- [22] LAMBRECHT, R.M., *Biological Models in Radiopharmaceutical Development*, Kluwer Academic (1996).
- [23] STASSEN, J.M., "Animal model to assess the safety and efficacy of thrombolytic agents", *New Therapeutic Agents in Thrombosis and Thrombolysis* (SASAHARA, A.A., LOSCALZO, J.L., Eds), Streiff MB, *Vena* (1997) 451–474.
- [24] TAILLEFER, R., et al., Comparison of early and delayed scintigraphy with ^{99m}Tc-apcitide and correlation with contrast-enhanced venography in detection of acute deep vein thrombosis, *J. Nucl. Med.* **40** (1999) 2029–2035.
- [25] KNIGHT, R., et al., The prevalence of positive Tc-^{99m} apcitide scintigraphy in the early postoperative period following total hip and knee arthroplasty, *Radiology* **213** (1999) 207.

PREPARATION OF IN-HOUSE DEXTRAN AND ITS CLINICAL APPLICATIONS IN SENTINEL NODE STUDIES, SIRIRAJ HOSPITAL

N. TOJINDA, S. CHIEWVIT, B. KHIEWVAN
Division of Nuclear Medicine, Siriraj Hospital
Email: sintj@mahidol.ac.th

S. DUMRONGPISUTIKUL
Division of Nuclear Medicine, Phramongkutklao Hospital

A. RATANAWICHITRASIN, S. TAWEEPRADITPOL
Department of Surgery, Siriraj Hospital

Bangkok, Thailand

Abstract

It is accepted that sentinel node biopsy (SLNB) plays an important role in the handling of breast cancer and malignant melanoma. To detect sentinel nodes (SLNs), several ^{99m}Tc compounds, including Dextran, can be used. The authors' Dextran kits, prepared in-house under the Phramongkutklao modified technique, have been used since their introduction in 2003. This aim of this study is to discuss the preparation procedure and the clinical applications in Siriraj Hospital and the preliminary results. The materials used are Dextran, stannous chloride, water for injection, HCl and NaOH. After dissolving Dextran in water for injection, $\text{Sn}_2\text{Cl}_2 \cdot 2\text{H}_2\text{O}$ in HCl is added, followed by pH adjustment to 6.5–7 using NaOH. The final volume is reached and then filtered through a 0.22 μm Millipore filter. The radiochemical purity (paper/acetone) showed purity of 98%, no bacterial growth was found and the bench life is up to 7 h. Technetium-99m-Dextran is requested by the surgeons for two main groups of patients—those with breast cancer and those with skin cancer. For breast cancer, 400 μCi (14.8 MBq) of the labelled compounds are requested to localize SLN using a gamma probe in the operation room together with detection by blue dye before SLNB. Mostly, a good agreement between these two techniques was achieved. For skin cancer, 4–5 mCi (148–185 MBq) is preferred. A good agreement with the blue dye was also obtained with better results for the ^{99m}Tc -Dextran, as deep SLNs could always be shown. In conclusion, the in-house Dextran kit is easily prepared and cost effective, giving satisfactory clinical usage.

1. INTRODUCTION

The sentinel lymph node (SLN) is the first lymph node that receives lymph from the anatomic site of the primary tumour [1]. It has been accepted that sentinel lymph node biopsy (SLNB) plays an important role in handling breast cancer and malignant melanoma [2]. The rationale for the adoption of SLNB for breast cancer is that, because of the progressive involvement of axillary nodes by tumour cells, the histology of this first lymph node would be representative of all the other axillary nodes [1]. Malignant melanoma is a malignant transformation of melanocytes and it has potential for nodal involvement (microscopic and macroscopic metastases) as well as distant metastasis. SLN was helpful in detecting micrometastasis or staging malignant melanoma without clinical metastasis. It then leads to SLNB and the management of the patients with pathological results of frozen and permanent sections showing malignancy involvement [4]. In the operation room, the dual systems (non-radioisotopic and radioisotopic) could be used to detect SLN. For radioisotopic tools, several ^{99m}Tc compounds can be used, such as $^{99m}\text{TcO}_4^-$ labelled with nanocolloids, antimony sulphur colloids, Dextran, etc. The radiopharmaceuticals used will be taken up by macrophage via phagocytosis [4] and will visualize the lymphatic channels leading from the sites of interstitial administration and be retained in the first lymph node(s). Purchasing these radiopharmaceuticals from commercial sources is costly and, therefore, unsuitable for the patients in government hospitals, including Siriraj Hospital. Since Dextran kit can be prepared in-house under the Phramongkutklo modified technique (patent pending) to give a satisfactory pilot study, it has been introduced in the Division of Nuclear Medicine and has been used in Siriraj Hospital since 2003.

2. MATERIALS AND METHODS

2.1. Manufacturing of the Dextran kit: Main materials

The components are Dextran (M.W. 70 000), stannous chloride dihydrate crystals ($\text{SnCl}_2 \cdot 2\text{H}_2\text{O}$), water for injection (WFI), HCl, and NaOH. After dissolving Dextran with WFI, a 4% stannous chloride in HCl solution is added followed by pH adjustment to 6.5–7 using NaOH. The final volume is made via WFI and the reagent is then passed through a 0.22 μm Millipore filter into N_2 purged vials, 0.5 mL in each aliquot as shown in Fig. 1. The vials can be kept in a freezer for at least six months and retain satisfactory radiochemical purity. For the safety of patients, bacteriological purity is checked for each batch of the

SESSION 2



FIG. 1. The in-house Dextran pharmaceutical prepared using the Phramongkutklao modified technique.

preparation by randomized sampling by the Department of Microbiology, Siriraj Hospital. Checking of the radiochemical purity is done using paper chromatography as a stationary phase and acetone as a mobile phase (paper/acetone system). Checking by ITLC-SG/acetone, ITLC-SG/MEK(methyl ethyl ketone), ITLC-SG/85% methanol, and paper/MEK systems was carried out several times. The bench life of the labelled Dextran was also studied throughout the day after labelling using the paper/acetone system. This was carried out six times on separate days. The particle size of the Dextran pharmaceutical (cold kit) was checked at the Faculty of Pharmacy, Mahidol University, using the Sub-Micron Particle Analyzer Coulter[®] Model N4 MD (photon correlation spectroscopy: dynamic light scattering).

2.2. Clinical applications in Siriraj Hospital

Technetium-99m-Dextran is requested by the surgeons in the Division of Head, Neck and Breast Surgery for use on patients with breast cancer, and in the Division of Plastic and Reconstruction Surgery for those with skin cancer (either malignant melanoma or squamous cell carcinoma).

For breast cancer, to detect SLN, some criteria are set for exclusion, including palpable lymph nodes, known metastases, prior extensive surgery in breast or axilla within 3 years, and a mass greater than 6 cm. In this paper data from 45 patients (mean age = 52.5 years, range 28–82 years) are included. Two categories are then used which are ‘without prior imaging’ and ‘with prior imaging’. The former is done to localize small tumours for SLNB using a gamma probe in the operation room without prior imaging at the Division of Nuclear Medicine. The latter has two steps: firstly, a pre-operation process is carried out at Nuclear Medicine to localize SLN via static imaging using a gamma camera (pre-operation lymphoscintigraphy), and secondly, the detection of the SLN using another administration of the labelled compound is carried out in the operation room using a gamma probe (Fig. 2).



FIG. 2. ^{99m}Tc -Dextran (left hand side) and a gamma probe (right hand side).

The values of the pre-operation process at Nuclear Medicine are: incremental increase in confidence that true SLN will be excised (while the surgeon can see all lymphatic drainage pathways via the images), small incision, faster procedure, and success with less radioactivity [5]. The gamma camera's wide field of view images the entire chest with the axillary and internal mammary node region visible in one field of view. In both categories, 400 μCi (14.8 MBq) of ^{99m}Tc -Dextran are used, and the detection through blue dye (1% isosulfan blue) is also performed in the operation room before SLNB (Fig. 2). The injection site is peri-areolar for the imaging study (pre-operation lymphoscintigraphy, Fig. 3) and peri-tumour for both radioisotope and dye techniques in the operation room. The injection procedure is either intradermal or subdermal.

For malignant melanoma, 4–5 mCi (148–185 MBq) of ^{99m}Tc -Dextran for injection is preferred, because the SLN is far from the cancer site. Dynamic as well as static imaging is then carried out in Nuclear Medicine and the locations of the SLNs found are marked with permanent ink as guidance, since it is difficult to locate an SLN via a gamma probe in the operation room only, owing to the distance between the SLN and the tumour (Fig. 4). If the pre-operation lymphoscintigraphy is done 1–3 days before the operation, then another



FIG. 3. Injection of ^{99m}Tc -Dextran via peri-areolar.



FIG. 4. ^{99m}Tc -Dextran, injection and (pre-operation) lymphoscintigraphy at Nuclear Medicine.

administration of the radiopharmaceutical will be given to the patient in the operation room. The SLN detection via blue dye is also carried out for purposes of comparison. Injection is subdermal around the tumour or surgical scar for the dual systems, as the lymphatic channel is located. Significantly higher counts than those of the background were 3:1 for imaging and at least 10:1 in the operation room [6].

The results are reported from the retrospective reviews of 14 patients (5 males, 9 females) with localized malignant melanoma. Their mean age was 59.79 years (range: 37–73 years), and they underwent pre-operative lymphoscintigraphy as well as surgery during the period 2003 to May 2005.

For both breast cancer and malignant melanoma cases, the gamma cameras used were Model Infinia I and II, and Varicam. The gamma probe used in the operation room was Navigator, Tyco. The statistical analyses were performed under Microsoft® Excel XP, and SPSS, version 10.

3. RESULTS AND DISCUSSION

3.1. Validation of the Dextran kit

The culture of the Dextran kit showed no growth after a 2 week incubation period for every lot tested. The radiochemical purity as checked by the paper/acetone system gave about 98–99% of the labelled compound at the origin and 1–2% of free pertechnetate at the solvent front, as shown in Fig. 5 [6, 7]. On the other hand, the ITLC-SG/acetone system showed an equivalent figure of 86–97%, ITLC-SG/MEK gave 81–96%, and paper/MEK 85–93% with the same pattern. Actually, the ITLC-SG/85% methanol has been tried a few times, resulting in 94–97% [8]. From the authors' (limited) experiences, some ITLC-SG systems seemed to give a wide range of radiochemical purity when separately tested, sometimes with high background. The reason for this is still

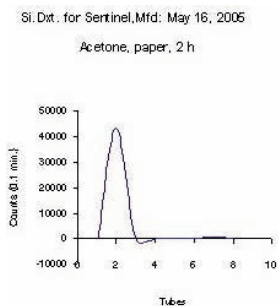


FIG. 5. Radiochemical purity of ^{99m}Tc -Dextran using the paper/acetone system.

unclear. However, these studies will be repeated again. Hydrolyzed reduced impurity was not tested, since Dextran is a starch by nature making it rare for it to be hydrolyzed or reduced, and also only minute amounts are used.

After labelling, the ^{99m}Tc -Dextran gave a radiochemical purity of about 98% (paper/acetone system) over 6–7 h, suggesting a very stable labelled compound or long bench life as shown in Fig. 6. The particle size was found to be around 100 nm, which is suitable for SLN studies, as it was recommended that a size of 100–200 nm was the best compromise between the need for effective and fast lymphatic drainage, and it was ideal for radioguided SLNB in breast cancer [6].

3.2. Clinical applications in Siriraj Hospital: Breast cancer

Using pre-operation lymphoscintigraphy by ^{99m}Tc -Dextran, SLNs could be detected and marked for the surgeons (Fig. 7). In the operating room, SLN detections followed by SLNB are shown in Figs 8 and 9. The SLN(s) would then be examined for malignancy by intra-operative frozen section.

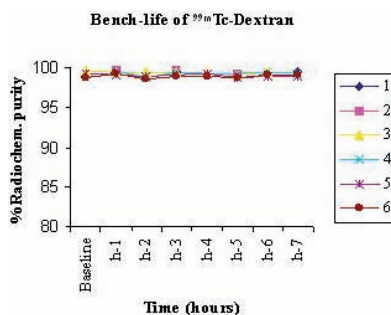


FIG. 6. Bench life of ^{99m}Tc -Dextran determined in six separate analyses.

SESSION 2

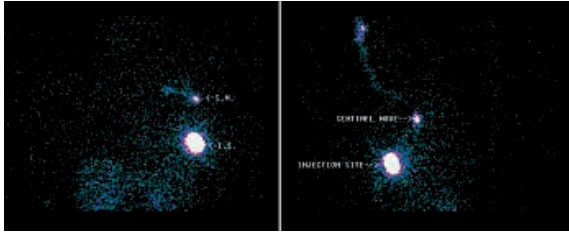


FIG. 7. ^{99m}Tc -Dextran demonstrated SLN under lymphoscintigraphy at Nuclear Medicine.



FIG. 8. Detection of SLN via a gamma probe in the operation room.

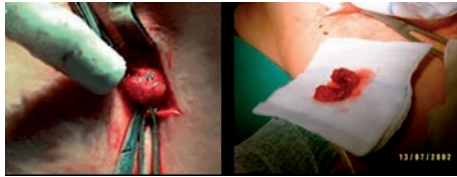


FIG. 9. Removal of SLN for frozen section.

The results of SLN detections in operation rooms via the dual systems are tabulated in Table 1. Those with positive malignancy findings (pathology) from the combined results ($n = 14$, 31.1%) underwent axillary lymph node dissection (ALND) to treat the micrometastases suggested. This surgery was not applied to the rest ($n = 31$, 68.9%) to avoid unnecessary complications including lymphedema, arm swelling, numbness/nerve injury, arm pain, seroma and infection.

The concordant and discordant results of SLN detections between ^{99m}Tc -Dextran and the dye methods as related to ALND are shown in Table 2. One discordance in the 'No ALND' column was the SLN demonstrated only by

TABLE 1. SENTINEL NODE DETECTION IN OPERATION ROOMS USING DUAL SYSTEMS

Parameter	Number of cases (<i>n</i>)	Time (min)*	SLN detection
^{99m} Tc-Dextran	45	22 (5–115)	45 in 45 (100%)
Blue dye	45	9 (3–74)	43 in 45 (95.6%)
Combined results	45		45 in 45 (100%)

* The mode was used, as it was not a normal distribution. The numbers in parentheses are the ranges.

^{99m}Tc-Dextran which was pathologically positive for malignancy. Of the two discordant results in the 'ALND' column, one was the SLN demonstrated by the labelled compound with a pathologically positive finding, while the other was demonstrated by blue dye. However, in most cases, a good agreement between the blue dye and the ^{99m}Tc-Dextran techniques was achieved with 93.3% concordance (42 in 45 cases). It demonstrated that the combined results provided more fruitful interpretations than formerly found [6].

3.3. Malignant melanoma

SLN could be detected in 13 out of 14 patients or 92.8% via ^{99m}Tc-Dextran and 4 out of 8 or 50% via blue dye, which was likely to be higher, if there were more patients for this group. The examples of the images taken in the Division of Nuclear Medicine are illustrated in Fig. 10 showing the injection

TABLE 2. THE DISCORDANT AND CONCORDANT RESULTS OF SLN DETECTION VIA THE DUAL SYSTEMS

Parameters		No ALND (cases)	ALND (cases)	Total (cases)
SLN detection via ^{99m} Tc-Dextran versus dye	Discordance	1	2	3
	Concordance	30	12	42
	Total	31	14	45

SESSION 2

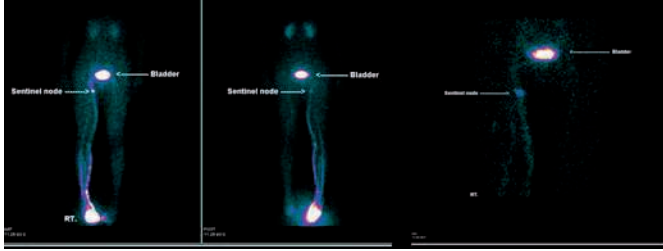


FIG. 10. SLN at the right inguinal region as demonstrated by ^{99m}Tc -Dextran administered in the Division of Nuclear Medicine.

site and the lesion at the right foot, and SLN at the right inguinal region. The location was then marked as a guideline for the surgeons in the operation room.

The results of clinical findings from lymph nodes, pathology, detection of SLN via ^{99m}Tc -Dextran, and detection of SLN via blue dye are tabulated in Table 3, suggesting that only clinical finding of negative lymph nodes (not palpable) was not enough to undertake a complete node dissection on the patients, who could afterwards be affected by the unnecessary complications which were the same as those who underwent ALND (lymphedema, numbness/nerve injury, arm/leg pain, seroma and infection). In addition, of the 8 patients whose SLNs were detected by the dual systems, concordant results were found in 5 cases, while discordant results were found in 3 cases of which the SLNs could be demonstrated by ^{99m}Tc -Dextran only. In malignant melanoma cases, it was rather difficult to observe SLNs via blue dye. However, it could be said that good agreement was obtained with the better results for the ^{99m}Tc -Dextran by which even deep SLNs could always be demonstrated.

The group of interest were patients with clinically non-palpable lymph nodes (node size < 1 cm, $n = 11$) of which SLNs could be observed in 10 of 11 patients via the ^{99m}Tc -Dextran technique. The results, together with pathological findings of malignancy and the management of the patients related, are shown in Table 4. Without SLN detection, the two patients would be missing from proper treatment. Besides, the eight patients would have undergone surgery unnecessarily, which may cause some complications. These expressed the usefulness of SLN detection by ^{99m}Tc -Dextran. The only one of 11 patients whose SLN could not be observed via either ^{99m}Tc -Dextran or blue dye was positive in pathological malignancy finding and underwent tumour removal (the tumour site was at the chest wall) together with complete node dissection.

TABLE 3. CLINICAL FINDINGS OF LYMPH NODES, PATHOLOGY, DETECTION OF SLN VIA ^{99m}Tc -DEXTRAN AND BLUE DYE

Patients	Clinical findings for lymph nodes ^a	Malignancy ^b (pathology)	SLN detection	
			^{99m}Tc -Dextran	Blue dye
1	Not palpable	negative	SLN detected	
2	Not palpable	negative	SLN detected	
3	Not palpable	negative	SLN detected	SLN not detected
4	Not palpable	negative	SLN detected	
5	Not palpable	positive	SLN detected	SLN detected
6	Palpable	negative	SLN detected	
7	Palpable	positive	SLN detected	
8	Not palpable	negative	SLN detected	SLN detected
9	Not palpable	negative	SLN detected	SLN not detected
10	Palpable	negative	SLN detected	
11	Not palpable	negative	SLN detected	SLN not detected
12	Not palpable	positive	SLN detected	SLN detected
13	Not palpable	negative	SLN detected	SLN detected
14	Not palpable	positive	SLN not detected	SLN not detected

^a 'Not palpable lymph nodes' referred to those with a size of less than 1 cm.

^b 'Negative' meant a negative result for malignancy, and 'positive' a positive result for malignancy.

TABLE 4. SLN DETECTION VIA ^{99m}Tc -DEXTRAN IN THE PATIENTS WITH CLINICALLY NEGATIVE LYMPH NODE FINDINGS

Clinically negative lymph node findings	SLN detection by ^{99m}Tc -Dextran	Malignancy (pathology)	Usefulness of SLN
11 out of 14 cases	Positive SLN detection in 10 cases out of 11	Positive malignancy in 2 cases out of 10	The patients received proper treatment for micrometastasis
		Negative malignancy in 8 cases out of 10	Complete node dissection was omitted

4. CONCLUSION

Pre-operation lymphoscintigraphy of SLNs provides useful information to the surgeons, e.g. location of the SLN prior to incision, and failure of the radiopharmaceutical is rare. The preparation of the in-house Dextran kit using the Phramongkutklao modified method is cost effective and not difficult, giving the ^{99m}Tc labelled compound a satisfactory radiochemical purity and long bench life. Moreover, its clinical applications in both groups of patients provided useful information for the surgeons to establish proper treatment for those with micrometastases and omit complete node dissection in those whose SLNs showed negative malignancy findings, thereby avoiding unnecessary complications. Thus, the in-house Dextran is a tool of choice for SLN detection.

ACKNOWLEDGEMENTS

The particle size determination was performed under the supervision of S. Puttipipatkachorn and J. Chingunpitak, Faculty of Pharmacy, Mahidol University. The authors appreciate the assistance given by A. Ngornrath Na Ayudhya, Ramathibodi Hospital, for her useful advice on radiochemical purity testing. Sincere thanks are offered to T. Tongpraparn for statistical analysis and to the radiological technologists involved in lymphoscintigraphy.

REFERENCES

- [1] COSTA, A., et al., Less aggressive surgery and radiotherapy is the way forward, *Curr. Opin. Oncol.* **16** (2004) 523–528.
- [2] VERA, D.R., et al., A synthetic macromolecule for sentinel node detection: ^{99m}Tc -DTPA-mannosyl-dextran, *J. Nucl. Med.* **42** (2001) 951–959.
- [3] RUSSELL-JONES, R., ACLAND, K., Sentinel node biopsy in the management of malignant melanoma, *Clinical and Experimental Dermatology* **26** (2001) 463–468.
- [4] FRIER, M., Radiopharmaceuticals for sentinel node detection, *Brazilian Archives of Biology and Technology* **45** (2002) 83–86.
- [5] MARIANI, G., et al., Radioguided sentinel lymph node biopsy in breast cancer surgery, *J. Nucl. Med.* **42** 8 (2001) 1198–1215.
- [6] YANG, K.T., et al., Quality control of ^{99m}Tc -labeled dextran for lymphoscintigraphy, *Eur. J. Nucl. Med.* **15** (1989) 171–173.
- [7] DASS, R.S., et al., Development of a dextran kit for labeling ^{99m}Tc and its evaluation for lymphoscintigraphy, *Nucl. Med. Biol.* **20** 5 (1993) 701–706.

- [8] HENZE, E., et al., Tc-99m dextran: A new blood-pool labeling agent for radio-nuclide angiocardiology, *J. Nucl. Med.* **23** (1982) 348–353.

COMPARATIVE STUDY OF ^{99m}Tc -EMB AND NATIVE EMB AND THE ROLE OF ^{99m}Tc -EMB IN RESISTANT MYCOBACTERIAL IMAGING

N. SINGH* **, A.K. SINGH*, A. BHATNAGAR*, G. MITTAL*,
T. RAVINDRANATH*

*Institute of Nuclear Medicine and Allied Sciences, DRDO
Email: namsingh1@yahoo.com

**Ambedkar Centre for Biomedical Research,
University of Delhi

Delhi, India

Abstract

Tuberculosis is a major opportunistic infectious disease responsible for the largest number of fatalities, even in the modern and technologically advanced world. Various radiopharmaceuticals have been used for the diagnostic and therapeutic study of tuberculosis but all suffer from certain limitations, such as non-specificity, insensitivity, etc. To this end, Ethambutol (EMB), an anti-tubercular drug, has been radiolabelled and used for resistant tuberculosis detection. Results of in vivo and in vitro studies with the ^{99m}Tc labelled EMB are presented.

1. INTRODUCTION

Tuberculosis is a dreaded infectious disease causing the greatest number of fatalities. The therapeutic potential of the anti-tubercular drug Ethambutol (EMB) is being utilized for the treatment of this granulomatous, opportunistic disease. Existing conventional diagnostic modalities (microbiological, molecular biology, chromatography, etc.) have their own proven utility but they suffer from certain limitations [1–5]. Radionuclidic emission based nuclear medicine modality utilizing radiolabelled EMB was used in this study for early detection and localization of resistant tubercular lesions.

2. MATERIALS AND METHOD

Radiocomplexation of EMB with ^{99m}Tc was performed and standardized using stannous mediated reduction of ^{99m}Tc . In vitro stability studies (i.e. serum and blood) were performed with ITLC to assess stability of the labelled compound. In vitro pharmacological studies such as uptake studies, MIC studies and CFU assays were performed to gauge the effect of radiocomplexation in the biological activity of the drug. In vitro pharmacological studies and organ distribution of ^{99m}Tc -EMB were conducted on New Zealand white rabbit and balb/c mice respectively at different time intervals up to 24 h and compared with native EMB [6, 7]. Imaging was performed in an animal model (thigh model with resistant tubercular lesion) [8] and subsequently in humans for further confirmation.

3. RESULTS

The labelling efficiency of ^{99m}Tc -EMB was found to be >95%. Only 3–4% of ^{99m}Tc leached out from the complex in 24 h of incubation in blood and serum, confirming its high stability. Biological studies indicated the similarity in the behaviour of labelled and native EMB. Drug uptake was also observed in resistant bacilli. Blood kinetics studies exhibited $V_d = 474 \text{ mL}$, $t_{1/2} = 17.7 \text{ h}$, $\text{Cl} = 18.5 \text{ mL/h}$ which was comparable to native EMB as indicated by Dollery [7] (see Table 1). Organ distribution indicated renal and hepatobiliary route of excretion. Scintigraphic studies under gamma camera in both the animal model and humans indicated normal biodistribution and efficacy of the tracer to localize in the resistant tubercular lesion (Figs 1–3).

TABLE 1. COMPARISON OF PHARMACOKINETICS OF ^{99m}Tc -EMB AND NATIVE EMB

^{99m}Tc -EMB	Native EMB
Distribution phase = 2 h	Distribution phase = 2–4 h
$t_{1/2} = 15.4 \text{ h}$	$t_{1/2} = 10\text{--}15 \text{ h}$
$V_d = 2.8 \text{ L/kg}$	$V_d = 3.1 \text{ L/kg}$
$\text{Cl} = 18.5 \text{ mL/h}$	$\text{Cl} = 15\text{--}20 \text{ mL/h}$
Plasma protein binding = 60%	Plasma protein binding = 10–40%

SESSION 2



FIG. 1. Normal biodistribution of $^{99m}\text{Tc-EMB}$ in New Zealand white rabbit.



FIG. 2. Normal biodistribution of $^{99m}\text{Tc-EMB}$ in human.

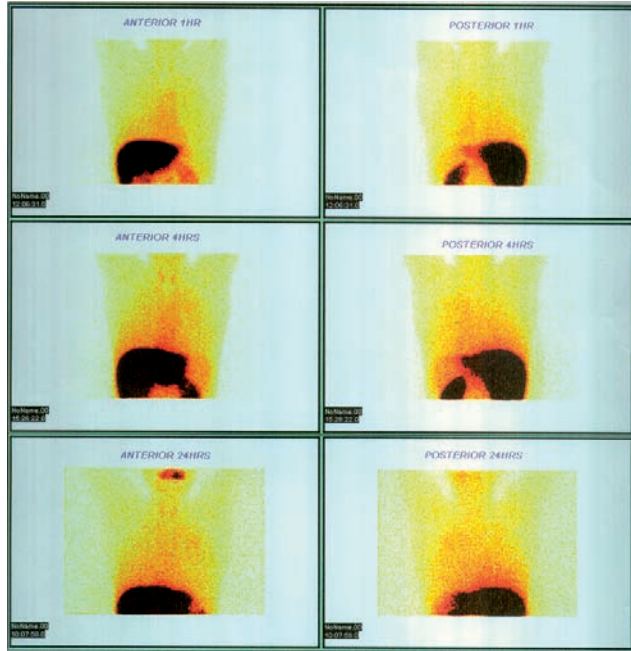


FIG. 3. Differential accumulation of $^{99m}\text{Tc-EMB}$ in patient with resistant pulmonary tuberculosis.

4. CONCLUSION

Technetium-99m-EMB is a highly specific and sensitive tracer for resistant tubercular detection.

REFERENCES

- [1] MERTENS, W., POWER, J., Utility of In-111-labeled leucocytes in patients completing high dose interleukin-2 therapy, Nucl. Med. Commun. **15** (1994) 73–80.
- [2] VORNE, M., SONI, J., LANTTO, T., POAKKINEN, S., Technetium-99m HMPAO labeled leucocytes in detection of inflammatory lesions: Comparison with gallium-67 citrate imaging, J. Nucl. Med. **30** (1989) 1332–1336.
- [3] PETERS, A., The utility of 99m-HMPAO-leucocytes for imaging infection, Sem. Nucl. Med. **24** (1994) 110–127.

SESSION 2

- [4] VINJAMURI, S.H., et al., Comparison of Tc-99m infection imaging with radio-labeled white cell imaging in the evaluation of bacterial infection, *Lancet* 346 (1996) 233–235.
- [5] HALL, A.V., et al., Evaluation of the efficacy of “^{99m}Tc-infecton” : A novel agent for detecting sites of infection, *J. Clin. Pathol.* **51** (1998) 215–219.
- [6] GENNARO, A.R., Remington’s pharmaceutical sciences. Harvey SC, Withrow CD. Basic pharmacokinetics. Mack Publishing, Easton, PA. 18th edn, 725–745.
- [7] DOLLERY, C., Therapeutic Drugs, Vol 2, Churchill Livingstone, 1–75.
- [8] SINGH, A.K., VERMA, J., BHATNAGAR, A., SEN, S., BOSE, M., Tc-99m isoniazid: A specific agent for diagnosis of tuberculosis, *World J. Nucl. Med* **4** (2003) 292–305.

TECHNETIUM CHEMISTRY AND
RADIOPHARMACEUTICALS: III

(Session 3)

Chairpersons

I. CARRIO

Spain

E.K.J. PAUWELS

Netherlands

TECHNETIUM RADIOPHARMACEUTICALS: APPLICATIONS IN NUCLEAR CARDIOLOGY

R.M.T. GIUBBINI

Nuclear and Nuclear Medicine Unit,
University and 'Spedali Civili' of Brescia,
Brescia, Italy
Email: giubbini@spedalicivili.brescia.it

Abstract

Single photon emission computed tomography (SPECT) with technetium labelled perfusion tracers is a consolidated tool for coronary artery disease diagnosis and for risk stratification. Technetium-99m labelled myocardial perfusion tracers have allowed a significant evolution in myocardial perfusion scintigraphy. Technical improvements in scintigraphic data acquisition, processing and analysis, such as SPECT and gated-SPECT, can be applied in current clinical practice as a consequence of the availability of perfusion tracers with optimal physical characteristics for gamma camera technology. The principal properties of commercially available tracers are analysed.

1. INTRODUCTION

Coronary artery disease is the premier killer in humans. Nuclear cardiology has demonstrated its clinical value during more than two decades of scientific and clinical experience. A large body of literature has shown that myocardial perfusion imaging, allowing simultaneous evaluation of perfusion and function, is a highly reliable non-invasive tool to provide both diagnostic and prognostic information. It is a useful tool for patient management at all stages of coronary artery disease. Myocardial perfusion studies allow confident clinical evaluations based on either positive or negative results. They can accurately distinguish between patients who need more aggressive invasive evaluation and treatment, and those who do not.

Myocardial perfusion imaging with single photon emission computed tomography (SPECT) during stress and rest is the procedure of choice for assessment of ischemic heart disease. Stress SPECT imaging is a 3-D modality that allows for a real time evaluation of myocardial perfusion. Over the years, it has benefited from technological standardization and has provided qualitative and quantitative analyses of myocardial perfusion, viability and left ventricle function.

SPECT is the most extensive imaging technique used and provides images of the heart using minute amounts of radiotracer that are injected intravenously. The images depict myocardial perfusion and delineate any ischemia or infarction in terms of site, severity and extent. It also simultaneously evaluates left ventricular function using wall motion, wall thickening, ejection fraction and volumes. SPECT derived variables can not only reliably detect coronary artery disease, but also stratify patients into different risk groups for future cardiac events. Examples of images are shown in Figs 1 and 2.



FIG. 1. Myocardial perfusion evaluated by SPECT. Normal case study (top) and patient with severe perfusion abnormality of anterior, septal and inferior walls (bottom).

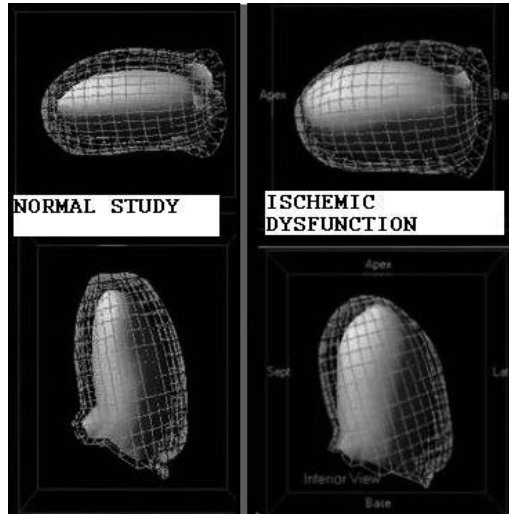


FIG. 2. Left ventricular function evaluated by gated-SPECT. Normal case study (left) and patient with severe ischaemic dysfunction (right).

2. MYOCARDIAL PERFUSION TRACERS

Since their introduction more than fifteen years ago, ^{99m}Tc labelled myocardial perfusion tracers have allowed a significant evolution in myocardial perfusion scintigraphy. Technical improvements in scintigraphic data acquisition, processing and analysis, such as SPECT and gated-SPECT can be applied in current clinical practice as a consequence of the availability of perfusion tracers with optimal physical characteristics for gamma camera technology.

Despite the maturity of SPECT imaging and the more favourable physical properties of ^{99m}Tc compared with ^{201}Tl , at present none of the ^{99m}Tc labelled agents that have been approved for clinical use has ideal biodistribution properties. A ^{99m}Tc labelled myocardial perfusion tracer with ideal biological characteristics is still the goal of many investigators. Favourable biological properties can be summarized as:

- Myocardial uptake proportional to blood flow with linear relationship at both low and high flow;
- High extraction fraction (ideal = 1);

- Favourable myocardial uptake and retention with minimal wash out and/or redistribution allowing appropriate timing for SPECT acquisition;
- Fast blood clearance with high heart to background ratio for early imaging;
- Fast lung clearance;
- Fast liver clearance and minimal residual abdominal activity interfering with scintigraphic acquisition;
- Easy kit preparation;
- In vitro and in vivo stability.

Many tracers have been synthesized, including ^{99m}Tc -sestamibi, ^{99m}Tc -tetrofosmin, ^{99m}Tc -teboroxime, ^{99m}Tc -N-NOET and ^{99m}Tc -furifosmin. Recently, Hatada et al. [1] reported on the use of a new technetium perfusion agent (NDBODC5) in a rat model. The agent has a more rapid clearance from the blood pool and from the liver than either sestamibi or tetrofosmin, suggesting that it may offer the potential for earlier imaging acquisition and less interference from abdominal activity.

However, only two imaging agents are currently commercially available, ^{99m}Tc -sestamibi and ^{99m}Tc -tetrofosmin, and, after thirty years, ^{201}Tl still has a considerable market, although the physical characteristics of this radionuclide are suboptimal for scintillation camera imaging. The potential advantages of a ^{99m}Tc labelled agent over ^{201}Tl are:

- The 140 keV photon energy of ^{99m}Tc (optimal for Anger gamma camera imaging) provides an improved resolution due to less Compton scatter, less tissue attenuation (in comparison to the low photon energy of 68–80 keV for ^{201}Tl).
- The shorter physical half-life of ^{99m}Tc (6 h as opposed to 73 h for ^{201}Tl) and the better radiation dosimetry permit the administration of a tenfold higher dose of a ^{99m}Tc labelled radiopharmaceutical. This yields better image quality and images which can be obtained in a shorter time period.
- The better counting statistics of ^{99m}Tc are advantageous for SPECT and gated-SPECT imaging, allowing simultaneous assessment of perfusion and function.
- First pass ventriculography can be also performed for the evaluation of right and left ventricular function.
- Since ^{99m}Tc is constantly available from an Mo- ^{99m}Tc generator, ^{99m}Tc labelled perfusion tracers are available 24 h in a nuclear medicine laboratory, allowing their use in the emergency room, coronary care or chest pain units at night and during weekends.

SESSION 3

The properties of the commercially available perfusion tracer are analysed in the following sections.

2.1. ^{99m}Tc -sestamibi

In the early 1980s, Jones et al. [2] reported on a new group of ^{99m}Tc labelled myocardial perfusion radiotracers, the ^{99m}Tc -isonitriles. Initial animal studies showed that the myocardial uptake of ^{99m}Tc -isonitriles was proportional to myocardial blood flow. The first member of the ^{99m}Tc -isonitrile family to be evaluated in humans was the hexakis (t-butyl-isonitrile)-technetium, known as ^{99m}Tc -TBI, whose use for imaging purposes was suboptimal due to an increased lung uptake and persistent liver uptake, masking defects of the inferior wall. The best ^{99m}Tc -isonitrile compound for imaging purposes that emerged from the research on this substance was the ^{99m}Tc -hexakis 2-methoxyisobutyl isonitrile, better known as sestamibi, ^{99m}Tc -MIBI or with the trademark name of Cardiolite that was approved by the US Food and Drug Administration at the end of the 1990s and subsequently introduced all over the world.

Technetium-99m-sestamibi is a monovalent cation with a central technetium core that is surrounded by six identical lipophilic ligands coordinated through the isonitrile carbon (Fig. 3). It is taken up by myocytes in proportion to regional myocardial blood flow. The cationic charge of the compound provides hydrophilic properties, while the six isonitrile groups allow hydrophobic interaction with cell membranes. The myocardial uptake of ^{99m}Tc -sestamibi is known to be dependent on cellular pH, mitochondrial derived membrane, electrochemical gradient and intact energy production pathways.

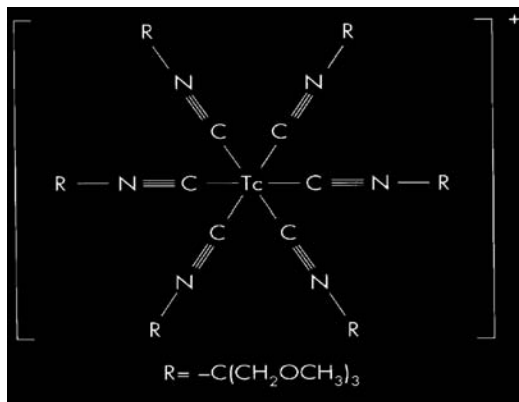


FIG. 3. ^{99m}Tc -sestamibi.

Piwnica-Worms et al. [3] demonstrated that the fundamental myocellular uptake mechanism of ^{99m}Tc -MIBI involved passive distribution across plasma and mitochondrial membranes and that at equilibrium ^{99m}Tc -MIBI was sequestered within mitochondria by the large negative transmembrane potentials. Technetium-99m-MIBI kinetics appeared to be dependent on sarcolemmal integrity and to a lesser extent on aerobic metabolism. Glover et al. [4] showed that ^{99m}Tc -sestamibi was rapidly taken up by non-ischemic, mild to moderate and severe ischemic myocardium, and that the initial myocardial uptake of ^{99m}Tc -sestamibi was linearly related (r value of 0.97) to the regional myocardial blood flow at rates up to approximately $2.0 \text{ mL}\cdot\text{g}^{-1}\cdot\text{min}^{-1}$. However, at higher flow rates, there is a plateau in the myocardial distribution versus flow curve, resulting in an underestimation of coronary blood flow. Leppo and Meerdink [5] performed a side by side comparison of ^{201}Tl and ^{99m}Tc -MIBI during variable blood flow levels in isolated rabbit hearts. When coronary flow was varied from 0.52 to $3.19 \text{ mL}\cdot\text{g}^{-1}\cdot\text{min}^{-1}$, myocardial extraction for MIBI averaged 0.38 ± 0.09 (SD) whereas ^{201}Tl myocardial extraction averaged 0.73 ± 0.10 (p less than 0.001). Net extraction, which was calculated using end points of 1.8–4.9 min, averaged 0.41 ± 0.15 for MIBI and was less than the ^{201}Tl net extraction of 0.57 ± 0.13 (p less than 0.001). The mean capillary permeability–surface area product for MIBI ($0.44 \pm 0.13 \text{ mL}\cdot\text{g}^{-1}\cdot\text{min}^{-1}$) was one third of ^{201}Tl ($1.30 \pm 0.45 \text{ mL}\cdot\text{g}^{-1}\cdot\text{min}^{-1}$; p less than 0.001). However, parenchymal cell permeability–surface area product for MIBI ($47.58 \pm 25.85 \text{ mL}\cdot\text{g}^{-1}\cdot\text{min}^{-1}$) was much higher than ^{201}Tl ($6.52 \pm 6.51 \text{ mL}\cdot\text{g}^{-1}\cdot\text{min}^{-1}$; p less than 0.0001), and apparent cellular volume of distribution for MIBI ($15.15 \pm 3.31 \text{ mL/g}$) was also higher than ^{201}Tl ($10.19 \pm 4.00 \text{ mL/g}$; p less than 0.01). The net result of these differences in myocellular kinetics of the two radiopharmaceuticals is that very little difference is observed in the initial myocardial accumulation when both are imaged in vivo.

2.2. ^{99m}Tc -tetrofosmin

Technetium-99m-tetrofosmin (Fig. 4) was the third ^{99m}Tc labelled myocardial perfusion imaging agent to be approved and made commercially available (^{99m}Tc -teboroxime was the second after ^{99m}Tc -sestamibi but it was immediately withdrawn from the market owing to its unfavourable characteristics for in vivo imaging). Technetium-99m-tetrofosmin showed faster clearance from both the liver and the lung than that of ^{99m}Tc -sestamibi. Another difference was that the kit preparation did not require a high temperature heating period that was mandatory for sestamibi.

Technetium-99m-tetrofosmin is the generic name for 1,2-bis [bis (2-ethoxyethyl) phosphino] ethane (trade name Myoview). Tetrofosmin is a

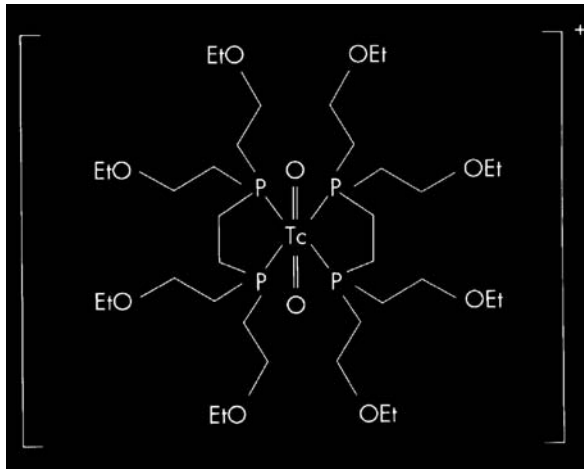


FIG. 4. ^{99m}Tc -tetrofosmin.

ligand that forms a lipophilic, cationic complex with ^{99m}Tc . Sinusas et al. [6] studied the initial myocardial uptake and clearance of ^{99m}Tc -tetrofosmin relative to microsphere flow in a canine model of ischemia during pharmacological vasodilatation. Myocardial ^{99m}Tc -tetrofosmin activity correlated linearly with microsphere flow ($r = 0.84$). Similar to ^{99m}Tc -MIBI, relative ^{99m}Tc -tetrofosmin activity underestimated flow in the higher flow ranges ($>2.0 \text{ mL}\cdot\text{g}^{-1}\cdot\text{min}^{-1}$) and overestimated flow in the low flow ranges ($<0.2 \text{ mL}\cdot\text{g}^{-1}\cdot\text{min}^{-1}$). Technetium-99m-tetrofosmin cleared rapidly from the blood and was retained in the myocardium. Resting target to background activity ratios (heart:lung = 3.57 ± 1.01 ; heart:liver = 0.58 ± 0.04) were acceptable 10 min after injection. It was concluded that ^{99m}Tc -tetrofosmin as a myocardial perfusion tracer was suitable for the assessment of myocardial perfusion in humans.

In a review by Dahlberg and Leppo [7], the myocardial deposition of radiolabelled perfusion agents for the non-invasive assessment of regional coronary blood flow was evaluated. They pointed out that ^{201}Tl and the ^{99m}Tc labelled compounds sestamibi, teboroxime and tetrofosmin showed differing myocardial extraction and retention. The maximum extraction of tetrofosmin was 0.37 suggesting a capillary-tissue permeability surface similar to that of ^{99m}Tc -sestamibi. In comparison, the maximum extraction value for ^{201}Tl is 0.73, for ^{99m}Tc -teboroxime 0.81, and for ^{99m}Tc -sestamibi 0.39. However, ^{99m}Tc -tetrofosmin has the lowest net extraction among the four compounds — 0.23 (c.f. ^{201}Tl : 0.57, ^{99m}Tc -sestamibi: 0.41, and ^{99m}Tc -teboroxime: 0.67). Higley et al.

[8] and Sridhara et al. [9] studied the kinetics of tetrofosmin in humans. After a stress injection, the myocardial uptake of ^{99m}Tc -tetrofosmin, although relatively stable over time, slightly decreases from 1.3 of the injected dose at 5 min to 1.0 at 2 h after the injection. From 5 min to 120 min post-injection, liver uptake decreases from 3.2 to 0.5, lung uptake decreases from 1.2 to 0.2, while gall bladder activity increases from 0.5 to 3.2, and the gastrointestinal tract activity increases from 2.0 to 8.7. From 5 min to 60 min after ^{99m}Tc -tetrofosmin injection, the heart to lung ratio increases from 4.0 ± 1.1 to 5.9 ± 1.3 and the heart to liver ratio increases from 0.8 ± 0.3 to 3.1 ± 3.0 . After a rest injection, the myocardial activity of ^{99m}Tc -tetrofosmin remains relatively constant over time with an uptake of 1.2 of the injected dose at 5 min and 1.0 at 2 h after the injection. From 5 min to 120 min post-injection, liver uptake decreases from 7.5 to 0.9, lung uptake decreases from 1.7 to 0.3, while gall bladder activity increases from 0.8 to 5.3, and the gastrointestinal tract activity increases from 2.9 to 13.8. From 5 min to 60 min after ^{99m}Tc -tetrofosmin injection, the heart to lung ratio increases from 3.1 ± 1.8 to 7.3 ± 4.4 and the heart to liver ratio increases from 0.4 ± 0.1 to 1.2 ± 0.8 . No significant ^{99m}Tc -tetrofosmin myocardial redistribution was found with a slow myocardial washout of approximately 4–5 per hour after exercise and 0.4–0.6 per hour after a rest injection.

3. CONCLUSIONS

Two ^{99m}Tc labelled radiopharmaceuticals for myocardial perfusion imaging are now commercially available. They show similar kinetics in humans and allow high quality clinical studies to be undertaken. However, tracers with higher extraction fractions and linear uptakes in comparison to myocardial flow remain the goal of pharmacological research. It is likely that with newest agents and a constant improvement in gamma camera technology and software development (attenuation, scatter, motion correction) an absolute quantification of myocardial tracer uptake and of coronary flow measurement will be achieved in the next years.

REFERENCES

- [1] HATADA, K., et al., ^{99m}Tc -N-DBODC5, a new myocardial perfusion imaging agent with rapid liver clearance: comparison with ^{99m}Tc -sestamibi and ^{99m}Tc -tetrofosmin in rats, *J. Nucl. Med.* **45** 12 (2004) 2095–2101.

SESSION 3

- [2] JONES, A.G., et al., Biological studies of a new class of technetium complexes: The hexakis(alkylisonitrile)technetium(I) cations, *Int. J. Nucl. Med. Biol.* **11** 3–4 (1984) 225–234.
- [3] PIWNICA-WORMS, D., KRONAUGE, J.F., CHIU, M.L., Uptake and retention of hexakis (2-methoxyisobutyl isonitrile) technetium(I) in cultured chick myocardial cells: Mitochondrial and plasma membrane potential dependence, *Circulation* **82** 5 (1990) 1826–1838.
- [4] GLOVER, D.K., OKADA, R.D., Myocardial kinetics of Tc-MIBI in canine myocardium after dipyridamole, *Circulation* **81** 2 (1990) 628–637.
- [5] LEPPA, J.A., MEERDINK, D.J., Comparison of the myocardial uptake of a technetium-labeled isonitrile analogue and thallium, *Circ. Res.* **65** 3 (1989) 632–639.
- [6] SINUSAS, A.J., et al., Technetium-99m-tetrofosmin to assess myocardial blood flow: Experimental validation in an intact canine model of ischemia, *J. Nucl. Med.* **35** 4 (1994) 664–671.
- [7] DAHLBERG, S.T., LEPPA, J.A., Myocardial kinetics of radiolabeled perfusion agents: Basis for perfusion imaging, *J. Nucl. Cardiol.* **2** 1 (1994) 189–197.
- [8] HIGLEY, B., et al., Technetium-99m-1,2-bis[bis(2-ethoxyethyl) phosphino]ethane: Human biodistribution, dosimetry and safety of a new myocardial perfusion imaging agent, *J. Nucl. Med.* **34** 1 (1993) 30–38.
- [9] SRIDHARA, B.S., et al., Comparison of myocardial perfusion imaging with technetium-99m tetrofosmin versus thallium-201 in coronary artery disease, *Am. J. Cardiol.* **72** 14 (1993) 1015–1019.

IMAGING ONCOGENE MRNA FOR EARLY DIAGNOSIS OF CANCER

N. SHANTHLY*, M.R. ARUVA*, K. ZHANG*, C.A. CARDI*,
T. XIOBING**, E. WICKSTROM**, M.L. THAKUR*

*Department of Radiology
Email: Mathew.Thakur@jefferson.edu

**Department of Biochemistry and Molecular Pharmacology

Thomas Jefferson University,
Philadelphia, Pennsylvania
United States of America

Abstract

In 2005 breast cancer attacked approximately 210 000 and took the lives of 40 000 women in the United States of America. Standard screening with breast self-examination and mammography, recommended to minimize breast cancer morbidity, miss 10–20% (up to 40% in young women) of breast cancer. Moreover, if an abnormality is found, an invasive diagnostic procedure is required to determine if the breast contains hyperplasia, atypia, or cancer. Approximately 80% of invasive procedures detect a benign pathology. Breast cancer cells express a gene product, cell surface receptor VPAC1, so named because the endogenous growth hormones vasoactive intestinal peptide and pituitary adenylate cyclase activating peptide bind to VPAC1 receptors with high affinity. VPAC1 receptors are overexpressed on 100% of human breast cancer cells. Cyclin D1 is a key regulator of the cell cycle and overexpressed in 50–80% of breast cells, whereas it is low or absent in normal breast tissues. The human breast cancer cell line MCF7 displays elevated levels of CCND1 mRNA, encoding cyclin D1, and an elevated level of IGF1R mRNA, encoding insulin-like growth factor 1 receptor. The authors hypothesize that ^{99m}Tc or ^{64}Cu labelled VIP analogues, or a peptide nucleic acid (PNA) chimera specific for IGFI receptor and CCND1 mRNA, will permit the early imaging of breast cancer by planar, SPECT or PET methods. The authors synthesized, characterized and administered i.v. ^{99m}Tc -AcGly-D (Ala)-Gly-Gly-aminobutanoyl-VIP (TP3654), ^{64}Cu diaminedithiol-aminobutanoyl-VIP (TP3982), ^{99m}Tc -AcGly-D(Ala)-Gly-Gly-PNA-D(Cys-ser-lys-Cys) chimera (WT4185) and ^{64}Cu -DOTA-PNA-D(cys-ser-lys-cys) WT4348. A 12mer, CTGGTGTTCAT nucleic acid sequence served as the PNA and 3 or 4 mer mismatched PNAs as negative controls. Using ^{99m}Tc -TP3654, the authors have successfully imaged human breast cancers not detectable by current modalities. In athymic, nude mice bearing MCF-7 human breast cancer xenografts, ^{64}Cu -TP3982 tumour uptake was 85 times greater than ^{99m}Tc -TP-3654 and with ^{64}Cu -

WT4348 twice as high as that of ^{99m}Tc -WT4185. PET imaging was performed using a MOSAIC (Philips) animal PET scanner. Fusion imaging was facilitated by ImTek animal computed tomography scanner.

1. INTRODUCTION

Cancer is a complex and formidable disease of humankind. Biochemically, it is a multistep process in which normal, healthy cells in the body undergo mutations in the genes that normally regulate cell division. Cancer cells differ from the normal by genetic alterations that affect the growth regulatory mechanism. Early detection of a malignant tumour is vital in the initiation of therapy and can save lives. Medical imaging plays a major role for diagnosis of an early form of cancer, to stage the disease, to assess treatment response, to identify recurrent disease, to map the tumour extent and to determine the distant spread.

Besides plain radiography and ultrasonography, the other procedures used for morphological examinations are computed tomography (CT) and magnetic resonance imaging (MRI). Scintigraphic imaging modalities such as single photon emission computerized tomography (SPECT) and positron emission tomography (PET) and the hybrid systems, such as PET/CT, not only complement the morphological images but also provide functional information on the disease status.

Targeting the overexpressed receptor proteins or mRNA precursors on the surface or within the cancer cells forms the basis for inhibiting the adverse functions of the abnormally proliferating cell as well as for detecting their abnormality. Many radiopharmaceuticals have emerged as tumour specific agents, targeting specific tumour markers for diagnosis and therapy. Tumours of neural crest origin have been imaged with ^{123}I labelled to meta-iodobenzylguanidine (mIBG) and treated with ^{131}I -mIBG [1–3]. The uptake of ^{123}I -mIBG promoted by an active energy dependent type 1 amine mechanism, is proportional to the number of neurosecretory granules. Though tumours such as pheochromocytoma and neuroblastoma have benefited from this agent, other gastropancreatic tumours of the same origin have not had the same effect. In recent years, the focus was shifted to somatostatin receptors (SSTR), which are expressed in a variety of tumours. Five types of SSTR have been identified. The somatostatin analogues with specific affinity for these receptors were labelled with several radionuclides and used as non-invasive imaging tools to identify the malignancy in its early form. Molecular studies have revealed that ^{111}In -octreotide binds specifically with high affinity to SSTR2, which are expressed on the cell membranes of neuroendocrine gastropancreatic tumours

such as carcinoids, gastrinomas, islet cell tumours, insulinomas, glucagonomas and VIPomas. Indium-111-octreotide (Octreoscan®) is now available for the management of SSTR positive neuroendocrine malignancy [4–6]. However, ^{111}In -octreotide has been less successful in breast cancer, small cell carcinoma of the lung and lymphomas. Another somatostatin receptor analogue, $^{99\text{m}}\text{Tc}$ -depreotide (NeoTect), with higher sensitivity and specificity for cancers of the lung has been developed [7–9]. Monoclonal antibodies function as receptor agonists [10–13]. Radiolabelled antibodies have been used successfully to detect some cancers. Monoclonal antibodies, being homogenous in nature, are ideal for the discrimination of cellular antigens and can reveal qualitative and quantitative differences in the antigenic composition of normal and malignant cells. Hence, they have been applied in the detection and early diagnosis of cancer, staging procedures and in therapy. For diagnostic applications, monoclonal antibodies are labelled with either $^{99\text{m}}\text{Tc}$ or ^{111}In because of the ease of preparation, suitable energy for standard camera imaging and the compatibility of their half-lives for the clearance of the antibody proteins in vivo. Whole antibodies and large fragments are usually labelled with the longer half-life of ^{111}In , while the smaller antibody Fab' fragments that are expected to have rapid blood clearance are labelled advantageously with the shorter half-life $^{99\text{m}}\text{Tc}$. The first monoclonal antibody approved by the US Food and Drug Administration for imaging tumours was ^{111}In -Satumomab pentetide (CYT-103), an ^{111}In labelled immunoconjugate of the B72.3 monoclonal antibody, which reacts with cell surface mucin-like glycoprotein antigen TAG-72 [14]. Adenocarcinomas of breast, ovarian and colorectal cancers express TAG-72. The use of this monoclonal antibody has been limited to ovarian and colon cancers [15–17]. Another monoclonal antibody, Herceptin® (Trastuzumab), has been approved as a therapeutic agent in metastatic breast cancer over-expressing HER2 oncogene. It can be used either alone or as an adjuvant to chemotherapy. Various techniques used to evaluate the association of HER2/neu and breast cancer include southern blotting, fluorescence in situ hybridization, immunohistochemistry, enzyme immunoassays and polymerase chain reaction methods. Among the listed techniques, the fluorescence in situ hybridization technique and immunohistochemistry on frozen sections and enzyme immunoassays on fresh tumour cytosolic protein were found to produce consistent results in identifying gene amplification [18]. Technetium-99m labelled monoclonal antibodies to HER2/neu protein has revealed promising results [19].

The above agents, however, do not recognize the early changes expressed in the genetic material, which have been identified in malignant tumours. The earliest signals, i.e. oncogene expression, once detected, can initiate therapy.

Molecular imaging of gene expression provides functional information unlike the other imaging modalities, which provide morphological details.

As with SSTR or CD20, the other and perhaps equally prominent yet less addressed cell surface oncogene products are the VPAC (vasoactive and pituitary adenylate cyclase) receptors. Studies have identified the significance of vasoactive intestinal peptide (VIP) receptors and their overexpression in such tumours as breast, exocrine pancreatic, gastric, prostate and colonic cancers. Generally, the receptor density is higher than that of somatostatin [20]. Technetium labelled VIP analogues in human studies have detected tumours that express these receptors [21] including those that were not detected by the existing scintigraphic methods. Investigators have also used ^{125}I labelled DNA antisense to image gene expression [22]. In this approach there were several limiting factors including rapid in vivo metabolism and poor transport across the cells. Tian et al. used $^{99\text{m}}\text{Tc}$ and ^{64}Cu radiolabelled peptide nucleic acid (PNA) antisense probes conjugated with a ligand, which was more specific in targeting the precancerous cells with high expression of oncogenes [23, 24].

Technetium-99m has always been the radioisotope of choice for imaging because it emits the ideal 140 KeV gamma photons and has the short half-life of 6 h which reduce the unnecessary radiation burden on patients. Since the PET scanner has better spatial resolution than the planar or SPECT scanner, PET imaging has gained considerable attention. Copper-64, with its half life of 12.7 h, high energy and β emissions (β^+ 655 keV(17.4%) and β^- 573 keV(30%), is a useful PET tracer, and has been successfully labelled to antisense probes for microPET imaging of experimental tumour in small animals. Molecular imaging of genetic expression has emerged as a non-invasive tool to map early malignant changes. The authors discuss the outcome of molecular imaging in relation to exogenous VIP receptors and endogenous oncogene expression in breast cancer.

2. SCINTIGRAPHY IN BREAST CANCER

The most common non-cutaneous malignancy in the United States of America is breast cancer [25]. Though the best screening procedure for the early diagnosis of breast cancer is mammography [26], it is known to miss 40% of breast cancer in young women [27]. The sensitivity is found to be less in patients with increased breast density and those on estrogen replacement therapy [28, 29]. Radionuclide imaging has been a vital tool in the staging of breast cancer and in detecting metastatic disease. All scintigraphic modalities have been used in breast imaging. It was an incidental finding in a patient with carcinoma of the right breast who was undergoing an angiocardigraphic

procedure with ^{99m}Tc -hexakis-2-methoxy-isobutyl-isonitrile (^{99m}Tc -sestamibi) [30], a positively charged agent that changed the spectrum in breast scintigraphy. Technetium-99m-sestamibi studies were easy to perform with no discomfort to the patient and the resultant images were of excellent quality because of the 140 keV photon flux from ^{99m}Tc . Several studies carried out with ^{99m}Tc -sestamibi have found it to be more sensitive than mammography in localizing lesions in dense breasts. Sensitivities of 86% in detecting palpable lesions and 63% in non-palpable lesions have been reported [31]. Sensitivity in imaging involved lymph node is less than 60%. Sestamibi uptake has been correlated to mitochondrial activity, tumour angiogenesis and expression of Pgp protein, which is related to multidrug resistance [32–34]. However, some benign lesions with high mitochondrial activity are also known to be positive with sestamibi scans [35]. The ultimate diagnosis is therefore finalized from an invasive biopsy. The other methods, such as sentinel node mapping and radio immunoscintigraphy, aim at detection of metastases and not the primary tumour. Fluorine-18-FDG has been used for breast tumour imaging since 1984 [36] and has been attributed to only 70% of breast cancer uptake at the best owing to the slow metabolic rate of breast cancers. The other factor contributing to the uptake is the overexpression of glucose transport [37, 38]. Since the ^{18}F -FDG is based on glucose metabolism, it is less sensitive for slow growing breast cancer and is also non-specific [39–42]. Another agent, 16α -(^{18}F)-fluoro- 17β -estradiol, which is specific for estrogen receptors, also presents the same limitations [43]. A review of various studies using ^{18}F -FDG has revealed high sensitivity and specificity for tumours greater than 1.5 cm. The tumours are usually palpable at this stage or are picked up by other conventional methods [44].

Hence, the need exists for a better procedure to detect breast cancer in the early stage. It is now evident that alterations in oncogenes induce uncontrolled changes at the cellular level, which result in neoplastic transformation. A change in mRNA is present in the early pre-invasive breast cancer [45]. Therefore, functional molecular imaging aimed at targeting the genomic changes at the cellular level is likely to provide more information about the early development of breast cancer.

3. EXOGENOUS GENE RECEPTOR IMAGING

Among the various peptides identified, the VIP is overexpressed in high density in breast, ovarian, colon and prostate carcinomas and their metastatic lesions [46–49]. VIP is a 28 amino acid peptide, which was initially isolated from porcine intestine [50]. It is a hydrophobic basic peptide containing three Lysine

(numbers 15, 20 and 21) and two Arginine (12 and 14) residues besides a histidine residue at N-terminal and an amidated C-terminal. This structure is common to humans, pigs and rats. All 28 amino acids are required for high affinity binding and biological activity [51]. Two types of VIP receptor (VIP1 and VIP2) have been detected on the cell membranes of normal intestinal and bronchial epithelial cells [20, 52, 53]. These receptors are overexpressed on cells of such tumours as colon, pancreatic adenocarcinomas and carcinoids [52–57]. Similarly, pituitary adenylate cyclase activated peptide (PACAP) is a 38 amino acid peptide, which was isolated from bovine hypothalamus [58]. It was found to stimulate accumulation of intra and extra cellular cAMP in monolayer cultures of rat anterior pituitary cells [59]. PACAP, a member of VIP family, is ten times more potent than VIP in stimulating adenylate cyclase in pituitary cells [59]. Like VIP, it has a histidine residue at N-terminal and an amidated C-terminal. Three gene receptors, PACAP 1, 2 and 3, have been identified. Gottscall et al. isolated 27 amino acid PACAP (PACAP₂₇) from bovine hypothalamus and came to the conclusion that PACAP₂₇ and PACAP₃₈ were equally active and came from a single 176 amino acid precursor [59]. PACAP₂₇, with IC₅₀ of 1.5nM, binds with high affinity to VIP1, VIP2 and PACAP 1, 2 and 3 receptors, whereas VIP₂₈ binds with high affinity (1.5nM) only to VIP1 and VIP2 receptors [60, 61]. This, in principle, renders PACAP better for imaging breast cancer, which overexpresses both VIP and PACAP (VPAC1 or VPAC2) receptors. Following the PACAP homology, the receptors are named as VPAC1 (VIP1 and PACAP2 combined) and VPAC2 (VIP2 and PACAP3 combined).

Using ¹²⁵I-VIP₂₈, it was observed that VPAC1 receptors are overexpressed (100%) in breast cancers, including 15 metastatic lesions [46, 62]. The receptor density was several times higher than SSTR. VPAC1 receptors had lower expression on normal cells than on the malignant breast cancer cells [20, 46, 62–64] although the difference in receptor expression was not quantified. Others have observed high expression (10⁴/cell) of VPAC1 receptors [65]. They are internalized after binding to VIP₂₈. The above property enables tumour imaging in relation to normal organs [63, 65]. Increased density and overexpression of VPAC1 receptors were noted on breast cancer cells for which ¹²⁵I- PACAP₂₇ has a high affinity (Kd 1.5nM) [62, 66, 67]. PACAP₂₇ receptors are also expressed on various other tumour cells [60, 62, 66–73].

VIP labelled with a suitable radionuclide can serve as a sensitive non-invasive molecular imaging tool for the detection of early malignancy. Several radioisotopes such as ¹²³I, ^{99m}Tc, ¹⁸F and ⁶⁴Cu have been used for labelling. Taking advantage of the 2-tyrosine residues at positions 10 and 22, VIP was labelled with ¹²³I and used for patient studies. However, the radiolabelling procedure is time consuming and required separation of the mono-iodo and

di-iodo products. In order to be able to label VIP with ^{99m}Tc , the peptide was modified. The molecular modification was focused on the carboxy (C) terminus at asparagine (Asn) [74].

An analogue of VIP, TP3654, was synthesized using the above modification and labelled to ^{99m}Tc . Promising results were obtained [75]. The VIP was modified at Asn²⁸C terminus by the addition of a spacer Aba²⁹ (4-amino butyric acid) and amino acids Gly³⁰- Gly³¹-(d)-Ala³²-Gly³³. The Gly-(d)-Ala-Gly-Gly is the chelating moiety for labelling with ^{99m}Tc and ^{64}Cu . This tetrapeptide provides the N4 configuration which binds strongly to ^{99m}Tc , thus improving the labelling procedure [75]. Once labelled to ^{99m}Tc , it was stable for >6 h. Functional studies of the analogue TP3654 revealed uncompromised biological activity equivalent to that of native VIP₂₈ with specific binding to VIP receptor expressing tumours both in animal models and humans [75, 76]. The capability of ^{99m}Tc -TP3654 to detect human breast tumours was studied in xenografts bearing estrogen dependent T47D human breast cancer cells. The results were compared with ^{125}I -VIP and ^{111}In -DTPA-octreotide and ^{99m}Tc -sestamibi. Tissue distribution and specific tumour uptake was compared for the above agents at 2 h and 24 h following the administration of each agent using cohorts of 5 mice each. At 24 h, the tumour uptake was high with ^{99m}Tc -TP3654 (Table 1).

The tumour to muscle (T/M) and tumour to blood (T/B) ratios with ^{99m}Tc -TP3654 were higher ($p < 0.01$) than those with ^{125}I -VIP. Tumours were clearly detected with ^{99m}Tc -TP3654 but were undetectable with ^{111}In -DTPA-octreotide due to the low tumour uptake. The high muscle uptake with ^{99m}Tc -sestamibi also prevented tumour detection. Biodistribution of ^{99m}Tc -TP3654 in immune compromised mice bearing human colon cancer cell line LS174T also indicated a high retention of activity in the tumours when compared to ^{111}In -octreotide. Studies in human volunteers revealed no adverse reactions. Renal uptake, though high in the initial 30 min, reduced markedly by 24 h. Specificity of ^{99m}Tc -TP3654 to the VPAC1 expression was demonstrated in patients with malignancy by administering the agent and performing scintigraphy. Of the 11 patients studied, 9 had concordance with the other modalities and 2 with abnormal scintigraphy were confirmed exclusively by histology and receptor expression [21, 75, 77].

Encouraged by these results, the investigation was focused on procuring images with higher sensitivity and better resolution. PET provides the above qualities by resolving small lesions with high sensitivity and mapping the physiological function and metabolic changes at the molecular level. The VIP analogue TP3654 was labelled successfully to ^{64}Cu for PET imaging. TP3982, another VIP analogue specific for VPAC1 receptors, was also synthesized and labelled to both ^{99m}Tc and ^{64}Cu . Extensive study, including biodistribution and PET imaging in estrogen dependent human T47D breast tumour cell lines in immune compromised mice, was carried out and revealed promising results. Both

TABLE 1. COMPARISON OF 24 h TISSUE DISTRIBUTION EXPRESSED AS %ID/g \pm S.D. OF ^{99m}Tc -TP3654 WITH ^{125}I -VIP, ^{111}In -OCTREOTIDE AND ^{99m}Tc -MIBI IN IMMUNE COMPROMISED MICE BEARING ESTROGEN DEPENDENT T47D HUMAN BREAST CANCER CELLS ($n = 5$)

Tissue	^{99m}Tc -TP3654	^{111}In -octreotide	^{99m}Tc -sestamibi
Muscle	0.03 \pm 0.00	0.01 \pm 0.00	0.75 \pm 0.03
Intestine	0.06 \pm 0.01	0.13 \pm 0.02	0.06 \pm 0.01
Heart	0.05 \pm 0.00	0.02 \pm 0.00	0.83 \pm 0.32
Lung	0.12 \pm 0.02	0.06 \pm 0.00	0.04 \pm 0.00
Blood	0.06 \pm 0.01	0.01 \pm 0.00	0.06 \pm 0.04
Spleen	0.64 \pm 0.08	0.10 \pm 0.03	0.03 \pm 0.01
Kidney	5.46 \pm 1.23	3.60 \pm 1.63	0.41 \pm 0.09
Liver	1.34 \pm 0.29	0.22 \pm 0.04	0.22 \pm 0.03
Tumour	0.20 \pm 0.05	0.09 \pm 0.01	0.18 \pm 0.00
T/M ratio*	6.26 \pm 2.09	6.10 \pm 1.79	0.25 \pm 0.01
T/B ratio**	3.41 \pm 0.62	8.99 \pm 1.58	3.32 \pm 1.77

Note: P values for ^{99m}Tc -TP3654 and ^{111}In -octreotide were significant (<0.01) for all tissues. P values for ^{99m}Tc -TP3654 and ^{99m}Tc -MIBI were significant (<0.01) for all tissues except for intestine, where ($P = 0.04$).

* T/M ratio: Tumour to muscle ratio.

** T/B ratio: Tumour to blood ratio

analogues were stable (98%) in vivo and ex vivo when incubated with 100 mol excess diethylenetriaminepentaacetic acid (DTPA), human serum albumin (HAS) or cysteine. A 4 h urine sample revealed the agent was stable in vivo [78]. Comparison of the VIP, which was modified at the C-terminal by the addition of diaminedithiol (N_2S_2) chelator with ^{99m}Tc - N_2S_2 -VIP and ^{99m}Tc (N_4)-VIP (TP3654), was carried out. Biodistribution in nude mice bearing T47D human breast cancer cell line revealed significant tumour uptake with ^{99m}Tc -TP3982 when compared with ^{99m}Tc -TP3654. The tumour to blood ratio at 24 h was better than that at 4 h. The ^{64}Cu -TP3982 showed more uptake in the tumour than the ^{99m}Tc -TP3982 and the accumulation in the tumour increased over the next 24 h. The tumour activity was found to be 21.2 times more at 4 h and 22.1 times more at 24 h. The equivalent when compared with ^{99m}Tc -TP3654 was 45 times at 4 h and 74 times at 24 h (Tables 2 and 3). MicroPET imaging of animals also confirmed the above results with good activity in the tumours with ^{64}Cu -TP3982 (Fig. 1) [78].

SESSION 3

TABLE 2. TISSUE DISTRIBUTION (%ID/g) OF ^{99m}Tc -TP3654 AND ^{99m}Tc -TP3982 IN NUDE MICE BEARING T47D ($n = 5$) (Reproduced from Ref. [78] with permission)

Tissue	4 h			24 h		
	^{99m}Tc -TP3654	^{99m}Tc -TP3982	p	^{99m}Tc -TP3654	^{99m}Tc -TP3982	p
Muscle	0.09 ± 0.01	0.29 ± 0.07	0.01	0.04 ± 0.01	0.17 ± 0.04	0.00
Intestine	0.18 ± 0.05	0.64 ± 0.15	0.01	0.05 ± 0.01	0.28 ± 0.03	0.00
Heart	0.10 ± 0.00	1.25 ± 0.11	0.01	0.06 ± 0.01	0.47 ± 0.03	0.00
Lung	0.17 ± 0.01	0.90 ± 0.11	0.01	0.16 ± 0.09	0.54 ± 0.05	0.00
Blood	0.21 ± 0.02	0.82 ± 0.08	0.01	0.12 ± 0.02	0.23 ± 0.01	0.00
Spleen	0.19 ± 0.05	1.98 ± 0.38	0.01	0.11 ± 0.02	1.29 ± 0.08	0.00
Kidney	18.99 ± 3.75	7.70 ± 1.26	0.01	3.52 ± 0.40	5.18 ± 0.45	0.01
Liver	1.12 ± 0.08	10.13 ± 1.69	0.01	0.33 ± 0.04	6.11 ± 0.50	0.00
Tumour	0.24 ± 0.08	0.51 ± 0.05	0.01	0.23 ± 0.13	0.77 ± 0.12	0.00
T/M ratio*	2.73 ± 1.09	1.86 ± 1.59	0.01	6.28 ± 3.09	4.83 ± 1.31	0.05
T/B ratio**	1.16 ± 0.29	0.63 ± 0.12	0.01	1.98 ± 1.44	3.29 ± 0.55	0.04

* T/M ratio: Tumour to muscle ratio.

** T/B ratio: Tumour to blood ratio.

Thus external gene receptor targeting does have a definite role in the management of certain tumours as explained Table 2 and 3)above. But some of these receptors are expressed in normal tissues albeit at low density and it remains to be seen if it may limit the use of these probes.

4. ENDOGENOUS GENETIC TARGETING

The mutated forms of regulatory proteins lead to overproduction of growth factor and increased expression of proteins that inhibit apoptosis. Oncogenic mutations are usually dominant and though several mutations are required to actually produce a cancer, one oncogene can trigger abnormal cell proliferation and increase the probability of other mutations. The oncogenes are activated by point mutations, chromosomal aberrations, gene amplification and DNA rearrangements [79–81]. Based on the function, the oncogenes can encode cytoplasmic relays in intracellular signalling pathways or encode transcription factors, which activate transcription of growth promoting genes or

TABLE 3. TISSUE DISTRIBUTION (%ID/g) OF ^{64}Cu -TP3982 AND $^{99\text{m}}\text{Tc}$ -TP3982 IN NUDE MICE BEARING T47D ($n = 5$) (Reproduced from Ref. [78] with permission)

Tissue	4 h			24 h		
	^{64}Cu -TP3982	$^{99\text{m}}\text{Tc}$ -TP3982	p	^{64}Cu -TP3982	$^{99\text{m}}\text{Tc}$ -TP3982	p
Muscle	1.77 ± 0.33	0.29 ± 0.07	0.01	2.68 ± 0.30	0.17 ± 0.04	0.00
Intestine	8.31 ± 2.83	0.64 ± 0.15	0.01	8.97 ± 3.03	0.28 ± 0.03	0.00
Heart	3.90 ± 1.07	1.25 ± 0.11	0.01	6.41 ± 1.92	0.47 ± 0.03	0.00
Lung	50.40 ± 8.06	0.90 ± 0.11	0.01	11.02 ± 5.13	0.54 ± 0.05	0.00
Blood	2.27 ± 0.08	0.82 ± 0.08	0.01	2.80 ± 0.97	0.23 ± 0.01	0.00
Spleen	4.12 ± 1.52	1.98 ± 0.38	0.01	4.74 ± 1.61	1.29 ± 0.08	0.00
Kidney	9.08 ± 3.23	7.70 ± 1.26	0.01	10.56 ± 3.59	5.18 ± 0.45	0.01
Liver	25.69 ± 2.73	10.13 ± 1.69	0.01	21.15 ± 8.08	6.11 ± 0.50	0.00
Tumour	10.81 ± 2.12	0.51 ± 0.05	0.01	17.04 ± 0.73	0.77 ± 0.12	0.00
T/M ratio*	6.42 ± 2.30	1.86 ± 1.59	0.01	6.43 ± 0.86	4.83 ± 1.31	0.05
T/B ratio**	5.96 ± 4.32	0.63 ± 0.12	0.01	6.99 ± 3.40	3.29 ± 0.55	0.04

*T/M ratio: Tumour to muscle ratio.

**T/B ratio: Tumour to blood ratio.

encode growth factors or their receptors or genes encoding other proteins. There are more than 5000 oncogenes. Of these, the common oncogene products and oncogenes found in cancer cells are HER2 (human epidermal growth factor receptor, also known as c-erbB-2/neu), CCND1, MYC, RAS, Bcl2 and SRC. The other classes of genes implicated in tumourogenesis are the tumour suppressor genes p53, APC, BRCA and Rb, which are capable of encoding nuclear or cytoplasmic proteins or proteins of unknown cellular locations.

5. ONCOGENES IN BREAST CANCER

The oncogenes, which have been implicated in the tumourogenic process resulting in breast cancer, are the CCND1, HER2, MYC, and the tumour suppressor p53 [82]. IGF1 receptor encodes a 1388 amino acid G protein, which is vital to the cell division process. IGF1 is amplified in primary and metastatic

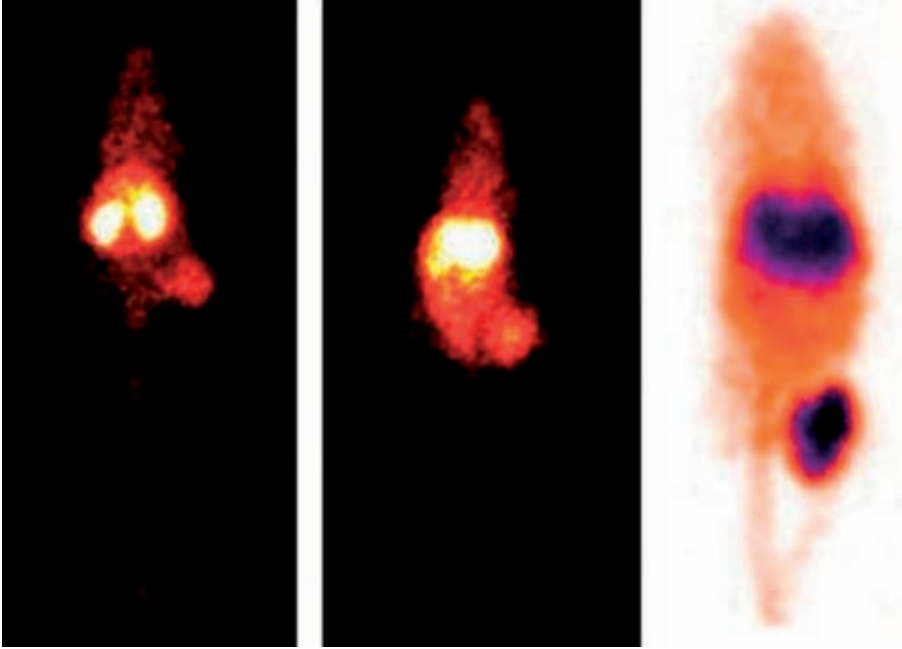


FIG. 1. 24 h PET images of T47D human breast cancer bearing nude mice receiving ^{99m}Tc -TP3654 (left), ^{99m}Tc -TP3982 (centre) and ^{64}Cu -TP3982 (right). Gamma camera images were acquired in posterior position. The gray scale in the first two gamma camera images was 0 to 50. The 1 mm coronal PET image of the mouse, which received ^{99m}Cu -TP3982, shows enhanced uptake in the tumour. The tumour in each mouse is located in the right flank (reproduced from Ref. [78] with permission).

cancer and the amplified gene has been observed in about 70% of tumours, especially in metastases [83].

The process of cell proliferation is also dependent on cyclin D1. Deregulation of cyclin D1 has been implicated in the development of breast cancer and other malignancies. Cyclin D1 gene amplification has been observed in primary breast tumours and those expressing estrogen receptors. The other noteworthy observation is the increase in cyclin D1 mRNA levels in premalignant atypical ductal hyperplasia with a potential to develop into in situ carcinoma of the breast. In the case of intermediate and poorly differentiated estrogen receptors, positive ductal carcinoma in situ and overexpression of the cyclin D1 protein have been observed [84–87]. About 50–80% of breast cancers overexpress cyclin D1 [88].

The *myc* family consists of the *cMYC*, *LMYC*, *NMYC*, *BMYC* and *SMYC*. The *BMYC* and *SMYC* suppress malignant transformation and exhibit a different function from the other *MYC* proteins [89]. Gene amplification has

been described [90] that causes genetic rearrangements leading to the breakage and resealing of chromosomes. The NMYC gene is amplified in numerous cell lines from human neuroblastoma and few of retinoblastoma [91]. The genomic amplification of NMYC appears to correlate with the prognosis of neuroblastoma [92]. Amplification by 16–200 fold has been noted in retinoblastoma cell lines [93, 94] and 5–170 fold in small cell lung cancer [95]. Tissues from patients with adenocarcinoma of the lung and those with untreated neuroblastoma have revealed amplification of NMYC [96, 97]. As regards BMYC, though expressed in similar levels in fetal and adult tissues, the highest levels were in the adult brain, hence designated as BMYC [98].

MYC was first isolated from chick embryo and was found to be homologous to the oncogene (VMYC) of the avian myelocytomatosis virus MC29 [99]. The MYC protein consists of a nuclear phosphoprotein of 65 KDa encoded in a helix–loop–helix leucine transcription factor, which activates growth promoting genes. A variety of transcriptional and suppressor proteins control the expression of MYC. Alteration in the MYC protein has been implicated in breast cancer and invasive bladder cancer. MYC is amplified and overexpressed in about 30% of in situ and advanced stages of breast cancer [87, 100]. The MYC protein has been identified in other tumours as well, such as B-cell lymphoma [101], Burkitt's lymphoma [102–104] and lung cancer [105]. Amplification of MYC has also been identified in small cell lung cancer [106]. Human promyelocytic leukemia and colon cancer cell lines also reveal amplification. In Burkitt's lymphoma the gene is translocated.

HER2 is located on chromosome 17q and encodes the human epidermal growth factor receptor type 2. Normal cells express HER2 in moderate levels. Amplification of this gene causes an increase in cell proliferation and also influences tumour growth, spread and response to therapy. The tumours, which overexpress this oncogene, may be more aggressive. HER2 is amplified in breast (25–30% amplification is seen in invasive breast cancer), ovarian and stomach cancers [107–109].

The p53 gene is located on chromosome 17 and produces a protein which acts as a transcription factor and prevents unregulated cell growth. The p53 protein is a negative regulator of cell proliferation and blocks the G1/S phase [110–112]. Mutations in p53 have been reported in 30% of breast cancers and 70% of colon cancers. The mutant allele is retained in 40% of breast cancers and 91% of colon cancers [113–119]. The p53 protein interacts with the DNA, hence when any damage to the DNA is detected, p53 can trigger apoptosis. The mutations in p53 may be sporadic events or inherited. In general, all cells carry the defect in those individuals who have inherited the defective copy of the gene. Two or more independent mutations are usually required for cancer to develop in those who have not inherited the gene.

So far, oligonucleotide sequences targetted against IGF1R, CCND1, MYC, KRAS, HER2 and the tumour suppressor p53 have been found to inhibit the abnormal cell proliferation in cancer [120–126]. Mitogen activated T cells are known to initiate the transcriptionally silent genes from the G0 to the G1/S stages. MYC is inhibited at the G1/S stage by antisense oligonucleotides [127]. A similar effect had been observed when antisense pentadecadeoxy-nucleotide targetted against MYC mRNA was used in promyelocytic leukemia cells [123].

The MYC activates cyclin D1 to induce the cells into S phase. A flow cytometry study of the cyclins in estrogen receptor positive human breast cancer cell line MCF-7 and tissue specimens of human breast carcinomas have revealed that these proteins are overexpressed in aneuploid and highly proliferative breast carcinomas [128] and hence cyclin D1 levels are useful indicators to predict the prognosis and overall survival. Estrogens regulate the MYC and cyclin D1 expression and function by a transcription mediated process. Cyclin D1 shows increased levels in the presence of estrogen stimulation in mammary cells [129–131]. In estrogen receptor positive tumours, overexpression of cyclin D1 mRNA has a direct correlation with a bad prognosis. High levels are thought to aid in the development of endocrine resistant disease [132]. Estrogen receptor and/or progesterone receptor positive breast cancer cells overexpress both CCND1 and IGF1R whereas overexpression of HER2 and MYC is typically seen in estrogen receptor negative breast cancer cells [133, 134]. Previous studies have proved the cytostatic effect of MYC antisense phosphorothioate oligonucleotide on the growth of estrogen independent MDA-MB-231 cell line. In estrogen stimulated cells, there was 75% inhibition of cell growth [135]. Antisense inhibition of cMYC mRNA in MCF-7 cells resulted in a decrease in the cyclin D1 expression and DNA synthesis. Similar effects were noted when the cells were treated with antiestrogen agents [131, 136].

From the above known factors, the authors hypothesize that for identification of the concerned mRNA, oligonuclides specific to the nature of each cancer cell need to be synthesized. Making use of such specific ligands that will not only attach themselves to the overexpressed mRNA in the cancer cells but can enter the cell would be ideal. Antisense oligonucleotides and antisense peptide nucleic acids (PNAs) are capable of recognizing and binding to the mRNA thereby entering the cell. Radiolabelling with gamma emitters such as ^{99m}Tc or positron emitting agents such as ^{64}Cu would render them highly useful as non-invasive, safe tools for detecting cancer in its earliest form.

On the basis of the above hypothesis, PNAs have been synthesized (Fig. 2). [82] and radiolabelled and extensive studies in breast and pancreatic cancer cell lines have revealed promising results. Basically, PNAs are synthetic

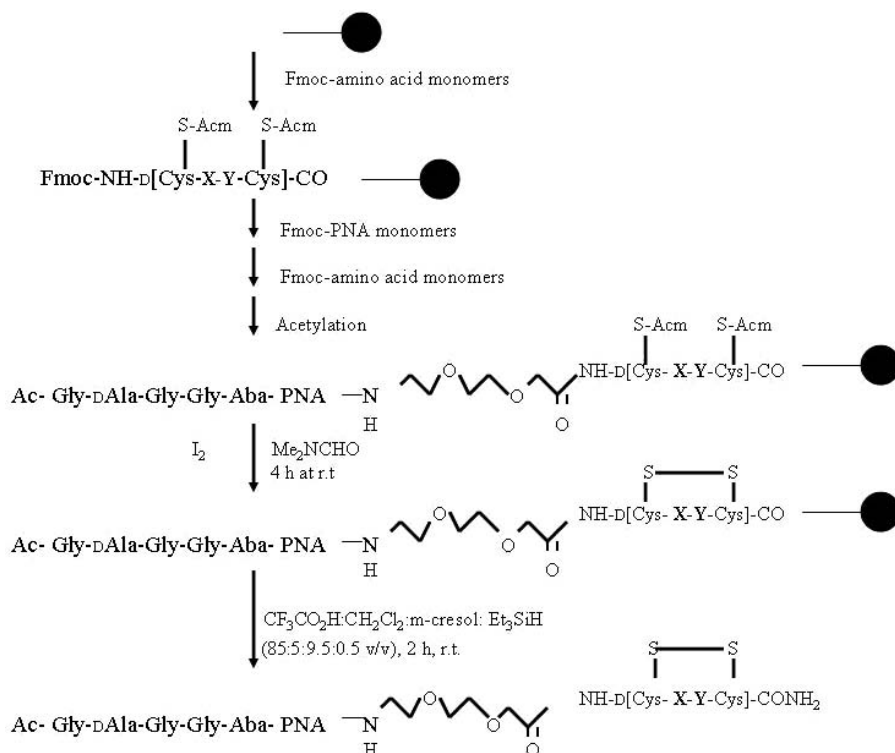


FIG. 2. Schematic representation of PNA synthesis PNA: 12-mer complementary to mRNAs of *CCND1*, *MYC*, *KRAS* and mismatched sequences. *X* and *Y* are ligand targeting to *IGF1R*: *X* = Ser, *Y* = Lys and for the mismatched peptide: *X* = Ala, *Y* = Ala (reproduced from Ref. [143] with permission).

analogues of DNA where the nucleobases are linked to a pseudo-peptide polymer backbone made of N-(2-aminoethyl) glycine units (Fig. 3) [82]. They hybridize to DNAs or RNAs with high affinity and specificity, essentially because of the uncharged and flexible polyamide backbone [137, 138]. They are also stable against nucleases and proteases and the solid phase synthesis [139]. Unlike the normal DNA, the PNA hybridization does not degrade the bound mRNA by RNase H [140]. When hybridized to RNA, the PNAs function in two ways: by targeting the mRNA to block protein synthesis and by inhibiting the enzymatic activities of ribonucleoproteins. When bound to the DNA, the gene transcription may be arrested or an artificial open complex may be created to promote transcription [141]. Addition of ligands enhances the cellular uptake [142].

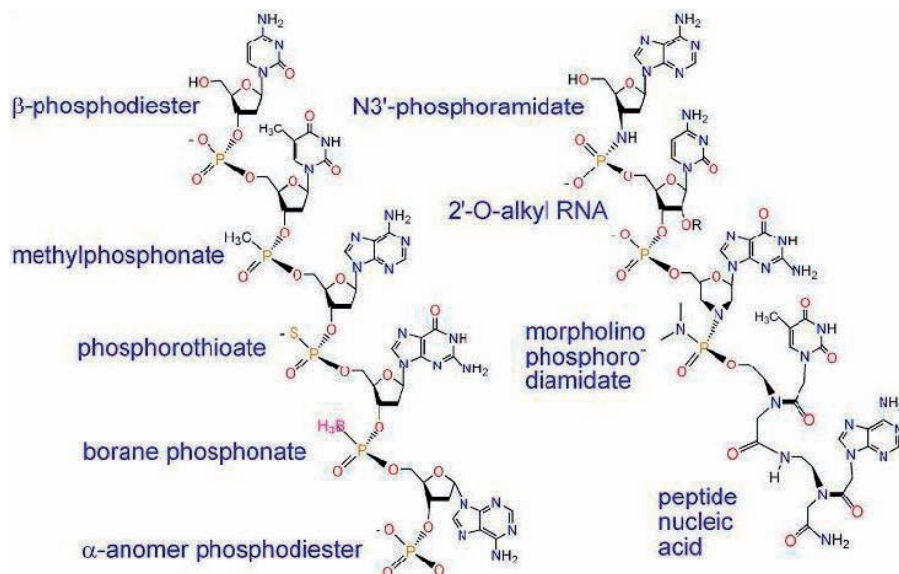


FIG. 3. Oligonucleotide backbone derivatives (reproduced from Ref. [82] with permission).

6. SYNTHESIS AND RADIOLABELLING OF PNA PROBES

Peptide-PNA-peptide probes have been synthesized by simultaneous use of peptide and DNA synthesizers [23, 143]. The authors later modified their technique and scaled up the process from 2 μ mol to 100 μ mol. Continuous solid phase synthesis was carried out such that the PNA probes carried cyclized peptide ligand analogues. The following sections describe the successful outcome of some of the probes, which are listed in Table 4.

6.1. Probe specific for MYC mRNA

A pentapeptide chelator-PNA, N-Gly-d-Ala-Gly-Gly-Aba-GCATCGTCGCGG, named WT3613 and specific for MYC mRNA was synthesized as described by Tian et al. [23] and labelled to ^{99m}Tc [144] (Fig. 4). A PNA mismatch control N-Gly-d-Ala-Gly-Gly-Aba-GCATGTCTGCGG (WT3629) was also synthesized. The chimeras were labelled to ^{99m}Tc and examined on a reverse phase high performance liquid chromatography column for the presence of unbound radioactivity [144]. Later, studies were carried out on a MYC

TABLE 4. ONCOGENE PROBES: SEQUENCE AND FUNCTION

Oncogene probe	Target/function	6.1. Chelator	PNA peptide sequence
WT3613	c-myc mRNA	Gly-D-Ala-Gly-Gly	GCATCGTCGCGG
WT3629	c-myc mRNA PNA mismatch	Gly-D-Ala-Gly-Gly	GCATGTCTGCGG
WT4261	myc mRNA and IGF1R	Gly-D-Ala-Gly-Gly	GCATCGTCGCGG-(Gly)4-D(Cys-Ser-Lys-Cys)
WT4185	CCND1 mRNA and IGF1R	AcGly-D(Ala)-Gly-Gly	CTGGTGTTCAT-D(Cys-Ser-Lys-Cys)
WT4172	CCND1 PNA mismatch	AcGly-D(Ala)-Gly-Gly	CTGGACAACCAT-D(Cys-Ser-Lys-Cys)
WT4113	CCND1 Peptide mismatch	AcGly-D(Ala)-Gly-Gly	CTGGTGTTCAT-D(Cys-Ala-Ala-Cys)
WT990	PNA-free	Gly- D (Ala)-Gly-Gly-Aba-(Gly)4	D(Cys-Ser-Lys-Cys)
WT4219	myc PNA antisense	AcGly-D(Ala)-Gly-Gly-aminobutanoate	GCATCGTCGCGG-D(Cys-Ser-Lys-Cys)
WT4235	myc PNA mismatch	AcGly-D(Ala)-Gly-Gly-aminobutanoate	GCATGTCTGCGG-D(Cys-Ser-Lys-Cys)
WT4351	Kras PNA antisense	SBTG2-DAP	GCCAACAGCTCC-D(Cys-Ser-Lys-Cys)
WT4433	Fluoresceinyl PNA antisense	SFX	CTGGTGTTCAT- D(Cys-Ser-Lys-Cys)
WT4361	Fluoresceinyl peptide mismatch	SFX	CTGGTGTTCAT- D(Cys-Ala-Ala-Cys)

mRNA and IGF1R specific cyclized chelator-PNA-peptide, N-Gly-d-Ala-Gly-Gly-Aba-GCATCGTCGCGG-(Gly)4-d(Cys-Ser-Lys-Cys) named WT4261 [82]. The use of d-aminoacids in the synthesis of the cyclic peptide analogue of IGF1 was found to improve the cellular uptake and the stability. Among them, JB3, d(Cys-Ser-Lys-Ala-Pro-Lys-Leu-Pro-Ala-Ala-Tyr-Cys) was found to inhibit the growth of cancer cells [145]. Tian et al. [82] used a smaller cyclized d-aminoacid sequence JB9, d(Cys-Ser-Lys-Cys) [d(CSKC)] for conjugating with the PNA (Fig. 5) [82]. The N-terminus of the d-aminoacid was then extended to accommodate the PNA specific for the IGF1R mRNA (Fig. 6) [24].

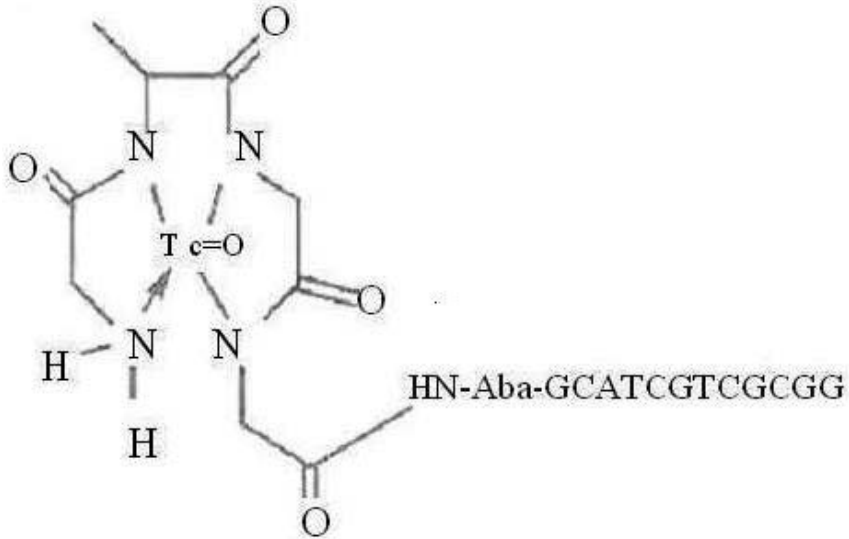


FIG. 4. Structure of *N*-Gly-d-Ala-Gly-Gly-Aba-GCATCGTCGCGG [WT3613], specific for *cMYC* mRNA (reproduced from Ref. [144] with permission).

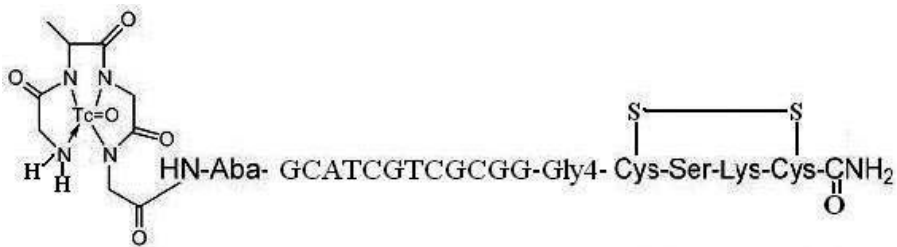


FIG. 5. ^{99m}Tc chelate PNA-peptide specific for *MYC* RNA and *IGF1R* (reproduced from Ref. [82] with permission).



FIG. 6. PNA-peptide specific for *IGF1R* mRNA and *IGF1* receptor (reproduced from Ref. [24] with permission).

6.2. Probe specific for CCND1 mRNA and IGF1R

The IGF1 analogue d(Cys-Ser-Lys-Cys) was assembled by 9-fluorenyl methoxy carbonyl (Fmoc) coupling followed by the incorporation of the linker aminoethoxyethoxyacetic acid (AEEA) and PNA monomers into the N-terminus of the peptide resin. The chelator Fmoc-Gly- d-Ala-Gly-Gly-Aba was then coupled to the N-terminus of the PNA-peptide, acetylated and the cysteine residues cyclized [146]. The purified cyclized peptide-PNA-peptide chimera AcGly-d-Ala-Gly-Gly-Aba-CTGGTGTTCAT-AEEA-d(CSKC), WT4185, was specific for CCND1 mRNA and IGF1R labelled to ^{99m}Tc [146]. Labelling to ^{99m}Tc was carried out by conjugating with the N_4 chelator, Gly-d-Ala-Gly-Gly-aminobutanoate (GDAGGB). The chimera, WT4185 (Fig. 7) [146], was tested along with a PNA mismatch control, WT4172, AcGDAGGB-CTGGACAACCAT-AEEA-d(CSKC), IGF1 peptide alanine substitution control, WT4113, AcGDAGGB-CTGGTGTTCAT-AEEA-d(CysAlaAlaCys) and the PNA free control, WT990, AcGDAGGB-(Gly)₄-d(CSKC). For internalization studies, fluorescent probes were synthesized by solid phase coupling of 6-(fluorescein-5-carboxamido)hexanoic acid, succinimidyl ester to the AEEA-PNA-peptide. WT4433 was designated to the fluorescent PNA antisense chimera and WT4361 to the fluorescent PNA mismatch [146].

6.3. Probe specific for MYC mRNA and IGF1R

Another cyclized peptide-PNA-peptide chimera, AcGly-d-Ala-Gly-Gly-Aba-GCATCGTCGCGG-AEEA-d(CSKC), WT4219, specific for MYC mRNA and IGF1R was synthesized, purified and labelled to ^{99m}Tc following the procedure described above. The PNA mismatch, AcGly-d-Ala-Gly-Gly-

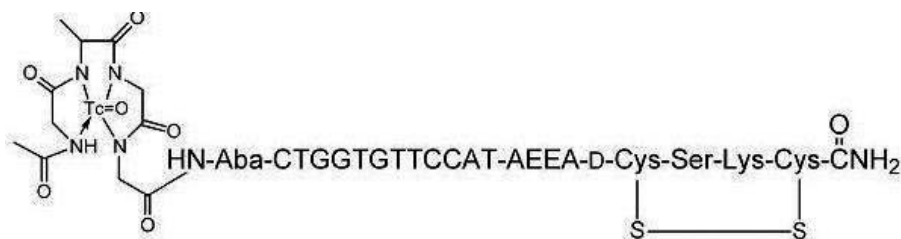


FIG. 7. Structure of ^{99m}Tc -AcGlyD(Ala)GlyGlyAba-CTGGTGTTCAT-AEEA-D(CysSerLysCys), WT4185, chelator-PNA-peptide designed to bind to IGF1R, to be internalized and hybridize with CCND1 mRNA (reproduced from Ref. [146] with permission).

Aba-GCATGTCTGCGG-AEEA-d(CSKC), WT4235 was also synthesized for *in vitro* and *in vivo* studies [147].

6.4. Probe specific for KRAS mRNA

For PET imaging, the peptide analogue d(CSKC) was modified by extending the C to N by Fmoc [24] by using S-benzoyl thioglycolic acid (SBTG) moiety as the chelator and linking the same to the amine groups in diaminopropanoate (DAP). AEEA was used as a spacer and this was followed by DAP and the chelator moiety SBTG to create the final mutant sequence, SBTG₂DAP-PNA-peptide chimera, specific for KRAS mRNA and the IGF1R (WT4315) which was labelled to ⁶⁴Cu (Fig. 8) [24].

7. CELLULAR INTERACTIONS AND IN VIVO STUDIES OF THE ABOVE PROBES

7.1. Probe specific for MYC mRNA

The pentapeptide chelator-PNA, N-Gly-d-Ala-Gly-Gly-Aba-GCATCGTCGCGG, WT3613 specific for MYC mRNA, labelled to ^{99m}Tc was studied in xenografts bearing BT474 estrogen receptor or MCF7: IGF1R, estrogen receptor plus human breast cancer cells along with the mismatch control WT3629. Biodistribution in the tumours, which were allowed to grow to up to 1 cm in diameter, revealed a twofold uptake at 4 h with the antisense probe, when compared with the control. The tumour activity decreased significantly at 24 h for both the control and the antisense probes. Quantification of cMYC mRNA in untreated MCF7 human breast cancer cell line as well as

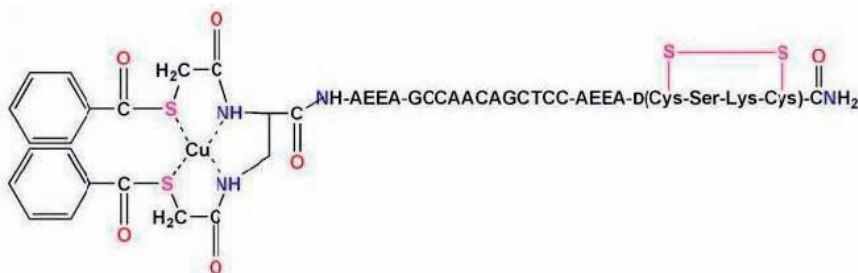


FIG. 8. Cu-64-SBTG₂DAP-PNA-peptide specific for KRAS mRNA and IGF1 receptor (reproduced from Ref. [24] with permission).

MCF7 treated with the peptide PNA chimera WT3613 using real time polymerase chain reaction (RT-PCR) did not, however, reveal any difference between the treated and untreated cells [144]. However, cellular interaction with MCF-7 cells carried out under similar settings with N-Gly-d-Ala-Gly-Gly-Aba-GCATCGTCGCGG-(Gly)₄-d(Cys-Ser-Lys), where the d(Cys-Ser-Lys) represented the peptide ligand, revealed a fourfold inhibition of the RT-PCR products. It can hence be assumed that purified cMYC-myc antisense peptide-PNA-peptide probe will hybridize more accurately to the mRNA. Planar scintigraphic imaging at 4 and 2 h post-administration of ^{99m}Tc labelled WT3613 (MYC-PNA-probe without the IGF1 analogue) and the mismatch WT3629 was studied in cohorts of 5 immuno compromised mice bearing MCF7: IGF1R, estrogen receptor plus human breast cancer cells. The PNA free control used was WT990- Gly-d-Ala-Gly-Gly-Aba-(Gly) 4-d(Cys-Ser-Lys-Cys). The tumour xenografts revealed a higher uptake of the myc-PNA antisense, whereas the myc mismatch probe WT3629 revealed no change to either the cellular or tissue distribution, thus proving the role of ^{99m}Tc-peptide-PNA probes in the imaging of gene expression in malignancy [144].

7.2. Probe specific for CCND1 mRNA and IGF1R

The cyclized peptide-PNA-peptide chimera WT4185, AcGDAGGB-CTGGTGTTCAT-AEEA-d(CSKC), specific for CCND1 mRNA and IGF1R was internalized by the MCF7 human breast cancer cells and down regulation of the cyclin D1 protein (by 56%) was observed when injected into the xenografts. Tissue distribution revealed significant retention in the xenografts 12 h post-administration of the antisense probe as did the scintigraphy. The tumour intensity at 24 h was sevenfold higher than the contralateral normal site. These observations were not seen in the mismatches and the control sequences (Fig. 9, [146]).

7.3. Probe specific for MYC mRNA and IGF1R

The chelator-PNA-peptide chimera, specific for myc mRNA and IGF1R, AcGDAGGB-GCATCGTCGCGG-AEEA-d(CSKC), WT4219, was also labelled to ^{99m}Tc and studied in xenografts bearing MCF7:IGF1R. There was a steady increase in tumour to blood and tumour to muscle ratios over 24 h. The tumours were also readily detected on the scintigraphy. The PNA mismatch, AcGDAGGB-GCATGTCTGCGG-AEEA-d(CSKC), WT4235, synthesized and tested as above however did not reveal tumour uptake [147] (Fig. 10 [24]).

Besides studying the internalization of the PNA-peptide chimeras by MCF7:IGF1R cells, oncogene expression in estrogen receptor negative, BT474

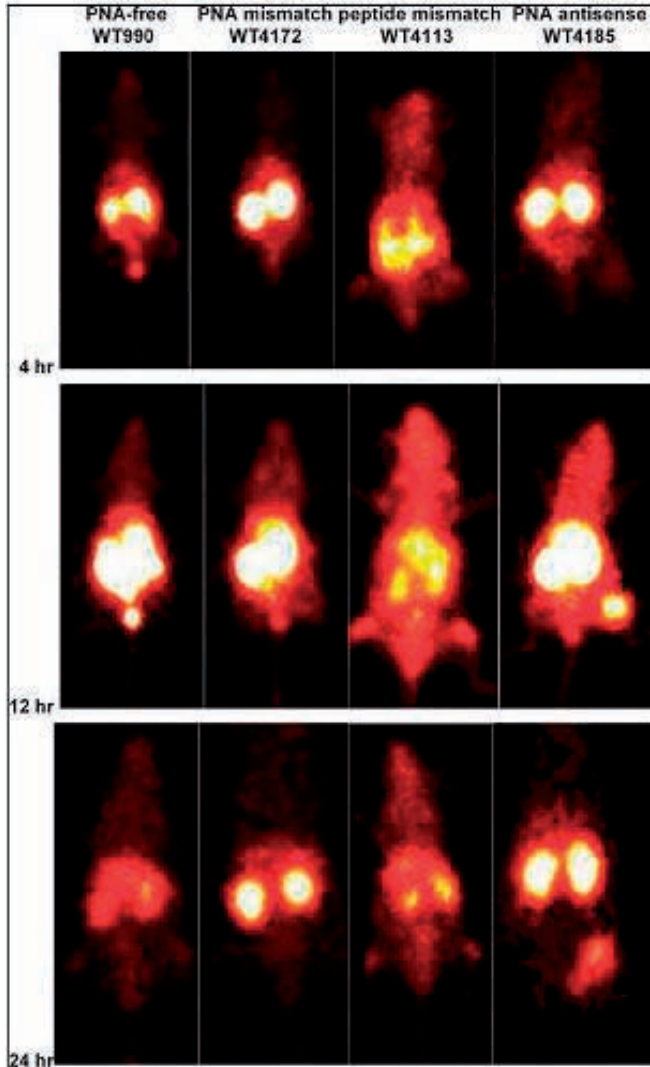


FIG. 9. Scintigraphic images of ^{99m}Tc labelled probes in nude mice bearing human MCF7:IGF1R estrogen receptor positive breast tumour cell xenografts. Images were acquired 4, 12, and 24 h post-injection of the PNA-free control probe, WT990, the PNA mismatch control probe, WT4172, the peptide mismatch control probe, WT4113, and the PNA antisense probe, WT4185 (reproduced from Ref. [146] with permission).

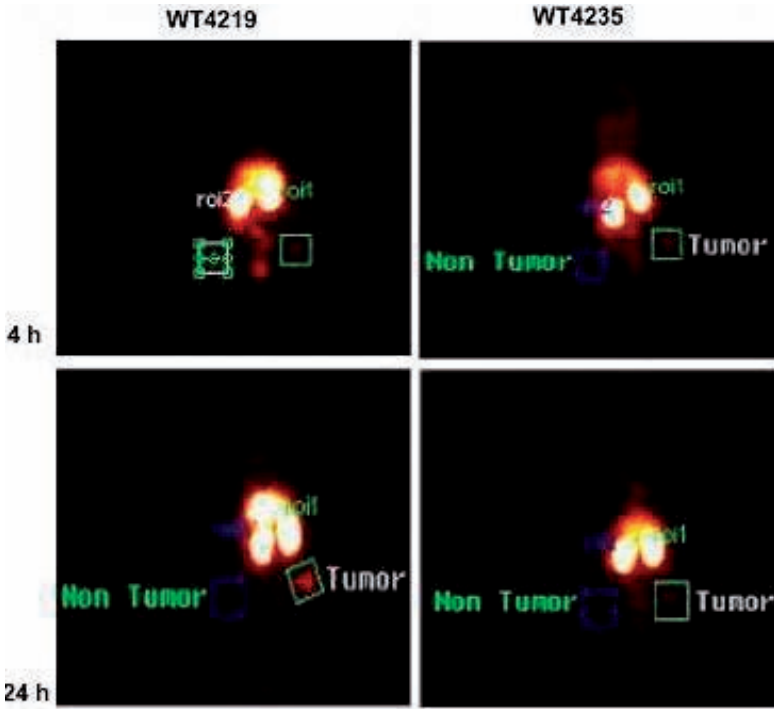


FIG. 10. Scintigraphic images of ^{99m}Tc labelled AcGDAGGB-PNA-peptides 4 and 24 h post-injection in immunocompromised mice bearing human MCF7:IGF1R estrogen receptor plus breast tumour cell xenografts. Left: ^{99m}Tc -WT4219 MYC antisense probe; right: ^{99m}Tc -WT4235 MYC mismatch control (reproduced from Ref. [24] with permission).

human breast cancer cells, which overexpress HER2 and MYC oncogenes, was compared with MCF7:IGF1R human breast by quantitative reverse transcription polymerase chain reaction. Approximately 8000 MYC mRNAs and 8000 CCND1 mRNAs per MCF7:IGF1R cell were estimated [24]. The injected MYC probe ^{99m}Tc -WT4219 and the CCND1 probe ^{99m}Tc -WT4185 were thus found to bind to 5% and 10% of the MYC and CCND1 mRNAs respectively [24].

8. IMAGING ONCOGENE EXPRESSION IN OTHER CANCERS

The encouraging results noted above suggest that imaging oncogenes could be applied to patients with high risk of breast malignancy and similar

SESSION 3

probes for other oncogenes could be synthesized and labelled to ^{99m}Tc or ^{64}Cu , rendering this an easy invasive tool for the early detection of other cancers as well.

Favourable results have been observed with KRAS specific probes. KRAS mutation has been observed in 90% of pancreatic cancers [148]. In vitro and in vivo studies in pancreatic cancer cell lines have demonstrated anti-proliferative activity with KRAS phosphorothionate oligonucleotides [125]. The KRAS antisense probe, WT4351 [SBTG₂DAP-AEEA-GCCAACAGCTCC-AEEA-D(CSKC)], was synthesized and labelled with ^{99m}Tc as well as ^{64}Cu . Cellular interactions with AsPC1 human pancreatic cancer cell line revealed about 2000 KRAS mRNA/cell for AsPC1 [24, 149]. Studies in xenografted human pancreatic cancer cell line AsPC1 revealed tumour to contralateral muscle image intensity ratios of 5.4 at 4 h and 2.7 at 24 h after injection of the ^{99m}Tc labelled probe. PET images of ^{64}Cu -KRAS antisense probe, WT4351, in tumour bearing mice revealed tumour to muscle image intensity ratios of 2.0 at 4 h and 3.0 at 24 h [149], (Fig. 11 [24]).

KRAS mutations have also been noted in colon cancer. Of the colon cancers, 30% are attributed to the changes in KRAS [150]. Primary and metastatic colon cancers are known to overexpress Gyanyl Cyclase C (GC-C), a receptor for the heat stable enterotoxin STa produced by *Eschericia coli*

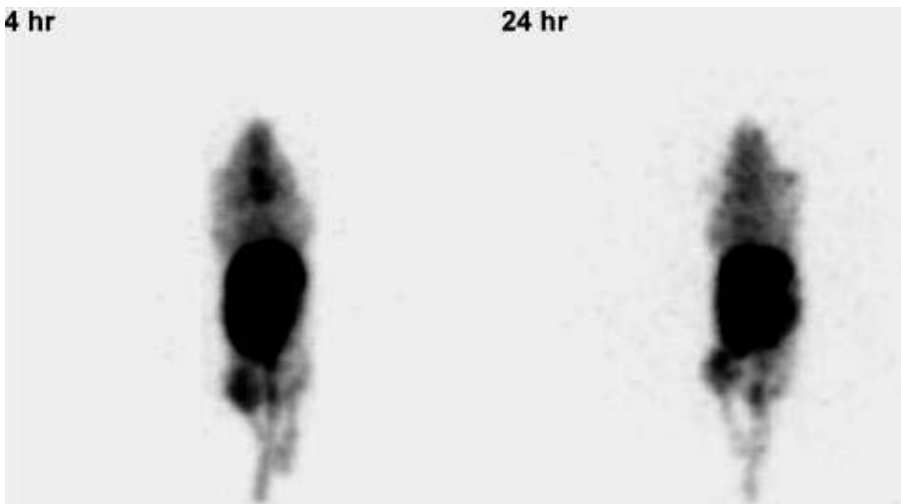


FIG. 11. PET imaging of ^{64}Cu -WT4351, SBTG₂DAP-KRAS PNA-peptide in AsPC1 pancreatic xenografts 4 and 24 h post-injection of the probe (reproduced from Ref. [24] with permission).

[151]. STa is made up of 13 amino acids where the enterogenic toxicity is attributed to the cys 5 to cys 17 residues. An analogue of STa was designed by replacing the cys 6 and cys 17 by two Ala residues and in vitro tests have asserted that it is comparable to the natural STa [143].

As stated earlier, amplification of the gene or overexpression of the HER2/neu protein has been identified in breast cancers. Breast cancer cells are known to overexpress a tyrosine kinase receptor, ERBB2. A hundredfold increase in expression has been reported when compared with normal cells. Gene amplification and increased transcription are the other changes which have been documented [152–155]. The ERBB2 gene encodes an 185KDa protein, *erb2*, that is found on the surface of secretory epithelial cells. Monoclonal antibodies specific to the ERBB2 protein have been used to decrease the expression of this gene as described earlier in this text. The phosphorothioate oligonucleotide probe labelled to ^{99m}Tc and specific for HER2 mRNA was studied in the SKBR3 cell line, which overexpresses HER2. However, the probe as well as the scrambled control exhibited similar equivocal results (S. Basu, E. Wickstrom, and M.L.Thakur, unpublished data, 1995). Intracellular delivery of antisense phosphorothioate oligomers by the addition of Lipofecin were found to down regulate the overexpressed ERBB2 in 33% of the SK-BR3 breast cancer cells. The antisense CTCATGGT-GCTCAC and the scrambled control CGCCTTATCCGTAGC were both tested. The effect of the control was only 4.5% [156]. More work is in progress with ^{64}Cu labelling using DOTA-PNA-peptide chimera.

9. DISCUSSION

In a malignant cell, the earliest change noted is the genomic mutation that leads to uncontrolled cell division and targeting these changes are critical in the diagnosis and management. Synthesis of chelator-peptide-PNA by continuous solid phase has yielded stable probes for imaging the MYC, CCND1, IGF1R and KRAS oncogenes. The initial study by Rao et al. revealed that the c MYC antisense probe WT3613 that lacked the receptor specific ligand revealed tumour activity. But the effects on c MYC mRNA in the MCF7 human breast cancer cell lines were better with the antisense probe with the ligand. This led to the modification in the synthesis of a chelator PNA- peptide WT4261 specific for MYC mRNA and IGF1R. The terminal amino group needed to be acetylated which enables cyclization of the disulphide bonds onto the PNA-peptide sequence [82]. The PNA was thus conjugated with the cyclic peptide analogue of IGF1, d(Cys-Ser-Lys-Cys) which improved the stability. Cyclized peptide-PNA-peptide probe chimera specific for CCND1 mRNA and IGF1R

(WT4185) synthesized using the above modification and labelled successfully to ^{99m}Tc revealed encouraging results in terms of internalization by the human breast cancer cell line MCF7. The probe also down regulated the CCND1 levels after internalization. The control probes did not show the above properties. Further research led to the synthesis of WT4219, another peptide-PNA-peptide probe specific for MYC mRNA and IGF1R and WT4315, which target KRAS mRNA. The listed chimera have been successfully labelled to ^{99m}Tc and the WT4315 to both ^{99m}Tc as well as PET agent ^{64}Cu . The images on xenografts bearing human breast and pancreatic cancer cell lines have been efficient in localizing the tumours, which did not exceed 1 cm. PNAs were chosen because they were more stable than normal DNA and hybridize more specifically to RNA. Radiolabelling and scintigraphy, as well as PET imaging, can detect gene expression in cancer cells as seen in the examples described in the above. The procedure is non-invasive and specific and has proven its efficiency in respect of oncogenes such as MYC, CCND1, KRAS and also in exogenous receptors such as VPAC1 in animal models. More work is in progress with respect to PET imaging and also identifying genetic expression in early pancreatic and prostate cancer.

10. CONCLUSION

Cancer is a complex and lethal disease. Experts advocate that if diagnosed early, an aggressive therapeutic intervention can be initiated, early enough to arrest its growth and further spread, This may spare patients from severe morbidity and mortality.

Advances in genomics and proteomics have provided a wealth of knowledge on the biological basis of cancer and thereby provided a host of biomarkers that can be targetted specifically to identify, early enough, the cells that have undergone genomic modulations that initiate abnormal cell proliferation.

The authors' studies [21, 23, 24, 75–78, 82, 123–125, 129, 143, 144, 146, 147], although in their infancy, have paved the way for a novel genomic approach that promise to utilize the specific biomarkers expressed exogenously and endogenously that not only take advantage of the biomedical basis of tumourogenesis but also of the recent advances in imaging instrumentation that have improved image resolution extensively.

The successful translational research of today is the clinical practice of tomorrow. It is to be hoped that this genomic approach will, sooner or later, help patients with regard to the early and accurate diagnosis not only of breast cancer but other cancers as well.

ACKNOWLEDGEMENTS

The work was supported by NIH grants CA109231 and CA 42960, 1R24 CA86307, Department of Energy grant ER63055.

REFERENCES

- [1] BOMANJI, J., CONRY, B.G., BRITTON, K.E., REZNEK, R.H., Imaging neural crest tumours with ¹²³I-metaiodobenzylguanidine and X-ray computed tomography: a comparative study, *Clin. Radiol.* **39** (1988) 502–506.
- [2] HOEFNAGEL, C.A., VOUTE, P.A., DE KRAKER, J., MARCUSE, H.R., Radionuclide diagnosis and therapy of neural crest tumors using iodine-131 metaiodobenzylguanidine, *J. Nucl. Med.* **28** (1987) 308–314.
- [3] SHAPIRO, B., SISSON, J.C., SHULKIN, B.L., GROSS, M.D., ZEMPEL, S., The current status of radioiodinated metaiodobenzylguanidine therapy of neuroendocrine tumors, *Q. J. Nucl. Med.* **39** (1995) 55–57.
- [4] KRENNING, E.P., et al., Localisation of endocrine-related tumours with radioiodinated analogue of somatostatin, *Lancet* **1** (1989) 242–244.
- [5] KRENNING, E.P., et al., Somatostatin receptor scintigraphy with indium-111-DTPA-D-Phe-1- octreotide in man: metabolism, dosimetry and comparison with iodine-123-Tyr-3-octreotide, *J. Nucl. Med.* **33** (1992) 652.
- [6] KRENNING, E.P., et al., Somatostatin receptor scintigraphy with ¹¹¹In-DTPA-D-Phe1 and ¹²³I-TYR₃-octreotide: the Rotterdam experience with more than 1,000 patients, *Eur. J. Nucl. Med.* **20** (1993) 716–731.
- [7] BLUM, J.E., HANDMAKER, H., LISTER-JAES, J., RINNE, N., A multi center trial with a somatostatin analogue ^{99m}Tc depreotide in the evaluation of solitary pulmonary nodules, *Chest* **117** (2000) 1232–1238.
- [8] WEINER, R.E., THAKUR, M.L., Radiolabeled peptides in oncology: role in diagnosis and treatment, *Bio Drugs* **19** (2005) 145–163.
- [9] WEINER, R.E., THAKUR, M.L., Radiolabeled peptides in the diagnosis and therapy of oncological diseases, *Appl. Radiat. Isot.* **57** (2002) 749–763.
- [10] DREBIN, J.A., LINK, V.C., GREENE, M.I., Monoclonal antibodies specific for the neu oncogene product directly mediate anti-tumor effects in vivo, *Oncogene* **2** (1988) 387–394.
- [11] STANCOVSKI, I., et al., Mechanistic aspects of the opposing effects of monoclonal antibodies to the ERBB2 receptor on tumor growth, *Proc. Natl. Acad. Sci. USA* **66** (1991) 8691–8695.
- [12] BACUS, S.S., et al., Tumor-inhibitory monoclonal antibodies to the HER-2/Neu receptor induce differentiation of human breast cancer cells, *Cancer Res.* **52** (1992) 2580–2589.

SESSION 3

- [13] MAIER, L.A., et al., Requirements for the internalization of a murine monoclonal antibody directed against the HER-2/neu gene product c-erbB-2, *Cancer Res.* **51** (1991) 5361–5369.
- [14] ABDEL-NABI, H., et al., In-111-labeled monoclonal antibody immunoscintigraphy in colorectal carcinoma: safety, sensitivity, and preliminary clinical results, *Radiology* **175** (1990) 163–171.
- [15] PINKAS, L., ROBINS, P.D., FORSTROM, L.A., MAHONEY, D.W., MULLAN, B.P., Clinical experience with radiolabelled monoclonal antibodies in the detection of colorectal and ovarian carcinoma recurrence and review of the literature, *Nucl. Med. Commun.* **20** (1999) 689–696.
- [16] DOERR, R.J., ABDEL-NABI, H., KRAG, D., MITCHELL, E., Radiolabeled antibody imaging in the management of colorectal cancer, Results of a multi-center clinical study, *Ann. Surg.* **214** (1991) 118–224.
- [17] SURWIT, E.A., et al., Clinical assessment of 111In-CYT-103 immunoscintigraphy in ovarian cancer, *Gynecol. Oncol.* **48** (1993) 285–292.
- [18] ROSS, J.S., FLETCHER, J.A., The HER-2/neu oncogene in breast cancer: Prognostic factor, predictive factor, and target for therapy, *The Oncologist* **3** (1998) 237–252.
- [19] ALLAN, S.M., et al., Clinicoradioimmuno-localization with a rat monoclonal antibody directed against C-erb B2, *Cell Biophys* **24** (1994) 93–98.
- [20] VIRGOLINI, I., et al., Cross-competition between vasoactive intestinal peptide and somatostatin for binding to tumor cell membrane receptors, *Cancer Res.* **54** (1994) 690–700.
- [21] THAKUR, M.L., et al., 99mTc-labeled vasoactive intestinal peptide analog for rapid localization of tumors in humans, *J. Nucl. Med.* **41** (2000) 107–110.
- [22] SHI, N., BOADO, R.J., PARDRIDGE, W.M., Antisense imaging of gene expression in the brain in vivo, *Proc. Natl. Acad. Sci. USA* **97** (2000) 14709–14714.
- [23] TIAN, X., WICKSTROM, E., Continuous solid-phase synthesis and disulfide cyclization of peptide-PNA-peptide chimeras, *Org. Lett.* **4** (2002) 4013–4016.
- [24] TIAN, X., et al., External imaging of CCND1, MYC, and KRAS oncogene mRNAs with tumor-targeted radionuclide-PNA-peptide chimeras, *Ann. N.Y. Acad. Sci.* **1059** (2005) 106–144.
- [25] AMERICAN CANCER SOCIETY, 2004: Cancer facts and figures.
- [26] PRIMIC-ZAKELJ, M., Screening mammography for early detection of breast cancer, *Ann. Oncol.* **10** (Suppl.) (1999) 121–127.
- [27] LANNIN, D.R., et al., Difficulties in diagnosis of carcinoma of the breast in patients less than fifty years of age, *Surg. Gynaecol. Obstet.* **177** (1993) 457–462.
- [28] ROSENBERG, R.D., et al., Effects of age, breast density, ethnicity, and estrogen replacement therapy on screening mammographic sensitivity and cancer stage at diagnosis: review of 183,134 screening mammograms in Albuquerque, New Mexico, *Radiology* **209** (1998) 511–518.
- [29] BUIST, D.S.M., PORTER, P.L., LEHMAN, C., TAPLIN, S.H., WHITE, E., Factors contributing to mammography failure in women aged 40–49 years, *J. Natl. Cancer Inst.* **96** (2004) 1432–1440.

- [30] CHITI, A., et al., Case report: technetium-99m-hexakis-2-methoxy-isobutyl-isonitrile imaging of breast cancer and myocardial infarction in the same patient, *Tumori* **80** (1994) 480–481.
- [31] BOMBARDIERI, E., et al., Nuclear medicine advances in breast cancer imaging, *Tumori* **87** (2001) 277–287.
- [32] SCOPINARO, F., et al., Technetium-99m sestamibi: an indicator of breast cancer invasiveness, *Eur. J. Nucl. Med.* **21** (1994) 984–987.
- [33] LIU, Z., et al., Imaging recognition of inhibition of multidrug resistance in human breast cancer xenografts using 99mTc-labeled sestamibi and tetrofosmin, *Nucl. Med. Biol.* **32** (2005) 573–583.
- [34] CORDOBES, M.D., et al., Technetium-99m-sestamibi uptake by human benign and malignant breast tumor cells: correlation with *mdr* gene expression, *J. Nucl. Med.* **37** (1996) 286–289.
- [35] PAPPO, I., HORNE, T., WEISSBERG, D., WASSERMAN, I., ORDA, R., The usefulness of MIBI scanning to detect underlying carcinoma in women with acute mastitis, *Breast J.* **6** (2000) 126–129.
- [36] BEANEY, R.P., LAMMERTSMA, A.A., JONES, T., MCKENZIE, C.G., HALNAN, K.E., Positron emission tomography for in vivo measurement of regional blood flow, oxygen utilization and blood volume in patients with breast carcinoma, *Lancet* **1** (1984) 131–134.
- [37] BROWN, R.S., WAHL, R.L., Overexpression of GLUT-1 glucose transport in human breast cancer: an immunohistochemical study, *Cancer* **72** (1993) 2979–2985.
- [38] PAUWELS, E.K.J., STURM, E.J., BOMBARDIERI, E., CLETON, F.J., STOKKEL, M.P., Positron-emission tomography with (18F) fluorodeoxyglucose, *J. Cancer Res. Clin. Oncol.* **126** (2000) 549–559.
- [39] WALTER, C., et al., Clinical and diagnostic value of preoperative MR mammography and FDG-PET in suspicious breast lesions, *Eur. Radiol.* **13** (2003) 1651–1656.
- [40] AVRIL, N., et al., Breast imaging with positron emission tomography and fluorine-18 fluorodeoxyglucose: use and limitations, *J. Clin. Oncol.* **18** (2000) 3495–3502.
- [41] WAHL, R.L., SIEGEL, B.A., COLEMAN, R.E., GATSONIS, C.G., PET STUDY GROUP, Prospective multicenter study of axillary nodal staging by positron emission tomography in breast cancer: a report of the staging breast cancer with PET Study Group, *J. Clin. Oncol.* **22** (2004) 277–285.
- [42] MCDONOUGH, M.D., DEPERI, E.R., MINCEY, B.A., The role of positron emission tomographic imaging in breast cancer, *Curr. Oncol. Rep.* **6** (2004) 62–68.
- [43] VAN BROCKLIN, H.F., POMPER, M.G., CARLSON, K.E., WELCH, M.J., KATZENELLENBOGEN, J.A., Preparation and evaluation of 17-ethynyl-substituted 16 alpha-[18F]fluoroestradiols: selective receptor-based PET imaging agents, *Int. J. Rad. Appl. Instrum.* **19 B** (1992) 363–374.
- [44] BOMBARDIERI, E., CRIPPA, F., PET imaging in breast cancer, *Q. J. Nucl. Med.* **45** (2001) 245–256.

SESSION 3

- [45] MA, X.J., et al., Gene expression profiles of human breast cancer progression, *Proc. Natl. Acad. Sci. USA* **100** (2003) 5974–5979.
- [46] REUBI, J.C., In vitro identification of vasoactive intestinal peptide receptors in human tumors: implications for tumor imaging, *J. Nucl. Med.* **36** (1995) 1846–1853.
- [47] VIRGOLINI, I., Vasoactive intestinal peptide receptor scintigraphy, *J. Nucl. Med.* **36** (1995) 1732–1739.
- [48] REUBI, J.C., Regulatory peptide receptors in human hepatocellular carcinomas, *Gut* **45** (1999) 766–774.
- [49] RADERER, M., et al., Comparison of iodine-123 vaso active intestinal peptide receptor scintigraphy and indium-111-CYT-103 immunoscintigraphy, *J. Nucl. Med.* **37** (1996) 1480–1487.
- [50] SAID, S.I., MUTT, V., Polypeptide with broad biological activity: Isolation from small intestine, *Science* **169** (1970) 1217–1218.
- [51] MOODY, T.W., Peptides and growth factors in non-small cell lung cancer, *Peptides* **17** (1996) 545–555.
- [52] BLUM, A.M., et al., Murine mucosal T cells have VIP receptors functionally distinct from those on intestinal epithelial cells, *J. Neuroimmunol.* **39** (1992) 101–108.
- [53] COUVINEAU, A., LABURTHE, M., The human vasoactive intestinal peptide receptor: molecular identification by covalent cross-linking in colonic epithelium, *J. Clin. Endocrinol. Metab.* **61** (1985) 50–55.
- [54] PAUL, S., SAID, S.I., Characterization of receptors for vasoactive intestinal peptide solubilized from the lung, *J. Biol. Chem.* **262** (1987) 158–162.
- [55] SREEDHARAN, S.P., ROBICHON, A., PETERSON, K.E., GOETZL, E.J., Cloning and expression of the human vasoactive intestinal peptide receptor, *Proc. Natl. Acad. Sci. USA* **88** (1991).
- [56] EL BATTARI, A., et al., Solubilization of the active vasoactive intestinal peptide receptor from human colonic adenocarcinoma cells, *J. Biol. Chem.* **263** (1988) 17685–17689.
- [57] SVOBODA, M., DE NEEF, P., TASTENOY, M., CHRISTOPHE, J., Molecular characteristics and evidence for internalization of vasoactive-intestinal-peptide (VIP) receptors in the tumoral rat-pancreatic acinar cell line AR 4-2 J, *Eur. J. Biochem.* **176** (1988) 707–713.
- [58] MIYATA, A., et al., Isolation of a novel 38 residue-hypothalamic polypeptide which stimulates adenylate cyclase in pituitary cells, *Biochem. Biophys. Res. Commun.* **164** (1989) 567–574.
- [59] GOTTSCHALL, P.E., TATSUNO, I., MIYATA, A., ARIMURA, A., Characterization and distribution of binding sites for the hypothalamic peptide, pituitary adenylate cyclase-activating polypeptide, *Endocrinology* **127** (1990) 272–277.
- [60] HARMAR, T., LUTZ, E., Multiple receptors for PACAP and VIP, *Trends Pharmacol. Sci.* **15** (1994) 97–99.
- [61] ZIA, F., et al., Pituitary adenylate cyclase activating peptide receptors regulate the growth of non-small cell lung cancer cells, *Cancer Res.* **55** (1995) 4886–4891.

- [62] REUBI, J.C., et al., Vasoactive intestinal peptide/pituitary adenylate cyclase activating peptide receptor subtypes in human tumors and their tissues of origin, *Cancer Res.* **60** (2000) 3105–3112.
- [63] VIRGOLINI, I., et al., Vasoactive intestinal peptide-receptor imaging for the localization of intestinal adenocarcinomas and endocrine tumors, *N. Engl. J. Med.* **331** (1994) 1116–1121.
- [64] GESPACH, C., BAWAB, W., DE CREMOUX, P., CALVO, F., Pharmacology, molecular identification and functional characteristics of vasoactive intestinal peptide receptors in human breast cancer cells, *Cancer Res.* **48** (1988) 5079–5083.
- [65] MOODY, T.W., et al., (Arg15, Arg21) VIP: evaluation of biological activity and localization to breast cancer tumors, *Peptides* **19** (1998) 585–592.
- [66] ZIA, H., et al., Breast cancer growth is inhibited by vasoactive intestinal peptide (VIP) hybrid, a synthetic VIP receptor antagonist, *Cancer Res.* **56** (1996) 3486–3489.
- [67] ZIA, H., et al., PACAP receptors are present on breast cancer cell lines, *Am. Assoc. Cancer Res.* **38** (1997) 117.
- [68] LE MEUTH, V., et al., Characterization of binding sites for VIP-related peptides and activation of adenylate cyclase in developing pancreas, *Am. J. Physiol.* **260** (1991) G265–274.
- [69] BASILLE, M., GONZALEZ, B.J., FOURNIER, A., VAUDRY, H., Ontogeny of pituitary adenylate cyclase-activating polypeptide (PACAP) receptors in the rat cerebellum: a quantitative autoradiographic study, *Brain Res. Dev.* **82** (1994) 81–89.
- [70] VERTRONGEN, P., CAMBY, I., DARRO, F., KISS, R., ROBBERECHT, P., VIP and pituitary adenylate cyclase activating polypeptide (PACAP) have an antiproliferative effect on the T98G human glioblastoma cell line through interaction with VIP2 receptor, *Neuropeptides* **30** (1996) 491–496.
- [71] OLIANAS, M.C., ENNAS, M.G., LAMPIS, G., ONALI, P., Presence of pituitary adenylate cyclase-activating polypeptide receptors in Y-79 human retinoblastoma cells, *J. Neurochem.* **67** (1996) 1293–1300.
- [72] LELIEVRE, V., BECQ-GIRAUDON, L., MEUNIER, A.C., MULLER, J.M., Switches in the expression and function of PACAP and VIP receptors during phenotypic interconversion in human neuroblastoma cells, *Neuropeptides* **30** (1996) 313–322.
- [73] PARKMAN, H.P., PAGANO, A.P., RYAN, J.P., PACAP and VIP inhibit pyloric muscle through VIP/PACAP-preferring receptors, *Regul. Pept.* **71** (1997) 185–190.
- [74] FUJIBAYASHI, Y., et al., Comparative studies of Cu-64-ATSM and C-11-acetate in an acute myocardial infarction model: ex vivo imaging of hypoxia in rats, *Nucl. Med. Biol.* **26** (1999) 117–121.
- [75] PALLELA, V.R., THAKUR, M.L., CHAKDER, S., RATTAN, S., 99mTc-labeled vasoactive intestinal peptide receptor agonist: functional studies, *J. Nucl. Med.* **40** (1999) 352–360.

SESSION 3

- [76] RAO, P.S., et al., 99m Tc labeled VIP analog: Evaluation for imaging colorectal cancer, *Nucl. Med. Biol.* **28** (2001) 445–450.
- [77] THAKUR, M.L., et al., Imaging tumors in humans with Tc-99m-VIP, *Ann. N.Y. Acad. Sci.* **921** (2000) 37–44.
- [78] THAKUR, M.L., et al., PET imaging of oncogene overexpression using 64Cu-vasoactive intestinal peptide (VIP) analog: Comparison with 99mTc-VIP analog, *J. Nucl. Med.* **45** (2004) 1381–1389.
- [79] TAWN, E.J., Chromosome changes in human cancer — are they pointers to mechanisms of initiation?, *Radiat. Oncol. Investig.* **5** (1997) 97–102.
- [80] ALITALO, K., Amplification of cellular oncogenes in cancer cells, *Med. Biol.* **62** (1984) 304–317.
- [81] SEEMAYER, T.A., CAVENEE, W.K., Molecular mechanisms of oncogenesis, *Lab. Invest.* **60** (1989) 585–599.
- [82] TIAN, X., et al., Imaging oncogene expression, *Ann. N.Y. Acad. Sci.* **1002** (2003) 165–188.
- [83] ARMENGOL, G., et al., DNA copy number changes and evaluation of MYC, IGF1R, and FES amplification in xenografts of pancreatic adenocarcinoma, *Cancer Genet. Cytogenet.* **116** (2000) 133–141.
- [84] BUCKLEY, M.F., et al., Expression and amplification of cyclin genes in human breast cancer, *Oncogene* **8** (1993) 2127–2133.
- [85] GILLET, C., et al., Amplification and overexpression of cyclin D1 in breast cancer detected by immunohistochemical staining, *Cancer Res.* **54** (1994) 1812–1817.
- [86] ZWIJSEN, R.M., et al., Cdk independent activation of estrogen receptor by cyclin D1, *Cell* **99** (1997) 405–415.
- [87] VOS, C.B., TER HAARI, N.T., PETERSE, J.L., CORNELISSE, C.J., VAN DER VIJVER, M.J., Cyclin D1 gene amplification and over expression are present in ductal carcinoma in situ of the breast, *J. Pathol.* **187** (1999) 279–284.
- [88] WEINSTAT-SASLOW, D., et al., Overexpression of cyclin D mRNA distinguishes invasive and in situ breast carcinomas from non-malignant lesions, *Nat. Med.* **12** (1995) 1257–1260.
- [89] RYAN, K.M., BIRNIE, G.D., Myc oncogenes: the enigmatic family, *Biochem. J.* **314** (1996) 713–721.
- [90] DALLA FAVERA, R., WONG-STAAAL, F., GALLO, R.C., Oncogene amplification in promyelocytic leukemia cell line HL-60 and primary leukemia cells of the same patient, *Nature* **299** (1982) 61–63.
- [91] SCHWAB, M., et al., Enhanced expression of the human gene N-myc consequent to amplification of DNA may contribute to malignant progression of neuroblastoma, *Proc. Natl. Acad. Sci. USA* **81** (1984) 4940–4944.
- [92] NAKAGAWARA, A., IKEDA, K., TSUDA, T., HIGASHI, K., N-myc oncogene amplification and prognostic factors of neuroblastoma in children, *J. Pediatr. Surg.* **22** (1987) 895–898.

- [93] SESHADRI, R., MATHEWS, C., NORRIS, M.D., BRIAN, M.J., N-myc amplified in retinoblastoma cell line FMC-RB1, *Cancer Genet. Cytogenet.* **33** (1988) 25–27.
- [94] LEE, W.H., MURPHREE, A.L., BENEDICT, W.F., Expression and amplification of the N-myc gene in primary retinoblastoma, *Nature* **309** (1984) 458–460.
- [95] NAU, M.M., Human small-cell lung cancers show amplification and expression of the N-myc gene, *Proc. Natl. Acad. Sci. USA* **83** (1986) 1092–1096.
- [96] SAKSELA, K., BERGH, J., NILSSON, K., Amplification of the N-myc oncogene in an adenocarcinoma of the lung, *J. Cell Biochem.* **31** (1986) 297–304.
- [97] BRODEUE, G.M., SEEGER, R.C., SCHWAB, M., VARMUS, H.E., BISHOP, J.M., Amplification of N-myc in untreated human neuroblastomas correlates with advanced disease stage, *Science* **224** (1984) 1121–1124.
- [98] INGVARSSON, S., ASKER, C., AXELSON, H., KLEIN, G., SUMEGI, J., Structure and expression of B-myc, a new member of the myc gene family, *Mol. Cell Biol.* **8** (1988) 3168–3174.
- [99] VENNSTROM, B., SHEINESS, D., ZABIELSKI, J., BISHOP, J.M., Isolation and characterization of c-myc, a cellular homolog of the oncogene (v-myc) of avian myelomatosis viral strain 29, *Virology* **42** (1982) 773–779.
- [100] BERNS, E.M., et al., C-myc amplification is a better prognostic factor than HER2/neu amplification in primary breast cancer, *Cancer Res.* **52** (1992) 1107–1013.
- [101] ADAMS, J.M., CORY, S., Myc oncogene activation in B and T lymphoid tumours, *Proc. R. Soc. Lond.* **226 B** (1985) 59–72.
- [102] TAUB, R., et al., A novel alteration in the structure of an activated c-myc gene in a variant t(2;8) Burkitt lymphoma, *Cell* **37** (1984) 511–520.
- [103] HORTNAGEL, K., et al., The role of immunoglobulin kappa elements in c-myc activation, *Oncogene* **10** (1995) 1393–1401.
- [104] SHTIVELMAN, E., HENGLEIN, B., GROITL, P., LIPP, M., BISHOP, J.M., Identification of a human transcription unit affected by the variant chromosomal translocations 2;8 and 8;22 of Burkitt lymphoma, *Proc. Natl. Acad. Sci. USA* **86** (1989) 3257–3260.
- [105] BERGH, J.C., Gene amplification in human lung cancer: The myc family genes and other proto-oncogenes and growth factor genes, *Am. Rev. Respir. Dis.* **142** (1990) S20–26.
- [106] LITTLE, C.D., NAU, M.M., CARNEY, D.N., GAZDAR, A.F., MINNA, J.D., Amplification and expression of the c-myc oncogene in human lung cancer cell lines, *Nature* **306** (1983) 194–196.
- [107] SLAMON, D.J., et al., Studies of the HER-2/neu proto-oncogene in human breast and ovarian cancer, *Science* **244** (1989) 707–712.
- [108] MENDELSON, J., BASELGA, J., The EGF receptor family as targets for cancer therapy, *Oncogene* **27** (2000) 6550–6565.
- [109] HOLBRO, T., CIVENNI, G., HYNES, N.E., The ErbB receptors and their role in cancer progression, *Exp. Cell Res.* **284** (2003) 99–110.

SESSION 3

- [110] DILLER, L., p53 functions as a cell cycle control protein in osteosarcomas, *Mol. Cell Biol.* **10** (1990) 5772–5781.
- [111] MICHALOVITZ, D., HALEVY, O., OREN, O., Conditional inhibition of transformation and of cell proliferation by a temperature-sensitive mutant of p53, *Cell* **62** (1990) 671–680.
- [112] MARTINEZ, J., GEORGOFF, I., MARTINEZ, J., LEVINE, A.J., Cellular localization and cell cycle regulation by a temperature-sensitive p53 protein, *Genes Dev.* **5** (1991) 151–159.
- [113] LEVINE, A.J., MOMAND, J., FINLAY, C.A., The p53 tumour suppressor gene, *Nature* **351** (1991) 453–456.
- [114] HOLLSTEIN, M., SIDRANSKY, D., VOGELSTEIN, B., HARRIS, C.C., p53 mutations in human cancers, *Science* **253** (1991) 49–53.
- [115] DAVIDOFF, A.M., HUMPHREY, P.A., IGLEHART, J.K., MARKS, J.R., Genetic basis for p53 overexpression in human breast cancer, *Proc. Natl. Acad. Sci. USA* **88** (1991) 5006–5010.
- [116] BORRESEN, A.L., et al., Constant denaturant gel electrophoresis as a rapid screening technique for p53 mutations, *Proc. Natl. Acad. Sci. USA* **M** (1991) 8405–8409.
- [117] PROSSER, J., THOMPSON, A.M., CRANSTON, G., EVANS, H.J., Evidence that p53 behaves as a tumour suppressor gene in sporadic breast tumours, *Oncogene* **5** (1990) 1573–1579.
- [118] BAKER, S.J., et al., Chromosome 17 deletions and p53 gene mutations in colorectal carcinomas, *Science* **244** (1989) 217–221.
- [119] BAKER, S.J., et al., p53 gene mutations occur in combination with 17p allelic deletions as late events in colorectal tumorigenesis, *Cancer Res.* **50** (1990) 7717–7722.
- [120] ANDREWS, D.W., et al., Results of a pilot study involving the use of an antisense oligodeoxynucleotide directed against the insulin-like growth factor type I receptor in malignant astrocytomas, *J. Clin. Oncol.* **19** (2001) 2189–2200.
- [121] CARROLL, J.S., PRALL, O.W., MUSGROVE, E.A., SUTHERLAND, R.L., A pure estrogen antagonist inhibits cyclin E-Cdk2 activity in MCF-7 breast cancer cells and induces accumulation of p130-E2F4 complexes characteristic of quiescence, *J. Biol. Chem.* **275** (2000) 38221–38229.
- [122] SMITH, J.B., WICKSTROM, E., Antisense c-myc and immunostimulatory oligonucleotide inhibition of tumorigenesis in a murine B-cell lymphoma transplant model, *J. Natl. Cancer Inst.* **90** (1998) 1146–1154.
- [123] WICKSTROM, E.L., et al., Human promyelocytic leukemia HL-60 cell proliferation and c-myc protein expression are inhibited by an antisense pentadecadeoxynucleotide targeted against c-myc Mrna, *Proc. Natl. Acad. Sci. USA* **85** (1988) 1028–1032.
- [124] WICKSTROM, E., BACON, T.A., WICKSTROM, E.L., Down-regulation of c-MYC antigen expression in lymphocytes of Emu-c-myc transgenic mice treated with anti-cmyc DNA methylphosphonates, *Cancer Res.* **52** (1992) 6741–6745.

- [125] WICKSTROM, E., TYSON, F.L., Differential oligonucleotide activity in cell culture versus mouse models (CHADWICK, D., CARDEW, G., eds), *Oligonucleotides as Therapeutic Agents*, Vol 209, Wiley, London (1997) 124–137.
- [126] BISHOP, M.R., et al., Ex vivo treatment of bone marrow with phosphorothioate oligonucleotide OL(1)p53 for autologous transplantation in acute myelogenous leukemia and myelodysplastic syndrome, *J. Hematother.* **6** (1997) 441–446.
- [127] HEIKKILA, R., et al., A c-myc antisense oligodeoxynucleotide inhibits entry into S phase but not progress from G0 to G1, *Nature* **328** (1987) 445–449.
- [128] COLLECCHI, P., et al., Cyclins of phases G1, S and G2/M are over expressed in aneuploid mammary carcinomas, *Cytometry* **42** (2000) 254–260.
- [129] WICKSTROM, E., et al., Oncogene mRNA imaging with 99mTc-chelator-PNA-peptide, *Russ. Chem. Bul. (Int. Ed.)* **51** (2002) 1083–1099.
- [130] PAREZ-ROGER, I., KIM, S.H., GRIFFITHS, B., SEWING, A., LAND, H., Cyclins D1 and D2 mediate myc induced proliferation via sequestration of p27^{kip1} and p21^{cip1}, *Embo. J.* **18** (1999) 5310–5320.
- [131] DOISNEAU-SIXOU, S.F., et al., Estrogen and antiestrogen regulation of cell cycle progression in breast cancer cells, *Endocr. Relat. Cancer* **10** (2003) 179–186.
- [132] KENNY, F.S., Overexpression of cyclin D1 messenger RNA predicts for poor prognosis in estrogen receptor-positive breast cancer, *Clin. Cancer Res.* **5** (1999) 2069–2076.
- [133] SURMACZ, E., Growth factor receptors as therapeutic targets: strategies to inhibit the insulin-like growth factor I receptor, *Oncogene* **22** (2003) 6589–6597.
- [134] BERNS, E.M., Prevalence of amplification of the oncogenes c-myc, HER2/neu, and int-2 in one thousand human breast tumours: correlation with steroid receptors, *Eur. J. Cancer* **28** (1992) 697–700.
- [135] WATSON, P.H., PON, R.T., SHIU, R.P., Inhibition of c-myc expression by phosphorothioate antisense oligonucleotide identifies a critical role for c-myc in the growth of human breast cancer, *Cancer Res.* **51** (1991) 3996–4000.
- [136] CARROLL, J.S., SWARBRICK, A., MUSGROVE, E.A., SUTHERLAND, R.L., Mechanisms of growth arrest by c-myc antisense oligonucleotides in MCF-7 breast cancer cells: implications for the antiproliferative effects of antiestrogens, *Cancer Res.* **62** (2002) 3126–3131.
- [137] EGHOLM, M., PNA hybridizes to complementary oligonucleotides obeying the Watson-Crick hydrogen-bonding rules, *Nature* **365** (1993) 566–568.
- [138] LARSEN, H.J., BENTIN, T., NEILSON, T., Antisense properties of peptide nucleic acid, *Biochem. Biophys. Acta.* **1489** (1999) 159–166.
- [139] BUCHARDT, O., EGHOLM, M., BERG, R.H., NEILSON, P.E., Peptide nucleic acids and their potential applications in biotechnology, *Trends Biotechnol.* **11** (1993) 384–386.
- [140] BONHAM, M.A., et al., An assessment of the antisense properties of RNase H-competent and steric-blocking oligomers, *Nucleic Acids Res.* **23** (1995) 1197–1203.
- [141] GOOD, L., NIELSEN, P.E., Progress in developing PNA as a gene-targeted drug, *Antisense Nucleic Acid Drug Dev.* **7** (1997) 431–437.

SESSION 3

- [142] SOOMETS, U., HALLBRINK, M., LANGEL, U., Antisense properties of peptide nucleic acids, *Front Biosci.* **4** (1999) 782–786.
- [143] TIAN, X., et al., Tumor targeting peptide-PNA-peptide chimeras for imaging overexpressing oncogene mRNAs, *Nucleosides Nucleotides Nucleic Acids* **24** (2005) 1085–1091.
- [144] RAO, P.S., et al., ^{99m}Tc-peptide-peptide nucleic acid probes for imaging oncogene mRNAs in tumours, *Nucl. Med. Commun.* **24** (2003) 857–863.
- [145] PIETRZKOWSKI, Z., et al., Inhibition of cellular proliferation by peptide analogues of insulin-like growth factor 1, *Cancer Res.* **52** (1992) 6447–6451.
- [146] TIAN, X., et al., External imaging of CCND1 cancer gene activity in experimental human breast cancer xenografts with ^{99m}Tc-peptide-peptide nucleic acid-peptide chimeras, *J. Nucl. Med.* **45** (2004) 2070–2082.
- [147] TIAN, X., et al., Noninvasive molecular imaging of MYC mRNA expression in human breast cancer xenografts with a [^{99m}Tc] peptide-peptide nucleic acid-peptide chimera, *Bioconjug. Chem.* **16** (2005) 70–79.
- [148] MU, D.Q., PENG, Y.S., XU, O.J., Values of mutations of K-ras oncogene at codon 12 in detection of pancreatic cancer: 15-year experience, *World J. Gastroenterol.* **10** (2004) 471–475.
- [149] CHAKRABARTI, A., ARUVA, M.R., SAJANKILA, S.P., THAKUR, M.L., WICKSTROM, E., Synthesis of novel peptide nucleic acid-peptide chimera for non-invasive imaging of cancer, *Nucleosides Nucleotides Nucleic Acids* **24** (2005) 409–414.
- [150] ADJEI, A.A., Blocking oncogenic ras signaling for cancer therapy, *J. Natl. Canc. Inst.* **93** (2001) 1062–1074.
- [151] CARRITHERS, S.L., et al., Guanylyl cyclase C is a selective marker for metastatic colorectal tumors in human extraintestinal tissues, *Proc. Natl. Acad. Sci. USA* **93** (1996) 14827–14832.
- [152] VAN DE VIJVER, M.J., et al., Neu-protein overexpression in breast cancer: Association with comedo-type ductal carcinoma in situ and limited prognostic value in stage II breast cancer, *Engl. J. Med.* **319** (1988) 1239–1245.
- [153] BARNES, D.M., et al., An immunohistochemical evaluation of c-erbB-2 expression in human breast carcinoma, *Br. J. Cancer* **58** (1988) 448–452.
- [154] KRAUS, M.H., POPESCU, N.C., AMSBAUGH, S.C., KING, C.R., Overexpression of the EGF receptor-related proto-oncogene erbB-2 in human mammary tumor cell lines by different molecular mechanisms, *Embo. J.* **6** (1987) 605–610.
- [155] PRESS, M.F., JONES, L.A., GODOLPHIN, W., EDWARDS, C.L., SLAMON, D.J., HER-2/neu oncogene amplification and expression in breast and ovarian cancers, *Prog. Clin. Biol. Res.* **354** (1990) 209–221.
- [156] VAUGHIN, J.P., et al., Antisense DNA downregulation of the ERBB2 oncogene measured by a flow cytometric assay, *Proc. Natl. Acad. Sci. USA* **92** (1995) 8338–8342.

SYNTHESIS AND EVALUATION OF ^{99m}Tc -KANAMYCIN AND ^{99m}Tc -ISONIAZID FOR INFECTION IMAGING

M. JEHANGIR*, A. MUSHTAQ*, S.A. MALIK**, S. ROOHI*

*Isotope Production Division,
Pakistan Institute of Nuclear Science and Technology
Email: mustansar@pinstech.org.pk

**Department of Biological Sciences,
Quaid-e-Azam University

Islamabad, Pakistan

Abstract

Infection continues to be a major cause of morbidity and mortality worldwide. Nuclear medicine has an important role in aiding the diagnosis of particularly deep seated infections. Established techniques such as radiolabelled leucocytes are sensitive and specific for inflammation but do not distinguish between infective and non-infective inflammation. There has been no recognized 'gold standard' for imaging sites of infection or inflammation until now. The challenge for nuclear medicine in infection imaging is to build on infection specific radiopharmaceuticals. This article describes the synthesis of ^{99m}Tc -Kanamycin and ^{99m}Tc -Isoniazid and their evaluation as infection imaging agents in animal models. Direct methods for labelling of Kanamycin and Isoniazid with ^{99m}Tc were exploited which are simple, rapid and efficient and do not require bifunctional chelating agents. Labelling efficiency depends on ligand/reductant ratio, pH and volume of reaction mixture. Radiochemical purity and stability of ^{99m}Tc -Kanamycin and ^{99m}Tc -Isoniazid was determined by thin layer chromatography. Biodistribution studies of both labelled complexes were performed on rats and rabbits. In vitro binding of ^{99m}Tc -Kanamycin to *S. aureus* bacteria was assessed. For comparison purposes, binding of ^{99m}Tc -Ciprofloxacin to bacteria was also performed. The localization kinetics of radiolabelled ^{99m}Tc -Kanamycin and ^{99m}Tc -Isoniazid were studied in the developed animal model and the images taken with a gamma camera. Results show that ^{99m}Tc -Kanamycin and ^{99m}Tc -Isoniazid complexes are quite stable and radiochemical purity of $\geq 95\%$ is maintained for up to 6 h. A significantly higher accumulation of ^{99m}Tc -Kanamycin was seen at the sites of *S. aureus* infected animals. Scintigraphy studies on rabbits also show that ^{99m}Tc -Isoniazid initially accumulated in infective lesions of *S. aureus* in rabbits not because of hypervascularity, but because of its non-specificity for *S. aureus* the residency of ^{99m}Tc -Isoniazid was low and it showed rapid washout from the lesion, whereas residency of tubercular lesion was high and it remained in the tubercular lesion in the delayed images also.

1. INTRODUCTION

At the dawn of the 21st century, infection still remains a major cause of mortality and morbidity globally, although the developing countries bear the greatest burden. Tuberculosis and multidrug resistant bacteria are increasing at an alarming rate and provide diagnostic, therapeutic and infection control challenges. Clinicians use a variety of clues, e.g. clinical, laboratory and radiological tests, to aid diagnosis and influence decision making. Although commonly employed and useful, the demonstration of a lesion by conventional radiological techniques such as X ray, ultrasound, computed tomography (CT) and magnetic resonance imaging (MRI), depends on the presence of structural abnormalities. In addition they are neither inflammation nor infection specific.

The introduction of radiopharmaceuticals in nuclear medicine has enhanced infection imaging because it depends on the demonstration of pathophysiological and pathobiological changes which occurs earlier in the infection process. Established techniques such as radiolabelled leucocytes [1], immunoglobulin [2, 3], colloids [4], neutrophils and cytokines [5], are inflammation specific but unable to distinguish between infective and non-infective lesions.

The challenge for nuclear medicine in infection imaging in the 21st century is to build on the recent trend towards the development of more infection specific radiopharmaceuticals, such as radiolabelled anti-infectives (e.g. ^{99m}Tc -Ciprofloxacin [6]). In addition to aiding early diagnosis of infection, through serial imaging these agents might prove very useful in monitoring the response to, and determining the optimum duration of, anti-infective therapy. Hence, the expanding range of radiopharmaceuticals over the last few years, such as radiolabelled anti-infectives, which aim to be infection specific, has been of particular interest to clinical microbiologists and infectious disease physicians as well as specialists in nuclear medicine [7–9].

Kanamycin sulphate is a bactericidal antibiotic, which acts by inhibiting the synthesis of protein in susceptible microorganisms. Kanamycin is used for treatment of infections when penicillin or other less toxic drugs cannot be used. Infections treated include bone, respiratory tract, skin, soft tissue and abdominal infections, complicated urinary tract infections, endocarditis, septicaemia, and enterococcal infections.

Isonicotinic acid hydrazide (Isoniazid) is one of the most effective agents in tuberculosis therapy. It inhibits the synthesis of long chain fatty acids (mycolic acid) in the cell wall of mycobacterium tuberculosis [10]. Studies on introduction of ^{11}C and ^{123}I on a substituent of the pyridine ring of Isoniazid have been published [11, 12]. Isoniazid derivatized with 2-iminothiolane has

been labelled with ^{99m}Tc by a conventional method and has shown promising results as a tubercular lesion imaging agent [13].

In the present studies, the authors optimized the direct labelling of Isoniazid and Kanamycin with ^{99m}Tc , which was quite simple. Radiochemical purity, stability, bacteria binding assay, in vivo biodistribution studies in rats and scintigraphy studies in rabbit were also evaluated.

2. METHODOLOGY

2.1. Kanamycin

2.1.1. Formulation of ^{99m}Tc -Kanamycin

Labelling of Kanamycin with ^{99m}Tc was done using $\text{SnCl}_2 \cdot 2\text{H}_2\text{O}$ as reducing agent. Optimum conditions of radiolabelling, such as the amount of reducing agent, pH and time of the reaction were determined. To determine the optimal amount of reducing agent, 5–30 μg of $\text{SnCl}_2 \cdot 2\text{H}_2\text{O}$ was used. The pH was adjusted by using HCl/NaOH . The reaction mixture volume used in all experiments was 2 ± 0.1 mL. After addition of all reagents, $^{99m}\text{TcO}_4^-$ (~370 MBq) in saline was injected into the vial. All experiments were carried out at room temperature ($22^\circ \pm 2^\circ\text{C}$). The maximum radiolabelling yield (>95%) was obtained with a reaction mixture containing: Kanamycin, 5 mg; $\text{SnCl}_2 \cdot 2\text{H}_2\text{O}$, 20 μg ; pH~7; ^{99m}Tc 370–500 MBq; and a reaction mixture volume of ~2 mL.

2.1.2. Quality control

The radiochemical yield of ^{99m}Tc -Kanamycin was checked by thin layer chromatography (TLC). Free $^{99m}\text{TcO}_4^-$ in the preparation was determined by using Whatman paper no. 3 as the stationary phase and acetone as the mobile phase. Reduced and hydrolyzed activity was determined by using instant TLC (ITLC-SG strips, Gelman Sciences) as the stationary phase and 0.5M NaOH as the mobile phase. Radiocolloids were also determined by passing the preparation through 0.22 μm bacteria filters (Millipore Filter Corp). Activity remaining on the filter and in solution was counted in a gamma counter (Ludlum).

2.1.3. Stability of ^{99m}Tc -Kanamycin

The stability of ^{99m}Tc -Kanamycin was checked for 6 h at room temperature. The distribution of radioactivity on chromatographic strips was

measured by a 2π scanner (Berthold, Germany). Alternatively, the strips were cut into 1 cm segments and counted in a gamma counter.

2.1.4. *In vitro* stability with human serum

Stability of the ^{99m}Tc -Kanamycin was studied *in vitro* [13]. 1.8 mL of normal human serum was mixed with 0.2 mL of ^{99m}Tc -Kanamycin and incubated at 37°C . During incubation, 0.2 mL aliquots were withdrawn at different time intervals up to 24 h and subjected to chromatography for determination of ^{99m}Tc -Kanamycin, reduced/hydrolysed ^{99m}Tc and free $^{99m}\text{TcO}_4^-$.

2.1.5. *In vitro* binding of ^{99m}Tc -Kanamycin to bacteria

In vitro binding of ^{99m}Tc -Kanamycin to *S. aureus* bacteria was assessed by the method described elsewhere [14]. Overnight cultures of bacteria, *S. aureus* ATCC 25923, were prepared in brain heart infusion broth (BHI, Oxoid) in a shaking water bath at 37°C . 0.1 mL of sodium phosphate buffer (Na-PB) containing ~ 5 MBq of ^{99m}Tc -Kanamycin was transferred to a test tube. 0.8 mL of 50% (v/v) of 0.01M acetic acid in Na-PB containing approximately 1×10^8 viable bacteria was added. The mixture was incubated for 1 h at 4°C and then centrifuged for 5 min at 2000g at 4°C . The supernatant was removed and the bacterial pellet was gently resuspended in 1 mL of ice cooled Na-PB and recentrifuged. The supernatant was removed and the radioactivity in the bacterial pellet was determined by gamma counter. The supernatants were also counted. The radioactivity related to bacteria was expressed in per cent of the added ^{99m}Tc activity bound to viable bacteria in regard to total ^{99m}Tc activity. For comparison purposes, binding of ^{99m}Tc -DTPA and ^{99m}Tc -Ciprofloxacin to bacteria was also performed.

2.1.6. Biodistribution studies in infected rats

A turbid suspension containing 2×10^8 colony forming units of *S. aureus* in 0.2 mL of saline was injected into the right thigh muscle of the rats ($n = 3$). After 24 h, when visible swelling appeared in the infected thigh, 0.2 mL of ^{99m}Tc -Kanamycin (~ 37 MBq) was injected via the tail vein. The rats were sacrificed using ether anesthesia after definite time periods and a biodistribution study was performed. One millilitre samples of blood were taken by cardiac puncture and weighed. Activity in total blood was calculated by assuming blood volume equates to 6.5% of body weight. The whole animals were then weighed and dissected. Samples of infected muscle, normal muscle, liver, spleen, lung, kidney, stomach, and heart were weighed and the activity

was measured using a gamma counter. The results were expressed as the per cent uptake of injected dose per organ.

The results of the ^{99m}Tc -Kanamycin and other compounds' bacterial uptake were analysed by an analysis of variance. The level of significance was set at 0.05.

2.1.7. ^{99m}Tc -Kanamycin scintigraphy

0.3 mL saline containing 2×10^8 colony forming units of viable *S. aureus* ATCC 25923 was injected into the left thigh muscle of rabbits. After 48 h, a significant swelling appeared at the site of injection. Each animal was placed on a flat hard surface with both hind legs spread out and all legs fixed with surgical tape. Diazepam (5 mg) was injected into the right thigh muscle. ^{99m}Tc -Kanamycin (~15 MBq) was then injected intravenously into the marginal ear vein. Immediately after injection, dynamic acquisition with both thighs in focus was done for 120 min by using a gamma camera. For the biodistribution study of the radiotracer, whole body acquisition was done at 15 min, 1 h and 2 h after injection.

2.2. Isoniazid

2.2.1. Formulation of ^{99m}Tc -Isoniazid

In the formulation of ^{99m}Tc -Isoniazid, the amount of Isoniazid was fixed at 2 mg. To determine the optimal amount of reducing agent, 50–200 μg of $\text{SnCl}_2 \cdot \text{H}_2\text{O}$ was used. The pH was adjusted by using HCl/NaOH . The maximum radiolabelling yield (>95%) was obtained with the reaction mixture containing 2 mg of Isoniazid: $\text{SnCl}_2 \cdot \text{H}_2\text{O}$ 100 μg ; pH~7; ^{99m}Tc 370–500 MBq; and a reaction mixture volume of ~2 mL. All the experiments were carried out at room temperature ($22^\circ \pm 2^\circ\text{C}$). The effect of various factors (pH, amount of reducing agent) on the labelling efficiency was also determined. Freeze dried kit of Isoniazid for labelling of ^{99m}Tc was also prepared. The stability and quality control of freeze dried kit are under investigation.

2.2.2. Quality control

Radiochemical yield of ^{99m}Tc -Isoniazid was checked by ascending TLC. ITLC-polysilicic acid (ITLC-SA, Gelman Sciences) paper strips as the stationary phase and Tetrahydrofuran as the mobile phase were used to separate the free $^{99m}\text{TcO}_4^-$, reduced/hydrolysed ^{99m}Tc and labelled Isoniazid. Reduced and hydrolysed activity was retained at the point of application ($R_f = 0$) whereas free

$^{99m}\text{TcO}_4^-$ moved away with the solvent front ($R_f = 0.9$) leaving ^{99m}Tc -Isoniazid at $R_f = 0.6$. The stability of ^{99m}Tc -Isoniazid was checked for 6 h at room temperature. The distribution of radioactivity on chromatographic strips was measured by a 2π scanner (Berthold, Germany) or cut into 1 cm segments and counted in a gamma counter.

2.2.3. Paper electrophoresis

The charge of the ^{99m}Tc -Isoniazid complex was determined by paper electrophoresis using a phosphate buffer of pH6.9 as the electrolyte and Whatman no. 1 paper as the support. The sample was run at a constant voltage of 300 V for 1 h. The strip was cut into 1 cm pieces and counted in a well-type gamma counter.

2.2.4. Biodistribution in rats

Biodistribution of ^{99m}Tc -Isoniazid in various organs was studied in Sprague-Dawley rats (200–225 g, $n = 3$) after injection of 15–20 MBq of tracer through the tail vein at 0.5, 4 and 24 h as described in Section 2.1.6.

2.2.5. Induction of experimental infection in rabbits

The *S. aureus* infection was induced in the right thigh muscle of rabbits as described in Section 2.1.7. Tubercular lesions were developed in the left thigh of the rabbits by administering a subcutaneous injection of 10^6 cells/mL of live *Mycobacterium tuberculosis* in the growing phase. Swelling, redness and hyperthermia were evident in *S. aureus* infective/inflammatory lesions after 48 h, whereas swelling and cold abscesses were evident in the tubercular lesion after ~3 weeks. The aspiration cytology of the lesions showed the presence of *S. aureus* in the infectious lesion and *M. tuberculosis* in the tubercular lesion, thereby confirming the origin of these lesions.

2.2.6. ^{99m}Tc -Isoniazid scintigraphy

Animals were sedated by giving intramuscular injection of Diazepam (5 mg) 10 min before imaging. 0.2 mL of ^{99m}Tc -Isoniazid containing 100–125 MBq was then injected intravenously into the marginal ear vein. Imaging was performed at different time intervals after tracer administration up to 12 h using a gamma camera (single headed Siemen's integrated ORBITER gamma camera).

3. RESULTS AND DISCUSSION

The direct method of labelling Kanamycin and INH with ^{99m}Tc was used, which is simple, rapid, efficient and does not require bifunctional chelating agents. The various chelates of ^{99m}Tc , which serve as radiopharmaceuticals, are formed by interaction between specific chelating agents and a reduced form of ^{99m}Tc . In order to form bonds with technetium, the chelator must contain electron donors such as nitrogen, oxygen and sulphur. The space between multiple electron donor atoms is required to allow several bonds to form with the central metal. Kanamycin has several functional groups such as $-\text{NH}_2$, $-\text{OH}$ and $-\text{O}-$ with which to form bonds with ^{99m}Tc . Although details of the chemistry of formation and molecular structure are unknown, ^{99m}Tc -Kanamycin and ^{99m}Tc -Isoniazid are assumed to be chelate complexes with one or more ligands attached to reduced ^{99m}Tc .

The structure of Kanamycin A [15] and Isoniazid are shown in Figs 1 and 2. The Kanamycin molecule contains 6-deoxy-6-amino-D-glucose (6-D-glucosamine) and 3-deoxy-3-amino-D-glucose (3-D-glucosamine) moieties linked by α -glycosidic bonds to the 4 and 6 positions of deoxystreptamine. Isoniazid is a pyridine derivative of nicotinamide. The chemical name of Isoniazid is isonicotinic acid hydrazide and its molecular formula is $\text{C}_6\text{H}_7\text{N}_3\text{O}$.

3.1. Kanamycin

Labelling efficiency, radiochemical purity and stability were assessed by a combination of ascending paper chromatography and ITLC on silica gel. In paper chromatography using acetone as the solvent, free $^{99m}\text{TcO}_4^-$ moved

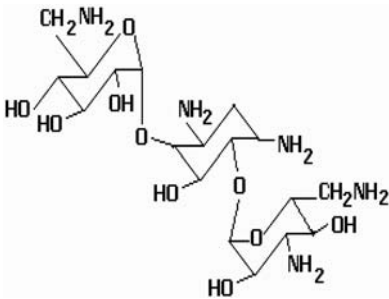


FIG. 1. Structure of Kanamycin.

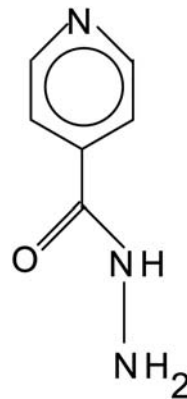


FIG. 2. Structure of Isoniazid.

towards the solvent front ($R_f = 1$), while ^{99m}Tc -Kanamycin and reduced/hydrolysed ^{99m}Tc remained at the point of spotting. In ITLC-SG chromatography using 0.5M NaOH as the solvent, reduced/hydrolyzed ^{99m}Tc remained at the point of spotting, whereas ^{99m}Tc -Kanamycin and free $^{99m}\text{TcO}_4^-$ moved towards the solvent front. Radiocolloids were also determined by passing the preparation through sterile filters (0.22 μm). In this technique, radiocolloids were retained on the filter, while ^{99m}Tc -Kanamycin and free $^{99m}\text{TcO}_4^-$ passed through it. The results obtained by both methods were in excellent agreement. The amount of radiocolloid in the final preparations was $\leq 2.0\%$.

The effect of various factors on the labelling efficiency of Kanamycin with ^{99m}Tc was also determined. Figure 3 shows that at low pH (2–5) the labelling efficiency was at a minimum (75%), while at pH6–7 the labelling efficiency of ^{99m}Tc -Kanamycin was $>97\%$. In basic media at pH8, the labelling efficiency was decreased (60–72%). Hence, further experiments were performed at pH6–7. The amount of the reducing agent $\text{SnCl}_2 \cdot 2\text{H}_2\text{O}$ which gave the highest labelling efficiency was 15–20 μg ; hence 20 μg of $\text{SnCl}_2 \cdot 2\text{H}_2\text{O}$ was chosen (Fig. 4).

The complexation of ^{99m}Tc with Kanamycin was not rapid and maximum labelling efficiency was achieved after 30 min (Fig. 5). The resulting complex of ^{99m}Tc -Kanamycin was quite stable and labelling of $\geq 98\%$ was maintained for up to 6 h (Fig. 5). The final formulation for the radiotracer ^{99m}Tc -Kanamycin was: Kanamycin 5 mg; $\text{SnCl}_2 \cdot 2\text{H}_2\text{O}$ 20 μg ; pH6–7; ^{99m}Tc 370–500 MBq; reaction mixture volume ~ 2 mL and incubation time 30 min at room temperature. The results of in vitro stability with normal human serum at 37°C shows there was almost no increase in free pertechnetate or reduced/hydrolyzed ^{99m}Tc up to 24 h. The total impurities were $< 5\%$ (Table 1).

In vitro binding of ^{99m}Tc -Kanamycin to bacteria was comparable to ^{99m}Tc -Ciprofloxacin [16]. Binding of ^{99m}Tc -Kanamycin was in the range of 40–50% ($n = 4$), while binding of ^{99m}Tc -Ciprofloxacin, a promising agent for the

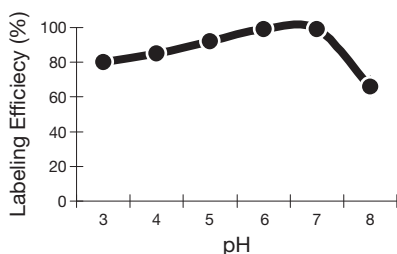


FIG. 3. Effect of pH on the labelling efficiency of ^{99m}Tc -Kanamycin ($n = 4$ per experiment).

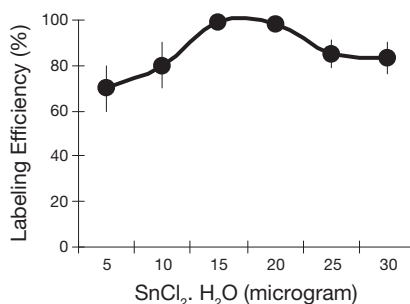


FIG. 4. Effect of $\text{SnCl}_2 \cdot 2\text{H}_2\text{O}$ amount on the labelling efficiency of ^{99m}Tc -Kanamycin ($n = 4$).

SESSION 3

TABLE 1. IN VITRO STABILITY OF ^{99m}Tc -KANAMYCIN IN NORMAL HUMAN SERUM ($n = 4$)

Incubation time (h)	^{99m}Tc -Kanamycin	Free pertechnetate	Colloid
1	98.0 ± 1.8	1.2 ± 0.1	1.0 ± 0.2
2	97.6 ± 1.7	1.6 ± 0.3	1.4 ± 0.3
4	96.8 ± 1.7	1.9 ± 0.4	1.6 ± 0.4
24	96.4 ± 1.3	2.2 ± 0.5	1.9 ± 0.6

diagnosis of bacterial infection [17, 18], ranged from 40 to 65% ($n = 4$). In vitro binding of ^{99m}Tc -DTPA (kidney/brain imaging agent) to bacteria was <8% ($n = 3$) (Fig. 6). Varying amounts of Kanamycin (2.5–50 µg) showed similar binding efficiency with bacteria (Fig. 7).

The tissue distribution of ^{99m}Tc -Kanamycin expressed as a percentage of injected dose per organ (%ID/organ) in rats with bacterial inflammations induced, 0.5, 4 and 24 h after intravenous administration is presented in Table 2. The ^{99m}Tc -Kanamycin was rapidly distributed after intravenous injection as shown by the renal elimination, although liver uptake is also significant. The high hydrophilic character of ^{99m}Tc -Kanamycin is in accordance with its predominant renal clearance. It is assumed that ^{99m}Tc -Kanamycin is stable in vivo, since insignificant activity was noticed in the thyroid and stomach during biodistribution studies.

Table 2 also presents data on the infected thigh and normal thigh radioactivity obtained at 0.5, 4 and 24 h after administration of ^{99m}Tc -Kanamycin. At 0.5, 4 and 24 h the target thigh/normal thigh radioactivity ratio indicated that higher binding affinity to the infection induced with *S. aureus* was observed.

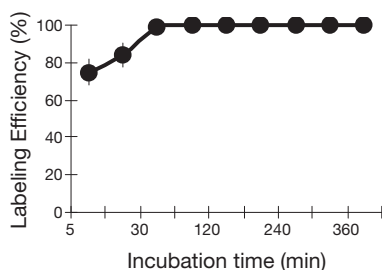


FIG. 5. Rate of complexation of ^{99m}Tc with Kanamycin and stability of ^{99m}Tc -Kanamycin ($n = 4$).

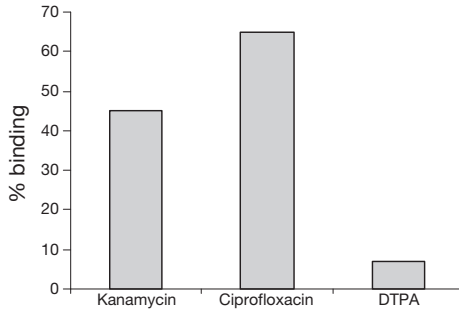


FIG. 6. Comparison of in vitro binding of Kanamycin, Ciprofloxacin and DTPA with viable *S. aureus*.

The highest target/non-target ratio reached >2 at 0.5 h and remained >2 up to 24 h post-injection of ^{99m}Tc-Kanamycin.

Whole body images of infected rabbits at 15 min, 1 h and 2 h after ^{99m}Tc-Kanamycin administration are presented in Fig. 8 (a, b and c). *S. aureus* infection in rabbit thigh was visualized as an area of increased tracer accumulation just after injection of labelled Kanamycin. The infection is clearly visible at 15 min post-administration, whereas at 1 h and 2 h, owing to increase in urinary bladder activity, the infection sites are poorly visualized compared to the 15 min image. Target to background ratios obtained from the region of interest (analysis of ^{99m}Tc-Kanamycin) ranged from 2.5 to 4:1. In vitro studies and animal experiments have shown that ^{99m}Tc-Kanamycin localizes in bacteria infected sites significantly. Owing to the ease of ^{99m}Tc-Kanamycin preparation and infection uptake, it may provide an alternative to ^{99m}Tc-Ciprofloxacin in a variety of patients referred for infection evaluation [19–22].

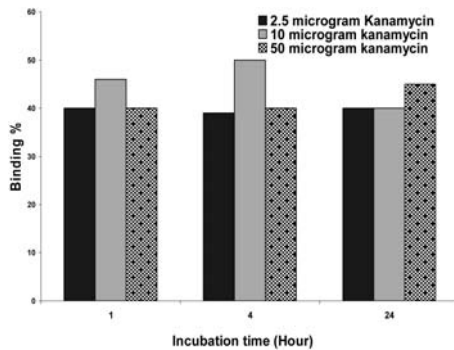


FIG. 7. In vitro binding of ^{99m}Tc-Kanamycin to viable *S. aureus* (n = 4 per experiment).

SESSION 3

TABLE 2. BIODISTRIBUTION DATA IN PER CENT INJECTED DOSE PER TOTAL ORGAN FOR ^{99m}Tc -KANAMYCIN at 0.5, 4 AND 24 h AFTER INTRAVENOUS ADMINISTRATION IN INFECTED RABBITS (MEAN \pm SD, $n = 4$)

Organ	0.5 h	4 h	24 h
Infected muscle	0.85 \pm 0.13	2.71 \pm 0.66	1.18 \pm 0.21
Normal muscle	0.34 \pm 0.08	1.15 \pm 0.12	0.48 \pm 0.08
Liver	22.25 \pm 3.32	16.98 \pm 3.45	7.98 \pm 1.73
Spleen	2.57 \pm 0.71	2.78 \pm 0.77	1.20 \pm 0.30
Lung	0.75 \pm 0.23	0.88 \pm 0.23	0.50 \pm 0.15
Kidney	23.45 \pm 3.88	10.67 \pm 2.10	2.82 \pm 0.50
Urine	20.56 \pm 3.56	50.55 \pm 4.34	65.44 \pm 6.65
Stomach	0.56 \pm 0.12	0.43 \pm 0.08	0.21 \pm 0.02
Heart	1.12 \pm 0.20	0.37 \pm 0.06	0.27 \pm 0.08
Blood	8.44 \pm 1.55	6.54 \pm 1.11	1.00 \pm 0.25

3.2. Isoniazid

Labelling efficiency, radiochemical purity and stability were assessed by TLC. ITLC-Polysilicic acid (ITLC-SA, Gelman Sciences) paper strips as the stationary phase and Tetrahydrofuran as the mobile phase were used to separate the free $^{99m}\text{TcO}_4^-$, reduced/hydrolysed ^{99m}Tc and labelled Isoniazid.

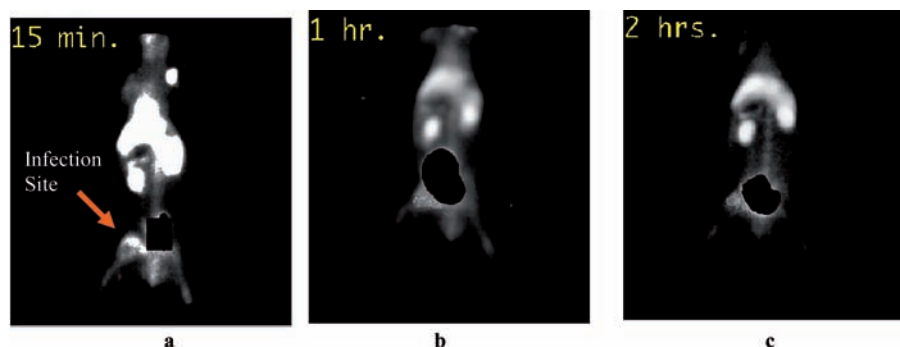


FIG. 8. Whole body gamma camera image of rabbit injected with ^{99m}Tc -Kanamycin at (a) 15 min post-administration, (b) 1 h post-administration, (c) 2 h post-administration. The urinary bladder is masked with lead foil in all figures and arrow indicates the site of infection.

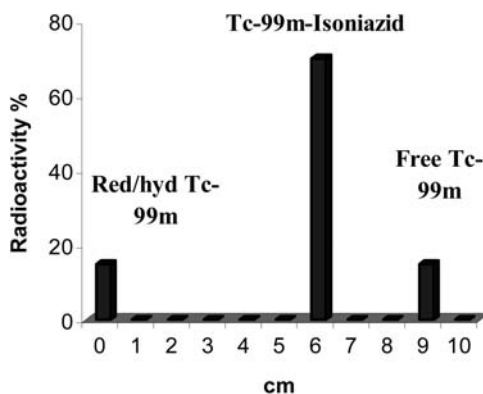


FIG. 9. Radiochromatogram showing positions of reduced/hydrolysed ^{99m}Tc , ^{99m}Tc -Isoniazid and free ^{99m}Tc .

Reduced and hydrolysed activity was retained at the point of application ($R_f = 0$) whereas free $^{99m}\text{TcO}_4^-$ moved away with the solvent front ($R_f = 0.9$) leaving ^{99m}Tc -Isoniazid at $R_f = 0.6$ (Fig. 9).

The amount of the reducing agent, $\text{SnCl}_2 \cdot 2\text{H}_2\text{O}$, which gave the highest labelling efficiency was 100 μg (Fig. 10). The effects of pH are shown in Fig. 11. At low pH (<4) the maximum labelling efficiency was 65%, while at pH6 and 8 the labelling efficiency of ^{99m}Tc -Isoniazid is around 80%, whereas maximum labelling of Isoniazid with ^{99m}Tc was achieved at pH7 (>99%). The complexation of ^{99m}Tc with Isoniazid was rapid and within 10 min maximum labelling efficiency was achieved. The resulting complex of ^{99m}Tc -Isoniazid was quite stable and labelling efficiency of $\geq 98\%$ was maintained for up to 6 h at room temperature (Fig. 12). The final formulation for the radiotracer ^{99m}Tc -Isoniazid was: Isoniazid 2 mg; $\text{SnCl}_2 \cdot 2\text{H}_2\text{O}$ 100 μg ; pH7; ^{99m}Tc 370–1100 MBq; reaction mixture volume ~2 mL and incubation time of 10 min at room temperature.

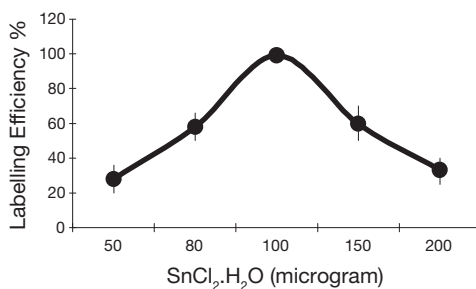


FIG. 10. Effect of reducing agent $\text{SnCl}_2 \cdot \text{H}_2\text{O}$ amount on the labelling efficiency of ^{99m}Tc -Isoniazid.

SESSION 3

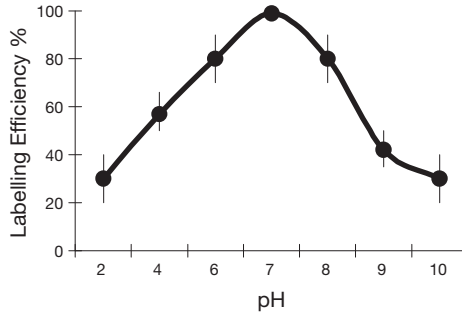


FIG. 11. Effect of pH on labelling efficiency of ^{99m}Tc-Isoniazid.

Paper electrophoresis study showed a neutral charge on the ^{99m}Tc-Isoniazid complex. Results are shown as activity migrated per centimetre towards anode or cathode from the point of application. More than 87% activity of labelled Isoniazid remained at the point of application, whereas ^{99m}TcO₄⁻ moved towards the anode (Fig. 13).

Biodistribution of ^{99m}Tc-Isoniazid at 0.5, 4 and 24 h was studied in rats (Fig. 14). Maximum uptake was found in kidneys (15%, 8% and 2.5% at 0.5, 4 and 24 h, respectively) indicating renal excretion of ^{99m}Tc-Isoniazid. High accumulation was recorded in the liver (10%, 11% and 4% at 0.5, 4 and 24 h, respectively) and significant radioactivity was also seen in the intestines (8%, 6% and 1% at 0.5, 4 and 24 h, respectively) indicating hepatobiliary excretion of the complex. Maximum uptake of tracer in bone, lungs, heart and spleen was <1.5% at 0.5 h. The standard error of the experiment was found to be <1% for all the organs. Negligible uptake, less than 2% in the stomach up to 24 h, confirmed good in vivo stability of the complex.

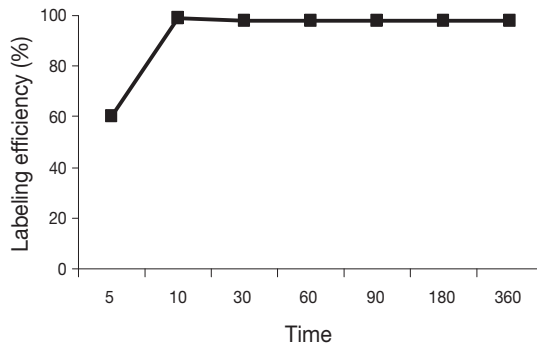


FIG. 12. Effect of incubation time on the labelling efficiency of ^{99m}Tc-Isoniazid.

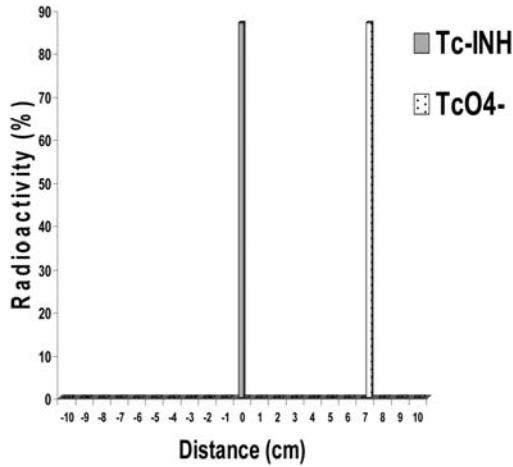


FIG. 13. Paper electrophoresis of ^{99m}Tc-Isoniazid in phosphate buffer of pH6.9 and Whatman paper as support. The samples were run at a constant voltage of 300 V for 1 h.

The suitability of ^{99m}Tc-Isoniazid prepared by the direct labelling method was evident in scintigrams of the rabbits. Tubercular lesion could be visualized in all the three rabbits at 2 h after administration of ^{99m}Tc-Isoniazid. To study the specificity of ^{99m}Tc-Isoniazid for tubercular lesion, a rabbit having *S. aureus*

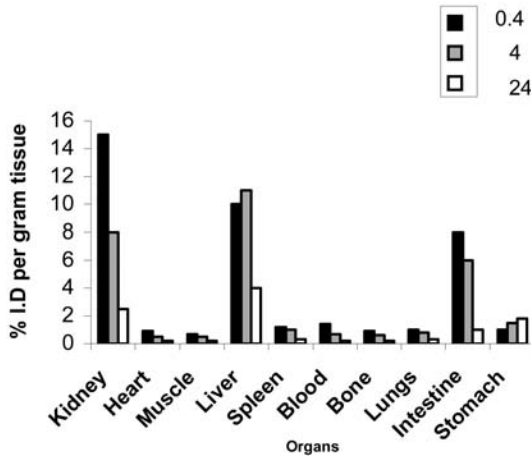


FIG. 14. Biodistribution of ^{99m}Tc-Isoniazid in Sprague-Dawley rats. The rats were administered 20–25 MBq of ^{99m}Tc-Isoniazid intravenously and radioactivity was measured after 0.5, 4 and 24 h.

SESSION 3

in the right thigh and tubercular lesion in the left thigh was injected with 100 MBq of ^{99m}Tc -Isoniazid. There was more accumulation of the tracer in the tubercular lesion compared with the *S. aureus* infection. Delayed images revealed clearance of activity from the non-tubercular lesion, while uptake becomes more specific for the tubercular lesion (Fig. 15a–c). The ^{99m}Tc -Isoniazid initially accumulated in infective lesions of *S. aureus* in rabbits as the result of hypervascularity (Fig. 15b), but because of its non-specificity for *S. aureus*, the residency of ^{99m}Tc -Isoniazid was low and it showed rapid washout from the lesion (Fig. 15c), whereas residency of tubercular lesion was high and it also remained in the tubercular lesion in the delayed images. These results suggest that ^{99m}Tc -Isoniazid prepared by the direct labelling method is quite a promising tracer, as is shown by an indirect labelling method [13].

4. CONCLUSION

The methodology for radiolabelling of Kanamycin and Isoniazid with ^{99m}Tc has been developed and standardized. The resulting complex of ^{99m}Tc -Kanamycin and ^{99m}Tc -Isoniazid, prepared by the direct labelling approach is simple, straightforward and stable with high labelling efficiency. It is also concluded from the above study that:

- ^{99m}Tc -Kanamycin is able to localize in bacterial infection induced by *S. aureus* in animal models.

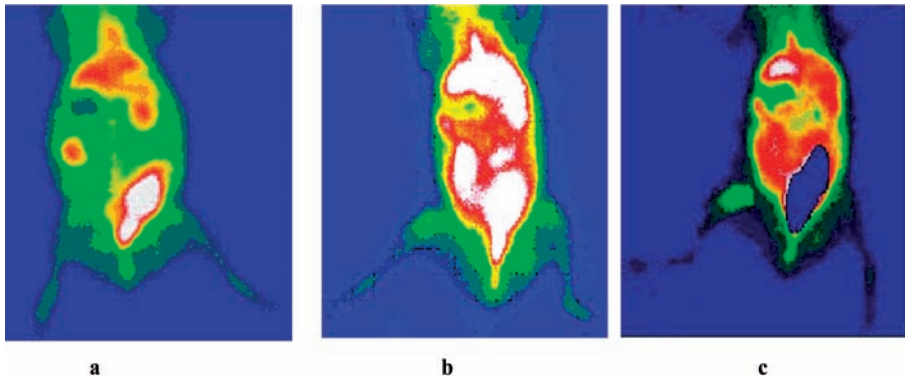


FIG. 15. Scintigram of a rabbit at (a) 0.5 h, (b) 2 h and (c) 12 h after administration of ^{99m}Tc -Isoniazid showing tubercular and *S. aureus* lesion in left and right thigh, respectively.

- The Biological activity (in vitro) of ^{99m}Tc -Kanamycin and ^{99m}Tc -Ciprofloxacin in comparable.
- The ^{99m}Tc -Isoniazid complex shows specific accumulation in *M. tuberculosis* lesions in the animal model.

ACKNOWLEDGEMENTS

The authors are thankful to S. Pervez, B. Khan and I. Haider for useful discussions and to the Department of Nuclear Medicine, Pakistan Institute of Engineering and Applied Sciences, Islamabad, for providing use of the gamma camera facility. The authors also acknowledge the animal house of the National Institute of Health, Islamabad, Pakistan for the provision of animals and help in the induction of *M. tuberculosis* infection in rabbits.

REFERENCES

- [1] THAKKUR, M.L., et al., J. Nucl. Med. **37** (1996) 1789.
- [2] CALAME, W., et al., J. Nucl. Med. **20** (1993) 490.
- [3] WELLING, M.M., FEITSMA, R.I.J., W. CALAME, W., PAUWELS, E.K.J., Nucl. Med. Commun. **18** (1997) 1057.
- [4] DE SCHRIJVER, M., STREULE, K., R. SENEKOWITSCH, R., FRIDRICH, R., Nucl. Med. Commun. **8** (1987) 895.
- [5] SIGNORE, A., CHIANELLI, M., R. BEI, R., OYEN, W., MODESTI, A., Eur. J. Nucl. Med. **30** (2003) 149.
- [6] OH, S.J., et al., Synthesis of ^{99m}Tc -ciprofloxacin by different methods and its biodistribution, Appl. Radiat. Isot. **5** (2002) 193–200.
- [7] BECKER, W., GOLDENBERG, D.M., WOLF, F., The use of monoclonal antibodies and antibody fragments in the imaging of infectious lesions, Semin. Nucl. Med. **24** (1994) 142–153.
- [8] CORSTENS, F.H.M., VAN DER MEER, J.W.M., Nuclear medicine's role in infection and inflammation, Lancet **354** (1999) 765–770.
- [9] WAREHAM, D., DAS, S.S., BRITTON, K., Imaging infection, In Infection highlights 1999-2000, ed. M.H. Wilcox, Health Press Limited, Oxford (2000) 81–87.
- [10] TAKAYAMA, K., SCHNOES, H.K., ARMSTRONG, E.L., BOYLE, R.W., Site of inhibitory action of isoniazid in the synthesis of mycolic acids in mycobacterium tuberculosis, Lip. Res. **16** (1975) 308–317.
- [11] SOMAWARDHANA, C.W., SAJJAD, M., LAMBRECHT, R.M., Synthesis of 2- ^{123}I and ^{124}I -Iodoisonicotinic Acid Hydrazide- potential radiotracer for tuberculosis, Appl. Radiat. Isot. **42** (1991) 215–220.

SESSION 3

- [12] SOMAWARDHANA, C.W., SAJJAD, M., LAMBRECHT, R.M., Radiopharmaceutical for differential diagnosis of tuberculosis: synthesis of 2-^[11C] Cyano-Isonicotinic Acid Hydrazide, *Appl. Radiat. Isot.* **42** (1991) 559–562.
- [13] SINGH, A.K., VERMA, J., BHATNAGAR, A., SEN, S., BOSE, M., Tc-99m Isoniazid: A specific agent for diagnosis of tuberculosis, *World J. Nucl. Med.* **2** (2003) 292–305.
- [14] WELLING, M.M., PAULUSMA-ANNEMA, A., BALTER, H.S., PAUWELS, E.K.J., NIBBERING, P.H., *Eur. J. Nucl. Med.* **27** (2000) 292.
- [15] WINTER, D.F., et al., *Eur. J. Nucl. Med.* **28** (2001) 570.
- [16] OH, S.J., et al., *Appl. Radiat. Isot.*, **57** (2002) 193.
- [17] OBRADOVIC, V., et al., *World J. Nucl. Med.* **2** (2003) 269.
- [18] CORN, M.J., et al., *The Chemistry of Kanamycin*, *Ann. N.Y. Acad. Sci.* **76** (1958) 27.
- [19] BRITTON, K.E., et al., *Eur. J. Nucl. Med.* **24** (1997) 553.
- [20] DAS, S.S., BRITTON, K.E., *World J. Nucl. Med.* **2** (2003) 173.
- [21] LARIKKA, M.J., et al., *Nucl. Med. Commun.* **23** (2002) 167.
- [22] CORSTENS, F.H.M., VAN DER MEER, J.W.M., *Lancet* **354** (1997) 765.

PREPARATION OF ^{99m}Tc -PENTAVALENT DMSA AND ITS UPTAKE BY BENIGN BONE DISEASES*

N. BOUCEKKINE, S.A. ZEMOUL, F. MOUAS, R. BENLABGASS,
S. HANZAL, A. KHELIFA, F. MECHKEN, M. HABECHE,
K. BELLAZOUG, B. BENCHELAGHEM, S.E. BOUYOUCHEF
Department of Nuclear Medicine,
CHU Bab El Oued,
Algiers, Algeria
Email: nadiaboucekkine@yahoo.fr

Abstract

^{99m}Tc -(V)DMSA is a tumour seeking agent that is known for its capability to detect medullary thyroid carcinoma and to be suitable in the detection of tumoral recurrence and/or its metastasis. However, DMSA V could also accumulate in soft tissue tumours, in lung cancer, metastatic diseases, brain tumours and some benign bone diseases. ^{99m}Tc -(V)DMSA can be reliably prepared by addition to the DMSA(III) of concentrated NaHCO_3 . A simple and efficient chromatography analysis uses an ITLSC-SG/MEC in butanol/acetic acid/water (3:2:3) to calculate the ratio DMSA(V):DMSA(III) and the amount of free pertechnetate. Its mechanism of accumulation has been thought to be related to its avidity to some cancer cells but it is also related to glucose mediated acidosis. The uptake of DMSA by benign bone disease has been studied in 68 patients with a known primary cancer, including patients with thyroid medullary carcinoma. An uptake of the DMSA V by benign bone diseases was noticed in more than 80% of the 68 patients, and that could lead to a misinterpretation of the DMSA V total body scan and make for an increased number of false positives in the detection of metastasis or recurrence. This was also confirmed in patients with thyroid medullary carcinoma.

* Although a presentation was given, only the abstract was made available.

NOVEL TECHNETIUM CHEMISTRY AND
RADIOPHARMACEUTICALS: I

(Session 4)

Chairpersons

R. ALBERTO
Switzerland

M. VENKATESH
India

WHAT ROLE FOR ^{99m}Tc RADIOPHARMACEUTICALS IN THE AGE OF MOLECULAR IMAGING?

A. DUATTI
Laboratory of Nuclear Medicine,
Department of Radiological Sciences,
University of Ferrara,
Ferrara, Italy
Email: dta@unife.it

Abstract

Molecular imaging is a new paradigm that is currently emerging in the field of medical and biological sciences as a novel tool for exploring fundamental biological processes at the molecular level in integrated living organisms. Nuclear imaging is a sensitive methodological approach that employs radiolabelled probes to investigate biomolecular interactions. This approach may ultimately lead to a deeper understanding of the route through which single biochemical pathways are grouped to form networks of biological processes controlling the behaviour of a whole organism. Technetium-99m radiopharmaceuticals are playing an important role in this new scenario and are currently expanding the applications of these tracers, particularly through the use of high resolution small animal scanners. This review briefly illustrates some of the recent results in this area and the potential developments that may further stimulate the research interest in ^{99m}Tc imaging agents.

1. THE MOLECULAR IMAGING PARADIGM

Molecular imaging is a technique that makes use of single molecules, or generates signals from molecules, to image the structure and function of living systems at the molecular level [1–3]. The image obtained displays specific molecular components of structures or molecular functions. Molecular medicine represents the merger of modern biology and medicine. In this new paradigm, diseases are viewed as resulting from internally and externally derived molecular errors that instruct cells to transform into the phenotypes of disease. Since its first appearance, nuclear imaging was an intrinsically molecular technology because it always requires the use of radiolabelled molecular probes to collect information from a specific biological target. Positron emission tomography (PET) uses positron labelled molecules to

image biomolecular processes such as metabolism, cell communication and gene expression, whereas single photon emission computed tomography (SPECT) employs molecules labelled with single photon emitters to perform the same task. Nuclear imaging benefits greatly from molecular probes originating from biochemistry and pharmaceuticals, which potentially allow the monitoring of a high number of fundamental biological processes. In contrast, it suffers from a relatively poor spatial resolution compared with other imaging modalities such as computed tomography (CT) and magnetic resonance imaging (MRI). However, the recent advent of small animal scanners having a submillimetre resolution has dramatically improved the quality of images collected with nuclear techniques [4–6], thus opening the door for an extensive application of nuclear imaging methods to the investigation of biological mechanisms and their entangled networks.

In PET imaging, spatial resolution has an intrinsic lower limit that cannot be overcome as a result of the path always travelled by the emitted positron before annihilation. Some theoretical calculations set this limit approximately at 0.5 mm for ^{18}F . In contrast, there is no basic limitation for SPECT and, at least in principle, spatial resolution could be indefinitely improved to well below the submillimetre scale. This characteristic of SPECT imaging makes molecular probes labelled with single photon emitters particularly attractive for fundamental biological studies. Moreover, the readily available $^{99\text{m}}\text{Tc}$ radiopharmaceuticals, conjoined with the favourable nuclear properties of this radionuclide, would provide a very convenient tool for molecular imaging in small animals.

However, the true challenge in approaching molecular imaging with $^{99\text{m}}\text{Tc}$ radiopharmaceuticals is to identify specific molecular probes capable of targeting a variety of biomolecular processes. To attain this goal, precise structural features should be imparted to a $^{99\text{m}}\text{Tc}$ complex, and this requirement always raises formidable chemical problems because of the metallic character of this transition element. Despite this, $^{99\text{m}}\text{Tc}$ radiopharmaceuticals have been successfully employed in molecular imaging applications and further advances in the structural design of these tracers may help to increase their role in current studies of biomolecular processes at a fundamental level. Representative examples of the use of $^{99\text{m}}\text{Tc}$ compounds in molecular imaging investigations will be briefly reviewed here, along with some future trends in the development of new effective $^{99\text{m}}\text{Tc}$ imaging agents.

2. THE MACHINERY OF MOLECULAR IMAGING

Since its very first application, nuclear medicine has essentially been a molecular imaging technology. This conclusion stems naturally from the consideration that, unlike other imaging modalities, nuclear medicine makes use of very small objects, such as single molecules, to perform its diagnostic task. As with other molecular imaging applications, nuclear imaging requires fixation of a signal emitting molecule (e.g. one containing a radioactive label) within the cell or tissue where the target is expressed. There are several different mechanisms by which this can be achieved. In the receptor–ligand model, one signal molecule (the ligand) binds with high affinity to a specific site on a target molecule through a receptor–target interaction. Key requirements for this type of imaging are the specificity and affinity of the receptor–ligand interaction, as well as the receptor density itself. The receptor–ligand pair does not necessarily have to mimic a naturally occurring interaction. The antigen–antibody model is essentially a variant of the receptor–ligand model. Again, the critical parameters are specificity, affinity and receptor density. In the transporter–substrate model, the signal molecule is accumulated within a cell or tissue compartment by a mechanism involving the interaction of the signal molecule with a single transporter, which must be uniquely present or absent in a process of disease. In the enzyme–substrate model, the target molecule is an enzyme that chemically modifies the signal molecule, fixing its biodistribution. A single molecule of enzyme can interact with many substrate molecules, multiplying the signal intensity.

3. APPROACHES TO THE DESIGN OF ^{99m}Tc IMAGING AGENTS

There are essentially two conceptual strategies for the design of new ^{99m}Tc radiopharmaceuticals, which go under the names of (i) a bifunctional (or pendant) approach, and (ii) an integrated approach, respectively [7]. Both strategies are based on the first selection of a convenient biologically active molecule or drug having a specific biological behaviour. After this step, however, the two methods diverge. The bifunctional approach literally suggests appending the bioactive group to a metal complex through a suitable linkage. This can be conveniently accomplished using a so-called bifunctional ligand that could be represented as a composite molecule, combining a strong chelating group for the radiometal with the biomolecule by means of a suitable linker. After the radiometal has been encaged by the chelating system, the resulting ‘conjugate’ complex retains the bioactive group into its structure as an appended side chain. Instead, the other procedure, the integrated approach,

puts its focus on the selected biomolecule itself that may serve as a mould for assembling the structure of the final ^{99m}Tc receptor radiopharmaceutical. The key step is to identify a region in its structure that is not essential for preserving its biological properties. The final radiopharmaceutical, therefore, is assembled by replacing this non-essential part with a metal containing fragment having a molecular shape and dimension similar to that of the substituted portion of the original biomolecule in order to fit almost exactly into the same position. Obviously, the ultimate success of both design strategies lies in their capability to keep unaltered the intrinsic biological behaviour of the starting biomolecule.

A key theoretical advantage of the two approaches outlined above originates from their representation of the molecular structure of a radioactive tracer as consisting of different 'pieces' or 'fragments', which can be, at least in principle, conveniently assembled to build up the final radiopharmaceutical. However, the merging of the various fragments to yield a stable product is not always simple to accomplish and, for practical purposes, this has been obtained only through the application of the bifunctional approach.

In recent years, an alternative approach to the problem of assembling the various parts of a receptor specific ^{99m}Tc radiopharmaceutical has emerged. This method is based on the chemical properties of certain types of substitution labile technetium complexes which show a marked reactivity only towards ligands having some specific set of coordinating atoms. In these complexes, a few coordination positions are occupied by a set of ligands that are tightly bound to the metal centre. The resulting strong ligand field allows a significant stabilization of the metal oxidation state, preventing the complex from undergoing oxidation–reduction reactions. The remaining positions of the coordination arrangement are usually spanned by weakly bound ligands that could be easily replaced by some other incoming ligand carrying a specific set of donor atoms. As a consequence, the reaction between the precursor complex and the hypothetical incoming ligand is expected to be kinetically favoured and should produce the final substituted complex in very high yield. Such a behaviour can be efficiently exploited for assembling a 'robust' ^{99m}Tc fragment with a biomolecule including the appropriate set of coordinating atoms. The high affinity of the precursor 'metal fragment' for the specific donor set on the bioactive ligand would ensure the perfect fitting of these two molecular building blocks to form the final, combined complex.

The first example of the application of the metal fragment approach [8, 9] was based on the chemical properties of the precursor, aquo-carbonyl, metal complex $[\text{}^{99m}\text{Tc}(\text{CO})_3(\text{H}_2\text{O})_3]^+$. In this species, the fragment $[\text{}^{99m}\text{Tc}(\text{CO})_3]^+$ constitutes the chemically inert portion of the complex. The three water molecules are weakly coordinated and, thus, can be easily replaced by some substituting ligand having the appropriate set of donor atoms. Under these

conditions, the reaction between the metal fragment $[\text{}^{99\text{m}}\text{Tc}(\text{CO})_3]^+$ and the incoming ligand becomes highly selective, allowing the efficient assemblage of these two pieces to afford the final complex. Therefore, the precursor complex $[\text{}^{99\text{m}}\text{Tc}(\text{CO})_3(\text{H}_2\text{O})_3]^+$ can be conveniently used as a synthon for the synthesis of a variety of $^{99\text{m}}\text{Tc}$ carbonyl derivatives.

Very recently, a second definite example of the metal fragment approach was found during the study of the synthesis of a novel class of asymmetrical nitrido heterocomplexes [10, 11]. It was found that this novel type of mixed ligand complexes was efficiently prepared by reacting the precursor complex $[\text{}^{99\text{m}}\text{Tc}(\text{N})(\text{PXP})\text{Cl}_2]$ (PXP = diphosphine ligand) with bidentate chelating ligands carrying π -donors as coordinating atoms. In these reactions, the arrangement of atoms $[\text{}^{99\text{m}}\text{Tc}(\text{N})(\text{PXP})]^{2+}$, composed by a $\text{Tc}\equiv\text{N}$ group coordinated to a chelating diphosphine ligand PXP, behaves as a 'robust' metal fragment, and the two chlorine atoms can be easily displaced by the incoming π -donor ligand to afford the asymmetrical complex $[\text{}^{99\text{m}}\text{Tc}(\text{N})(\text{PXP})(\text{L})]^{0/+}$. Thus, the metal synthon $[\text{}^{99\text{m}}\text{Tc}(\text{N})(\text{PXP})]^{2+}$ could be conveniently utilized to obtain a very broad class of asymmetrical nitrido Tc(V) complexes with a variety of bidentate ligands.

4. $^{99\text{m}}\text{Tc}$ ANALOGUES OF ^{18}F -FDG

The advent of a true $^{99\text{m}}\text{Tc}$ analogue of ^{18}F -FDG would revolutionize the current nuclear medicine scenario, but this goal seems tremendously difficult to achieve for reasons that will be clarified below. Several attempts have been made to append a glucose moiety to a $^{99\text{m}}\text{Tc}$ fragment with the purpose of obtaining a final conjugated complex that is recognized by some glucose transporter. The $^{99\text{m}}\text{Tc}$ tricarbonyl synthon was linked to a glucose derived bifunctional ligand [12]. Unfortunately, the resulting compound was not recognized by the glucose transport system. A recent report described results with a bifunctional ligand formed by a glucose moiety linked to a N2S2 chelating system [13]. The resulting $^{99\text{m}}\text{Tc}$ -oxo complex displays some promising properties, but the full biological evaluation of this new agent is still far from being completed. Some years ago, a $^{99\text{m}}\text{Tc}$ complex incorporating two thioglucose ligands symmetrically positioned around a $[\text{}^{99\text{m}}\text{TcN}]^{2+}$ core on the basal plane of a square pyramidal arrangement was reported [14], but the biological properties of this compound were not explored further.

5. IMAGING OF GENE EXPRESSION

Paradoxically, the most simple ^{99m}Tc compound, namely the ubiquitous tetraoxo anion, $[\text{}^{99m}\text{TcO}_4]^-$, currently constitutes one of the most promising imaging agents for monitoring gene expression. Imaging of gene expression requires the use of highly specific imaging probes, sensitive systems producing high resolution images and appropriate amplification. Reporter gene imaging is one of the potential approaches that has been utilized to study promoter/regulatory elements, inducible promoters and endogenous gene expression. A reporter gene is an exogenous gene that has been artificially inserted into a targetted cell or tissue and whose product has an activity that is readily distinguishable from that of native genes within the cell. Reporter gene imaging involves the visualization of transcriptional and post-transcriptional regulation products of target gene expression, and of specific intracellular protein-protein interactions. This can be accomplished by introducing into the living subject a radiolabelled probe whose distribution is closely sensitive to the intracellular presence of the product of reporter gene expression. Regulatory regions of genes (promoters/enhancers) can be cloned and used to drive transcription of the reporter gene and of a specific gene of interest. Thus, the expression of the gene of interest can be monitored by coupling it to the same promoter of the reporter gene into the target. When the reporter gene expression is revealed by the selective interaction of its genetic product with the radiolabelled probe, this can ultimately reveal the expression of the gene under investigation [15]. Two approaches are possible to adapt the reporter gene concept for PET or SPECT. The reporter gene can be introduced in such a way that it encodes for an enzyme that is capable of trapping a specific tracer through the action of that enzyme. The second approach uses a reporter gene that encodes for an intracellular and/or extracellular receptor capable of binding a tracer.

Iodine uptake occurs across the membrane of thyroid follicular cells through an active transporter process mediated by a sodium iodide symporter (NIS). NIS is an integral protein of the basolateral membrane of thyroid follicular cells. The NIS catalyzed active accumulation of iodide from the interstitium into the cell is achieved against an electrochemical gradient. In addition to iodide, several other anions are transported by NIS ($\text{I}^- > \text{SeCN}^- > \text{SCN}^- > \text{ClO}_3^- > \text{NO}_3^-$). NIS also transports technetium pertechnetate and rhenium perrhenate. The only apparent common denominator of these well transported substrates is anionic monovalency and a size closer to that of the iodide ion. It has been shown that gene transfer of NIS into a variety of cell types confers increased radioiodine and $[\text{}^{99m}\text{TcO}_4]^-$ uptake by up to several hundredfold. Thus, the NIS gene can be efficiently employed as a reporter gene for imaging

gene expression and [$^{99m}\text{TcO}_4$] $^-$ utilized as a radioactive reporter probe [16–18].

6. OUTSIDE THE BRAIN

In recent years, a number of useful ^{99m}Tc radiopharmaceuticals intended for different targets have been developed, particularly with peptides, using the bifunctional approach. In this area, various biological processes have been successfully monitored as briefly outlined below [3].

Imaging of inflammation would ideally require an imaging agent showing rapid localization to an infectious focus, with enough specificity to distinguish bacterial infection from aseptic inflammation. The first molecular targeting agents were antigranulocyte antibodies. Antigens targeted have included NCA-90 (CD66c), expressed on activated neutrophils [19], as well as NCA-95 (142) and CD15 (SSEA-1) [20, 21]. Most of these preparations have been labelled with ^{99m}Tc using hydrazinonicotinamide as a linker. Several peptide agents have been investigated. Chemotactic peptides binding receptors on granulocytes in acute inflammation have shown superior localization to infected sites. However, even at imaging doses, these agents are capable of inducing marked granulocytopenia. Similar effects have hindered the introduction of agents targeting receptors for interleukin-2 in chronic inflammation, although imaging characteristics have been promising [22]. Other targets currently under study include bacterial receptors for cationic peptides derived from human ubiquicidine [23] and the HLA class-II-like antigen expressed on B lymphocytes and monocytes [24].

Apoptosis, or programmed cell death, is an active, energy dependent mechanism for the elimination of cells that have been injured, infected, or immunologically recognized as harmful or superfluous. As part of the apoptotic mechanism, phosphatidylserine, a phospholipid normally sequestered on the inner leaflet of the cell membrane, is translocated to the external leaflet. A 35-kDa endogenous human protein, annexin V, binds to exposed phosphatidylserine with an affinity in the nanomolar range. ^{99m}Tc -annexin V was initially prepared by derivatization with hydrazinonicotinamide [25] and has been used to image apoptosis. While the degree of uptake of annexin V correlates well with the extent of cell death, uptake is not completely specific for apoptosis, as it can also be seen in cellular necrosis and in severe metabolic stress [26, 27].

Angiogenesis is a basic mechanism allowing solid tumours to grow. A high number of natural proangiogenic and antiangiogenic factors have been identified. The $\alpha_5\beta_3$ integrin is expressed on vascular endothelial cells during angiogenesis and vascular remodelling [28]. The integrin binds several

ligands in the extracellular matrix, each containing the motif -Arg-Gly-Asp- (RGD). Cyclic peptides labelled with ^{99m}Tc and containing RGD sequences have high affinity and selectivity for $\{\alpha\}\nu\beta 3$ integrin [29].

A ubiquitous problem that frequently plagues molecular imaging applications of ^{99m}Tc radiopharmaceuticals originates from non-specific uptake that sometimes makes image quality questionable, particularly when accumulation of activity is low due to the intrinsic properties of the biological target. Improvements in this field could be achieved through the development of novel ligand systems imparting superior biodistribution characteristics to the resulting conjugate complex. In this context, the use of the metallic fragments $[\text{}^{99m}\text{Tc}(\text{CO})_3]^+$ and $[\text{}^{99m}\text{Tc}(\text{N})(\text{PNP})]^{2+}$ may prove useful. As an example of this type of advancement, recently some derivatives of the $[\text{}^{99m}\text{Tc}(\text{N})(\text{PNP})]^{2+}$ fragment incorporating an enzyme sensitive diphosphine (PNP) and a peptide sequence having affinity for receptors expressed on metastatic cells were found to exhibit dramatic washout properties from normal liver, thus allowing the visualization of metastatic processes in this tissue (Fig. 1).

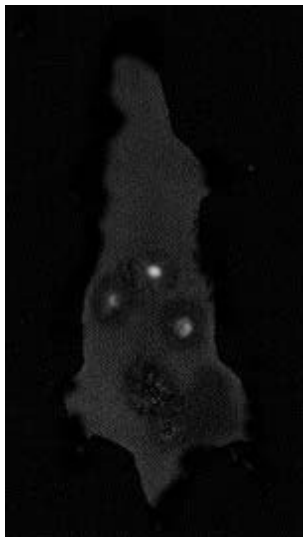


FIG. 1. Example of a derivative of the $[\text{}^{99m}\text{Tc}(\text{N})(\text{PNP})]^{2+}$ fragment incorporating an enzyme sensitive diphosphine (PNP) and a peptide sequence having affinity for receptors expressed on metastatic cells.

7. INSIDE THE BRAIN

Crossing the blood brain barrier (BBB) is a real challenge, not only for ^{99m}Tc radiopharmaceuticals, but also for a large number of drugs. The delivery of a chemical compound to the brain poses dramatic problems and, usually, there are strict requirements to be simultaneously fulfilled (e.g. lipophilicity and receptor affinity) [30]. Though the pendant approach has been used for designing the receptor specific imaging agent ^{99m}Tc -TRODAT1 [31], which essentially still remains the only ^{99m}Tc derivative capable of penetrating the BBB while maintaining affinity for D2 receptors, this method does not appear to be the most suitable for all situations. The integrated approach may help to overcome some difficulty, but the design of the structure of the bioactive radiopharmaceutical, fashioned on the molecular mould of some bioactive drug, always appears to be critical from the chemical point of view, though some recent successful examples have been reported in an attempt to develop ^{99m}Tc imaging agents for amyloid plaques [32]. Classes of ^{99m}Tc complexes which showed extensive BBB penetration are $^{99m}\text{TcO-N2S2}$ and $^{99m}\text{TcO-3+1}$ complexes [30], and $^{99m}\text{TcN-bis(dithiocarbamato)}$ complexes [11]. The basic molecular structures of these complexes could be conveniently used as molecular frames for shaping the structure of the final ^{99m}Tc brain imaging agent, while imparting receptor affinity for some specific target through an extensive modification of the lateral functional groups.

REFERENCES

- [1] WEISSLEDER, R., MAHMOOD, U., Molecular imaging, *Radiology* **219** (2001) 316–333.
- [2] MASSOUD, T.F., GAMBHIR, S.S., Molecular imaging in living subjects: seeing fundamental biological processes in a new light, *Genes & Developments* **17** (2003) 545–580.
- [3] BRITZ-CUNNINGHAM, S.H., ADELSTEIN, S.J., Molecular targeting with radionuclides: State of the science, *J. Nucl. Med.* **44** (2003) 1945–1961.
- [4] KING, M.A., et al., Introduction to the physics of molecular imaging with radioactive tracers in small animals, *J. Cell Biochem.* **39** (Suppl.) (2002) 221–230.
- [5] HUMM, J.L., et al., From PET detectors to PET scanners, *Eur. J. Nucl. Med. Mol. Imaging* **30** (2003) 1574–1597.
- [6] BEEKMAN, F.J., et al., U-SPECT-I : A novel system for submillimeter-resolution tomography with radiolabeled molecules in mice, *J. Nucl. Med.* **46** (2005) 1194–1200.

- [7] HOM, R.K., KATZENELLEBOGEN, J.A., Technetium-99m-labeled receptor-specific small-molecule radiopharmaceuticals: Recent developments and encouraging results, *Nucl. Med. Biol.* **24** (1997) 485–498.
- [8] ALBERTO, R., et al., A novel organometallic aqua complex of technetium for the labeling of biomolecules: synthesis of $[^{99m}\text{Tc}(\text{OH}_2)_3(\text{CO})_3]^+$ from $[^{99m}\text{TcO}_4]^-$ in aqueous solution and its reaction with a bifunctional ligand, *J. Am. Chem. Soc.* **120** (1998) 7987–7988.
- [9] SCHIBLI, R., SCHUBIGER, P.A., Current use and future potential of organometallic radiopharmaceuticals, *Eur. J. Nucl. Med.* **29** (2002) 1529–1542.
- [10] BOLZATI, C., et al., Chemistry of the strong electrophilic metal fragment $[\text{Tc}(\text{N})(\text{PXP})]^{2+}$ (PXP = diphosphine ligand): A novel tool for the selective labeling of small molecules, *J. Am. Chem. Soc.* **124** (2002) 11468–11479.
- [11] BOSCHI, A., et al., Development of technetium-99m and rhenium-188 radiopharmaceuticals containing a terminal metal-nitrido multiple bond for diagnosis and therapy, *Top. Curr. Chem.* **252** (2005) 85–115.
- [12] SCHIBLI, R., et al., Synthesis and in vitro characterization of organometallic rhenium and technetium glucose complexes against Glut 1 and hexokinase, *Bioconjug. Chem.* **16** (2005) 105–112.
- [13] BANERJEE, S.R., et al., A new bifunctional amino acid chelator targeting glucose transporter, *J. Nucl. Med.* **45** (2004) 465.
- [14] UCCELLI, L., et al., “Incorporation of a glucose moiety in a technetium-99m nitrido compound”, X International Symposium on Radiopharmaceutical Chemistry (Proc. Symp. Kyoto, 1993) 6–7.
- [15] PHELPS, M.E., Positron emission tomography provides molecular imaging of biological processes, *Proc. Nat. Acad. Sci. USA* **97** (2000) 9226–9233.
- [16] LEE, W.W., et al., Imaging of adenovirus-mediated human sodium iodide symporter gene by $^{99m}\text{TcO}_4$ scintigraphy in mice, *Nucl. Med. Biol.* **31** (2004) 31–40.
- [17] CHUNG, J-K., Sodium iodide symporter: its role in nuclear medicine, *J. Nucl. Med.* **43** (2002) 1188–1200.
- [18] YANG, H.S., et al., Imaging of human sodium-iodide symporter gene mediated by recombinant adenovirus in skeletal muscle of living rats, *Eur. J. Nucl. Med. Mol. Imaging* **31** (2004) 1304–1311.
- [19] SKEHAN, S.J., et al., Mechanism of accumulation of ^{99m}Tc -sulesomab in inflammation, *J. Nucl. Med.* **44** (2003) 11–18.
- [20] PALESTRO, C.J., et al., Osteomyelitis: diagnosis with ^{99m}Tc -labeled antigranulocyte antibodies compared with diagnosis with ^{111}In -labeled leukocytes—initial experience, *Radiology* **223** (2002) 758–764.
- [21] SCIUK, J., et al., Comparison of technetium 99m polyclonal human immunoglobulin and technetium 99m monoclonal antibodies for imaging chronic osteomyelitis: first clinical results, *Eur. J. Nucl. Med.* **18** (1991) 401–407.
- [22] RENNEN, H.J., et al., Specific and rapid scintigraphic detection of infection with ^{99m}Tc -labeled interleukin-8, *J. Nucl. Med.* **42** (2001) 117–123.
- [23] WELLING, M.M., et al., Radiochemical and biological characteristics of ^{99m}Tc -UBI 29–41 for imaging of bacterial infections, *Nucl. Med. Biol.* **29** (2002) 413–422.

SESSION 4

- [24] JUWEID, M., et al., ^{99m}Tc -LL1: A potential new bone marrow imaging agent, *Nucl. Med. Commun.* **18** (1997) 142–148.
- [25] BLANKENBERG, F.G., et al., In vivo detection and imaging of phosphatidylserine expression during programmed cell death, *Proc. Natl. Acad. Sci. USA* **95** (1998) 6349–6354.
- [26] NARULA, J., et al., Annexin-V imaging for noninvasive detection of cardiac allograft rejection, *Nat. Med.* **7** (2001) 1347–1352.
- [27] HOFSTRA, L., et al., Visualisation of cell death in vivo in patients with acute myocardial infarction, *Lancet* **356** (2000) 209–212.
- [28] ELICEIRI, B.P., CHERESH, D.A., Role of α_v integrins during angiogenesis, *Cancer J.* **3** (Suppl.) (2000) S245–S249.
- [29] SU, Z.F., et al., In vitro and in vivo evaluation of a technetium-99m-labeled cyclic RGD peptide as a specific marker of $\alpha_v\beta_3$ integrin for tumor imaging, *Bioconjug. Chem.* **13** (2000) 561–570.
- [30] JOHANNSEN, B., PIETZSCH, H.-J., Development of technetium-99m-based CNS receptor ligands: Have there been any advances?, *Eur. J. Nucl. Med.* **29** (2002) 263–275.
- [31] KUNG, M.P., et al., [^{99m}Tc]TRODAT-1: A novel technetium-99m complex as a dopamine transporter imaging agent, *Eur. J. Nucl. Med.* **24** (1997) 372–380.
- [32] ZHUANG, Z.P., et al., Biphenyls labeled with technetium 99m for imaging β -amyloid plaques in the brain, *Nucl. Med. Biol.* **32** (2005) 171–184.

^{99m}Tc EDDA/HYNIC-TOC: A SUITABLE RADIOPHARMACEUTICAL FOR RADIOGUIDED SURGERY OF NEUROENDOCRINE

J. FETTICH*, S. REPSE*, M. SNOJ**, M. ZITKO-KRHIN*,
S. MARKOVIC*

*University Medical Centre Ljubljana
Email: jure.fettich@kclj.si

**Institute of Oncology

Ljubljana, Slovenia

Commercially available ¹¹¹In-DTPA-octreotide is a well-established radiopharmaceutical for imaging of neuroendocrine tumours (NET) expressing somatostatine receptors. Its analogue [Tyr³] octreotide can also be successfully radiolabelled with ^{99m}Tc. Compared with ¹¹¹In labelled preparation, the advantages of ^{99m}Tc labelled [Tyr³] octreotide are: energy of gamma rays more suitable for registration using gamma detectors and shorter half life, allowing use of higher activities and lower tracer uptake by the kidneys. Its pharmacokinetic properties do not differ significantly from commercially available ¹¹¹In-DTPA-octreotide [1]. For reasons stated above, the authors propose ^{99m}Tc labelled [Tyr³] octreotide for radioguided surgery of NET using a gamma probe.

Four patients, two with clinical and biochemical signs and symptoms of gastrinoma, one with biochemical evidence of carcinoid and the other with those of insulinoma underwent surgery. In all patients a markedly increased ^{99m}Tc labelled [Tyr³] octreotide uptake by the tumour (grades III and IV) was clearly seen on planar scintigraphy and SPECT, while all investigations, including contrast CT, MRI and endoscopical US were negative or inconclusive in all patients except the patient with the carcinoid, where the tumour was seen also on CT.

[^{99m}Tc-ethylendiaminediacetic acid-hydrazinonicotinamide-D-Phe¹ Tyr³] octreotide (^{99m}Tc-EDDA/HYNIC-TOC) was prepared according to the protocol suggested by von Guggenberg [2]. Radiochemical purity was determined using reversed phase gradient HPLC (a 125 mm × 4 mm HP ODS hypersil column, 0.02M phosphate buffer of pH6.2/acetonitrile at a flow rate 1 mL/min). Indicative retention time of ^{99m}Tc peptide complex was at 14 min

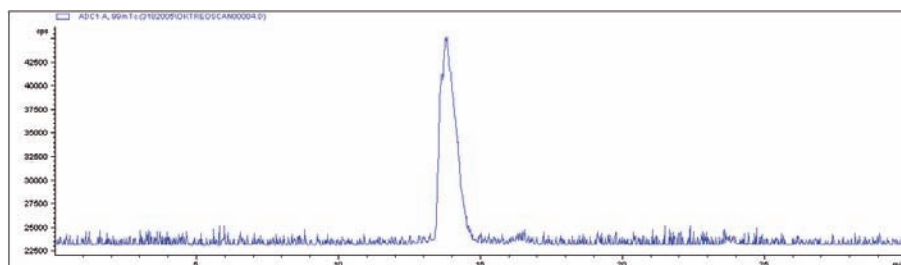


FIG. 1. HPLC radiochromatogram of ^{99m}Tc -EDDA/HYNIC-TOC.

(Fig. 1). Radiochemical purity above 95% was achieved in all cases. Following radiolabelling, the radiopharmaceutical was sterilized by filtration using a 0.22 μm filter.

Ten micrograms of peptide labelled with 600 MBq of ^{99m}Tc were injected IV 4 h prior to surgery. Using a gamma probe, the surgeons were able to localize the tumours successfully in all cases. The intraoperative count rate over the tumour was more than three times higher than the radioactivity detected elsewhere in the operating field. After removal of the tumours, a high level of radioactivity of the excised tissue was confirmed *ex vivo* by gamma probe and gamma camera measurements, and the nature of the tumours was confirmed by histology.

All patients were clinically, biochemically and scintigraphically disease free on follow-up three months after surgery. The authors conclude that ^{99m}Tc labelled [Tyr³] octreotide is the radiopharmaceutical of choice for radioguided surgery of NET owing to its physical and biological properties. In the hands of surgeons experienced in the use of the gamma probe, this approach seems to be superior to the traditional surgical technique, making surgery of NET shorter and easier, as well as increasing success of operative treatment of NET.

REFERENCES

- [1] PEITL, P., FETTICH, J., SLODNJAK, I., HOJKER, S., Comparison of ^{99m}Tc -EDDA/HYNIC and ^{111}In -DTPA-Octreotide uptake in patients without known pathology, *Eur. J. Nucl. Med.* **31** 2 (2004) 308.
- [2] VON GUGGENBERG, E., et al., Preparation via coligand exchange and characterisation of (^{99m}Tc -EDDA-HYNIC-D-Phe1, Tyr3) octreotide (^{99m}Tc -EDDA-HYNIC-TOC), *J. Lab. Comp. Radiopharm.* (2003).

COMPARATIVE IN VITRO AND IN VIVO EVALUATION OF A SERIES OF NOVEL BOMBESIN-LIKE PEPTIDES

E. GOURNI, P. BOUZIOTIS, M. PARAVATOU,
S. XANTHOPOULOS, S.C. ARCHIMANDRITIS,
A.D. VARVARIGOU

Institute of Radioisotopes and Radiodiagnostic Products,
NCSR 'Demokritos'

Email: egourni@yahoo.gr

M. FANI

Biomedica Life Sciences S.A.

G. LOUDOS

Biomedical Simulations and Imaging Laboratory, NTUA

Athens, Greece

Abstract

Bombesin (BN) is a peptide exhibiting a high affinity for the gastrin releasing peptide (GRP) receptor, which is overexpressed by a variety of tumours, such as breast or prostate cancer. The aim of the present work is the study of a series of novel BN-like peptides, by investigation of the radiochemical and radiopharmacological behaviour of the complexes they form with the nuclides $^{185/187}\text{Re}$ and $^{99\text{m}}\text{Tc}$. The derivatives under study are: BN1: Cys-*Aca*-BN[2-14], BN1.1: Gly-Gly-Cys-*Aca*-BN[2-14], BN1.2: MeGly-Gly-Cys-*Aca*-BN[2-14], BN1.3: (Me)₂Gly-Gly-Cys-*Aca*-BN[2-14] and BN1.4: Cys-Gly-Cys-*Aca*-BN[2-14] where *Aca* represents 6-amino-n-hexanoic acid. The $^{185/187}\text{Re}$ complexes were formed via the precursor Re-gluconate. The radiolabelling of the derivatives with $^{99\text{m}}\text{Tc}$ was performed via the precursor $^{99\text{m}}\text{Tc}$ -gluconate. The authors' efforts were focused on the comparative assessment of the radiolabelling conditions of the BN analogues with $^{99\text{m}}\text{Tc}$, so that the final radiolabelled products could have the maximum specific activity. The stability of the radiolabelled products was studied over time. The capability of the new peptides to tag cancer cells was evaluated in epithelial prostate cancer cells (PC3). Thus, the authors examined whether the new BN-derivatives, as well as their complexes with $^{185/187}\text{Re}$, inhibit [^{125}I -Tyr⁴]-BN binding. The in vivo behaviour of the $^{99\text{m}}\text{Tc}$ labelled BN-like peptides was evaluated in normal mice. In addition, for the most promising radiolabelled peptide the stability in human plasma was studied. Also, biodistribution and scintigraphic studies were assessed in prostate cancer models.

1. INTRODUCTION

A variety of tumours express neuropeptide receptors on their surface in higher density than most healthy tissues. The overexpression of peptide receptors in human tumours is of considerable clinical interest and they serve as a potential target for tumour imaging with radiolabelled peptides that bind specifically to these receptors. Peptides that selectively interact with specific receptors may be used as carriers to direct diagnostic or therapeutic radionuclides to receptor bearing organs. One such receptor binding peptide is bombesin (BN). BN is a 14 amino-acid peptide isolated from frog skin, with a high affinity for the gastrin releasing peptide (GRP) receptor [1, 2].

Several analogues of BN have been radiolabelled with a variety of radionuclides for diagnostic and therapeutic applications. This is because a variety of human tumours, such as small cell lung, prostate, breast, gastric, colorectal and pancreatic cancers, are known to express receptors specific for BN-like peptides [3–6]. BN/GRP receptors present on various cancer cells may be important for the early diagnosis of cancers with radiolabelled BN-like peptides.

With the object of preparing new radiopharmaceuticals for cancer diagnosis/therapy, the authors have designed, synthesized and studied a series of new BN-like peptides [7]. These peptides form complexes with the radiometal ^{99m}Tc ($T_{1/2} = 6.0$ h), which is ideal for diagnostic purposes, as well as with $^{185/187}\text{Re}$, which has similar chemical properties to Tc. In all the derivatives, X-Aca-BN[2-14] NH_2 of the study, the metal chelating group X has been conjugated to the N-terminal amine of Gln-Arg-Leu-Gly-Asn-Gln-Trp-Ala-Val-Gly-His-Leu-Met(CONH_2), (BN[2-14] NH_2) via 6-amino-hexanoic acid (Aca). The metal chelating group X in each case is one of the following: Gly-Gly-Cys (BN1.1), MeGly-Gly-Cys (BN1.2), $\text{Me}_2\text{Gly-Gly-Cys}$ (BN1.3), Cys-Gly-Cys (BN1.4), where MeGly refers to methylglycine and Me_2Gly refers to dimethylglycine.

The authors' efforts were focused on the comparative assessment of the radiolabelling conditions of the BN analogues with ^{99m}Tc . Next, for the in vitro evaluation of the peptide derivatives, the cancer cell line PC3 (epithelial prostate cancer cells), overexpressing BN-R, was used. More specifically, the authors examined whether the novel X-Aca-BN[2-14] NH_2 derivatives, as well as the respective $^{185/187}\text{Re-X-Aca-BN[2-14]NH}_2$ complexes, inhibit [$^{125}\text{I-Tyr}^4$]-BN cancer cell binding. Finally, the in vivo behaviour and the pharmacokinetic properties of the radiolabelled peptides were studied and evaluated, comparatively, in normal mice, with emphasis on the kinetics of the complexes and their uptake in organs, overexpressing BN receptors, such as the pancreas. The preliminary results mentioned above warranted further investigation of the

^{99m}Tc -BN1.1 BN derivative so its stability in human plasma was studied. Also, biodistribution and scintigraphic studies were assessed in prostate cancer models.

2. MATERIALS AND METHODS

[Tyr⁴]BN was purchased from Sigma. [¹²⁵I-Tyr⁴]BN was purchased from Amersham (100 μL , 10 μCi , 2000 Ci/mmol). KReO_4 was obtained from Sigma-Aldrich (Austria). Technetium-99m in the form of $\text{Na}^{99m}\text{TcO}_4$ in physiological saline, was eluted from a commercial ^{99}Mo - ^{99m}Tc generator (Mallinckdrodt Medical B.V.). Solvents for high performance liquid chromatography (HPLC) were of analytical grade; they were further filtered through 0.22 μm membrane filters (Millipore, Milford, United States of America). The BN derivatives were synthesized by the Fmoc method in the Immunopeptide Chemistry Laboratory of the Institute of Radioisotopes and Radiodiagnostic Products of the National Center for Scientific Research 'Demokritos'. The human prostate adenocarcinoma cell line was obtained from the American Type Culture Collection. For cell culturing, Dulbeccos's modified eagle medium, fetal bovine serum, penicillin/streptomycin, L-glutamine and trypsin/EDTA solution were purchased from PAA Laboratories (Austria). The bovine serum albumin (BSA), glutamax, hepes, bacitracin, aprotinin and PMSF used were obtained from Sigma-Aldrich (Austria).

2.1. Formation of Re(V)O complexes

Re(V)-complexes were prepared by ligand exchange reaction of the Re(V)-gluconate precursor with the BN derivatives according to the literature [8]. The reaction took place at 70°C, at a 1:1 metal:ligand molar ratio. The novel complexes were analysed by RP-HPLC.

2.2. Labelling with ^{99m}Tc

A solid mixture containing 1.0 g Na-gluconate, 2.0 g NaHCO_3 and 15 mg SnCl_2 was homogenized and kept dry [9, 10]. A quantity (6 mg) of the above mixture was dissolved in 2.0 mL of a $\text{Na}^{99m}\text{TcO}_4$ solution, containing 1480 MBq (40 mCi) of ^{99m}Tc . An aliquot of the above solution, containing 740–925 MBq (20–25 mCi) of ^{99m}Tc was added to 0.03–0.1 mg of the peptide under study. The mixture was left at room temperature and the exchange reaction was completed in 30 min.

2.3. Cell culture

The human PC3 adenocarcinoma cell line was maintained in Dulbecco's modified eagle medium supplemented with 1% fetal bovine serum, 1% L-glutamine, 1% penicillin/streptomycin, 1% glutamax, hepes 50mM, aprotinin 1 µg/mL, PMSF 0.25mM and 0.125% BSA. Cells were cultured at 37°C in a humidified incubator in an atmosphere containing 5% CO₂ and passaged weekly.

2.4. Competition binding assays

Competition binding experiments were performed using a PC3 cell line. [Tyr⁴]BN served as the control peptide and [¹²⁵I-Tyr⁴]BN as the radioligand [11–13]. In brief, cells were placed at confluence in 24 well plates with 35 000 cpm [¹²⁵I-Tyr⁴]BN in the presence of increasing concentrations of the different BN analogues (0–1000nM). After 1 h at 37°C, cells were washed twice with a cold binding buffer and then solubilized with 1N NaOH. Radioactivity was determined in a (NaI) γ counter (Packard).

2.5. Plasma incubation

Human blood was collected in heparinized polypropylene tubes, immediately centrifuged for 15 min at 5000 rpm at 4°C and the plasma collected [11]. Samples of the ^{99m}Tc-BN1.1 derivative were then incubated with the fresh plasma at 37°C and aliquots were withdrawn at 15 min and 2 h intervals. Ethanol was added to the latter in a 2:1 EtOH/aliquot v/v ratio, the samples were centrifuged at 35 000 rpm for 10 min and supernatant fractions were passed through a Millex GV filter (0.22 µm) prior to the HPLC analysis being conducted.

2.6. Biodistribution in normal mice

Female Swiss mice (average weight 25 g) were used for the biodistribution studies in groups of five animals per time point, the new ^{99m}Tc-BN derivatives being administered intravenously into the tail vein. Each mouse received a 100 µL aliquot in saline. Animals were sacrificed by ether anesthesia at preselected time points post-injection. The main organs were weighed and counted. The animals of an additional group were, each, co-injected with 100 µL of native BN (1 mg/mL) and 100 µL of the labelled peptide. These animals were sacrificed 1 h post-injection. Biodistribution data were calculated as the per cent injected dose per gram (%ID/g), using an appropriate standard.

2.7. Biodistribution in tumour bearing mice

For tumour implantation, approximately 5×10^6 PC3 cells in 0.2 mL saline were injected subcutaneously into the thigh of 5 female nude mice. Tumours developed approximately 3 weeks post-inoculation. Biodistribution studies were carried out at 1 h post-injection of the ^{99m}Tc -BN1.1 derivative as described above. The percentages of the injected dose per gram (%ID/g) of tissue were measured.

3. RESULTS AND DISCUSSION

3.1. Formation of Re(V)O complexes

The formation of $^{185/187}\text{Re}$ complexes of the BN-like peptides was successfully performed by the exchange reaction with preformed Re(V)-gluconate. The rhenium complexes were purified by RP-HPLC. HPLC analysis indicated the formation of a single species in each case. The retention times of the pure peptides, eluted from the chromatographic column, as well as those of the respective $^{185/187}\text{Re}$ complexes are reported in Table 1. $^{185/187}\text{Re}$ -BN1.3 could not be isolated.

3.2. Labelling with ^{99m}Tc

Technetium-99m labelling was easily performed at room temperature. As demonstrated by RP-HPLC, the radiolabelled peptides formed a single radioactive species in all cases. The obtained ^{99m}Tc -BN-like peptides remained stable for at least six hours post-labelling. The results of the radiolabelling are summarized in Table 2. Since the $^{185/187}\text{Re}$ -BN and the ^{99m}Tc -BN conjugates have similar retention times in RP-HPLC, it can be deduced that conjugates of both metals have the same structure [14, 15].

TABLE 1. RETENTION TIMES OF THE PURE PEPTIDES AND THEIR RESPECTIVE $^{185/187}\text{Re}$ COMPLEXES

Peptide	Pure peptide Retention time (min)	$^{185/187}\text{Re}$ complex Retention time (min)
BN 1.1	8.71	10.01
BN 1.2	8.33	11.26
BN 1.3	8.99	not isolated
BN 1.4	9.35	11.39

TABLE 2. RESULTS OF THE RADIOLABELLING OF THE BN-LIKE PEPTIDES

Peptide	Quantity (μg)	Radioactivity (mCi)	Yield %	Retention time (min)
BN 1.1	100	20	98	10.88
	30	25	98	10.88
BN 1.2	100	20	>95	11.13
BN 1.3	100	20	>95	11.38
BN 1.4	100	20	>95	11.68

It is obvious from the above table that the maximum specific activity was obtained for the BN1.1 derivative.

3.3. Competition binding assays

The binding capability of the BN derivatives for the GRP-R was determined on a human androgen insensitive PC3 prostate cancer cell line, reported to predominantly express BN-R2. The IC_{50} values calculated were found in the sub-nanomolar range and were comparable to those of Tyr⁴-BN. Binding data were analysed and IC_{50} values were calculated by non-linear regression according to a one site model using the PRISM4 program (Graph Pad Software, San Diego, USA) (Table 3).

TABLE 3. INHIBITION OF [¹²⁵I-Tyr⁴]BN BINDING TO PC3 CELLS BY DIFFERENT BN ANALOGUES

Compound	IC_{50} (nM)
Tyr ⁴ -BN	1.24
BN 1.1	0.59
^{185/187} Re-BN 1.1	1.13
BN 1.2	0.72
^{185/187} Re-BN 1.2	0.76
BN 1.3	0.76
^{185/187} Re-BN 1.3	not isolated
BN 1.4	1.36
^{185/187} Re-BN 1.4	1.42

The *in vitro* binding studies of the novel BN analogues demonstrated that they have a high GRP-R binding affinity (Table 3). In parallel, the $^{185/187}\text{Re}$ complexes were examined and also found to have an affinity for the GRP-R. It should be noted that the BN derivatives themselves show a slightly higher affinity than their $^{185/187}\text{Re}$ complexes towards PC3 cancer cells [11, 12]. This is probably due to the alteration of the peptide's ternary structure during the formation of the complex. From the data in Table 3 it is obvious that the derivative with the highest affinity for the GRP-R is BN-1.1. Also, the IC_{50} value of the $^{185/187}\text{Re}$ -BN1.1 complex is almost similar to that of Tyr⁴-BN, thus it is assumed that the respective $^{99\text{m}}\text{Tc}$ complex should also have a high affinity for the GRP-R.

3.4. Plasma incubation

The stability of the most promising radiolabelled peptide, the $^{99\text{m}}\text{Tc}$ -BN1.1 derivative, was studied in human plasma (Table 4). The incubation of the derivative in human plasma, under conditions which mimic the human organism (37°C), showed that the labelled peptide derivative remains stable at approximately 80%, even after 2 h post-incubation.

3.5. Biodistribution in normal mice

In the biodistribution studies, all the derivatives under evaluation presented rapid blood clearance, as shown by the data summarized in Tables 5 and 6. The new $^{99\text{m}}\text{Tc}$ conjugates cleared rapidly from the blood and were eliminated mainly through the renal/urinary pathway. Uptake in the pancreas was high and specific, as demonstrated by the effective *in vivo* blockade of this organ, in the animals co-injected with a high dose of native BN. Intestinal uptake can be attributed mainly to the GRP-R, expressed in this tissue, given that it was substantially reduced in the animals co-injected with native BN [11].

Biodistribution evaluation of the $^{99\text{m}}\text{Tc}$ labelled peptides shows that all the radiolabelled conjugates clear efficiently from the blood and are eliminated

TABLE 4. STABILITY OF THE $^{99\text{m}}\text{Tc}$ -BN1.1 DERIVATIVE IN HUMAN PLASMA

	Time	Stability
In human plasma	15 min	95%
	2 h	80%

TABLE 5. BIODISTRIBUTION OF THE NOVEL ^{99m}Tc LABELLED DERIVATIVES (*Tissue distribution data at 30, 60 and 120 min post-injection. Five animals were used per time point and results are given as mean \pm standard deviation of %ID/g*)

Tissue		BN 1.1	BN 1.2	BN 1.3	BN 1.4
Blood	30 min	1.2 \pm 0.2	0.7 \pm 0.1	1.4 \pm 0.4	0.6 \pm 0.1
	60 min	1.1 \pm 0.7	2.0 \pm 0.3	1.8 \pm 0.3	3.2 \pm 1.7
	120 min	0.4 \pm 0.1	0.4 \pm 0.1	1.0 \pm 0.1	0.1 \pm 0.0
Liver	30 min	2.3 \pm 0.8	4.1 \pm 1.7	3.0 \pm 1.9	3.8 \pm 1.6
	60 min	2.7 \pm 0.8	4.2 \pm 1.4	1.8 \pm 0.6	9.6 \pm 5.5
	120 min	1.1 \pm 0.6	1.2 \pm 0.5	1.9 \pm 0.8	3.1 \pm 2.2
Total intestines	30 min	2.4 \pm 1.3	8.7 \pm 2.5	5.6 \pm 1.9	9.3 \pm 2.2
	60 min	7.3 \pm 2.2	10.5 \pm 3.2	3.4 \pm 1.6	3.3 \pm 1.8
	120 min	6.4 \pm 0.8	9.8 \pm 1.4	6.4 \pm 1.1	15.7 \pm 0.8
Kidney	30 min	9.2 \pm 2.1	4.3 \pm 1.0	11.0 \pm 3.2	3.7 \pm 0.1
	60 min	4.6 \pm 1.6	5.8 \pm 0.9	7.2 \pm 1.6	14.7 \pm 4.5
	120 min	3.7 \pm 1.6	1.6 \pm 0.4	6.4 \pm 1.8	0.6 \pm 0.1
Pancreas	30 min	11.3 \pm 3.6	7.7 \pm 3.4	12.8 \pm 2.7	10.3 \pm 1.7
	60 min	5.1 \pm 0.5	7.3 \pm 1.0	3.0 \pm 0.4	6.7 \pm 2.5
	120 min	3.6 \pm 1.7	3.0 \pm 0.8	6.7 \pm 0.9	0.6 \pm 0.2
Urine (%ID/organ)	30 min	20.4 \pm 4.9	6.5 \pm 0.9	26.6 \pm 7.0	3.9 \pm 0.5
	60 min	19.5 \pm 5.6	20.5 \pm 1.0	21.8 \pm 0.3	12.3 \pm 0.3
	120 min	33.8 \pm 3.6	46.0 \pm 3.6	34.3 \pm 4.2	23.3 \pm 4.6

TABLE 6. BLOCKING EXPERIMENT (*Tissue distribution data at 60 min post-injection. Animals were co-injected with a high dose of native BN. The results are given as mean \pm standard deviation of %ID/g*)

Tissue	BN 1.1	BN 1.2	BN 1.3	BN 1.4
Blood	3.0 \pm 1.6	2.1 \pm 0.9	2.7 \pm 0.8	3.5 \pm 0.2
Liver	4.4 \pm 3.2	9.5 \pm 5.8	3.5 \pm 1.7	10.0 \pm 2.8
Total intestines	3.8 \pm 0.7	9.9 \pm 3.9	2.2 \pm 0.6	3.3 \pm 1.7
Kidney	12.0 \pm 0.3	20.7 \pm 12.1	11.8 \pm 6.3	16.0 \pm 5.3
Pancreas	1.3 \pm 0.2	1.8 \pm 1.0	1.3 \pm 0.4	1.3 \pm 0.3
Urine (%ID/organ)	33.5 \pm 0.8	1.0 \pm 0.6	0.6 \pm 0.2	0.5 \pm 0.1

mainly through the kidneys to the urinary tract without any significant retention in the kidneys. High pancreas values render all the new BN derivatives possible candidates for imaging organs rich in BN receptors.

3.6. Biodistribution in tumour bearing mice

Gamma camera imaging of a nude mouse bearing prostate cancer, injected with the ^{99m}Tc -BN1.1 derivative, is presented in Fig. 1. The experimental tumour is clearly delineated 1 h post-injection. Biodistribution studies showed that the tumour uptake was $15.2 \pm 2.1\%$ ID/g and the tumour to non-tumour ratio was 30.

4. CONCLUSION

A series of novel BN-like peptides has been synthesized, isolated and characterized by analytical methods. The radiolabelling of these peptides led to the formation of a single radioactive species with a yield of over 95% in all cases. The BN1.1 derivative is the one that was labelled with the maximum specific radioactivity. The ^{99m}Tc -BN-1.1 compound remains stable with time and in human plasma. To date these in vitro findings show that the cold peptides exhibit a slightly higher affinity than their complexes with $^{185/187}\text{Re}$ towards the cancer cell line PC3, which overexpresses the BN receptor subtype II. The in vivo behaviour and the pharmacokinetic properties of the radiolabelled derivatives were studied and evaluated by performing biodistribution studies on normal mice. It was found that the elimination of the derivatives

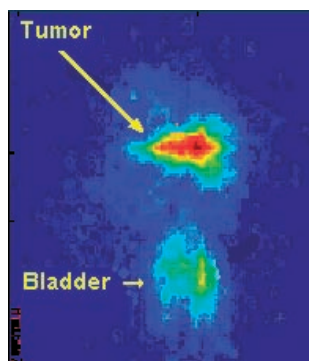


FIG. 1. Gamma scintigrams of a nude mouse injected with the ^{99m}Tc -BN1.1 derivative.

took place mainly via the urinary and, to a lesser extent, the hepatobiliary systems. The pancreas uptake was shown to be specific. Preliminary in vivo studies of the most promising radiolabelled peptide, ^{99m}Tc -BN-1.1, in nude mice bearing prostate cancer showed a clear delineation of the experimental tumour and a tumour to non-tumour ratio of 30.

REFERENCES

- [1] OKARVI, S.M., Recent development in ^{99m}Tc -labeled peptide-based radiopharmaceuticals: an overview, *Nucl. Med. Commun.* **20** (1999) 1093–1112.
- [2] OKARVI, S.M., AL-JAMMAZ, I., Synthesis, radiolabeling and biological characteristics of a bombesin peptide analog as a tumor imaging agent, *Anticancer Res.* **23** (2003) 2745–2750.
- [3] PANSKY, A., et al., Gastrin releasing peptide-preferring bombesin receptors mediate growth of human renal cell carcinoma, *J. Am. Soc. Nephrol.* **11** (2000) 1409–1418.
- [4] MOODY, T.W., PERT, C.B., GAZDAR, A.F., CARNEY, D.N., High levels of intracellular bombesin characterize human small cell lung carcinoma, *Science* **214** (1981) 1246–1248.
- [5] MARKWALDER, R., REUBI, J.C., Gastrin-releasing peptide receptors in the human prostate: Relation to neoplastic transformation, *Cancer Res.* **59** (1999) 1152–1159.
- [6] GUGGER, M., REUBI, J.C., GRP receptors in nonneoplastic and neoplastic human breast, *Am. J. Pathol.* **155** (1999) 2067–2076.
- [7] VARVARIGOU, A.D., BOUZIOTIS, P., ZIKOS, C., SCOPINARO, F., DE VINCENTIS, G., Gastrin releasing peptide (GRP) analogues for cancer imaging, *Cancer Bioth. Radiopharm.* **19** (2004) 219–229.
- [8] JANKOWSKY, R., KIRSCH, S., REICH, T., SPIES, H., JOHANNSEN, B., Solution structure of rhenium(V) oxo peptide complexes of glycylglycylcysteine and cysteinylglycine as studied by capillary electrophoresis and X-ray absorption spectroscopy, *J. Inorg. Bioch.* **70** (1998) 99–106.
- [9] COSTOPOULOS, B., et al., Radiochemical and radiobiological evaluation of a synthetic peptide labelled with ^{99m}Tc , *Nucl. Med. Commun.* **18** (1997) 474–481.
- [10] VARVARIGOU, A.D., et al., Synthesis, chemical, radiochemical and radiobiological evaluation of a new ^{99m}Tc -labeled Bombesin-like peptide, *Cancer Bioth. Radiopharm.* **17** 3 (2002) 317–326.
- [11] NOCK, B., [^{99m}Tc]Demobesin 1, a novel potent bombesin analogue for GRP receptor-targeted tumor imaging, *Eur. J. Nucl. Med.* **30** (2003) 247–258.
- [12] LA BELLA, R., A ^{99m}Tc (I)-postlabeled high affinity Bombesin analogue as a potential tumor imaging agent, *Bioconjugate Chem.* **13** (2002) 599–604.

SESSION 4

- [13] SMITH, C.J., Radiochemical investigations of $^{99m}\text{Tc-N}_3\text{S-X-BBN}[7-14]\text{NH}_2$: An in vitro/in vivo structure-activity relationship study where X=0-, 3-, 5-, 8-, and 11-carbon tethering moieties, *Bioconjugate Chem.* **14** (2003) 93–102.
- [14] BAIDOO, K.E., et al., Design, synthesis and initial evaluation of high-affinity technetium bombesin analogues, *Bioconjugate Chem.* **9** (1998) 218–225.
- [15] LIBSON, K., et al., Kinetics and mechanism of ligand substitution on analogous technetium (V) and rhenium(V) complexes, *Inorg. Chim. Acta.* **12** (1973) 23–35.

[^{99m}TcN]-N-BENZYL PIPERIDINE DITHIOCARBONATE: A POTENTIAL SIGMA RECEPTOR IMAGING AGENT

D. SATPATI*, K. BAPAT*, S. BANERJEE*, K. KOTHARI*,
H.D. SARMA**, M. VENKATESH*

*Radiopharmaceuticals Division
Email: drishtys@apsara.barc.ernet.in

**Radiation Biology & Health Sciences Division

Bhabha Atomic Research Centre
Mumbai, India

Abstract

With an aim of preparing a specific agent for targeting sigma receptors, 4-amino-N-benzyl piperidine was functionalized to a dithiocarbamate derivative and radiolabelled with the preformed [^{99m}TcN]²⁺ core. Radiolabelling yield of the complex, [^{99m}TcN]-4-dithiocarbamate-N-benzyl piperidine, as determined by HPLC was found to be >98%. Pharmacokinetics of the product was determined by performing normal biodistribution in Swiss mice. Receptor specificity of the radiolabelled complex was tested by carrying out in vitro and in vivo blocking studies with (+) pentazocine, a sigma receptor specific agent. In the in vitro studies, cell uptake of ~2% was observed with MCF-7 cells as well as with fibrosarcoma cells, which reduced to ~0.2% and 0.9% respectively after pre-incubation with pentazocine. Biodistribution studies in normal mice showed brain uptake of 0.6 ± 0.05%ID/g at 5 min post-injection, which reduced to 0.3 ± 0.06 %ID/g at 2 h post-injection. Uptake in other organs known to exhibit sigma receptors at 5 min post-injection (%ID/g) was found to be: 10% (heart), 23% (lungs), 31% (liver) and 22% (kidneys). Administration of pentazocine one hour prior to the injection of [^{99m}TcN]-4-dithiocarbamate-N-benzyl piperidine resulted in a decrease in accumulation of radioactivity in these organs (%ID/g) to a significant extent and was found to be: brain (not detected), 6.8% (heart), 13.9% (lungs), 14.8% (liver) and 14.9% (kidneys).

1. INTRODUCTION

Sigma receptors are non-opiate, non-dopaminergic membrane bound proteins that possess a high affinity for neuroleptic drugs [1]. It is reported that there are two subtypes of sigma receptor, namely sigma-1 and sigma-2. [³H](+)-

pentazocine selectively labels sigma-1 sites whereas di-o-tolyl guanidine is used for the labelling of both sigma-1 and sigma-2 sites [2, 3, 4]. Besides the central nervous system, sigma receptors are widely distributed in peripheral tissues such as liver, kidneys, lungs, gonads and ovaries [5]. Sigma receptors are known to be overexpressed in various human tumours such as melanoma, breast cancer, small cell lung carcinoma, prostate cancer and tumours of neural origin. The high density of sigma receptors in these tumours makes them excellent targets for designing tumour specific imaging agents [6]. The $[^{99m}\text{TcN}]^{2+}$ core forms stable complexes with N and S donors in a tetradentate array. In this respect dithiocarbamates (DTCs) are ideally suited for complexation. Since the $-\text{NH}_2$ group of piperidine is a pendant moiety, its facile derivatization to DTC provides a possible route for synthesis of the ligand under study. Unlike $[^{99m}\text{TcO}]^{3+}$ which leads to low specific activity complexes due to a requirement for an excess amount of ligand for stabilization, the high specific activity obtainable with $[^{99m}\text{TcN}]^{2+}$ owing to the requirement for low ligand concentration encourages its use in designing receptor specific agents. Various radioiodinated as well as ^{11}C and ^{18}F labelled derivatives of piperidine have been reported to be selective sigma-1 ligands and used for imaging human melanoma and non-small cell lung carcinoma [7, 8, 9]. However, there are few reports of sigma receptor ligands labelled with ^{99m}Tc [10]. The paper describes an effort made to radiolabel the derivatized piperidine DTC with a $[^{99m}\text{TcN}]^{2+}$ core offering high specific activity and leading to the formation of stable complexes.

The paper reports the chemical synthesis of the DTC derivative of 4-amino-N-benzyl piperidine (Pip-DTC) and its radiolabelling with a $[^{99m}\text{TcN}]^{2+}$ core. The evaluation of the complex was carried out by performing in vitro cell binding studies as well as competition studies using a sigma receptor specific ligand as a blocking agent. Biodistribution studies were carried out in mice to determine the pharmacokinetics and in vivo specificity of the complex.

2. MATERIALS AND METHODS

All reagents used were of commercial grade. The $^{99m}\text{TcO}_4^-$ was obtained from an in-house $^{99}\text{Mo}/^{99m}\text{Tc}$ column generator using normal saline. Commercial kit for preparation of $[^{99m}\text{TcN}]^{2+}$ precursor was obtained from CIS Bio International. Electrophoresis experiments were carried out using a 0.025M phosphate buffer (pH7.5) at 300V/cm for 1 h. HPLC analyses were performed on a Jasco PU 1580 system with a Jasco 1575 tunable absorption detector and an indigenously developed radiometric detector system using a C-18 reversed phase HiQ Sil (5 μm , 250 mm \times 4 mm) column. About 25 μL of

the test solution was injected into the column and the elution was monitored by observing the radioactivity profile. The flow rate was maintained at 1 mL/min. The gradient system consisting of eluting solvents H₂O (solvent A) and acetonitrile (solvent B) with 0.1% trifluoroacetic acid was used (0–28 min, 90% to 10% A; 28–30 min, 10% A; 30–32 min, 10% to 90% A). Mass spectra were recorded on a QTOF Micromass instrument using electron spray ionization in positive mode. Dulbecco's Modified Eagle's Medium (DMEM) and fetal calf serum were obtained from Sigma Chemicals Co. (USA), MCF-7 and fibrosarcoma cell lines were procured from the National Centre of Cell Sciences, Pune, India. All the animal experiments were carried out in compliance with the relevant national laws as approved by the local committee on the conduct and ethics of animal experimentation.

3. EXPERIMENTAL

3.1. 4-dithiocarbamato-N-benzyl piperidine (Pip-DTC)

4-amino-N-benzyl piperidine (50 mg, 0.26 mmol) was dissolved in diethyl ether and carbon disulphide (15 μ L, 0.25 mmol) was added to it, along with sodium hydroxide (4.8 mg, 0.12 mmol). A white precipitate was obtained immediately on addition of carbon disulphide. The reaction mixture was stirred at room temperature overnight. After 24 h, the solvent was removed and the product was purified using ammonia:methanol (5:95) as the eluting solvent in a silica gel column. The structure of Pip-DTC is shown in Fig. 1.

3.2. [^{99m}TcN]-4-dithiocarbamato-N-benzyl piperidine {[^{99m}TcN]-Pip-DTC}

A 0.1 mL methanol solution of 4-dithiocarbamato-N-benzyl piperidine (50 μ g, 0.2mM) was added to 1 mL of [^{99m}TcN]²⁺ precursor prepared using the

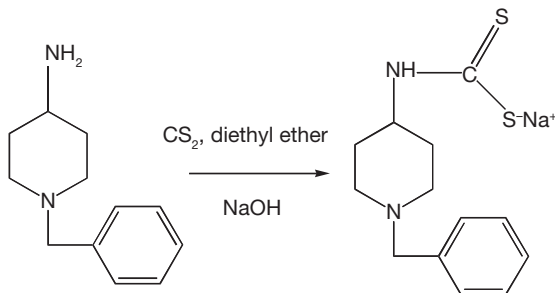


FIG. 1. Structure of Pip-DTC.

kit vial. The reaction mixture was incubated at room temperature for 30 min. The complex was characterized by TLC and HPLC (structure shown in Fig. 2).

3.3. Cell uptake studies

Cell uptake studies were carried out using two different cell lines, i.e. MCF-7 and fibrosarcoma. MCF-7 cells were propagated in DMEM supplemented with 10% fetal calf serum. After attaining confluency, the cells were centrifuged and suspended in plain DMEM. Fibrosarcoma cells were isolated from tumour bearing mice under aseptic conditions and suspended in DMEM. The tumour cells were washed twice and finally a suspension of $\sim 10^6$ – 10^7 cells/mL was prepared in 50mM tris-buffer (pH8) containing 0.2% BSA. Around 10^5 cells were incubated at 37°C for 60 min with the complex, [^{99m}TcN]-Pip-DTC and blanks were set up with ~ 100 – 500 fold cold compound and also with $^{99m}\text{TcO}_4^-$. Under similar conditions, inhibition studies were carried out by incubating $\sim 10^5$ cells with 100 μg of pentazocine along with the radiolabelled compound. After incubation, the cells were washed twice with ice cold assay buffer and centrifuged at 2000 rpm for 5 min. After removal of supernatant, the radioactivity associated with the cell pellet was counted.

3.4. Biodistribution and receptor blocking studies

Biodistribution studies were carried out in normal Swiss mice. 0.1 mL of [^{99m}TcN]-Pip-DTC (3–7 MBq) was injected via the tail vein. At 5 min and 2 h post-injection, animals were sacrificed and all the major organs were excised and weighed. The organs were counted in a NaI(Tl) flat geometry detector to calculate the percentage of injected dose per gram in the various organs.

Receptor blocking studies were carried out by intraperitoneal injection of 25 μg of pentazocine 1 h prior to the administration of the radiolabelled

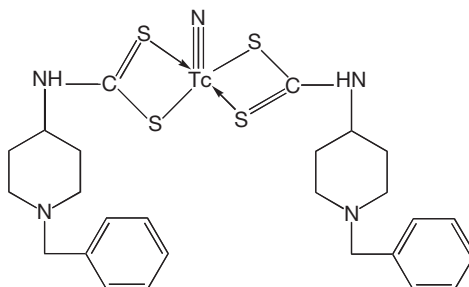


FIG. 2. Probable structure of [^{99m}TcN]-Pip-DTC.

complex. After 5 min post-injection of the complex, the animals were sacrificed and the percentage radioactivity associated with each organ was estimated.

4. RESULTS

N-benzyl piperidine is the basic pharmacophore used in several studies to prepare the radioiodinated benzamides for designing agents intended for studying sigma receptor affinity. With the aim of preparing ^{99m}Tc labelled agents specific for sigma receptors, the authors carried out functionalization of the amino group of 4-amino-N-benzyl piperidine. DTC derivative has been prepared by reaction with carbon disulphide and purified for subsequent labelling with a ^{99m}Tc -nitrido core. The $[\text{}^{99m}\text{TcN}]^{2+}$ core was prepared using the kit presented by the IAEA as a gift. The complex was then prepared by incubation of Pip-DTC with the $[\text{}^{99m}\text{TcN}]^{2+}$ core. The core as well as complex could be prepared with a >98% yield as determined by HPLC. In the HPLC gradient system, the nitrido core had a retention time of 4 min whereas the complex eluted as a single species had a retention time of 15 min.

As sigma receptors are overexpressed in variety of tumours, MCF-7 and fibrosarcoma cell lines were chosen for carrying out the in vitro studies. Though the cell uptake of the complex $[\text{}^{99m}\text{TcN}]$ -Pip-DTC was less (~2%) with both the cell lines, there was significant reduction in the cell uptake (75% and 55% respectively) when the cells were incubated with pentazocine, a sigma receptor specific drug, indicating receptor specificity of the complex. Pharmacokinetics of the product was carried out in normal Swiss mice. At 5 min post-injection, brain uptake of ~0.6% ID/g was observed which reduced to 0.3% ID/g at 2 h post-injection. Uptake in other vital tissues, such as heart, lungs, liver and kidneys expressing sigma receptors was also recorded and found to be 10%, 23%, 31% and 22% ID/g respectively. The receptor blocking experiment was carried out by administration of pentazocine 1 h prior to $[\text{}^{99m}\text{TcN}]$ -Pip-DTC, which led to a decrease in percentage radioactivity in heart, lungs, liver and kidneys of 6.8%, 13.9%, 14.8% and 14.9% ID/g at 5 min post-injection respectively. No radioactivity was observed in the brain after receptor blocking (Fig. 3). High uptake in the organs expressing sigma receptors and a decrease in radioactivity after injection of pentazocine suggest specificity of the complex. Since the experiments reveal that the complex exhibited the capability of crossing the blood brain barrier, it provides considerable insight with regard to potential applicability in designing an imaging agent for neural tumours which express sigma receptors.

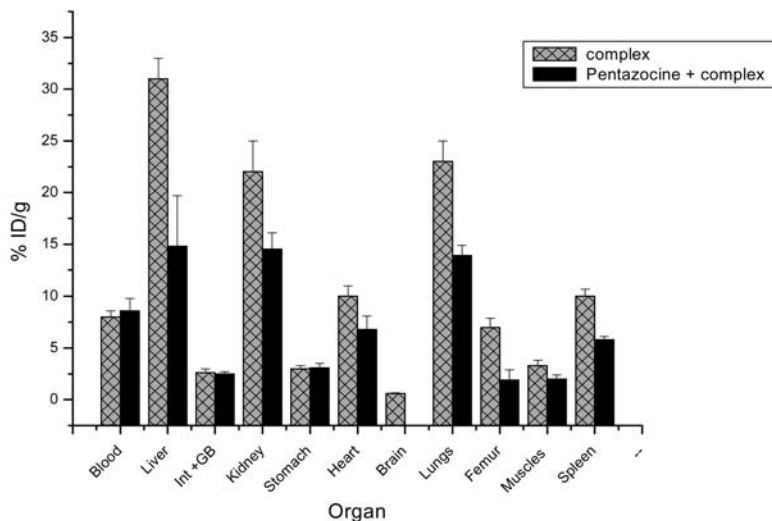


FIG. 3. *In vivo* receptor blocking studies of [^{99m}TcN]-Pip-DTC at 5 min post-injection in Swiss mice.

5. CONCLUSION

4-dithiocarbamate-N-benzyl piperidine could be synthesized with good yields and radiolabelled with a [^{99m}TcN] $^{2+}$ core with >98% yield. The product has shown uptake in the brain as well as in the organs expressing sigma receptors. The uptake in these organs was found to decrease on blocking the receptors with a specific drug, i.e. pentazocine. These studies indicate specificity of the product for sigma receptors. Further studies in tumour bearing mice are under way.

ACKNOWLEDGEMENTS

The authors are grateful to V. Venugopal, Director, Radiochemistry and Isotope Group, for his constant support and encouragement. The authors are also grateful to the IAEA for providing the ^{99m}Tc -nitrido kit.

REFERENCES

- [1] WALKER, J.M., et al., Sigma receptors: Biology and function, *Pharmacol. Rev.* **44** (1990) 355–402.
- [2] BOWEN, W.D., Sigma receptors: Recent advances and new clinical potentials, *Pharm. Acta Helv.* **74** (2000) 211–218.
- [3] BOWEN, W.D., DE COSTA, B.R., HELLEWELL, S.B., WALKER, J.M., RICE, K.C., [³H](+)-Pentazocine: A potent and highly selective benzomorphan-based probe for σ -1 receptors, *Mol. Neuropharmacology* **3** (1993) 117–126.
- [4] WEBER, E., et al., 1,3-Di(2-[5-³H] tolyl) guanidine: A selective ligand that labels σ type receptors for psychotomimetic opiates and antipsychotic drugs, *Proc. Natl. Acad. Sci. USA* **83** (1986) 8784–8788.
- [5] WOLFE, S.A., CULP, S.G., DE SOUZA, E.B., Sigma receptors in endocrine organs: Identification, characterization and autoradiographic localization in rat pituitary, adrenals, testis, and ovary, *Endocrinology* **124** (1989) 1160–1172.
- [6] VILNER, B.J., JOHN, C.S., BOWEN, W.D., Sigma-1 and sigma-2 receptors are expressed in a variety of human and rodent tumor cell lines, *Cancer Res.* **55** (1995) 408–413.
- [7] JOHN, C.S., VILNER, B.J., GEYER, B.C., MOODY, T., BOWEN, W.D., Targeting sigma receptor binding benzamides as in-vivo diagnostic and therapeutic agents for human prostate tumors, *Cancer Res.* **59** (1999) 4578–4583.
- [8] ZHAO, J., CHANG, R., CARAMBOT, P., WATERHOUSE, R.N., Radiosynthesis and in vivo study of [¹⁸F]1-(2-fluoroethyl)-4-[(4-cyanophenoxy)methyl] piperidine: A promising new sigma-1 receptor ligand, *J. Label Compd. Radiopharm.* **48** (2005) 547–555.
- [9] ISHIWATA, K., et al., Synthesis and preliminary evaluation of [¹¹C] NE-100 labeled in two different positions as a PET σ receptor ligand, *Nucl. Med. Biol.* **25** (1998) 195–202.
- [10] CHOI, S.R., et al., Development of Tc-99m labeled sigma-2 receptor specific ligand as a potential breast tumor imaging agent, *Nucl. Med. Biol.* **28** (2001) 657–666.

^{99m}Tc LABELLED PEPTIDE F11: A NEW POTENTIAL $\alpha_v\beta_3$ INTEGRIN ANTAGONIST FOR SCINTIGRAPHIC DETECTION OF TUMOURS

A. PERERA, A. PRATS, A. HERNÁNDEZ

Centre for Clinical Research

Email: alejandro.perera@infomed.sld.cu

O. REYES, M. BEQUET, N. SANTIAGO

Centre for Genetic Engineering and Biotechnology

R. LEYVA

Isotope Centre

E. FERNANDEZ

Institute of Pharmacy and Food

G. PIMENTEL

National Institute for Oncology and Radiobiology

Havana, Cuba

Abstract

The aim of the present work was to develop a peptide with the sequence Arg-Gly-Asp-Ser (polypeptide F11) and label it with ^{99m}Tc to obtain scintigraphic images in an animal model for tumour imaging. Polypeptide F11 was obtained by solid phase synthesis. The influence of the molar ratio of F11:Sn⁺² (1:0.5, 1:1, 1:2, 1:4) on the radiochemical purity of radiopharmaceutical was assessed. The stability of the radiolabelled peptide was tested by its incubation in 0.1M PBS (pH7.2), in a solution containing 30-fold molar excess of L-cysteine and in fresh human plasma, at room temperature for up to 24 h. One microgram (27.5–29.0 MBq) of ^{99m}Tc -F11 was injected through the ocular plexus of C57BL6 male mice to determine the biokinetics up to 24 h. Scintigraphic images were acquired after administration of 13 μg (67–74 MBq) of ^{99m}Tc -F11 to C57BL6 mice bearing B16 melanoma tumours and nude mice with A431 tumours. Using a 1.3-fold molar excess of stannous fluoride, a ^{99m}Tc labelling yield of $95.2 \pm 2.1\%$ and recovery from HPLC of $>92\%$ was attained. About 40% of the ^{99m}Tc bound to peptide was transchelated to L-cysteine at 24 h. Polypeptide F11 that resulted is sensitive to the action of chelating agents and peptidases in plasma. A significant binding to plasma proteins was seen by size exclusion HPLC. Renal uptake varied from 9.5% ID/g at 1 h to 4.0% ID/g at 24 h; thus it could be the main elimination pathway. The rest of the organs showed uptakes of less than 2.0% ID/g. Serum pharmacokinetics were fixed to a bicompartamental model with a $T_{1/2\alpha} = 43.1 \pm 13.5$ min and

$T_{1/2\beta} = 327 \pm 149$ min. Scintigraphic images showed an intense tumour uptake of the radiopharmaceutical. In conclusion, the ^{99m}Tc labelled peptide F11 could be a promising radiopharmaceutical for scintigraphic detection of tumours.

1. INTRODUCTION

Peptides are involved in a broad range of biological processes. Their low molecular weights impact in low antigenicity, fast clearance and rapid tissue penetration [1]. Furthermore, in contrast with monoclonal antibodies, peptides can be easily and cheaply obtained by solid phase synthesis with high purity [1]. These advantages have encouraged the assessment of different aminoacidic sequences as potential candidates for the study and therapy of several diseases, mainly in the field of oncology [1–4]. Tumour cells show a wide variety of receptors, which could be used as targets for radiolabelled molecules. Thus, there could be available a panel of peptides, each appropriate for a particular kind of cancer or, even better, a ‘universal’ peptide that binds to all tumour types [4]. The last alternative seems to be more reasonable and the integrins remain one of the most attractive targets [4]. Integrins are cell surface receptors that are involved in cell–cell and cell–matrix interactions [5–7]. They are heterodimeric glycoproteins consisting of α and β chains that are non-covalently linked on the cell surface [5–7].

The $\alpha_v\beta_3$ integrin is implicated in many pathological processes, such as osteoporosis, misregulated angiogenesis, tumour growth and tumour metastasis [8, 9]. This receptor is highly expressed on different malignancies such as osteosarcomas, neuroblastomas, glioblastomas, lung carcinomas, breast neoplasms, gastric carcinoma, prostate cancer, bladder carcinomas and invasive melanomas [6, 8–14].

Many integrins, including the $\alpha_v\beta_3$ receptor, act by recognizing the specific tripeptide sequence Arg-Gly-Asp (RGD) of their substrates [15]. Thus, a variety of radiolabelled RGD derivative peptides have been proposed for the diagnosis and therapy of malignant diseases [16, 17].

The aim of the present work was to develop a peptide with the sequence Arg-Gly-Asp-Ser and label it with ^{99m}Tc to obtain scintigraphic images in an animal model.

2. MATERIALS AND METHODS

2.1. Peptide

Polypeptide F11 contains a linear sequence Arg-Gly-Asp-Ser to recognize the $\alpha_v\beta_3$ receptor and another linear sequence (Ala-Gly-Gly-Gly) at the N-terminal to chelate ^{99m}Tc . It was obtained by solid phase synthesis in the Laboratory of Synthetic Peptides, Centre for Genetic Engineering and Biotechnology, Havana, Cuba.

Peptide was analysed by mass spectrometry and its purity determined by reverse phase high performance liquid chromatography (HPLC-RP). The purity of the obtained peptide was >95%.

2.2. ^{99m}Tc -labelling of F11

The labelling procedure was carried out at neutral pH, employing stannous fluoride as the reducing agent. The influence of molar ratio F11 Sn^{+2} (1:0.5, 1:1, 1:2, 1:4) on the radiochemical purity of the radiopharmaceutical was assessed. To 80 μg of F11 (100 μL) in 0.1M saline phosphate buffer (PBS) (pH8.5) was added stannous fluoride (Sigma, United States of America) in 100 μL of 0.3mM HCl and 740–1110 MBq of ^{99m}Tc from a freshly eluted $^{99}\text{Mo}/^{99m}\text{Tc}$ generator (Amersham, United Kingdom). The mixture was incubated for 20 min at room temperature. Results were represented by using a chart.

Labelled peptide was analysed by HPLC, using a reversed phase column, with in-line radiometric and UV detection ($\lambda = 205 \text{ nm}$) and a flow rate of 1 mL/min. The following solvent system was employed: pump A 0.1% trifluoroacetic acid in water; pump B 0.1% trifluoroacetic acid in acetonitrile; and the following gradient of pump B was used: 0–3 min 5%, 3–28 min 5% to 80%, 28–33 min 80% to 5%, 33–35 min 5%.

Quality control of ^{99m}Tc -F11 was also performed by paper chromatography using 1.0 cm \times 9.5 cm strips of Whatman 3MM and acetone ($R_f = 0.8$ –1.0 $^{99m}\text{TcO}_4^-$) and acetonitrile 50% ($R_f = 0.0$ radiocolloids) as mobile phases.

2.3. In vitro stability of the label

The stability of ^{99m}Tc -F11 in aqueous solution was tested by its incubation in 0.1M PBS (pH7.2) and in a solution containing a 30-fold molar excess of L-cysteine at room temperature for up to 24 h. Samples were analysed by HPLC-RP.

Stabilization in plasma was performed as follows: to 200 μL of ^{99m}Tc labelled peptide solution was added 1 mL of fresh human plasma and the solution incubated at room temperature. Control was prepared by diluting

200 μL with 1 mL of 0.1 PBS (pH7.2). Fifty microlitre samples were taken at 0, 1, 2, 4, 6 and 24 h intervals. Plasma proteins were precipitated with 70 μL of acetonitrile and the supernatant analysed by HPLC-RP.

2.4. Plasma protein binding assay

To 200 μL of $^{99\text{m}}\text{Tc}$ labelled peptide solution was added 1 mL of fresh human plasma and the solution incubated at room temperature. A control was prepared by diluting 200 μL of this solution with 1 mL of 0.1 PBS (pH7.2). Samples were analysed by size exclusion HPLC at 0, 2 and 5 h intervals. Elution was performed at a flow rate of 0.5 mL/min, using 20mM EDTA 0.1M PBS (pH7.0) as a mobile phase. Half-millilitre fractions were collected and the count rate measured in an automatic gamma counter.

The percentage of binding of $^{99\text{m}}\text{Tc}$ labelled peptides to plasma proteins was also determined by paper chromatography using 1.0 cm \times 9.5 cm strips of Whatman 3MM and acetonitrile 50% as the mobile phase. Plasma protein remained at the start, while labelled peptides migrated with the front.

2.5. Animal biodistribution

One microgram (27.5–29.0 MBq) of $^{99\text{m}}\text{Tc}$ -F11 was injected through the ocular plexus of C57BL6 male mice to determine the biokinetics. Blood samples were collected at 5, 15, 30 and 45 min and 1, 2, 4, 6, 8, 12 and 24 h intervals, and the activity in serum was analysed for pharmacokinetic purposes. Groups of three animals were sacrificed at 1, 4, 12 and 24 h intervals after administration. The percentage injected dose per gram of tissue (%ID/g) was determined for the following organs: heart, liver, kidneys, spleen, lungs, stomach, large intestine, small intestine, pancreas, thymus and femur.

Scintigraphic images were acquired 1, 3, 6 and 16 h after administration through a tail vein of 13 μg (67–74 MBq) of $^{99\text{m}}\text{Tc}$ -F11 to three C57BL6 mice bearing B16 melanoma tumours and three nude mice with A431 tumours, using a gamma camera (Sophy DS-7, Sopha Medical Systems, France) equipped with a pinhole collimator (2 mm). Imaging was performed by employing a 20% window centred on the 140 keV photopeak, a matrix size of 256 \times 256 pixels and 500 kcounts per view.

2.6. $^{99\text{m}}\text{Tc}$ labelling of peptide

Figure 1 shows the dependence of labelling efficiency on molar ratio of F11:Sn⁺². Use of a 1.3-fold molar excess of stannous fluoride attained a $^{99\text{m}}\text{Tc}$

SESSION 4

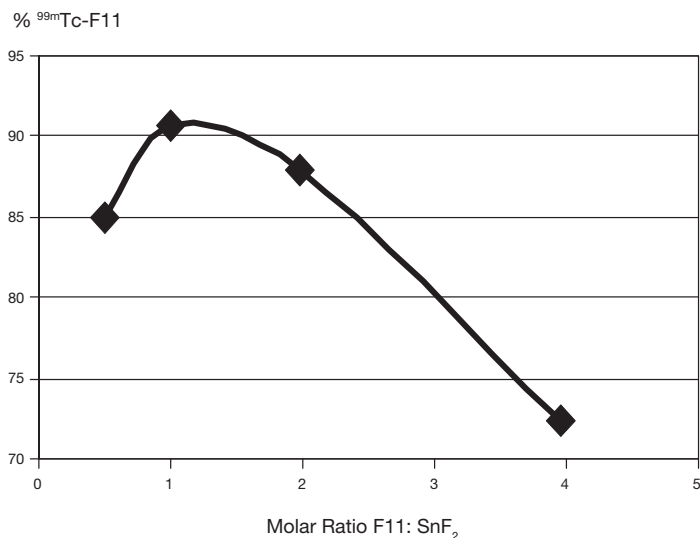


FIG. 1. Dependence of radiochemical purity of ^{99m}Tc-F11 on the molar ratio F11:SnF₂.

labelling yield of $95.2 \pm 2.1\%$ and recovery from HPLC was $>92\%$. A combined chromatogram and radiochromatogram of ^{99m}Tc-F11 is observed in Fig. 2.

2.7. In vitro stability of the label

The stability of the ^{99m}Tc-F11 in 0.1M PBS and in 30-fold molar excess of L-cysteine (L-cys) up to 24 h is summarized in Fig. 3. In the absence of cysteine, the radiolabelled peptide that resulted was sufficiently stable, with more than 90% of the activity remaining bound to the peptide at 24 h. Challenging the label with a 30-fold molar excess of L-cysteine was enough to transchelate about 40% of the metal after 24 h of incubation.

A shift in retention time of ^{99m}Tc-F11 was observed when the peptide was incubated in plasma, suggesting it could have some sensitivity to the action of peptidases in plasma and circulating chelating agents (such as glutathione and cysteine).

2.8. Plasma protein binding assay

Size exclusion HPLC was performed at selected times on samples incubated in plasma at room temperature in order to assess the affinity of ^{99m}Tc-F11 for plasma proteins. A significant binding to plasma proteins was demonstrated by size exclusion HPLC. The results are shown in Fig. 4.

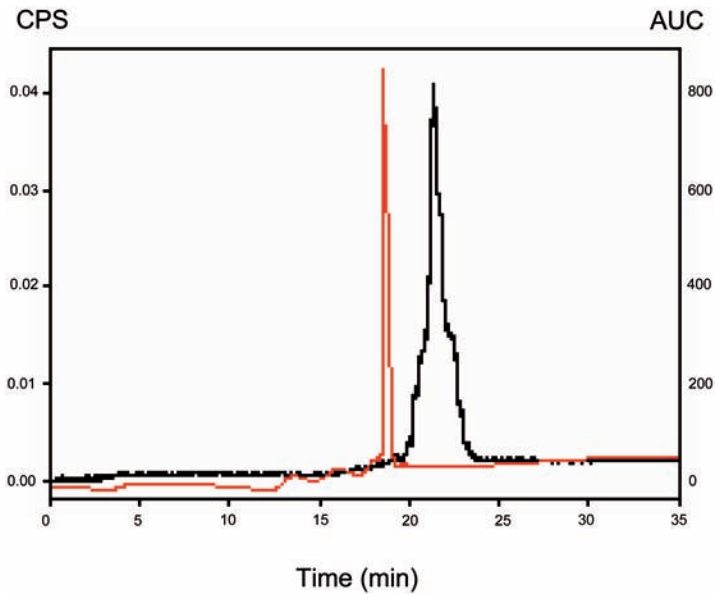


FIG. 2. Chromatogram (red line) and radiochromatogram (black line) of $^{99m}\text{Tc-F11}$.

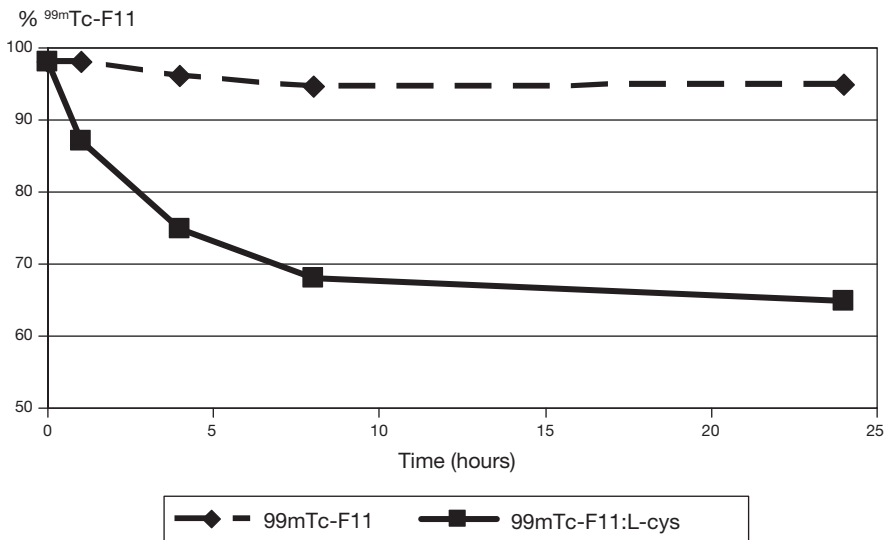


FIG. 3. Stability of $^{99m}\text{Tc-F11}$ in aqueous solutions.

SESSION 4

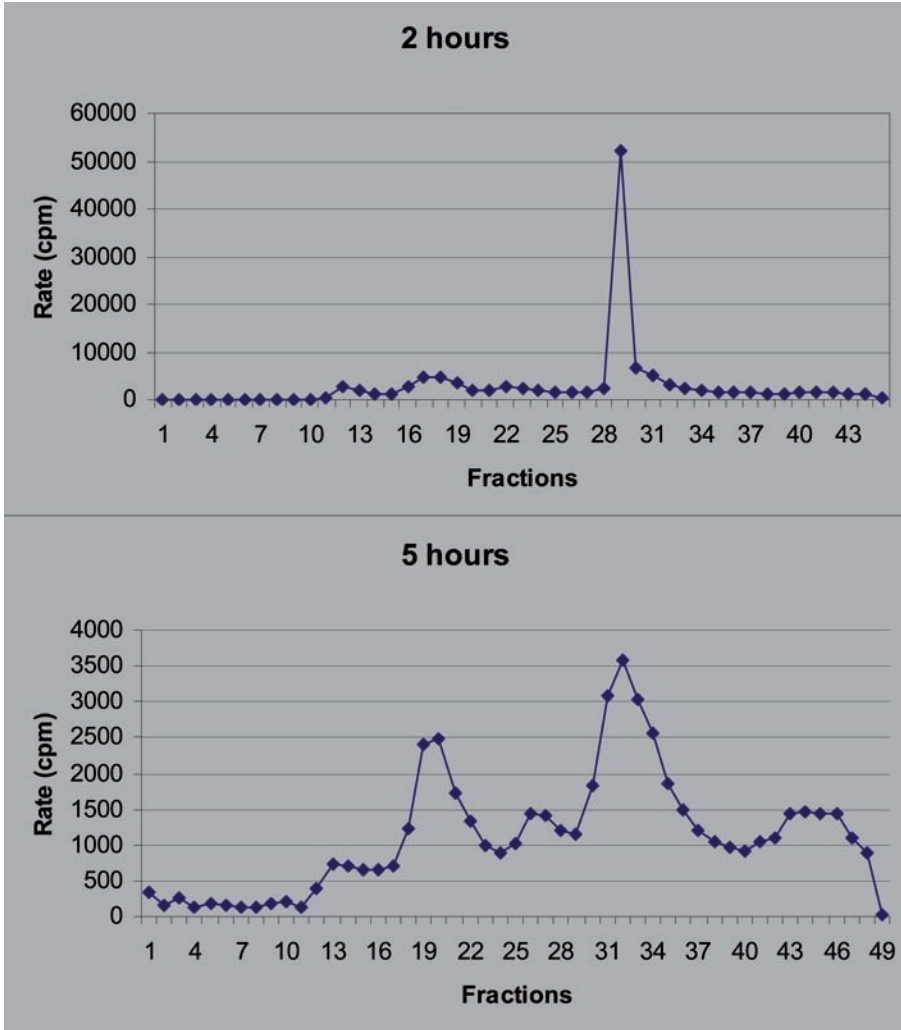


FIG. 4. Size exclusion HPLC of the samples of ^{99m}Tc -F11 incubated in plasma for 2 and 5 h. A significant binding to plasma proteins is observed.

2.9. Animal biodistribution

The main pharmacokinetic parameters, calculated assuming a bicompartamental model, are summarized in Table 1.

Figure 5 shows the biodistribution of ^{99m}Tc -F11 in the studied organs. The highest uptake of the label was observed in kidneys (9.5–4.0% ID/g). Also, an

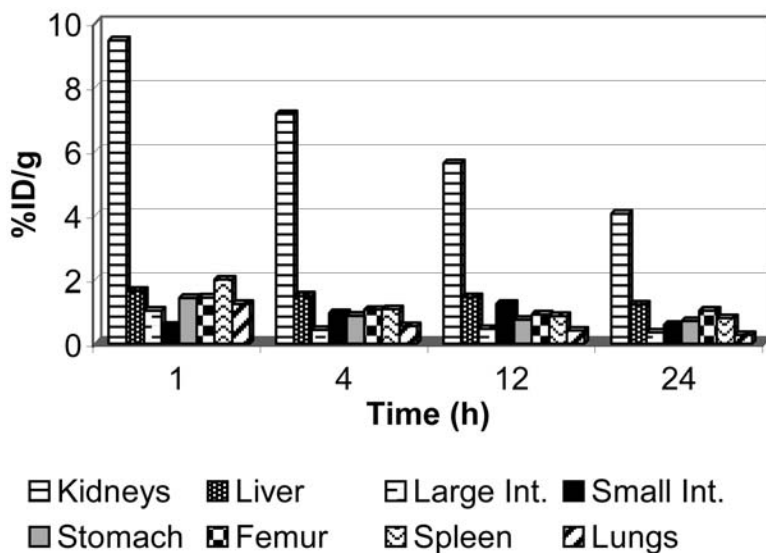


FIG. 5. Biodistribution of ^{99m}Tc-F11 in C57BL/6 mice.

TABLE 1. PHARMACOKINETIC PARAMETERS OF ^{99m}Tc-F11 IN SERUM OF C56BL/6 MICE

Parameters	Mean ± SD	Relative deviation (%)
C _{max} (%ID/mL)	56.6 ± 5.2	9.2
AUC (%IDmin/mL)	8814 ± 1139	12.9
T _{1/2α} (min)	43.1 ± 13.5	31.4
T _{1/2β} (min)	327 ± 149	45.5
MRT (min)	346 ± 128	37.1
V _d (mL)	6836 ± 660	9.6
Cl (mL/min)	0.0113 ± 0.0015	12.9

C_{max}: maximum concentration in serum; AUC: area under curve; T_{1/2}: half time of clearance; MRT: mean residence time; V_d: volume of dilution; Cl: clearance.

elevated activity was detected in urine ($49.2 \pm 6.7\%$ ID/g in 24 h). Thus, the urinary tract should be the main excretion pathway for ^{99m}Tc-F11. The other organs took up less than 2.0% ID/g (doses in the heart, thymus and pancreas were negligible).

Scintigraphic images showed a satisfactory uptake of radiopharmaceutical in the tumours (Fig. 6).

3. DISCUSSION

The tripeptidic chain Arg-Gly-Asp (RGD) is the primary recognition site to $\alpha_v\beta_3$ integrin and different peptides containing this sequence have been synthesized. Some of them have been labelled with proper radionuclides to assess, *in vivo*, the expression of the vitronectine receptor. Decapeptide α P2 contains two RGD sequences and a cysteine residue to facilitate ^{99m}Tc labelling [2, 20]. Haubner et al. [21] synthesized several derivative peptides from the structure ciclo-RGDFV, labelled them with ^{131}I and obtained autoradiographic images of nude mice xenografted with melanoma M21, breast carcinoma MaCaF and Balb/c with induced osteosarcomas to detect the expression of integrin $\alpha_v\beta_3$. Afterwards, the same authors labelled the ciclo-RGDFV peptides with ^{18}F for PET imaging of M21 tumours in nude mice [22]. Starting from these previous reports, polypeptide F11 was designed.

One of the most important causes of the *in vivo* instability of the radiopharmaceuticals is the transchelation of the technetium to other molecules such as glutathione and cystine. After which, cysteine challenge is widely used to assess the stability of Tc labelled peptides and proteins [18]. Pallela et al. [19] reported that the tetrapeptide sequence Gly-D-Ala-Gly-Gly was stable enough to challenge 100-fold molar excess of DTPA, HSA and L-cysteine up to 5 h. In the present study, ^{99m}Tc -F11 has the chelating sequence Ala-Gly-Gly-Gly and showed similar stability. Plasma stability assay offers the possibility of *in vitro* assessment of the proteolytic degradation of peptide backbone by plasma proteases, which represent the other main route of *in vivo* instability of radiolabelled peptides. In the present study, after 6 h incubation, the degradation started being significant. The introduction of unnatural amino acids in the peptide sequence such as D-optical isomers could minimize this breakdown.

Generally, peptides (mainly linear hydrophilic ones) are cleared from the blood by glomerular filtration and are then reabsorbed in the proximal tubules, where they can be degraded by peptidases [20, 23, 24]. The high levels of activity detected in kidneys suggested that F11 has a similar behaviour. The value of the clearance ($\text{Cl} = 0.0113 \pm 0.0015 \text{ mL/min}$) suggests a significant reabsorption of F11 in the kidneys. Cyclic peptides have shown less renal excretion and a higher hepatic uptake because of their lipophilic character [21, 22].

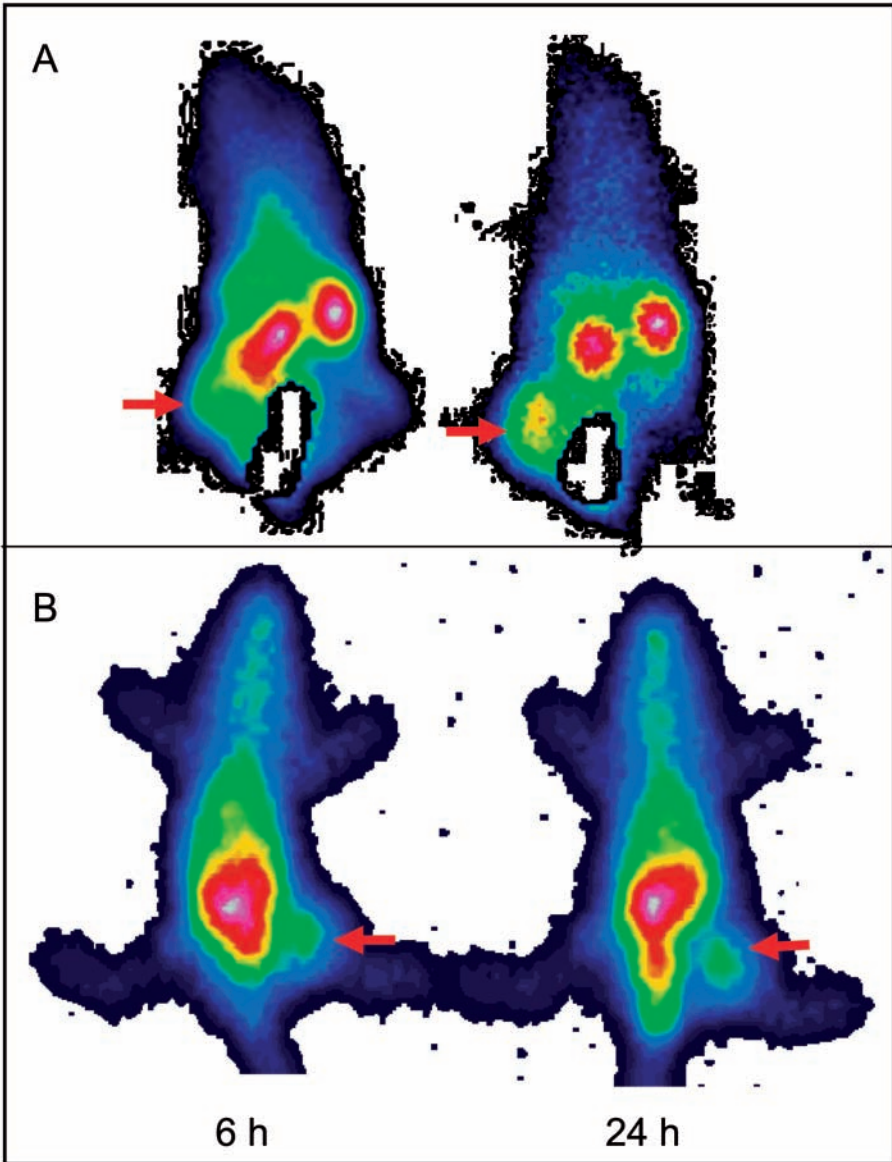


FIG. 6. Scintigraphic images of $^{99m}\text{Tc-F11}$ in a C57BL/6 mouse bearing a B16 tumour and a nude mouse bearing a A431 tumour at 6 and 12 h after IV administration.

SESSION 4

Usually, peptides show rapid blood kinetics due to their low molecular weight [3, 23]. Whilst some of them have a certain binding to plasma protein, most peptides show values of $T_{1/2\alpha}$ in the range of a few minutes [23, 24]. The pharmacokinetic profile could also influence the susceptibility to proteolytic degradation not only in plasma, but also during the transit through liver, kidneys and gastrointestinal tract. This process could destroy the molecule or even the binding with the radionuclide [23]. The affinity of F11 for plasma protein could impact the incremented value of $T_{1/2\beta}$ (327 ± 149 min). Nevertheless, the elevated value of virtual dilution volume (6836 ± 660 mL) suggests that the label was all distributed in vascular space and extravascular fluids.

4. CONCLUSION

The ^{99m}Tc labelled peptide F11 could prove a promising radiopharmaceutical for scintigraphic detection of tumours.

REFERENCES

- [1] WEINER, R.E., THAKUR, M.L., Radiolabeled peptides in diagnosis and therapy, *Sem. Nucl. Med.* **31** (2001) 296–311.
- [2] BOERMAN, O.C., OYEN, W.J.G., CORSTENS, F.H.M., Radio-labeled receptor-binding peptides: A new class of radiopharmaceuticals, *Sem. Nucl. Med.* **30** (2000) 195–208.
- [3] BLOK, D., FEITSMA, R.I.J., VERMEIJ, P., PAUWELS, E.J.K., Peptide radiopharmaceuticals in nuclear medicine, *Eur. J. Nucl. Med.* **26** (1999) 1511–1519.
- [4] MATHER, S.J., Radiolabelled peptides — promises and pitfalls, *Nucl. Med. Comm.* **21** (2000) 507–509.
- [5] HAUBNER, R., FINSINGER, D., KESSLER, H., Stereoisomeric peptide libraries and peptidomimetics for designing selective inhibitors of the $\alpha_v\beta_3$ integrin for a new cancer therapy, *Angew Chem. Int. Ed. Engl.* **36** (1997) 1374–1389.
- [6] KAWAHARA, E., OOI, A., NAKANISHI, I., Integrin distribution in gastric carcinoma: Association of β_3 and β_5 integrins with tumor invasiveness, *Pathol. Int.* **45** (1995) 493–500.
- [7] CLEZARDIN, P., Recent insights into the role of integrins in cancer metastasis, *Cell Mol. Life Sci.* **54** (1998) 541–548.
- [8] HAUBNER, R., et al., Radiolabeled $\alpha_v\beta_3$ integrin antagonists: A new class of tracers for tumor targeting, *J. Nucl. Med.* **40** (1999) 1061–1071.
- [9] ALBELDA, S.M., Biology of disease: role of integrins and other cell adhesion molecules in tumor progression and metastasis, *Lab. Invest.* **68** (1993) 4–17.

- [10] GLADSON, C.L., CHERESH, D.A., Glioblastoma expression of vitronectin and $\alpha v\beta 3$ integrin: Adhesion mechanism for transformed glial cells, *J. Clin. Invest.* **88** (1991) 1924–1932.
- [11] FALCIONI, R., et al., Expression of $\beta 1$, $\beta 3$, $\beta 4$, and $\beta 5$ integrins by human lung carcinoma cells of different histotypes, *Exp. Cell Res.* **210** (1994) 113–122.
- [12] GASPARINI, G., et al., Vascular integrin $\alpha v\beta 3$: a new prognostic indicator in breast cancer, *Clin. Cancer Res.* **4** (1998) 2625–2634.
- [13] ALBELDA, S.M., et al., Integrin distribution in malignant melanoma: association of the $\beta 3$ subunit with tumor progression, *Cancer Res.* **50** (1990) 6757–6764.
- [14] FELDING-HABERMANN, B., MUELLER, B.M., ROMERDAHI, C.A., CHERESH, D.A., Involvement of integrin αv gene expression in human melanoma tumorigenicity, *J. Clin. Invest.* **89** (1992) 2018–2022.
- [15] GURRATH, M., MULLER, G., KESSLER, H., AUMAILLEY, M., TIMPL, R., Conformation/ activity studies of rationally designed potent anti-adhesive RGD peptides, *Eur. J. Biochem.* **210** (1992) 911–921.
- [16] POETHKO, T., et al., Two-step methodology for high-yield routine radiohalogenation of peptides: ^{18}F -labeled-RGD and Octreotide analogs, *J. Nucl. Med.* **45** (2004) 892–902.
- [17] ONTHANK, D.C., et al., ^{90}Y and ^{111}In complexes of DOTA-conjugated integrin $\alpha v\beta 3$ receptor antagonist: Different but biologically equivalent, *Bioconjugate Chem.* **15** (2004) 235–241.
- [18] STALTERI, M.A., BANSAL, S., HIDER, R., MATHER, S.J., Comparison of the stability of technetium-labeled peptides to challenge with cysteine, *Bioconjugate Chem.* **10** (1999) 130–136.
- [19] PALLELA, V.R., THAKUR, M.L., CHAKDER, S., RATTAN, S., $^{99\text{m}}\text{Tc}$ -Labeled vasoactive intestinal peptide receptor antagonist: Functional studies, *J. Nucl. Med.* **40** (1999) 352–360.
- [20] SIVOLAPENKO, G.B., et al., Imaging of metastatic melanoma utilising a technetium- $^{99\text{m}}$ labelled RDG-containing synthetic peptide, *Eur. J. Nucl. Med.* **25** (1998) 1383–1389.
- [21] HAUBNER, R., et al., Radiolabeled $\alpha v\beta 3$ integrin antagonists: A new class of tracer for tumor targeting, *J. Nucl. Med.* **40** (1999) 1061–1071.
- [22] HAUBNER, R., et al., Noninvasive imaging of $\alpha v\beta 3$ integrin expression using ^{18}F -labeled RGD-containing glycopeptide and positron emission tomography, *Cancer Res.* **61** (2001) 1781–1785.
- [23] LISTER-JAMES, J., MOYER, B.R., DEAN, R.T., Pharmacokinetics considerations in the development of peptide-based imaging agents, *J. Nucl. Med.* **41** (1997) 111–118.
- [24] TREJTNAR, F., LAZNICEK, M., LAZNICKOVA, A., MATHER, S.J., Pharmacokinetics and renal handling of $^{99\text{m}}\text{Tc}$ -labeled peptides, *J. Nucl. Med.* **41** (2000) 177–182.

HYNIC-TOC LABELLED WITH ^{99m}Tc VIA AN INSTANT KIT FORMULATION: PRECLINICAL RESULTS

M. CIAVARO*, E. OBENAU*, G. FISZMAN**, S.G. DE CASTIGLIA*

*Centro Atómico Ezeiza, Comisión Nacional de Energía Atómica
Email: silgomez@cae.cnea.gov.ar

** Instituto A. Roffo, Universidad de Buenos Aires

Buenos Aires, Argentina

Abstract

The aim of this work was the development of an instant kit formulation based on a ^{99m}Tc labelling of HYNIC-TOC using a coligand exchange from tricine to EDDA. The preparation of the labelled conjugate was achieved at elevated temperature and under optimized conditions of pH, EDDA and stannous ion concentrations. Quality control tests were carried out to evaluate different parameters such as radiochemical purity, dissolution time, pH, stability of the kits during storage at 4°C, sterility, apyrogenicity and internalization in AR42J cells. ^{99m}Tc -EDDA/HYNIC-TOC was obtained with high radiochemical purity (>95%) and retained biological activity after it was prepared by addition of 0.2M Na_2HPO_4 to a kit, followed by 1.1GBq ^{99m}Tc pertechnetate and stored for a period of up to six months.

1. INTRODUCTION

Somatostatin is a peptide hormone containing 14 amino acids with a short biological half-life of only 2 min, which exhibits a wide spectrum of biological and oncological actions [1]. The expression of large numbers of high affinity somatostatin receptors by certain tumours makes it attractive but unsuitable owing to the short half-life for diagnostic application in nuclear medicine. For this reason several analogues have been synthesized which are more potent and longer acting than somatostatin itself [2, 3].

Imaging somatostatin receptor positive tumour with ^{111}In -diethylene triaminepentaacetic acid-D-Phe-octreotide (^{111}In -DTPA-octreotide) has become a widely used diagnostic procedure in clinical nuclear medicine [4].

This technique permits the localization and staging of tumours that express the appropriate somatostatin receptors, the most important of which is receptor subtype 2 (SSTR2).

However, ^{99m}Tc can be considered as the radiolabel of choice, with daily availability from a generator, and the ^{99m}Tc -EDDA/HYNIC-TOC is a promising new radiopharmaceutical with the potential to replace ^{111}In -DTPA-OCT as the radiopharmaceutical for somatostatin receptor scintigraphy [5].

The aim of this work was to develop a freeze-dried kit formulation for the instant preparation of ^{99m}Tc -EDDA/HYNIC-TOC in a high radiochemical yield to allow a further clinical evaluation in a nuclear medicine centre.

2. MATERIALS

Cold conjugated peptide HYNIC-TOC was provided by the IAEA from piCHEM. Tricine, EDDA and other chemicals were purchased from Sigma Chemical Co. The radionuclide was obtained from a $^{99m}\text{Mo}/^{99m}\text{Tc}$ generator eluted with saline (CNEA, Argentina).

3. METHOD

3.1. Labelling of HYNIC-TOC with ^{99m}Tc

Several experiments were carried out to obtain the parameters of the wet labelling solution. The preparation of the labelled conjugate was achieved at elevated temperature and under optimized conditions of pH, reaction time, and EDDA, tricine and stannous ion concentrations.

3.2. Direct labelling with tricine

The conjugate peptide was labelled with ^{99m}Tc using tricine as coligand [6]. Ten micrograms of HYNIC-TOC were incubated with 0.5 mL of fresh eluted $^{99m}\text{TcO}_4^-$ solution (296–370 MBq), 0.5 mL tricine solution (100 mg/mL in 25mM succinate buffer (pH5.0)) and 15 μL tin(II) solution (10 mg/5 mL HCl 0.1N) for 30 min at RT. Radiochemical purity was tested by HPLC, reverse phase, column: Delta Pack: 3.9 mm \times 150 mm, acetonitrile/0.01N phosphate buffer (pH6.2): 0–3min 0% ACN, 3–10 min 0–25% ACN, 10–20 min 25% ACN, 20–23 min 25–70% ACN, 26–27 min 70–0% ACN.

3.3. EDDA/tricine exchange labelling

A typical labelling of the conjugated peptide was as follows: 20 µg of HYNIC-TOC were incubated with 1 mL EDDA/tricine solution (equal volumes) of 40 mg tricine/mL PBS 0.2N (pH6.2) and 20 mg EDDA/mL NaOH 0.1N), 1 mL $^{99m}\text{TcO}_4^-$ in saline and 15 µL SnCl_2 solution (1 mg/1 mL HCl 0.1N) at 100°C for 10 min.

HYNIC-TOC was incubated with variable amounts of EDDA (0–20 mg), tricine(0–50 mg), $\text{SnCl}_2 \cdot 2\text{H}_2\text{O}$ (5–200 µg) and $^{99m}\text{TcO}_4^-$ (800 MBq) in order to optimize the labelling reaction. The pH (2.5–7.5), reaction time (0–30 min) and temperature (0–100°C) were also varied. One parameter was changed at a time. Radiochemical purity was tested by HPLC using the above system. ITLC was performed using MEK to determine the amount of free $^{99m}\text{TcO}_4^-$ ($R_f = 1$), 0.1N citrate buffer (pH5) to determine ^{99m}Tc coligand, $^{99m}\text{TcO}_4^-$ ($R_f = 1$) and methanol/1M ammonium acetate 1/1 for ^{99m}Tc colloid ($R_f = 0$).

3.4. Kit formulation

Several experiments were carried out to obtain the best kit formulation with regard to the parameters of the wet labelling solution. Four formulations were evaluated, two of them containing EDDA, HYNIC-TOC, tricine, stannous chloride and mannitol, one without tricine and one without conjugated peptide. EDDA and tricine were dissolved in various solutions of different pH, such as water, 0.1N NaOH and 0.2M phosphate buffer (pH6). Mannitol was the bulking agent (50 mg/vial) in all formulations. Table 1 shows the content of 1.2 mL of dispensed solution in sterile vials immediately before a lyophilization process of 24 h.

Labelling of the kit was performed as follows: Formulation I, adding 0.5 mL of 0.2M phosphate buffer (pH6) and the necessary activity of ^{99m}Tc pertechnetate freshly eluted, in 1.0 mL of saline; Formulation II, adding pertechnetate in saline only; Formulations III and IV, tricine or conjugated peptide was dissolved in 0.5 mL of 0.2M phosphate buffer (pH6) respectively and added to the vial before the pertechnetate. Finally, all the formulations were incubated in boiling water for 10 min.

3.5. Quality control tests

The radiochemical purity of ^{99m}Tc -EDDA/HYNIC-TOC prepared from different formulations was assessed by HPLC and ITLC. The limulus test and sterility assay were performed on a sample of each formulation. The stability of the lyophilized formulations was evaluated over a period of six months.

TABLE 1. DIFFERENT KIT FORMULATIONS FOR LABELLING HYNIC-TOC WITH ^{99m}Tc

EDDA	TRICINE	$\text{SnCl}_2 \cdot 2\text{H}_2\text{O}$	MANNITOL	HYNIC-TOC
10 mg/NaOH 0.1N	30 mg/phosphate buffer	20 $\mu\text{g}/\text{HCl}$ 0.1N	50 mg/phosphate buffer	20 $\mu\text{g}/\text{ethanol}$ 10%
10 mg/water (gently heated)		20 $\mu\text{g}/\text{HCl}$ 0.1N	50 mg/water	20 $\mu\text{g}/\text{ethanol}$ 10%
10 mg/water (gently heated)	30 mg/water	20 $\mu\text{g}/\text{HCl}$ 0.1N	50 mg/water	

An internalization assay was carried out according to a published procedure [7]. Briefly, AR42J cells were seeded at a density of 8×10^5 cells per well, grown to confluency for 48 h, washed and incubated with 300 000 cpm of the radiolabelled peptide and either PBS/0.5% BSA buffer alone or cold peptide (10 μM PBS/0.5% BSA buffer). After separation of the membrane bound radioligand fraction and the internalized radioligand fraction, all fractions were counted in a gamma counter. The per cent internalized activity was calculated on the basis that total activity comprises membrane bound plus internalized activity.

4. RESULTS

4.1. Radiolabelling of HYNIC-TOC with ^{99m}Tc

The HPLC profiles of the conjugated peptide labelled using direct labelling with tricine or EDDA/tricine exchange labelling are shown in Fig. 1. Only one peak was obtained for the labelled peptide using the second technique and after optimizing the parameters of the reaction. The final labelling solution contains 20 μg HYNIC-TOC, 30 mg tricine, 10 mg EDDA, 20 μg SnCl_2 and 555 MBq $^{99m}\text{TcO}_4^-$ in a 2 mL final volume. The labelled peptide was obtained after heating the solution in boiling water for 10 min.

4.2. Kit formulation

Radiochemical purity of the different kit formulations are shown in Table 2. These results were obtained immediately after lyophilization.

SESSION 4

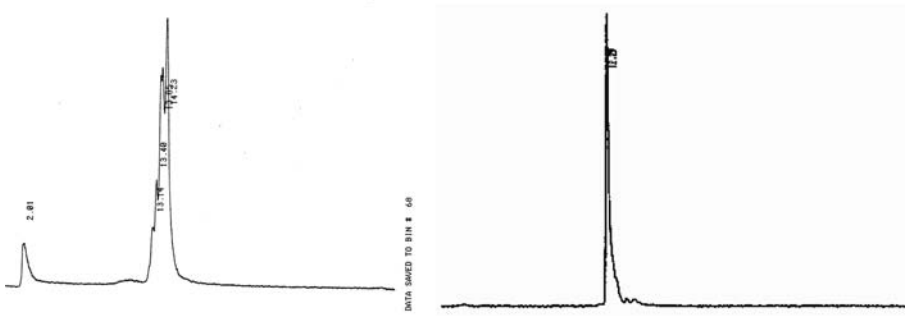


FIG. 1. HPLC chromatograms of the labelled peptide: (left) direct labelling with tricine, (right) EDDA/tricine exchange labelling.

TABLE 2. RADIOCHEMICAL PURITY OF THE DIFFERENT KIT FORMULATIONS

Formulation	HPLC results		ITLC results			
	Labelled peptide (%)	$^{99m}\text{TcO}_4^- + ^{99m}\text{Tc}$ coligand (%)	Labelled peptide (%)	^{99m}Tc coligand (%)	$^{99m}\text{TcO}_4^-$ (%)	$^{99m}\text{TcO}_2$ (%)
I	95.4	4.6	82.7	12.8	1.5	3.0
II	90.0	10.0	78.4	19.5	0.3	1.8
III	91.8	8.2	80.4	15.1	3.1	1.4
IV	98.0	2.0	91.8	3.5	0.6	4.2

4.3. Stability to storage

The kits were stored at 4°C and Fig. 2 shows the radiochemical purity results for the four formulations over a period of six months.

There were no significant differences between HPLC and ITLC results of formulation IV ($p < 0.05$). Formulations II and III showed a drop in radiochemical purity to 70% within six months. There were significant differences between HPLC and ITLC results for formulation I ($p < 0.05$). The radiochemical purity values determined by HPLC did not drop below 90% during the period studied.

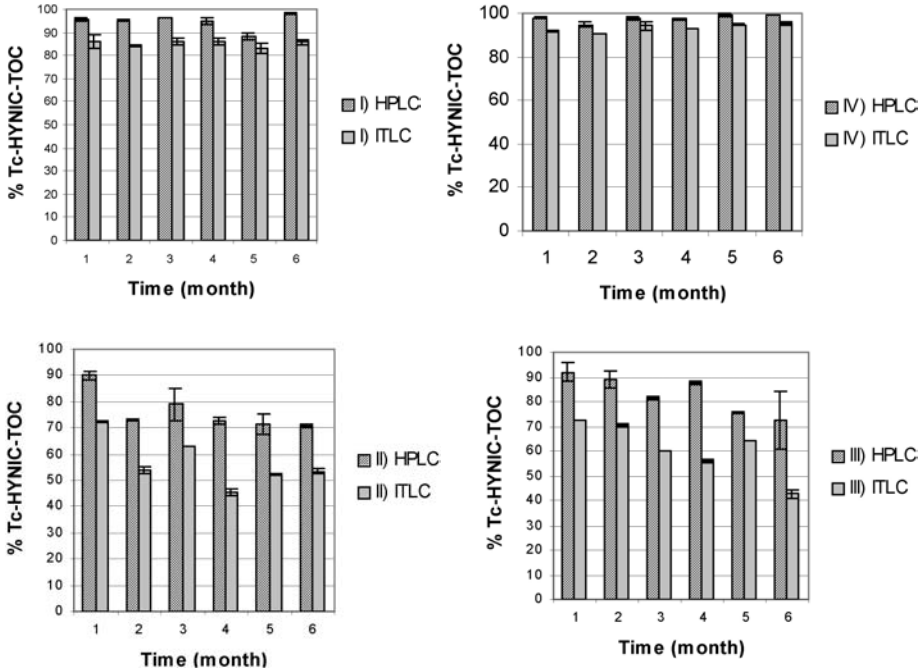


FIG. 2. Radiochemical purity results (HPLC and ITLC) of kit formulations (I-IV) stored for up to six months.

4.4. Internalization

The rate of internalization into SSTR positive AR42J cells is shown in Fig. 3. Expressed as a percentage of bound activity, a result of $93.1 \pm 0.48\%$ was obtained at 2 h.

5. DISCUSSION

This study was designed to develop a simple and reliable kit formulation for the labelling of HYNIC-TOC with ^{99m}Tc and suitable for diagnosis of neuroendocrine tumours. The labelled peptide was obtained with radiochemical purities higher than 95% within 15 min after addition of pertechnetate solutions to optimized HYNIC-TOC lyophilized kits.

The parameters of the wet labelling reaction have been optimized for use in the kit formulation and although the preparation conditions of the wet labelling required a final pH of 7.2, a lower pH (4.5) of the freeze-drying

SESSION 4

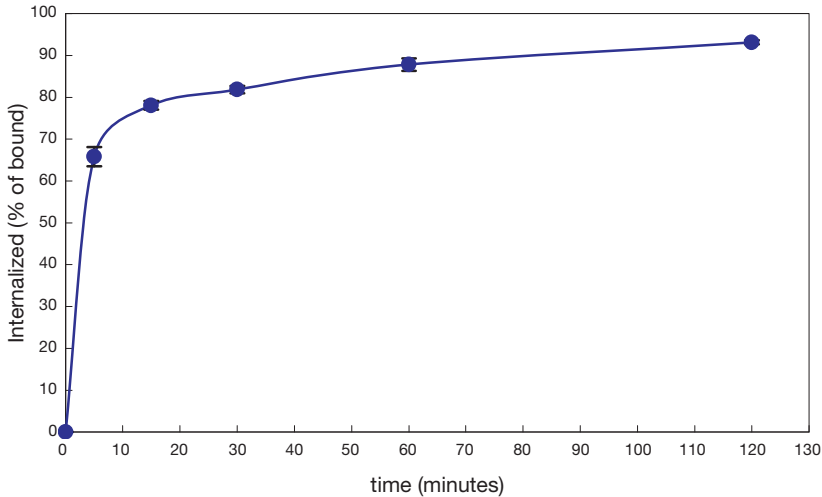


FIG. 3. Internalization of the radiolabelled peptide obtained via a kit preparation versus time.

solution was necessary in order to obtain a high radiochemical purity (formulation I). It is important to note that the labelling procedure from lyophilized kits I occurred at pH6.2 after the addition of 0.5 mL of buffer phosphate.

Summarizing the results, optimized lyophilized kit contains 10 mg EDDA, 30 mg Tricine, 20 μg $\text{SnCl}_2 \cdot 2\text{H}_2\text{O}$, 50 mg mannitol and 20 μg HYNIC-TOC. After reconstitution with 0.5 mL buffer phosphate followed by 1.1 GBq of pertechnetate and incubating at 100°C over 10 min, the HPLC chromatogram showed 95.4% of labelled peptide. However, the ITLC chromatograms showed 82.7% of labelled peptide while labelled coligand was seen as the principal impurity. The authors have also evaluated a fourth formulation that does not contain the conjugated peptide as it is mentioned above. Labelling of this formulation (IV) showed radiochemical purity values higher than 95% over six months and the results from ITLC studies showed no significant differences with HPLC values. It is important to note that high radiochemical purity values were obtained when labelling a lyophilized formulation that does not contain the conjugated peptide. In this case, the pH of the freeze-drying formulation was 4.5 and radiochemical purity values are in agreement with the literature [7]; the authors have also obtained values of >90% independent of pH. This can be explained as being due to the formation of hidrazone impurities resulting from the reaction of aldehyde and ketone impurities with the HYNIC-peptide conjugate [8] during the process of manufacturing the lyophilized kit.

Protein binding as determined by Centricon 30 ultrafiltration showed a stable protein binding instead of a significant increase over time found for labelled HYNIC-TOC conjugate using tricine as coligand [6].

In conclusion, it is possible to obtain ^{99m}Tc -EDDA/HYNIC-TOC after labelling a freeze-dried kit formulation (I). Further clinical evaluation would be necessary.

ACKNOWLEDGEMENTS

The authors would like to express their gratitude to the IAEA for having provided the conjugated peptide.

REFERENCES

- [1] SCHALLY, A.V., Oncological applications of somatostatin analogs, *Cancer Res.* **48** (1988) 6977–6985.
- [2] VIRGOLINI, I., et al., In vitro and in vivo studies of three radiolabelled somatostatin analogues: ^{123}I -Octreotide, ^{123}I -Tyr-3-Oct and ^{111}In -DTPA-Phe-1-Oct, *Eur. J. Nucl. Med.* **23** 10 (1996) 1388–1399.
- [3] BAKKER, W., et al., In vivo use of radioiodinated somatostatin analogue: dynamics, metabolism, and binding to somatostatin receptor-positive tumors in man, *J. Nucl. Med.* **32** 6 (1991) 1184–1188.
- [4] VISSER, T., et al., Somatostatin receptor scintigraphy with Indium-111-DTPA-Phe-1-Octreotide in man: metabolism, dosimetry and comparison with iodine-123-Tyr-3-Octreotide, *J. Nucl. Med.* **33** 5 (1992) 652–658.
- [5] DECRISTOFORO, C., et al., ^{99m}Tc -EDDA/HYNIC-TOC: A new ^{99m}Tc labelled radiopharmaceutical for imaging somatostatin receptor positive tumours: First clinical results and intra-patient comparison with ^{111}In -labelled octreotide derivatives, *Eur. J. Nucl. Med.* **27** 9 (2000) 1318–1325.
- [6] OBENAU, E., CRUDO, J., EDREIRA, M., VIAGGI, M., DE CASTIGLIA, S.G., “Somatostatin analogues labelled with ^{99m}Tc ”, *^{99m}Tc Labelled Peptides for Imaging of Peripheral Receptors*, IAEA-TECDOC-1214, IAEA, Vienna (2001) 17–27.
- [7] VON GUGGENBERG, E., MIKOLAJCZAK, R., JANOTA, B., RICCABONA, G., DECRISTOFORO, C., Radiopharmaceutical development of a freeze-dried kit formulation for the preparation of [^{99m}Tc -EDDA-HYNIC-D-Phe¹, Tyr³]-Octreotide, a somatostatin analog for tumor diagnosis, *J. Pharm. Sci.* **93** (2004) 2497–2506.
- [8] HARRIS, D.T., et al., Synthesis of stable hydrazones of a hydrazinonicotinyl-modified peptide for the preparation of ^{99m}Tc -labeled radiopharmaceuticals, *Bioconjugate Chem.* **10** (1999) 808–814.

INDIGENOUS CAPACITY BUILDING
IN RADIOPHARMACEUTICALS

(Session 5)

Chairpersons

R.S. KAMEL
IAEA

N. RAMAMOORTHY
IAEA

INDIGENOUS CAPACITY BUILDING IN RADIOPHARMACEUTICALS: SAUDI ARABIAN EXPERIENCE

M.M. VORA

Cyclotron and Radiopharmaceuticals Department,
King Faisal Specialist Hospital and Research Centre,
Riyadh, Saudi Arabia
Email: vora@kfshrc.edu.sa

Abstract

Easy availability of radiopharmaceuticals is a key element in the application of radioisotopes in health care. Furthermore, creating self-sufficiency within the country and the geographical region further enhances this prospect. Manufacture of radiopharmaceutical began at King Faisal Specialist Hospital and Research Centre (KFSH&RC) in 1983 with the installation of the CS-30 (26.4 MeV) cyclotron, with the intention not only to make available the cyclotron products for the country and the geographical region, but also to establish a contemporary research programme. Consequently, a PET scanner was installed at KFSH&RC in 1995. Currently, the centre routinely produces several SPECT and PET radiopharmaceuticals supporting around 40 nuclear medicine facilities within the country and the geographical region. A key motivating and driving force has been the goal of becoming a comprehensive radiopharmaceuticals manufacturing facility and making the country self-sufficient in all its radiopharmaceutical needs. Consequently, 2000 witnessed the introduction of ^{131}I based products for diagnosis as well as for therapy. GMP is the cornerstone of any radiopharmaceuticals manufacturing programme. The KFSH&RC is a perfect example of how this operational and guiding principle has been applied and evolved over the years, culminating in an effective quality management system (ISO 9001:2000) for manufacturing high quality radiopharmaceuticals. The programme building has been 'work in progress'. For efficient functioning, the staff must be well qualified and appropriately trained to achieve the mission of the organization. This has been achieved through selective staffing, followed by extensive on the job training, as well as didactic education, including various IAEA programmes for specific training. The year 2005 marked the beginning of an expansion of the KFSH&RC's programme entailing construction of a new building; provision of a state of the art cyclotron (30 MeV), a small cyclotron dedicated for PET isotopes production and additional production laboratories; and installation of a $^{99\text{m}}\text{Tc}$ generator and cold kit manufacturing facility. The paper covers the past, present and future of radiopharmaceuticals manufacturing at KFSH&RC, encompassing programme building and the striving for self-sufficiency.

1. INTRODUCTION

Undoubtedly, the easy and reliable availability of radiopharmaceuticals is the key element for application of radioisotopes in health care and for the viable practice of nuclear medicine. Apart from the industrialized nations, however, on-demand availability of radiopharmaceuticals is invariably a limiting factor in many developing countries, essentially depriving people of the full benefit of nuclear medicine for good health. In most instances, such an unfavourable situation arises from the absence of indigenous manufacturing, or from difficult logistics of importation from a manufacturing site to the point of use. As a result, compromised patient care can become a real issue for those nations lacking indigenous manufacturing capabilities, and which have to depend upon importation of these products. Furthermore, as the new imaging technologies find wider application (e.g. PET), developing nations could not possibly derive benefits of progress in the absence of indigenous manufacturing capabilities.

For obvious reasons then, the easy and dependable availability of these time limited products is highly desirable in order to spread the benefits of modern medicine globally.

Clearly, the most logical solution is the establishment of indigenous manufacturing capability and creation of self-reliance, thus breaking the barrier of geographical isolation.

A reason often cited for the absence of indigenous capacity is that of cost. In addition to the shortage of resources, which can be prohibitively expensive for some developing countries, there is also a lack of qualified personnel, severely limiting application of technology.

In spite of this seemingly unfavourable situation, the establishment of indigenous manufacturing is a real possibility in most developing countries. For implementation of a successful programme, attention must be focused on such key factors as creative vision, sound planning, commitment of resources and, most importantly, development of a workforce with technical expertise.

This presentation is intended to serve as an example for developing countries of how it may be possible to develop a programme that grows over the years and subsequently evolves as an all-encompassing programme to fulfil the radiopharmaceutical needs required for the comprehensive practice of nuclear medicine and indeed the needs of a nation's citizens.

At King Faisal Specialist Hospital & Research Centre (KFSH&RC), one such programme began in the early 1980s with a vision and commitment of the administration. It began with the installation of a facility for the production of cyclotron based radiopharmaceutical products for medical imaging and also for the establishment of a contemporary research programme in radiotracer devel-

opment. Over the two decades since the production of the first batch of radiopharmaceuticals in 1983, there has been a paradigm shift to expand manufacturing activity to encompass virtually all radiopharmaceuticals (including the non-cyclotron based radiopharmaceuticals) used routinely in a nuclear medicine facility. Consequently, the KFSH&RC is committed to establishment of a comprehensive manufacturing facility (self-reliance) serving the radiopharmaceutical needs of the country and indeed the geographical region.

Presented below is the past, present and envisioned future of radiopharmaceuticals manufacturing at KFSH&RC, encompassing programme building and moving towards self-sufficiency.

2. PERSONNEL, TRAINING AND EDUCATION

People are the most valuable asset in any organization. For a manufacturing facility to become successful and to improve continually, a well-qualified and appropriately trained staff is a primary requirement. Moreover, it's about developing in the staff a 'culture' that spells quality. In most developing countries, there is no lack of qualified and capable individuals per se. What could be lacking, however, is the level of experience and training for specific job functions. Therefore, to build human resources in developing countries, a viable solution is to establish a tailored and focused training programme at the technical and scientific level.

In many developing countries, new technology is invariably acquired through technology transfer in the form of either experts from an industrialized country establishing the protocols, or the technology being purchased outright. What happens next is an important issue for the viability and sustainability of the programme. The organization must ensure the transfer of knowledge, not just the technology.

The radiopharmaceuticals manufacturing programme at KFSH&RC, initially only involving the cyclotron facility, is an example of a highly successful technology transfer. All the protocols and procedures were initially established by the external experts, which became the foundation for current operations, as well as for the future growth encompassing comprehensive manufacturing capabilities.

At KFSH&RC, it was also realized that people are the most important component of a viable programme. For efficient functioning, the staff must be well qualified and appropriately trained to achieve the mission of the organization. This has been achieved through staff selection based upon educational background appropriate for the assigned job function, followed by extensive on the job training, as well as didactic and continuing education. Consequently, the

facility has had a good mix of young and experienced staff at any given time. Furthermore, use has been made of various IAEA programmes to provide specific training and fellowships for in-depth exposure at other centres. With embarkation upon new programmes, continuing education remains key to the ultimate success of the entire programme.

3. PHYSICAL RESOURCES: INFRASTRUCTURE AND EQUIPMENT

An essential requirement for a viable manufacturing facility is an adequate and appropriate infrastructure, taking into account specific design considerations for personnel safety, as well as product safety. In addition to its physical structure, the facility must also be furnished with appropriate equipment for efficient production and quality control. The extent of facility design and space allocation depends largely upon the scope of the programme. A certain minimum structure must include production areas (hot cells, fume hoods, clean rooms), quality control laboratories and storage.

The KFSH&RC facility was designed initially with the intention of producing only the cyclotron based radionuclides and radiopharmaceuticals. To achieve this goal, a medium energy cyclotron was selected for optimum capability of isotope production. In addition to manufacturing conventional isotopes, it was intended to establish a research programme for developing new radiotracers through an active R&D programme. Consequently, provision of four different types of particle beam and seven beam lines presented the option of producing a variety of radioisotopes.

With the cyclotron at the centre of activity, the facility was designed to include support laboratories and associated areas. These included target preparation and enriched materials recovery laboratories, hot cells for remote processing of the irradiated targets, clean air areas for radiopharmaceuticals manufacturing and aseptic handling, a radiochemistry laboratory for developmental work, quality control laboratories, and packaging and storage areas. Radiation protection considerations were addressed through adequate shielding and monitoring. Radioactive waste management necessitated facilities for temporary storage of the solid as well as liquid wastes, prior to terminal disposal.

It must be emphasized that the facility was less than ideal from the outset; specifically the clean air environment. Over the years, periodic modifications of the facility became essential. For example, progressive improvement in the environment surrounding the laminar flow cabinets (Class A) ultimately resulted in the currently used clean room set-up with laminar flow cabinets

(Class A) being placed in a Class B environment with access being controlled through a Class C area. Such progression has culminated in a facility that is more compatible with requirements and this has enhanced confidence in the quality of production.

An integral component of an appropriate infrastructure is the equipment used in manufacturing and quality control. For reproducibility and for enhanced confidence, attention must be given not only to the variety and pieces of equipment, but also to its calibration and maintenance. Furthermore, continuous improvements and modernization mandate replacements at regular intervals. For example, at KFSH&RC, the classical method of thin layer chromatography was gradually replaced with high performance liquid chromatography.

4. PRODUCTION

4.1. Radioisotope production

For facilities engaged in manufacturing cyclotron based radiopharmaceuticals, the production of isotopes is the first step, unlike the facilities engaged in production of $^{99}\text{Mo}/^{99\text{m}}\text{Tc}$ generators and cold kits. Whether it is production of isotopes or cold kits, sufficient information is available in the published literature to allow the user to develop their own protocols. An important consideration in developing protocols (standard operating procedures) is that the method should not only be efficient, it should also be simple, fast, and reproducible. Invariably, a substantial amount of experimental work is required to adapt the published procedures to the conditions prevailing at a new facility. Moreover, developmental work is necessary to ensure reliability in manufacturing and consistent conformity of the radiochemical bulk material to required specifications. This is where the experience and technical know-how of the staff become essential to the success of the programme.

At KFSH&RC's cyclotron facility, radioisotope production protocols were derived mainly from the experience of the staff and from available literature. Application of a systematic development programme entailed a logical sequence of activities. As a result, a sustainable programme for manufacturing radioisotopes and subsequently the radiopharmaceuticals came into existence and continued to be built upon for the future (Table 1).

Some of the development activities included:

- Target design and irradiation parameters;
- Deposition of enriched material on targets through electroplating;

TABLE 1. CURRENTLY PRODUCED ISOTOPES AT THE KFSH&RC CYCLOTRON FACILITY

Isotope	Activity at EOB (typical) (mCi)	Number of batches manufactured to date
I-123	550	3400
Tl-201	850	1100
Ga-67	950	1300
Rb-81/Kr-81m	40	5400
F-18	900	2100
N-13	100	750

- Radiochemical procedures for processing irradiated targets;
- Bulk radiochemical qualification specifications and tests;
- Enriched materials recovery processes.

As with any new facility that has experienced teething problems, protocols were eventually developed for production of various radionuclides of required specifications, and in the required quantities.

4.2. Radiopharmaceutical production

4.2.1. General

Manufacturing radiopharmaceuticals is the topic of discussion of this paper. Naturally, a great deal of attention will be focused on this activity in an organization aiming to manufacture radiopharmaceuticals.

Broadly speaking, radiopharmaceuticals may be divided into two primary categories: diagnostics and therapeutics. On the other hand, cold kits for ^{99m}Tc generators form a special category since these are not exactly radiopharmaceuticals nor conventional pharmaceuticals. Regardless of the category, all these products are pharmaceuticals and therefore must be manufactured as such.

Considering the fact that more than 80% of all procedures in a nuclear medicine facility are performed with just one isotope, ^{99m}Tc , any facility planning to serve as a regional centre for radiopharmaceuticals should logically consider production of $^{99}\text{Mo}/^{99m}\text{Tc}$ generators and the associated cold kits. In a developing country, therefore, this endeavour would be the most reasonable enterprise and also the most readily achievable objective. Immense benefits to society are practically a foregone conclusion from such an endeavour.

SESSION 5

Using the KFSH&RC facility as an example, it could be said that ^{99m}Tc generator manufacture could have been included as an integral component of the facility from the beginning of the project. Instead, establishment of the cyclotron facility was the objective at that time. It will be seen later that this scenario is about to change in near future.

The foremost requirement for manufacturing radiopharmaceuticals is that the products conform to required specifications of purity, efficacy and safety. Product conformity must also be achieved with consistency and with reliability. This is particularly true for an organization serving the national need as regards radiopharmaceuticals.

The most practical way to achieve a high level of quality assurance is the application of good manufacturing practice (GMP) guidelines (e.g. WHO, USFDA). The GMP is the minimum standard that must be applied by the manufacturer. In most countries, the manufacture of radiopharmaceuticals according to GMP guidelines is a regulatory requirement. In those rare instances where such requirements are not yet implemented, adaptation and enforcement of GMP regulations in the manufacture of radiopharmaceuticals is only a matter of time.

The application of GMP in a workplace in a developing country poses a challenge for a number of reasons: limited resources, staff limitations and, most importantly, the philosophy of operation. Furthermore, maintaining strict compliance with GMP guidelines requires a great deal of organizational commitment, including human and physical resources. The manufacturer must develop an operational philosophy which is transmitted to all levels within the organization. This is one area in which proper training and commitment of staff towards best work ethics is of paramount importance.

At the KFSH&RC facility, GMP guidelines were implanted and implemented since production of the very first batch of radiopharmaceutical. The ultimate aim is to ensure consistency resulting in product conformity, batch after batch. Although all procedures in use today have been 'tried and tested', experience has shown that there is always room for improvement. In this regard, the manufacturing programme at KFSH&RC has been, and continues to be, 'work in progress'.

Operational guidelines on continuous quality improvement, and investment of time and effort in this exercise proved beneficial, which is evident from the fact that >98.5% of all product batches conformed to the required product specifications in the first product run. Two decades of experience have shown that even the well-established protocols and procedures necessitate attention to detail to ensure repetitive reliability.

Experience has also shown that once the infrastructure is in place and the operational philosophy has been defined, it is a matter of sound application to

develop production protocols. Consequently, continuous experimental and developmental work has culminated in the production of a relatively comprehensive range of radiopharmaceuticals manufactured at the facility, as discussed below.

4.2.2. Cyclotron based radiopharmaceuticals

Initially, radiopharmaceutical production at KFSH&RC was entirely based on cyclotron produced isotopes. The most commonly used products were made readily available, boosting nuclear medicine practice in Saudi Arabia. As will be discussed later, production activities were expanded and continue to be expanded to encompass more cyclotron based products, as well as some non-cyclotron products (Tables 2, 3 and 4).

The potential of positron emission tomography (PET) as the diagnostic imaging tool of the future was recognized at KFSH&RC while the technology was still in its infancy, as exemplified by the installation of a PET camera (PC-4200, TCC) in the early 1980s. Several positron emitting radiotracers were developed at that time. However, the real PET scanner and PET radiopharmaceuticals production were established in 1995.

TABLE 2. CYCLOTRON BASED RADIOPHARMACEUTICALS CURRENTLY MANUFACTURED AT KFSH&RC

Radiopharmaceutical	First production	Batches produced to date
Sodium iodide I-123 capsules	February 1983	3350
Sodium iodide I-123 oral solution	March 1983	3200
Gallium citrate Ga-67 injection	April 1983	1300
Thallium chloride Tl-201 injection	July 1983	1150
Krypton Kr-81m gas generator	March 1984	5350
Sodium iodohippurate I-123 injection	July 1984	3100
Sodium iodide I-124	October 1987	50
m-Iodobenzylguanidine sulphate I-123 injection	April 1990	800
Fluorine F-18 2FDG injection	January 1995	2100
Nitrogen-13 ammonia injection	February 1995	750

SESSION 5

TABLE 3. OTHER PRODUCTS NOT CURRENTLY MANUFACTURED*

Radiopharmaceutical	First production
Indium chloride In-111 injection	December 1984
Indium oxine In-111	July 1987
In-DTPA	September 1989
I-123 IPPA	September 1991
I-123 IMP	May 1994

* Production discontinued due to limited usage.

TABLE 4. NON-CYCLOTRON PRODUCTS CURRENTLY PRODUCED

Radiopharmaceutical	First production
Sodium iodide I-131 capsules (various dosage forms)	August 2000
Sodium iodide I-131 oral solution (various dosage forms)	September 2000
m-Iodobenzylguanidine sulphate I-131 injection (diagnostic)	July 2001
Carbon-14 urea capsules	July 2004
m-Iodobenzylguanidine sulphate I-131 injection (therapeutic)	September 2004

4.2.3. Non-cyclotron radiopharmaceuticals

The great majority of radiopharmaceuticals used for diagnosis or for therapy are based on the non-cyclotron isotopes, of which ^{99m}Tc and ^{131}I are the two most widely used.

Having available the necessary infrastructure and the technical know-how, and also the GMP in place, it was relatively simple to establish the manufacture of several ^{131}I products within the facility. Although this isotope is reactor produced and is not manufactured in Saudi Arabia, it is readily available as radiochemical bulk from external sources. KFSH&RC developed production protocols for the manufacture of a wide range of ^{131}I products from imported radiochemical bulk material.

Manufacture of the value added ^{131}I radiopharmaceuticals is a perfect example of what a facility can achieve with minimal resource expenditure. The

^{131}I radioisotope is easily procurable at very reasonable cost from a number of reactor facilities around the world. The striking advantages realized from indigenous manufacture of the ^{131}I radiopharmaceuticals are the cost effectiveness, from a manufacturer's view, and the utility, from the user's point of view. As a result, the ^{131}I based products now comprise ~20% of all radiopharmaceutical products distributed by KFSH&RC to the users.

It is quite natural that the facility should be engaged in manufacturing $^{99}\text{Mo}/^{99\text{m}}\text{Tc}$ generators. Although attempts have been made to establish a $^{99\text{m}}\text{Tc}$ generator production plant for quite a few years through technology transfer, as well as through the facility's development efforts, it is only now that the project is being implemented. Along with the generator, KFSH&RC is also developing production protocols for the most common cold kits to prepare $^{99\text{m}}\text{Tc}$ radiopharmaceuticals, which are scheduled to become available in 2006.

5. QUALITY CONTROL AND QUALITY ASSURANCE

Control and assurance of quality are the cornerstones of any radiopharmaceuticals manufacturing programme. A product ready to use in a patient must conform to all the required specifications of an injectable radiopharmaceutical, which is assessed through analysis and measurement. However, further assurance of quality in a product is provided through a quality assurance programme that encompasses a wider view of quality, including control of all possible factors that may have a bearing on product quality. Any organization planning to establish a manufacturing facility must institute a solid quality assurance programme.

As discussed earlier, many developing countries have formulated their own quality standard for manufacturing radiopharmaceuticals. KFSH&RC experience shows that sound application of GMP provides the backbone for engineering quality into the products being manufactured. Radiopharmaceuticals manufacturing at KFSH&RC has followed international guidelines of GMP from the outset. However, it would be incorrect to say that GMP and quality assurance was fully operational from day one. As the facility gained experience, however, the extent of application increased continually, and evolved over time, with continuous improvements. This evolution is a result not only of experience, but also of the commitment to quality, culminating in an effective quality management system that is applicable today. As a result, the facility manages to manufacture radiopharmaceutical products that conform consistently to the pre-established specifications, as shown in Table 5.

SESSION 5

TABLE 5. PRODUCT BATCH DISPOSITION

Year	Batches produced	Batches rejected	Batches conforming to specifications (%)
2000	1111	9	99.2
2001	1285	34	97.4
2002	1209	15	98.8
2003	1151	17	98.5
2004	1099	6	99.5

6. REGIONAL DISTRIBUTION

As already discussed, domestic manufacturing improves product availability and hence the practice of nuclear medicine, thereby benefiting the patient; the most obvious advantage being ready availability of radiopharmaceuticals for patient use.

Prior to establishment of the KFSH&RC production facility, radiopharmaceuticals were being imported (which is still the case for ^{99m}Tc generator and cold kits). However, with its programme, the facility has filled the gap of cyclotron based radiopharmaceuticals to the point that presently, most nuclear medicine facilities in Saudi Arabia utilize its products. Product availability within hours of a request being made is a convenience enjoyed by nuclear medicine physicians.

Presently, the cyclotron facility routinely produces six cyclotron isotopes (^{201}Tl , ^{67}Ga , ^{81m}Kr , ^{123}I , ^{18}F and ^{13}N) which are subsequently formulated into nine different radiopharmaceuticals. Approximately 25 batches of radiopharmaceuticals are manufactured weekly and this supports ~40 nuclear medicine facilities within the country and the geographical region (Table 6).

7. R&D

In support of the on-going manufacturing programme and for future growth, it is desirable that the manufacturing facility engages in R&D. A continuous infusion of new ideas is the backbone for growth. For this activity, it is essential that the staff is technology 'savvy' and is enthusiastic about 'making a difference'.

TABLE 6. RADIOPHARMACEUTICALS SUPPLIED (2000–2004)

Year	Units supplied*
2000	13686
2001	13072
2002	13921
2003	13555
2004	11125

* More than 200 000 radiopharmaceutical unit doses distributed since inception (1983 to October 2005).

At KFSH&RC, the presence of staff with advanced education and technical experience has paid dividends in the form of developing ‘new’ products. Furthermore, the junior staff is well trained to carry out developmental work under the supervision of the senior staff. For example, after establishing the initial group of routine radiopharmaceuticals, development work through the joint efforts of the production and the research staff culminated in the production of a number of products including: In-oxine, ^{123}I IPPA, ^{123}I IMP, ^{131}I products, PET products and ^{14}C urea. R&D activities also led to development of production protocols for, at that time, non-conventional isotopes: ^{124}I and ^{211}At . In fact, KFSH&RC patented the methodology for production of the ^{124}I isotope (US Patent # 5019323 of 28 May 1991).

In developing countries, technology is often acquired through technology transfer from developed countries. In the absence of such possibilities, however, it is not impossible to collaborate with other centres for exchange of information, or to learn through published literature (e.g. IAEA TEDOCs). Knowing the value of indigenous manufacturing of $^{99\text{m}}\text{Tc}$ generators, KFSH&RC began developing its own production protocols for the generator and for cold kits.

8. FUTURE PLANS

A key motivating and driving force for the facility has been the goal of becoming a comprehensive radiopharmaceuticals manufacturing facility in the region. To this end, 2005 marked the establishment of just one such facility through expansion of the programme that entails:

- A new building (presently under construction);

SESSION 5

- A state of the art 30 MeV cyclotron (installed in 2006–2007);
- A small cyclotron dedicated for PET isotopes (installed in May 2006);
- Radiopharmacy laboratories (clean rooms, automation (2006–2007));
- ^{99m}Tc generators plant (to be installed in 2007);
- Cold kits manufacturing (on-going);
- Centralized radiopharmacy (2007).

9. CONCLUSION

For most developing countries, the aim of establishing domestic manufacturing, and therefore building capacity and self-reliance, is not a pipe dream; it is a real possibility. A comprehensive facility can be realized if there is motivation and driving forces that include administrative commitment, commitment of resources, building the infrastructure and preparing the technical work force. The potential for expansion of radioisotope applications and the benefits to developing countries is enormous. While striving for capacity building and self-reliance, it is imperative that quality management is woven into the fabric of planning.

Interest in PET is growing at a brisk pace worldwide. Many developing countries are considering the possibility of establishing such a facility. Whether it is the contemporary modality such as PET or the conventional facility manufacturing ^{99m}Tc generators and cold kits, it would take a concerted effort by experienced and novice staff to fulfil the goal.

The Saudi Arabian experience is meant to illustrate this very idea of evolution and maturity through experience. The purpose of this paper is to share our experiences by discussing development of our programme with respect to current and future plans.

ACKNOWLEDGEMENTS

Past and present staff of the Cyclotron and Radiopharmaceuticals Department, and the administration of KFSH&RC.

TRENDS IN INDIGENOUS RADIOISOTOPE AND RADIOPHARMACEUTICAL PRODUCTION IN BANGLADESH

M.Z. ABEDON, M.A. HAQUE
Radioisotope Production Division,
Institute of Nuclear Science and Technology,
Atomic Energy Research Establishment,
Dhaka, Bangladesh
Email: mzabedin@dhaka.net

Abstract

The Radioisotope Production Division (RIPD) of the Institute of Nuclear Science and Technology started producing radioisotopes for medical use in 1987, as soon as the 3 MW TRIGA Mark-II research reactor started operation. There are 17 nuclear medicine centres in Bangladesh and the RIPD partially meets domestic demand for medical radioisotopes, the balance being imported. The RIPD routinely produces ^{131}I solution and $^{99\text{m}}\text{Tc}$ generator and from October 2005 it was scheduled to substitute the import of these items by indigenous production. The RIPD is planning to establish a $^{99\text{m}}\text{Tc}$ cold kit manufacturing facility by 2007–2008.

1. INTRODUCTION

There are 17 nuclear medical centres in Bangladesh which are distributed more or less uniformly all over the country, and the primary objective of the Radioisotope Production Division (RIPD) of the Institute of Nuclear Science and Technology is to meet domestic demand for radioisotopes and radiopharmaceuticals [1].

The RIPD started producing instant $^{99\text{m}}\text{Tc}$ by irradiating natural MoO_3 in the research reactor in 1987. Solvent extraction of $^{99\text{m}}\text{Tc}$ with methyl ethyl ketone was used in this production. The $^{99\text{m}}\text{Tc}$ produced was routinely used in three nuclear medical centres located in Dhaka. The RIPD also produced portable sublimation generators from irradiated titanium molybdate but this method was discontinued due to inconsistent yield and contamination problems.

In 1997, a facility for the production of sterile $^{99\text{m}}\text{Tc}$ chromatographic generator was installed at the RIPD with technical assistance from BRIT

(India) under an IAEA technical cooperation project (BGD 4014). This facility is capable of producing four generators per batch. Using this plant, the RIPD produced four generators per batch and supplied the four nuclear medicine centres of the country [2, 3]. In order to meet the entire demand for ^{99m}Tc generators in the country, a plant with the capacity to produce 50 generators (15 GBq each) per batch was installed at the RIPD in May 2005 under an IAEA technical cooperation project (BGD 2010). Using this plant, the RIPD now produces 12 generators per week (the current demand of the country) and supplies these to the users [4].

The RIPD produces ^{131}I solution by irradiating natural TeO_2 using the dry distillation method. There are two dry distillation systems in the production lead shielded box for alternate use. The production capacity of the plant is sufficient to meet the country's entire demand for ^{131}I . A plant for diagnostic and therapeutic ^{131}I capsule production has recently been installed and test production of diagnostic ^{131}I capsules has been successful. Therapeutic capsule production will be started when the ^{131}I solution having the required radioactive concentration becomes available.

The demand for in vivo ^{99m}Tc kit in Bangladesh is more than 6000 vials per year. A programme to establish a kit preparation facility at the RIPD has been included in the three year (2005–2008) rolling plan of the Government.

2. $^{99}\text{Mo}/^{99m}\text{Tc}$ SOLVENT EXTRACTION GENERATOR

The RIPD started producing instant ^{99m}Tc by irradiating natural MoO_3 in the research reactor in 1987. A ^{99m}Tc solvent extraction generator plant was installed at the RIPD with technological assistance provided by Isocommerz of the former German Democratic Republic under an IAEA technical cooperation project. In this system, the relative differences in the distribution coefficients of pertechnetate and molybdate for methyl ethyl ketone was used as the basis of separation in the solvent extraction generator. Pertechnetate is preferentially extracted into methyl ethyl ketone from alkaline molybdate solution. Produced ^{99m}Tc was routinely used in three nuclear medical centres located in Dhaka until 1993.

3. $^{99}\text{Mo}/^{99m}\text{Tc}$ CHROMATOGRAPHIC GENERATOR

In order to solve the problem of sending instant ^{99m}Tc to remote nuclear medicine centres of the country, a plant for production of column chromatographic ^{99m}Tc generators was installed at the RIPD through an IAEA technical

cooperation project (BGD 4014) with technological assistance from BRIT (India). In this generator, the relative differences in the distribution coefficients of MoO_4^- and TcO_4^- on alumina were used. The passage of physiological saline through an alumina bed containing adsorbed $\text{MoO}_4^-/\text{TcO}_4^-$ elutes TcO_4^- quantitatively. The generator production facility consists of two lead shielded boxes separated by a fume hood. Each lead shielded box is equipped with manipulators, tongs, lead glass, etc., and in-cell equipment for processing fission ^{99}Mo and production of four generators at a time. Fission molybdenum is introduced into the processing lead shielded boxes via the fume hood. The facility is so planned that the two lead shielded boxes will be used alternately for production. This is necessary for maintenance of a clean atmosphere and on radiation safety grounds. The RIPD has produced four generators (15 GBq each) per batch fortnightly since 1998 and 105 batches of $^{99\text{m}}\text{Tc}$ generator have been produced in this plant and supplied to the four nuclear medicine centres in the country. The user's responses regarding the performance of these generators and quality of $^{99\text{m}}\text{TcO}_4^-$ obtained from them were quite satisfactory [5, 6].

The existing $^{99\text{m}}\text{Tc}$ generator plant is only capable of producing four generators per batch and the country's weekly requirement is 12–17 generators (some centres need weekly supply, others fortnightly). In order to meet domestic demand, a new IAEA technical cooperation project (BGD 2010) was initiated for 2003–2004 and a plant was installed at the RIPD in May 2005. Since October 2005, the RIPD has been routinely producing 12–14 generators per week, matching domestic demand. This plant was designed and installed with technological assistance from Hans Waelischmiller GmbH of Germany and with financial assistance provided by the IAEA [7].

A computer controlled on-line sterile filtration and loading system for production of $^{99\text{m}}\text{Tc}$ generator has been developed and used in this plant. This plant is capable of producing 50 generators (15 GBq) per batch and the production facility complies with the GMP requirements for radiopharmaceuticals.

A special type of filter is used for this on-line filtration. This filter is a combination of hydrophilic and hydrophobic membranes which allows passage of both aqueous solution and air. The same type of filtration unit is used in the generator assembly for terminal filtration.

The main obstacle in development of the on-line loading system was the existence of the air filter at one of the inlet needles of the generator hardware. This difficulty has been overcome by the introduction of a pneumatically controlled glass column adaptor. First, the loading solution is transferred to the adaptor and then the adaptor is pneumatically connected to the on-line system.

This new plant consists of two lead shielded boxes. One is used for chemical processing and dispensing of ^{99}Mo solution and the other for sterile filtration and generator loading. Usually radioisotope lead shielded boxes are maintained under negative pressure to prevent the release of any radionuclide during operation, but for aseptic loading of the generator a positive pressure is required. To overcome this difficulty, a small laminar flow module is installed above the loading area of the lead shielded box which provides a Class 100 (Class A; ISO 5) clean area during the loading process and the overall pressure of the lead shielded box is maintained negative.

This chromatographic $^{99\text{m}}\text{Tc}$ generator production is based on fission produced ^{99}Mo . The main features of this generator are: (1) cold generator assembly, (2) dry column generator, (3) terminal filtration, (4) small elution volume (minimum volume for full elution is 3 mL), (5) elution volume can be selected by volume controller, (6) adequate radiation protection for the users, (7) sterile and non-pyrogenic $^{99\text{m}}\text{Tc}$ eluate, and (8) reuseable generator hardware, etc.

The generators produced at the RIPD are comparable with the best quality generators available on the world market. This facility enables Bangladesh to produce a sufficient number of high quality $^{99\text{m}}\text{Tc}$ generators locally. Figure 1 shows the RIPD's increased production of generators.

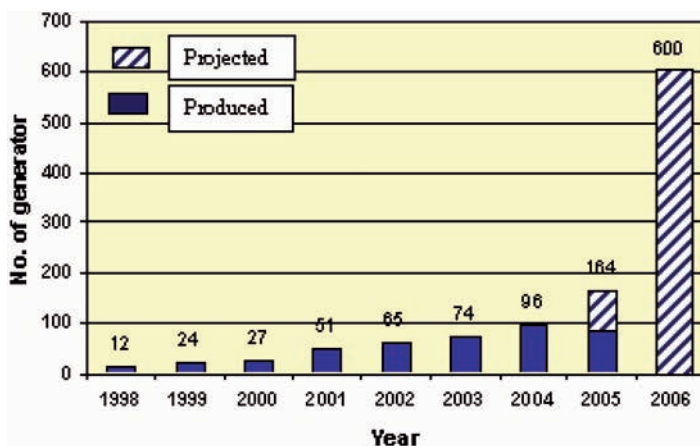


FIG. 1. Production data of $^{99\text{m}}\text{Tc}$ generators at RIPD.

4. PRODUCTION OF ^{131}I

A plant for the production of ^{131}I was installed at the RIPD in 1987. Iodine-131 is produced from an irradiated TeO_2 target. Tellurium-130 (natural abundance 33.4%) captures neutrons to produce $^{131\text{m}}\text{Te}$, which transforms into ^{131}I by beta emission.

Tellurium dioxide in a finely crystalline form and sealed in a quartz ampoule is irradiated in the reactor and after two days of cooling it is heated to about 730°C . Iodine-131 is released and transferred by air stream into a trap filled with $\text{Na}_2\text{CO}_3/\text{NaHCO}_3$ buffer. More than 99% of the iodine is absorbed as sodium iodide at pH7–9. This plant is suitable for the production of 370 GBq of ^{131}I per batch.

Recently, two new furnaces with compact control systems have been installed in the old ^{131}I production hot cell for separation of ^{131}I . The operating temperature and air flow for these systems have been optimized and separation efficiency of ^{131}I was found to be >90%. The optimum sublimation efficiency for the new furnace was found to occur at $730\text{--}750^\circ\text{C}$ and at an air flow rate of $2.6\text{ cm}^3/\text{min}$ [8].

The RIPD produces ^{131}I every week and its quality (radiochemical purity, radionuclidic purity, pH range, etc.) was found to lie within permissible limits. The isotope is supplied to the nuclear medicine centres for diagnostic and therapeutic applications. The user report is very satisfactory. Yearly production and projected targets are shown in Fig. 2.

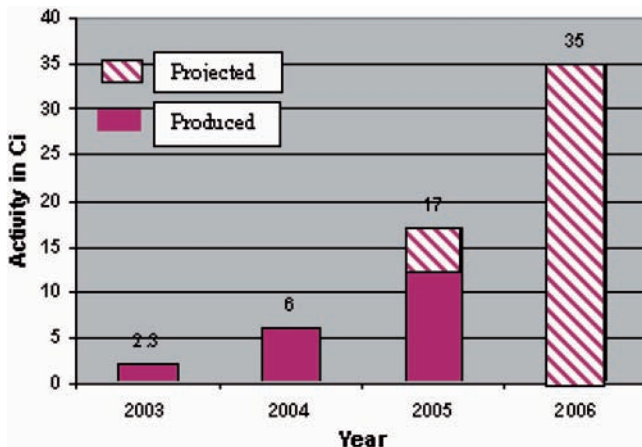


FIG. 2. Production data of ^{131}I at RIPD from 2003.

5. PRODUCTION OF ^{131}I CAPSULES

Iodine-131 capsules of 1.85, 2.78 and 3.70 GBq are used for thyroid ablation therapy and capsules of 37–74 MBq are used for diagnosis in the nuclear medicine centres. Present demand for ^{131}I therapeutic capsules in the country is about 56 GBq/week.

In order to produce ^{131}I capsules locally, a plant was installed at the RIPD in 2001. The facility can be used for the production of both diagnostic and therapeutic capsules. Inert material used to fill the capsules is composed of a mixture of dry Na_2HPO_4 , ascorbic acid and $\text{Na}_2\text{S}_2\text{O}_3$ powder in a 10:1:1 ratio.

The plant will be used for ^{131}I therapy capsule production by importing ^{131}I solution with higher radioactivity concentration.

6. IN VIVO $^{99\text{m}}\text{Tc}$ COLD KIT PRODUCTION FACILITY

The demand for various in vivo $^{99\text{m}}\text{Tc}$ cold kits in Bangladesh numbers more than 6000 vials per year. In order to produce kits locally, a programme to establish a kit manufacturing facility at the RIPD has been initiated through an IAEA technical cooperation project proposal (2007–2008).

7. CONCLUSIONS

The RIPD routinely produces ^{131}I and $^{99\text{m}}\text{Tc}$ generator and supplies to the nuclear medicine centres of the country. At present, production matches demand within the country. The users' responses with regard to the indigenous products are quite satisfactory. By 2008, the division plans to install an in vivo $^{99\text{m}}\text{Tc}$ kit manufacturing facility for supplying kits locally. The aim is to achieve self-sufficiency in production and supply of the main items of radioisotopes and radiopharmaceuticals used in Bangladesh.

REFERENCES

- [1] ABEDIN, M.Z., HAQUE, M.A., Production and Supply of Medical Isotopes from Radioisotope Production Division, 10th National Conference and International Symposium of Bangladesh Society of Nuclear Medicine, 11th February 2005, Dhaka, Bangladesh, Printed in Bangladesh Journal of Nuclear Medicine **8** 1 (2005) 43.
- [2] ABEDIN, M.Z., MOHSIN ALI, M.D., Radionuclidic Characteristics of the ^{99m}Tc-Generator Produced at the Institute of Nuclear Science & Technology, AERE, Savar, Bangladesh Journal of Nuclear Medicine **2** 1 (1999) 3-5.
- [3] ABEDIN, M.Z., MOHSIN ALI, M.D., Quality Control of ^{99m}Tc-Generator Produced at the Institute of Nuclear Science & Technology, Internal Report, INST, AERE, Savar, INST-69/RID-12 (1998).
- [4] NOVOTNY, D., WAGNER, G., Automation in generator technology. Technical recommendation and production of sterile generator and the post-elution concentration. Report of the 1st Research Coordination Meeting on Development of Generator Technologies for Therapeutic Radionuclides, 4-8 October 2004, IAEA, Vienna (2004) 50.
- [5] ABEDIN, M.Z., YASMIN, L., RAHMAN, H., HOSSAIN, A., CHAKRABARTI, K.L., Quality Assurance of RIPD Tc-99m Generators, 2nd AGM of ARCCNM and 8th National Conference of Bangladesh Society of Nuclear Medicine, 6-8 February 2003, Dhaka, Bangladesh, Abstract Printed in Bangladesh Journal of Nuclear Medicine **6** 1 (2003) 72.
- [6] HOQUE, R., et al., Elution performance and clinical experience ⁹⁹Mo/^{99m}Tc generator of RIPD, INST, Savar, Bangladesh. Bangladesh Journal of Nuclear Medicine **4** (2001) 85-88.
- [7] ABEDIN, M.Z., et al., Some Experiences on Chromatographic Tc-99m Generator Production, International Conference on Current Trnds in Radiopharmaceuticals, October 21-23 (2003), PINSTECH & NORI, Islamabad, Pakistan (Published in the Conference proceedings).
- [8] HAQUE, M.A., et al., Installation of new I-131 production system & its Performance, 9th National Conference of Bangladesh Society of Nuclear Medicine, 9th January (2004), Dhaka, Bangladesh (Published in the Conference proceedings).

EXPERIENCE IN THE PRODUCTION OF PAKGEN ^{99}Mo - $^{99\text{m}}\text{Tc}$ GENERATORS

M.M. ISHFAQ, H. NIZAKAT, K.M. BASHAR, M. JEHangIR
Isotope Production Division, PINSTECH,
Islamabad, Pakistan
Email: mishfaq@pinstech.org.pk

Abstract

A facility for the production of ^{99}Mo - $^{99\text{m}}\text{Tc}$ generators, along with a clean room system was established at PINSTECH by the IAEA under a technical cooperation project (PAK/4/04) with finance of US \$200 000. This generator production facility comprises three clean rooms: (i) preparatory room (grade D), (ii) generator loading room (grade C), and (iii) quality control room (grade B). The materials used for generator preparation are transferred through airlocks while dress change rooms are provided for personnel entry. Two hot cells equipped with in-cell equipment are installed in a generator production room. The prepared generators are transferred via conveyor belt to the quality control room for measuring elution efficiency and ^{99}Mo breakthrough. Regular production of Pakgen $^{99\text{m}}\text{Tc}$ generators started in January 2003. More than 1900 Pakgen $^{99\text{m}}\text{Tc}$ generators with calibrated activities (five days reference date) ranging from 300 to 600 mCi of ^{99}Mo have been supplied to various nuclear medical centres in Pakistan. Before preparation, the generator bodies and the various sections of the Generator Production Laboratory are cleaned and disinfected. During preparation, the required calculated activity of ^{99}Mo is loaded on the columns of pre-assembled generators by pre-wash, loading and post-wash steps and the quality of the generator is checked by elution efficiency and molybdenum breakthrough of eluate obtained after one hour of the post-wash step. All these calculations are carried out using the MOGEN-I computer program developed in Visual Basic 6 software. This software is suitable for recording and acquitting commercial data and monitoring production and quality control. All Pakgen $^{99\text{m}}\text{Tc}$ generators are test eluted before shipment. Quality tests performed include: elution efficiency, molybdenum breakthrough, radiochemical purity, chemical purity, radionuclidic purity, sterility and apyrogenicity. The eluate fulfils the quality control criteria prescribed by the IAEA and the European Pharmacopoeia. In hospitals, the Pakgen $^{99\text{m}}\text{Tc}$ generators showed optimum performance in terms of elution yields, molybdenum breakthrough, labelling yields and quality of gamma scans.

1. INTRODUCTION

The rapid development of nuclear medicine has been contingent on the availability of the radionuclide ^{99m}Tc ($T_{1/2} = 6 \text{ h}$), whose nuclear properties are ideal for organ imaging [1]. The progeny radionuclide ^{99m}Tc is formed from the β^- decay of the parent ^{99}Mo ($T_{1/2} = 66 \text{ h}$). Technetium-99m decays by isomeric transition to ^{99}Tc by 140 keV gamma photons; at this energy the photons have adequate tissue penetration. In a chromatographic generator based on alumina, the eluted $^{99m}\text{TcO}_4^-$ by saline can be used for imaging various organs (bone, kidney, heart, brain, liver, spleen, lung, stomach, etc.) after preparation of ^{99m}Tc labelled radiopharmaceuticals.

Previously, Pakistan imported ~20 ^{99}Mo - ^{99m}Tc generators (cost US \$500 000) loaded with ~10 Ci of fission ^{99}Mo for use in medical centres/hospitals from Amersham Inc. in the United Kingdom. To overcome the problem associated with import of the generators, such as hard currency, increasing price, import policies, delay and changes in supply schedules, etc., the IAEA was approached with respect to the provision of a facility for the production of ^{99}Mo - ^{99m}Tc generators conforming to international standards. During 1998, a contract between the IAEA, the Institute of Isotopes (Budapest, Hungary (contractor)) and PINSTECH (Islamabad, Pakistan) was signed under an IAEA technical cooperation project (PAK/4/40) [2]. Under this project, the contractor provided a clean laboratory, two hot cells and in-cell equipment amounting to the value of US \$200 000 while PINSTECH provided a HVAC unit with all local facilities. Radioactive commissioning of the Generator Production Laboratory (GPL) was carried out in early 2000.

Regular production of Pakgen ^{99m}Tc generators started in September 2003 using fission ^{99}Mo obtained from NEC, South Africa. More than 1900 Pakgen ^{99m}Tc generators with calibrated activities (five day reference date) ranging from 300 to 600 mCi of ^{99}Mo have been supplied to various nuclear medical centres in Pakistan.

2. PRODUCTION OF PAKGEN ^{99m}Tc GENERATORS

2.1. Theoretical considerations

2.1.1 Alumina as an adsorbent for ^{99}Mo

The ^{99m}Tc generator based on a chromatographic separation of ^{99m}Tc from ^{99}Mo using alumina as adsorbent is still the common method. The adsorption of the molybdate ion on alumina is strongly affected by pH owing to changes in the chemical structure of the molybdate ion (Fig. 1). The retention

SESSION 5

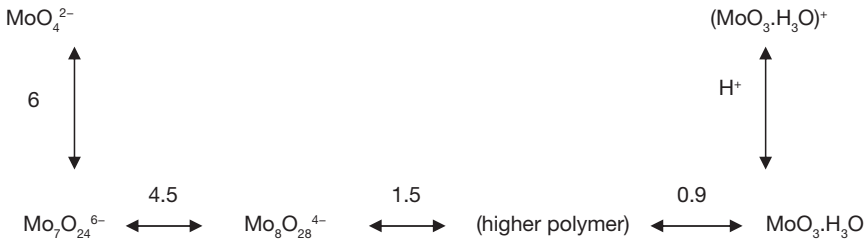


FIG. 1. Charge on the molybdate ion at various pH values.

of Mo molecules in polymeric form is very high on the alumina column as compared to Tc molecules in acidic conditions (pH~2.9). Alumina (acidic) having a grain size of 100–200 mesh is the most appropriate adsorbent as it allows a good flow pattern, optimum adsorption of Mo and good elution yield. The concentration profile of a 3 g alumina column in a Pakgen generator was determined by collection of 1 mL of eluate. The yield of $^{99\text{m}}\text{Tc}$ per mL eluate is presented in Fig. 2. More than 90% of the activity of $^{99\text{m}}\text{Tc}$ is concentrated in the first 5 mL of eluate.

2.1.2. Kinetics of growth and decay of the ^{99}Mo – $^{99\text{m}}\text{Tc}$ – ^{99}Tc system

The growth and decay of ^{99}Mo – $^{99\text{m}}\text{Tc}$ – ^{99}Tc is followed by a well known decay sequence [1] as depicted in Fig. 3.

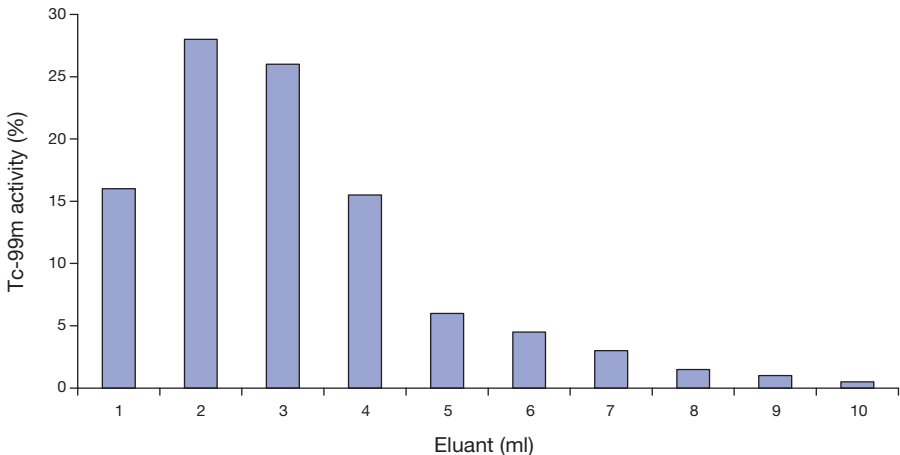


FIG. 2. Elution profile of $^{99\text{m}}\text{Tc}$ (3 g alumina in column).

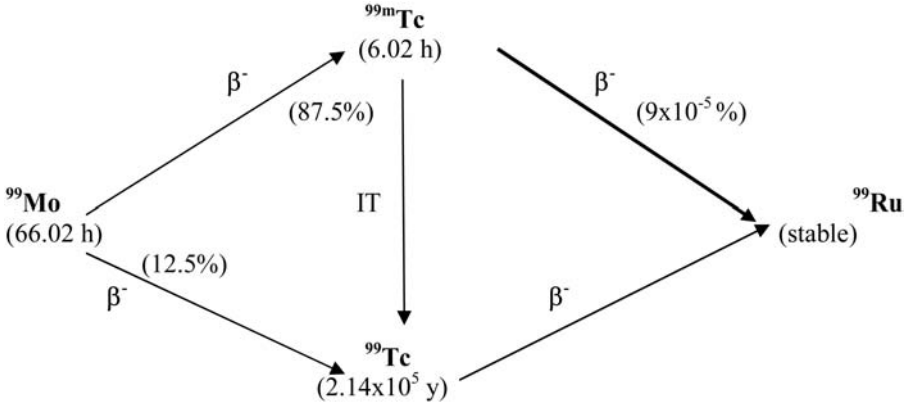


FIG. 3. Decay sequences of ^{99}Mo to ^{99}Ru .

The decay scheme shows that 12.5% of the atoms are converted directly into ^{99}Tc while 87.5% pass to the metastable state $^{99\text{m}}\text{Tc}$. From the decay scheme shown in Fig. 3, the following expressions may be derived:

The activity of ^{99}Mo atoms at any time, t;

$$A_1 = A_1 e^{-\lambda_1 t}$$

The activity of $^{99\text{m}}\text{Tc}$ at time, t:

$$0.875 \lambda_2$$

$$A_2 = \frac{0.875 \lambda_2}{(\lambda_2 - \lambda_1)} A_1 [e^{-\lambda_1 t} - e^{-\lambda_2 t}] + (A_2)_0 e^{-\lambda_2 t}$$

$$(\lambda_2 - \lambda_1)$$

Where λ_1 and λ_2 are decay constants and A_1 and A_2 are activities of ^{99}Mo and $^{99\text{m}}\text{Tc}$ respectively.

For ^{99}Mo and $^{99\text{m}}\text{Tc}$, the values of λ_1 and λ_2 are such that a state of transient equilibrium will be achieved after $^{99\text{m}}\text{Tc}$ has gone through a maximum value. However, the $^{99\text{m}}\text{Tc}$ activity will never exceed the ^{99}Mo activity because only 87.5% of the disintegration of ^{99}Mo results in $^{99\text{m}}\text{Tc}$.

All the theoretical calculations were carried out using the MOGEN-I computer program which was developed in Visual Basic 6 software. This software takes into account mathematical equations for theoretical calculation

SESSION 5

of generator parameters using ^{99}Mo – $^{99\text{m}}\text{Tc}$ – ^{99}Tc decay schemes; otherwise these calculations are laborious and time consuming. This software is suitable for recording and acquitting commercial data and monitoring production and quality control.

2.1.3. *Requirements of the clean room system*

The objective of good manufacturing practice is to use advanced techniques and quality assurance to minimize the risk of product contamination and to generate products of standard quality. Production of sterile medicinal products should be carried out in clean areas whose entry should be through change rooms for personnel and through airlocks for materials. Clean areas should be maintained to an appropriate standard of cleanliness and supplied with air, which has passed through filters of an appropriate efficiency. The various operations of component preparation, product preparation, filling, etc., should be carried out in separate areas within the clean area.

Clean areas for the production of sterile products are classified according to the required characteristics of the air into grades A, B, C and D. The cleanest room (A or B category) is essential for the production of $^{99\text{m}}\text{Tc}$ freeze-dried kits because no post-sterilization is possible owing to easy decomposition of products. However, for the products where sterilization is possible before administration, a laboratory of C category is required. Sterilized $^{99\text{m}}\text{Tc}$ solution is obtained by providing Millipore filters in the Pakgen $^{99\text{m}}\text{Tc}$ generators; hence, a C category clean laboratory is necessary for the production of $^{99\text{m}}\text{Tc}$ generators. Air and bacteriological characteristics of clean rooms are given in Table 1.

According to US standards, the classification is: Class 100 (grade A), Class 1000 (grade B), Class 10 000 (grade C) and Class 100 000 (grade D).

In the clean areas, all exposed surfaces should be smooth in order to minimize the shedding or accumulation of particles or microorganisms and to permit the repeated application of cleaning agents.

Changing rooms should be designed as airlocks and used to provide separation of different stages. Airlocks should not be opened simultaneously. An interlocking system should be operated to prevent the opening of more than one door at a time. A filtered air supply should maintain a positive pressure relative to surrounding areas.

The sanitation of clean areas is important. They should be cleaned frequently and thoroughly with disinfectants. Monitoring should be undertaken regularly in order to detect the development of resistant strains.

TABLE 1. AIR CLASSIFICATION SYSTEM FOR THE MANUFACTURE OF STERILE PRODUCTS

Grade	Max. permitted number of particles per m ³ equal to or above:		Max. permitted number of viable microorganisms per m ³
	0.5 µm	5 µm	
A (Laminar air flow)	3520	29	Less than 1
B	35 200	293	7
C	352 000	2930	10
D	3 520 000	29 300	100

2.2. Practical aspects

2.2.1. GPL

The GPL illustrated in Fig. 4 comprises three clean rooms, consisting of (i) a preparatory room (grade D), (ii) a generator loading room (grade C), and (iii) a quality control room (grade B). Two different areas, one for the loading of ⁹⁹Mo activity and entry of raw materials and the other for the packing of generators are provided. The materials used for generator preparation are transferred through airlocks from one area to another. The dress change rooms are provided for personnel entry. Two hot cells equipped with in-cell equipment are installed in a generator loading room. The prepared generators are transferred via conveyor belt to the quality control room. Finally, the finished generators are packed in the packaging area for transportation [3].

2.2.2. Disinfection of GPL

Prior to starting production, the GPL was disinfected using Incidin[®] extra. Floors, walls and ceiling were washed with diluted disinfecting agent. The inside surfaces of hot cells were disinfected by spraying with 70% ethanol. The filtered airflow was then switched on. After these preparations, entry into the aseptic laboratory was allowed only by personnel wearing sterile protective clothing (mask, boots, gloves, aprons, caps, etc.).

SESSION 5

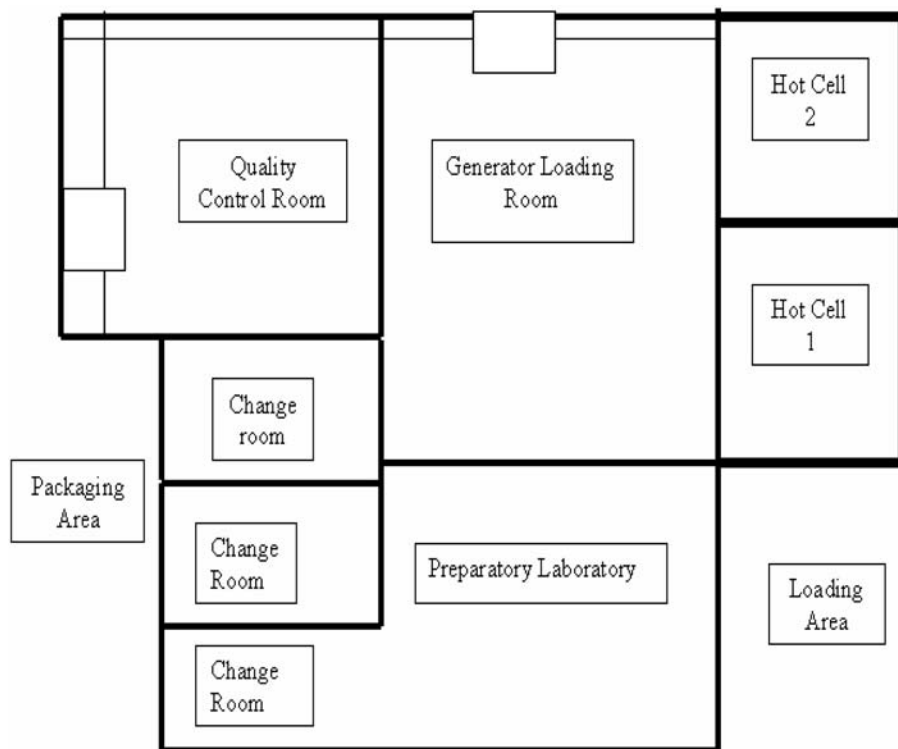


FIG. 4. Layout of GPL.

2.2.3. Preparation of alumina glass columns

The required glass columns were filled with Al_2O_3 (acidic) 100–200 mesh (3 g) using the standard procedure. These columns were sterilized in an oven at 150°C for two hours and then stored in a desiccator.

2.2.4. Assembly of generator bodies

Various parts of the generators were sprayed with 70% ethanol in the preparatory room. After drying, the prepared alumina columns were connected to SS tubes and these assemblies were inserted into the lead generator containers. The assembled generator bodies were transferred to the generator loading room. Prepared generator bodies were placed in series for ^{99}Mo dispensing.

2.2.5. Preparation of reagents

1N nitric acid physiological saline solution of pH3.5, pH4.5 and 0.2N sodium hydroxide were prepared by using sterilized and pyrogen free water and saline.

2.2.6. Checking of equipment and instruments in hot cells

The pH meter, balance, magnetic stirrer, air bubbler, peristaltic pumps, hydraulic lift, tygon tube connections, activity meter, remote tongs and vacuum system were checked. The on-line manometer was also checked for appropriate negative pressure (−4 cm) in hot cells.

2.2.7. Transfer of required amounts of reagents into hot cells

Various amounts of desired chemicals, such as H_2O_2 , HNO_3 , NaOH , and syringes and stock bottles filled with sterile distilled water were placed into hot cells before transfer of ^{99}Mo bulk bottle. 250 mL of pre-wash and post-wash solutions each were filled in headers attached to hot cell II.

2.3. Production technology

2.3.1. Description of Pakgen ^{99m}Tc generator

The Pakgen generator is a system by which a sterile, pyrogen free solution of ^{99m}Tc as sodium pertechnetate can be obtained. This solution is eluted from an alumina chromatographic column on which fission produced ^{99}Mo is adsorbed. The glass column is fitted with a G-2 filter disc at the bottom and closed at both ends by rubber stoppers and aluminium caps. A stainless steel needle with one end connected to the bottom of the column and the other end fitted with a Millipore filter is to receive a vacuum vial to elute the column. Another stainless steel needle with one end connected to the top of the column while the other end, having a spike (a double needle), is to receive a saline vial. The column and the needles are protected by cylindrical lead shielding with a minimum thickness of 40 mm (Fig. 5). The whole system is placed in a cover made of galvanized iron. The Pakgen is delivered in polystyrene packing in a plastic bucket [4].

SESSION 5

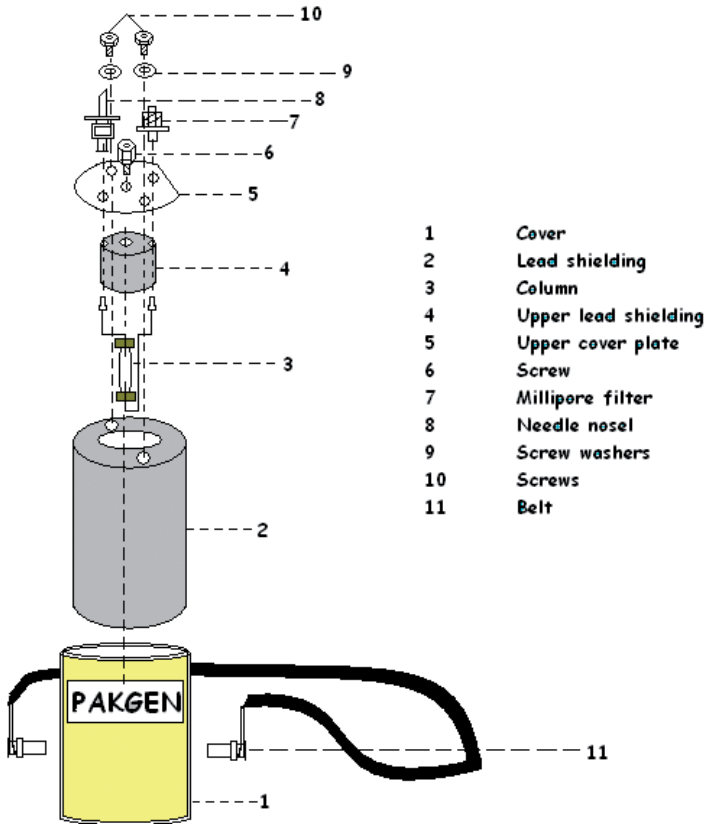


FIG. 5. Parts of Pakgen ^{99m}Tc generator.

2.3.2. Loading/dispensing of ⁹⁹Mo from stock bottle on generator columns

From the stock solution, a 1 mL aliquot was taken by long needle syringe and injected into a sealed vial. Activity was measured in an activity meter. The tubing system was rinsed with 1 mL of ⁹⁹Mo solution. Prepared generator bodies were placed on the conveyor. The calculated volume of ⁹⁹Mo was filled by means of the peristaltic pump. The volume of ⁹⁹Mo was determined on a weight basis using a balance. The generators were filled with activity one by one. At the filling position, the first generator is at the pre-wash position, the second is at the filling position and the third is at the post-wash position.

2.3.3. Assembly and packaging of generators

The prepared generators were fitted with membrane filter, spike and injection needle onto the ends of the column under the LAF. Protective caps were put onto the injection needle and spike. After performing the control elution, generators were transferred to the packaging area where they were supplied with labels indicating batch number, activity reference date and expiry date.

3. QUALITY CONTROL OF PAKGEN ^{99m}Tc GENERATORS

The quality control criteria set by the IAEA and various pharmacopoeias [5–7] for ^{99m}Tc generator and ^{99m}Tc eluate are based on various controls on the eluate from the generator, which are essential to ensure that the eluate is suitable for preparing ^{99m}Tc labelled radiopharmaceuticals and safe to administer to patients. However, quick elution tests are performed to estimate the elution yield of ^{99m}Tc and ^{99}Mo breakthrough during the production process for releasing the generators.

3.1. Quick elution tests

Elution from the Pakgen ^{99m}Tc generator (quick test) was taken after a one hour post-wash step and the activity of the eluate for ^{99m}Tc and ^{99}Mo were measured to determine elution efficiency of ^{99m}Tc and breakthrough of ^{99}Mo .

3.1.1. Elution yield of ^{99m}Tc / ^{99}Mo breakthrough

The elution efficiency of a generator can be defined simply as the proportion of the ^{99m}Tc present in the system that is separated during the elution process and is usually expressed as a percentage. From experience with the molybdate ^{99}Mo pertechnetate– ^{99m}Tc system, using an alumina adsorbent and sodium chloride eluant, the loss of elution efficiency is due to radiation induced reduction which gives a non-elutable technetium species. It has been suggested that the hydrated electron is the species responsible for the reduction. It is important, both to the producer and to the end user, that the radiation induced chemical effects be minimized or reversed. The presence of water within the system is detrimental to the efficient operation of the generator; this has led to the development of a ‘dry’ generator such as Pakgen, where residual eluant is removed from the alumina bed at the end of each elution cycle.

The activity of eluted ^{99m}Tc was measured in a dose calibrator. This vial was then put into a lead canister (6 mm thick lead) and ^{99}Mo activity was measured by a dose calibrator (attenuation factor of 3.5 for ^{99}Mo). As test elution is performed one hour after post-rinse, only 10% of the total ^{99m}Tc is generated. Resulting data were used for calculating the elution yield of ^{99m}Tc and ^{99}Mo breakthrough by using MOGEN-I software.

3.2. Radionuclidic purity

Radionuclide purity is that proportion of radioactivity due to ^{99m}Tc compared to the total activity measured. The presence of traces of other radionuclides can increase radiation exposure. As a starting material, fission ^{99}Mo is obtained from South Africa. The purity level of fission produced ^{99}Mo is very high, as shown in Table 2. This product specification is a certificate of guarantee in the final quality control report.

3.3. Radiochemical purity

Radiochemical purity of a radiopharmaceutical preparation refers to the fraction of the stated radionuclide present in the stated form. Although pertechnetate is the most stable valence state of technetium, lower valency species have, however, been detected in generator eluate.

Between 5 and 10 μL of ^{99m}Tc eluate was dropped onto three pieces of 1.5 cm \times 15 cm chromatographic paper (ITLC-SG, Gelman) at a point 1.5 cm from one end of the strips. The strips were placed into a developing vessel containing a 4:1 mixture of acetone:2N HCl, without allowing the liquid level to reach the eluate drop. The developing time was \sim 15 min. Strips were dried and

TABLE 2. RADIONUCLIDE PURITY CERTIFICATE BY NTP RADIOISOTOPES, SOUTH AFRICA

Radionuclide	Purity (%)	Technique
Mo-99	0.1	γ spectrometry
I-131	5×10^{-3}	
Ru-103	5×10^{-3}	
Sr-89	6×10^{-5}	β spectrometry
Sr-90	6×10^{-6}	
α emitters	1×10^{-7}	α spectrometry
other γ emitters	0.01	γ spectrometry

scanned with a 2π -scanner for radioactivity determination; $^{99m}\text{TcO}_4^-$ is found at R_f 0.85–1.0 value.

3.4. Chemical purity

Eluted ^{99m}Tc may contain chemical impurities, originating from either the generator bed or the eluant, which could detrimentally affect the clinical application of the radionuclide. Probably the chemical impurity most commonly reported is aluminium and H_2O_2 . The aluminium content should be $<20 \mu\text{g/mL}$, whereas the limit for H_2O_2 should be $<10 \mu\text{g/mL}$ of ^{99m}Tc eluate. These tests were performed using standard kits. Table 3 shows the characteristics of the Pakgen ^{99m}Tc generator.

3.5. Biological control

Biological control is concerned with sterility and apyrogenicity. Since the ^{99m}Tc eluted from a generator will normally be used directly or following

TABLE 3. CHARACTERISTICS OF ^{99m}Tc ELUATE OBTAINED FROM PAKGEN ^{99m}Tc GENERATOR

Quality	Eluate purity limit	Methodology	Results
Characteristic	A clear colourless solution of ^{99m}Tc with half-life of 6 h emits gamma radiation of 140 keV	Visual, gamma counting	A clear colourless solution
pH	4–8	pH meter and pH paper	5.5–6.5
Radiochemical purity	Not less than 95% as pertechnetate Al $< 20 \mu\text{g/mL}$	TLC and paper chromatography Chemical test	More than 98% Al $< 4 \text{ mg/mL}$
Chemical purity	$\text{H}_2\text{O}_2 < 10 \mu\text{g/mL}$		$\text{H}_2\text{O}_2 < 3 \text{ mg/mL}$
Yield of ^{99m}Tc	90–110%	Ionization chamber	90–110%
Breakthrough of ^{99}Mo	$<0.01\%$ of ^{99m}Tc activity	6 mm lead container in ionization chamber	$<0.01\%$ of ^{99m}Tc activity

SESSION 5

chemical formulation as an intravenous injection, attention must be paid to sterility and apyrogenicity. It is well established that the chromatographic generator effectively filters microorganisms that eluate from manufactured sterile generators and that these do not require terminal autoclaving as a further safeguard before injection.

3.5.1. Sterility test

A sterility test in accordance with the pharmacopoeia normally lasts 14 days. This period, however, is too long for ^{99m}Tc generators. For this reason, it is permitted to use the product before the sterility test has been completed. For the sterility test, a medium for aerobic and anaerobic microorganisms (thioglycolate medium) and a medium for fungi (fluid sabouraud medium) are necessary. Details are available in Refs [5–7].

3.5.2. Apyrogenicity test

Since the apyrogenicity test is much less time consuming, it is feasible for ^{99m}Tc prior to use in humans. The rabbit test takes about four hours and involves injecting the pertechnetate into the ear and measuring the course of temperature in at least three animals. Details of rabbit testing are described in all well known pharmacopoeias [5–7]. The limulus amoebocytal lysate forms a gel in the presence of endotoxin if incubated for 60 min at a temperature of 37°C. Details and directions for this test are available in pharmacopoeias.

3.6. Areas and personnel dosimetry

Protective clothing, overshoes and surgical gloves were worn by personnel involved in the production and quality control of generators. Personnel dosimetry was carried out by TLD and pocket dosimeters. The maximum dose received by any operator was <3 mrem. Smear tests of GPL were performed three times, first after opening the bulk ^{99}Mo solution in the hot cell, and second after loading the generators and lastly after completion of the whole process. Samples were also collected from the trap bottle on the vacuum line. The health physicist reported no incident to personnel or area contamination.

3.7. Radioactive waste management

As total volume of the ^{99}Mo stock solution and rinsing solution were dispensed into produced generators, nominal activity of ^{99}Mo solution is

expected. Radioactive waste was generated only by eluting generators (^{99m}Tc , $T_{1/2} = 6$ h). By evaporation, contamination on bottle and tygon tube walls is also expected. Plastic bottles that contained ^{99}Mo bulk solution, used up chromatographic columns, plastic tubes and cotton swabs (for wiping) are included as solid radioactive waste. As generator components are proposed to be recycled, decayed alumina columns have to be taken out from generators. Although after six weeks every radioisotope found on the column is below the exemption activity level, decayed columns would be disposed of as radioactive waste. The ~300 mL of elution liquid and ~100 mL of rinse water contain mainly ^{99m}Tc , while negligible amounts of ^{99}Mo are also expected. After four weeks in storage, it will be handed over to the 'radwaste' management group.

4. CONCLUSION

Under an IAEA technical cooperation project (PAK/4/04), the Institute of Isotopes in Budapest, Hungary, designed, manufactured and installed a ^{99m}Tc generator loading facility at PINSTECH. From January 2003, regular production of Pakgen ^{99m}Tc generators utilizing fission ^{99}Mo (>36 Ci) imported from South Africa has been carried out on a weekly basis and more than 1900 consignments of these generators, with activities ranging from 300 mCi to 600 mCi (reference activity), have been supplied to ~20 different hospitals in Pakistan. More than 97% of the generators showed optimum performance in terms of elution efficiency of ^{99m}Tc , ^{99}Mo breakthrough and radiochemical purity. Similarly, the eluate obtained from these generators showed optimum labelling efficiency with radiopharmaceutical freeze-dried kits. Less than 2% of generators showed low ^{99m}Tc yields. This might be due to channelling of the alumina bed during transportation as more than 80% of these generators were recovered by consecutive elution with saline.

REFERENCES

- [1] BOYD, R.E., *Radiochemica Acta*, 30 (3) (1982) 123.
- [2] CONTRACT between THE INTERNATIONAL ATOMIC ENERGY AGENCY, THE INSTITUTE OF ISOTOPES CO., LTD and Government of Pakistan represented by the PAKISTAN INSTITUTE OF NUCLEAR SCIENCE AND TECHNOLOGY (PINSTECH) concerning the design, manufacture, installation and commissioning of a ^{99m}Tc Generator Loading Facility at PINSTECH in Nilore, Islamabad, Pakistan (1997), IAEA, Vienna.

SESSION 5

- [3] JEHANGIR, M., MUSHTAQ, A., ISHFAQ, M.M., Generator Production Laboratory (GPL) and Its Safety Assessment, Rep. IPD-Rep-1, Aug. 2002, Pinstech, Islamabad (2002).
- [4] INTERNATIONAL ATOMIC ENERGY AGENCY. Regulations for the Safe Transport of Radioactive Material, Safety Standard Series No. ST-1, IAEA, Vienna (1996).
- [5] UNITED STATES PHARMACOPOEIA (1980).
- [6] EUROPEAN PHARMACOPOEIA (1997).
- [7] BRITISH PHARMACOPOEIA (1980).

BIONT – A NEW CENTRE FOR PET RADIOPHARMACEUTICALS PRODUCTION IN CENTRAL EUROPE

P. RAJEC, F. MACÁŠEK, P. KOVÁČ

BIONT a.s.,

Bratislava, Slovakia

Email: rajec@biont.sk

Abstract

BIONT a.s. is a joint stock company that was established in January 2005 as a 'ready to act' facility constructed as a part of Slovakia's cyclotron centre. All its facilities represent state of the art technology for research and production of radionuclides for PET. The layout of the facility was designed for a dual beam cyclotron Cyclone 18/9 and GMP zone for producing PET radiopharmaceuticals. Core parts of the facility were built with the help of the IAEA under two technical cooperation grants during 1997–2004. Cyclone 18/9 is equipped with six targets: two aqueous targets for $^{18}\text{F}^-$ (Nb and Ag), one gas target for $^{18}\text{F}_2$ production, an aqueous target for ^{13}N , and a gas target each for $^{15}\text{O}_2$ and $^{11}\text{CO}_2$. An external beam is constructed for a solid target. The production area includes eight lead shielded boxes with new modules for 2- ^{18}F]FDG and ^{18}F]DOPA synthesis, a dry methylation module for preparation of ^{11}C -methyl iodide precursor, a system designed for ^{13}N]NH₃ and ^{15}O]H₂O production, an automatic dispensing unit, and all necessary auxiliary equipment. A quality control laboratory is equipped with GC, HPLC, TLC scanner, UV-VIS spectrometer, gamma spectrometer and LAL test equipment. A radiopharmaceuticals R&D laboratory is equipped with two shielded chambers, a mini-cell for synthesis modules, and a dispensing cell for an automatic dispensing module. The LC-MS system is dedicated to precursors and radiopharmaceutical analysis. The laboratory also includes a laminar shielded box with dose calibrator, centrifuge, lyophilizer, ultra pure water production unit and other laboratory equipment. The adjacent PET centre, built as a nuclear medicine clinic equipped both with PET/CT and SPECT/CT, allows PET diagnostics also with ultra short lived tracers such as ^{11}C , ^{13}N , and ^{15}O . The design of the microPET unit will also be able to use the same radionuclides. All units are directed under the systems of GMP, good automated manufacturing practice, good practice of control laboratories and GLP, and the quality management system of the company is built under the umbrella of the ISO 9001:2000 standard.

1. EQUIPMENT

1.1. Cyclotron Cyclone 18/9

For production of short lived PET radionuclides, the cyclotron Cyclone 18/9 (IBA, Belgium) is used. It accelerates negative H^- ions to a fixed energy of 18 MeV and D^- ions to 9 MeV with beam intensities up to 80 μA for protons and 40 μA for deuterons. The construction of the cyclotron also allows simultaneous dual target bombardment. The independent exit ports allow installation of up to eight targets. At present there are six targets and one external beam line installed and one external beam target equipped with COSTIS (IBA) solid targetry.

Targets installed on the cyclotron are all of IBA design and comprise:

- Three liquid targets with a niobium and silver body, two of them for $^{18}F^-$ and the third for $^{13}NH_3$ production;
- Three gaseous targets for $^{11}CO_2$, $^{15}O_2$ and $^{18}F_2$ production; and
- An external beam target COSTIS (compact solid target irradiation system).

The radionuclide transportation system consists of Teflon capillary for $^{18}F^-$, metal tubes for ^{11}C and $^{18}F_2$, and a pneumatic switching box (SAS unit, Tema Sinergie) for automatic transport line selection to hot cells. The automatic control system based on programmable logic control allows fully automatic radionuclide production (target filling, irradiation and transport to the hot cells).

COSTIS is especially designed for irradiation of solid targets using helium cooling of the targets on the front side. The external beam line allows research and development of new target configurations and offers the new possibility for radionuclide production suitable for medical application. The system has been chosen for pilot production of the SPECT compatible PET radionuclides in the laboratory (IAEA grant SLR/2/2002).

1.2. Production of radiopharmaceuticals

The production and quality control of radiopharmaceuticals are in accordance with principles of current good manufacturing practice. All the equipment was qualified to be manufactured at a plant which met ISO 9001:2000, EN 45014, Pharmaceutical Inspection Convention and GALP standards.

SESSION 5

Manufacture takes place in a 40 m² clean room of class C with class D auxiliary rooms. The production area includes six 70 mm lead shielded boxes (SMC1/70 and SMC2/70 (Tema Sinergie)) for housing the synthesis modules (GE Medical Systems):

- TracerLab FX_{FDG} and TracerLab MX_{FDG} modules for the nucleophilic synthesis of 2-[¹⁸F] fluoro-deoxyglucose (¹⁸F- FDG) radiopharmaceutical;
- TracerLab FX_{DOPA} for electrophilic [¹⁸F]DOPA synthesis;
- A dry methylation module, TracerLab FX_C, for preparation of [¹¹C] methyl iodide precursor and synthetic reactor with HPLC separation possibility;
- Further boxes are designed for [¹³N]NH₃ and [¹⁵O]H₂O production.

For manual dispensing of short lived PET (¹¹C) radiopharmaceuticals a laminar shielded box NMC1/70 is available equipped with a DDS-A (Tema Sinergie) filling station for FDG in syringes.

A new type of automatic dispensing unit (DDS-V) in a shielded isolator DMC 2/70 with a LaCalhén (now Central Research Laboratories) double door sealed transfer system and hydrogen peroxide vapour sterilization was developed by Tema Sinergie for dispensing the thermally labile radiopharmaceuticals under aseptic conditions.

Dispensing unit DDS-V is used as a fully automatic filling station for FDG in vials which grants radiological protection to operators and preserves sterility of the product. A single use sterile kit allows for safe operation and avoids product contamination. The integrity of the filter is checked after the filling of vials by determination of the bubble point (Palltronic). The equipment is based on an accurate peristaltic pump and ionization chamber dose calibrators CRC 15 PET (Capintec, Inc.), whose operation is controlled by PC. The automatic dose drawing station allows for safe and quick drawing of a dose of FDG into a vial without any intervention of the operator; it can load batches of radiopharmaceutical both directly from a synthesis module and from a lead shielded vial.

Auxiliary equipment includes a hydrogen peroxide vapour generator VHP 100P (Steris), purified water production, 'pass through' washing and sterilizer units. All equipment installed under IQ, OQ and PQ qualification was completely validated for radiopharmaceutical production.

2. MANUFACTURING ENVIRONMENT

The manufacturing environment is critical for product quality and many parameters are controlled:

- Temperature;
- Humidity;
- Overpressure of production rooms and under pressure in hot cells;
- Air movement;
- Microbial contamination;
- Particulate contamination.

The air handling system was designed to protect contamination from environment operators and cross-contamination of the product with adequate, validated cleaning procedures, appropriate levels of protection of product and correct air pressure cascade. Appropriate dress (type of clothing, proper changing rooms), validated sanitation and adequate transfer procedures for materials and personnel were designed with maximum care. Filtered air entering to the production room is 100% exhausted and three stage filtration (G4, F9, H14 filters) produces an air suitable for a class C room. The temperature in the production room is kept to $23 \pm 2^{\circ}\text{C}$, humidity is $45 \pm 15\%$ and overpressure in the operator room 20 ± 5 Pa. The data are continually measured and stored in the central control system to judge their adequacy with respect to good manufacturing practice. The entire preparatory work is done in class C auxiliary rooms in a class A laminar microbiological box.

3. QUALITY CONTROL LABORATORY

A quality control laboratory has been built in accordance with the principles of good practice for control laboratories and provided with the following analytical instruments:

- Gas chromatograph (Perkin Elmer) with flame ion, thermal conductivity and radiometric detectors;
- High performance liquid chromatographs with refractive index, radiometric, electrochemical and fluorescence detectors (Perkin Elmer, Raytest);
- Thin layer chromatography scanner (Bioscan);
- Gamma spectrometer and dose calibrators (Canberra Packard);
- Bacterial endotoxins LAL test (Pyroquant Diagnostik); and
- UV-VIS spectrometer (Perkin Elmer).

SESSION 5

The data are collected in the Laboratory Information and Managing System and transferred to the analytical certificate of the radiopharmaceutical.

4. INFORMATION SYSTEM

The information system for radiopharmaceuticals was developed with up to date software according to the recommendation of 21 CFR Part 11 (electronic signature) and validated according to the principle of GAMP 4. It is an integrated IT system and data from all equipment used for production are integrated to the system as well as data from environmental monitoring. The system is installed on a server and files are fully protected. No users can access the system without an administrator giving them access. Every change in the field is time, date and user ID stamped. Records of all steps during preparation have an electronic signature. The system creates final protocols and electronic batch records from the production.

5. RESEARCH AND DEVELOPMENT

The radiopharmaceutical research and development laboratory is equipped with two shielded chamber mini-cells (Hans Wälischmiller) for a synthesis module, and a HWM dispensing cell for an automatic dispensing module.

A liquid chromatograph–mass spectrometric system, LC-MS (Agilent 1100) with PET radiometric detector (Canberra Packard), is dedicated to the precursors and radiopharmaceutical analysis. The laboratory also includes a laminar shielded box, cooled high speed centrifuge, lyophilizer, ultra pure water production unit, batch calibrator and other laboratory equipment.

6. THE PRESENT STATE

Technical tests and operation qualification of manufacturing facilities were performed. Standard operation procedures and personnel training were accomplished.

Validated production of [^{18}F] FDG according to current good manufacturing practice in the module Tracerlab MX was performed and documented.

The synthesis modules for [^{18}F]FDG, [^{18}F]DOPA and [^{11}C]methyl iodide were installed and qualified.

A microPET unit for PET radiopharmaceutical testing was installed at the Institute of Experimental Endocrinology of the Slovak Academy of Sciences.

External audit of the Institute of Nuclear Physics of the Academy of Sciences of the Czech Republic was passed as a condition of FDG manufacturing by BIONT a.s. under its registration for FDG radiopharmaceuticals in Slovakia and the Czech Republic.

Pharmaceutical inspection by the Slovak State Drug Control Institute for the good manufacturing practice certificate is under way, and a licence from the Slovak Ministry of Health for drug production is expected.

Studies of the chemical and radiation stability of FDG using the LC-MS system were published and continue to be used in the development of quality control of FDG.

Research on ^{124}I and $^{94\text{m}}\text{Tc}$ production using Cyclone 18/9 solid targetry was launched.

7. CONCLUSION

BIONT a.s. is a new centre for PET radiopharmaceutical production in Slovakia. All its facilities represent state of the art technology for research and radionuclide production. The centre is able to produce enough PET radiopharmaceuticals to supply all Slovak hospitals equipped with PET scanners or SPECT coincidence detectors and to the hospitals close enough to our centre in neighbouring regions of Austria, the Czech Republic, Hungary and Poland.

CAPACITIES AND CURRENT ACTIVITIES OF THE CYCLOTRON AND NUCLEAR MEDICINE DEPARTMENT AT NRCAM

K.K. MOGHADDAM

Cyclotron and Nuclear Medicine Department,
Nuclear Research Center for Agriculture and Medicine (NRCAM),
Karaj, Islamic Republic of Iran
Email: kkamali@nrcam.org

Abstract

The Cyclotron and Nuclear Medicine Department at the Nuclear Research Center for Agriculture and Medicine (NRCAM) has a cyclotron accelerator (model Cyclone 30) which is a fixed frequency, dual beam extraction system with capabilities to produce a proton beam in the 15–30 MeV energy range, and a deuteron beam in the 7–15 MeV range, with maximum output currents of 350 μA and 150 μA respectively. This department consists of laboratories and sections such as: electrochemical, inorganic chemistry, labelling, radioisotope production hot laboratories, quality control, nuclear medicine, etc. Accordingly, the department is capable of producing various radioisotopes and radiopharmaceuticals, conforming, in terms of quality and quantity, to international standards. The widely used products in nuclear medicine manufactured at the facility include ^{201}Tl , ^{67}Ga , $^{81\text{m}}\text{Kr}$, ^{111}In , ^{18}F FDG, ^{123}I , ^{103}Pd and ^{57}Co . Of these radioisotopes and radiopharmaceuticals, ^{201}Tl , ^{67}Ga , and $^{81\text{m}}\text{Kr}$ are produced routinely every week and sent to about 35 hospitals and nuclear medicine centres around the country. In order to gain knowledge in the routine production of ^{103}Pd and ^{57}Co radioisotopes, an IAEA technical cooperation programme was initiated (IRA/04/032). There are also some new IAEA technical cooperation projects under consideration. The production of ^{123}I by the new technique of bombarding the ^{123}Te isotope with protons and gaining knowledge of producing the seed form of ^{103}Pd for use in brachytherapy are some of these new suggested technical cooperation projects. With regard to international safety principles, radiation protection and environmental protection rules, this department aims to choose the quality management standard system ISO 9001-2000 for its radiopharmaceutical production. The paper introduces the cyclotron and nuclear medicine department at NRCAM, its facilities, current activities and future goals, as well as demonstrating the indigenous capacity to produce radiopharmaceuticals.

1. INTRODUCTION

The Atomic Energy Organization of Iran established a research centre for the application of nuclear techniques in agriculture and medicine in 1986. This centre was allocated a 104 hectare site at Karaj, 40 km west of Tehran. The cyclotron project for producing radioisotopes along with research and development in the field of nuclear physics was approved in 1992. Related buildings and their associated laboratories with 5000 m² of infrastructure were constructed. Eventually the Cyclotron and Nuclear Medicine Department (CNMD) was established and started work in 1995. The main part of this department is a cyclotron accelerator (Cyclone 30), which has been installed at the site by IBA of Belgium.

This cyclotron is a fixed frequency, dual beam extraction system which was designed as a negative ion accelerator for ease of beam extraction and for its lower levels of harmful radiation. This accelerator has the capability to produce proton beams with output energy ranging from 15 to 30 MeV and a maximum current of 350 μ A, as well as deuteron beams with output energy ranging from 7.5 to 15 MeV and a maximum current of 150 μ A [1].

2. INFRASTRUCTURE OF THE CNMD

2.1. Facilities

This department consists of laboratories and sections such as: electro-chemical, labelling, inorganic chemistry, gamma spectroscopy, quality control, biological and bacterial control, radioisotope production hot laboratories, PET chemicals, ^{81m}Kr radioisotope production and nuclear medicine (which has a coincidence dual head SPECT system). Figure 1 shows the schematic diagram of this department and its facilities.

2.2. Scientific staff

At the present time (2005) the scientific staff working at the CNMD number around 30. This consists of 10 PhDs (two nuclear technologists, two nuclear engineers, one chemical engineer, one biochemist, one nuclear pharmacist, two pharmacists and one nuclear medicine), 8 M.Sc.s (two nuclear engineers, one analytical chemist, one medical physicist, one robotic, one electronic, one telecommunication and one medical radiation engineer) and 7 B.Sc.s with experience in physics, chemistry, electronics, radiology and

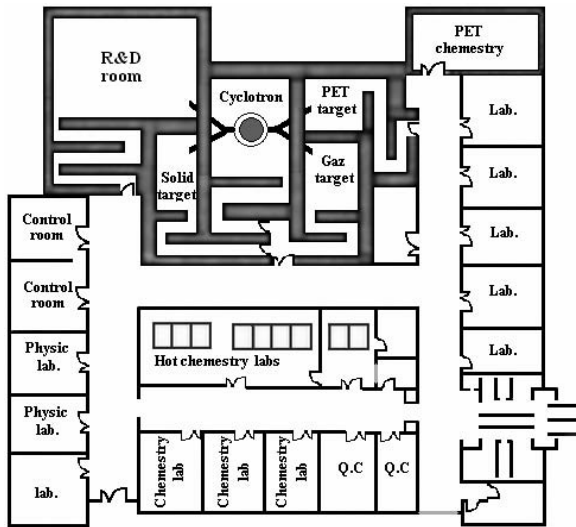


FIG. 1. Schematic diagram of the CNMD.

mechanics. In addition, 5 experienced technicians provide assistance to the scientific staff.

2.3. Working groups

In order to achieve the goals of the CNMD, in applied and fundamental research on nuclear physics as well as medical radioisotopes and radiopharmaceuticals production and research using cyclotron accelerator, this department has been divided into working groups and offices according to their related duties. The position and interrelation between these groups and offices are shown in Fig. 2.

3. OVERALL STRATEGY

The CNMD's main overall strategy is to use the beam outlet of the cyclotron accelerator for producing various radioisotopes and radiopharmaceuticals which are important in the field of nuclear medicine. These products, after passing through some standard quality control, will then be ready for use and will be sent to the nuclear medical centres or hospitals around the country for the diagnosis and treatment of various diseases. The second strategy is to

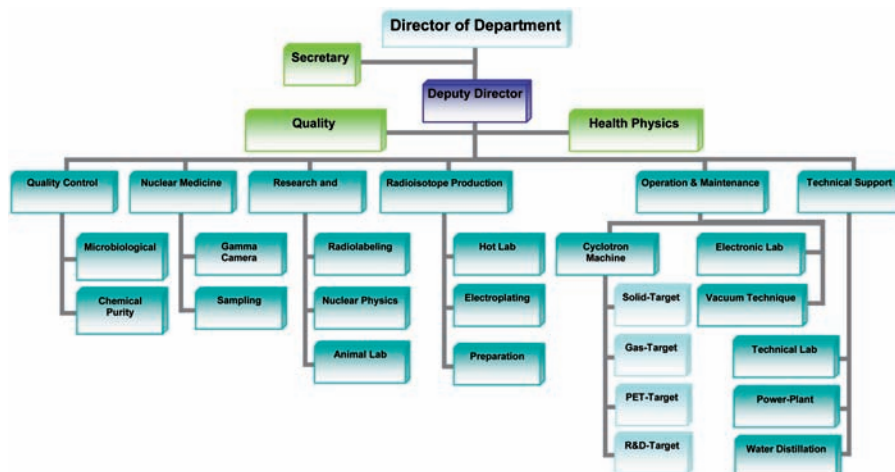


FIG. 2. Organizational chart of the CNMD (groups and offices).

use the outlet beam of the cyclotron accelerator for fundamental and applied research in the field of nuclear physics as well as research on producing new medical radioisotopes or new pharmaceuticals.

4. QUALITY POLICY FOR THE CNMD

At this time, the main activities of the CNMD are the production and research on some of the diagnostic and therapeutic radioisotopes, such as ^{201}Tl , ^{67}Ga , $^{81\text{m}}\text{Kr}$, ^{111}In , ^{18}FDG , ^{103}Pd and ^{123}I , with a quality that is in accordance with international standards.

This department, with due regard for safeguard principles, radiation protection rules and environment protection, and in order to strive for continuous quality improvement and customer satisfaction, has chosen quality management system of ISO9001-2000 as the standard and has committed itself to reach the following principal aims:

- Production of radioisotopes and radiopharmaceuticals in accordance with international standards;
- Research and production of new radioisotopes and radiopharmaceuticals;
- Timely delivery of radiopharmaceuticals;

SESSION 5

- Promoting nuclear physics in the country;
- Promoting joint research projects with universities and research institutions on national and international levels.

In order to reach the above goals, the NRCAM management system has encouraged the efforts, participation and coordination of all employees, as well as promoting employee's scientific qualifications and applying advanced technologies, as well as economizing available resources.

5. CURRENT ACTIVITIES AND PROJECTS

5.1. Routine production radioisotopes and radiopharmaceuticals

At this time, at the CNMD, the most important diagnostic medical radioisotopes and radiopharmaceuticals being produced or awaiting production in the near future, are ^{201}Tl , ^{67}Ga , $^{81\text{m}}\text{Kr}$, ^{111}In , ^{57}Co , ^{18}F FDG, ^{123}I , plus therapeutic radioisotope ^{103}Pd . Of these radioisotopes and radiopharmaceuticals, ^{201}Tl , ^{67}Ga and $^{81\text{m}}\text{Kr}$ are routinely produced and sent weekly to the about 35 hospitals or nuclear medicine centres around the country. If merited by customer demand, ^{111}In and ^{57}Co radioisotopes can also be produced. The specification and medical application of these routinely produced radioisotopes or radiopharmaceuticals are shown in Table 1.

TABLE 1. ROUTINELY PRODUCED RADIOISOTOPES AND RADIO-PHARMACEUTICALS AT CNMD

Radionuclide	Medical application	Specification	Chemical form	Half-life
Thallium-201	Heart disease	Colourless, sterile, isotonic pH5-7, 37 MBq/mL	Thallium chloride (injection)	73.5 h
Gallium	Tumours and inflammation	Colourless, sterile, isotonic pH6-8, 37 MBq/mL	Gallium citrate (injection)	67.5 h
Krypton-81m	Lung disease (ventilation/perfusion)	($^{81\text{m}}\text{Kr}/^{81}\text{Rb}$) generator	Gaseous	$^{81\text{m}}\text{Kr}$: 3.3 s ^{81}Rb : 4.6 h

Total production of these routinely produced radioisotopes and radiopharmaceuticals at the CNMD during the past 5 years (2000–2004) is shown in Fig. 3 [2].

5.2. Working potentials

With respect to the facilities and scientific staffs at CNMD, besides the production of radioisotopes and radiopharmaceuticals, there exists the capability to undertake other activities such as:

- Quality control of new radiopharmaceuticals, including radionuclide purity, radiochemical and chemical purity, microbiological purity (sterility, pyrogen), pH and isotonicity;
- Analysis of radiopharmaceutical samples with TLC, HPLC, IR, RTLC, electrophoresis, UV and gamma spectroscopy techniques;
- Bombarding of various samples with 15–30 MeV proton beam as well as 7.5–15 MeV deuteron beam, according to customer demands;
- Testing the effect of new radiopharmaceuticals on animals;
- Gamma imaging using SPECT for different parts or organs of the human body which had previously undergone treatment with radiopharmaceuticals as well as PET radiopharmaceuticals (such as FDG), using the dual head gamma camera with coincidence system (model: DST-XL, SMV);
- Designing and fabricating various kind of solid, liquid or gaseous targets to produce new radioisotopes, using cyclotron outlet beams;
- Producing a neutron beam (which can be used in new projects) by proton bombardment of targets such as beryllium or deuterium.

5.3. Research projects

The most important approved research projects in the field of nuclear medicine or nuclear physics which are now in progress at CNMD are as follows:

- Production and quality control of [^{18}F]FDG;
- Development of ^{111}In radiopharmaceutical production;
- Design and construction of ^{103}Pd production system;
- Design and construction of a system for production of ^{123}I radioisotope using enriched ^{124}X gas target technology;
- Design and construction of the targets for the production of ^{11}C ;
- Technical design and provision of subordinate cyclotron systems;

SESSION 5

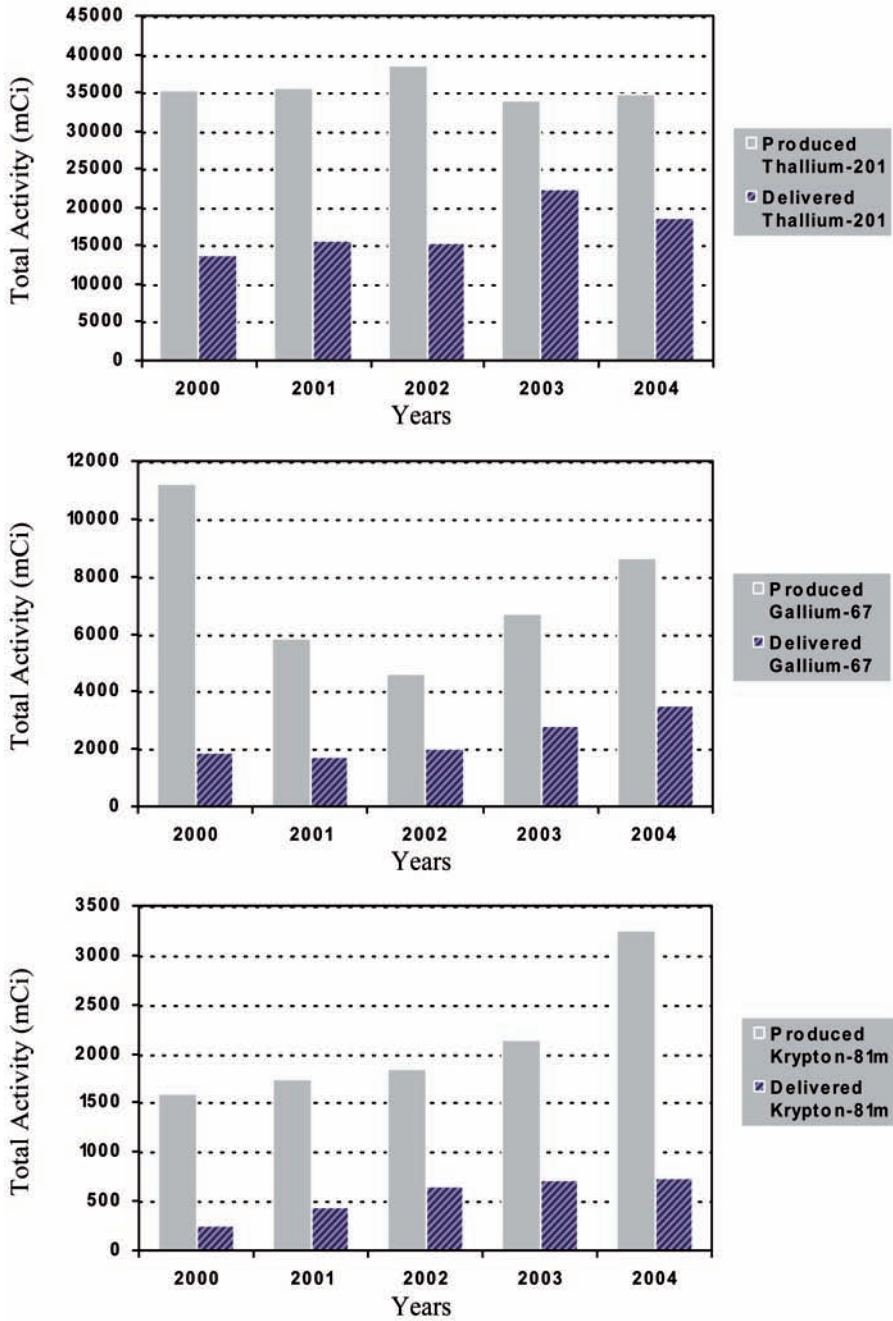


FIG. 3. Total production of ^{201}Tl , ^{67}Ga and $^{81\text{m}}\text{Kr}$ during the period 2000–2004.

- Presenting an improved radiochemical method for FDG to increase the yield, decreasing the synthesis time and its quality control;
- Introduction of an optimum method for radiochemical separation of ^{67}Ga ;
- Production of ^{18}F -FTHA radiopharmaceutical for diagnostic purposes;
- Labelling of proteins with radioactive fluorine and iodine;
- Labelling of chitosan with ^{67}Ga , quality control of the product and investigation of distribution and therapeutic effect on the cancerous tissues of mice by administering directly to the lesion;
- Preparation of MIBG kit labelled with ^{123}I ;
- Feasibly study of solid target coating with gold;
- Radiation protection optimization in NRCAM cyclotron department;
- Measurement of neutron spectrum produced from ^{203}Tl target bombarded by proton, using scintillation detector NE-213;
- Production and quality control of ^{64}Cu Pyruvaldehyde-bis-(N^4 -methylthio-semicarbazone) for PET and targeted therapy applications;
- Production and quality control of ^{66}Ga for PET applications and preparation of ^{66}Ga]citrate, ^{66}Ga]-DOTA-HIgG, ^{66}Ga]oxine and ^{66}Ga]bleomycin labelled compounds;
- Design and fabrication of prototype standard sealed point sources and plastic vials using ^{57}Co radioisotope produced in the CNMD;
- Design and construction of heavy concrete and borated concrete for gamma and neutron shields;
- Analysis and performance improvement of cyclotron Tl and FDG target rooms' shielding;
- Dosimetric parameters determination of the first model of ^{103}Pd seed produced in NRCAM.

5.4. Published papers

Over the years, the scientific staff at the CNMD, according to their research activities and the results achieved from them, have prepared and submitted articles and papers for presentation at various national and international conferences and publication in journals around the world. Some of the most important of these papers which have been recently published in international journals (ISI degree) are as follows:

JALILIAN, A.R., et al., Radiosynthesis of ^{75}Se]5-ethyl 4-methyl 1,2,3-selenadiazoles, *J. App. Radiat. Isot.* **60** (2004) 659–663.

SESSION 5

MOGHADDAM, K.K., NASSERI, M.M., Recognition of internal structure of unknown objects with simultaneous neutron and gamma radiography, *J. Appl. Radiat. Isot.* **61** (2004) 461–464.

JALILIAN, A.R., et al., Preparation of [⁶⁶Ga]Blomycin complex as a possible PET radiopharmaceutical, *J. Radioanal. Nucl. Chem.* **264** (2005) 617–621.

JALILIAN, A.R., SARDARI, S., SARDARI, D., Application of radioisotopes in antifungal research and fungal diseases studies, *J. Curr. Med. Chem. Anti-Infective Agents* **3** (2004) 325–337.

JALILIAN, A.R., et al., Radiosynthesis of [¹⁸F]-5-[2-(2-chlorophenoxy)phenyl]-1,3,4-oxadiazole-2-yl-4-fluorobenzoate a labeled for benzodiazepine receptors, *J. Radioanal. Nucl. Chem.* **260** 20 (2004) 373–377.

SADEGHI, M., et al., Thick rhodium electrodeposition on copper backing as the target for production of palladium-103, *J. Radioanal. Nucl. Chem.* **262** 3 (2004) 665–672.

SADEGHI, M., VAN DEN WINKEL, P., AFARIDEH, H., HAJI-SAEID, M., Crack-free, thick rhodium deposition on copper substrate using sulfate bath (Rhodex solution), *J. Radioanal. Nucl. Chem.* **265** 3 (2005) 455–458.

ROSHANFARZAD, P., JALILIAN, A.R., SABET, M., Production and quality control of ⁶⁵Zn radionuclide, *J. Nukleonika* **50** (2005) 97–103.

JALILIAN, A.R., et al., Development of ¹¹¹In-DTPA-human polyclonal antibody complex for the long-term, *J. Nukleonika* **50** (2005) 91–96.

5.5. Projects in cooperation with the IAEA

In the CNMD there are also some recent/current TC and CRP research projects which have the cooperation and support of the IAEA. The names of these projects are as follows:

Production of Palladium-103 and Cobalt-57 (IAEA TC project (code no.: IR/04/032));

Development and quality control of in-house radiopharmaceuticals for infection in HIV/AIDS positive patients (IAEA CRP, code no.: 324-E1-RC-978-1 (started September 2004));

Development and enhancement of radiopharmaceuticals in accordance with GMP (good manufacturing practice) (IAEA TC project, code no.: IRA/2/007).

In addition to these, a regional training course was conducted in 2004 under the TC project (code no. IRA/2/007) entitled GMP in Cyclotron-Produced Radiopharmaceuticals. Twenty trainees from the Islamic Republic of Iran, Kazakhstan, Saudi Arabia and the Syrian Arab Republic participated in this training course.

6. FUTURE GOALS

In accordance to the existing facilities and scientific staff capabilities at CNMD, it was considered important to gain knowledge of the routine production of at least one new medical radioisotope or radiopharmaceutical each year, up to the 2010. In 2005, the projects for routine production of ^{18}F FDG, ^{123}I and ^{103}Pd radioisotopes and radiopharmaceuticals were finished.

^{18}F FDG is the most well-known radiopharmaceutical used in the PET technique for oncology and cardiology. Iodine-123 is another widely used radioisotope which is going to replace ^{131}I in nuclear medicine centres because of its better characteristics in the diagnosis of thyroid diseases, such as its shorter half-life, no unwanted beta ray emission dose to the patients, better energy of gamma ray emission for taking image with gamma camera, etc. Palladium-103 is also a famous radioisotope which has been used recently to treat some diseases such as prostate cancer by the brachytherapy technique.

In addition to the activities and projects mentioned above, the following future aims and goals for defining new research projects as well as starting new activities are progressing. These new activities or research projects first of all are defined in order to improve the working condition of previous ones, such as increasing the radiopharmaceuticals production efficiency, increasing radiation protection safety standards, optimizing the recovery process for raw radioisotope material, etc. Furthermore, they are defined in order to produce new useful medical radioisotopes or radiopharmaceuticals as well as trying to produce neutron beams and therefore start a new research project in the field of nuclear physics or using the neutron beam for some nuclear application such as neutron activation analysis or neutron radiography. Planned projects include:

- Design and construction of a system for producing ^{123}I through $^{123}\text{Te}(p,n)^{123}\text{I}$ reaction;

SESSION 5

- Producing ^{103}Pd in the form of seed for malignant tumour treatment using the brachytherapy technique;
- Producing a neutron beam by bombarding a beryllium or deuterium target with a proton beam;
- Design and construction of a neutron activation analysis system for material analysis;
- Design and construction of a neutron radiography system;
- Research on producing new radioisotopes for use in PET such as ^{13}N and ^{15}O ;
- Research and development for increasing the production efficiency of ^{201}Tl , ^{67}Ga , $^{81}\text{Rb}/^{81\text{m}}\text{Kr}$ and ^{111}In radioisotopes in order to be able to cater for increased domestic demand in the near future.

REFERENCES

- [1] ION BEAM APPLICATIONS CO., Cyclone-30-CI cyclotron accelerator, Technical Manual, IBA, Belgium (1995).
- [2] CYCLOTRON & NUCLEAR MEDICINE DEPARTMENT (CNMD), Annual reports, NRCAM, AEOI, Karaj (2001–2005).

REACTOR BASED RADIONUCLIDES
AND GENERATORS

(Session 6)

Chairpersons

M. JEHANGIR

Pakistan

R. MIKOLAJCZAK

Poland

PRODUCTION OF THERAPEUTIC RADIONUCLIDES IN MEDIUM FLUX RESEARCH REACTORS

M. VENKATESH, S. CHAKRABORTY

Radiopharmaceuticals Division,
Bhabha Atomic Research Centre,
Mumbai, India

Email: meerav@apsara.barc.ernet.in

Abstract

Therapeutic applications of radionuclides have been growing rapidly. Several potential therapeutic radionuclides offer a choice of optimal therapeutic effect for varied situations. However, the feasibility for production of these isotopes dictates their use in practice. Most radionuclides used in vivo for therapy are β^- emitters produced in nuclear research reactors. Neutron flux (ϕ) plays an important role in determining the feasibility of production of the desired nuclide. Internationally, of the research reactors (~54) used for radioisotope production, only a few (7) have high flux ($>5 \times 10^{14} \text{ n}\cdot\text{cm}^{-2}\cdot\text{s}^{-1}$) capabilities while most (26) are of medium flux ($1-5 \times 10^{14} \text{ n}\cdot\text{cm}^{-2}\cdot\text{s}^{-1}$). Apart from ϕ , the production reaction, the cross-section for neutron absorption (σ), the natural abundance of the target nuclide are also important parameters that influence the production feasibility while the amounts and the specific activities needed play a vital role in the utility of the isotope produced. Nuclides such as ^{177}Lu can be produced in large amounts in moderate flux reactors owing to high σ . In some cases (e.g. ^{177}Lu , ^{153}Sm), capture of epithermal/fast neutrons could significantly enhance the yields and specific activities. No carrier added grade radionuclides could be obtained from indirect reactions such as neutron capture followed by emission of charged particles (e.g. ^{32}P), decay such as beta (e.g. ^{131}I) or EC (e.g. ^{125}I) or fission (e.g. $^{90}\text{Y}/^{90}\text{Sr}$). However, one should be wary of the needs for extensive chemical separations and possible concomitant production of radionuclidic impurities. The use of enriched targets has helped in certain cases to obtain large amounts of high specific activity products and in some cases helps to prevent co-produced radionuclidic impurities (e.g. ^{175}Yb). Several radionuclides suitable for a variety of situations can be successfully produced in moderate flux reactors. Among these, a fresh approach could enable use of nuclides such as ^{142}Pr , ^{170}Tm and therapy using mixed nuclides such as ^{186}Re and ^{188}Re .

1. INTRODUCTION

The application of radiation and radioisotopes in medicine is as old as the discovery of radiation itself and in the past century this field has developed

steadily into several specialist fields in medicine such as radiation oncology, diagnostic nuclear medicine, therapeutic nuclear medicine, diagnostic in vitro radiometric techniques and radiation processing of medical products. However, these specialist areas have grown at different rates, reaching milestones at different times. Therapeutic radiopharmaceuticals, the beginning of which could be considered to be the use of ^{131}I and ^{32}P in the late 1940s for the treatment of thyroid cancers/hyperthyroidism and polycythemia vera respectively, have registered a steady and rapid growth in the past 10–15 years. The availability of newer specific targeting molecules and the feasibility of producing radionuclides with optimal nuclear characteristics for various applications are major causes of this upward trend. Therapeutic effect in radiopharmaceuticals is achieved by the high LET radiations such as α , β^- , e^- (Auger or Coster-Kronig or conversion). Most of the therapeutic radiopharmaceuticals employ β^- emitters, which are generally neutron rich and are produced in nuclear research reactors. However, a small abundance of low energy (80–200 keV) gammas are preferred for dosimetric calculations and imaging the localization of the radiopharmaceutical. Among the parameters that govern the production feasibility of an isotope, the neutron flux is an important one. Internationally there are about 54 research reactors producing radioisotopes, of which 21 have $\phi < 10^{14} \text{ n}\cdot\text{cm}^{-2}\cdot\text{s}^{-1}$, 26 have $\phi \sim 1\text{--}5 \times 10^{14} \text{ n}\cdot\text{cm}^{-2}\cdot\text{s}^{-1}$ and 7 high flux reactors with $\phi > 5 \times 10^{14} \text{ n}\cdot\text{cm}^{-2}\cdot\text{s}^{-1}$ [1]. Although the list of potential therapeutic radionuclides is very large, those in actual use are much fewer owing to the production logistics and practical limitations. An overview of the therapeutic radionuclides that can be produced in medium flux nuclear research reactors is attempted here.

2. REQUIREMENTS OF RADIONUCLIDES FOR THERAPY

Currently, therapy using radiation and radioisotopes can be considered to be effected by teletherapy, brachytherapy and in vivo application of radiopharmaceuticals. While teletherapy, the oldest and most widely used modality, most often employs ^{60}Co , brachytherapy is performed using a wider range of nuclides such as ^{137}Cs , ^{192}Ir , ^{103}Pd , ^{106}Ru and ^{125}I . However, a large variety of nuclides are reported to be suitable for in vivo therapeutic radiopharmaceutical applications [2], most of which are for treatment of various kinds of cancers, followed by palliation of skeletal pain due to metastatic cancerous lesions. Treatment of conditions such as hyperthyroidism using radioiodine is a well established and widely used modality and radiation synoviorthesis using radiopharmaceuticals has been practised in some countries for a long time. Apart from these, the applicability of radiation in the form of a radiopharmaceutical

employed via a balloon as in angioplasty, for prevention of restenosis of blood vessels (endovascular radionuclide therapy (EVRT)), has been explored in the past few years. Unlike the diagnostic radionuclide, the requirements for a therapeutic radionuclide will be to a large extent governed by the exact application. Table 1 lists some common applications of therapeutic radiopharmaceuticals.

Therapeutic nuclides, unlike the diagnostic ones, are required to produce the therapeutic effect and hence would need to be administered in adequate quantities, depending on the size of the lesion to be treated. This results in the need for large amounts of therapeutic nuclides. For example, typically 1.11–1.85 GBq (30–50 mCi) of ^{153}Sm or ^{90}Y is used per patient for bone pain palliation or antibody/peptide based therapy which would demand processing of these isotopes at TBq (Ci) levels in the initial stages [10]. Additionally, the short half-lives of most isotopes employed in radiopharmaceuticals augment the quantities required. While the choice of the nuclide depends on the energy of the emitted radiation, the half-life and the desired volume of irradiation, the requirements in terms of quantities and specific activities will depend upon the end use. For example, radiolabelled peptides or antibodies that will have to

TABLE 1. COMMON APPLICATIONS OF THERAPEUTIC RADIOPHARMACEUTICALS

Application	Products currently used (*denotes under trial)	Specific requirements/ comments
Treatment of thyroid cancer; thyrotoxicosis	^{131}I iodide	Very common; high radioactive concentration and large amounts
Pain palliation in skeletal metastasis	$^{89}\text{Sr}^{+2}$, ^{153}Sm -EDTMP, ^{186}Re -HEDP, ^{177}Lu -phosphonate*	Large potential; large amounts may be required
Treatment of cancers of prostate, colon, breast, ovary, non-Hodg. Lym., etc.	^{90}Y , ^{131}I labelled antibodies (CD-20, HLA-DR, TAG72.3, Mucin)	High specific activity and large amounts; multiple doses required
Cancers expressing peptide receptors	$^{177}\text{Lu}/^{90}\text{Y}$ labelled peptides: Lanreotide;, DOTA-TATE; VIP analogues; gastrin; neuropeptides; neurokinin; gastrin; glucagon, etc.	High specific activity and large amounts; multiple doses required
Synoviorthesis	^{90}Y , ^{166}Ho , ^{32}P labelled particles	Increasing utility
EVRT	^{90}Y , ^{166}Ho , $^{188}/^{186}\text{Re}$ based products*	Yet to be established

target the receptors or antigens on the cancer cells will have to be labelled at very high specific activities while preparations such as radiocolloids used in the treatment of liver cancers or for radiation synoviorthesis do not impose such requirements. Thus, ^{90}Y from $^{89}\text{Y}(n,\gamma)^{90}\text{Y}$ can be used in former applications while ^{90}Y -lanreotide for treating somatostatin expressing cancers requires ^{90}Y from the ^{90}Sr - ^{90}Y generator. Hence, in order to consider the production feasibility of an isotope in a reactor, a holistic view of the production routes involved as well as the needs of the specific application with respect to the amounts of activity and the specific activity will need to be taken. Table 2 lists the reactor produced radionuclides that have potential for use in therapy, though this is not exhaustive. The list includes established radionuclides such as ^{60}Co , ^{137}Cs used in teletherapy/brachytherapy, nuclides that may be capable of being produced in reactors but which are predominantly produced in accelerators and a few alpha emitters which are seldom used and are not listed.

From these tables it can be seen that a reasonable range of nuclides is possible to be used for varied purposes. A molecule that will target the DNA of the cancer cell could be labelled with an Auger electron emitter such as ^{125}I . However, a molecule that will barely reach the tumour mass needs to be tagged with a nuclide emitting higher penetrating radiations such as hard betas [7]. Alpha particles with high LET and range of action limited to just a cell, need extremely good targeting strategies for their application. The actual application in real situations, however, is seen to be limited to a few isotopes such as ^{90}Y , ^{131}I , ^{32}P , ^{153}Sm and ^{188}Re owing to practical limitations.

3. FACTORS OF IMPORTANCE

In order to review the utility of medium flux reactors for production of therapeutic radionuclides, several factors need to be considered. The primary considerations arise from the production reaction on neutron capture, namely $N = N_0\sigma\phi(1 - e^{-\lambda t})$; where σ is the neutron absorption cross-section, ϕ is the neutron flux, N_0 the initial number of target nuclei dependent on the isotopic abundance, λ the decay constant of the nuclide and t the time duration of irradiation.

While the intrinsic factors λ and σ are not amenable to changes, ϕ depends on the reactor design and the irradiation position used, which is not very flexible. Duration of irradiation, although flexible, can be varied only within reasonable limits for practical purposes. Target nuclides present in 100% natural abundance such as ^{165}Ho have an inherent advantage over target nuclides present in much smaller proportions.

SESSION 6

TABLE 2. RADIONUCLIDES WITH THERAPEUTIC POTENTIAL

Radionuclide	$T_{1/2}$	Mode of decay	E_{\max} of particle (MeV)	Production route
<i>β^- particle emitters</i>				
^{32}P	14.26 d	β^-	1.71	$^{32}\text{S}(\text{n,p})^{32}\text{P}$
^{47}Sc	3.3 d	β^-, γ	0.44, 0.6	$^{45}\text{Sc}(2(\text{n},\gamma))^{47}\text{Sc}$
^{67}Cu	2.6 d	β^-, γ	0.58	$^{67}\text{Zn}(\text{n,p})^{67}\text{Cu}$
^{89}Sr	50.53 d	β^-	1.49	$^{88}\text{Sr}(\text{n},\gamma)^{89}\text{Sr}$; $^{89}\text{Y}(\text{n,p})^{89}\text{Sr}$
^{90}Y	64.10 h	β^-	2.21	$^{235}\text{U}(\text{n,f})^{90}\text{Sr}(\beta^-)^{90}\text{Y}$ (generator)
^{103}Ru	39.3 d	β^-, γ	0.72, 0.22	$^{235}\text{U}(\text{n,f})^{103}\text{Ru}$
^{106}Ru	1 y	β^-	0.039	$^{235}\text{U}(\text{n,f})^{106}\text{Ru}$
^{109}Pd	13.5 h	β^-, γ	1.027, 0.45	$^{108}\text{Pd}(\text{n},\gamma)^{109}\text{Pd}$
^{105}Rh	35.36 h	β^-, γ	0.57	$^{104}\text{Ru}(\text{n},\gamma)^{105}\text{Ru}(\beta^-)^{105}\text{Rh}$
^{115}Cd	44.6 d	β^-, γ	1.11	$^{114}\text{Cd}(\text{n},\gamma)^{115}\text{Cd}$
^{131}I	8.02 d	β^-, γ	0.97	$^{130}\text{Te}(\text{n},\gamma)^{131}\text{Te}(\beta^-)^{131}\text{I}$
^{153}Sm	1.9 d	β^-, γ	0.81	$^{152}\text{Sm}(\text{n},\gamma)^{153}\text{Sm}$
^{165}Dy	2.3 h	β^-, γ	1.28, 1.19	$^{164}\text{Dy}(\text{n},\gamma)^{165}\text{Dy}$
^{166}Dy	3.4 d	β^-, γ	0.404	$^{164}\text{Dy}(2(\text{n},\gamma))^{166}\text{Dy}$
^{166}Ho	27 h	β^-, γ	1.85	$^{165}\text{Ho}(\text{n},\gamma)^{166}\text{Ho}$
^{169}Er	9.3 d	β^-, γ	0.34	$^{168}\text{Er}(\text{n},\gamma)^{169}\text{Er}$
^{170}Tm	128.6 d	β^-, γ	0.96, 0.88	$^{169}\text{Tm}(\text{n},\gamma)^{170}\text{Tm}$
^{175}Yb	4.18 d	β^-, γ	0.47	$^{174}\text{Yb}(\text{n},\gamma)^{175}\text{Yb}$
^{177}Lu	6.73 d	β^-, γ	0.49	$^{176}\text{Lu}(\text{n},\gamma)^{177}\text{Lu}$
^{186}Re	90.64 h	β^-, γ	1.07	$^{185}\text{Re}(\text{n},\gamma)^{186}\text{Re}$
^{188}Re	17 h	β^-, γ	2.12	$^{187}\text{Re}(\text{n},\gamma)^{188}\text{Re}$ $^{186}\text{W}(2(\text{n},\gamma))^{188}\text{W}(\beta^-)^{188}\text{Re}$ (generator)
^{198}Au	2.7 d	β^-, γ	0.96	$^{197}\text{Au}(\text{n},\gamma)^{198}\text{Au}$
^{199}Au	3.1 d	β^-, γ	0.45, 0.29, 0.24	$^{198}\text{Pt}(\text{n},\gamma)^{199}\text{Pt}(\beta^-)^{199}\text{Au}$
<i>Auger/conversion electron emitters</i>				
^{125}I	60 d	EC	X rays and low energy Auger e^-	$^{124}\text{Xe}(\text{n},\gamma)^{125}\text{Xe}(\text{EC})^{125}\text{I}$
$^{117\text{m}}\text{Sn}$	14 d	IT	126, 129 keV conversion e^-	$^{116}\text{Sn}(\text{n,g})^{117\text{m}}\text{Sn}$; $^{117}\text{Sn}(\text{n}, \text{n})^{117\text{m}}\text{Sn}$
<i>α particle emitters</i>				
^{213}Bi	45.6 m	α (2.1%), β^+ (97.8%)	5.87	^{233}U (several successive decays)

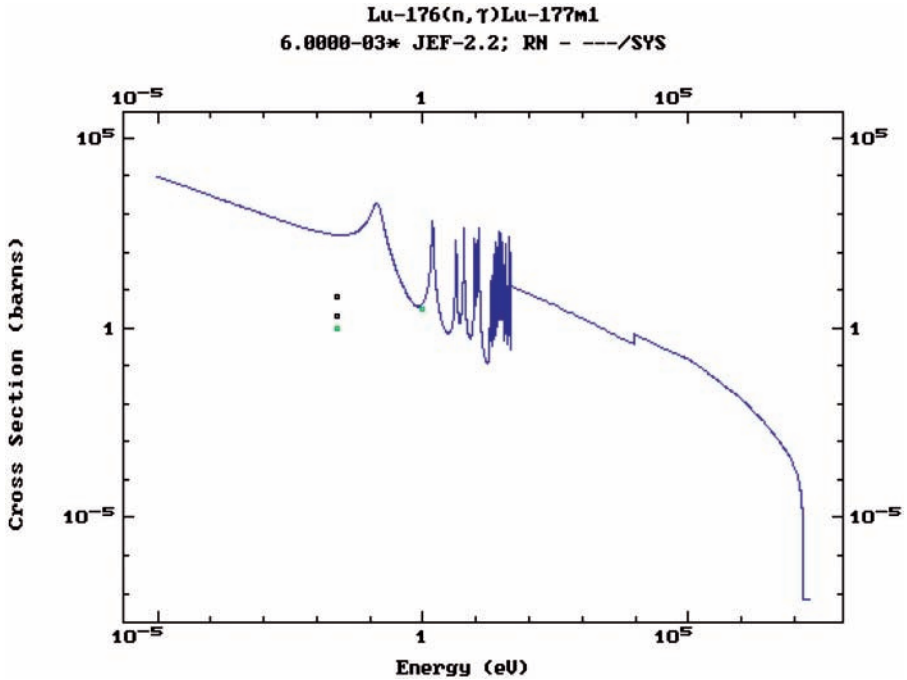


FIG. 1. Neutron absorption cross-section for $^{176}\text{Lu}(n,\gamma)^{177}\text{Lu}$ reaction.

Epithermal and fast neutrons contribute significantly to the production yields and the specific activities in some cases such as ^{153}Sm and ^{177}Lu , owing to the high capture cross-sections in the higher energy regions [11, 12]. Figure 1 shows the capture cross-section of ^{176}Lu for production of ^{177}Lu [13]. If the irradiation position in the reactor provides a flux of thermal as well as higher energy neutrons, the yields for such nuclei could be very high.

It has been the authors' experience that the yields of ^{177}Lu are nearly 2.7 times the theoretical yield with respect to thermal neutron capture alone [12], under various irradiation conditions ($\phi = 1.4 \times 10^{13} - 1 \times 10^{14} \text{ n}\cdot\text{cm}^{-2}\cdot\text{s}^{-1}$; duration of irradiation 7–21 d).

If σ is too small, as in the case of ^{88}Sr (0.0057b), the probability becomes too low, necessitating high flux reactors. The abundance of the target nuclide is another factor that could determine the feasibility of regular production and use of the product nuclide. Radionuclides such as ^{33}P , which may be preferred for certain applications over ^{32}P , suffers from the fact that adequate amounts cannot be produced owing to the low abundance of ^{33}S (0.75%) augmented with very low σ (in mb for fast neutrons) for the (n,p) reaction. Thus, generally, the commonly used radioisotopes originate from targets that are present in

SESSION 6

reasonably large amounts in nature. Use of enriched isotopes is one way to obtain higher yields in both the above situations of low σ and low abundance. Although use of enriched target isotopes can help to augment the production, where their abundances are low the increase is generally not orders of magnitude higher. Additionally, the cost of enriched targets is very high when the natural abundance is low. This would make the process economically unfavourable, except when the unused target atoms can be recovered for reuse. Such recovery is possible when the product nuclide is an element different from the target as in the case of indirect reactions or sequential reactions following neutron capture. However, very careful separation becomes essential in such cases. For example, enriched ^{124}Xe used for production of ^{125}I can be separated and recovered. Similarly, if enriched ^{130}Te is used for preparation of ^{131}I , separation of ^{131}I by dry distillation would leave the target intact in the reaction vessel which can be reused. On the other hand, unused enriched ^{152}Sm used to obtain ^{153}Sm cannot be recovered. Hence, the use of enriched targets will have to be resorted to judiciously. Enriched ^{152}Sm is often used for obtaining high specific activity ^{153}Sm for making bone pain palliation agents. Although high specific activity tracers are not essential for bone pain palliation agents, the limits on the total amount of ligand that can be injected into the patients, in turn, limits the total amount of radiometal that can be used. In some cases, use of enriched target isotopes would be beneficial for avoiding concomitant production of unwanted radionuclides by neutron capture of the co-existing isotopes. For example, in the case of ^{175}Yb , Yb nat. yields $\sim 2.2\text{--}2.6\text{ MBq}/\mu\text{g}$ ^{175}Yb with $^{169}\text{Yb} + ^{177}\text{Lu}$ impurities, while ^{174}Yb 99% yields $\sim 7.4\text{--}9.3\text{ MBq}/\mu\text{g}$ ^{175}Yb of $>99.9\%$ RN purity [14]. In certain other cases, such as ^{186}Re , a well recognized therapeutic radionuclide, moderate flux reactors could be used for its production, if a highly enriched ^{185}Re target is used.

Often in the production of radionuclides, particularly when large amounts and high specific activities are desired, irradiation duration is optimized to obtain maximum yields, referred to as saturation yields. Based on the production equation, as a rule of thumb, irradiation for a duration 3–4 times the $T_{1/2}$ of the product is adhered to. This works well for straight reactions and isotopes such as ^{166}Ho are produced by irradiation for 3–4 d. However, when concomitant production of undesired radionuclides is possible, the duration of irradiation may have to be optimized based on the isotopic composition of the target and the yields of all the isotopes under consideration under the given conditions of irradiation. For example, in the production of ^{125}I by irradiation of Xe gas ($^{124}\text{Xe}(n,\gamma;\text{EC})^{125}\text{I}$), other isotopes of iodine such as ^{126}I and ^{127}I are co-produced due to multiple possibilities. In such cases, the irradiation is carried out for a short time (a few days) to achieve low quantities of ^{126}I in the product [15]. In some cases, where the burnup is high due to high σ , long durations of

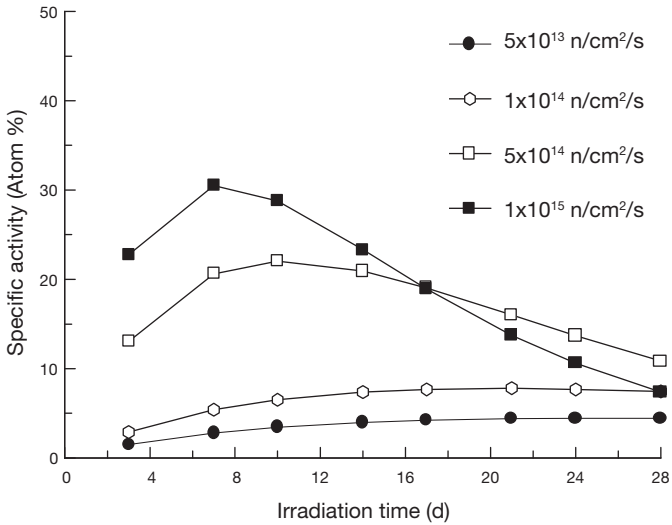


FIG. 2. Buildup of ^{177}Lu activity with duration of irradiation at different neutron flux.

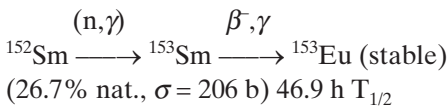
irradiation could be counter-productive, resulting in lower yields. This is depicted in the Fig. 2, where theoretically calculated data for the production of ^{177}Lu by thermal neutron capture is exemplified. However, the actual situation has to be experimentally decided, as factors other than just thermal neutron capture could contribute.

When high specific activity products are required, as in the case of receptor targeting agents, the choice of nuclides that can be used becomes limited, since radiative neutron capture yields radionuclides of the same element, leading to specific activities lower than the maximum possible. A few radionuclides, such as ^{177}Lu , that can be produced by high capture cross-section (n,γ) reactions, however, can still be produced in adequately high specific activities [12]. The route of production of the isotope assumes an important role when high specific activity products are desired. Reactions such as (n,γ) followed by a transmutation leading to a radionuclide of a different element (n,p , and $n,\text{fission}$) have made it possible to obtain isotopes such as ^{131}I , ^{32}P , ^{137}Cs in high specific activities (no carrier added n.c.a. grade), using a moderate flux reactor. At the Bhabha Atomic Research Centre, large amounts of ^{131}I are regularly produced using the $^{130}\text{Te}(n,\gamma; \beta^- \text{ decay})^{131}\text{I}$ route. Radionuclides obtained from a generator, such as $^{90}\text{Sr}/^{90}\text{Y}$ and $^{188}\text{W}/^{188}\text{Re}$ offer the advantages of n.c.a. grade high specific activity products and the possibility for easy multiple use at the hospital radiopharmacy. Despite the absence of a gamma component that could help in dosimetry and imaging, the use of ^{90}Y in many of

the radiolabelled antibodies and peptides for treatment of large lesions is due to such logistic advantages. The parent ^{90}Sr can be obtained in large amounts from the fission of ^{235}U . Although enriched ^{235}U is irradiated specifically for production of nuclides by the fission route ($^{235}\text{U}(\text{n},\text{f})^{131}\text{I}; ^{90}\text{Sr}; ^{137}\text{Cs}$), long lived nuclides such as ^{90}Sr ($T_{1/2}$ 28.8 y) and ^{137}Cs ($T_{1/2}$ 30 y) can also be efficiently recovered from the waste from processed irradiated fuel [16]. However, it should be noted that the separation of the desired radionuclide from the others present would be necessary, could be challenging and needs to be carried out very efficiently. Some details and typical data for therapeutic radionuclides that can be produced in moderate flux reactors are given below.

Phosphorus-32: ^{32}P is a widely used, well-established nuclide produced by $^{32}\text{S}(\text{n},\text{p})^{32}\text{P}$ reaction in moderate flux reactors. The role of epithermal and fast neutrons is significant in the production of radionuclides, particularly in threshold reactions. Phosphorus-32 yields from one of the reactors, Cirus ($\phi_{\text{th}} = 1 \times 10^{13} \text{ n}\cdot\text{cm}^{-2}\cdot\text{s}^{-1}$; 2% ϕ_{fast}), are more than twice those of another reactor, Dhruva ($\phi_{\text{th}} = 1 \times 10^{14} \text{ n}\cdot\text{cm}^{-2}\cdot\text{s}^{-1}$; 1% ϕ_{fast}). Typically, on irradiation of 100 g of natural sulphur for 90 d, ^{32}P yields are ~45 GBq (1.2 Ci) in Dhruva and 100 GBq (2.7 Ci) in Cirus.

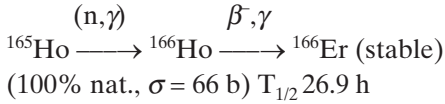
Samarium-153: ^{153}Sm with 46.9 h $T_{1/2}$, 810 keV $E_{\beta\text{-max}}$ and 103 keV (28.3%) γ photon, is also an established useful therapeutic radionuclide for various therapeutic applications. Samarium-153 can be produced in adequate specific activity by irradiating the natural Sm_2O_3 target with acceptable radionuclidic purity. The specific activity and radionuclidic purity could be enhanced further by the use of an enriched $^{152}\text{Sm}_2\text{O}_3$ target if required.



Typically, on a 7 d irradiation at a thermal neutron flux of $3 \times 10^{13} \text{ n}\cdot\text{cm}^{-2}\cdot\text{s}^{-1}$, yields of ^{153}Sm were 11 GBq/mg (300 mCi/mg) with natural targets and ~44 GBq/mg (1200 mCi/mg) with enriched (98% ^{152}Sm) targets. Contribution from epithermal neutrons leads to higher yields. The average levels of radionuclidic impurity burden at 2 d after production are 0.37 kBq (10 nCi) ^{154}Eu , 5.55 kBq (150 nCi) ^{155}Eu and 37 kBq (1 μCi) ^{156}Eu per 37 MBq (1 mCi) of ^{153}Sm in the case of natural Sm target. In the case of 98% ^{152}Sm enriched target, the level of ^{154}Eu was of similar value, while the ^{155}Eu and ^{156}Eu burdens were negligible compared to those for natural targets.

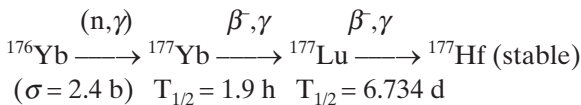
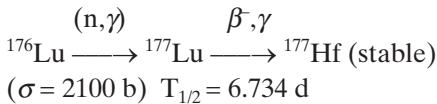
Holmium-166: ^{166}Ho , with 26.9 h $T_{1/2}$, $E_{\beta\text{-max}}$ of 1.85 MeV and 81 keV γ rays (6%), is yet another promising therapeutic radionuclide being used in some countries for treatment and being explored for various therapeutic applications

worldwide. A major advantage of ^{166}Ho is that it can be produced in adequate quantities, in high specific activities and with high radionuclidic purities by irradiating natural Ho targets in reactors with medium thermal neutron flux.



Irradiation of a Ho_2O_3 target at a thermal neutron flux of $3 \times 10^{13} \text{ n}\cdot\text{cm}^{-2}\cdot\text{s}^{-1}$ for 7 d yielded ^{166}Ho with a specific activity of $\sim 7.5 \text{ GBq/mg}$ (200 mCi/mg). The specific activity can easily be enhanced two- to threefold, by carrying out irradiations at positions in the reactor with a higher neutron flux. The formation of $^{166\text{m}}\text{Ho}$ ($T_{1/2} = 1200 \text{ y}$), along with ^{166}Ho , has been cited as one disadvantage. However, the authors' repeated experiments have yielded ^{166}Ho without any detectable contamination with $^{166\text{m}}\text{Ho}$, since the radioactivity due to $^{166\text{m}}\text{Ho}$ produced will be insignificant in short irradiations owing to its very long half-life, although the neutron capture cross-sections are nearly equal.

Lutetium-177: The potential of ^{177}Lu for use in in vivo targeted therapy is well recognized. β^- particles with E_{max} of 497 keV (78.6%), 384 keV (9.1%) and 176 keV (12.2%) offer therapeutic efficacy with a mean tissue penetration of 0.67 mm, while the γ photons of 113 keV (6.4%) and 208 keV (11%) are ideally suited for imaging the in vivo localization. The 6.734 d physical $T_{1/2}$ of ^{177}Lu though is relatively longer than many other therapeutic radionuclides used in radiopharmaceuticals and is comparable to ^{131}I and therefore will be logistically advantageous for supply to distant places. Lutetium-177 can be produced in reactors having moderate to high thermal neutron flux, by two different routes [12, 17]; either by (n,γ) reaction of a Lu_2O_3 (natural 2.6% ^{176}Lu or enriched ^{176}Lu) target or by irradiation of a Yb_2O_3 target followed by radiochemical separation of ^{177}Lu from Yb isotopes.



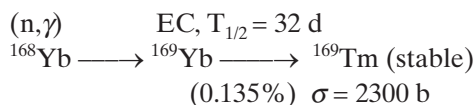
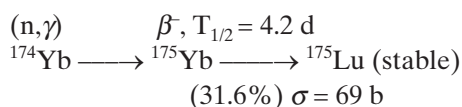
These routes lead to products having different specific activities. Direct (n,γ) activation of natural Lu_2O_3 powder produces low specific activity ^{177}Lu . The specific activity, however, can be enhanced by using a target enriched in

^{176}Lu and by irradiating for an optimal duration. The second route gives high specific activity n.c.a. grade ^{177}Lu . However, in this route, radiochemical separation of ^{177}Lu activity from the irradiated Yb_2O_3 target is crucial because of the radionuclidic purity requirement. In the laboratory, irradiation of a natural Lu (2.6% ^{176}Lu) target at a moderate thermal neutron flux of $3 \times 10^{13} \text{ n}\cdot\text{cm}^{-2}\cdot\text{s}^{-1}$ for 7 d yielded ^{177}Lu with a specific activity of 5.6–6.7 MBq/ μg . This could be used in agents for palliation of bone pain for skeletal metastasis as well as for radiation synovectomy of small/medium joints. On the other hand, by using 64% enriched ^{176}Lu target (cost ~60 times that of natural Lu target) and carrying out irradiations at ϕ of $\sim 9 \times 10^{13} \text{ n}\cdot\text{cm}^{-2}\cdot\text{s}^{-1}$ for 21 d, ^{177}Lu was obtained with a specific activity of ~850 MBq/ μg (~21 atom%), which is quite suitable for receptor specific radiopharmaceuticals for targeted tumour therapy. This could obviate the need for tedious radiochemical separation using a Yb target to obtain high specific activity ^{177}Lu . The radionuclidic purity of ^{177}Lu produced from both natural and enriched targets was ~100% as ascertained by analysing the γ ray spectrum of the irradiated targets after radiochemical processing. It is worthwhile mentioning that there is the possibility of formation of $^{177\text{m}}\text{Lu}$ ($T_{1/2} = 160.5 \text{ d}$; β^- and IT decay) on thermal neutron bombardment of a Lu_2O_3 target. However, the γ ray spectrum of the irradiated Lu target did not show any significant peak corresponding to the photopeaks of $^{177\text{m}}\text{Lu}$. This is expected as the radioactivity due to $^{177\text{m}}\text{Lu}$ produced will be insignificant and below the detectable limit on a 7 d irradiation owing to its long half-life and comparatively low cross-section ($\sigma = 7 \text{ b}$) for its formation. Attempts were made to assay any trace amounts of $^{177\text{m}}\text{Lu}$ activity by recording the γ ray spectrum of a sample aliquot, after complete decay of ^{177}Lu activity showed the presence of trace amounts of $^{177\text{m}}\text{Lu}$. The average level of the radionuclidic impurity burden in ^{177}Lu due to $^{177\text{m}}\text{Lu}$ was found to be 5.5 kBq of $^{177\text{m}}\text{Lu}$ /37 MBq of ^{177}Lu (150 nCi / 1 mCi) at EOB. Since $^{177\text{m}}\text{Lu}$ eventually decays to ^{177}Lu , the desired nuclide, the presence of a small amount (0.015% at EOB) should be acceptable.

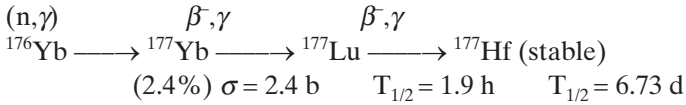
Rhenium-186/187: Both ^{186}Re and ^{188}Re have been used for therapy. Rhenium-186 ($T_{1/2} = 90 \text{ h}$) decays to stable ^{186}Os with the emission of β^- ($E_{\text{max}} = 1.07 \text{ MeV}$), accompanied by 137 keV (9%) γ photon, while ^{188}Re ($T_{1/2} = 16.9 \text{ h}$) decays to stable ^{188}Os with the emission of 2.12 MeV β^- (E_{max}) followed by emission of 155 keV (15%) γ photon. As Re belongs to the same group as Tc, radionuclides of Re are often preferred for therapy owing to their chemical similarity to Tc. The possibility of studying the pharmacokinetics using a Tc labelled molecule, before launching on a Re labelled molecule, has steered many groups to take up Re isotopes for development of radiopharmaceuticals. However, often, Re chemistry is not identical to that of Tc, owing to its tendency to oxidize back to a +7 state.

As mentioned earlier, obtaining ^{188}Re from a $^{188}\text{W}/^{188}\text{Re}$ generator would be ideal, for which ^{188}W ($T_{1/2} = 69.4$ d) will have to be produced by successive neutron capture of a ^{186}W target. This is not feasible in moderate flux reactors. However, irradiation of targets enriched in ^{185}Re and ^{187}Re would yield appreciable amounts of ^{186}Re and ^{188}Re (σ of 110 b and 75 b, respectively). Use of natural Re (37.4% ^{185}Re , 62.6% ^{187}Re) would result in production of both ^{186}Re and ^{188}Re in comparable amounts. In such cases, cooling of the target after irradiation to allow ^{188}Re ($T_{1/2} = 19$ h) to decay would give adequately pure ^{186}Re . Typically, on irradiation of natural Re metal at a thermal neutron flux of $3 \times 10^{13} \text{ n}\cdot\text{cm}^{-2}\cdot\text{s}^{-1}$ for 7 d, 6.7–7.4 GBq/mg of total $^{186/188}\text{Re}$ will be obtained of which 2.7–3.0 GBq/mg will be ^{186}Re . After 7 d cooling for complete decay of ^{188}Re , the specific activity of ^{186}Re will be 670–740 MBq/mg [18], which may be adequate for a pain palliation agent. However, this amounts to uneconomic utilization and unfavourable production logistics. As a result, an enriched ^{185}Re target is used for large scale production of ^{186}Re for therapeutic applications. Typically, on 7d irradiation of 98% ^{185}Re at a thermal neutron flux of $3 \times 10^{13} \text{ n}\cdot\text{cm}^{-2}\cdot\text{s}^{-1}$, ~ 7.34 GBq/mg ^{186}Re can be obtained, which can be used for therapy. However, since both ^{186}Re and ^{188}Re can be used for treating similar sized lesions (5–11 mm maximum tissue range), although their tissue penetration ranges are not close, a strategy to use a mixture of both nuclides may be effective. The dosimetry calculations in this situation would be more involved and complex, but, nevertheless, possible. If treatment with mixed isotopes is accepted, moderate flux reactors could yield high amounts of these isotopes for therapy.

Ytterbium-175: ^{175}Yb too possesses excellent radionuclidic properties, namely a $T_{1/2}$ of 4.185 d, β^- emission (80%) with $E_{\text{max}} = 0.48$ MeV, γ photons of 113 keV (1.9%), 282 keV (3.1%) and 396 keV (6.5%), and is suitable for radiotherapy of small lesions. As in the case of ^{177}Lu , the relatively long half-life of ^{175}Yb is a logistical advantage. Ytterbium-175 can be produced by thermal neutron bombardment of natural ytterbium or a ^{174}Yb enriched target ($\sigma = 69$ b). However, use of a natural ytterbium target results in radionuclidic impurities of ^{169}Yb and ^{177}Lu .



SESSION 6



Of these, ${}^{169}\text{Yb}$ ($T_{1/2} = 32 \text{ d}$) decays by electron capture (100% k electron capture) followed by the emission of Auger electrons of low yield and the principle γ photons are of reasonably low energy (177 keV (22.5%), 197 keV (35.9%)). Hence, it is envisaged that the presence of low amounts of ${}^{169}\text{Yb}$ should not cause any serious problem in the in vivo application of ${}^{175}\text{Yb}$. On the other hand, the presence of ${}^{169}\text{Yb}$ will be useful in extended studies of the pharmacological characteristics of the ${}^{175}\text{Yb}$ labelled radiopharmaceuticals in biological systems. Lutetium-177 is the other radionuclidic impurity, itself a therapeutic radionuclide. The radionuclidic characteristics of ${}^{177}\text{Lu}$ as well as its chemical properties are very similar to those of ${}^{175}\text{Yb}$. Hence, the presence of ${}^{177}\text{Lu}$ in very small quantities in the ${}^{175}\text{Yb}$ produced should not restrict the use of the latter in in vivo therapy.

Typically, on irradiation of a natural Yb target at a thermal neutron flux of $3 \times 10^{13} \text{ n}\cdot\text{cm}^{-2}\cdot\text{s}^{-1}$ for 7 d, 2.2–2.6 MBq/ μg of ${}^{175}\text{Yb}$ was produced to ~95% radionuclidic purity (with ~3% of ${}^{169}\text{Yb}$ and ~2% of ${}^{177}\text{Lu}$). Under the same conditions, 98.6% ${}^{174}\text{Yb}$ enriched Yb yielded ${}^{175}\text{Yb}$ with a specific activity of ~7.5 MBq/ μg and ~100% radionuclidic purity [14].

4. CONCLUSION

Several well-established therapeutic radionuclides can thus be produced in medium flux reactors in adequate quantities and of acceptable specific activity. However, exploration to identify new therapeutic radionuclides continues to satisfy the need for varied uses. A few, such as ${}^{142/143}\text{Pr}$, ${}^{170}\text{Tm}$ and ${}^{141}\text{Ce}$, have the potential to be used in therapy and have been explored for production feasibility in medium flux reactors [19]. Additionally, mixed radionuclide therapy, as in the case of ${}^{186}\text{Re}$ and ${}^{188}\text{Re}$, would merit a fresh appraisal owing to the ease of large scale production in many centres and could open possibilities for production in medium flux reactors.

ACKNOWLEDGEMENTS

The authors are grateful to V. Venugopal, Director, Radiochemistry & Isotope Group, BARC for his support and encouragement for the radioisotope production programme. K.V. Vimalnath, K.C. Jagadeesan and P.V. Joshi, our colleagues, are gratefully acknowledged for their efforts and help in providing the production data for the various radionuclides mentioned in this article.

REFERENCES

- [1] OECD NUCLEAR ENERGY AGENCY, Beneficial Uses and Production of Isotopes, Nuclear Energy Agency, OECD Publication, No. 5293, 2005.
- [2] VOLKERT, W.A., GOECKELER, W.F., EHRHARDT, G.J., KETRING, A.R., Therapeutic radionuclides : Production and decay property considerations, *J. Nucl. Med.* 32 (1991) 174-185.
- [3] NEVES, M., KLING, A., LAMBRECHT, R.M., Radionuclide production for therapeutic radiopharmaceuticals, *Appl. Radiat. Isot.* 57 (2002) 657-664.
- [4] VOLKERT, W.A., HOFFMAN, T.J., Therapeutic radiopharmaceuticals, *Chem. Rev.* 99 (1999) 2269-2292.
- [5] QAIM, S.M., Therapeutic radionuclides and nuclear data, *Radiochim. Acta* 89 (2001) 297-302.
- [6] MIRZADEH, S., MAUSNER, L.F., GARLAND, M.A., "Reactor-produced medical radionuclides", *Radiochemistry and Radiopharmaceutical Chemistry in Life Sciences* (VERTES, A., NAGY, S., KLENCZAR, Z., Eds), 1st edn, Kluwer Academic Publishers, Amsterdam (2003) 1-46.
- [7] Radionuclides for Therapy (Proc. 4th Bottstein Colloquium, 1986) Villeggen, Switzerland, (1986) (SCHUBIGER, P.A., HASLER, P.H., Eds).
- [8] EHRHARDT, G.J., KETRING, A.R., AYRES, L.M., Reactor-produced radionuclides at the University of Missouri Research Reactor, *Appl. Radiat. Isot.* 49 (1998) 295-297.
- [9] CUTLER, C.S., et al., Current and potential therapeutic uses of lanthanide radioisotopes, *Cancer Biotherapy Radiopharm.* 15 (2000) 531-545.
- [10] MAUSNER, L.F., SRIVASTAVA, S.C., Selection of radionuclides for radioimmunotherapy, *Med. Phys.* 20 (1993) 503-509.
- [11] RAMAMOORTHY, N., SARASWATHY, P., DAS, M.K., MEHRA, K.S., ANANTHAKRISHNAN, M., Production logistics and radionuclidic purity aspects of ¹⁵³Sm for radionuclide therapy, *Nucl. Med. Commun.* 23 (2002) 83-89.
- [12] PILLAI, M.R.A., et al., Production logistics of ¹⁷⁷Lu for radionuclide therapy, *Appl. Radiat. Isot.* 59 (2003) 109-118.
- [13] <http://www-nds.iaea.org/ngatlas/>
- [14] CHAKRABORTY, S., et al., Feasibility study for production of ¹⁷⁵Yb: A promising therapeutic radionuclide, *Appl. Radiat. Isot.* 57 (2002) 295-301.

SESSION 6

- [15] MARTINHO, E., NEVES, M.A., FREITAS, M.C., ^{125}I Production: Neutron Irradiation Planning, *Appl. Radiat. Isot.* 10 (1984) 933-938.
- [16] VENKATESH, M., et al., Complexation Studies with ^{90}Y from a Novel ^{90}Sr - ^{90}Y Generator, *Radiochim. Acta* 89 (2001) 1-5.
- [17] LEBEDEV, N.A., NOVGORODOV, A.F., MISIAK, R., BROCKMANN, J., ROSCH, F., Radiochemical separation of no-carrier-added ^{177}Lu as produced via the $^{176}\text{Yb}(n,\gamma)^{177}\text{Yb} \rightarrow ^{177}\text{Lu}$ process, *Appl. Radiat. Isot.* 53 (2000) 421-425.
- [18] UNNI, P.R., KOTHARI, K., PILLAI, M.R.A., Radiochemical Processing of Radionuclides for Targeted Therapy, IAEA-TECDOC-1228 (2001)90-98.
- [19] VIMALNATH, K.V., et al., Prospects and problems in the production of Pr-143 for RNtherapy applications, *Radiochim. Acta* 93(2005)1-8.

THE CONTINUING IMPORTANT ROLE OF HIGH FLUX RESEARCH REACTORS FOR PRODUCTION OF THERAPEUTIC RADIOISOTOPES*

F.F. KNAPP, Jr.*, S. MIRZADEH*, M.A. GARLAND**

*Nuclear Medicine Program
Email: knappffjr@ornl.gov

** Process Engineering Research Group

Nuclear Science and Technology Division,
Oak Ridge National Laboratory,
Oak Ridge, Tennessee,
United States of America

Abstract

Research reactors play a central role for the production of medical radioisotopes for therapeutic applications. Examples produced by ‘direct’ radiative (n,γ) neutron capture with adequate specific activity in modest flux reactors include ^{186}Re and ^{153}Sm for bone pain palliation, and ^{177}Lu for cancer therapy. When adequate specific activity cannot be obtained by radiative capture with modest thermal flux, another strategy employed involves ‘indirect’ production via beta decay of reactor produced parents, where the change in the atomic number permits separation of the product, such as classical production of ^{131}I from decay of ^{131}Tl and no carrier added (n.c.a) ^{177}Lu from decay of reactor produced ^{177}Yb . Research reactors are categorized herein as having ‘high’ flux when the thermal flux ($\text{n}\cdot\text{cm}^{-2}\cdot\text{s}^{-1}$) is $>10^{14}$ and ‘very high’ when the thermal flux $>10^{15}$. Availability of very high thermal flux will provide higher specific activity products and thus higher yields per target mass, also conserving target material and requiring less target volume. Examples of when very high flux is required include production of ^{188}W — for the ^{188}W – ^{188}Re generator system — and $^{117\text{m}}\text{Sn}$, a conversion electron emitter. Very high flux also permits the direct production of high specific activity (70–80 Ci/mg Lu) ^{177}Lu (theoretical value 109 Ci/mg) from highly enriched ^{176}Lu , which is expected to be more cost effective than production/purification via the

* The submitted manuscript was authored by a contractor of the US Government under contract DE-ACO5-00OR22725.

indirect route in modest flux reactors. The indirect production of $^{195\text{m}}\text{Pt}$ — an Auger electron emitter — from ^{193}Ir is only practical at high flux. Thorium-229, the parent of ^{225}Ac for the ^{225}Ac – ^{213}Bi generator — can be produced by irradiation of ^{226}Ra . This route is being evaluated as an alternative source to extraction from ^{233}U . In this paper the unique capabilities of very high flux reactors are reviewed for the production of high specific activity therapeutic radioisotopes which cannot be practically produced in lower flux research reactors.

1. INTRODUCTION

Nuclear reactors continue to play an important role in providing neutron rich radioisotopes for nuclear medicine [1–6]. Many reactor produced radioisotopes thus decay by beta particle emission and are of interest for a variety of routine therapeutic applications in nuclear medicine and oncology. In some cases the decay products from the reactor produced products (i.e. from generator systems) are also used for these applications.

Widely practised clinical applications with therapeutic radioisotopes include cancer therapy, treatment of arthritis (radionuclide synovectomy) and palliation of bone pain resulting from metastases to the skeleton. These routine applications require reliable availability of the required radioisotopes at reasonable costs. The use of both reactor produced gamma and, in particular, beta emitting radioisotopes for the inhibition of arterial restenosis following high pressure balloon angioplasty—primarily for the coronary vessels—has more recently paved the way for use of drug eluting stents.

Radionuclide generators prepared from reactor produced radioisotopes are of particular interest since repeated elution can inexpensively provide many patient doses [7–10]. This aspect is expected to be especially important for providing a source of radioisotopes to remote sites, especially in developing regions, which involve long distances and expensive distribution costs, as has been discussed for the ^{188}W – ^{188}Re and ^{90}Sr – ^{90}Y generators [11]. Therapeutic applications using both unsealed (radiopharmaceuticals for nuclear medicine) and sealed sources (for radiation oncology) are major growth areas in nuclear medicine and oncology. There is thus a rapidly increasing requirement for therapeutic radioisotopes, many of which are reactor produced. The goal of this paper is to review briefly the production of several key reactor produced radioisotopes of current interest in very high flux research reactors. Examples of several key radioisotopes, for which very high thermal flux permits production, include ^{188}W , $^{117\text{m}}\text{Sn}$, $^{195\text{m}}\text{Pt}$ and ^{229}Th . The requirement for other capabilities such as target volume and target handling facilities are issues that also have to be considered.

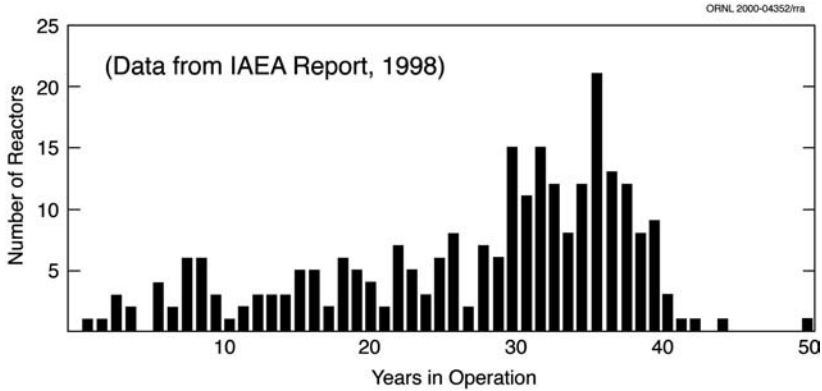


FIG. 1. Summary of years of operation for reactors operating in 1998 (source: IAEA [12]).

2. RESEARCH REACTOR FOR MEDICAL RADIOISOTOPE PRODUCTION

The last IAEA published compilation on research reactors [12] summarized the reactors which were available internationally in 1998 (297), including those used for medical radioisotope production. This information is now available from a convenient IAEA web page found at <http://www.iaea.org/worldatom/rrdb/>. Figure 1 contains data published in the IAEA 1998 report which summarizes the population of research reactors as a function of years of operation, vividly illustrating that many research reactors are in the 20-40 year age range.

More recent data from the IAEA have been combined with the 1998 summary [12] in Fig. 2. While the trend during the growth years 1940–1970 witnessed significantly more reactors being commissioned than being shut down, after 1970 this trend was reversed as the decommissioning of older reactors began. Fortunately, more recent data available from the IAEA for the period 1998–2005 reflect a change in this trend with the number of new reactors under construction/commissioning equal to the number of reactors being decommissioned.

A significant number of research reactors are still operating worldwide and a summary of key ‘high’ and ‘very high’ thermal flux reactors used for medical radioisotope production is described in Table 1. The present status, however, is that many currently operating research reactors are 20–30 years old. In addition, several key reactors have recently been permanently taken out

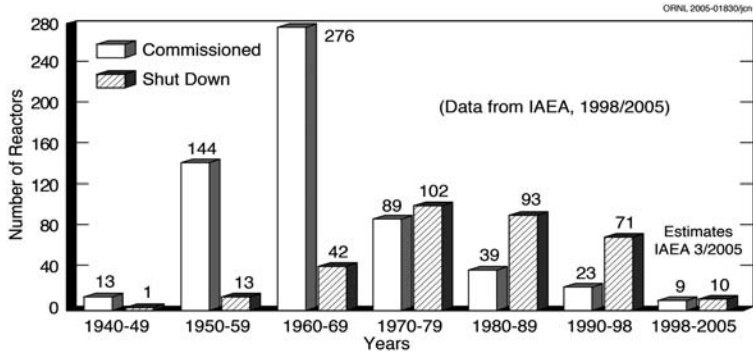


FIG. 2. Summary of reactors commissioned and shut down between 1940 and 2005 (source: IAEA).

of service, including the High Flux Reactor (HFBR, Brookhaven, United States of America), the Fast Flux Test Facility (FFTF, Hanford, USA) and the Studsvik Materials Testing R2 and R2-0 Reactors (Sweden). The data in Table 1 are expressed in an alternative format in Fig. 3, in which recent data provided by the IAEA have been added to the 1998 published data [12] to illustrate the total number of operating research reactors.

Fortunately, data provided by the IAEA database illustrate that several new reactors have either recently been started or are planned for construction in several countries (Table 2).

3. HIGH FLUX REACTOR PRODUCTION OF MEDICAL RADIOISOTOPES

Specific activity is generally proportional to the reactor thermal neutron flux and the thermal neutron capture cross-section. High flux reactors can thus generally produce proportionately higher specific activity products. In the case of fission products, high thermal flux is not required and fission products such as ^{99}Mo and ^{90}Sr (fission product parent of ^{90}Y) can be produced in adequate yields in low or modest flux reactors. The availability of high thermal flux is particularly important when the desired products are produced by multiple neutron capture. In the case of production via two successive neutron captures, the reactor neutron flux is an important factor for this reaction pathway and production values vary as a function of the square of the thermal neutron flux; doubling the flux thus increases the specific activity by a factor of four. Key examples of current interest include ^{188}W produced from irradiation of

SESSION 6

TABLE 1. EXAMPLES OF HIGH/VERY HIGH FLUX RESEARCH REACTORS*

Reactor	Critical	Country	Max. $n\cdot\text{cm}^{-2}\cdot\text{s}^{-1} \times 10^{14}$
Very high flux research reactors			
SM(3)	1961	Dimitrovgrad, Russian Federation	50
HFIR	1965	Oak Ridge, USA	25
BR2	1961	Mol, Belgium	10
High flux research reactors			
MURR	1966	Columbia, USA	6
MARIA	1974	Swierk, Poland	4.5
HANARO	1995	Taejeon, Rep. of Korea	4
NRU	1957	Chalk River, Canada	4
HFR	1965	Petten, Netherlands	2.7

* IAEA data 2005.

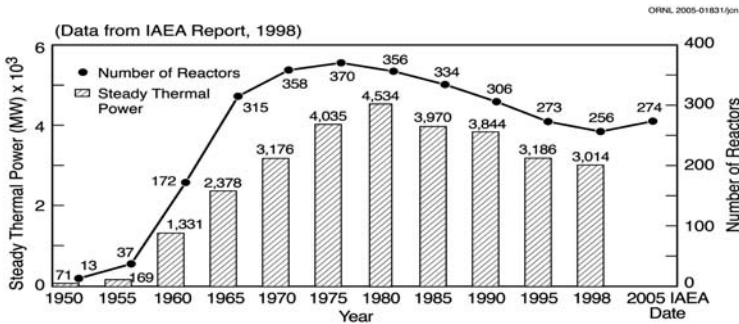


FIG. 3. Summary of reactors operating and steady power levels during the period 1950–2005 (source: IAEA).

enriched ^{186}W by the $^{186}\text{W}(n,\gamma)\text{--}^{187}\text{W}(n,\gamma)\text{--}^{188}\text{W}$ route [13–16] and ^{166}Dy produced from ^{164}Dy , $^{164}\text{Dy}(n,\gamma)\text{--}^{165}\text{Dy}(n,\gamma)\text{--}^{166}\text{Dy}$ [17]. Holmium-166 can be produced directly from neutron irradiation of ^{165}Ho (mono-isotopic in nature) but long lived $^{166\text{m}}\text{Ho}$ (half-life 1200 y; 810 keV (57%) and 712 keV (54%) gammas) is also produced. As an alternative, ^{166}Dy produced from ^{164}Dy [17] provides carrier free ^{166}Ho (containing no $^{166\text{m}}\text{Ho}$), which is separated by HPLC methods.

TABLE 2. STATUS OF KEY NEW RESEARCH REACTORS (IAEA 2005)

Reactor designation	Country	Expected start date	Peak thermal flux	Power level
FRM-II	Germany	2004	3E14	20 MW
MNSR	Nigeria	2004	1E12	(30 kW)
TRIGA-II	Morocco	2005	4E13	2 MW
OPAL	Australia	2006	3E14	20 MW
CARR	China	2006	Not known	60 MW
PIK	Russian Federation	Not known	4E15	100 MW
Pool type	Thailand	Not known	1E14	5 MW
Maple 1 & 2	Canada	Not known	2E14	10 MW

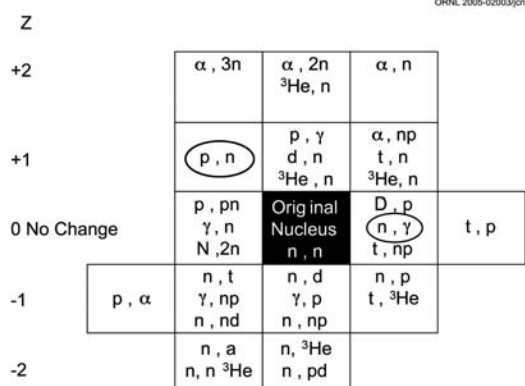


FIG. 4. Summary of changes in Z as a function of nuclear reaction.

3.1. Specific activity is often compromised by the ‘direct’ production pathway

Since many therapeutic radioisotopes are produced in research reactors by direct radiative neutron capture, Z does not change and the desired product atoms cannot be practically separated from the target atoms which often thus considerably reduce the product specific activity (Fig. 4). Contamination of reactor produced radioactive products with target materials is often in contrast to accelerator production of radioisotopes, where proton capture—(p,n) reaction for instance—changes Z and the challenge is the availability of

ORNL 2005-0199Wajon

Reactor Production of Radioisotopes

No Change in Z – Target and Product Atoms Cannot be Separated

Incident Neutron	Target Nucleus	Process	Example	Change in Z Atomic Number
		 γ Radiative Capture $[n,\gamma]$	Lu-176 \rightarrow Lu-177	0
		 γ Inelastic Scattering $(n,n'\gamma)$	Sn-117 \rightarrow Sn-117 m	0
		 $(n,2n)$	Au-197 \rightarrow Au-196	0

FIG. 5. Examples of nuclear reactions with no change in Z and dilution of product atoms with target.

methods for the effective separation of the desired radioactive product atoms from the target material. High specific activity radioisotopes are often required for radiolabelling agents which target a limited number of cellular binding sites, which is required to avoid receptor saturation. This is particularly true with many receptor binding agents, including peptide targeting agents such as bombesin and substance P, and alternative production methods have been pursued which favour production in higher flux reactors.

Examples of common reactor production pathways where Z does not change are summarized in Fig. 5 and include the production of ^{177}Lu by the $^{176}\text{Lu}(n,\gamma)^{177}\text{Lu}$ radiative pathway. Since Z does not change, the product ^{177}Lu atoms cannot be practically separated from the non-activated ^{176}Lu target atoms. However, in this case the very high thermal neutron cross-section of 2090 b results in rapid target burnup and, as discussed later, this permits production of relatively high specific activity ^{177}Lu in even low to modest thermal flux reactors. Tin-117m is a radioisotope which has been of interest for sometime because of its versatile organometallic and coordination chemistry. The half-life of 15 d allows maintenance of an inventory and shipment to distant sites. In addition to the emission of a gamma photon for imaging (159 keV, 86%), interest in the use of $^{117\text{m}}\text{Sn}$ for therapy results from its emission of low energy conversion electrons. Unfortunately, the low cross-section ($\sigma = 19$ mb) limits the specific activity by direct production in even very high flux reactors. However, the specific activity of $^{117\text{m}}\text{Sn}$ can be considerably increased compared to the $^{116}\text{Sn}(n,\gamma)^{117\text{m}}\text{Sn}$ radiative pathway by the inelastic scattering $^{117}\text{Sn}(n,n'\gamma)^{117\text{m}}\text{Sn}$ route [18]. Because the epithermal flux cross-section is higher, use of the higher energy neutron flux available in higher flux

Reactor Production of Radioisotopes

Z Changes – Permitting Separation of Product Atoms from Target Atoms

Incident Neutron	Target Nucleus	Process	Example	Change in Z Atomic Number
		Fission	U-235 → Sr-90	Multiple Products
		[n,p], [n,α]	Zn-67 → Cu-67	-2
		[n,np] Beta decay product	Ni-58 → Co-57 Yb-177 → Lu-177	-1 +1

FIG. 6. Examples of nuclear reactions where the desired product is obtained from decay of the initial product, allowing separation of n.c.a. products with increased specific activity.

reactors permits an increase in the specific activity by a factor of three [18]. Another example is the uncommon but known (n,2n) pathway, such as that used for the production of ^{196}Au from ^{197}Au .

3.2. ‘Indirect’ production pathways can significantly increase specific activity

There are strategies for indirect reactor production pathways, such as the well-known production of ^{131}I from the $^{130}\text{Te}(n,\gamma)^{131}\text{Te}(\beta\text{-decay})^{131}\text{I}$ route. Other examples are illustrated in Fig. 6 and most notably include fission products, the (n,p) reaction for the reactor production of ^{67}Cu and the isolation of radioactive products such as n.c.a. ^{177}Lu formed by beta decay of the initial neutron activated product, ^{177}Yb . In this approach, Z changes by beta particle emission, for instance, and if effective chemical separation methods are available, the n.c.a. desired radioactive product can be separated from the target atoms. Examples of other such ‘batch’ chemical separations of the product formed by β^- decay of the reactor produced parent include ^{111}Ag , ^{77}As and ^{199}Au . Silver-111 is readily obtained by anion exchange and chromatographic separation of ^{111}Pd and the 7.47 d half-life readily permits shipment to other sites. Silver can be complexed with functionalized tetraazaheterocycles for attachment to antibodies or other therapeutic agents. Arsenic-77 is readily separated from the ^{77}Ge reactor produced product and has a chemistry similar to that of phosphorus, permitting preparation of arsonates and other

potentially useful species. The last example, ^{199}Au , has been of interest for many years and can be attached to antibodies.

4. VERY HIGH FLUX IS REQUIRED FOR PRODUCTION OF ^{188}W

The increasing use of unsealed radioactive targeting agents for cancer treatment and other therapeutic applications requires the routine availability of cost effective radioisotopes. Rhenium-188 is a key example of a high energy beta emitting therapeutic radioisotope that is readily available carrier free from the alumina-based ^{188}W (half-life 69 d)– ^{188}Re (half-life 16.9 h) generator system [19, 20]. Rhenium-188 has many attractive properties for a wide variety of therapeutic applications, which include emission of a 2.12 MeV beta particle, a 155 keV (15%) gamma photon for imaging and versatile chemistry for attachment to a variety of targeting molecules. These properties make ^{188}Re an important candidate for applications where deep tissue penetration is a benefit. Emission of gamma photons which can be readily imaged (155 keV, 15%) is an added benefit which permits evaluation of biodistribution, pharmacokinetics and dosimetry estimates. The long parent half-life and consistent generator performance result in a shelf life of several months. The 24 h post-generator ^{188}Re elution 62% in-growth and high elution yields (75–85%) result in daily yields of about 50%, with consistently low ^{188}W parent breakthrough ($<10^{-6}$). Simple post-elution concentration methods have been developed to provide very high specific volume solution for ^{188}Re radiolabelling (>700 mCi/mL saline from 1 Ci generator) [19, 20].

A variety of ^{188}Re labelled therapeutic radiopharmaceuticals and devices have been developed, and over 60 physician sponsored clinical trials are currently in progress throughout the world with applications in nuclear medicine, oncology and interventional cardiology. One important application is palliation of metastatic bone pain with ^{188}Re -HEDP—which is readily prepared from a simple ‘kit’ [21, 22] and is a cost effective alternative to other available agents, especially in developing regions. Recent studies have demonstrated enhancement of progression free interval and survival time by repeated ^{188}Re -HEDP injections [21]. Post-percutaneous transluminal coronary angioplasty treatment of arterial segments using liquid filled balloons with ^{188}Re perrhenate or MAG3 is an efficacious and cost effective approach for uniform vessel wall dose delivery for inhibition of hyperplasia. Other applications include the use of the ^{188}Re labelled antiNCA95 (CD66) antibody in conjunction with external beam irradiation as an effective method for myeloablation/conditioning prior to stem cell transplantation in leukemia patients. In addition, the ^{188}Re -P2045 peptide has been developed for the treatment of

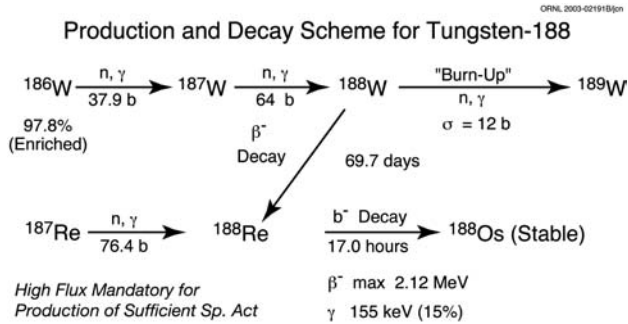


FIG. 7. Scheme for reactor production of ^{188}W .

small cell/non-small cell lung tumours, and ^{188}Re labelled antibodies are being evaluated for tumour therapy. Therapy of refractory liver cancer is being explored by site-specific catheter delivery of ^{188}Re -B20 albumin particles and ^{188}Re -Lipiodol is being used in several countries, including an IAEA sponsored multicentre trial at ten sites [23]. In the developing world, use of the ^{188}W - ^{188}Re generator also represents a particularly convenient and cost effective system for providing the ^{188}Re therapeutic radioisotope. Use of the ^{188}W - ^{188}Re generator in a centralized radiopharmacy would be expected to optimize the costs and use of ^{188}Re .

Tungsten-188 is a key example of where a very high thermal flux is required for the production of sufficient specific activity for practical use of the adsorption based ^{188}W - ^{188}Re generator [8]. Low specific activity ^{188}W requires the use of larger amounts of alumina for the generator column, thus increasing the eluant volume and decreasing the ^{188}Re activity/volume (mCi/mL). The increase in specific activity using very high flux reactors is dramatically illustrated (Fig. 7) for the production of ^{188}W from enriched ^{186}W by the $^{186}\text{W}(n,\gamma)^{187}\text{W}(n,\gamma)^{188}\text{W}$ pathway. Cross-sections for both the ^{186}W and ^{187}W neutron capture pathways are relatively small and there is competing burnup of the ^{188}W product (Fig. 7, [24]). In addition, the significant self-shielding that has been observed and evaluated using the solid ^{186}W targets [25] as a strategy to increase the ^{188}W yield/target volume [26] is a factor which decreases the ^{188}W specific activity. The authors have had extensive experience over the last several years in HFIR production of ^{188}W , from both enriched ^{186}W tungsten metal and tungsten oxide targets [8]. The metallic powder targets are usually processed by oxidation with hydrogen peroxide and/or hypochlorite in the presence of a base and oxide targets are dissolved in a base with concomitant oxidation [8, 24]. The reactor production yields of ^{188}W [8, 24] are about one order of magnitude lower than the calculated values for the $^{186}\text{W}(n,\gamma)^{187}\text{W}$ ($\sigma =$

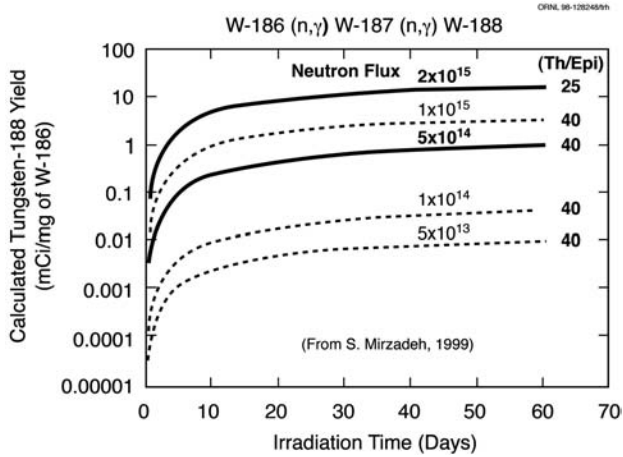


FIG. 8. Production of ^{188}W as a function of thermal neutron flux. Values estimated using the LAURA code [27, 28].

37.9 ± 0.6 b) and $^{187}\text{W}(n,\gamma)^{188}\text{W}$ ($\sigma = 64 \pm 10$ b) reactions. The neutron burnup cross-section for the $^{188}\text{W}(n,\gamma)^{189}\text{W}$ nuclear reaction is one factor which has been recently shown to contribute to the reduced production yields observed for ^{188}W [24]. By irradiation of ^{188}W , a value of 12.0 ± 2.5 b has been calculated for this neutron burnup cross-section [24].

The calculated specific activity values of ^{188}W as a function of the thermal neutron flux are shown in Fig. 8 and vividly demonstrate a dramatic increase with increasing flux and that a minimal thermal flux of 10^{15} is required to produce a specific activity of only about 1 Ci/g ^{186}W . Figure 9 shows the actual production values in the ORNL HFIR and the deviation from the theoretical values.

5. PRODUCTION OF $^{117\text{m}}\text{Sn}$ BY INELASTIC REACTION

Tin-117m is produced with relatively low specific activity (5–6 mCi/mg) by neutron irradiation of enriched ^{116}Sn . Specific activity can be increased in the HFIR by a factor of about three by using the $^{117}\text{Sn}(nn',\gamma)^{117\text{m}}\text{Sn}$ inelastic route (20–22 mCi/mg) [18]. In contrast to the other radioisotopes of current interest for palliation, $^{117\text{m}}\text{Sn}$ decays by conversion electron emission. The low energy conversion electrons travel only a very limited distance in tissue, which may preclude potential bone marrow depression, which can be a limiting factor with high energy β^- emitting radioisotopes. Potential advantages of $^{117\text{m}}\text{Sn}$ are the absence of high energy beta particles, the emission of a gamma photon of

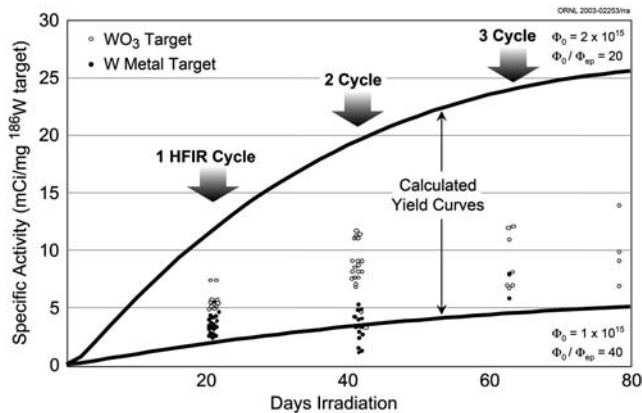


FIG. 9. Production of ^{188}W in the ORNL HFIR compared with the theoretical production yields.

nearly optimal energy for imaging and high metastatic uptake of tin(IV)-DTPA. Production of $^{117\text{m}}\text{Sn}$ in a nuclear reactor involves radiative capture by the (n,γ) route by irradiation of enriched ^{116}Sn , or via the inelastic $(n,n'\gamma)$ route by irradiation of enriched ^{117}Sn . The authors have evaluated both these routes in detail using the ORNL HFIR [18], where specific activity values of 8–10 mCi/mg from enriched ^{117}Sn after a long irradiation time (1 cycle = 24 d) are routinely obtained.

6. HIGH FLUX DIRECT PRODUCTION OF MULTI-CURIE LEVELS OF VERY HIGH SPECIFIC ACTIVITY ^{177}Lu IS ADVANTAGEOUS COMPARED WITH INDIRECT PRODUCTION IN MODEST FLUX REACTORS

The reactor produced radiolanthanide examples of current broad interest include ^{177}Lu and ^{166}Ho , both of which can be produced by direct — $^{176}\text{Lu}(n,\gamma)^{177}\text{Lu}$ and $^{165}\text{Ho}(n,\gamma)^{166}\text{Ho}$ — and also via indirect production routes: $^{176}\text{Yb}(n,\gamma)^{177}\text{Yb}(\beta\rightarrow\text{decay})^{177}\text{Lu}$ and $^{164}\text{Dy}(2n,\gamma)^{166}\text{Dy}(\beta\rightarrow\text{decay})^{166}\text{Ho}$. While reactor indirect production routes can often provide high specific activity products, the disadvantages can include the modest production rates of the parent radioisotopes at lower flux (^{177}Yb). In addition, large target volumes may be required and processing constraints include time requirements and costs. The reactor production facilities required depend on specific activity requirements, the particular application and economics. For ^{177}Lu , in particular,

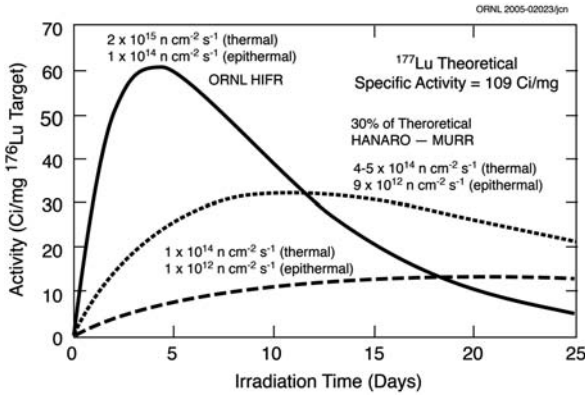


FIG. 11. Reactor production of ^{177}Lu from ^{176}Lu as a function of thermal neutron flux.

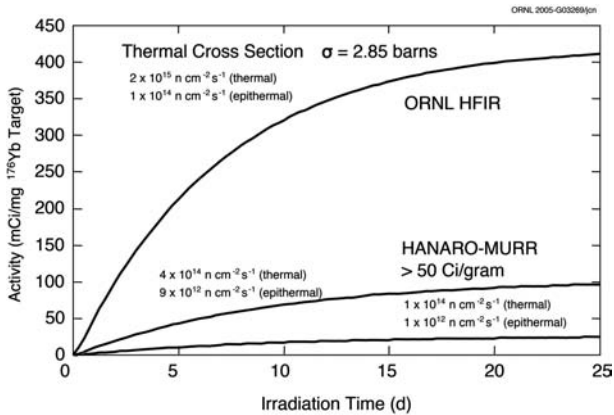


FIG. 12. Reactor production of ^{177}Lu from ^{176}Yb as a function of thermal neutron flux.

in a very high flux reactor with capabilities for on-line access to the reactor core. As illustrated in Fig. 11, the theoretical maximum specific activity of 109 Ci/mg Lu is approached when very high thermal flux is available.

As an alternative, the indirect production of ^{177}Lu by beta decay of reactor produced ^{177}Yb as a function of thermal flux is illustrated in Fig. 12 [29]. Production via this pathway would, in principle, allow the use of modest thermal flux reactors. However, the combination of factors, including the large target volume required, the large amounts of adsorbent which would be required for effective column separation, the time factor required for column separation and the relatively large volumes of radioactive acidic wastes would

suggest that this approach would not be cost effective on the large scale which would be required to provide the activity levels of ^{177}Lu needed for large scale clinical trials or for routine clinical use.

7. INDIRECT PRODUCTION OF $^{195\text{m}}\text{Pt}$ IN A HIGH FLUX REACTOR

Other promising examples of indirect routes utilizing a very high flux reactor for production of radioisotopes for which the utility has not yet been fully established include $^{195\text{m}}\text{Pt}$ and ^{229}Th . The potential availability of $^{195\text{m}}\text{Pt}$ with adequate specific activity is of widespread interest because of the therapeutic potential of Auger electron emitting radioisotopes. Platinum-195m decay results in the emission of 33 electrons per decay and this radioisotope may thus have the potential for effective therapy of cellular internalized radiopharmaceuticals. Platinum-195m is also of interest as a tracer for studies of the biokinetics and therapeutic mechanism of widely used platinum based antitumour agents such as *cis*-dichlorodiammineplatinum(II) ('*Cis*-platinum'–'*Cis*-DDP') and carboplatinum. Both of these applications require much higher specific activity material than is currently available (~1 mCi/mg). The authors have evaluated inelastic neutron scattering, $^{195}\text{Pt}(n,n',\gamma)^{195\text{m}}\text{Pt}$, as a possible route to provide higher specific activity $^{195\text{m}}\text{Pt}$ than can be obtained via the traditional radiative thermal neutron capture, $^{194}\text{Pt}(n,\gamma)^{195\text{m}}\text{Pt}$ [18]. Such direct neutron capture routes provide specific activity values of only ~1 mCi/mg platinum, even at the highest thermal neutron flux available at the core of the HFIR. In some cases, the yield from the (n,n') neutron scattering reaction has been found to be higher than that obtained from the (n, γ) neutron capture reaction, such as the threefold increase described earlier for production of $^{117\text{m}}\text{Sn}$. In the case of $^{195\text{m}}\text{Pt}$, however, the relative gain in specific activity was found to be only about 1.4 [16].

The indirect production of $^{195\text{m}}\text{Pt}$ from the decay of reactor produced $^{195\text{m}}\text{Ir}$ (Fig. 13) represents a new approach for significantly increasing the specific activity of $^{195\text{m}}\text{Pt}$ for biomedical research [16, 30, 31]. For the separation of platinum from iridium, the reported equilibrium constants (K_d) for thiourea complexes of iridium(IV) and platinum(IV) on AG-50W \times 4 cation exchange resin in 0.1–1.0M HCl/0.1–0.2M thiourea are ~3.5 for Ir, and 1.5×10^3 to 1.5×10^4 for platinum. In 0.1–1.0M HCl and in the absence of thiourea, the K_d of platinum is only 1.4. The authors found that the separation of microscopic levels of $^{195\text{m}}\text{Pt}$ from macroscopic levels of iridium can be achieved using this approach and the authors expect this approach to be a practical and effective method for routine hot cell separation of n.c.a. $^{195\text{m}}\text{Pt}$ from the iridium target

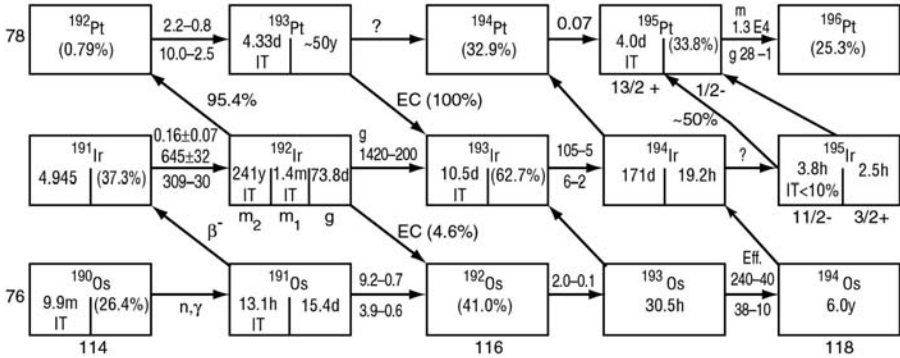


FIG. 13. Reactor production of ^{195m}Pt by the direct irradiation of ^{194}Pt and ^{195}Pt and by indirect irradiation of ^{176}Yb .

($^{195m}\text{Ir}/^{192}\text{Ir}$). The production of ^{195m}Pt by the $^{193}\text{Ir}(n,\gamma)^{194}\text{Ir}(n,\gamma)^{195}\text{Ir}(\beta^- \text{ decay})^{195m}\text{Pt}$ route is expected to make this important radioisotope available with a specific activity of 70–100 mCi/mg. Since there is broad interest in the nuclear medicine/oncology community for the use of Auger electron emitting radioisotopes for targeted tumour cell therapy, the attachment of ^{195m}Pt to intracellular targeted peptides and other agents is expected to represent a new opportunity for cancer treatment via Auger electron therapy.

8. REACTOR PRODUCTION OF ^{229}Th FROM ^{226}Ra MAY OFFER AN ALTERNATIVE TO SEPARATION FROM ^{233}U

Another example of broad current interest is ^{229}Th , the parent of ^{225}Ac , used for the ^{225}Ac - ^{213}Bi generator system. Thorium-229 is available in limited supply from the decay of ^{233}U , or ^{225}Ac can be accelerator produced by the $^{226}\text{Ra}(p,2n)^{225}\text{Ac}$ route. Because of the benefits of the long half-life of ^{229}Th ($T_{1/2} = 7340$ y), another route which is being explored is the reactor production of ^{229}Th by the $^{226}\text{Ra}(3(n,\gamma))(2\beta^- \text{ decay})^{229}\text{Th}$ route (Fig. 14) [32].

In a preliminary small scale irradiation experiment in the ORNL HFIR [32], a 43.5 μg target of ^{226}Ra nitrate was irradiated for one reactor cycle (~ 24 d) at a thermal neutron flux of 10^{15} $\text{n}\cdot\text{cm}^{-2}\cdot\text{s}^{-1}$, with a thermal:epithermal ratio of ~ 20 . The yield of ^{229}Th was about 31 μCi per mg of ^{226}Ra per reactor cycle. Although at the end of bombardment the activity of the ^{228}Th and ^{227}Ac contaminants co-produced with ^{229}Th were 951 and 56 times higher, even from a mixture of ^{228}Th and ^{229}Th , high purity ^{225}Ac can be obtained by initial extraction of radium from thorium and then extracting ^{225}Ac from the radium

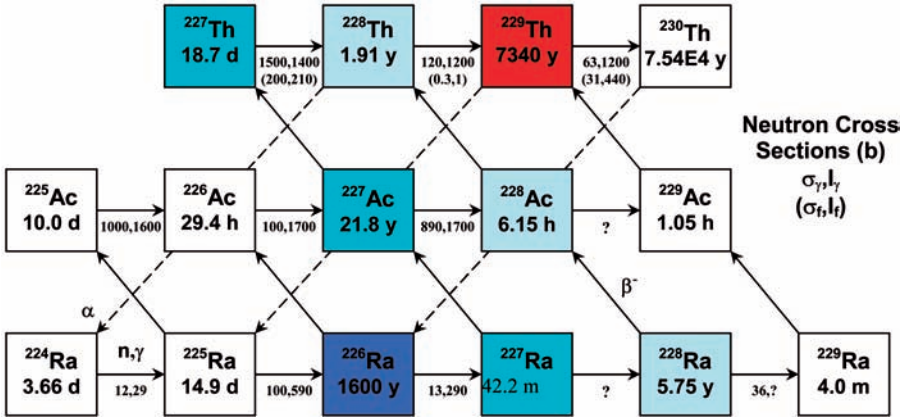


FIG. 14. Reactor production of ^{229}Th from ^{226}Ra .

mixture, since ^{224}Ra , the progeny of ^{228}Th decays by α emission to ^{220}Rn with no β^- decay to ^{224}Ac . The ^{229}Th yields under these conditions were ~ 50 times larger than those predicted. In contrast, the experimental to theoretical yields for ^{228}Th and ^{227}Th were 1.4 and 1.0, respectively. The lack of neutron capture cross-section data for the intermediate ^{227}Ra and ^{228}Ac radionuclides hampers any theoretical calculations. The results from these preliminary measurements suggest that production of ~ 300 mCi of ^{229}Th would be possible from irradiation of one gram of ^{226}Ra in the target position of HFIR for one year. Subsequent recycling of the ^{226}Ra target could theoretically result in an increase in the ^{226}Ra yield resulting from the formation of ^{228}Ra (Fig. 15).

The limited availability of ^{229}Th necessitates investigation of alternative production routes for ^{229}Th , ^{225}Ra and ^{225}Ac because of the broad interest in the clinical applications of ^{213}Bi . Uranium-233 is currently the only source available from which to obtain high purity ^{229}Th . The demand for ^{225}Ac already exceeds the levels of ^{225}Ac that can be currently provided (~ 500 mCi/y) from decay of the available 150 mCi ^{229}Th inventory available at ORNL. In fact, if predictions are accurate, the demand may soon even exceed the levels of ^{229}Th present in the ^{233}U stockpile. Estimates predict that only ~ 38 g of ^{229}Th (~ 8 Ci) — which is only about ~ 80 times the current ORNL available ^{229}Th — could be extracted from the entire ^{233}U stockpile, although routine processing is unfeasible because of the very high costs and security issues. For these reasons, alternative accelerators and reactor production routes are being evaluated for the production of ^{229}Th , ^{225}Ra and ^{225}Ac .

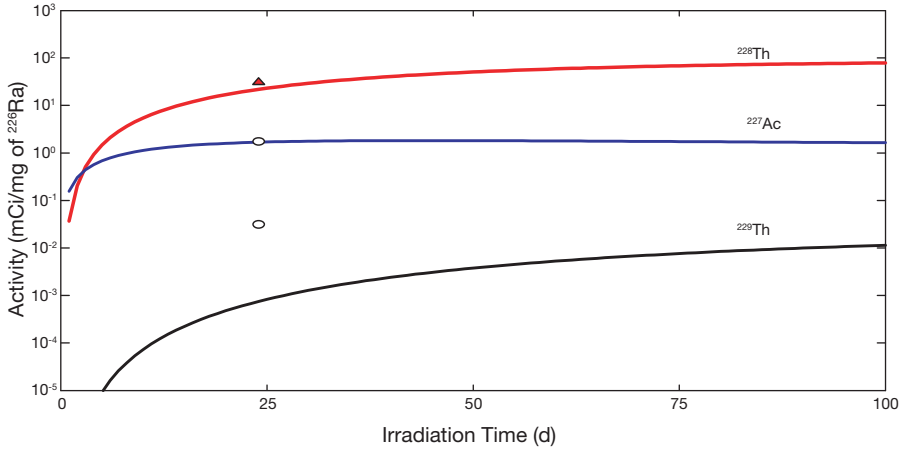


FIG. 15. Comparison of calculated production yields and experimental yields at the ORNL HFIR for ^{228}Th , ^{227}Ac and ^{229}Th .

9. SUMMARY AND CONCLUSIONS

Research reactors continue to have a central role in the production of medical radioisotopes, not only via fission to provide ^{99}Mo and ^{90}Sr , but also via traditional pathways for production of ^{131}I and a variety of other therapeutic radioisotopes with emerging important therapeutic applications. The availability of very high thermal flux reactors represents a unique capability for production of high specific activity radioisotopes which cannot be produced with adequate specific activity or in adequate activity levels by lower flux reactors or alternative production methods. These examples include ^{188}W (i.e. for ^{188}Re), $^{117\text{m}}\text{Sn}$ and $^{195\text{m}}\text{Pt}$, which are potent Auger emitters for potential therapeutic applications. Initial promising experimental data suggest that reactor production of ^{229}Th is feasible.

ACKNOWLEDGEMENTS

ORNL is managed by UT Battelle, LLC, for the US Department of Energy, under contract No. DE-AC05-00OR22725.

REFERENCES

- [1] MIRZADEH, S., MAUSNER, L.F., GARLAND, M., Reactor-Produced Medical Radioisotopes, *In*, Handbook of Nuclear Chemistry, Volume 4, Chapter 3, pp. 1–46; A. Vertes, N. S. Klencsar, Editors; Kluwer Academic Publishers, Amsterdam (2003).
- [2] KNAPP, F.F., Jr., MIRZADEH, S., BEETS, A.L., Reactor Production and Processing of Therapeutic Radioisotopes for Applications in Nuclear Medicine, *J. Radioanalyt. Nucl. Chem. Lett.*, 205 (1996) 93.
- [3] KNAPP, F.F., Jr., MIRZADEH, S., BEETS, A.L., DU, M., Production of Therapeutic Radioisotopes in the ORNL High Flux Isotope Reactor for Applications in Nuclear Medicine, Oncology and Interventional Cardiology, *J. Radioanalyt. Nuc. Chem.* 263 (2005) 503.
- [4] KNAPP, F.F., Jr., BEETS, A.L., MIRZADEH, S., ALEXANDER, C.W., HOBBS, R.L., Production of Medical Radioisotopes in the ORNL High Flux Isotope Reactor (HFIR) for Cancer Treatment and Arterial Restenosis Therapy after PTCA, *Czech. J. Physics* 49 (1999) Suppl. S1-Part II, 799.
- [5] MIKOLAJESZAK, R., PARUS, J.L., Reactor Produced Beta-Emitting Nuclides for Nuclear Medicine, *World J. Nucl. Med.* 4 (2005) 184.
- [6] INTERNATIONAL ATOMIC ENERGY AGENCY, Manual for Reactor Produced Radioisotopes, IAEA-TECDOC-1340, IAEA, Vienna (2003).
- [7] ROESCH, F., KNAPP, F.F., Jr., Radionuclide Generators, *In*, Handbook of Nuclear Chemistry, Volume 4, Chapter 3, pp. 81-118; A. Vertes, N.S. Klencsar, Editors; Kluwer Academic Publishers, Amsterdam (2003).
- [8] KNAPP, F.F., Jr., CALLAHAN, A.P., BEETS, A.L., MIRZADEH, S., HSIEH, B.-T., Processing of Reactor-Produced Tungsten-188 for Fabrication of Clinical Scale Alumina-Based Tungsten-188/Rhenium-188 Generators, *Appl. Rad. Isot.* 45 (1994) 1123.
- [9] KNAPP, F.F., Jr., MIRZADEH, S., The Continuing Important Role of Radionuclide Generator Systems for Nuclear Medicine, *Eur. J. Nucl. Med.* 21 (1994) 1151.
- [10] MIRZADEH, S., KNAPP, F.F., Jr., Biomedical Radionuclide Generators Systems, *J. Radioanalyt. Nucl. Chem.* 203 (1996) 469.
- [11] INTERNATIONAL ATOMIC ENERGY AGENCY, Development of Generator Technologies for Therapeutic Radionuclides, Rep. Research Coordination Meeting (333-F2-RC-958), IAEA, Vienna (2004).
- [12] INTERNATIONAL ATOMIC ENERGY AGENCY, Nuclear Research Reactors in the World 1998 Edition, Reference Data Series No. 3, IAEA, Vienna (1999).
- [13] KNAPP, F.F., Jr., CALLAHAN, A.P., BEETS, A.L., MIRZADEH, S., HSIEH, B.-T., Processing of Reactor-Produced ^{188}W for Fabrication of Clinical Scale Alumina-Based $^{188}\text{W}/^{188}\text{Re}$ Generators, *Appl. Radiat. Isot.* 45 (1994) 1123.

- [14] KNAPP, F.F., Jr., MIRZADEH, S., BEETS, A.L., DU, M., Therapeutic Radioisotope Production in the High Flux Isotope Reactor (HFIR), *J. Label Compounds. Radiopharm.* 46 (Suppl. 1) (2003) S320.
- [15] PONSARD, B., et al., The Tungsten-188/Rhenium-188 Generator: Effective Coordination of Tungsten-188 Production Between the HFIR and BR2 Reactors, *J. Radioanalyt. Nucl. Chem.* 257 (2003) 169.
- [16] KNAPP, F.F., Jr., et al., Reactor-Produced Radioisotopes from ORNL for Bone Pain Palliation, *Appl. Radiat. Isot.* 49 (1998) 309.
- [17] DADACHOVA, E., MIRZADEH, S., LAMBRECHT, R.M., HETHERINGTON, E., KNAPP, F.F., Jr., Separation of Carrier-Free Holmium-166 from Neutron-Irradiated Dysprosium Targets, *Anal. Chem.* 66 (1995) 4272.
- [18] MIRZADEH, S., KNAPP, F.F., Jr., ALEXANDER, C.W., MAUSNER, L.F., Evaluation of the Neutron Inelastic Scattering for Radioisotope Production, *Appl. Radiat. Isot.* 48 (1997) 441.
- [19] KNAPP, F.F. Jr., Use of Rhenium-188 for Cancer Treatment, *Cancer Biotherapy and Radiopharm.* 13 (1998) 337.
- [20] KNAPP, F.F., Jr., et al., Development of the Alumina-Based Tungsten-188/Rhenium-188 Generator and Use of Rhenium-188-Labeled Radiopharmaceuticals for Cancer Treatment, *Anticancer Research* 17 (1997) 1783.
- [21] PALMEDO, H., et al., Repeated Bone Targeted Therapy for Hormone-Refractory Prostate Carcinoma: Randomized Phase II Trial with the New, High-Energy Radiopharmaceutical Rhenium-188-HEDP, *J. Clin. Oncol.* 21 (2003) 2869.
- [22] KNAPP, F.F., Jr., et al., Reactor-Produced Radioisotopes from ORNL for Bone Pain Palliation, *Appl. Radiat. Isot.* 49 (1998) 309.
- [23] SUNDRAM, F.X., et al., Phase I Study of Transarterial Rhenium-188 HDD Lipiodol in Treatment of Inoperable Primary Hepatocellular Carcinoma - A Multicentre Evaluation, *World J. Nucl. Med.* 1 (2002) 5.
- [24] MIRZADEH, S., KNAPP, F.F., Jr., LAMBRECHT, R.M., Burn-up Cross Section of Tungsten-188, *Radiochemica Acta*, 77 (1997) 99.
- [25] GARLAND, M., Neutronic Effects on Tungsten-186 Double Neutron Capture, PhD thesis, University of Maryland, 2004.
- [26] MIRZADEH, S., DU, M., BEETS, A.L., KNAPP, F.F., Jr., Thermoseparation of Neutron-Irradiated Tungsten from Re and Os, *Indust. Engineer. Chem. Res.* 39 (2000) 3169.
- [27] MIRZADEH, S., WALSH, P., Numerical Evaluation of the Production of Radio-nuclides in a Nuclear Reactor - Part I, *Appl. Radiat. Isot.* 49 (1998) 379.
- [28] MIRZADEH, S., WALSH, P., Numerical Evaluation of the Production of Radio-nuclides in a Nuclear Reactor - Part II, *Appl. Radiat. Isot.* 49 (1998) 383.
- [29] BEETS, A.L., DU, M., MIRZADEH, S., KNAPP, F.F., Jr., Method for Preparation of High Specific Activity Reactor-Produced Lutetium-177, U.S. Patent No. 6,716,353, Issued April 5, 2004.
- [30] MIRZADEH, S., DU, M., BEETS, A.L., KNAPP, F.F., Jr., High Specific Activity Platinum -195m, U.S. Patent No. 6,804,319, Issued October 12, 2004.

SESSION 6

- [31] MIRZADEH, S., DU, M., BEETS, A.L., KNAPP, F.F., Jr., New Method for Preparation of High Specific Activity Platinum-195*m* for Medical Therapy, U.S. Patent No. 6,751,280, Issued June 15, 2004.
- [32] BOLL, R.A., GARLAND, M., MIRZADEH, S., Reactor Production of Thorium-229. Proceedings, 4th Symposium on Alpha Radioimmunotherapy, Dusseldorf, Germany, June 28-29, 2004.

TECHNOLOGICAL LINE FOR PRODUCTION OF CARRIER FREE ^{188}Re IN THE FORM OF STERILE ISOTONIC SOLUTION OF SODIUM PERRHENATE(VII)

E. ILLER*, Z. ZELEK**, M. KONIOR**, K. SAWLEWICZ*,
J. STANISZEWSKA*, R. MIKOLAJCZAK*, U. KARCZMARCZYK***

*Radioisotope Centre POLATOM
Email: e.iller@polatom.pl

** POLATOM Ltd
Otwock-Świerk

***National Institute of Public Health, Warsaw

Poland

Abstract

The radiometric properties of ^{188}Re create convenient conditions for medical application of this radionuclide. A growing interest with respect to the possible use of ^{188}Re for radioimmunotherapy, radionuclide synovectomy and bone pain palliation has been observed, chiefly due to the favourable characteristics of ^{188}Re ($T_{1/2} = 16.98$ h), emitting β^- particles with an average energy of 764 keV ^{188}Re and 155 keV gamma photons (15% γ radiation). The mentioned properties allow for in vivo biodistribution evaluation of ^{188}Re labelled ligands by means of a gamma camera. At the Radioisotope Centre POLATOM, the technology for production of sterile and isotonic solution of ^{188}Re has been developed. The technology enables preparation of carrier free ^{188}Re in the form of a sterile isotonic solution of sodium perrhenate(VII) with a total activity of 185 GBq and a radiochemical purity of 99.9%. The batches of sodium perrhenate(VII) ^{188}Re obtained are distributed to national nuclear medicine centres.

1. INTRODUCTION

The radiometric properties of ^{188}Re create advantageous conditions for the medical application of this radionuclide. Rhenium-188 belongs to the group of beta-gamma emitters (average energy of beta particles 784 keV, gamma

photons 155 keV (15%), $T_{1/2} = 16.9$ h) and exhibits chemical reactivity similar to ^{99m}Tc and can thus be converted to the chemical forms required for preparation of various therapeutic radiopharmaceuticals. The ^{188}Re radionuclide is produced as a result of ^{188}W decay. The ^{188}W parent ($T_{1/2} = 69$ d) is obtained by double neutron capture of ^{186}W in a nuclear reactor following the reaction scheme $^{186}\text{W} (n, \gamma) \Rightarrow ^{187}\text{W} (n, \gamma) \Rightarrow ^{188}\text{W}$. This reaction occurs with low efficiency and requires $5 \times 10^{14} \text{ n}\cdot\text{cm}^{-2}\cdot\text{s}^{-1}$ thermal neutron flux for production of a specific activity of $>0.3\text{--}0.4$ Ci/g. Such conditions are available at the SM in Dimitrograd and the HFIR in Oak Ridge. The high energy beta emission of ^{188}Re ($E = 2.12$ MeV) is particularly well suited when effective deep tissue penetration is required (maximum penetration 10 mm). In addition, its gamma emission permits quantitative gamma camera imaging for evaluation of biokinetics and dosimetric estimations.

A number of important therapeutic applications of ^{188}Re have been developed over the past two decades and have demonstrated the use of ^{188}Re as an effective alternative to the more expensive and/or less readily available therapeutic radioisotopes. These clinical trials include the use of ^{188}Re -HEDP and DMSA for the treatment of metastatic bone pain, various ^{188}Re labelled HDD/Lipiodol and DEDC/Lipiodol radioembolytic therapy of hepatocellular carcinoma. More recently, the use of ^{188}Re colloid for radionuclide synovectomy has been found effective for treatment of refractory disease.

At the Radioisotope Centre POLATOM, the technology of production of sterile and isotonic solution of ^{188}Re has been elaborated. A technological line consisting of five lead shielded chambers has been built following both pharmaceutical requirements and environmental regulations [1].

2. LABORATORY OPERATIONS

In the literature can be found descriptions of several types of $^{188}\text{W}\text{--}^{188}\text{Re}$ generator, where such materials as Dowex, zirconium oxides, alumina and tungstate of Zr, Ti, Co and Mo were used for filling the generator columns [2–4].

The best elution efficiency was obtained when alumina was used for filling the generator columns. Taking into consideration those literature reports of other investigations, alumina was selected as the filler material for the generator columns.

The adsorption of tungstate solution on two types of alumina has been investigated over a wide range of pH (9.7–2.5) and temperature (0–34°C) in the presence of chloride, acetate, nitrate and phosphate ions. Alumina for filling the generator columns was first activated using 0.9% NaCl in 0.001M HCl to obtain pH3. Tungsten-188 in the form of tungstenic acid was slowly fed onto the

SESSION 6

column (flow rate of 0.1 mL/min). After ^{188}W deposition, the alumina column was washed with 0.9% NaCl. For the eluates of ^{188}Re in 0.9% NaCl, a concentration system has been proposed consisting of anion and cation exchange resins. The obtained solution was purified and concentrated in the chromatographic system consisting of cation exchanger AG-50W-X12 resin, 200–400 mesh hydrogen form and anionic column Accel Plus QMA Light, where the perrhenate ions were concentrating.

The Na^+ cations replace the H^+ ions on the cationic exchanger (Ag-50W-X12, Bio-Rad), then the H^+ ions bind to acetate ions and elute as acetic acid. The $^{188}\text{ReO}_4^-$ ions pass through the column and are stopped on the anionic column (Sep-Pak Plus QMA Light). The column is first washed with water to remove acetic acid and then $^{188}\text{ReO}_4^-$ ions are eluted in 1–2 mL of 0.9% NaCl [5, 6].

3. QUALITY CONTROL

An important part of the technology is quality control of the obtained product, especially when the product is intended for medical purposes. The quality of eluated ^{188}Re perrhenate solution was checked by means of paper chromatography using 0.9% NaCl as the developing solution to evaluate its radiochemical purity. Chemical purity of the eluate was determined using an ICP-optical emission spectrometer (Optima 33000XL, Perkin-Elmer) with special consideration given to the presence of tungsten, aluminium and zirconium. Radionuclide purification of the eluates was checked by gamma spectrometry. This covered the overall assessment of radionuclide impurities related to the ^{188}Re activity and ^{188}W breakthrough. As a result of the investigations carried out the quantitative specification of sodium perrhenate(VII) solution has been elaborated (Table 1).

4. TECHNOLOGICAL LINE FOR PRODUCTION OF CARRIER FREE ^{188}Re

Concurrently with the laboratory work, in those cases where the results obtained proved the correctness of the design and construction of the technological line for sodium perrhenate(VII) production, construction of a line consisting of lead chambers was commenced. On the basis of the previously developed procedures of filling and elution of the generator, and also taking into account the requirements formulated for the final products, a technological line for processing of sodium tungstate was constructed [7, 8].

TABLE 1. SPECIFICATION OF SODIUM PERRHENATE(VII) ^{188}Re SOLUTION

Tests	Requirement	Method
Identification:		Visual inspection
Characters	Colourless, clear solution	
Identity		
Gamma ray spectrum	Presence of specific γ lines: E γ = 155.06 E γ = 477.96 E γ = 633.00	Gamma ray spectrometry
pH	5.5–7.5	Potentiometry
Radionuclide purity	>99.9%	Gamma ray spectrometry
Radiochemical purity	\geq 98%	Paper chromatography
Chemical purity	Not more than: 5 ppm Pb, Al, Ba, Ni 10 ppm B, Zn 15 ppm W 20 ppm Si, Mg, Ca	ICP-OES
Sterility	Sterile	Direct inoculation
Bacterial endotoxins	<0.125 EU/mL	LAL test

The line consists of five lead shielded chambers in which the following operations are carried out:

- (a) Unloading of active material;
- (b) Loading of ^{188}W solution on alumina packed chromatographic column;
- (c) Elution of ^{188}Re in the form of sodium perrhenate;
- (d) Concentration of the eluate;
- (e) Dosage of ^{188}Re solution to vials and its sterilization;
- (f) Vial removal from technological line.

The obtained solution of ^{188}Re is recommended for medical applications as a precursor to radiopharmaceuticals production, therefore the air inside the production chambers must meet the purity requirements.

In chambers I and V, air should be classified into class C. Also, the air inside the room where the technological line is situated should fulfil the class D requirements of purity.

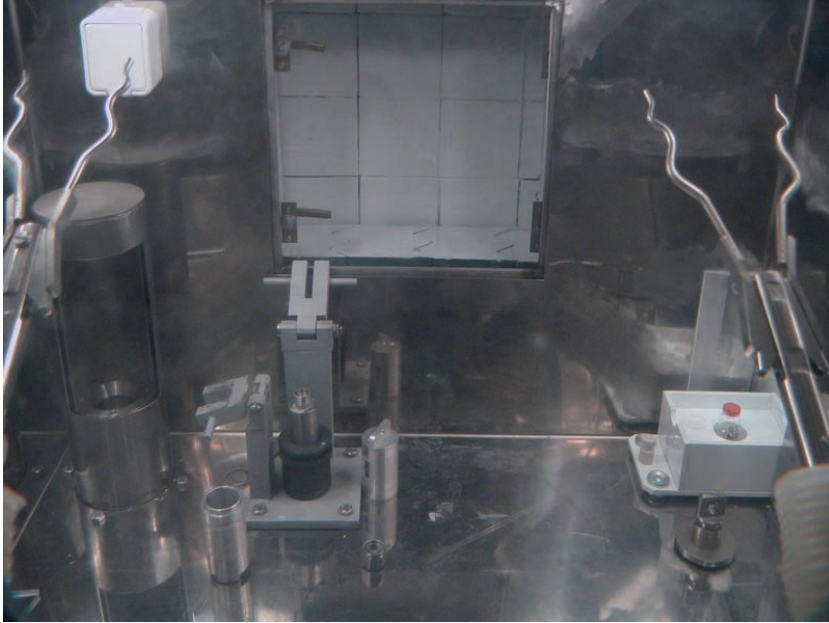


FIG. 1. View of chamber I.

Chamber I is intended for unloading of the irradiation target material: sodium tungstate ^{188}W , currently imported from RIAR in the Russian Federation, possesses the following specifications (Fig. 1):

- (a) Sodium tungstate in sodium hydroxide solution;
- (b) ^{188}W specific activity 186–322 GBq/g;
- (c) ^{187}W – ^{188}W activity ratio 6.0–0.2%;
- (d) Total gamma emitter activity ratio 0.30–0.01%;
- (e) Solvent concentration (sodium hydroxide) 0.16–0.80 mol/L;
- (f) Tungsten concentration 26–83 g/L.

Chamber I is equipped with the following devices to facilitate carrying out the above operations:

- (a) A lift enabling the transport of active material from cellar to chamber;
- (b) Equipment for opening of the capsules containing the ^{188}W solution;
- (c) A pneumatic syringe to effect removal of active solution from the capsule.

The capsule with active material is delivered to the chamber through the cellar by means of a pneumatic lift. In the chamber, the capsule is placed in a



FIG. 2. View of chamber II.

special holder and the ^{188}W solution is removed by means of a syringe and transferred to a beaker. Next, the capsule is flushed with a few millilitres of 0.3M NaOH and the washout is added to the active solution. The beaker containing this solution is transported to the second chamber (Fig. 2).

In chamber II, the sodium tungstate is heated and sodium hypochloride, acetic acid and hydrochloric acid are added. The purpose of this operation is the transformation of sodium tungstate into tungstic acid solution of pH2–3. The acid solution is slowly fed into the generator column filled with alumina.

Chamber II is equipped with:

- (a) Magnetic mixer with heating;
- (b) Thermocouple;
- (c) Holder of generator columns;
- (d) Storage for worn out columns.

In the third chamber, elution of sodium perrhenate from the generator column takes place. As eluent, 0.9% NaCl is used. After elution, chloride anions are removed from the sodium perrhenate when the eluate is passed through the column with AgNO_3 supported on Dowex 50W-X4. Next, perrhenate anions are adsorbed on an anionic column and are finally removed by isotonic saline.

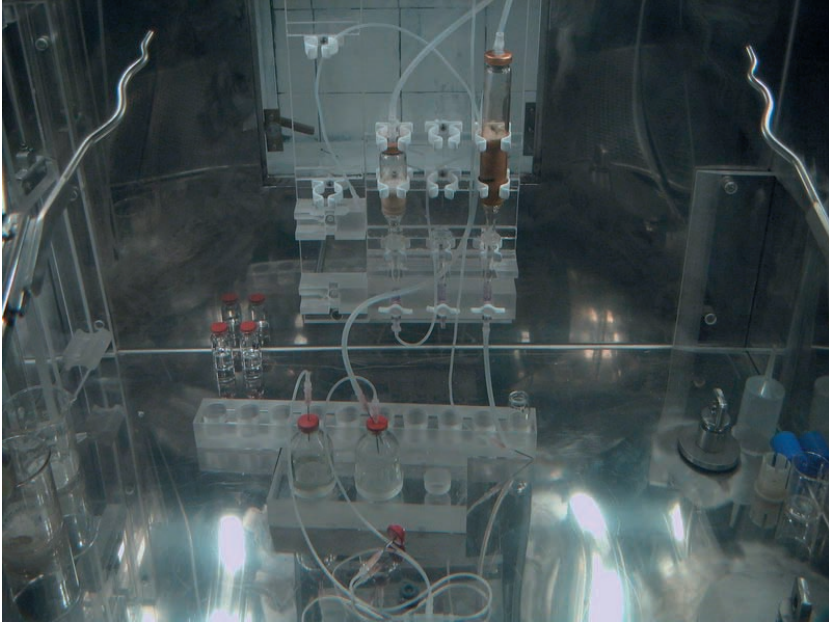


FIG. 3. View of chamber III.

The fourth chamber serves a similar purpose to chamber III except that in addition portioning of the rhenium solution and conducting measurements of its activity are performed here (Figs 3 and 4).

The following equipment is installed in chamber IV:

- (a) Holders of generator columns, and concentration and purification columns;
- (b) Sealer;
- (c) Dosage pipette;
- (d) Seal remover;
- (e) Radiometric chamber 4 Π geometry.

Chamber V is destined for sterilization of the final product and its unloading. Also, it can be used for delivery of auxiliary equipment to the technological line.

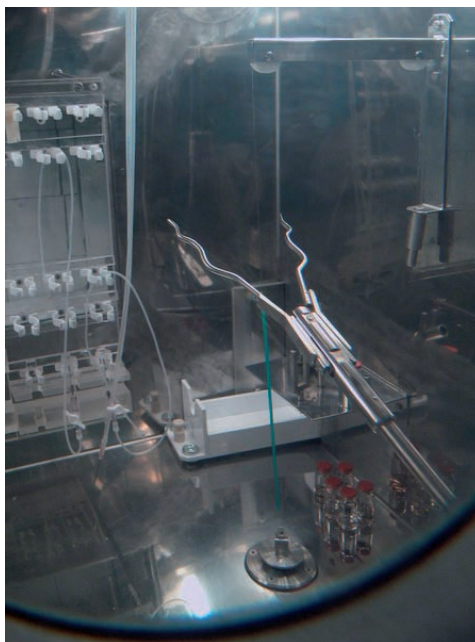


FIG. 4. View of chamber IV.

5. CONCLUSION

The developed technology has enabled preparation of carrier free ^{188}Re in the form of a sterile isotonic solution of sodium perrhenate(VII) with a total activity of 185 GBq and a radiochemical purity of 99.9%. The series of sodium perrhenate(VII) products obtained are distributed to national nuclear medicine centres.

REFERENCES

- [1] INTERNATIONAL ATOMIC ENERGY AGENCY, Development of Generator Technologies for Therapeutic Radionuclides, Rep. Research Coordination Meeting (333-F2-RC-958), IAEA, Vienna (2004).
- [2] BRODSKAYA, G.A., GAPUROVA, O.U., "Development of high-activity $^{188}\text{W}/^{188}\text{Re}$ generator" Radiokimiya, 35 (1993) 92-97.

SESSION 6

- [3] DADACHOV, M., LAMBRECHT, R.M., HETHERINGTON, E., "An improved Tungsten $^{188}\text{W}/^{188}\text{Re}$ gel generator based on zirconium tungstate". J. Radioanal. Nucl. Chem. Letters, 188 (1994) 267-278.
- [4] DADACHOV, M., LAMBRECHT, R.M., " $^{188}\text{W}/^{188}\text{Re}$ gel generator based on metal tungstates" J. Radioanal. Nucl. Chem. Letters, 200 (1995) 211-221.
- [5] SAWLEWICZ, K., et al., Elaboration of technology for production of W-188/Re-188 generator. Internal Report of RC POLATOM, No 11, 1999.
- [6] SAWLEWICZ, K., et al., Exploitation investigation of W-188/Re-188 generator. Internal Report of RC POLATOM, No 15, 2000.
- [7] KONIOR, M., ZELEK, Z., Optimisation of manufacturing parameters of W-188/Re-188 generators. Internal Report of RC POLATOM, No 24, 2004.
- [8] POLATOM, Technological – dosimetric instruction for production of sodium perrhenate (VII) Re-188 POLATOM, 31.03.2005.

HYDROXYAPATITE BASED ^{99}Mo - $^{99\text{m}}\text{Tc}$ AND ^{188}W - ^{188}Re GENERATOR SYSTEMS

F. MONROY-GUZMÁN*, V.E. BADILLO-ALMARAZ**,
J.A. FLORES DE LA TORRE**, J. COSGROVE***, F.F. KNAPP, Jr.***

*ININ, Carretera Mexico-Toluca
Email: fmg@nuclear.inin.mx

** Universidad Autónoma de Zacatecas, CREN, Zacatecas

Mexico

*** Nuclear Science and Technology Division,
Oak Ridge National Laboratory, Oak Ridge, Tennessee,

United States of America

Abstract

This paper describes studies evaluating the use of hydroxyapatite as the adsorbent material for both ^{99}Mo - $^{99\text{m}}\text{Tc}$ and ^{188}W - ^{188}Re generator systems. Hydroxyapatite is an insoluble solid with anion exchange properties. A study of the sorption behaviour of ^{99}Mo , $^{99\text{m}}\text{Tc}$, ^{188}W and ^{188}Re on hydroxyapatite in NaCl medium was evaluated by batch experiments. The results demonstrated that while ^{99}Mo , $^{99\text{m}}\text{Tc}$ and ^{188}Re are not adsorbed by the hydroxyapatite in NaCl solutions ($K_d < 5$), ^{188}W is strongly adsorbed ($K_d > 500$). On the basis of these measurements, hydroxyapatite ^{188}W - ^{188}Re generator systems were then constructed and eluted in NaCl solutions. The hydroxyapatite based ^{188}W - ^{188}Re generator performances are presented.

1. INTRODUCTION

Radioisotope generator systems have traditionally played a central role in nuclear medicine by providing short lived radioisotopes for research and clinical applications [1-4]. Technetium-99m (half-life 6 h) is the most widely used radionuclide in diagnosis and ^{188}Re (16.9 h) is a particularly attractive candidate for therapeutic applications. These radioisotopes are usually provided by the ^{99}Mo - $^{99\text{m}}\text{Tc}$ and ^{188}W - ^{188}Re generator systems in which ^{99}Mo and ^{188}W are adsorbed onto an alumina chromatographic column and the less

strongly bound $^{99m}\text{TcO}_4^-$ and $^{188}\text{ReO}_4^-$ are eluted with isotonic saline solutions. Alternative adsorbent materials have also been investigated in order to improve the performance of these generators. In the case of ^{99}Mo – ^{99m}Tc generator systems, hydrous zirconium oxide [5], manganese dioxide [6, 7], 1X8 Dowex resins [8], NCA [9] and reverse phase chromatography using 2-ethylhexyl phosphoric acid on kieselguhr [10] have been reported while for the ^{188}W – ^{188}Re generators the most published studies relate to adsorption of W and Re using anion exchangers [11–13] activated carbon [14] or zirconium dioxide [15]. Nevertheless, in these systems, the separation of rhenium or technetium from tungsten or molybdenum is usually performed with mineral acids which are incompatible with the medical applications and require additional steps to remove the acids.

Hydroxyapatite is an insoluble solid with anion exchange properties which has been proposed for retaining fission products from nuclear wastes [16]. For this reason, the authors have proposed evaluation of hydroxyapatite as a potential adsorbent material for both ^{99}Mo – ^{99m}Tc and ^{188}W – ^{188}Re generator systems. Sorption studies were designed in order to study the affinity of hydroxyapatite for these radionuclides and to provide evidence of the feasibility of this system. The performance of the generator systems constructed using hydroxyapatite was evaluated.

2. SORPTION STUDIES

2.1. Experimental

All chemicals used were of analytical grade. Bio-Gel HTP hydroxyapatite ($\text{Ca}_{10}(\text{PO}_4)_6(\text{OH})_2$) from Bio-Rad was used. The hydroxyapatite was washed with 0.4M and 0.04M NaH_2PO_4 solutions at pH6.5. It was then dried at 40°C for 24 h and sieved. A 200–400 mesh was used to determine the distribution coefficients of the hydroxyapatite particles.

2.1.1. Radionuclides

Tungsten-187 was produced by irradiation of 250 mg of tungsten oxide (WO_3) in the TRIGA MARK III Reactor at ININ at a neutron fluence rate of $1.6 \times 10^{12} \text{ n}\cdot\text{cm}^{-2}\cdot\text{s}^{-1}$ for 100 s. The oxide was dissolved in a 9M NaOH solution and H_2O_2 , and adjusted to pH7 with 12M HCl.

The ^{99}Mo , ^{99m}Tc and ^{188}Re were provided by ININ's Radioactive Material Department as solutions of sodium ^{99}Mo -molybdate ($\text{Na}_2^{99}\text{MoO}_4$) (MDS Nordion), sodium ^{99m}Tc -pertechnetate ($\text{Na}^{99m}\text{TcO}_4$) and sodium ^{188}Re -

SESSION 6

perrhenate ($\text{Na}^{188}\text{ReO}_4$) derived from the elution of ^{99}Mo - $^{99\text{m}}\text{Tc}$ (GETEC, ININ, Mexico) and ^{188}W - ^{188}Re (ORNL) generators respectively.

The sodium ^{188}W -tungstate solutions ($\text{Na}_2^{188}\text{WO}_4$) were provided by ORNL (37 kBq/ μL).

All radioactivity measurements were performed with a coaxial gamma detector HPGe (Canberra 7229P) connected to a PC multichannel analyser (ACUSSPECT-A, Canberra).

2.1.2. Determination of distribution coefficients

Distribution coefficients (Kd) for static conditions were determined by the radiotracer technique in 0.9% NaCl as a function of pH. For this purpose, 25 mL of a 0.9% NaCl solution (V_{sol}) was mixed with 250 mg (m_h) of the hydroxyapatite. The pH of the 0.9% NaCl solutions was adjusted at different values with 0.1M NaOH and a pH>5 was established in order to avoid the dissolution of the hydroxyapatite which is unstable in acid media [16, 17].

Solid and aqueous solutions were brought to equilibrium by shaking the mixture for 14 d and then 100 μL of the radioactive solutions (3.7 kBq/ μL) added containing $^{99}\text{MoO}_4^{2-}$, $^{187}\text{WO}_4^{2-}$, $^{99\text{m}}\text{TcO}_4^-$ or $^{188}\text{ReO}_4^-$. The mixture was again shaken for 24 h. Three reference solutions were prepared with the same amount of radioactive solution in 25 mL of 0.9% NaCl solution. Finally, the hydroxyapatite and the liquid phase were separated by centrifugation. The distribution coefficients of radionuclides were determined by comparing the activity of a 2 mL aliquot of the liquid phase (A_{sol}) with that of 2 mL of the three reference solutions (A_{stand}). Distribution coefficients were determined by means of the following equation:

$$K_d = \frac{\text{Activity per gram of hydroxyapatite}}{\text{Activity per mL of solution}} = \left(\frac{A_{\text{stand}} - A_{\text{sol}}}{A_{\text{sol}}} \right) \left(\frac{V_{\text{sol}}}{m_h} \right)$$

The corresponding photopeaks used to calculate the Kd value were 739.4 keV for ^{99}Mo , 141 keV for $^{99\text{m}}\text{Tc}$, 685.74 keV for ^{187}W and 155 keV for ^{188}Re .

2.1.3. Separation factor

From the Kd values were calculated the separation factors ($\alpha_{\text{A,B}}$) which are defined as the ratio of the distribution coefficients of two adsorbed solutes measured under the same conditions:

$$\alpha_{A,B} = \frac{Kd_A}{Kd_B}$$

By convention, the solutes designated as A and B are chosen so as to make $\alpha > 1$. For column chromatography, this separation factor is the relative retention value calculated for two adjacent peaks and provides information about the feasibility to separate the solutes A and B.

2.2. Results

2.2.1. Sorption of W, Re, Mo and Tc on hydroxyapatite

The effect of the 0.9% NaCl solution pH on the sorption of Mo(VI), Tc(VII), W(VI) and Re(VII) on hydroxyapatite is shown in Fig. 1. Technetium and rhenium present Kd values in the range 0–3 mL/mg in the pH range studied. These values do not show a specific tendency in connection with the pH, although the molybdenum shows an increase in the Kd values as the NaCl solutions become more basic. However, its Kd values are as weak as those of technetium and rhenium. These data demonstrate that technetium, rhenium and molybdenum are not retained on the hydroxyapatite under these conditions.

In the case of tungsten, the Kd values follow an exponential decay model ($y = ae^{-bx}$). The tungsten is retained on hydroxyapatite at $\text{pH} < 7.5$ and not adsorbed at $\text{pH} > 7.5$. The Kd values decrease abruptly from $\text{pH} 6.5$ and at about $\text{pH} 7.9$ they are practically zero. The highest Kd value (~ 400 mL/mg) is obtained at $\text{pH} \sim 6.5$.

The $\alpha_{\text{Mo,Tc}}$ and $\alpha_{\text{W,Re}}$ separation factors shown in Fig. 2 were calculated from the Kd values presented in Fig. 1. It is important to note that high α values indicate a more favourable separation between the elements while α values of less than 1 mean an impracticable separation. According to the authors' data, technetium and molybdenum cannot be separated using 0.9% NaCl solutions, while rhenium and tungsten can be separated with 0.9% NaCl solutions at $\text{pH} < 7.5$.

In conclusion, the hydroxyapatite can be only used as an adsorbent of the ^{188}W – ^{188}Re generators, assuming that 0.9% NaCl solutions at $\text{pH} < 7.5$ are employed as eluant.

Adsorption studies of molybdenum, technetium, tungsten and rhenium on hydroxyapatite using 0.01M CaCl_2 solution eluants were also performed. However, these data are not presented in this work [18].

SESSION 6

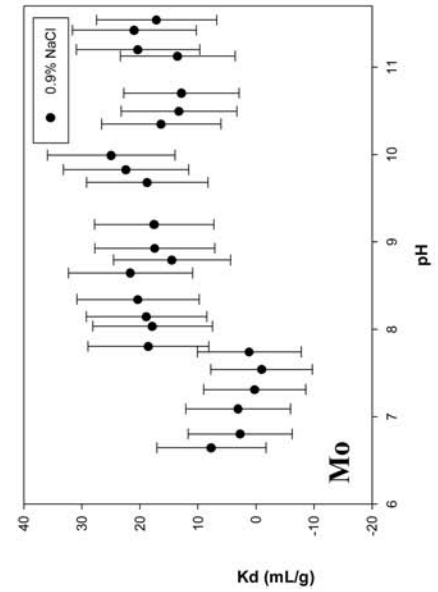
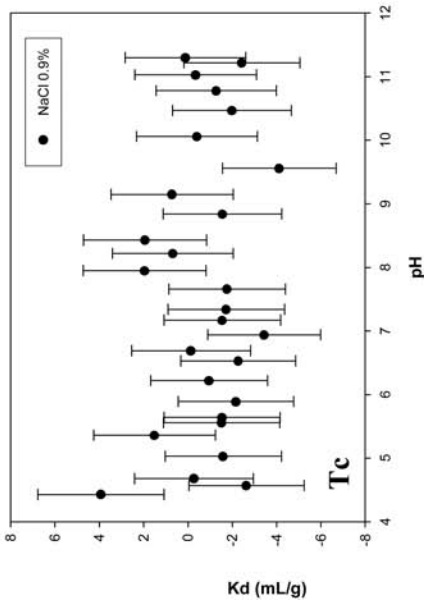
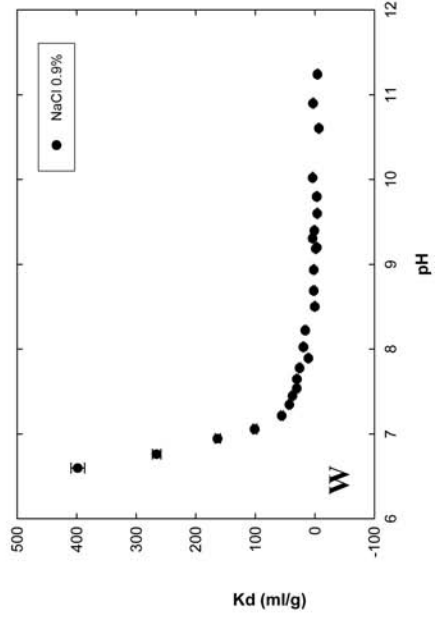
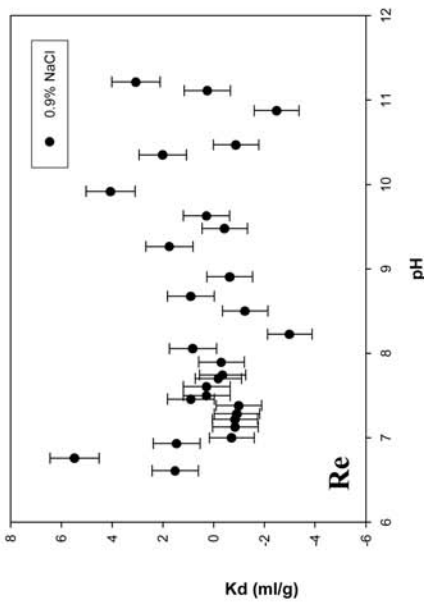


FIG. 1. Sorption behaviour of Tc, Mo, Re and W on hydroxyapatite as a function of pH in 0.9% NaCl.

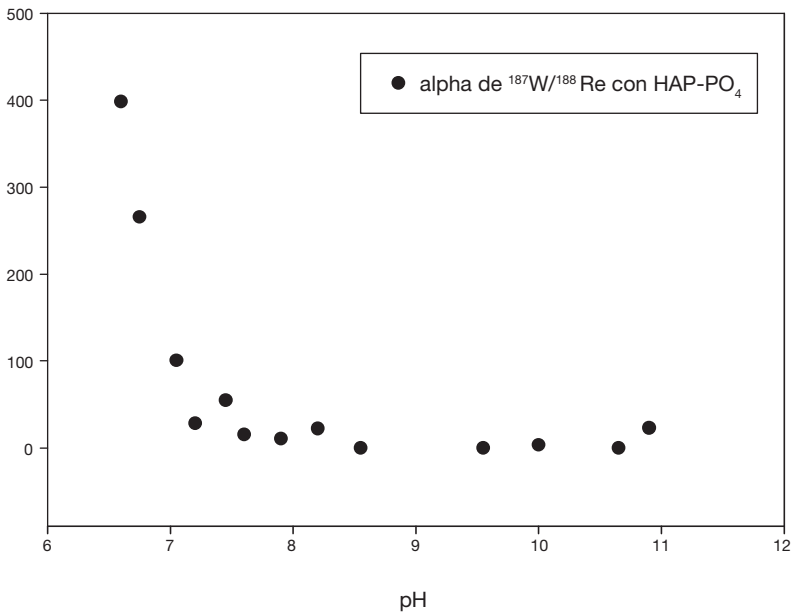
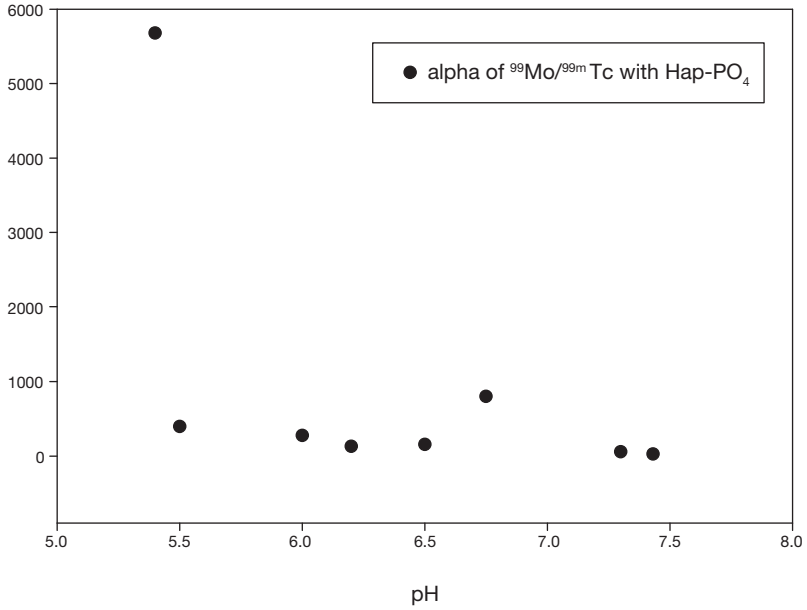


FIG. 2. Separation factor of Mo and Tc ($\alpha_{\text{Mo}, \text{Tc}}$) and W and Re ($\alpha_{\text{W}, \text{Re}}$) on hydroxyapatite as a function of pH in 0.9% NaCl.

3. PREPARATION OF ^{188}W - ^{188}Re GENERATORS

From the results of the adsorption data obtained in the previous section for tungsten and rhenium, hydroxyapatite based ^{188}W - ^{188}Re generators were constructed. The effect of the 0.9% NaCl solution pH and the particle size of the hydroxyapatite on the ^{188}W - ^{188}Re generator performance were evaluated.

3.1. Experimental

3.1.1. Preparation and analysis of generators

Poly-Pre chromatography columns (0.8 cm \times 4 cm) from Bio-Rad were filled with hydroxyapatite (500 mg) previously mixed in the selected medium where $^{188}\text{WO}_4^{2-}$ is strongly retained while $^{188}\text{ReO}_4^-$ is weakly adsorbed. The medium under investigation was then percolated through the column. The generators were eluted every 3 d over a period of one month. The ^{188}Re elution profile was obtained by collecting a volume fraction and measuring under well-defined geometric conditions. The elution efficiency was calculated by comparing the experimental and theoretical activities of $^{188}\text{ReO}_4^-$. The radionuclide purity of the $^{188}\text{ReO}_4^-$ eluates were determined in relation to the ^{188}W activities present in the elutions. These eluates were measured after 10 d for 3600 s in the photopeak of 155 keV.

The radiochemical purity of the ^{188}Re eluates was determined by TLC using silica gel 60 F254 TLC aluminium sheet as the solid phase and acetonitrile as the mobile phase. The $^{188}\text{ReO}_4^-$ R_f was 1.

The presence of phosphates in the eluates (chemical purity) was determined by AQUANAL® Professional Vario H powder packs (Riedel-deHaën) using photometry.

3.2. Results

3.2.1. Performance of hydroxyapatite based ^{188}W - ^{188}Re generators

3.2.1.1. Effect of NaCl solution pH

The sorption data for the tungsten and rhenium on hydroxyapatite in NaCl solutions showed the feasibility of separating both elements if the pH of the NaCl solutions is less than 7.5 (see Section 2). The pH values of the 0.9% NaCl solutions used for elution of the hydroxyapatite based ^{188}W - ^{188}Re generators were 5.5, 6.0, 6.3 and 6.5, in order to evaluate the effect on the performance of the generators (see Table 1). These pH values were selected

TABLE 1. PERFORMANCE OF HYDROXYAPATITE BASED ^{188}W - ^{188}Re

0.9% NaCl pH	Size particle (μm)	Eluate volume (mL)	Average ^{188}Re elution efficiency (%)	Average ^{188}W breakthrough (%)	^{188}Re radiochemical purity (%)	Phosphates ($\mu\text{g}/\text{cm}^3$)	pH eluates
5.5	38-75	5.4	44.8	0.0530	99.2	>1000	6.5
6.0	38-75	4.6	71.0	0.0346	93.5	>1000	6.5
6.3	38-75	5.1	65.7	0.0339	96.2	>1000	6.5
6.5	38-75	3.5	66.1	0.0280	99.3	>1000	6.5
6.3	75-150	4.4	67.4	0.0401	94.1	>1000	6.5
6.3	38-75	5.1	65.7	0.0339	96.2	>1000	6.5
6.3	38	2.1	64.0	0.0811	89.9	>1000	6.5

SESSION 6

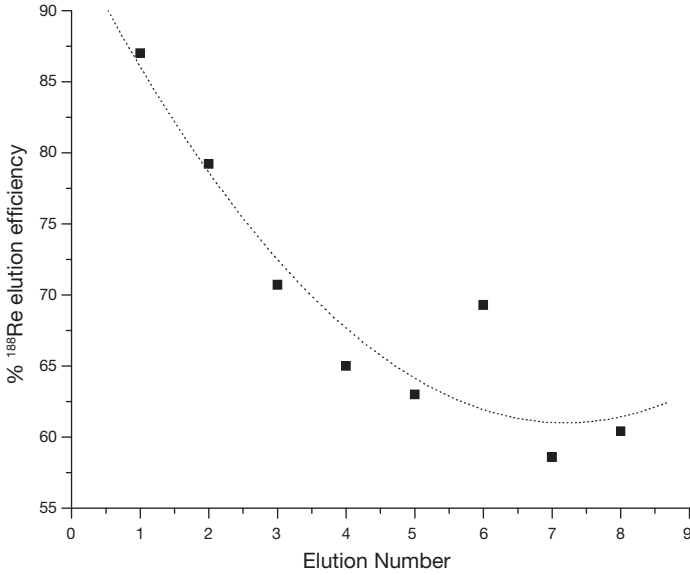


FIG. 3. Behaviour of hydroxyapatite based ¹⁸⁸W-¹⁸⁸Re elution efficiency as a function of the elution number.

because the best separation factors ($\alpha_{W,Re}$) in these experimental conditions were obtained at $pH < 6.6$. It is important to note that the 0.9% NaCl solutions have an initial pH of about 6. In fact, the lowest pH value shown in Fig. 1 corresponds to the 0.9% NaCl solutions without pH adjustment, and this pH value increased to about 6.5 after reaching equilibrium. All the ¹⁸⁸Re eluates obtained in this study presented a pH value of 6.5 and phosphate concentrations of more than 1000 ppm (see Table 1). In addition, the efficiencies decreased in each elution following an exponential decay model (see Fig. 3) tending to elution efficiency values of about 65% in all the generators except for the generator eluted with 0.9% NaCl solution at pH5.5 which presented the lowest elution efficiencies (35–60%).

The highest average elution efficiency was obtained in the generator eluted with 0.9% NaCl solutions at pH6, while the lowest efficiency and highest ¹⁸⁸W breakthrough resulted when using 0.9% NaCl solutions at pH5.5. The efficiency of the generators eluted from 0.9% NaCl solutions at pH values of more than 6 tends to be about 65%.

During the washing and the first elution of the generators (see Table 2), traces of ¹⁹¹Os and ¹⁹²Ir in the ¹⁸⁸Re eluates were detected. The ¹⁹¹Os and ¹⁹²Ir are co-produced during reactor production of ¹⁸⁸W from irradiation of ¹⁸⁶W as has been described earlier [15]. The washing presented the highest percentage

TABLE 2. RADIONUCLIDE PURITY OF THE ^{188}Re ELUATES

0.9% NaCl pH	Particle size (μm)	Elution no.	^{191}Os breakthrough (%)	^{192}Ir breakthrough (%)	^{188}W breakthrough (%)
5.5	38–75	washing	5.52E4	2.08E3	0.1089
		1	1.93E4	3.65E4	0.0177
6.0	38–75	washing	4.83E4	1.90E3	0.0055
		1	5.87E5	1.91E4	0.0066
6.3	38–75	washing	7.59E4	2.85E3	0.0078
		1	5.10E5	2.25E4	0.0079
6.5	38–75	washing	2.67E4	2.41E3	0.0011
		1		5.52E5	0.0008
6.3	75–150	washing	2.43E4	2.47E3	0.0134
		1		1.21E4	0.0016
6.3	38–75	washing	7.59E4	2.85E3	0.0078
		1	5.10E5	2.25E4	0.0079
6.3	38	washing	3.29E4	2.70E3	0.0023
		1		1.49E4	0.0043

of ^{191}Os ($\sim 5 \times 10^{-4}$) and ^{192}Ir ($\sim 1 \times 10^{-3}$) breakthrough which decreased by about ten times in the first elution and disappeared from the second elution. The percentages of ^{188}W breakthrough tend to increase from the fifth elution (Fig. 4), therefore, the average ^{188}W breakthroughs shown in the Table 1 are larger than those summarized in Table 2. The lowest and highest average ^{188}W breakthrough values and elution volumes were obtained in the generators eluted with 0.9% NaCl solution at pH6.5 and 5.5, respectively. All the generators presented radiochemical purities of more than 93%. The chemical form of the rhenium in the eluates is consequently $^{188}\text{ReO}_4^-$.

3.2.1.2. Effect of the hydroxyapatite particle size

The hydroxyapatite particle size has no significant effect on the efficiency of the ^{188}W – ^{188}Re generators. The efficiencies obtained were about 65% and all the ^{188}Re eluates presented pH values of 6.5 and phosphate concentrations of more than 1000 ppm, whereas the elution volumes and the percentage ^{188}W breakthroughs decreased with a diminution of the hydroxyapatite particle size.

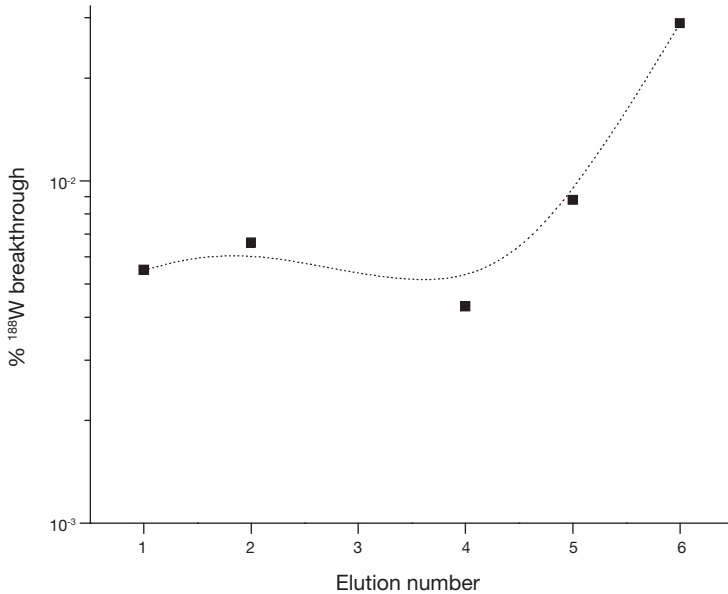


FIG. 4. Percentage ¹⁸⁸W breakthrough behaviour of the hydroxyapatite based ¹⁸⁸W-¹⁸⁸Re generator.

4. DISCUSSION

The tungsten and molybdenum form MoO_4^{2-} and WO_4^{2-} anions at pH values >5.5 and concentrations $<10^{-3}\text{M}$ [19, 20] and in accordance with the authors' radiochemical purity (see Table 1) determinations of the rhenium eluates, this element is present as ReO_4^- .

The anion retention on hydroxyapatite can be explained by surface properties [16], in particular the existence of surface calcium sites is suggested by several authors [21, 22] pointing to ligand exchange as the mechanism of the anionic surface hydroxyl reaction. For the basic solutions, the weak sorption of MoO_4^{2-} , TcO_4^- and ReO_4^- anions may be interpreted in terms of the competition between these anions and the hydroxyl species, whose source is the solution pH regulator, NaOH, for these same Lewis acid sites. This replacement of the surface group by the hydroxyl group has been observed on this solid in another study [16] which investigated the sorption of phosphate ions on these calcium sites, concluding that the calcium metal ion is a Lewis acid, i.e. the OH group may be replaced by another Lewis base supplied by the solution. The results of the authors sorption studies appear to agree with these hypotheses for the basic medium, although at $\text{pH}<7$ only the WO_4^{2-} ion was adsorbed on the

hydroxyapatite. Considering that the WO_4^{2-} , MoO_4^{2-} , ReO_4^- , TcO_4^- and Cl^- anions are Lewis bases (electron donors), it is possible to assume that the WO_4^{2-} and Cl^- anions are stronger electron donors than MoO_4^{2-} , ReO_4^- and TcO_4^- anions and the Lewis acid–base reaction between WO_4^{2-} and Ca of the hydroxyapatite and Cl^- and Ca are favoured. For that reason the ReO_4^- is not retained in the ^{188}W – ^{188}Re generator eluted with 0.9% NaCl solutions.

The decrease in the generator efficiency with the elution number could be attributed to the reduction of the Re(VII) to Re(IV). This hypothesis is based on the fact that the Tc(IV) in NaCl solutions is slowly retained on alumina. Two adsorption mechanisms of the Tc(IV) on alumina have been suggested: (1) Tc(IV) species present a higher affinity for the hydroxyl than the Tc(VII) and (2) the precipitation of the TcO_2 caused by an increase in its concentration on the alumina [21]. Considering that the hydroxyapatite also has hydroxyl groups, it is possible that the Re(VII) presents the same behaviour as Tc(VII) and can be reduced to Re(IV). In order to reduce this effect it is recommended that the generator be dried completely after each elution or that an oxidant agent be added to the eluant solution, as has been described earlier for the alumina based system [23].

The release of phosphate ions during the elution of the generators could be connected with (1) the release or sorption of the calcium or phosphate ions to reach the solubility equilibrium of the hydroxyapatite, that is, the dissolution of the hydroxyapatite caused by the medium's conditions (pH, electrolyte concentration); or (2) the replacement of the phosphate groups in the hydroxyapatite by the WO_4^{2-} ions. On the other hand, Mo(VI) adsorption studies on hydroxyapatite at different NaCl concentrations have shown that the distribution coefficient of the Mo(VI) is lower at low concentrations and rises with increasing NaCl concentration [17]. This effect is attributed to the Donnan potential produced by the anion and cation concentration differences between the hydroxyapatite and the solution. Equilibrium is established in which the tendency of the ions to level out the existing concentration differences is balanced by the action of the electric field [24]. Consequently, it is possible that the Donnan equilibrium also causes the release of the phosphate ions during the elution of the ^{188}W – ^{188}Re generators with the 0.9% NaCl solutions.

The variation of the ^{188}W breakthrough percentages in the ^{188}Re eluates with the elution number ranges from values of 10^{-3} or less, to 10^{-2} . This could be considered a disadvantage of the hydroxyapatite based ^{188}W – ^{188}Re generators with respect to the alumina based systems, which present ^{188}W breakthrough percentages of about 10^{-5} to 10^{-3} [25, 26]. However, the evident release of phosphate ions during the elution of the generators allows the authors to deduce that the increase in the ^{188}W breakthrough percentages is possibly caused by the dissolution of the hydroxyapatite by the NaCl solutions, which

SESSION 6

could be reduced by washing with phosphate or calcium solutions after each elution with 0.9% NaCl. In order to prove this hypothesis additional experiments are required.

5. CONCLUSIONS

Hydroxyapatite does not retain Mo(VI), Tc(VII) and Re(VII) in 0.9% NaCl solutions at pH>6. The W(VI) is adsorbed on hydroxyapatite in 0.9% NaCl solutions at pH values in the range 6.5–7.5. The sorption on hydroxyapatite depends on the pH of the medium. The sorption mechanism of the anions on hydroxyapatite can be explained by the replacement of the hydroxyl or phosphate groups by the other anions. It is feasible to construct ^{188}W – ^{188}Re generators based on hydroxyapatite in a 0.9% NaCl medium but not ^{99}Mo – $^{99\text{m}}\text{Tc}$ generators. The decrease in hydroxyapatite based ^{188}W – ^{188}Re generator efficiency can be attributed to the reduction of Re(VII) to Re(IV) which is slowly adsorbed by the hydroxyl groups.

ACKNOWLEDGEMENTS

This work was supported by IAEA research contract No. 12879. Gratitude is also expressed (F. Monroy-Guzmán) to The United States–Mexico Foundation for Science (FUMEC-AMC) (Summer stay in EU 2005) and ORNL, managed by UT Battelle, LLC, for the US Department of Energy, under contract No. DE-AC05-00OR22725.

REFERENCES

- [1] ROESCH, F., KNAPP, F.F., Jr., "Radionuclide Generators", in Handbook of Nuclear Chemistry, Volume 4, Chapter 3, pp. 81-118; A. Vertes, N. S. Klencsar, Editors; Kluwer Academic Publishers, Amsterdam (2003).
- [2] MIRZADEH, S., KNAPP, F.F., Jr., "Biomedical Radionuclide Generators Systems", *Invited Review*, Centennial Issue - Discovery of Radioactivity, In, *J. Radioanalyt. Nucl. Chem.*, 203, 469-486 (1996).
- [3] MIRZADEH, S., KNAPP, F.F., Jr., "Biomedical Radionuclide Generators Systems", *Invited Review*, for publication in the Centennial Issue - *Discovery of Radioactivity*, *Journal of Radioanalyt. Nucl. Chem.* (1995), 203, 469-486 (1996).
- [4] KNAPP, F.F., Jr., MIRZADEH, S., "The Continuing Important Role of Radionuclide Generator Systems for Nuclear Medicine", *Invited Review Article*, *Eur. Jour. Nucl. Med.*, 21, 1151-1166 (1994).

- [5] PINAJIAN, J.J., A technetium-99m generator using hydrous zirconium oxide. *Int. J. App. Rad. Isot.*, 17 (1966) 664-670.
- [6] MELONI, S., BRANDONE, A., A new technetium-99m generator using manganese dioxide. *Inter. J. App. Rad. Iso.*, 19 (1964) .
- [7] SERRANO GÓMEZ, J., Sorción de iones MoO_4^{2-} , en la hidrotalcita calcinada y separación del $^{99\text{m}}\text{Tc}$ generador. Ph.D. Thesis Metropolitan Autonomous University. Mexico, (2002).
- [8] CHATTOPADHYAY, S., DAS, M.K., SARKAR, B.R., RAMAMORTHY, N., Separation of pertechnetate from molybdate by anion-exchange chromatography: Recovery of $^{99\text{m}}\text{Tc}$ from (n,γ) ^{99}Mo and suitability for use in central radiopharmacy (CRPh). *Radiochim. Acta.* 90 (2002) 417.
- [9] BONARDI, M., BIRATTARI, C., GROPPI, F., SABBIONI, E., Thin-target excitation functions, cross-section and optimized thick-target yields for $^{\text{nat}}\text{Mo}(p,xn)^{94\text{g},95\text{m},95\text{g},96(\text{m}+\text{g})}\text{Tc}$ nuclear reactions induced by protons from threshold up to 44 MeV. No Carrier added radiochemical separation and quality control. *App. Rad. Isot.* 57 (2002) 617-635.
- [10] D'OLIESLAGER, W., INDESTEEGE, J., D'HONT, M., Separation of molybdenum and technetium on di-2-ethylhexylphosphoric acid (D-2-ehpa)-kieselguhr. *Talanta.* 22 (1975) 395-399.
- [11] KURODA, R., ISIDA, T., SEKI, T., OGUMA, K., *Chromatographia*, 15 (1982) 223.
- [12] LEE, B., IM, H.-J., LUO, H., HAGAMAN, E.W., DAI, S., Synthesis and Characterization of Periodic Mesoporous Organosilicas as Anion Exchange Resins for Perrhenate Adsorption. *Langmuir*, 21 (2005)5372 -5376.
- [13] KHALID, M., MUSHTAQ, A., IQBAL, M.Z., Sorption of tungsten(VI) and rhenium(VII) on various ion-exchange materials. *Separation Science and Technology*, 36(2001)283 – 294.
- [14] LOSKUTOV, A.I., ANDRIANOV, S.F., SIMONOV, E.G., KUZIN, I.A., *Zh. Prikl. Khim.* 49 (1976) 728.
- [15] MALISHEV, K.W., SMIRNOV, V.V., *Radiokhymica*, 17 (1975) 249.
- [16] BADILLO-ALMARAZ, V.E., “Etude des mécanismes de retention d’actinides et de produits de fission sur l’hydroxyapatite”. Ph. D. Thesis. University of Paris XI, Paris (1999).
- [17] VÁZQUEZ-GUERRERO, S., BADILLO-ALMARAZ, V.E., MONROY-GUZMÁN, F., “Influencia del electrolito en el fijación de ^{99}Mo en hidroxiapatita como matriz del generador $^{99}\text{Mo}/^{99\text{m}}\text{Tc}$ ”. (Proc. XVI SNM Annual Meeting and XXIII SMSR Annual Meeting, Oaxaca, 2005) SNM, Oaxaca Mexico (2005) (CD-ROM file EX6/1).
- [18] AGUILAR-DORADO, I.C., MONROY-GUZMÁN, F., BADILLO-ALMARAZ, V.E., Estudio de la viabilidad de la hidroxiapatita como matriz del generador $^{99}\text{Mo}/^{99\text{m}}\text{Tc}$. (Proc. International Joint Meeting Cancun 2004 LAS/ANS-SNM-SMSR, XV SNM Annual Meeting and XXII SMSR Annual Meeting). SNM, Cancún, Mexico (2004) (CD-ROM file EX7/1).

SESSION 6

- [19] HSIEH, B.T., CALLAHAN, A.P., BEETS, A.L., TING, G., KNAPP, F.F., Jr., Ascorbic Acid/Saline Eluant Increases Re-188 Yields After "Wet" Storage of W-188/Re-188 Generators, *Appl. Radiat. Isot.* 47 (1996) 23-26
- [20] TYTKO, H.K., GLEMSER, O., Isopolymolybdates and Isopolytungstates, *Advances Inorganic Chemistry and Radiochemistry*. Vol. 19, Academic Press, USA. (1976).
- [21] STAMMOSE, D., Propriétés physico-chimiques des aluminés γ : application au générateur isotopique molybdène-technétium“. Ph. D. Thesis. University of Paris VI, Paris (1983).
- [22] WU, L., FORSLING, W., SCHINDLER, P.W., Surface Complexation of calcium mineral in aqueous solution. 1. Surface protonation at fluoroapatite-water interfaces. *J. Coll. Inter. Sci.* 147(1), (1991)178-185.
- [23] CASES, J.M., JACQUIER, P., SMANI, S.M., POIRIER, J.E., BOTTERO, J.Y., Propriétés électrochimiques superficielles des apatites sédimentaires et flottabilité. *Revue de l'Industrie Minérale*. Janvier-Février, 1-2, (1989).
- [24] HELFFERICH, F., Ion Exchange. Dover, USA. 1995.
- [25] KNAPP, F.F., Jr., Use of Rhenium-188 for Cancer Treatment,” *Cancer Biotherapy and Radiopharm.*, 13(5), 337-349 (1998).
- [26] KNAPP, F.F., Jr., et al., Development of the Alumina-Based Tungsten-188/Rhenium-188 Generator and Use of Rhenium-188-Labeled Radiopharmaceuticals for Cancer Treatment, *Anticancer Research*, 17 (1997) 1783–1796.

FOSTERING DEVELOPMENT EFFORTS TOWARDS (a) SMALL SCALE LOCAL PRODUCTION OF ^{99}Mo FROM LEU TARGETS AND (b) GEL GENERATOR FOR $^{99\text{m}}\text{Tc}$ USING (n, γ) ^{99}Mo : THE IAEA ROLE

N. RAMAMOORTHY*, I. GOLDMAN**, P. ADELFRANG**

*Division of Physical and Chemical Sciences
Email: N.Ramamoorthy@iaea.org

** Division of Nuclear Fuel Cycle and Waste Technology

International Atomic Energy Agency,
Vienna

Technetium-99m is the most widely used radioisotope in diagnostic nuclear medicine in the world with almost 40 000 procedures performed every day [1]. It is commonly obtained by eluting an alumina column loaded with ^{99}Mo of high specific activity obtained by thermal neutron fission of ^{235}U . Highly enriched uranium (HEU) targets of >95% ^{235}U are in use for this purpose [2]. Four commercial companies, namely, MDS Nordion (Canada), IRE (Belgium), Mallinckrodt (Netherlands) and Nuclear Technology Products (South Africa) cater for most of the ^{99}Mo needs using HEU targets. ANSTO (Australia) and CNEA (Argentina) are among the other few producers. The former is at present using uranium dioxide pellets enriched to 2.2% ^{235}U , while the latter is using LEU targets, i.e. <20% ^{235}U content. The former is also slated to switch over to using LEU targets of <20% ^{235}U after the commissioning of a new reactor facility. In order to assure secure availability of ^{99}Mo , several research reactors are used for irradiating uranium targets. The need for far more assured research reactor irradiation services is being highlighted by industrial companies engaged in radioisotope production [2].

Measures advocated for reducing nuclear proliferation risks warrant that any materials of weapons potential be phased out of conventional commercial trade and HEU is high on the list. The Reduced Enrichment for Research and Test Reactors (RERTR) programme is a major initiative in this regard from the US Department of Energy, which is handled by the Argonne National Laboratory (ANL). The main activities involve supporting the conversion of HEU fuels to LEU fuels in research reactors and the return of fresh and spent HEU fuel to the country of origin. Another related aim has been the

development and deployment of LEU targets for production of fission produced ^{99}Mo ('fission moly'). Accordingly, ANL developed a technology for production of 'fission moly' using LEU targets and the process know-how, referred to as the 'modified Cintichem process', is available for adaptation by interested Member States [3]. This method uses an LEU foil target, while an alternative target is a mini-plate target, developed by CNEA [3]. There are two processing routes: the alkaline dissolution and the acid dissolution methods. Both methods involve multiple stages of ion exchange chromatography for separation and subsequent purification of ^{99}Mo . The scope for separation of ^{131}I as a by-product has also been demonstrated.

Switching over to the use of LEU targets over a defined period of time by all the major industrial producers of ^{99}Mo would be necessary, but owing to associated commercial aspects such a discussion is beyond the purview of this paper.

Amongst the alternative $^{99\text{m}}\text{Tc}$ delivery systems feasible using $(n,\gamma)^{99}\text{Mo}$ of low-medium specific activity, the gel generator based on zirconium molybdate- ^{99}Mo (Zr^{99}Mo) is attractive in terms of user friendliness, thanks to the convenience of column operation [4, 5]. This would be a good substitute for the chromatographic alumina column generator, if there is ready access to $(n,\gamma)^{99}\text{Mo}$ of specific activity 0.5–1 Ci/g of Mo and process technology along with reliable process gadgets for gel preparation. Procedures for preparation as well as evaluation of the clinical utility of gel generators are successfully established, but the process is demanding in terms of remote handling facilities for robust and safe operation [5–7].

The concept of post-elution concentration of perrhenate and pertechnetate mooted by the ORNL group and the growth of centralized radiopharmacy service providers have given a fillip to the prospects of using large gel bed (10–25g) generators loaded with $(n,\gamma)^{99}\text{Mo}$ through the dual purpose use of the secondary trap column of alumina for ^{99}Mo necessary for Zr^{99}Mo gel generators [8, 9]. The effective use of the alumina trap column for 'purification-cum-concentration' of pertechnetate after eluting the large gel bed with deionized water has widened the scope of utility of gel generators, even when faced with the modest specific activities of ^{99}Mo . This fruitful outcome of the post-elution concentration option augurs well for the wider adaptation of gel generator technology [9]. The need for a large quantity of MoO_3 target for reactor irradiation, radionuclidic impurities in the irradiated material and their fate while preparing $^{99\text{m}}\text{Tc}$ gel generator systems have posed interesting challenges, but have been addressed satisfactorily [10].

In the annual meetings of the RERTR, several presentations were made and lately through sessions dedicated to production of ^{99}Mo using LEU targets [3]. Following the RERTR meeting in November 2004 in Vienna, a consultants

meeting was held by IAEA to review the various issues and to consider formulating a coordinated research project (CRP). The extensive work and good results reported in the case of the above two systems form the basis of the CRP launch recommended by the consultants meeting. Comparative assessment of production logistics and the quality control testing aspects of deriving ^{99}Mo from the HEU and LEU targets have been reported by ANL [3]. Small scale production of ‘fission moly’ is envisaged locally in many participant centres under the CRP, with ANL and CNEA providing the technical know-how for production of ^{99}Mo using LEU targets.

By virtue of the vast literature available on gel generators [4–7, 9, 10] and the strategy for exploiting dual use of the alumina trap column for post-elution concentration [9], the Zr^{99}Mo gel generator system appears promising, despite technical complexities. This gel generator option to utilize local production of $(n,\gamma)^{99}\text{Mo}$ will be pursued by a few other participants of the CRP, i.e. those having access to research reactors of suitable flux and assured operational features. Technical know-how for gel generators is expected to be available from India/Brazil.

In view of the need for securing reliable, diverse sources of ^{99}Mo and to discourage the use of HEU targets for ‘fission moly’ production, all options for the local production of ^{99}Mo and prospects of novel delivery systems for $^{99\text{m}}\text{Tc}$ merit attention, not only in developing countries, but also in developed countries. The IAEA will foster such efforts.

REFERENCES

- [1] http://www.mds.nordion.com/master_dex.asp?page_id=12
and <http://www.radioisotopes.co.za/>.
- [2] BONET, H., DAVID, B., PONSARD, B., “Production of ^{99}Mo in Europe: Status and Perspectives”, 9th International Topical Meeting RRFM, Budapest, Hungary, www.euronuclear.org/pdf/RRFM2005-postersession4.pdf (2005) 20.
- [3] <http://www.rertr.anl.gov/MO99.html>
- [4] and <http://www.cnea.gov.ar/xxi/para-conocer/uranio/>.
- [5] EVANS, J.V., et al., “A new generator for technetium-99m”, Proc. 3rd World Congress of World Fed. of Nucl. Med. Biol. (RAYNAUD, C., Ed.), Pergamon Press, Paris (1982) 1592.
- [6] INTERNATIONAL ATOMIC ENERGY AGENCY, Alternative Technologies for $^{99}\text{Tc}^{\text{m}}$ Generators, IAEA-TECDOC-852, IAEA, Vienna (1996).
- [7] <http://www.iaea.org/publications>.
- [8] SARASWATHY, P., et al., $^{99\text{m}}\text{Tc}$ gel generators based on zirconium molybdate— ^{99}Mo : Part I and Part II, *Radiochim. Acta* 83 (1997) 97, 103.

- [9] SARASWATHY, P., et al., "Evaluation of preparation and performance of gel column $^{99}\text{Tc}^{\text{m}}$ generators based on zirconium molybdate— ^{99}Mo ", Modern Trends in Radiopharmaceuticals for Diagnosis and Therapy, IAEA-TECDOC-1029, IAEA, Vienna (1998) 385.
- [10] KNAPP, F.F., Jr., et al., "Use of a new tandem cation/anion exchange system with clinical-scale generators provides high specific volume solutions of technetium-99m and rhenium-188", *ibid.*, 419.
- [11] SARKAR, S.K., et al., High radioactive concentration of $^{99\text{m}}\text{Tc}$ from zirconium molybdate – ^{99}Mo gel generator using an acidic alumina column for purification cum concentration, *Nucl. Med. Commun.* 25 (2004) 597.
- [12] SARASWATHY, P., Studies on the separation, characterization and evaluation of technetium-99m: Applicability to ^{99}Mo - $^{99\text{m}}\text{Tc}$ generator for medical use, Ph.D. Thesis, University of Mumbai, Mumbai, India (2002).

NOVEL TECHNETIUM CHEMISTRY
AND RADIOPHARMACEUTICALS: II

(Session 7)

Chairpersons

A. VERBRUGGEN

Belgium

M.R.A. PILLAI

IAEA

NOVEL TECHNETIUM CHEMISTRY AND RADIOPHARMACEUTICALS

Tc(V), Tc(III) or Tc(I) – which way to go for keeping Tc radiopharmaceuticals alive?

R. ALBERTO, S. KUNZE, S. MUNDWILER, B. SPINGLER

Institute of Inorganic Chemistry,

University of Zurich,

Zurich, Switzerland

Email: ariel@aci.unizh.ch

Abstract

Novel ^{99m}Tc based radiopharmaceuticals which have found market introduction are rare. Despite enormous research efforts over the past 10 years, only very few new compounds (^{99m}Tc or ^{188}Re) contribute to public health. New radiopharmaceuticals may belong to the class of perfusion or targeting agents in which a complex is conjugated to a receptor binding molecule. While other techniques are developing very rapidly, ^{99m}Tc based radiopharmacy risks losing its leading role in nuclear medicine to PET or MRI. Despite the authors' pessimistic view for the future of ^{99m}Tc research, ^{186}Re – ^{188}Re and other therapeutic radionuclides will fuel research in group 7 chemistry. Of course, many scientific papers can still be produced (which is as important as finding a novel radiopharmaceutical), but the ultimate goal should be the contribution to public health. The question arises as to why the situation is as described and how it can be changed (rapidly). This paper aims at a critical review of the limitations and requirements demanded for finding a novel radiopharmaceutical. The main focus here will be put on the underlying chemistry. Research in radiopharmaceutical chemistry should follow a 'top-down' strategy, to meet requirements from the market and production in clinics. Synthons are required for this drug finding process. Currently, 4 or 5 precursors are available, namely $[\text{Tc}=\text{O}]^{3+}$, $[\text{TcO}_2]^+$ and $[\text{Tc}=\text{N}]^{2+}$ core from Tc being in the oxidation state +V, Tc(III) chemistry and $[\text{Tc}(\text{CO})_3]^+$ chemistry in the +I valency [1]. The HYNIC approach represents another strategy but suffers from an as yet undefined core. All of these approaches are likely to be successful from a coordination chemistry point of view. The presentation will critically emphasize their weak and strong points with regard to different kinds of biomolecules. The search for novel cores and strategies is not at its end and a number of hypothetical cores and methodologies will be proposed to complement the available ones, underlining the importance of basic Tc chemistry.

1. NEW CORES

During the past few years, the progress in radiopharmaceutical chemistry has been critically reviewed several times [1–7]. A closer look at these reviews reveals that the progress made towards novel radiopharmaceuticals is comparably small. A current IAEA coordinated research project is dedicated to the exploration of the radiopharmacy with new ^{99m}Tc cores in order to expand the ‘palette’ of potential targeting molecules. New cores offer new possibilities, based solely on the fact that the new cores represent synthons that should better adapt to the physicochemical and biological properties of targeting vehicles. The chemistry will briefly be discussed in order to assess if the new cores will expand the field of novel radiopharmaceuticals.

Besides the availability of new cores as a base for new radiopharmaceuticals, one must also ask whether the lack of the latter ones is only a result of inadequate chemistry and biological behaviour or if other aspects play a role of similar, or even superior, importance. The following flow chart overviews the various science dependent and independent factors impacting on a successful development of radiopharmaceuticals (Fig. 1).

One of the most important but hardly controllable aspects is represented by the first section in Fig. 1. Since contributions to public health care represent

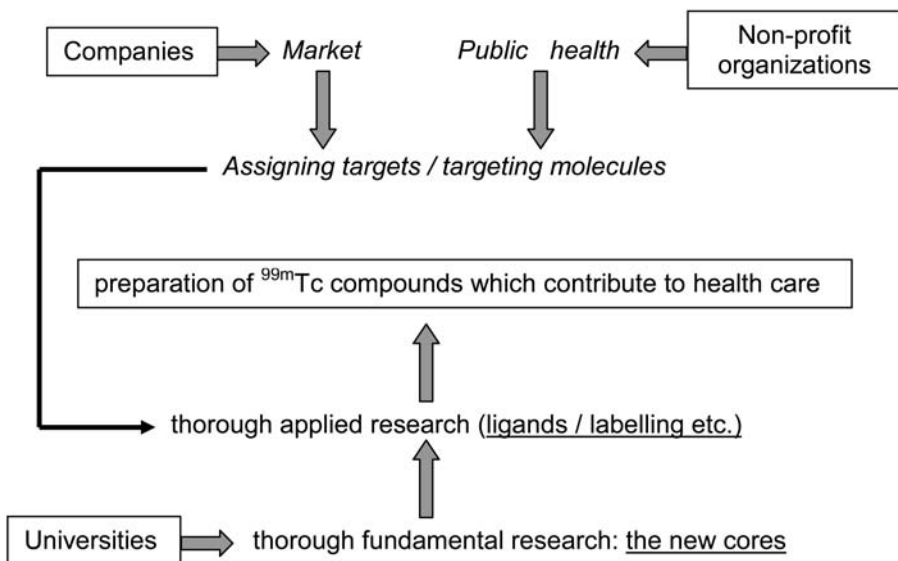


FIG. 1. A general flow chart depicting the different interactions between research and public health.

SESSION 7

the ultimate goal of radiopharmaceutical chemistry, a thorough market study is crucial for the selection of a targeting vehicle. Depending on the standpoint and background of the analyser, different criteria might apply. Companies by nature validate the financial outcome as being of prime importance whereas governmental organizations might be more interested in the number of people profiting from new imaging or treating agents. An excellent example of this situation is given by Aids and malaria or other diseases which are not very attractive for companies but which represent a major problem for the quality of life in many countries. It should be emphasized at this point that the two approaches to what is important need to be weighed equally, but it is crucial to merge these aspects for the good of both parties. Market analysis does not only include financial benefits but also intellectual property, market introduction aspects and other factors for which companies are experts. On the other hand, non-profit organizations also have a strong influence on, and responsibility for, the direction of research. Research projects must emphasize targeting vehicles which are not only pure research products but which also have the chance of becoming a product in less affluent countries. According to the experience of the authors, such studies and designations are hardly ever done with the required quality. Hence, the study of new cores as described in the following part will only be successful for broader publicity if these points are more seriously considered by both companies and international organizations.

It will certainly be more motivating for scientists doing the research to work with molecules that have real prospects for contributing to public health (and financial benefit) rather than just studying and comparing labelling techniques with new cores and compounds which can 'only' be published. Clearly, publishing basic research is of the highest importance for all of us, but the two arguments, doing something reasonable as regards practical application and doing good research are not mutually exclusive but complementary. The new cores to be described below are an excellent base but a thorough market study by companies and by non-profit organizations is an indispensable prerequisite to the sustainable and longer term development of radiopharmaceuticals.

As outlined above, chemists have to take care about the second part of the diagram shown in Fig. 1. It is clear that a thorough market study does not help much if the science behind it is not available. From surveying the recent literature it is clear that the corresponding science such as labelling techniques, biological studies etc., is available and that it does not, in principle, matter if Tc(V), Tc(III) or Tc(I) is selected, the question is rather for which targeting vehicle which core is the most appropriate. It will be seen in the following part that all cores, owing to the fact that they are chemically very different, are complementary rather than competing, and that the appropriate core has to be selected for a particular problem. In fact, this situation is very useful since it

expands substantially the possibilities for labelling. Before the introduction of the new cores, the most commonly used ^{99m}Tc moiety was, and still is, $[\text{Tc}=\text{O}]^{3+}$, with Tc being in the oxidation state +V. Despite being very attractive and still the most widely studied in the context of radiopharmaceuticals, its flexibility is rather limited, or in other words, tetradentate ligands are more or less the only choice. Still, success has been achieved and TRODAT [8–11] merits emphasis as well as Depreotide [12–15] and more recently Demobesine [16–19].

The palette of promising cores has been expanded substantially in the past few years. Without taking the time sequence of development into account, several new moieties have been introduced in recent years: the $[\text{TcN}]^{2+}$ moiety by Duatti and co-workers [20–24], the Tc(III) core by Pietzsch, Seifert and co-workers [25–28] and the $[\text{Tc}(\text{I})(\text{CO})_3]^+$ core by the authors' group [29–32]. The basic features of the cores actually available are depicted in Fig. 2 in which the three new cores are shown at the extreme right.

The basic chemistry of the three cores has been studied in detail and their chemical behaviour and stability are known. Furthermore, labelling chemistry has been developed and biomolecules have been labelled. For a number of corresponding perfusion agents or targeting molecules, *in vitro* and *in vivo* studies have been performed as well. For the $[\text{TcN}]^{2+}$ and $[\text{Tc}(\text{CO})_3]^+$ precursors, kits are available that make routine studies on a reproducible basis possible. Depending on the biomolecule, labelling is possible in a one or two step procedure. The stability of the formed complexes is high but they still differ in their properties and, hence, the potential biomolecules and radiopharmaceuticals derived from these complexes could also have different properties. The $[\text{TcN}]^{2+}$ core is very flexible with respect to the chemistry and the ligand conjugated to the biomolecule. Its introduction into a biomolecule can be considered as a kind of [3+2] approach. The tridentate ligand, usually with a combination of PNP donors, is variable, however, and the toxicity and stability of the phosphines have to be considered. The remaining two sites are then bound to a bidentate ligand, usually attached to the targeting molecule and there can be a vast combination of S, N and O and even other donors. The

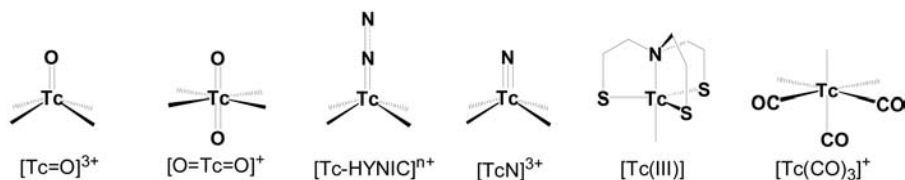


FIG. 2. The basic cores developed in ^{99m}Tc radiopharmaceuticals.

variability of the pentadentate complex can be fine tuned with respect to the target and the biomolecule.

The situation is somewhat similar with the Tc(III) approach. Here, the tetradentate ligand is less flexible in respect of the combination of donors, usually a tetradentate umbrella such as the NS3 ligand. The electronic properties of the Tc(III) centre in combination with this '4' ligand result in the unique feature that only one further monodentate ligand is introduced, usually a soft donor such as an isocyanide or a phosphine; others are possible as well. The striking aspect of the Tc(III) approach is the fact that only a simple monodentate ligand has to be attached to the biomolecule and no special care in respect of stereochemistry has to be taken into account. The precursor is synthesized from Tc(III)EDTA, a synthon that can conveniently be produced under ambient conditions. The Tc(III) approach is still less flexible than the $[\text{TcN}]^{2+}$ approach since the chemistry is more or less fixed. As it is, it can only be altered by the introduction of functionality in the carbon backbone and this will, however, lead to enantiomers. A big advantage of the Tc(III) approach is still the fact that the $^{99\text{m}}\text{Tc}$ building block is small and has a molecular weight of 294 D, which is low in comparison to $[\text{TcN}]^{2+}$ with the PNP coligand (depending on the nature of PNP, of course). Besides molecular weight, the topology of the Tc(III) precursor is a strong advantage, since it is small and highly symmetric, without active groups pointing out of the topology of the overall complex. The lipophilicity might be considered a disadvantage, however, and as outlined above, the complementary aspect of the different cores predestines this core probably for CNS receptor ligands.

The $[\text{Tc}(\text{CO})_3]^+$ approach fits well in this series of new cores. A one or two step labelling procedure is feasible, different s can be introduced to 'fine tune' the biological properties and the building block is also of comparably low molecular weight (268 D without further s) [33]. Hydro- and lipophilicity can be varied over a broad range and a combination of mono-, bi- and tridentate ligands is possible [6]. An advantage of the $[\text{Tc}(\text{CO})_3]^+$ approach is the possibility of direct labelling. Since complexes formed with a d^6 centre are generally robust, a special design of the donor is not a prerequisite for stable labelling. This is exemplified with the labelling of vitamin B12 from which a new radiopharmaceutical emerged that entered preclinical trials early in 2006. The cyano group attached to the central Co(III) metal in B12 represents a kind of 'inorganic' nitrile ligand. The authors found that it represents, as organic nitriles do, an excellent coordinating group for the $[\text{Tc}(\text{CO})_3]^+$ moiety. One of the three coordinating sites in $[\text{Tc}(\text{CO})_3]^+$ is occupied by the nitrogen of the cyanide, whereas the two remaining sites are occupied by water or, potentially, by bidentate s [34]. The approach is shown in Fig. 3.

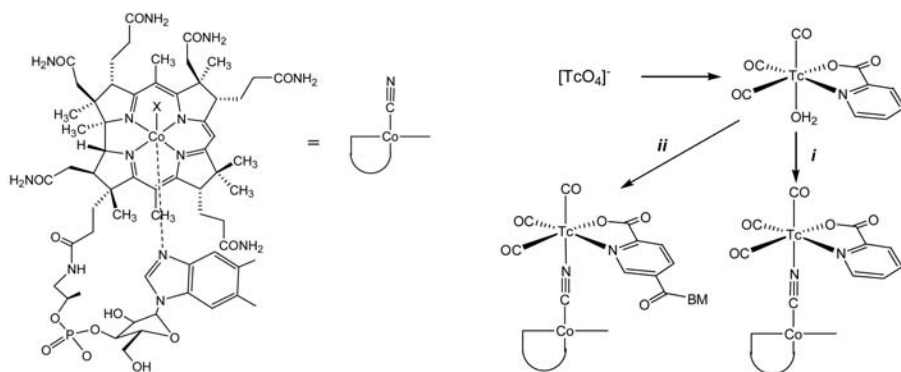


FIG. 3. Direct labelling of vitamin B12 through the cyano group bound to Co(III). A bidentate chelator can be introduced before labelling (pathway i) or the metal can mediate the introduction of an additional molecule (pathway ii).

Surprisingly, once bound to the cyanide, the conjugate is very stable and the complex not released. Studies on mice showed fast clearance through the kidneys with the B12 conjugate still being intact in the urine. A further unexpected finding is the fact that the two remaining water ligands are hardly exchanged by competing coordinating groups from, for example, serum proteins or other molecules present in serum. It is therefore also very difficult to introduce a bidentate ligand after coordination of $[\text{Tc}(\text{CO})_3]^+$ to B12 whereas introduction of a bidentate ligand and subsequent binding to B12 is easy. The X ray structure of the rhenium analogue is shown in Fig. 4.

As one of the advantages of all the three new cores is ligand flexibility, the bidentate chelators can here be varied to a large extent, enabling a systematic screening of biological properties and receptor binding. The metal centre can even be used to mediate the attachment of additional molecules such as fluorescence markers or pharmacologically active molecules such as antibiotics and it also offers the possibility of undertaking sound basic research with the clear intent of finding an application in public health care.

This short example, similar ones are also available for the other two cores, illustrates the enormous potential behind new radiopharmaceutical chemistry. Flexibility allows the assignment of new targets and new cores to enrich the armoury of radiopharmacy.

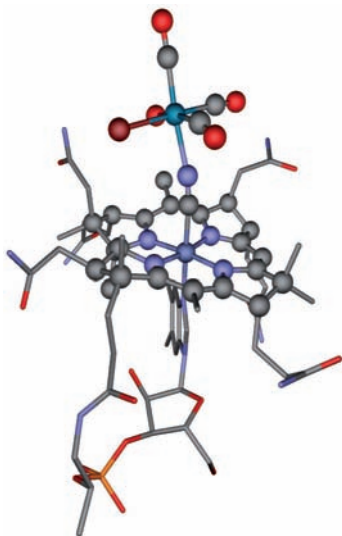


FIG. 4. X ray structure analysis of $\text{CN-}[\text{Re}(\text{OH})_2(\text{CO})_3]^+$ [34].

2. CONCLUSION

Which way to go to keep radiopharmacy alive? As outlined above and exemplified with the newly available cores, the answer to this question is probably less related to chemistry or biology than to other aspects influencing the target dedicated development of new radiopharmaceuticals. Taken together, the new (and the old) cores are an excellent base for producing new $^{99\text{m}}\text{Tc}$ based radiopharmaceuticals with potential for financial benefit but also for contributions to non-profit health care. Thus, the chemistry is at this point not the bottleneck anymore but is, rather, the thorough assignment of an appropriate target. Finally, it should not be concluded that chemistry has done its best and cores or methodologies are available for all possibilities. The analysis of the current situation should rather encourage the search for further cores, also an essential aspect for keeping $^{99\text{m}}\text{Tc}$ based radiopharmacy and nuclear medicine alive.

ACKNOWLEDGEMENTS

The authors acknowledge the Swiss National Science Foundation, Tyco-Mallinckrodt Med. Inc., Petten, Netherlands and Solidago Ag, Bern, Switzerland for their financial support.

REFERENCES

- [1] SCHIBLI, R., SCHUBIGER, P.A., *Eur. J. Nucl. Med. Mol. I.*, 29, **2002**, 1529.
- [2] ALBERTO, R., *Technetium*, CCCII, 5, **2004**, 127.
- [3] ALBERTO, R., *Eur. J. Nucl. Med. Mol. I.*, 30, **2003**, 1299.
- [4] WELCH, M., *Eur. J. Nucl. Med. Mol. I.*, 30, **2003**, 1302.
- [5] *Radiochemistry and Radiopharmaceutical Chemistry in "Life Sciences"*. **2003** Kluwer Academic Publisher, Dordrecht.
- [6] ALBERTO, R., PAK, J.K., VAN STAVEREN, D., MUNDWILER, S., BENNY, P., *Biopolymers*, 76, **2004**, 324.
- [7] BANERJEE, S.R., et al., *Nucl. Med. Biol.*, 32, **2005**, 1.
- [8] LU, C.S., et al., *J. Nucl. Med.*, 45, **2004**, 49.
- [9] KRAUSE, K.H., DRESEL, S.H., KRAUSE, J., LA FOUGERE, C., ACKENHEIL, M., *Neurosc. Biobehav. Rev.*, 27, **2003**, 605.
- [10] TOTH, G., et al., *J. Labelled Compd. Radiopharm.*, 46, **2003**, 1067.
- [11] HUANG, W.S., LEE, M.S., LIN, S.Z., CHEN, C.Y., WEY, S.P., *J. Nucl. Med.*, 44, **2003**, 233p.
- [12] WEINER, R.E., THAKUR, M.L., *Biodrugs*, 19, **2005**, 145.
- [13] SHAH, T., BUSCOMBE, J., CAPLIN, M., *Eur. J. Endocrin.*, 152, **2005**.
- [14] GAO, Z.R., BIRSACK, H.J., BUCERIUS, J., *Clin. Nucl. Med.*, 30, **2005**, 60.
- [15] BAATH, M., et al., *Eur. J. Nucl. Med. Mol. I.*, 31, **2004**, S215.
- [16] MAINA, T., et al., *J. Nucl. Med.*, 46, **2005**, 823.
- [17] NOCK, B.A., et al., *J. Med. Chem.*, 48, **2005**, 100.
- [18] NOCK, B.A., et al., *Eur. J. Nucl. Med. Mol. I.*, 31, **2004**, S280.
- [19] NOCK, B., et al., *Eur. J. Nucl. Med. Mol. I.*, 30, **2003**, 247.
- [20] DUATTI, A., BOSCHI, A., UCCELLI, L., *Braz. Archives Biol. Technol.*, 45, **2002**, 135.
- [21] DUATTI, A., BOLZATI, C., UCCELLI, L., ZUCCHINI, G.L., *Trans. Met. Chem.*, 22, **1997**, 313.
- [22] BOLZATI, C., et al., *Bioconjugate Chem.*, 14, **2003**, 1231.
- [23] BOLZATI, C., et al., *J. Am. Chem. Soc.*, 124, **2002**, 11468.
- [24] BOSCHI, A., DUATTI, A., UCCELLI, L., *Contrast Agents Iii: Radiopharmaceuticals - from Diagnostics to Therapeutics*, 252, **2005**, 85.
- [25] SEIFERT, S., et al., *Appl. Rad. Isotopes*, 53, **2000**, 431.
- [26] PIETZSCH, H.J., et al., *Inorg. Chem.*, 40, **2001**, 59.
- [27] PIETZSCH, H.J., et al., *Bioconjugate Chem.*, 14, **2003**, 136.

SESSION 7

- [28] SEIFERT, S., et al., *Bioconjugate Chem.*, 15, **2004**, 856.
- [29] ALBERTO, R., et al., *J. Am. Chem. Soc.*, 120, **1998**, 7987.
- [30] ALBERTO, R., SCHIBLI, R., WAIBEL, R., ABRAM, U., SCHUBIGER, A.P., *Coord. Chem. Rev.*, 190-192, **1999**, 901.
- [31] BERNARD, J., et al., *Inorg. Chem.*, 42, **2003**, 1014.
- [32] SCHIBLI, R., KATTI, K.V., HIGGINBOTHAM, C., VOLKERT, W.A., ALBERTO, R., *Nucl. Med. Biol.*, 26, **1999**, 711.
- [33] MUNDWILER, S., KUNDIG, M., ORTNER, K., ALBERTO, R., *Dalton T.*, **2004**, 1320.
- [34] KUNZE, S., ZOBİ, T., KURZ, P., SPINGLER, B., ALBERTO, R., *Angew. Chem. Int. Ed.*, 43, **2004**, 5025.

NEW ^{99m}Tc -CYTECTRENE PIPERIDINE COMPOUND AS A SPECIFIC BRAIN IMAGING AGENT

M. SAIDI, M. TRABELSI, A. MEKNI

Centre National des Sciences et Technologies Nucléaires,

Sidi Thabet, Tunisia

Email: m.saidi@cnstn.rnrt.tn

Radiopharmaceuticals that bind to CNS receptors *in vivo* are useful for understanding the pathophysiology of several neuropsychiatric disorders.

For the diagnosis of these pathophysiological processes it is important to develop radioligands capable of binding specifically to well-defined CNS receptors in order to evaluate their density and distribution in the brain.

Owing to the availability, low cost and optimal radiation properties of ^{99m}Tc , there is a considerable interest in the development of ^{99m}Tc radiopharmaceuticals for imaging CNS receptors using single photon emission tomography.

Biodistribution studies in rats of cyclopentadienyl technetium tricarbonyl conjugates of piperidine derivatives [1–3] showed that ^{99m}Tc -cytectrenes, containing in their structure an N-methylpiperidine and an N-isopropyl piperidine, accumulated in the brain regions with different binding specificity. Therefore, the authors studied the biobehaviour of a new cytectrene (Fig. 1) in which the piperidine was not substituted.

Furthermore, in order to improve the reaction conditions for eventual routing use, the authors carried out radiochemical labelling following the tricarbonyl concept of Alberto et al. [4], without the need for $\text{Mn}(\text{CO})_5\text{Br}$.

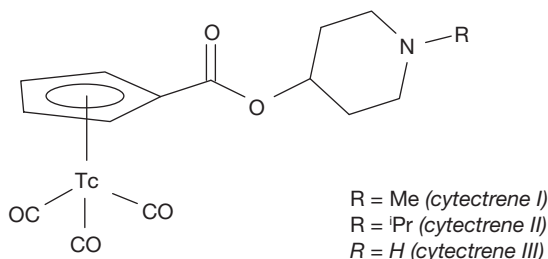


FIG. 1. Proposed structure of ^{99m}Tc -tricarbonyl-cytectrenes.

The *in vivo* uptake of the ^{99m}Tc ligands in the whole rat brain and specific brain regions was investigated. Samples of brain regions (cerebellum, colliculi, diencephalons, hippocampus, striatum, medulla, frontal cortex, parietal cortex and occipital cortex) were identified, removed, weighed and their radioactivity measured.

The highest uptake was observed in the striatum and in the cortex regions (Fig. 2). Receptor binding assays in rat brain homogenates and blocking studies are necessary to determine further data concerning specificity, selectivity and non-specific binding of this compound.

REFERENCES

- [1] SAIDI, M., et al., *J. Labelled Cpd. Radiopharm.* **44** (2001) 603-618.
- [2] KRETZSCHMAR, M., SAIDI, M., BERGMANN, R., *Annual Report FZR 363* (2002) 53.
- [3] SAIDI, M., et al., *Annual Report FZR 394* (2003) 24.
- [4] ALBERTO, R., et al., *J. Am. Chem. Soc.* **123** (2001) 3135.

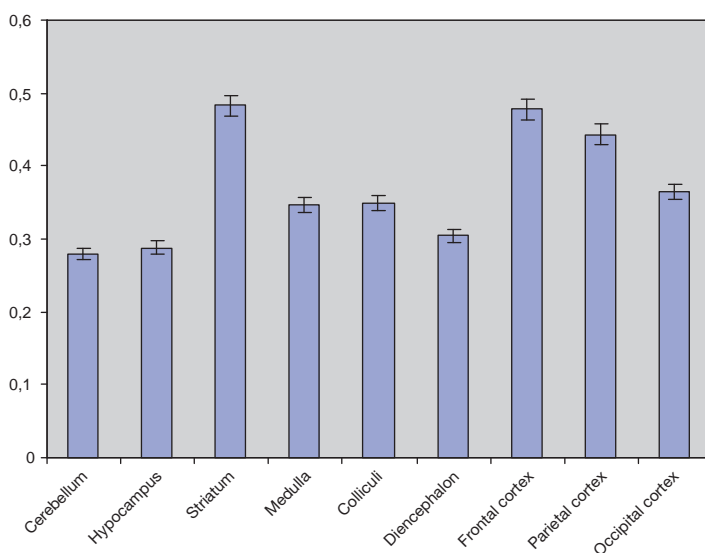


FIG. 2. *In vivo* uptake of ^{99m}Tc -cytectrene in different parts of rat brain.

**TRICARBONYLTECHNETIUM(I) COMPLEXES WITH
NEUTRAL BIDENTATE LIGANDS — N-METHYL-2-
PYRIDINECARBOAMIDE AND N-METHYL-2-
PYRIDINECARBOTHIOAMIDE**
Experimental and theoretical studies

J. NARBUTT*, M. ZASEPA-LYCZKO*, M. CZERWINSKI**,
R. SCHIBLI****

*Institute of Nuclear Chemistry and Technology
Email: jnarbutt@ichtj.waw.pl

** Jan Dlugosz University

Czestochowa, Poland

***Paul Scherrer Institute,
Villigen, Switzerland

Abstract

Two kinds of $[\text{Tc}(\text{CO})_3\text{LB}]$ complexes were obtained and studied, where L is either a neutral chelating ligand with N, S donor atoms, N-methyl-2-pyridinecarbothioamide, L_{NS} , or its analogue with N, O donor atoms, N-methyl-2-pyridinecarboamide, L_{NO} , and B is a monovalent anion or H_2O . The complexes were prepared both with $^{99\text{m}}\text{Tc}$ at n.c.a. level ($\text{B} = \text{OH}^-$ or H_2O) and with ^{99}Tc in milligram quantities ($\text{B} = \text{Cl}^-$). The complexes were investigated by HPLC, IR and paper electrophoresis. Also, advanced (DFT) quantum chemistry calculations on the $[\text{Tc}(\text{CO})_3\text{LCl}]$ complexes were made.

1. INTRODUCTION

The chemistry of tricarbonyltechnetium(I) complexes, the derivatives of organometallic aqua-ion *fac*- $[\text{Tc}(\text{CO})_3(\text{H}_2\text{O})_3]^+$ (**1**), with a chelating ligand in the molecule, has developed quickly in the last decade [1]. These thermodynamically stable and kinetically inert $^{99\text{m}}\text{Tc}$ chelates are good candidates for radiopharmaceuticals or their precursors. Owing to the softness of the Tc(I) centre, chelators with soft donor atoms are preferred as the ligands. Widely studied in this respect are bi- and tridentate derivatives of pyridine and/or

imidazole (aromatic N donors) in combination with other donor atoms, in particular sulphur. The aim of the present study is to select ligands that form very stable tricarbonyl complexes of Tc(I), which after further functionalization can appear as precursors for radiopharmaceuticals of the second generation.

2. EXPERIMENTAL

$\text{Na}[^{99\text{m}}\text{TcO}_4]$ was eluted from a $^{99}\text{Mo}/^{99\text{m}}\text{Tc}$ generator using 0.9% saline. Synthesis of the precursor **1** in water was carried out according to Alberto's low pressure method [2, 3] and/or by using potassium boranocarbonate [4]. The complexes at n.c.a concentrations were obtained from **1** by adding a methanol solution of L to the precursor solution in the PBS buffer to reach $[\text{L}] = 10^{-3}\text{M}$, followed by heating the mixture at 37°C or 75°C for 10–60 min. The ^{99}Tc complexes were prepared in water–methanol solution by adding a little excess of the ligand to the precursor solution and heating the mixture at 50°C . The ligands were synthesized by Dr. J. Mieczkowski, as described elsewhere [5, 6].

HPLC-RP studies were performed using a Nucleosil C-18 column and the 0.05M TEAP buffer–methanol gradient, the flow rate being 1 mL/min. Determination of the IR spectra was carried out in KBr pellets using a Perkin Elmer 16 PC FT-IR spectrophotometer.

Advanced (DFT) quantum chemistry calculations were performed [7] using three parameter Becke functionals of B3LYP type with the Lanl2dz basis set and Berny geometry optimization algorithm. The numerical calculations, based on the GAUSSIAN-98 program, were carried out using Cray J90 and Cray Y-MP supercomputers.

3. RESULTS AND DISCUSSION

The DFT calculations optimized the gas phase structures of the ligands and their complexes. The results confirm the authors' expectations based on the X ray diffraction studies on the analogous rhenium complexes [5, 6] that each ligand coordinates the metal centre bidently via the pyridine nitrogen and the X atom ($\text{X} = \text{O}$ or S), forming a five membered chelate ring (Fig. 1).

This conclusion is supported by the similarity of the IR spectra of the technetium complexes studied (Figs 2 and 3) to those of their rhenium analogues [5, 6]. Two characteristic peaks of CO vibrations (2026 and 1928 cm^{-1}) confirm the existence of the $^{99}\text{Tc}(\text{CO})_3$ core in the complexes studied.

The yield of the $[\text{C}^{99\text{m}}\text{Tc}(\text{CO})_3\text{L}_{\text{NX}}\text{B}]$ complexes ($\text{B} = \text{H}_2\text{O}$ and/or OH^-) was studied by HPLC. After 40 min incubation at 75°C the $[\text{C}^{99\text{m}}\text{Tc}(\text{CO})_3\text{L}_{\text{NS}}\text{B}]$

SESSION 7

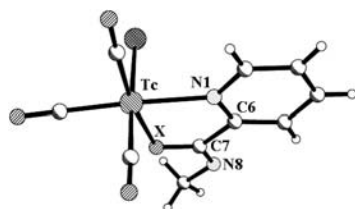


FIG. 1. Gas phase structures of the ligands and their complexes.

complex was obtained with nearly 100% yield (Fig. 4), while the yield of $[^{99m}\text{Tc}(\text{CO})_3\text{L}_{\text{NO}}\text{B}]$ was lower (53–84% depending on the pH of the complex formation (Fig. 5)). Two forms of the complexes were observed: cationic ($\text{B} = \text{H}_2\text{O}$), eluted as peak 2 on the chromatograms and neutral ($\text{B} = \text{OH}^-$), eluted as peak 3 (Figs 4 and 5). The equilibrium between these two forms depends on

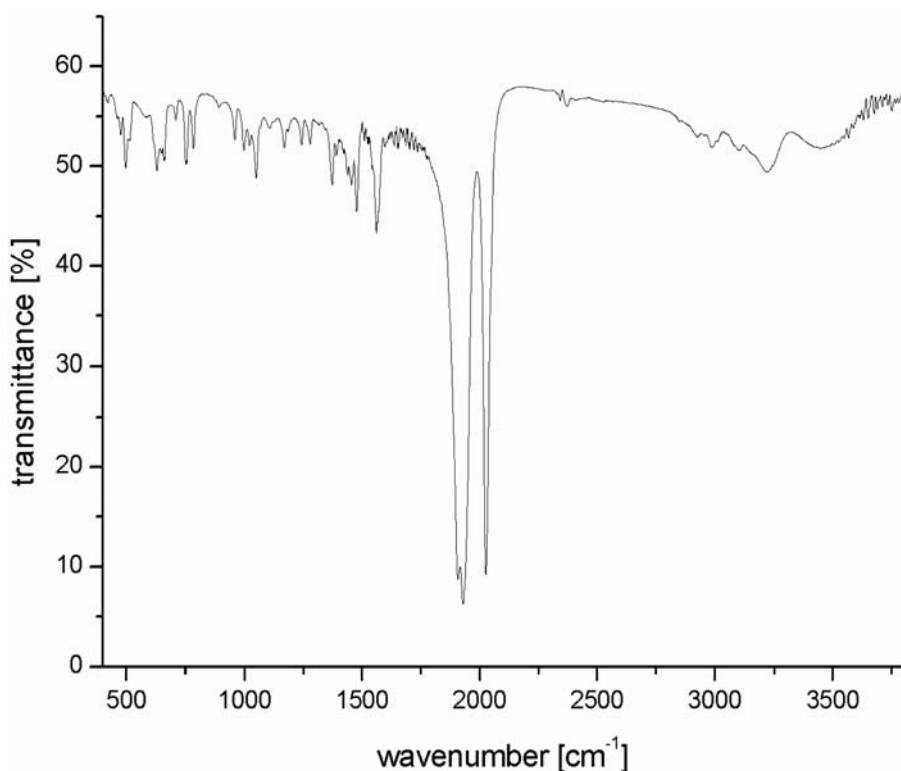


FIG. 2. IR spectrum of $[\text{Tc}(\text{CO})_3\text{L}_{\text{NS}}\text{Cl}]$; $\text{L}_{\text{NS}} = N\text{-methyl-2-pyridinecarbothioamide}$.

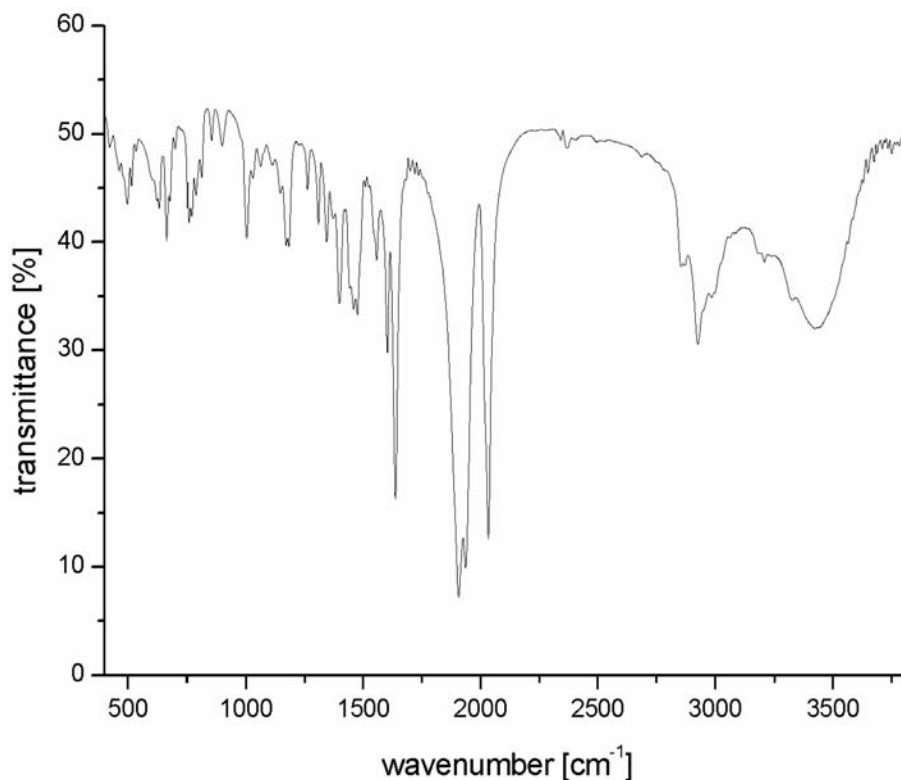


FIG. 3. IR spectrum of $[Tc(CO)_3L_{NO}Cl]$ (contaminated with L_{NO}); L_{NO} = *N*-methyl-2-pyridinecarboamide.

the complex and on the pH of the complex formation; it is shifted to over 90% of the neutral form at $pH > 7$ (Fig. 4) for $[^{99m}Tc(CO)_3L_{NS}B]$, but for $[^{99m}Tc(CO)_3L_{NO}B]$ the cationic form predominates (from 50% at pH3 to 64% at pH10 (Fig. 5)). The easier hydrolysis of $[Tc(CO)_3L_{NS}(H_2O)]^+$ evidenced stronger coordination of the H_2O ligand to the Tc atom in the complex with the L_{NS} ligand than in the complex with the L_{NO} ligand. However, that was rather unexpected under the assumption of stronger coordination of the L_{NS} than L_{NO} ligand, supported by the higher yields of the former complex (see below) and by the results of the quantum chemistry calculations [7].

The co-existence of two forms of the complexes, cationic and neutral, was also confirmed by paper electrophoresis. Under the experimental conditions (see above) two peaks appeared on the electropherograms: that remaining at the starting point corresponded to the neutral form, while that moving to the cathode corresponded to the cationic form.

SESSION 7

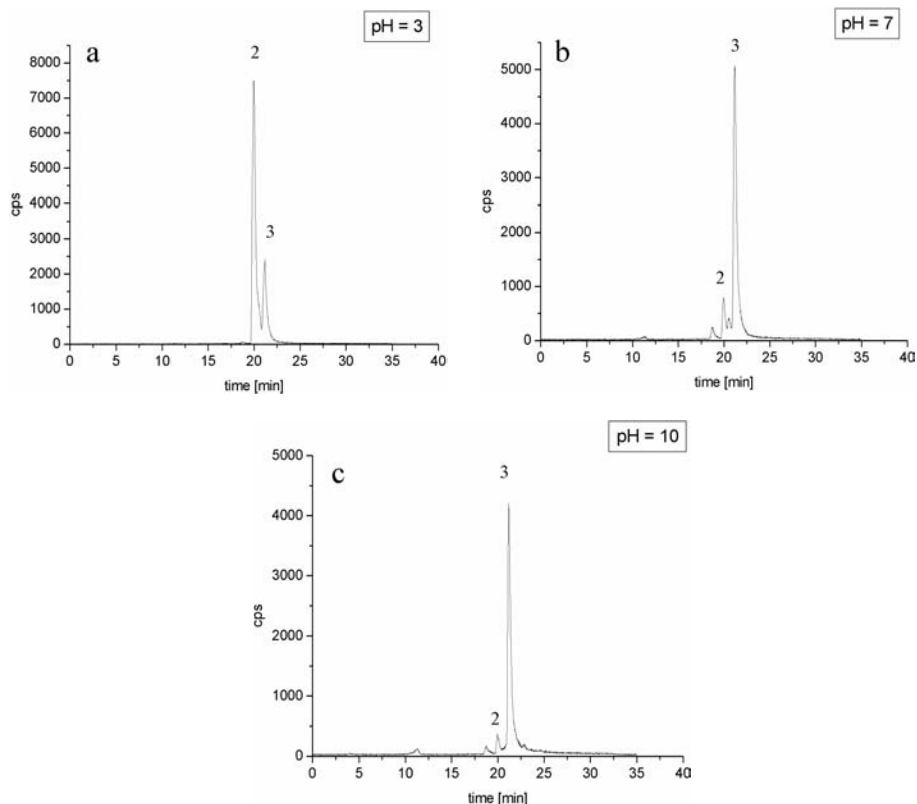


FIG. 4. HPLC chromatograms of the $[^{99m}\text{Tc}(\text{CO})_3\text{L}_{\text{NS}}\text{B}]$ complexes obtained at different pH. Peak 2: $[^{99m}\text{Tc}(\text{CO})_3\text{L}_{\text{NS}}(\text{H}_2\text{O})]^+$, peak 3: $[^{99m}\text{Tc}(\text{CO})_3\text{L}_{\text{NS}}(\text{OH})]$. **a:** pH3, **b:** pH7 and **c:** pH10.

After having optimized the gas phase structures of **1**, its chloride form $[\text{Tc}(\text{CO})_3(\text{H}_2\text{O})_2\text{Cl}]$, both ligands were studied and for their $[\text{Tc}(\text{CO})_3\text{LCl}]$ complexes the authors calculated the total energies of these species and Mulliken charges on their atoms. The calculated charges on the atoms of the free ligands and of their chelates show that the transfer of electron density (charge) from L to $\text{Tc}(\text{CO})_3\text{Cl}$ in the chelate molecule is greater for $[\text{Tc}(\text{CO})_3\text{L}_{\text{NS}}\text{Cl}]$ (0.51 e) than for $[\text{Tc}(\text{CO})_3\text{L}_{\text{NO}}\text{Cl}]$ (0.37 e), which means that the $\text{Tc}-\text{L}_{\text{NS}}$ bond is more covalent than $\text{Tc}-\text{L}_{\text{NO}}$, i.e. the former ligand is more strongly bound.

However, the energy of complex formation, calculated as the differences between the total energies of the products and substrates in the gas phase, is more negative for $[\text{Tc}(\text{CO})_3\text{L}_{\text{NO}}\text{Cl}]$ (-201 kJ/mol) than for $[\text{Tc}(\text{CO})_3\text{L}_{\text{NS}}\text{Cl}]$

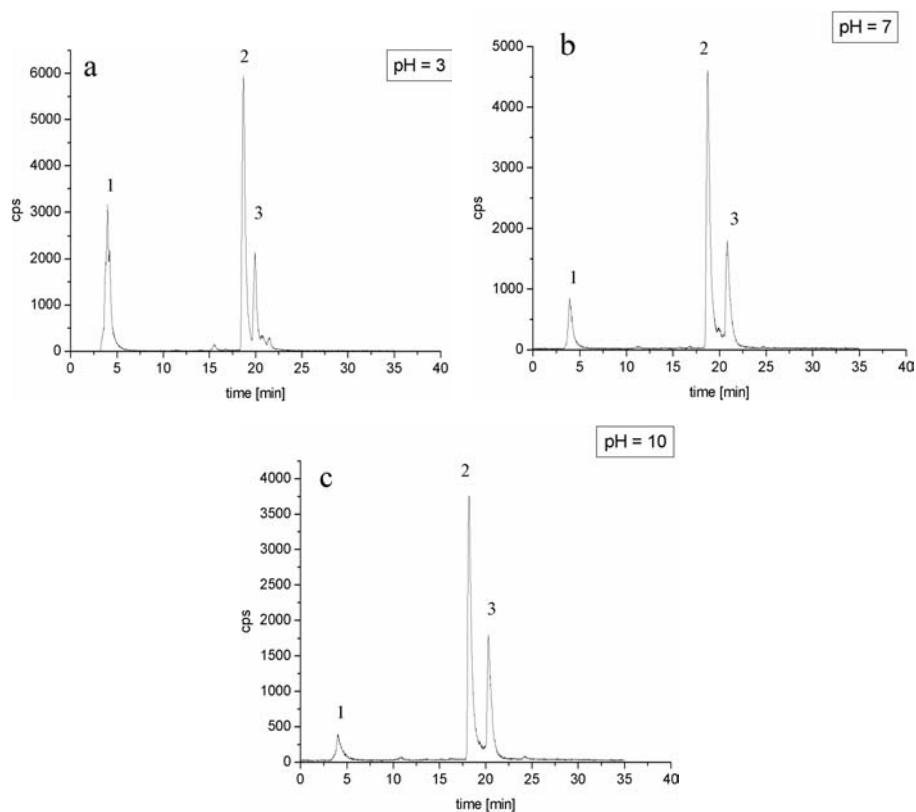


FIG. 5. HPLC chromatograms of the $[^{99m}\text{Tc}(\text{CO})_3\text{LNOB}]$ complexes obtained at different pH. Peak 1: precursor **1**, peak 2: $[^{99m}\text{Tc}(\text{CO})_3\text{LNO}(\text{H}_2\text{O})]^+$, peak 3: $[^{99m}\text{Tc}(\text{CO})_3\text{LNO}(\text{OH})]$. **a:** pH3, **b:** pH7 and **c:** pH10.

(-186 kJ/mol). One of the reasons for this contradiction is a stronger hydration in aqueous solution, where the chelates are formed, of the N–O donating ligand than of their N–S analogue, owing to stronger H bonds of water to the former species. The calculated difference in the hydration energies (~ 16 kJ/mol) is insufficient, however, to explain the contradiction. The other reason can be the stronger deformation of the chelate ring in the optimized structure of $[\text{Tc}(\text{CO})_3\text{L}_{\text{NS}}\text{Cl}]$ than in that of $[\text{Tc}(\text{CO})_3\text{L}_{\text{NO}}\text{Cl}]$. While the chelate rings in the crystals of the analogous rhenium(I) complexes are planar, i.e. the dihedral angle $\Theta(\text{N1-C6-C7-X}) = 0^\circ$, it is not so in the optimized $[\text{Tc}(\text{CO})_3\text{L}_{\text{NS}}\text{Cl}]$ molecules where $\Theta = 28.6^\circ$ in $[\text{Tc}(\text{CO})_3\text{L}_{\text{NS}}\text{Cl}]$, but only 7.3° in $[\text{Tc}(\text{CO})_3\text{L}_{\text{NO}}\text{Cl}]$. Also, the calculated Tc–S distance in $[\text{Tc}(\text{CO})_3\text{L}_{\text{NS}}\text{Cl}]$ (266 pm) is much longer than the experimental Re–S distance (244 pm) [5]. The

SESSION 7

stronger the deformation of the quasi-aromatic chelate ring, the less the structural stabilization due to the expected conjugation of p orbitals perpendicular to the ring plane. If the real structures of the chelates in solution are less deformed than those calculated, a significant contribution to the stability of the chelate with the L_{NS} ligand would be observed. The other reason for the difference in the energies of formation of the chelates can be the different ground state conformations of the free ligands in solution, owing to rotation around the C6–C7 axis. The calculated energy differences between the various gas state conformations of the ligands studied exceed 50 kJ/mol.

The question remains open as to why the $[Tc(CO)_3L_{NS}(H_2O)]^+$ cation hydrolyses more easily than $[Tc(CO)_3L_{NO}(H_2O)]^+$, despite expectations. The calculations carried out for the chloride complexes indicate a higher covalency of the Tc– L_{NS} bond than that of Tc– L_{NO} , which implies a weaker bonding of the B ligand. In fact, the calculated Tc–Cl distance is shorter in $[Tc(CO)_3L_{NO}Cl]$ (253.7 pm) than in $[Tc(CO)_3L_{NS}Cl]$ (255.5 pm) and the same relation is observed in the experimental structures of the analogous rhenium complexes [5, 6]. If the same relation was observed for B = H_2O , one might expect a greater polarization of the Tc–OH₂ bond and easier deprotonation (hydrolysis) of the $[Tc(CO)_3L_{NO}(H_2O)]^+$ complex. The DFT calculations on the $[Tc(CO)_3L_{NX}(H_2O)]^+$ complexes (to be carried out) will hopefully solve the problem.

The work is in progress. The DFT calculations may be considered a valuable tool for predicting the thermodynamic stability and other properties of metal complexes of interest for radiopharmaceutical chemistry.

ACKNOWLEDGEMENTS

The work was supported by a grant No. 4 TO9A 11023 from the Polish Committee for Scientific Research (KBN). The research stay of M. Zasepa-Lyczko at PSI was financed by the European Commission under Marie Curie Actions for the Transfer of Knowledge, contract No. MTKD-CT-2004-509224.

REFERENCES

- [1] MUNDWILER, S., KÜNDIG, M., ORTNER, K., ALBERTO, R., Dalton Trans., 1320-1328 (2004).
- [2] ALBERTO, R., et al., Transition Met. Chem., **22**, 597-601 (1997);
- [3] ALBERTO, R., SCHIBLI, R., WAIBEL, R., ABRAM, U., SCHUBIGER, A.P., Coord. Chem. Rev., **190-192**, 901-919 (1999).

- [4] ALBERTO, R., ORTNER, K., WHEATLEY, N., SCHIBLI, R., SCHUBIGER, A.P., *J. Am. Chem. Soc.* 2001, 123, 3135-3136.
- [5] FUKS, L., et al., *J. Organomet. Chem.*, **89**, 4751-4756 (2004).
- [6] GNIAZDOWSKA, E., FUKS, L., MIECZKOWSKI, J., NARBUTT, J., this Symposium.
- [7] NARBUTT, J., CZERWINSKI, M., ZASEPA-LYCZKO, M., NUCAR 2005 (Proc. DAE-BRNS Symp. Nuclear and Radiochemistry, Amritsar, India, 2005), 64-67.

MODIFIED BOMBESIN ANALOGUE WITH TECHNETIUM TRICARBONYL PRECURSOR AS PROSTATIC RADIODIAGNOSTIC AGENT

B.L. FAINTUCH*, E. MURAMOTO*, L. MORGANTI**,
R.M. CHURA-CHAMBI**, N. NASCIMENTO**,
E.G. GARAYOA***, P. BLAUENSTEIN***, P.A. SCHUBIGER***

*Radiopharmacy Center, Institute of Energetic and Nuclear Research
Email: faintuch@ipen.br

**Molecular Biology Center, Institute of Energetic and Nuclear Research
São Paulo, Brazil

***Center for Radiopharmaceutical Science, Paul Scherrer Institute,
Villigen, Switzerland

Abstract

Bombesin (BBN) and the molecularly related gastrin releasing peptide act as neurotransmitters and endocrine cancer cell growth factors on normal tissues as well as on neoplastic cells of various origins, including prostatic carcinomas and many breast carcinomas. The aim of the study was the evaluation of the labelling and biodistribution of modified BBN analogue with Tc-carbonyl core as a prostatic tumour diagnostic agent. BBN (7-14) was synthesized by substituting methionine (14) by norleucine and coupling the (N α His)Ac ligand for application of the Tc-carbonyl labelling technique. Radiochemical evaluation was done and biodistribution studies were performed in normal Swiss mice at 1.5, 4 and 24 h post-injection, and in nude mice bearing prostate cancer cells PC-3, 1.5 h post-injection. The yield of the tricarbonyl intermediate was greater than 90%. Radiochemical purity for the radiolabelled BBN was $86.3 \pm 1.2\%$. Biodistribution study results suggest that $^{99m}\text{Tc}(\text{CO})_3\text{-BBN}$ was mainly excreted by the hepato-biliary system and had high intestinal uptake. Tumour uptake was $1.15 \pm 0.05\%$ ID/g with tumour: blood and tumour: muscle ratios of 2.67 and 3.19, respectively. Scintigraphic imaging in nude mice bearing PC-3 cells showed a very low uptake by the tumour. Labelling conditions permitted a good yield. Nevertheless, the radiopharmaceutical did not show improved uptake by prostatic cell tumour, in comparison with findings observed without the modification in the molecule.

1. INTRODUCTION

Bombesin (BBN) is a 14 amino acid structure that belongs to the family of bombesin-like neuropeptides. It binds to receptors such as that of neuromedin B, the gastrin releasing peptide receptor and the orphan BBN subtype-3 receptor [1, 2]. BBN-like neuropeptides and their receptors also play a role in neoplasms. Stimulatory effects of the peptides on mitogenesis have been implicated in tumour growth of several human cancer cell lines such as lung, breast and prostatic cancers [3].

Blauenstein et al. have studied different radiolabelled BBN analogues [4–6]. Modifications of the BBN (7-14) molecule have been attempted in order to obtain derivatives that can increase plasma stability and provide easy labelling with radionuclides.

The finding that not only gastrin releasing peptide receptor is over expressed on human tumours but in some cases also neuromedin B and BB3 receptor subtypes led research groups to develop conjugates of the slightly modified BBN ligand [7].

The synthesis of Tc-carbonyl synthon has opened the door for $^{99m}\text{Tc(I)}$ peptide chemistry. The one step synthesis of the $[\text{}^{99m}\text{Tc}(\text{CO})_3(\text{H}_2\text{O})_3]^+$ complexes reported by Alberto and co-workers (1998) [8] by reduction of pertechnetate with sodium borohydride in aqueous solution in the presence of carbon monoxide, led to a new technique for development of biomolecules with radiopharmaceutical applications. Egli et al. (1999) have investigated the capability of amino acids and amino acid fragments to react with the ^{99m}Tc -tricarbonyl core [9]. It has been observed that ^{99m}Tc -tricarbonyl complexes which are coordinated with a tridentate chelating system exhibit good stability when challenged in human plasma, and also with excess cysteine, histidine or glutathione [10].

For radiolabelling the peptide with ^{99}Tc using the organometallic precursor $[\text{}^{99m}\text{Tc}(\text{CO})_3(\text{H}_2\text{O})_3]^+$, the peptide analogue was derivatized with a tridentate bifunctional chelator, N α -histidinyl acetate.

2. OBJECTIVE

The aim of the study was the evaluation of the labelling and biodistribution of modified BBN analogue with ^{99m}Tc -carbonyl core as a prostatic tumour diagnostic agent.

3. METHODS

Technetium-99m was obtained from an alumina based $^{99}\text{Mo}/^{99\text{m}}\text{Tc}$ generator locally supplied by the Radiopharmacy Center of the Institute of Energetic and Nuclear Research (IPEN/CNEN).

Reagents used in the study were purchased from Merck and Sigma-Aldrich Brazil Ltda. The CO gas was purchased from White Martins Gases Industriais SA, São Paulo, Brazil.

Peptide synthesis was performed in the solid phase following the Fmoc strategy. BBN (7-14) was synthesized by substituting methionine (14) by norleucine and coupling (N α His)Ac ligand for the application of the $^{99\text{m}}\text{Tc}$ -carbonyl labelling technique. The BBN analogue sequence is (N α His)-Ac-N-Gln-Trp-Ala-Val-Gly-His-Leu-Norleucin-NH₂.

3.1. Synthesis of $^{99\text{m}}\text{Tc}$ -carbonyl

The organometallic precursor was prepared according to a published procedure [8]. Briefly, 4.4 mg Na₂CO₃, 15 mg Na/K tartrate and 5.5 mg NaBH₄ were purged with carbon monoxide gas for 60 min. Then, 1 mL of Na $^{99\text{m}}\text{TcO}_4$ (1850 MBq) eluted from a generator was added. The vial was heated at 75°C for 35 min. The reaction was stopped in an ice bath. Then, the pH was adjusted to 7 using 0.2 mL of 1M HCl/1M phosphate buffer solution (2:1) previously nitrogenated.

3.2. Peptide labelling

To 50 μL of a $5 \times 10^{-4}\text{M}$ peptide solution was added 450 μL of $^{99\text{m}}\text{Tc}$ -carbonyl. The mixture was heated for one hour at 75°C and later cooled in an ice bath.

3.3. Quality control

Radiochemical evaluation was done by Whatman no.1 and TLC-Al method with solvent mixture MeOH/HCl 6M (99.5/0.5).

$^{99\text{m}}\text{Tc}(\text{CO})_3\text{-BBN}$ was also characterized by reverse phase high performance liquid chromatography on a Waters 600E system. The flow rate was 1 mL/min starting with a solvent composition of 95% of solvent A (0.1% TFA in water) and 5% of solvent B (0.1% TFA in ACN) and followed a linear gradient of 30% A:70% B from 0–25 min and 30% A:70% B to 5% A:95% B from 25–30 min.

The product was purified in a C18 SepPak cartridge before biological studies commenced. The impurities were eluted with water and $^{99m}\text{Tc}(\text{CO})_3\text{-BBN}$ with ethanol.

3.4. Biodistribution studies

Biodistribution studies were performed on normal Swiss mice ($n = 3$) at 1.5, 4 and 24 h post-injection and on nude mice bearing prostate cancer cells PC-3, 1.5 h post-injection. Scintigraphic images were documented for these last animals.

4. RESULTS AND DISCUSSION

The development of tracers based on BBN/GRP receptors for non-invasive scintigraphic evaluation would make possible the biochemical characterization of certain cancers and benefit patients by means of earlier therapeutic intervention. Previous studies [6, 9] of the $^{99m}\text{Tc}(\text{CO})_3^+$ core demonstrated its usefulness as a convenient platform for drug development.

The precursor $^{99m}\text{Tc}(\text{CO})_3(\text{H}_2\text{O})_3^+$ and the radiolabelled peptide were evaluated using paper chromatography for the first and TLC-Al for the second in the same mixture solvent. The R_f of the radiochemical species can be seen in Table 1.

The yield of the tricarbonyl intermediate was greater than 90%. The radiochemical purity of the radiolabelled BBN was $86.3 \pm 1.2\%$, with $R_t = 19.1$ (Fig. 1).

Biodistribution study results suggest that $^{99m}\text{Tc}(\text{CO})_3\text{-BBN}$ was mainly excreted by the hepato-biliar system and had high intestinal uptake as shown in Table 2. Tumour uptake was $1.15 \pm 0.05\%$ ID/g with tumour:blood and tumour:muscle ratios of 2.67 and 3.19, respectively (Table 3). Activity in the

TABLE 1. RETENTION FACTOR OF RADIOCHROMATOGRAM WHEN USING $^{99m}\text{Tc}(\text{CO})_3^+$

Radiochemical species	Whatman no. 1	TLC-Al
$^{99m}\text{TcO}_4^-$	0.5–0.6	0.7
$^{99m}\text{Tc}(\text{CO})_3$	0.8–0.9	0.0–0.2
$^{99m}\text{TcO}_2$	0.0	0.0
$^{99m}\text{Tc}(\text{CO})_3\text{-conjugate}$	0.9–1.0	0.7

SESSION 7

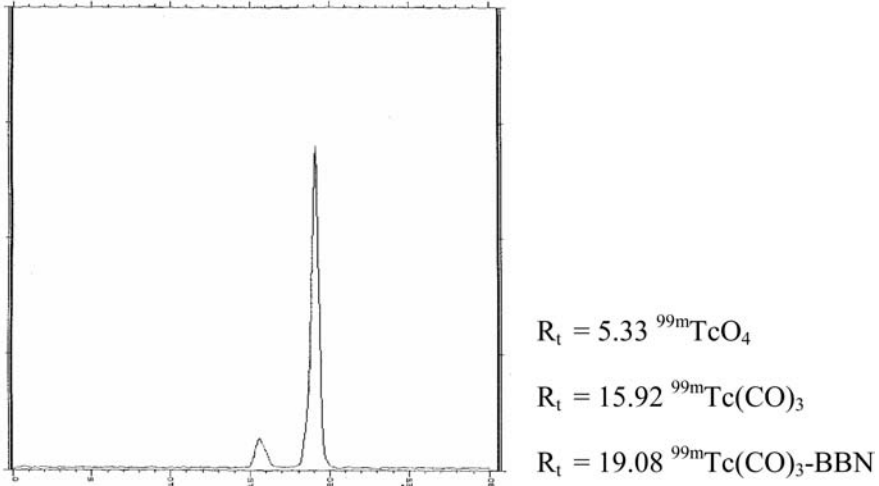


FIG. 1. Radiochromatogram of $^{99m}\text{Tc}(\text{CO})_3\text{-BBN}$.

pancreas was used as a measure of receptor binding. At 1.5 h post-injection, the activity was only $1.23 \pm 0.06\%$ ID/g. There was no significant uptake or retention in the stomach indicating minimal, if any, *in vivo* dissociation for

TABLE 2. BIODISTRIBUTION (%ID/g) OF $^{99m}\text{Tc}(\text{CO})_3\text{-BBN}$ IN NORMAL SWISS MICE AS A FUNCTION OF TIME AFTER INTRAVENOUS ADMINISTRATION (n = 3)

Organ	1.5 h	4 h	24 h
Blood	0.48 ± 0.13	0.15 ± 0.02	0.06 ± 0.02
Heart	0.33 ± 0.50	0.26 ± 0.08	0.02 ± 0.01
Lung	0.81 ± 0.03	0.28 ± 0.03	0.10 ± 0.01
Kidney	1.97 ± 0.23	0.39 ± 0.01	0.12 ± 0.01
Spleen	0.53 ± 0.04	0.16 ± 0.05	0.04 ± 0.01
Stomach	0.97 ± 0.33	0.70 ± 0.16	0.18 ± 0.05
Pancreas	1.31 ± 0.04	0.43 ± 0.04	0.05 ± 0.02
Liver	5.26 ± 0.24	2.40 ± 0.23	0.57 ± 0.14
Large intestine	2.05 ± 1.78	3.01 ± 1.09	1.12 ± 0.06
Small intestine	4.60 ± 0.85	0.97 ± 0.17	0.11 ± 0.02
Muscle	0.50 ± 0.11	0.15 ± 0.01	0.01 ± 0.01

Note: Values represent mean \pm SD (n = 3) of per cent of injected dose per gram.

TABLE 3. BIODISTRIBUTION OF $^{99m}\text{Tc}-(\text{CO})_3\text{-BBN}$ IN PROSTATE TUMOUR BEARING NUDE MICE (PC-3) 1.5 h AFTER INTRAVENOUS ADMINISTRATION (n = 3)

Organ	1.5 h	
	%ID/g	%ID/organ
Blood	0.43 ± 0.05	0.63 ± 0.05
Heart	0.48 ± 0.06	0.04 ± 0.01
Lung	1.22 ± 0.14	0.22 ± 0.04
Kidney	2.34 ± 0.25	0.73 ± 0.12
Spleen	0.82 ± 0.32	0.12 ± 0.07
Stomach	0.56 ± 0.04	0.10 ± 0.01
Pancreas	1.23 ± 0.06	0.27 ± 0.05
Liver	5.82 ± 0.27	6.02 ± 0.12
Large intestine	2.36 ± 0.81	0.81 ± 0.11
Small intestine	5.72 ± 1.17	5.56 ± 0.28
Muscle	0.36 ± 0.14	0.05 ± 0.01
Tumour	1.15 ± 0.05	0.40 ± 0.10
Tumour:blood	2.67	
Tumour:muscle	3.19	

^{99m}Tc from these ligands to produce $^{99m}\text{TcO}_4^-$. Scintigraphic imaging in nude mice bearing PC-3 cells showed a very low uptake by the tumour (Fig. 2).

Efforts have been made to design derivatized BBN analogues for binding and pharmacokinetic studies. Because BBN agonists are generally preferable to BBN antagonists for receptor specific internalization, most BBN analogues with an amidated C-terminus are directly involved in the specific binding interaction with the gastrin releasing peptide receptor and the truncated C-terminal heptapeptide sequence (BBN(8-14)) must be maintained or minimally substituted. Blauenstein et al. (2004) [11] synthesized many BBN analogues and the substitution of Leu13 by cyclohexylalanin brought better stability of the complex in plasma. The authors have not tested stability in plasma but tumour uptake did not indicate that replacement of Met by norleucine was worthy. Along with insignificant pancreas uptake, that failure may be related to the capability of the derivative to target gastrin releasing peptide receptor expressing cells in vivo.

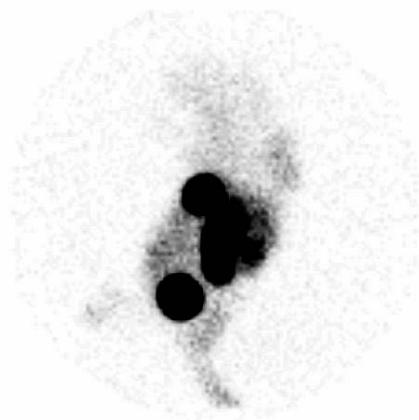


FIG. 2. Scintigraphic imaging of nude mice bearing prostate cancer tumour cells.

5. CONCLUSION

Labelling conditions permitted a good yield to be obtained. Substitution of the amino acid in position 14 by norleucine in the molecule had the advantage that no oxidation took place during synthesis and labelling, rendering it easier to work with this compound. Nevertheless, radiopharmaceutical analysis did not show improved uptake by prostatic cell tumour, in comparison with findings observed without this modification.

REFERENCES

- [1] MAINA, T., et al., Species differences of bombesin analog interactions with GRP-R define the choice of animal models in the development of CRP-R-targeting drugs, *J. Nucl. Med.* **46** (2005) 823.
- [2] FLEISCHMANN, A., WASER, B., GEBBERS, J.O., REUBI, J.C., Gastrin-releasing peptide receptors in normal and neoplastic human uterus: Involvement of multiple tissue compartments, *The Journal of Clinical Endocrinology & Metabolism* **90** 8 (2005) 4722.
- [3] MOODY, T.W., CHAN, D., FAHRENKRUG, J., JENSEN, R.T., Neuropeptides as autocrine growth factors in cancer cells, *Curr. Pharm. Des.* **9** (2003) 495.

- [4] BLAUENSTEIN, P., et al., Improving the tumor uptake of ^{99m}Tc -labeled neuropeptides using stabilized peptide analogues, *Cancer Biotherapy & Radiopharmaceuticals* **19** (2) (2004) 181.
- [5] LA BELLA, R., et al., In vitro and in vivo evaluation of a ^{99m}Tc (I)-labeled bombesin analogue for imaging of gastrin releasing peptide receptor-positive tumors, *Nucl. Med. Biol.* **29** (2002) 553.
- [6] LA BELLA, R., et al., A ^{99m}Tc (I)-postlabeled high affinity bombesin analogue as a potential tumor imaging agent, *Bioconj. Chem.* **13** 3 (2002) 599.
- [7] ZHANG, H., et al., Synthesis and evaluation of bombesin derivatives on the basis of pan-bombesin peptides labeled with Indium-111, Lutetium-177, and Yttrium-90 for targeting bombesin receptor-expressing tumors, *Cancer Research* **64** (2004) 6707.
- [8] ALBERTO, R., SCHIBLI, R., EGLI, A., SCHUBIGER, A.P., "A novel organometallic aqua complex of technetium for the labeling of biomolecules: Synthesis of $[\text{}^{99m}\text{Tc}(\text{OH}_2)_3(\text{CO})_3]^+$ from $[\text{}^{99m}\text{TcO}_4]^-$ in aqueous solution and its reaction with a bifunctional ligand", *J. Am. Chem. Soc.* **120** (1998) 7987.
- [9] EGLI, A., et al., Organometallic Tc- 99m -aquaion labels peptide to an unprecedented high specific activity, *J. Nucl. Med.* **40** (1999) 1913.
- [10] SCHIBLI, R., SCHUBIGER, P.A., Current use and future potential of organometallic radiopharmaceuticals, *Eur. J. Nucl. Med.* **29** (2002) 1529.
- [11] BLAUENSTEIN, P., et al., Improving the tumor uptake of ^{99m}Tc -labeled neuropeptides using stabilized peptide analogues, *Cancer Biotherapy & Radiopharmaceuticals* **19** 2 (2004).

SYNTHESES AND CHARACTERIZATION OF ^{99m}Tc -METOMIDATE AS THE $^{99m}\text{Tc}(\text{I})$ -TRICARBONYL-*(R)*-BIPYRIDINYL-MTO-CONJUGATE

R. SCHIBLI*, M. STICHELBERGER**, F. HAMMERSCHMIDT***,
M.L. BERGER⁺, I. ZOLLE⁺⁺

*Paul Scherrer Institute, Division of Radiopharmaceutical Chemistry,
Villigen

** CHUV, Service de Médecine Nucléaire, Lausanne

Switzerland

***Institute of Organic Chemistry, University of Vienna

⁺Center for Brain Research, Medical University of Vienna

⁺⁺Ludwig-Boltzmann-Institute of Nuclear Medicine, AKH-Wien
Email: ilse.zolle@univie.ac.at

Vienna, Austria

Abstract

Metomidate (MTO) is a potent and selective inhibitor of steroid 11 β -hydroxylation in the adrenal cortex. Labeled with a radionuclide it has gained importance for adrenal scintigraphy in patients with functional adrenal disorders. Since kit preparation would considerably enhance the availability of this radiotracer, the authors report labelling with ^{99m}Tc . For this purpose, two nucleophilic centres were introduced by replacing the phenyl ring of MTO with the bipyridinyl moiety, producing the BiPy-MTO precursor for bidentate binding with the tricarbonyl-technetium fragment. Structural derivatives of MTO were evaluated by the displacement of ^{131}I -IMTO from rat adrenal membranes. Complex formation using the kit IsoLink™ proceeded with high yield. Addition of the precursor to the $^{99m}\text{Tc}(\text{I})$ -tricarbonyl-complex and heating produced the $^{99m}\text{Tc}(\text{I})$ -tricarbonyl-*(R)*-BiPy-MTO-conjugate. Chemical characterization of the conjugate was obtained by HPLC, using the analogous Re(I)Br-tricarbonyl-*(R)*-BiPy-MTO-conjugate as a reference. The $^{99m}\text{Tc}(\text{I})$ -tricarbonyl-*(R)*-BiPy-MTO-conjugate was injected in mice and the kinetics of uptake and elimination were studied.

1. INTRODUCTION

Etomidate (*R*)-1-[1-phenylethyl]-1*H*-imidazole-5-carboxylic acid ethyl ester] (ETO) and the corresponding methyl ester (metomidate) are potent inhibitors of the adrenocortical P-450c11 enzyme system [1, 2], as demonstrated by the selective inhibition of cyt. P-450 species in adrenal cortex mitochondria [3]. The interaction with P-450c11 is stereospecific, the (*R*)-enantiomer (ETO) being a more potent inhibitor of adrenal cortex mitochondrial 11b-hydroxylation than (*S*)-ETO. These findings were confirmed by the displacement of ¹³¹I-IMTO binding (4-iodo-MTO) with structural derivatives of MTO verifying the lower binding potency of the (*S*)-enantiomer [4]. The authors have evaluated the functionality of the chiral C-atom and also the biochemical acceptance of replacing the phenyl ring. Compounds synthesized included demethyl-MTO (no chiral C-atom) and (*S*)-MTO [4]. As a replacement of the phenyl ring, pyridine and bipyridine were chosen, producing pyridinyl-MTO (Py-MTO) and bipyridinyl-MTO (BiPy-MTO), both as the demethylated achiral derivatives and as the biologically active (*R*)-enantiomers. Structural verification was obtained by ¹H- and ¹³C-NMR spectroscopy.

2. EXPERIMENTAL

2.1. Precursor synthesis

2.1.1. Synthesis of (*R*)-BiPy-metomidate

Replacement of the phenyl ring by the 2,2'-bipyridine moiety is based on the Mitsunobu reaction which had been adopted for the synthesis of MTO derivatives [4, 5]. Here, the (*S*)-configured 1-(2,2'-bipyridin-5-yl)ethanol was coupled with methyl 1*H*-imidazole-5-carboxylate at -30°C in THF providing the main product (70%, alkylation at N-1) and an isomeric side product (11%, alkylation at N-3), which had not been observed previously. According to Mitsunobu, coupling is performed at N-1 of imidazole with inversion of configuration at the chiral centre. Therefore, this method requires the synthesis of 1-(2,2'-bipyridin-5-yl)ethanol (building block 1) with (*S*)-configuration (Fig.1).

The synthesis of 1-(2,2'-bipyridin-5-yl)ethanol starts with the Stille coupling of 2-trimethylstannylpyridine and ethyl 5-chloronicotinate catalyzed by tetrakis(triphenyl-phosphane)palladium in 76% yield as described in the literature [6]. The resulting ester was saponified with sodium hydroxide in a mixture of ethanol/water to yield the corresponding sodium carboxylate. The dried product was converted to the acid chloride using thionylchloride. The

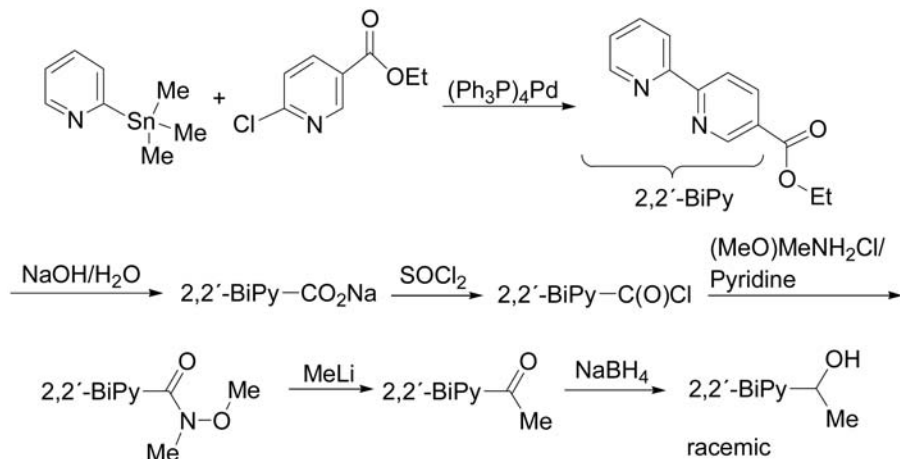


FIG. 1. Synthesis of building block 1: 1-(2,2'-bipyridin-5-yl)ethanol.

crude 2,2'-bipyridinyl-5-carbonyl chloride was reacted with N,O-dimethylhydroxylamine to produce an amide (Weinreb amide) isolated as an oil in 92% yield. Addition of methyllithium in dry THF to the Weinreb amide at low temperature furnished the 2,2'-bipyridin-5-yl methyl ketone as a crystalline solid (96%), which was reduced smoothly to the racemic substituted ethanol in 92% yield. Preparative HPLC on a chiral stationary phase (Chiracel OD) gave the enantiomerically pure secondary alcohols (ee 99% by analytical HPLC on Chiracel OD-H and ^1H NMR spectroscopy of the (*R*)-Mosher esters). The absolute configuration was assigned on the basis of the chemical shifts of relevant signals in the ^1H NMR spectra of the (*R*)-Mosher esters. The less polar enantiomer (by HPLC) had (*S*)-configuration, the more polar enantiomer had (*R*)-configuration.

The (*R*)-configured alcohol was transformed to the (*S*)-alcohol with the same enantiomeric excess (ee >99%) using the Mitsunobu reaction followed by saponification of the resulting ester.

The (*S*)-configured 1-(2,2'-bipyridin-5-yl)ethanol was coupled with methyl 1*H*-imidazole-5-carboxylate at -30°C in THF (Mitsunobu reaction) providing the main product (70%, alkylation at N-1) and an isomeric side product (11%, alkylation at N-3) (Fig. 2). The isomeric products were separated by flash column chromatography.

The product (alkylation at N-1) is a viscous oil: 1-[1-(2,2'-bipyridin-5-yl)ethyl]-1*H*-imidazole-5-carboxylic acid methyl ester; $[\alpha]_{\text{D}}^{20} = +66.7$ (*c* 0.73, acetone); anal. calcd. (%) for $\text{C}_{17}\text{H}_{16}\text{N}_4\text{O}_2$ (308.33) found: C 66.02, H 5.39; Calcd: C 66.22, H 5.23.

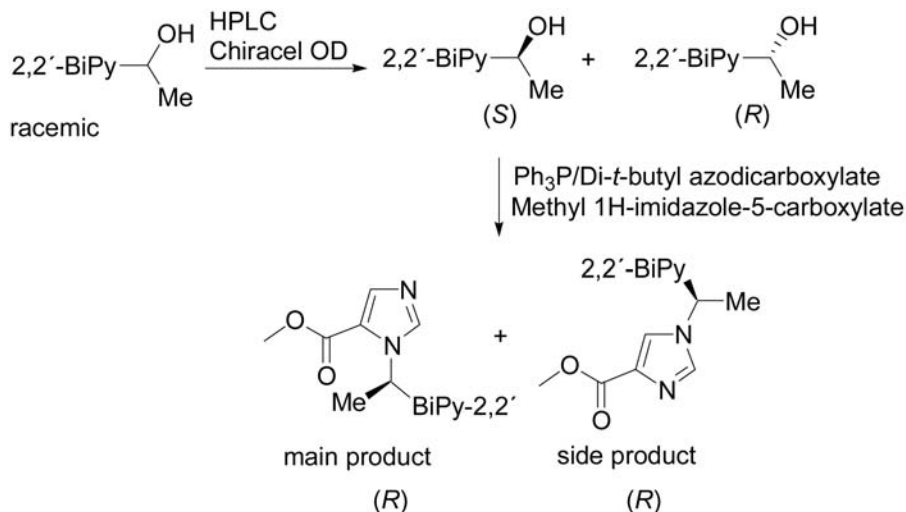


FIG. 2. Synthesis of (R)-BiPy-metomidate (modified Mitsunobu reaction).

2.1.2. Synthesis of achiral BiPy-MTO

The synthesis of MTO having no chiral centre (missing methyl group = dme) and of 2,2'-BiPy replacing the phenyl ring, has been performed according to the scheme shown in Fig. 3.

The intermediate ester obtained by Stille coupling was reduced with lithium aluminum hydride in dry THF to the alcohol in 78% yield. It was coupled by the Mitsunobu reaction using triphenylphosphane and diethyl azodicarboxylate with methyl 1*H*-imidazole-5-carboxylate at 0°C.

Two products were isolated, the main product (60%, m.p. 125–126°C, alkylation at N-1 of starting methyl 1*H*-imidazole-5-carboxylate, namely 1-(2,2'-bipyridin-5-yl)methyl]-1*H*-imidazole-5-carboxylic acid methyl ester) and a side product (6%, m.p. 130–131°C, alkylation at N-3 of starting methyl 1*H*-imidazole-5-carboxylate, namely 1-(2,2'-bipyridin-5-yl)methyl]-1*H*-imidazole-4-carboxylic acid methyl ester) which were separated by flash column chromatography.

2.1.3. Synthesis of Py-MTO derivatives

By analogy, (*S*)-1-(pyridin-3-yl)ethanol or (pyridin-3-yl)methanol were coupled with methyl 1*H*-imidazole-5-carboxylate producing (*R*)-Py-MTO of

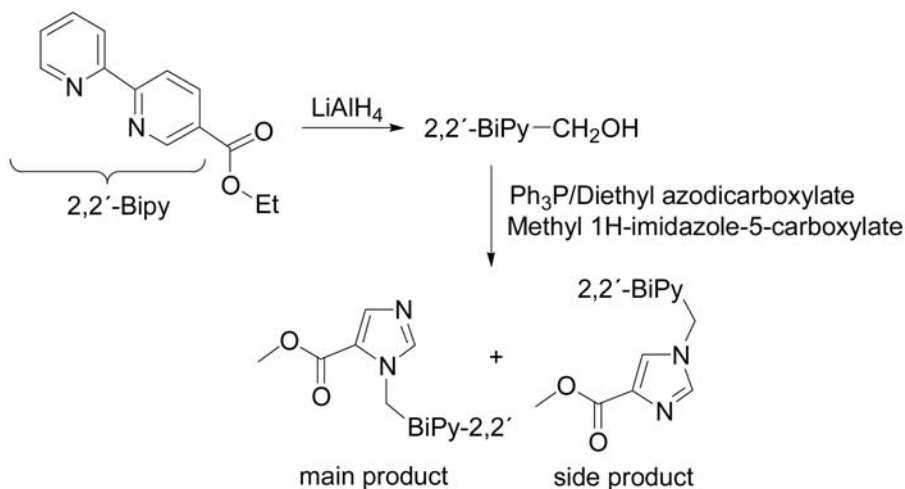


FIG. 3. Synthesis of achiral BiPy-metomidate.

high enantiomeric excess (ee 96%) or the achiral pyridinyl-derivative, respectively. Alkylation at N-3 of starting methyl 1*H*-imidazole-5-carboxylate was not observed.

2.2. Structure–affinity relationship studies

In vitro displacement studies were performed using ^{131}I -IMTO radioligand binding to rat adrenal membranes [4, 7]. Test compounds were used at concentrations between 0.1nM and 300 μM . Binding potency was expressed as the IC_{50} value.

Membranes prepared from rat adrenals were incubated with 20 000–40 000 counts/min of ^{131}I -IMTO together with 2nM carrier (resulting in a specific activity of 330–660 GBq/mmol) at 23°C for 20–30 min. Bound radioligand was isolated by filtration through glass fibre filters. Non-specific binding was determined with ETO (10 μM). The IC_{50} values were evaluated by non-linear, least squares regression analysis.

2.3. Labelling procedures

2.3.1. Formation of the $^{99m}\text{Tc}(\text{I})$ -tricarbonyl (*R*)-BiPy-MTO-conjugate

Cationic $^{99m}\text{Tc}(\text{H}_2\text{O})_3(\text{CO})_3^+$ [8, 9] was prepared using a kit formulation (IsoLink™, Mallinckrodt). To the IsoLink vial was added 1.0 mL of $\text{Na}[^{99m}\text{TcO}_4]$ (100–300 MBq) in saline. The reaction mixture was heated at 100°C for 20 min to form the $^{99m}\text{Tc}(\text{CO})_3(\text{H}_2\text{O})_3^+$ intermediate. After cooling to room temperature the solution was neutralized with 0.2 mL of a 1:2 mixture of 1M phosphate buffer (pH7.4) and 1M HCl. 0.2 mL (20–60 MBq) of the labelled tricarbonyl intermediate were added to a 10 mL vial containing 0.05 mL of a 10^{-2}M solution of *R*-BiPy-MTO in physiological phosphate buffer (PBS) and 0.25 mL of PBS. The mixture was heated at 75°C for 45 min. After cooling, a sample of the resulting solution was analysed by TLC and radio-HPLC. The radiochemical yield of the cationic $^{99m}\text{Tc}(\text{R-BiPy.MTO})(\text{H}_2\text{O})(\text{CO})_3^+$ conjugate was >85%. The ^{99m}Tc -*R*-BiPy-MTO-conjugate was purified on analytical HPLC column (Nucleosil 100-5 C₁₈, Macherey-Nagel) at a retention time (t_R) of 19.5–20.2 min. The organic solvent (methanol) was evaporated under a stream of nitrogen and the sample was further diluted with PBS to a final concentration of 10 MBq/mL. Figure 4 shows the reaction conditions for synthesis of the $^{99m}\text{Tc}(\text{I})$ -tricarbonyl-BiPy-MTO-conjugate. Formation of two isomers can be expected (see reaction with rhenium). However, the *R*- and *S*-isomers were not separated by the reversed phase HPLC column and were eluted as a single peak.

2.3.2. Synthesis of the $[\text{ReBr}(\text{R-BiPy-MTO})(\text{CO})_3]$ conjugate

The non-radioactive organometallic rhenium conjugate of *R*-BiPy-MTO was obtained as the corresponding hydrobromide salt $[\text{ReBr}(\text{R-BiPy-MTO})(\text{CO})_3]\cdot\text{HBr}$. The synthesis was performed by reacting 40 mg (52 μmol)

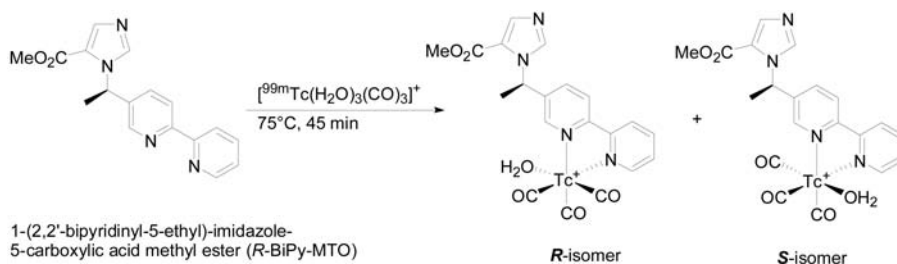


FIG. 4. Labelling of (*R*)-BiPy-MTO with the $^{99m}\text{Tc}(\text{I})$ -tricarbonyl complex.

of the preformed $[\text{ReBr}_3(\text{CO})_3]^{2-}$ intermediate with 15 mg (48 μmol) of *R*-BiPy-MTO precursor in 1 mL methanol at 50°C for 12 h, with stirring (Fig. 5). Conjugate formation was analysed by HPLC. The conjugate was precipitated directly from the reaction solution by addition of excess HBr (0.1M) as a yellow powder (yield 64%).

Re(I)Br-tricarbonyl-(*R*)-BiPy-MTO-conjugate; anal. calcd. (%) for $\text{C}_{19}\text{H}_{17}\text{Br}_2\text{N}_4\text{O}_5\text{Re}$ (725.91) found: C 32.02, H 2.83, N 7.74; Calcd: C 31.37, H 2.36, N 7.70.

Elemental analysis confirmed the proposed composition with a metal:ligand ratio of 1:1. NMR analysis indicated the formation of two isomers with a ratio of approx. 50:50. These were confirmed by HPLC analysis by two distinct signals with a t_R of 22.2 min and 22.4 min, respectively.

2.3.3. Biodistribution of ^{99m}Tc -metomidate in mice

Biodistribution studies were performed using female, adult BALB/c mice according to, and in compliance with, the Swiss Guidelines for Animal Care. Mice (average weight 25 g) were injected with aliquots of 100 μL of the conjugate solution (10 MBq/mouse) into the tail vein. Three animals were used per group. Tissues and organs were excised from the sacrificed animals at 2, 7, 30 and 60 min post-injection. The organs and tissues were weighed and the radioactivity measured in a gamma counter. Organ uptake was expressed as a percentage of the injected dose per organ (%ID/organ) and per gram of wet tissue mass (%ID/g).

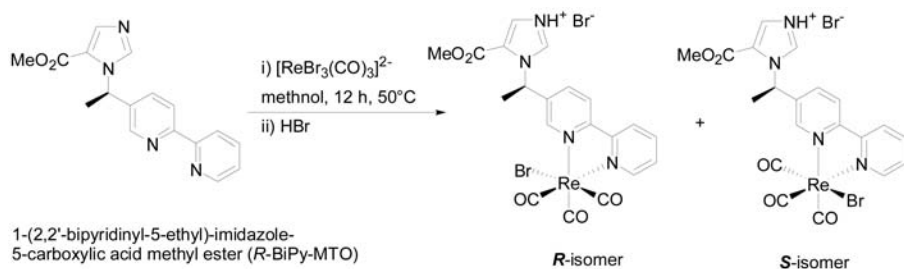


FIG. 5. Synthesis of Re(I)Br-tricarbonyl-(*R*)-BiPy-MTO-conjugate.

3. RESULTS

3.1. Precursor synthesis

Syntheses are based on the Mitsunobu reaction starting from methyl 1*H*-imidazole-5-carboxylate and from either (pyridin-3-yl)- and (2,2'-bipyridin-5-yl)methanol or (*S*)-1-(pyridin-3-yl)- and (*S*)-1-(2,2'-bipyridin-5-yl)ethanol of high enantiomeric excess (96% and 99%, respectively). The inversion of configuration and high regioselectivity of alkylation at N-1 underline the merits of this method for the synthesis of biologically active MTO derivatives.

3.2. Structure–affinity relationship studies

The IC₅₀ values (Table 1) demonstrate the high affinity of (*R*)-MTO in comparison with the (*S*)-enantiomer [7]. For comparison, the dme analogue (no chiral C-atom) is also listed (IC₅₀ = 28.8nM). The moderate decrease of binding affinity observed when the phenyl ring is replaced by pyridine (IC₅₀ = 20.7nM) is amplified in the cases of dme-Py-MTO (IC₅₀ = 870nM) and dme-BiPy-MTO (IC₅₀ = 1.1μM). Absence of the (*R*)-methyl substituent and replacement of phenyl are not tolerated. However, the biologically active (*R*)-enantiomers (*R*)-Py-MTO and (*R*)-BiPy-MTO exhibit adequate binding potency. The free MTO-acid is biologically inactive.

TABLE 1. DISPLACEMENT OF ¹³¹I-IMTO BY TEST COMPOUNDS

Inhibitor	IC ₅₀ values (nM)	(n)
(<i>R</i>)-Metomidate (MTO)	3.69 ± 1.92	(6)
(<i>S</i>)-MTO	492 ± 2.81	(4)
Dme-MTO	28.8 ± 10.9	(4)
(<i>R</i>)-Py-MTO	20.7 ± 3.80	(4)
Dme-Py-MTO	870 ± 240	(3)
Dme-BiPy-MTO	1100 ± 410	(7)
(<i>R</i>)-BiPy-MTO	179 ± 66.1	(3)
(<i>R</i>)-MTO-COOH	123 000 ± 41 000	(3)

3.3. Conjugate formation

The $^{99m}\text{Tc}(\text{I})$ -tricarbonyl-BiPy-MTO-conjugate was obtained with high radiochemical purity (>95%). The observed specific activity was generally >1 GBq/ μg . Purification by analytical HPLC produced the $^{99m}\text{Tc}(\text{I})$ -tricarbonyl-BiPy-MTO-conjugate with a t_{R} of 19.5–20.2 min. The ^{99m}Tc -intermediate and [^{99m}Tc]Na-pertechnetate would be eluted at 5 and 10 min, respectively; the free ligand *R*-BiPy-MTO eluted at 16.7 min. The corresponding neutral rhenium conjugate revealed a slightly higher retention time of 22.2–22.4 min than the corresponding cationic $^{99m}\text{Tc}(\text{I})$ -*R*-BiPy-MTO-conjugate.

3.4. Biodistribution in mice

Data obtained 30 min after the intravenous injection indicate accumulation of radioactivity in excretory organs, primarily in the liver and kidneys (Fig. 6). High renal activity indicates rapid hydrolysis of the intact ester and excretion of the labelled metabolite. Adrenal uptake corresponds to 5.5% ID/g tissue. While accumulation in the liver showed a moderate decrease in the next 30 min, renal activity decreased rapidly (32% in 30 min). No increase of adrenal activity was seen during this period.

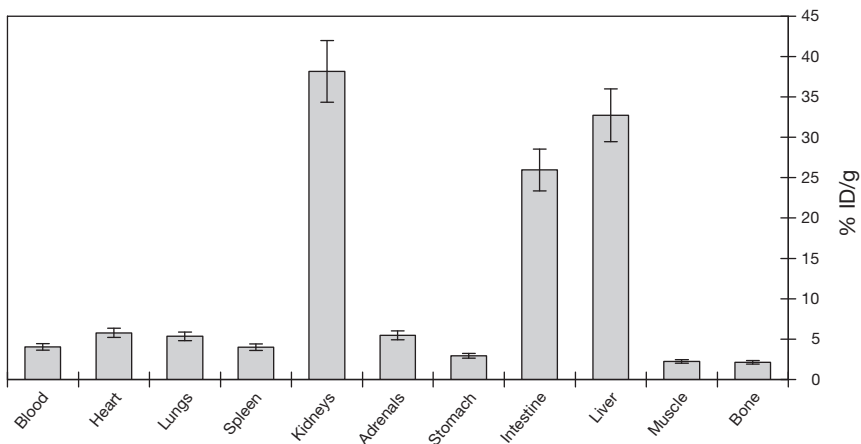


FIG. 6. Biodistribution of $^{99m}\text{Tc}(\text{I})$ -*R*-BiPy-MTO-conjugate 30 min post-injection in mice.

4. DISCUSSION

Replacement of the phenyl ring of (*R*)-MTO by pyridine or bipyridine showed a moderate loss of affinity in case of (*R*)-Py-MTO. The biologically active bipyridinyl-MTO displaced ^{131}I -IMTO binding from rat adrenal membranes with an IC_{50} of 180nM. As a result of affinity measurements it is expected that the $^{99\text{m}}\text{Tc}(\text{I})$ -tricarbonyl-*R*-BiPy-MTO-conjugate would exhibit specific binding to adrenocortical tissue despite the contribution of the unsaturated tricarbonyl moiety to unspecific binding.

Formation of the $^{99\text{m}}\text{Tc}(\text{I})$ -tricarbonyl-complex using a commercial kit was almost quantitative, coupling with the *R*-BiPy-precursor proceeded with high yield. HPLC separation produced the $^{99\text{m}}\text{Tc}(\text{I})$ -tricarbonyl-*R*-BiPy-MTO-conjugate with high chemical and radiochemical purities.

The biodistribution of $^{99\text{m}}\text{Tc}(\text{I})$ -tricarbonyl-*R*-BiPy-MTO-conjugate in mice showed high uptake in the liver (26% ID) and kidneys (11% ID) 2 min after IV injection. Liver uptake reached a maximum at 30 min after injection (31.2% ID) and stayed on a high activity plateau. Intestinal activity also showed a maximum at 30 min post-injection (14.9% ID), which decreased to 2.8% at 60 min. The elimination of activity by the kidneys decreased to 6.2% at 60 min. Renal activity is an indicator of enzymatic cleavage of the methyl ester producing the labelled, biologically inactive MTO-carboxylate anion. Rapid metabolization in mice might have affected the specific adrenal uptake, which did not exceed 5.5% ID/g tissue. Radioactivity in the blood pool may be partially explained by association of $[\text{}^{99\text{m}}\text{Tc}(\text{I})\text{-}(\text{R-BiPy-MTO})(\text{H}_2\text{O})(\text{CO})_3]^+$ with plasma proteins [10], measured in vitro (data not shown).

5. CONCLUSIONS

Formation of the $^{99\text{m}}\text{Tc}(\text{I})$ -tricarbonyl-complex using a commercial kit was quantitative, coupling with the BiPy-precursor proceeded with high yield. HPLC separation produced a pure $^{99\text{m}}\text{Tc}(\text{I})$ -tricarbonyl-*R*-BiPy-MTO-conjugate. Structural verification was obtained by analysis of the analogous *Re*(I)-tricarbonyl-*R*-BiPy-MTO-conjugate. Biodistribution in mice indicated rapid metabolism of the radiotracer and a moderate adrenal uptake. The labelled metabolite contributed to high accumulation of radioactivity in the kidneys.

SESSION 7

REFERENCES

- [1] ENGELHARDT, D., *Clin. Investig.* 72 (1994) 481-488.
- [2] BERGSTRÖM, M., et al., *J. Nucl. Med.* 41 (2000) 275-282.
- [3] VAN DEN BOSSCHE, H., et al., *Biochem. Pharmacol.* 33 (1984) 3861-3868.
- [4] SCHIRBEL, A., et al., *Radiochim. Acta*, 92 (2004) 297-303.
- [5] HAMMERSCHMIDT, F., et al., *Monatshefte Chem.* 136 (2005) 229-239.
- [6] GHADIRI, M.R., SOARES, C., CHOI, C., *J. Am. Chem. Soc.* 114 (1992) 825-831.
- [7] BERGER, M.L., SCHIRBEL, A., HAMMERSCHMIDT, F., ZOLLE, I., *Eur. J. Nucl. Med. & Molec. Imaging* 29 (Suppl. 1) S380 (2002).
- [8] NETTER, M., et al., *J. Labelled Compd. & Radiopharm.* Vol. 44: Suppl. 1, S624 (abstract) (2001).
- [9] ALBERTO, R., et al., *J. Am. Chem. Soc.* 120 (1998) 7987-7988.
- [10] SCHIBLI, R., et al., *Bioconjugate Chem.* 11, (2000) 345-351.

DIRECT LABELLING OF LIPIODOL WITH [¹⁸⁸RE(CO)₃]-CHELATES

M.M. SAW* **, F.X. SUNDRAM**, T.S. ANDY HOR*, Y.Y. KAI***,
R. ALBERTO⁺

*Department of Chemistry, National University of Singapore

**Department of Nuclear Medicine and PET, Singapore General Hospital

***National Institute of Education, Nanyang Technological University

Singapore

⁺Institute of Inorganic Chemistry, University of Zurich,
Zurich, Switzerland
Email: ariel@aci.unizh.ch

Abstract

Hepatocellular carcinoma is one of the ten most common tumours in the world. Internal radiation therapy has been used extensively in the management of hepatocellular carcinoma. Lipiodol, when injected through hepatic artery, accumulates in liver cancer cells and thus has been used as a vehicle for hepatocellular carcinoma targeting. The first and only attempt to label ¹⁸⁸Re covalently with Lipiodol was reported by Wang et al. by using the linker EDTB (EDTB = N,N,N',N'-terakis(2-benzimidazolylmethyl)-1,2-ethanediamine). The authors have synthesized bi- and tridentate ligand systems featuring long alkyl chains as Lipiodol surrogates and their [Re(CO)₃] complexes to be solved in Lipiodol. In the paper, direct labelling of the natural product Lipiodol with [Re(CO)₃]-metal fragments will be highlighted.

1. INTRODUCTION

Hepatocellular carcinoma is one of the ten most common tumours in the world [1] and the most frequent malignant tumour in large areas of Asia and Africa [2, 3]. Internal radiation therapy has been used extensively in the management of hepatocellular carcinoma such as ¹³¹I iodized poppy seed oil (LipiodolTM), ⁹⁰Y labelled microspheres or ¹⁸⁸Re-HDD/Lipiodol. The radiographic contrast medium LipiodolTM (GUERBET) is derived from natural

poppy seed oil. Lipiodol, when injected through hepatic artery, accumulates in liver cancer cells [4]. This makes arterially directed treatment of liver especially attractive, since the tumour can be made either ischemic or infused with cytotoxic agents while uninvolved liver is spared [5]. Most Lipiodol based internal radiation therapy approaches in the literature involve lipophilic radiometal complexes dissolved in, rather than covalently conjugated to, Lipiodol [6]. Covalent binding of a radionuclide other than ^{131}I to Lipiodol is challenging. The first and only attempt to label ^{188}Re covalently with Lipiodol was reported by Wang et al. using the linker EDTB (EDTB = N,N,N',N'-terakis(2-benzimidazolymethyl)-1,2-ethanediamine) affording EDTB conjugated Lipiodol [7]. Unfortunately, the exact structure of the labelled Lipiodol could not be verified and the toxicity of EDTB is unknown and therefore is an obstacle for further clinical trials.

Radioactive $^{186/188}\text{Re}$ is gaining prominence and significance as the main therapeutic radionuclide by virtue of its distinctive physical properties [8]. Currently, $[\text{M}(\text{OH}_2)_3(\text{CO})_3]^+$ ($\text{M} = {}^{99\text{m}}\text{Tc}$ or $^{186/188}\text{Re}$) has emerged as a versatile metal precursor [9]. The authors have synthesized bi- and tridentate ligand systems featuring long alkyl chains as Lipiodol surrogates and their $[\text{Re}(\text{CO})_3]$ complexes to be solved in Lipiodol [10]. In this article, direct labelling of the natural product Lipiodol with $[\text{Re}(\text{CO})_3]$ -metal fragments will be highlighted.

2. EXPERIMENTAL

2.1. General procedures and materials

Materials were purchased from commercial suppliers and used without further purification, unless otherwise specified. All reactions were carried out under purified nitrogen. $\text{Na}^{99\text{m}}\text{TcO}_4$ was eluted with 0.9% saline from ${}^{99}\text{Mo}$ - ${}^{99\text{m}}\text{Tc}$ generators purchased from Amersham Co. ^1H and ^{13}C -NMR spectra were recorded on Varian Mercury 200, Varian Gemini 300 and Bruker DRX500 spectrometers. The reported chemical shifts (in ppm) are relative to tetramethylsilane. Infrared spectra were recorded as pellets (KBr) using a Perkin Elmer FT-IR spectrometer. High performance liquid chromatography (HPLC) was performed on a Merk L7000 system using a Macherey-Nagel EC 250/3 Nucleosil 100-5 C18HD column for non-radioactive compounds and a Macherey-Nagel EC 250/3 Nucleosil 100-5 C18 column for radioactive compounds. The HPLC solvents used were 0.1% trifluoroacetic acid (solvent A) and HPLC grade methanol (solvent B). The general HPLC gradient (gradient 1) used is as follows: 0–3 min: 100% A; 3.1–9 min: 75% A:25% B; 9.1–20 min: linear gradient from 66% A (34% B) to 0% A (100% B); 20–28 min:

100% B; 28.1–30 min: 100% A. The flow rate was 0.5 mL/min. The HPLC gradient (gradient 2) used is as follows: 0–15 min 50% A; 15–30 min 100% B. The flow rate was 0.5 mL/min. Detection was performed at 220 nm for non-radioactive aliphatic compounds and at 250 nm for non-radioactive aromatic compounds. The detection of radioactive ^{99m}Tc and ^{186}Re compounds was performed with a Berthold LB506 radiodetector equipped with a NaI(Tl) scintillation detector. Mass spectra were recorded on a Merck M8000 HPLC/MS spectrometer with electrospray ionization (ESI) and a VG platform II instrument. All of the spectra are recorded in positive ion mode unless otherwise specified.

2.2. Synthesis of $[\text{NEt}_4]_2[\text{ReBr}_3(\text{CO})_3](1)$

$[\text{NEt}_4]_2[\text{ReBr}_3(\text{CO})_3]$ was synthesized according to the published procedure [11].

2.3. Synthesis of $[\text{Re}(2\text{-picolinate})(\text{OH})_2(\text{CO})_3](2)$

To a solution of 300 mg of **1** (0.4 mmol) dissolved in 4 mL of H_2O , 2-picolinic acid 48 mg (0.4 mmol) was added and stirred at 80°C for 14 h. A yellow precipitate was formed immediately. The precipitate was filtered off and washed with water affording 147 mg of greenish-yellow solid. (Isolated yield - 90%). HPLC: R_t 14.5 min (method – gradient 2), IR(cm^{-1}) (KBr): 3435(w), 2023(s), 1878(br, s), 1624 (m).

2.4. Synthesis of $[\text{Re}(\text{quinaldate})(\text{OH})_2(\text{CO})_3](3)$

To a solution of 101 mg of **1** (0.13 mmol) dissolved in 4 mL of H_2O , quinaldic acid 23 mg (0.13 mmol) was added and stirred at 80°C for 3 h. A yellow precipitate was formed immediately. Precipitate was filtered off and washed with water affording 59 mg of deep yellow solid. (Isolated yield – 98%). HPLC: R_t 14.7 min (method – gradient 1), ESI/MS m/z : 443.2 (100%) $[\text{M}-\text{H}_2\text{O}+\text{H}]^+$ (calcd. $\text{C}_{13}\text{H}_7\text{NO}_5\text{Re}$ 443.4), IR(cm^{-1}) (KBr): 3082(br, m) ν_{OH} , 2029(s), 1885(s) $\nu_{\text{C=O}}$, 1648(m), 1458(m), 1376(m), 773(m). ^1H NMR (CDCl_3 , ppm): 8.36 (d, 1H), 8.22 (d, 1H), 8.14 (d, 2H), 7.92 (t, 2H), 2.15 (s, 2H).

2.5. Synthesis of $[\text{Re}(\text{isoquinoline-1-carboxylate})(\text{OH})_2(\text{CO})_3](4)$

To a solution of 100 mg of **1** (0.13 mmol) in 4 mL of H_2O , isoquinoline-1-carboxylic acid 23 mg (0.13 mmol) was added and stirred at 75°C overnight. A deep orange precipitate was formed immediately. The precipitate was filtered

off and washed with water affording 58 mg of deep orange solid. The product is slightly soluble in water. (Isolated yield – 58%), HPLC: $R_t = 19.8$ min (method – gradient 1). ESI/MS m/z : 465.3 (100%) $[M-H_2O+Na]$ (calcd. $C_{13}H_6NNaO_3Re$ 466.0), 906.1 $[2(M-H_2O)+Na]^+$ (80%) (calcd. $C_{26}H_{12}N_2NaO_{10}Re_2$ 907), IR (cm^{-1}) (KBr): 3435(br, w) ν_{OH} , 2026(s), 1885(s) $\nu_{C=O}$, 1609 (m), 1585(m).

2.6. Synthesis of Lipiodol functionalized with 4-mercaptopyridine (5)

To a solution of 4-mercaptopyridine 239 mg (2.2 mmol) in 4 mL of methanol, 300 μ L of Et_3N (482 mg, 2.2 mmol) was added and stirred at room temperature for 15 min (pH10). Lipiodol 1 mL (≈ 2.5 mmol) was added and stirred at 60°C for 3 h. A 0.1 mL sample was taken and diluted with 2 mL of CH_3OH and injected into mass spectrometer. ESI/MS m/z : 548.3 (100%) $[M+H]^+$ (calcd. $C_{25}H_{43}INO_2S$ 548.2).

2.7. Lipiodol functionalized with imidazole (6)

To a solution of imidazole 136 mg (2 mmol) in 4 mL of methanol, 270 μ L of Et_3N (482 mg, 2.2 mmol) was added and stirred at room temperature for 15 min (pH10). Lipiodol 1 mL (≈ 2.5 mmol) was added and stirred at 65°C under reflux for 3 h. Solvent extraction was done with ethyl acetate and washed with water three times. Organic parts were collected and evaporated in vacuo affording deep yellow oil. ESI/MS m/z : 505.2 (100%) $[M+H]^+$ (calcd. $C_{23}H_{42}IN_2O_5$ 505.5).

2.8. Lipiodol functionalized with cysteine (7)

To a solution of L-cysteine 123 mg (1 mmol) dissolved in 4 mL of CH_3CN , Cs_2CO_3 245.3 mg (0.75 mmol) and 500 μ L of Lipiodol (≈ 1.5 mmol) were added and stirred at 55°C for 3 h. ESI/MS m/z : 554.9 (100%) $[M-CH_2CH_3 + K]^+$ (calcd. $C_{20}H_{38}IKNO_4S$ 554.1), HPLC: R_t 25.9 min.

2.9. $[Re(2\text{-picolinate})(5)(CO)_3]$ (8)

To a solution of 31 mg (0.04 mmol) of **1** dissolved in 2 mL of acetone, 2-picolinic acid 4.8 mg (0.04 mmol) was added and refluxed at 45°C for 30 min. 1 mL of **5** was added and stirred at 75°C overnight. ESI/MS m/z : 924 (100%) $[M-CH_3]^+$ (calcd. $C_{33}H_{44}IN_2O_7ReS$ 924.9).

2.10. [Re(quinaldate)(5)(CO)₃] (9)

To a solution of 0.5 mL of **5** in CH₃OH, 44 mg (1 mmol) of **3** was added and stirred at 80°C overnight. ESI/MS *m/z*: 974 [M-CH₃]⁺ (100%) (calcd. C₃₇H₄₅IN₂O₇ReS 975.1).

2.11. [Re(isoquinoline-1-carboxylate)(6)(CO)₃] (10)

To a solution of 0.5 mL of **6** in CH₃OH, 46 mg (1 mmol) of **4** was added and stirred at 80°C overnight. ESI/MS *m/z*: (negative mode) 947 [M-H]⁻ (calcd. C₃₆H₄₆N₃O₇ReI 946.2).

2.12. [Re(isoquinoline-1-carboxylate)(5)(CO)₃] (11)

To a solution of 1 mg (0.04 mmol) of **1** dissolved in 2 mL of CH₃OH, isoquinoline-1-carboxylic acid 7.3 mg (0.04 mmol) was added and stirred at 45°C for 30 min. 1 mL of **5** was added and stirred at 75°C overnight. ESI/MS *m/z* (negative mode): 992.5 [M-CH₃+OH]⁻ (calcd. C₃₇H₄₇IN₂O₈ReS 993.2).

2.13. 10-(Pyridin-4-ylsulphanyl)-octadecanoic acid ethyl ester (12)*Step (1): Synthesis of 10-bromo-octadecanoic acid*

Surface mediated hydrobromination of oleic acid was carried out by a published method [12]. Merck grade 60 silica gel absorbents were equilibrated with moisture in an oven (120°C atmosphere) for 72 h prior to use. The order of addition of precursors and surface catalysts were as described by the original author. To a solution of oleic acid 891 μL (1 g, 3.5 mmol) in 15 mL of CH₂Cl₂, 11 g of Merck grade 60 silica gel was added and stirred to get a suspension. Hydrobromic acid 300 μL (3.5 mmol) was added to the suspension and stirred at room temperature for 26 h. Reaction mixture immediately turned a deep orange. It was filtered off and washed with CH₂Cl₂ and evaporated in vacuo, affording 776 mg of red-orange oil. (Isolated yield – 60%) HPLC: R_t – 19.3 min (method – gradient 2, 220nm), ESI/MS *m/z*: 721.3 (100%) [2M-CH₂CH₃+Na]⁺ (calcd. C₃₄H₆₆Br₂NaO₄ 721.3).

Step (2): Synthesis of 10-bromo-octadecanoic acid ethyl ester

To a solution of 776 mg of 10-bromo-octadecanoic acid in 18 mL of CH₃CH₂OH, H₂SO₄ 300 μL (8% of the weight of ethanol) was added and refluxed at 75°C for 27 h. Crude product was filtered off, evaporated in vacuo,

extracted with ethyl acetate and washed with water three times affording 672 mg (2 mmol) of orange-red oil. (Isolated yield – 52%) HPLC: R_t – 22.4 min (method – gradient 2, 220nm), ESI/MS m/z : 298.9 (100%) $[M-Br-CH_3]^+$ (calcd. $C_{19}H_{38}O_2$ 298.3), 1H NMR ($CDCl_3$, ppm): 0.86-0.91 (t, $J = 6.75$ Hz, 3H), 1.26 (m, 20H), 1.31 (m), 1.42 (m, 2H), 1.62 (m, 2H), 1.63-1.82 (m, 4H), 2.27-2.32 (t, $J = 7.5$ Hz, 2H), 3.44-3.51 (m, 1H) (CH_2CHBr), 4.01-4.06 (m, 2H).

Step (3): Synthesis of 10-(pyridine-4-ylsulphanyl)-octadecanoic acid ethyl ester

4-mercaptopyridine 143 mg (1.3 mmol) was dissolved in 3 mL of CH_3CN and Cs_2CO_3 576 mg (1.8 mmol) was added and stirred for 15 min. 10-bromo-octadecanoic acid ethyl ester 450 mg (1.2 mmol) dissolved in 3 mL of CH_3CN was added and stirred at room temperature for 20 h. Crude product was purified by preparative HPLC (gradient 0.1%TFA: CH_3OH , flow rate – 40 mL/min) affording 239 mg of yellow-brown oil. (Isolated yield – 57%) 1H NMR ($CDCl_3$, ppm): 0.88-0.91 (t, $J = 6.71$ Hz, 3H), 1.26 (m), 1.32 (m) 3, 1.42 (m), 1.58-1.63 (m, 4H), 2.28-2.31 (t, $J = 7.52$ Hz, 2H), 2.78-2.81 (m, 1H) ($SCHCH_2$), 4.11-4.16 (q, $J = 7.1$ Hz, 2H), 7.63-7.64 (d, $J = 5.04$ Hz, 2H), 8.50-8.51 (d, $J = 5.26$ Hz, 2H), ^{13}C NMR ($CDCl_3$, ppm): 14.3, 14.5, 22.9, 25.2, 27.5, 29.3, 29.4, 29.5, 29.7, 29.9, 30.0, 32.1, 34.6, 53.6, 60.4, 121.1, 130.7, 174.1, ESI/MS m/z : 454.3 $[M+CH_3OH+H]^+$ (calcd. $C_{26}H_{48}NO_3S$ 454.3), HPLC: $R_t = 19.3$ min (method – gradient 2).

2.14. [Re(isoquinoline-1-carboxylate)(12)(CO)₃] (13)

To a solution of 84 mg (0.2 mmol) of **12** in 3 mL of CH_3OH , 92 mg (0.2 mmol) of **4** was added and stirred at 100°C under reflux for 20 h. Flash chromatography was done with $CH_2Cl_2:CH_3OH$ (200:1) (v/v) affording 141 mg of orange-red oil. (Isolated yield – 84%). 1H NMR ($CDCl_3$, ppm): 0.86-0.90 (t, $J = 5.55$ Hz, 3H), 1.25 (m), 1.26 (m), 1.28 (m), 1.53-1.55 (m, 2H), 1.60 (m, 2H), 2.26-2.31 (t, $J = 7.65$ Hz, 2H), 2.70-2.72 (m, 1H), 4.09-4.16 (t, $J = 7.1$ Hz, 2H), 7.27-7.28 (d, $J = 4.5$ Hz, 1H), 7.40-7.42 (d, $J = 6.9$ Hz, 1H), 7.77-7.88 (m, 3H), 7.91-7.94 (d, $J = 6.3$ Hz, 1H), 8.42-8.44 (d, $J = 5.4$ Hz, 2H), 8.73-8.76 (d, $J = 6.3$ Hz, 1H), 9.96 (s, 11H), 9.99 (s, 1H), ^{13}C NMR ($CDCl_3$, ppm): 14.0, 14.1, 22.5, 24.7, 26.4, 26.5, 28.9, 29.0, 29.1, 29.2, 29.3, 29.4, 29.6, 31.7, 33.5, 34.0, 34.2, 52.9, 60.1, 121.8, 127.2, 128.2, 129.1, 130.3, 130.7, 132.9, 138.1, 143.2, 149.5, 155.3, 173.3, 193.6, 196.5, 198.2 ($C\equiv O$), ESI/MS m/z : 840.9 (70%) $[M-CH_2CH_3+H]^+$ (calcd. $C_{36}H_{49}N_2O_7ReS$ 840.3), IR (KBr) (cm^{-1}): 2927(m) ν_{-CH_3} , 2854(m) ν_{-CH_2} , 2022(s) ν_{-CO} , 1916, 1891(s) ν_{-CO} , 1668 (m) $\nu_{-C=N}$, HPLC: $R_t = 22.1$ min (method – gradient 2), TLC: $R_f = 0.25$ (product) (UV active spot 254 nm) (mobile – $CH_2Cl_2:CH_3OH$ (200:1)).

3. RESULTS AND DISCUSSION

3.1. Labelling approach

A ligand entity that can connect Lipiodol to the metal centre chemically can be visualized through derivatization of Lipiodol such that it has the functionality to coordinate to the metal ($M = \text{Tc}$ or Re). Alternatively, the ligand on the metal ($M = \text{Tc}$ or Re) can be functionalized, such that it chemically condenses with Lipiodol or its derivative. The authors have covalently bonded Lipiodol with $[\text{Re}(\text{CO})_3]$ complexes by two different approaches (Fig. 1).

3.2. Analytical method

HPLC analysis of Lipiodol showed four closely packed peaks which are difficult to separate and thereby isolate the individual components. NMR study of this mixture is complicated. Thus, ESI/MS was chosen as the main analytical tool for studying direct labelling experiments as it is well known as an efficient method for characterization of metal complexes in solution in general [13]. Andy Hor et al. have reported the use of ESI mass spectrometry (ESI/MS) as a rapid, convenient and economical solution based technique for screening reactions of a wide range of platinum(II) and palladium(II) substrates [14]. The advantages of this approach include the accepted general agreement between mass spectrometric data and solution speciation [15].

3.3. ESI/MS base line study of Lipiodol

Poppy seed oil is a chemical mixture comprising mostly unsaturated fatty acids, namely linoleic acid **a** (66.4%) (FW 564.3) and monounsaturated oleic acid **b** (19.7%) (FW 438.4). It also contains a significant amount of saturated fatty acids, namely palmitic acid **c** (10.6%) (FW 284.5) and stearic acid **d** (2.9%) (FW 312.5) [16]. Molecular and aggregate ions detected by positive ion ESI/MS study of Lipiodol in methanol are shown in Table 1.

3.4. ESI/MS study of Lipiodol functionalized with BFC

Derivatized Lipiodols were characterized by ESI/MS. Complex **5** showed m/z 548.3 (100%) $[\text{M}+\text{H}]^+$, which is in accordance with mass value for 4-mercaptopyridine coordinated to 9,13-diiodo-octadecanoic acid ethyl ester, main component of Lipiodol (calcd. $\text{C}_{25}\text{H}_{43}\text{INO}_2\text{S}$ 548.2). Complex **6** showed m/z 505.2 (100%), which is in accordance with mass value for $[\text{M}+\text{H}]^+$ ($M =$

imidazole coordinated to 9,13-diiodo-octadecanoic acid ethyl ester) (calcd. $C_{23}H_{42}IN_2O_2$ 505.5) (Fig. 2). Likewise, complex **7** showed m/z 554.9 (100%), which is in accordance with the mass value for L-cysteine coordinated to 9,13-diiodo-octadecanoic acid ethyl ester minus $-CH_2CH_3$ which might have lost in ESI/MS condition plus potassium ion which came from the previous samples (calcd. $C_{20}H_{38}IKNO_4S$ 554.1).

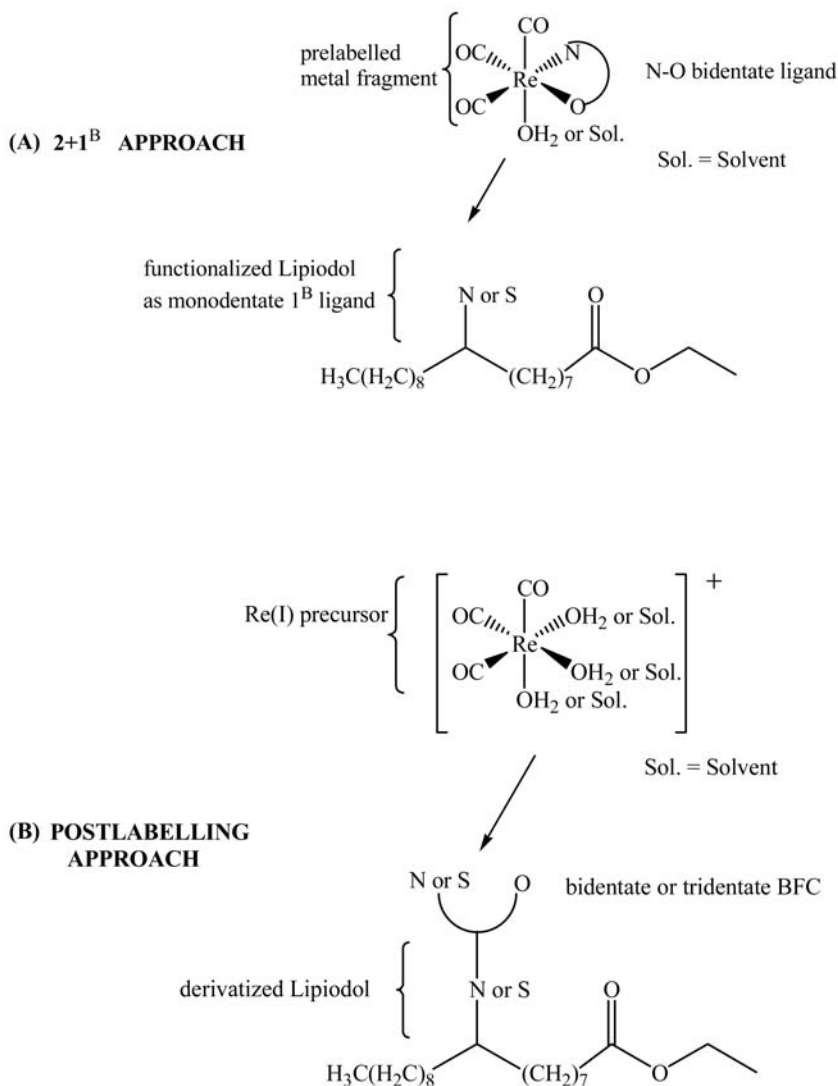


FIG. 1. Covalent bonding of Lipiodol with Re(I) complexes by two different approaches (A) and (B).

SESSION 7

TABLE 1. ESI/MS STUDY OF LIPIODOL IN METHANOL SHOWING MOLECULAR AND AGGREGATE IONS

m/z	Intensity	Relative conc. of parent compound	Principal ions
461.0	25%	19.7% (b)	[9- iodo-octadecanoic acid ethyl ester + Na] ⁺
531.3	20%	66.4% (a)	[9,13-diiodo-octadecanoic acid ethyl-ester - C ₄ H ₉ + Na] ⁺
586.8	100%	66.4% (a)	[9,13-diiodo-octadecanoic acid ethyl ester + Na] ⁺
898.6	18%	66.4% (a)	[9,13-diiodo-octadecanoic acid ethyl ester + octadecanoic acid ethyl ester + Na] ⁺
1024.3	45%	66.4% (a)	[2(9,13-diiodo-octadecanoic acid ethyl ester)- (CH ₂ CH ₃)+Na] ⁺
1149.9	47%	66.4% (a)	[2(9,13-diiodo-octadecanoic acid ethyl ester) + Na] ⁺

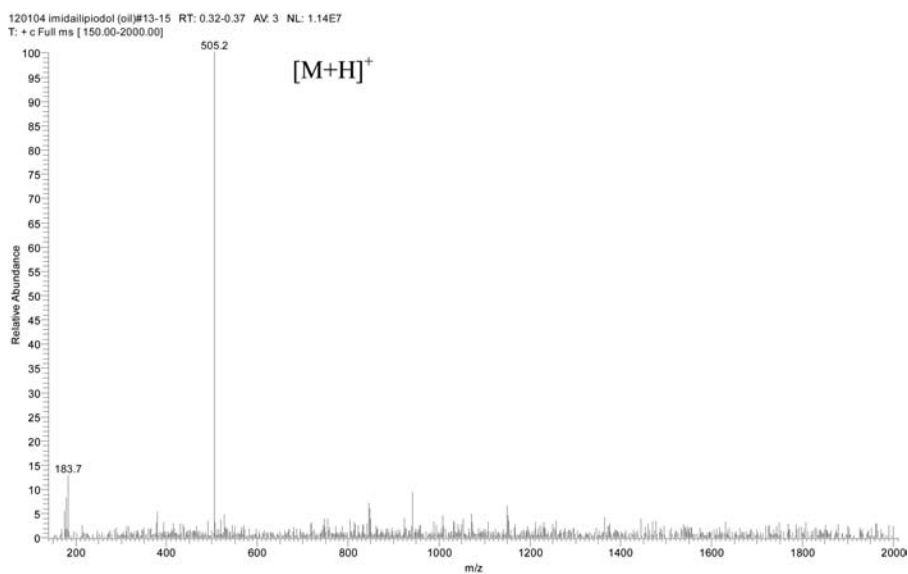


FIG. 2. ESI/MS spectrum of imidazole derivatized Lipiodol **6** (m/z 505.2 $[M+H]^+$, (calcd. $C_{23}H_{42}IN_2O_2$, 505.5).

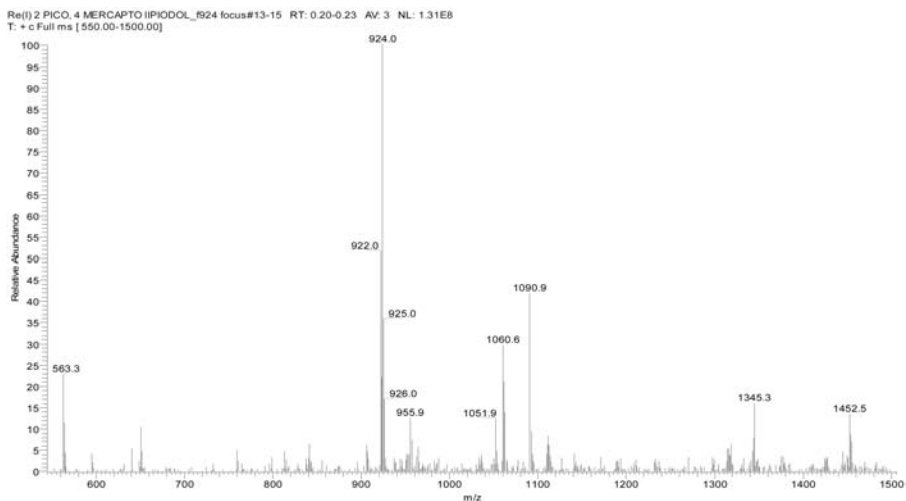


FIG. 3. ESI/MS spectrum of **8**, m/z 924 $[M-CH_3]^+$.

3.5. Coordination of functionalized Lipiodol with $[Re(CO)_3]$ -metal fragment

The authors studied $[Re(CO)_3]$ complexes coordinated to derivatized Lipiodol by ESI/MS. Three metal fragments, **2**, **3** and **4**, were used. The ESI/MS spectrum of complex **8** showed m/z 924 (100%) $[M-CH_3]^+$ (calcd. $C_{33}H_{44}N_2O_7ReS$ 924.9) (Fig. 3). The ESI/MS spectrum of **9** showed m/z 974 $[M-CH_3]^+$ (100%) (calcd. $C_{37}H_{45}IN_2O_7ReS$ 975.1). The ESI/MS spectrum (negative mode) of complex **10** showed m/z 947 $[M-H]^-$ (calcd. $C_{36}H_{46}N_3O_7ReI$ 946.2). The ESI/MS spectrum of complex **11** in negative mode showed m/z 994.7, which is in agreement with the molecular ion $[M-CH_3+OH]^-$ (calcd. $C_{37}H_{47}IN_2O_8ReS$ 993.2).

3.6. A Lipiodol mimic – functionalized oleate ethyl ester

Even though the authors' ESI/MS study of incorporation of $[Re(CO)_3]$ -metal fragments with functionalized Lipiodol clearly showed that direct labelling of Lipiodol with $[Re(CO)_3]$ is feasible, further characterization is very challenging. To overcome this problem the authors synthesized a Lipiodol mimic and its $[Re(CO)_3]$ -metal complex.

A Lipiodol mimic was developed by multistep synthesis starting from hydrobromination of oleic acid. Oleic acid was chosen as a model long chain fatty acid in this study rather than linoleic acid as the latter is more unsaturated

and will lead to multiple addition and formation of more isomers. The ^1H NMR spectrum of product 10-bromo-octadecanoic ethyl ester revealed loss of signal corresponding to the $-\text{CH}=\text{CH}-$ protons of oleic acid (5.5 ppm) and appearance of $-\text{CH}_2-\text{CH}-\text{Br}$ proton signal in 3.5 ppm denoting the disappearance of the double bond of oleic acid. 10-bromo-octadecanoic acid ethyl ester was functionalized with 4-mercaptopyridine in the presence of Cs_2CO_3 . The ESI/MS spectrum of the product **12** showed m/z 454.3, which is in agreement with $[\text{M}+\text{CH}_3\text{OH}+\text{H}]^+$ (calcd. $\text{C}_{26}\text{H}_{48}\text{NO}_3\text{S}$ 454.3). Spectroscopic data are in agreement with the proposed structure.

3.7. Coordination of $[\text{Re}(\text{isoquinoline-1-carboxylate})(\text{OH}_2)(\text{CO})_3]$ to (10-pyridin-4-ylsulphanyl-octadecanoic acid ethyl ester)

$[\text{Re}(\text{CO})_3]$ metal fragment **4** was coordinated to **12** affording **13** (Fig. 4) in high yield 84%. Characterization of the complex in solution was achieved by IR and NMR spectroscopy.

4. CONCLUSION

This study has proven that derivatization of the natural product Lipiodol with monodentate and polydentate ligands can be achieved by relatively simple

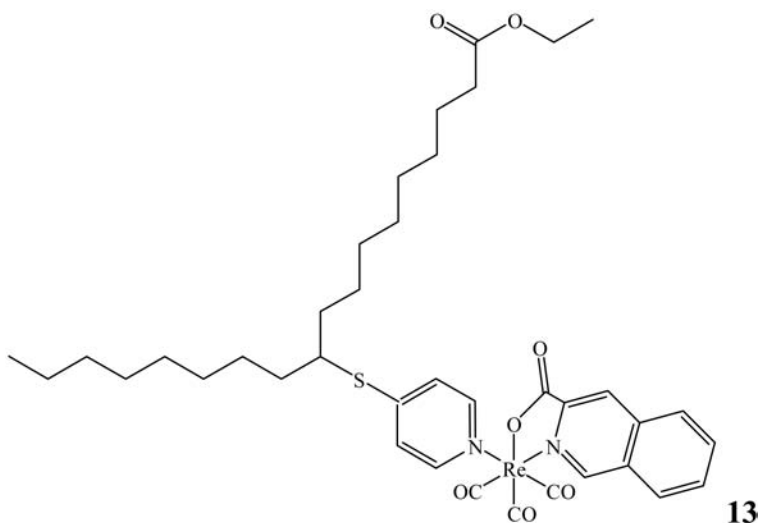


FIG. 4. Proposed structure of a Lipiodol mimetic directly labelled with $[\text{Re}(\text{CO})_3]$ -metal fragment.

synthetic routes. By using a versatile 2+1 mixed ligand approach or post-labelling approach, $[\text{Re}(\text{CO})_3]$ -metal fragment can be coordinated to derivatized Lipiodol, affording direct coordination of Lipiodol with either radioactive ^{186}Re , ^{188}Re or chemotherapeutic agents. Owing to the complexity of compounds in Lipiodol, a Lipiodol mimic, 10-Pyridin-4-ylsulphonyl-octadecanoic acid ethyl ester **12**, was synthesized and characterized. This Lipiodol mimic ligand and its $[\text{Re}(\text{CO})_3]$ -complex **13** have indirectly proved the possibility of similar structures in direct labelling of Lipiodol. The ultimate aim in the research and development of Lipiodol based drugs is direct covalent bonding of either radiometal or chemotherapeutic drugs which will give the best stability in the simplest and most direct approach. In this study, the authors have highlighted the simple, feasible and efficient methods for direct covalent bonding of the $[\text{Re}(\text{CO})_3]$ complex with Lipiodol. This approach might have significant impact on potential clinical applications in internal radiation therapy and chemoembolization therapy of hepatocellular carcinoma.

REFERENCES

- [1] WILLIAMS, R., RIZZO, P., *N. Engl. J. Med.* **1996**, 334, 728-729.
- [2] LIN, D.Y., LIN, S.M., LIAW, Y.F., *J. of Gastrol. & Hepatol.* **1997**, 12, 319.
- [3] OKUDA, K., et al., *Cancer*. **1985**, 56, 018.
- [4] NG, I.O., LAI, E.C., FAN, S.T., NG, M.M., SO, M.K., *Cancer*, **1995**; 76: 2443-48.
- [5] SIGURDSON, E.R., et al., *J. Clin. Oncol.* **1987**, 5, 1836-1840.
- [6] GARIN, E., et al., *Nucl. Med. Commun.* **2004**, 25, 1007.
- [7] WANG, S.J., et al., Jr. *Appl. Radiat. Isot.* **1996**, 47, 267.
- [8] MEASE, R.C., LAMBERT, C., *Seminars in Nuclear Medicine*, Radiochemistry Update, W B Saunders Company. **2001**, Oct, Vol XXXI, 4.
- [9] ALBERTO, R., et al., *J. Am. Chem. Soc.* **1998**, 120(31), 7987 - 7988.
- [10] SAW, M.M., et al., Complexes with the *fac*- $[\text{M}(\text{CO})_3]^+$ ($\text{M} = ^{99\text{m}}\text{Tc}$, Re) moiety and long alkyl chain ligands as Lipiodol surrogates. (manuscript in preparation for *Inorg. Chim. Acta*).
- [11] ALBERTO, R., et al., *J. Chem. Soc. Dalton Trans.* **1994**, 2815.
- [12] KROPP, P.J., *J. Am. Chem. Soc.* **1993**, 115, 3071.
- [13] BEARTANI, R., et al., *Inorg. Chim. Acta.* **2003**, 356, 357.
- [14] FONG, S.W.A., et al., *Inorg. Chim. Acta.* **2004**, 2081.
- [15] HENDERSON, W., NICHOLSEN, B.K., MCCAFFREY, L.J., *Polyhedron.* **1998**, 17, 4291.
- [16] BAILEY, A.E., FORMO, M.W., APPLEWHITE, T.H., *Bailey's Industrial oil and fat products*, 4th ed., Wiley, New York, 1985.

CHAIRPERSONS OF SESSIONS

Session 1	S. GOMEZ DE CASTIGLIA F.F. KNAPP, Jr.	Argentina United States of America
Session 2	A. DUATTI J. KÖRNYEI	Italy Hungary
Session 3	I. CARRIO E.K.J. PAUWELS	Spain Netherlands
Session 4	R. ALBERTO M. VENKATESH	Switzerland India
Session 5	R.S. KAMEL N. RAMAMOORTHY	IAEA IAEA
Session 6	M. JEHANGIR R. MIKOLAJCZAK	Pakistan Poland
Session 7	A. VERBRUGGEN M.R.A. PILLAI	Belgium IAEA

SECRETARIAT OF THE SYMPOSIUM

M.R.A. PILLAI	Scientific Secretary
K.K. SOLANKI	Scientific Co-Secretary
R. PERRICOS	Conference Services
L. BARRIOS	Conference Assistance
R.J. BENBOW	Proceedings Editor

IAEA PROGRAMME COMMITTEE

M. DONDI

M. HAJI-SAEID

R.S. KAMEL

M.R.A. PILLAI

N. RAMAMOORTHY
(*Chairperson*)

K.K. SOLANKI

The International Symposium on Trends in Radiopharmaceuticals (ISTR-2005) covered developments across the entire spectrum of radiopharmaceutical science, including radionuclide production and radiochemical processing; manufacture and quality control; advances in radiopharmaceuticals research; good manufacturing practices and regulatory aspects. Volume 1 covers technetium radiopharmaceuticals and radioisotope production in research reactors. Volume 2 covers cyclotron based isotopes, therapeutic and PET radiopharmaceuticals and radiopharmacy.

**INTERNATIONAL ATOMIC ENERGY AGENCY
VIENNA
ISBN 92-0-101707-3
ISSN 0074-1884**